NOVEL DIAGNOSTIC TOOLS AND BIOMARKERS IN HEMATOLOGIC MALIGNANCIES

EDITED BY: Mina Luqing Xu, Alejandro Gru, Julia T. Geyer and Andrew G. Evans
PUBLISHED IN: Frontiers in Oncology

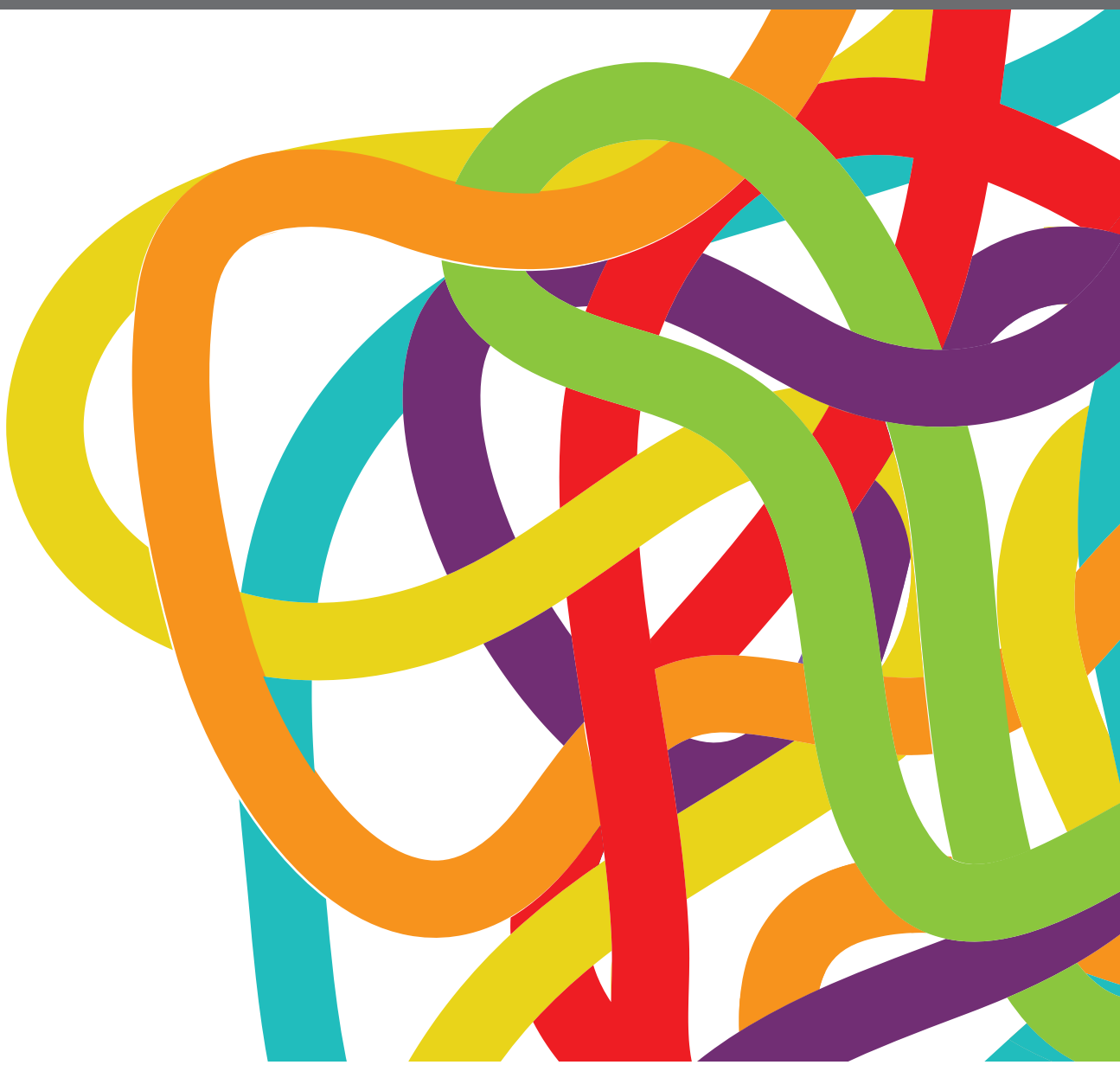

frontiers Research Topics

frontiers

ISSN 1664-8714
ISBN 978-2-88974-703-0
DOI 10.3389/978-2-88974-703-0

About Frontiers

Frontiers is more than just an open-access publisher of scholarly articles: it is a pioneering approach to the world of academia, radically improving the way scholarly research is managed. The grand vision of Frontiers is a world where all people have an equal opportunity to seek, share and generate knowledge. Frontiers provides immediate and permanent online open access to all its publications, but this alone is not enough to realize our grand goals.

Frontiers Journal Series

The Frontiers Journal Series is a multi-tier and interdisciplinary set of open-access, online journals, promising a paradigm shift from the current review, selection and dissemination processes in academic publishing. All Frontiers journals are driven by researchers for researchers; therefore, they constitute a service to the scholarly community. At the same time, the Frontiers Journal Series operates on a revolutionary invention, the tiered publishing system, initially addressing specific communities of scholars, and gradually climbing up to broader public understanding, thus serving the interests of the lay society, too.

Dedication to Quality

Each Frontiers article is a landmark of the highest quality, thanks to genuinely collaborative interactions between authors and review editors, who include some of the world's best academicians. Research must be certified by peers before entering a stream of knowledge that may eventually reach the public - and shape society; therefore, Frontiers only applies the most rigorous and unbiased reviews.
Frontiers revolutionizes research publishing by freely delivering the most outstanding research, evaluated with no bias from both the academic and social point of view. By applying the most advanced information technologies, Frontiers is catapulting scholarly publishing into a new generation.

What are Frontiers Research Topics?

Frontiers Research Topics are very popular trademarks of the Frontiers Journals Series: they are collections of at least ten articles, all centered on a particular subject. With their unique mix of varied contributions from Original Research to Review Articles, Frontiers Research Topics unify the most influential researchers, the latest key findings and historical advances in a hot research area! Find out more on how to host your own Frontiers Research Topic or contribute to one as an author by contacting the Frontiers Editorial Office: frontiersin.org/about/contact

NOVEL DIAGNOSTIC TOOLS AND BIOMARKERS IN HEMATOLOGIC MALIGNANCIES

Topic Editors:
Mina Luqing Xu, Yale University, United States
Alejandro Gru, University of Virginia Health System, United States
Julia T. Geyer, Weill Cornell Medical Center, United States
Andrew G. Evans, University of Rochester, United States

Citation: Xu, M. L., Gru, A., Geyer, J. T., Evans, A. G., eds. (2022). Novel Diagnostic Tools and Biomarkers in Hematologic Malignancies. Lausanne: Frontiers Media SA. doi: 10.3389/978-2-88974-703-0

Table of Contents

frontiers in Oncology

SYSTEMATIC REVIEW
published: 04 March 2021
doi: 10.3389/fonc.2021.632910

Clinical Value of ctDNA in Hematological Malignancies (Lymphomas, Multiple Myeloma, Myelodysplastic Syndrome, and Leukemia): A Meta-Analysis

Xiangyu Tan[1], *Han Yan*[1], *Lei Chen*[1], *Yuyang Zhang*[1] *and Chunyan Sun*[1,2]*

[1] Department of Hematology, Union Hospital, Tongji Medical College, Huazhong University of Science and Technology, Wuhan, China, [2] Collaborative Innovation Center of Hematology, Huazhong University of Science and Technology, Wuhan, China

Background: Circulating tumor DNA (ctDNA) has offered a minimally invasive approach for the detection and measurement of cancer. However, its diagnostic and prognostic value in hematological malignancies remains unclear.

Materials and methods: Pubmed, Embase, and Cochrane Library were searched for relating literature. Diagnostic accuracy variables and disease progression prediction data were pooled by the Meta-Disc version 1.4 software. Review Manager version 5.4 software was applied for prognostic data analysis.

Results: A total of 11 studies met our inclusion criteria. In terms of diagnosis, the pooled sensitivity and specificity were 0.51 (95% confidence intervals (CI) 0.38–0.64) and 0.96 (95% CI 0.88–1.00), respectively. The AUSROC (area under the SROC) curve was 0.89 (95%CI 0.75–1.03). When it comes to the prediction of disease progression, the overall sensitivity and specificity was 0.83 (95% CI 0.67–0.94) and 0.98 (95% CI 0.93–1.00), respectively. Moreover, a significant association also existed between the presence of ctDNA and worse progression-free survival (HR 2.63, 95% CI 1.27–5.43, $p = 0.009$), as well as overall survival (HR 2.92, 95% CI 1.53–5.57, $p = 0.001$).

Conclusions: The use of ctDNA in clinical practice for hematological malignancies is promising, as it may not only contribute to diagnosis, but could also predict the prognosis of patients so as to guide treatment. In the future, more studies are needed to realize the standardization of sequencing techniques and improve the detection sensitivity of exploration methods.

Keywords: circulating tumor DNA, hematological malignancies, lymphomas, multiple myeloma, myelodysplastic syndrome, leukemia, meta-analysis

OPEN ACCESS

Edited by:
Alejandro Gru, University of Virginia Health System, United States

Reviewed by:
Rehan Khan, Case Western Reserve University, United States
Deepshi Thakral, All India Institute of Medical Sciences, India

***Correspondence:**
Chunyan Sun
suncy0618@163.com

Specialty section:
This article was submitted to Hematologic Malignancies, a section of the journal Frontiers in Oncology

Received: *24 November 2020*
Accepted: *05 February 2021*
Published: *04 March 2021*

Citation:
Tan X, Yan H, Chen L, Zhang Y and Sun C (2021) Clinical Value of ctDNA in Hematological Malignancies (Lymphomas, Multiple Myeloma, Myelodysplastic Syndrome, and Leukemia): A Meta-Analysis. Front. Oncol. 11:632910. doi: 10.3389/fonc.2021.632910

INTRODUCTION

In recent years, significant progress in the diagnosis and treatment of hematological malignancies has been made. However, the current gold standard for disease diagnosis and monitoring, tissue or bone marrow (BM) biopsy, is invasive and painful. A further issue is that sampling a single tumor site during biopsy may not reveal all malignant clones (1).

Mandel and Metais first described the presence of DNA molecules in human plasma in 1948 (2). In 1994, Vasioukhin et al. described the presence of tumor-specific mutations in cell-free DNA (cfDNA) of patients with myelodysplastic syndrome (MDS) and acute myeloid leukemia (AML), demonstrating the significance of circulating tumor DNA (ctDNA) analysis in hematologic malignancies (3, 4). Unfortunately, due to the lack of sensitive and specific detection methods, the research on cfDNA is relatively behind. With the recent advent of new techniques, such as droplet digital polymerase chain reaction (ddPCR) and next-generation sequencing (NGS), tumor-derived fragmented DNA in the plasma or serum, known as ctDNA, has the ability to be one of the most sensitive, non-invasive biomarkers available for use in cancer patients (5). Compared with a classic biopsy, ctDNA is more convenient and presents minor procedural risk to the patient, with a less expensive price. And more importantly, ctDNA has been determined to have a half-time of 16 min to 2.5 h in circulation, which enables ctDNA analysis to be considered as a real-time snapshot of disease burden (6). In theory, ctDNA could also deliver more complete information regarding the patient's entire tumor burden, because the sample may represent all tumor DNA present in the circulation, without spatial limitations of the biopsy sampling of a single lesion within a single anatomic site (7).

Although many recent studies have focused on applications in hematological malignancies (8–13), the results are still unclear. Therefore, we performed a meta-analysis to estimate the clinical application value in patients with hematological malignancies.

METHODS

Search Strategy

We searched for studies in Pubmed, Embase, and Cochrane library with no restriction of publication date using key words "lymphomas AND ctDNA," "myeloma AND ctDNA," "myelodysplastic syndrome AND ctDNA," and "leukemia AND ctDNA."

Inclusion Criteria, Exclusion Criteria

Two reviewers evaluated potential articles independently, according to the inclusion and exclusion criteria mentioned below. Discrepancies were resolved by discussion until a consensus was reached.

Inclusion criteria: (1) retrospective and prospective observational cohort studies involving patients with lymphoma, multiple myeloma, myelodysplastic syndrome, or leukemia; (2) ctDNA was analyzed in patients; (3) information on the diagnostic, prognostic, or predictive value of ctDNA was provided; (4) prognostic studies had to report the results of a survival analysis in the form of a hazard ratio and 95 % confidence intervals; (5) a sample size≥5; (6) reported in English; and (7) participants were adults.

Exclusion criteria: (1) cell-free DNA without information of mutations; (2) circulating viral DNA; (3) lack of outcomes; and (4) conference abstracts, comments, reviews, case reports, or meta-analyses.

Data Extraction

Only full-text articles were taken into consideration. Extracted study characteristics included: first author, publication year, type of cancer, number of patients, ctDNA measurement method, and mutation evaluated in ctDNA. If the eligible studies provided survival data, hazard ration (HR) for overall survival (OS), progress-free survival (PFS), event-free survival (EFS), or disease progressing with 95% confidence interval (CI) they were extracted.

TABLE 1 | Results of diagnosis quality assessment of included studies according to the QUADAS-2 tool criteria.

Study	Risk of bias				Applicability concerns		
	Patients selection	Index text	Reference standard	Flow and time	Patients selection	Index text	Reference standard
Fontanilles, M.2017	L	L	L	L	L	L	L
Hickmann, A.K.2019	U	L	U	L	L	L	L
Mazzotti.C 2018	U	L	L	L	U	L	L
Sakata-Yanagimoto, M 2017	U	L	L	U	L	L	L
Watanabe, J. 2019 PCNSL	L	L	L	L	L	L	L

L: low risk of bias; H: high risk of bias; U: unclear risk of bias.

TABLE 2 | A study could be allocated one point for each of the seven criteria; in case of ambiguity, half a point was assigned.

Adapted REMARK criteria for quality assessment (1 point/criteria)	
1.	Case selection adequate (baselines from medical chart)
2.	States the marker examined and the aim of the study
3.	Reporting at least the following characteristics: disease stage, histology, and received treatment
4.	States the time and type of sampling (serum/plasma)
5.	States the assay methods used and provides a detailed protocol (at least cfDNA isolation, sequence method, and sequence depth)
6.	A clear description of the flow of patients through the study
7.	A clear description of the reasons for dropout

A study was included for further analysis when graded ≥ 5.5 points.

Abbreviations: ctDNA, circulating tumor DNA; BM, bone marrow; cfDNA, cell-free DNA; ddPCR, droplet digital polymerase chain reaction; NGS, next-generation sequencing; HR, hazard ration; OS, overall survival; PFS, progress-free survival; EFS, event-free survival; CI, confidence interval; PLR, positive likelihood ratios; NLR, negative likelihood ratios; DOR, diagnostic ratios; SROC, the summary receiver operating characteristic curve; EGFR, epidermal growth factor receptor; MRD, the minimal residual disease; MAF, the mutant allele fraction; MDS, myelodysplastic syndrome.

TABLE 3 | Prognostic studies were scored according to the criteria in **Table 2**.

Study	1	2	3	4	5	6	7	Total
Roschewski, M.2015	1	1	1	1	1	1	1	7
Assouline, S. E.2016	1	1	1	1	1	1	1	7
Kurtz, D. M.2018	1	0.5	1	1	0.5	1	1	6
Sarkozy, C.2017	1	1	1	1	0.5	1	1	6.5
Fontanilles, M. 2017	1	1	1	1	1	1	1	7
Hossain, N. M.2019	0.5	1	0.5	1	0.5	1	1	5.5
Qiong Li.2020	1	1	1	1	1	1	1	7

Studies' Quality Assessment

The results of diagnosis quality assessment were shown in **Table 1**. The quality of prognostic studies was assessed by an adapted version of the reporting recommendations for tumor marker prognostic studies (REMARK) criteria for biomarker studies (**Table 2**) (14). Detailed information on quality assessment about prognostic studies was shown in **Table 3**.

Statistical Analysis

Diagnostic variables, such as sensitivity, specificity, likelihood ratios [i.e., positive likelihood ratios (PLR) or negative likelihood ratios (NLR)], diagnostic ratios (DOR), and the summary receiver operating characteristic curve (SROC) were calculated and analyzed using the Meta-Disc software, version 1.4. The pooled HR and the 95% CIs for OS or PFS were analyzed by the Review Manager version 5.4 software. We used a random-effect model if significant heterogeneity was observed ($P < 0.05$ or $I^2 > 50\%$); if not, we would turn to a fixed-effect model.

RESULTS

A total of 996 articles were identified through the search (**Figure 1**). After screening, 273 duplicated studies were removed, and 674 studies were excluded based on their titles and abstracts. A further 39 studies were excluded for not fulfilling the inclusion criteria. Finally, a total of 11 studies were included in the meta-analysis. The details and main characteristics of included studies are summarized in **Table 4**.

ctDNA as Marker for Diagnosis in Hematological Malignancies

Five studies were pooled for the meta-analysis of diagnostic accuracy. As presented in **Figure 2**, the overall sensitivity and specificity was 0.51 (95% CI 0.38–0.64) and 0.96 (95% CI 0.88–1.00) respectively. The pooled PLR and NLR were 4.04 (95% CI 1.68–9.70) and 0.60 (95% CI 0.37–0.98), respectively. The area under the SROC was 0.89 and the DOR was 14.60 (95%CI 3.74–57.02).

ctDNA as Prognostic Marker in Hematological Malignancies

Three studies were pooled for the meta-analysis of disease progression prediction. As shown in **Figure 3**, the overall sensitivity and specificity was 0.83 (95% CI 0.67–0.94) and 0.98 (95% CI 0.93–1.00) respectively. The pooled PLR and NLR were 17.31 (95%CI 4.11–72.84) and 0.21 (95% CI 0.09–0.49), respectively. The DOR was 145.74 (95% CI 30.17–704.12).

Three articles with a total of 266 patients included analysis on the association of ctDNA and PFS in patients with hematological malignancies. A significantly worse PFS for ctDNA positive patients was observed(HR 2.63, 95% CI 1.27–5.43)(**Figure 4**). Moreover, there were four articles with 352 patients that included analysis on the association of ctDNA and OS with hematological malignancies. Patients who had ctDNA positive or higher ctDNA levels had a worse OS (HR 2.92, 95% CI 1.53–5.57) (**Figure 5**).

DISCUSSION

Since fragmented DNA was first found in the whole blood by Mandel and Metais, cfDNA and ctDNA have been applied in a variety of disciplines. For example, detection of ctDNA is an effective method to determine EGFR status in NSCLC, providing a more expedient measure to predict resistance to EGFR tyrosine kinase inhibitors and prognosis (25). A study showed that ctDNA monitoring may help identify hematologic cancer patients at risk for relapse in advance of established clinical parameters (8). However, the relationship between ctDNA and hematological malignancies remains unclear. Therefore, it is necessary to conduct comprehensive analysis illuminating the clinical utility of ctDNA in the diagnoses of patients with hematological malignancies and prognosis prediction.

Our pooled data have shown that the detection of ctDNA has an obvious advantage in hematological malignancies diagnosis specificity (specificity: 0.96, 95% CI 0.88–1.00). A phase 1 clinical trial which studied the clinical value of ctDNA in MDS showed that there was an excellent correlation ($r^2 = 0.84$; $P < 0.0001$) between the mutant allele fraction (MAF) of somatic mutations in BM and ctDNA across multiple matched time points (26). Another study on gene detection with 26 patients with MDS showed that the correlation of 52 somatic mutations detected in BM and ctDNA was also significant ($R^2 = 0.8272$, $P < 0.0001$) (13). These results imply that mutations in ctDNA may represent somatic mutations in tumor cells. So in this regard, ctDNA testing is a good alternative to biopsy because of its non-invasive advantages. However, in terms of test sensitivity, the present evidence showed no superiority of ctDNA over biopsy (sensitivity: 0.51, 95% CI 0.38–0.64). Hematologic tumors are highly heterogeneous, with various gene mutations in a tumor,

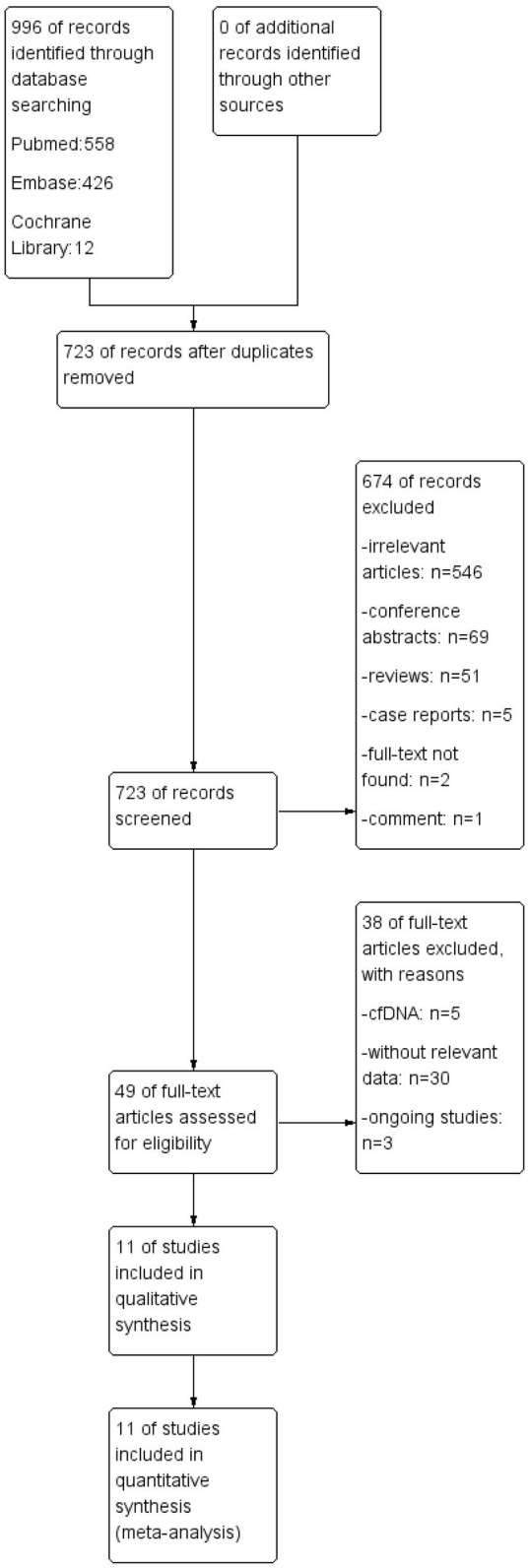

FIGURE 1 | Flow chartof selection process to enrolleligiblestudie.

which may be one of the main reasons for its lack of sensitivity. On the other hand, we pooled results of various tumors and mutations on account of the limited number of studies in our meta-analysis, which may lead to inaccurate results. Therefore, more accurate circulating gene targets need to be defined. To increase the sensitivity of ctDNA, there is a necessity to study the detection rate of ctDNA using a panel-based NGS approach, and panels should include the most-frequently mutated genes in tumor tissue.

The quantitative level of ctDNA has prognostic value for patients which could influence therapy choices (27, 28). Detection of ctDNA clearance during first-line chemotherapy can reflect tumor response to treatment, which may allow real-time adjustment of duration or intensity, or identification of patients at high risk of treatment failure (20). Similar to our results, studies by Herrera et al. also showed a correlation between ctDNA and disease progression as well as recurrence, whose multivariable model results show that detectable ctDNA was associated with increased risk of progression/death (HR 3.9, $P = 0.003$) and relapse/progression (HR 10.8, $P = 0.0006$) (29). Moreover, some studies indicated that detectable ctDNA was also associated with tumor volume, which means ctDNA is associated with tumor burden in patients (11, 24). Given the non-invasive nature and short half-life of ctDNA, its interim monitoring during therapy can provide a real-time assessment of tumor dynamics, allowing for an early indication of response or resistance to therapy. After treatment, ctDNA can be used for post-treatment monitoring. It can perform a similar function to surveillance imaging without the need for radiation exposure, which may potentially increase susceptibility to preclinical recurrence, and ultimately allow for early intervention (28, 30, 31). The study by Roschewski et.al. showed that patients developed detectable ctDNA a median of 3.5 months before clinical evidence of disease (20). Similarly, ctDNA detected relapse at a mean of 6 months before imaging detection in another study by Scherer et al. (32). These encouraging results suggest that ctDNA may help faster relapse detection, and allows subsequent therapy to be initiated before clinical progression. These findings will highly strengthen the value of ctDNA in clinical management of patients with hematological malignancies.

As is shown in our pooled data, the presence of ctDNA or higher levels of ctDNA is associated with a poorer PFS and OS. Sarkozy's study has a similar result to us, showing that patients with higher levels of ctDNA experienced a significantly shorter PFS than those with lower levels of ctDNA (median 15.3 months vs. not reached, $p = 0.004$) (23). Another study also showed that patients with detectable ctDNA have worse survival outcomes than those without (6). These results imply that ctDNA assessment could be a useful alternative endpoint for PFS and OS.

Several limitations in this study need to be addressed. Firstly, the lack of a well-accepted ctDNA gene target might contribute to the presence of bias. Secondly, due to the limited studies, we included little data which may lead to results' bias. Furthermore,

TABLE 4 | Major characteristics of enrolled studies.

No.	Study	Type of cancer	Number of patients	ctDNA measurement method	Mutation evaluated in ctDNA
1	Fontanilles, M. (14)	PCNSL	50	NGS	MYD88 c.T778C
2	Hickmann, A, K. (15)	PCNSL	6	NGS	MYD88, PIM1, BCL2, ETV6, KMT2D, LPHN3, PRDM1, CD79B, SOCS1, IRF4, MYC, FOXB1, LRP1B, HLA-B, LTF, EPHA5, EP400, SYNE1, BLNK, STAT3, FES, SEPT9, POLR3A, DPYD, TFE3, CSMD3, FAT1, KIT, MAGI1, TP53, ASXL1, SETD2, IDH2, MTRR, PBRM1, BCR, MN1, RNF213, TOP1, ATM, FANCM, CDKN1B, PAX5, FOXO1, MCL1, PTPRT, CARD11, PPM1D, DST, BCL10, TCL1A, FN1, HSP90AA1, NIN, SLCO1B1, HSP90AB1, ARID5B, ETS1, ERBB4, CCND2, HLA-C, ITGB2, EPHA3, BCL6, TBL1XR1, PCBP1, RECQL4, CREBBP, STAT4, MLLT3, KEAP1, BTK
3	Mazzotti,C. (16)	MM	37	NGS	IGH, IGK, IGL rearrangements
4	Sakata-Yanagimoto, M. (17)	PTCL	14	Targeted sequencing	G17V-RHOA
5	Watanabe, J. (18)	PCNSL	12	ddPCR	MYD88
6	Roschewski, M. (19)	DLBCL	126	NGS	VDJ rearrangements
7	Assouline, S. E. (20)	DLBCL	20	CAPP-seq and ddPCR	EZH2, MEF2B, CREBBP, EP300, MLL2, FAS, STAT6, TP53, MYD88, MLL3
8	Kurtz, D. M. (21)	DLBCL	217	CAPP-seq	ABCB11, ACTG1, AFF1, APC, B2M, BCHE, BCL10, BCL2, BCL6, BTG1, BTG3, BTK, CAPZA3, CARD11, CCND1, CCND3, DSEL, EGR1, EPHA7, RF1, IRF4, KRAS, LAMA1, MAP2K1, MC5R, MED12, MEF2B, PXDN, RASSF9, STAT6, ZFP42, ZMYM6, ZNF608, ZNF678, et al.
9	Sarkozy, C. (22)	FL	29	NGS	VDJ rearrangements
10	Hossain, N. M. (23)	DLBCL	6	NGS	immunoglobulin gene V(D)J rearrangements
11	Qiong, Li. (24)	ENTKL	65	NGS	ADAM3A, APC, ARID1A, ARID1B, ARID2, ASXL3, ATM, BCOR, BCORL1, CD28, CHD8, CREBBP, DDX3X, DNMT3A, EP300, EZH2, FYN, IDH2, IL2RG, JAK1, JAK3, KDM6A, KMT2A, KMT2D, MGA, NF1, NOTCH1, PRDM1, PTPN1, RHOA, SETD2, SOCS1, STAT3, STAT5B, STAT6, TET1, TET2, TNFRSF14, TP53, TRAF3, ZAP608

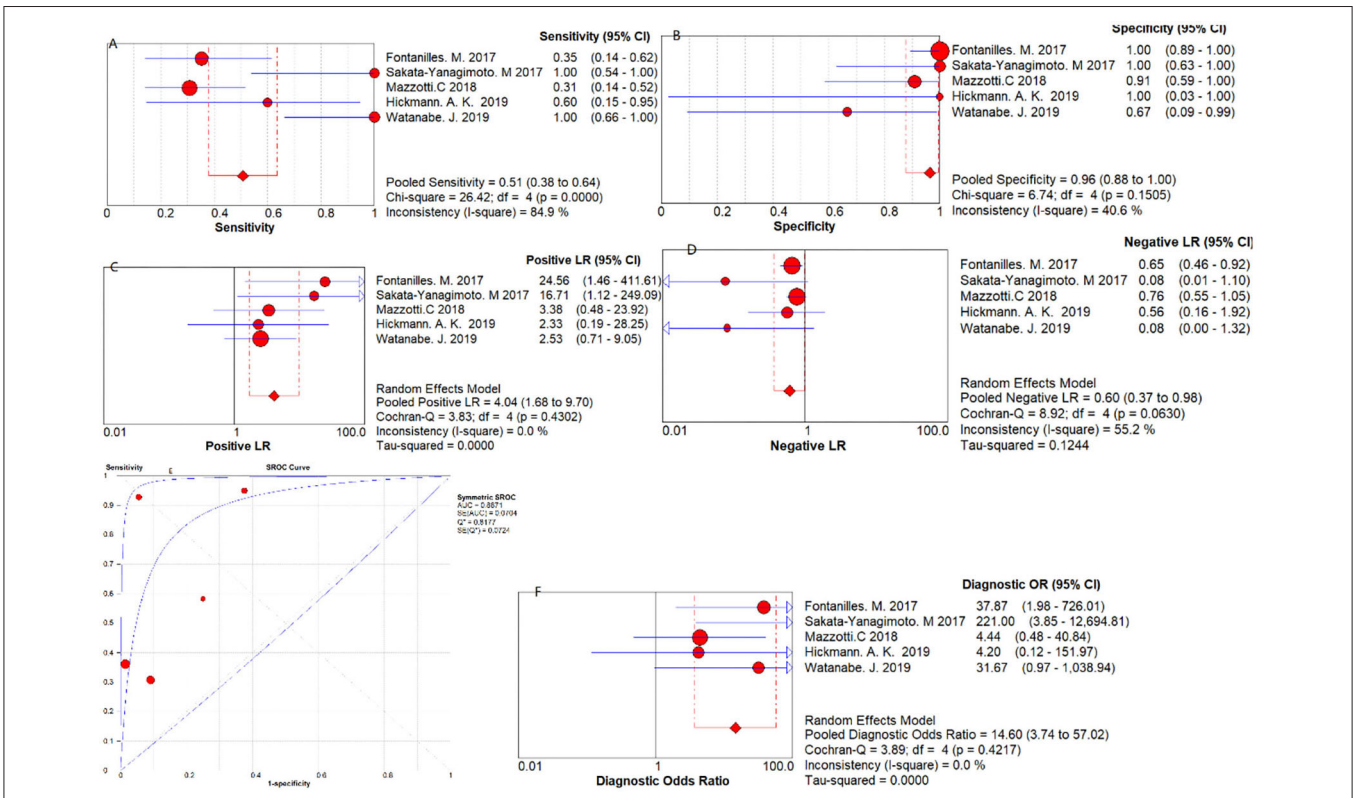

FIGURE 2 | Diagnostic accuracy forest plots. **(A)** Forest plots of overall sensitivity. **(B)** Forest plots of overall specificity. **(C)** Forest plots of positive likelihood ratio. **(D)** Forest plots of negative likelihood ratio. **(E)** Forest plots of SROC Curve. **(F)** Forest plots of diagnostic odds ratio.

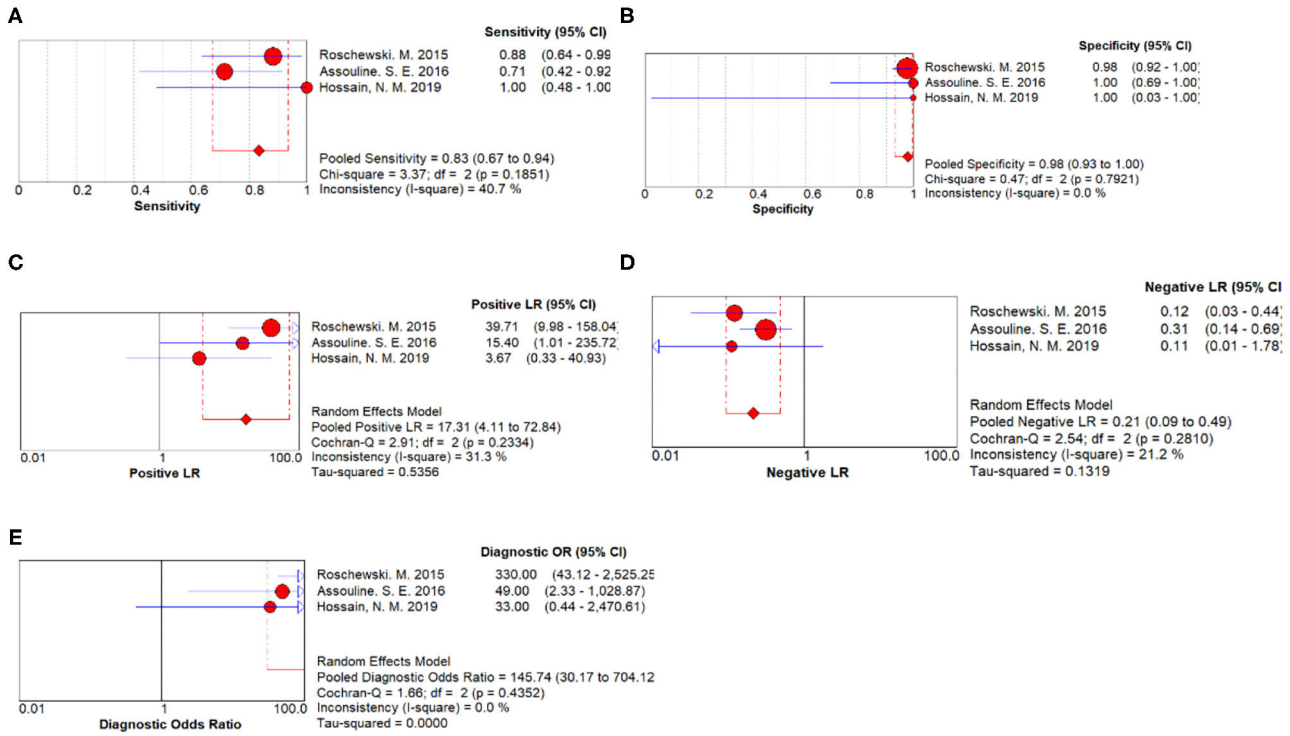

FIGURE 3 | Disease progression prediction forest plots. **(A)** Forest plots of overall sensitivity. **(B)** Forest plots of overall specificity. **(C)** Forest plots of positive likelihood ratio. **(D)** Forest plots of negative likelihood ratio. **(E)** Forest plots of diagnostic odds ratio.

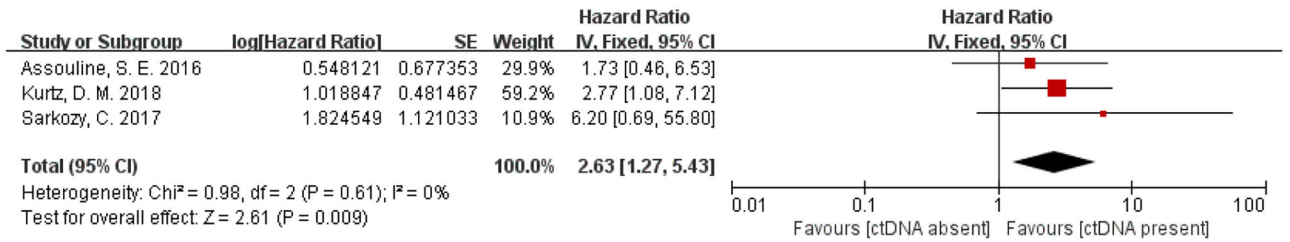

FIGURE 4 | Forest plot of a Fixed-effect meta-analysis of the prognostic role of ctDNA on progression-free survival.

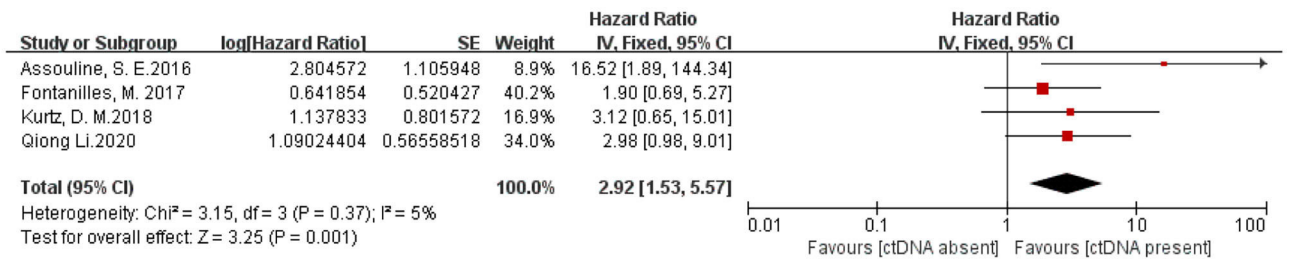

FIGURE 5 | Forest plot of a Fixed-effect meta-analysis of the prognostic role of ctDNA on overall survival.

the difference in detection method and materials, such as PCR primers or the equipment applied, is also an important source of study bias. Therefore, our conclusion might not be universal suitable.

Despite its preliminary nature, this study clearly indicated that the presence of ctDNA in hematological malignancies patients predicted unfavorable survival. Before its wide application in hematological malignancies patients, some concerns still need

to be addressed, including more accurate molecule targets and more suitable detection techniques. In a word, more prospective studies with consistent and standardized methodology are needed to further resolve these problems.

CONCLUSIONS

In summary, our meta-analysis revealed that the presence of ctDNA is related to a worse prognosis in patients with hematological malignancies (lymphomas, multiple myeloma, myelodysplastic syndrome, or leukemia). Moreover, ctDNA is a potential diagnostic biomarker in hematological malignancies, although the low diagnostic accuracy is a point of concern. The specificity and non-invasive nature of ctDNA testing, as well as its ability to reflect the patient's tumor burden in real time, makes it a potential substitute for biopsy. In the future, more studies are needed to realize the standardization of sequencing techniques and explore methods to improve detection sensitivity.

DATA AVAILABILITY STATEMENT

The original contributions presented in the study are included in the article/**Supplementary Material**, further inquiries can be directed to the corresponding author/s.

AUTHOR CONTRIBUTIONS

XYT and HY collected and analyzed the data and wrote the paper. LC analyzed the data. YYZ revised the paper. CYS conceived and designed this study, analyzed the data, and wrote the paper. All authors read, reviewed, and approved the final manuscript.

FUNDING

This work was supported by grants from the National Natural Science Foundation of China (Nos. 81974007 and 8167019 for CYS) and the Clinical Research Physician Program of Tongji Medical College, HUST (for CYS).

ACKNOWLEDGMENTS

We would like to thank the researchers and study participants for their contributions.

SUPPLEMENTARY MATERIAL

The Supplementary Material for this article can be found online at: https://www.frontiersin.org/articles/10.3389/fonc.2021.632910/full#supplementary-material

REFERENCES

1. Kubaczkova V, Vrabel D, Sedlarikova L, Besse L, Sevcikova S. Cell-free DNA—minimally invasive marker of hematological malignancies. *Eur J Haematol*. (2017) 99:291–9. doi: 10.1111/ejh.12925
2. Mandel P, Metais P. The nucleic acids in blood plasma in humans. *C R Seances Soc Biol Fil*. (1948) 142:241–3.
3. Vasioukhin V, Anker P, Maurice P, Lyautey J, Lederrey C, Stroun M. Point mutations of the N-ras gene in the blood plasma DNA of patients with myelodysplastic syndrome or acute myelogenous leukaemia. *Br J Haematol*. (1994) 86:774–9. doi: 10.1111/j.1365-2141.1994.tb04828.x
4. Postel M, Roosen A, Laurent-Puig P, Taly V, Wang-Renault SF. Droplet-based digital PCR and next generation sequencing for monitoring circulating tumor DNA: a cancer diagnostic perspective. *Expert Rev Mol Diagn*. (2018) 18:7–17. doi: 10.1080/14737159.2018.1400384
5. Wan JCM, Massie C, Garcia-Corbacho J, Mouliere F, Brenton JD, Caldas C, et al. Liquid biopsies come of age: towards implementation of circulating tumour DNA. *Nat Rev Cancer*. (2017) 17:223–38. doi: 10.1038/nrc.2017.7
6. Merker JD, Oxnard GR, Compton C, Diehn M, Hurley P, Lazar AJ, et al. Circulating tumor DNA analysis in patients with cancer: American society of clinical oncology and college of american pathologists joint review. *J Clin Oncol*. (2018) 36:1631–41. doi: 10.1200/JCO.2017.76.8671
7. Nakamura S, Yokoyama K, Yusa N, Ogawa M, Takei T, Kobayashi A, et al. Circulating tumor DNA dynamically predicts response and/or relapse in patients with hematological malignancies. *Int J Hematol*. (2018) 108:402–10. doi: 10.1007/s12185-018-2487-2
8. Kis O, Kaedbey R, Chow S, Danesh A, Dowar M, Li T, et al. Circulating tumour DNA sequence analysis as an alternative to multiple myeloma bone marrow aspirates. *Nat Commun*. (2017) 8:15086. doi: 10.1038/ncomms15086
9. Nakamura S, Yokoyama K, Shimizu E, Yusa N, Kondoh K, Ogawa M, et al. Prognostic impact of circulating tumor DNA status post–allogeneic hematopoietic stem cell transplantation in AML and MDS. *Blood*. (2019) 133:2682–95. doi: 10.1182/blood-2018-10-880690
10. Chen F, Pang D, Guo H, Jiang X, Liu S, Huang L, et al. Clinicopathological characteristics and mutational profiling of adult t-cell lymphoblastic lymphoma in a chinese population. *Cancer Manage Res*. (2020) 12:3003–12. doi: 10.2147/CMAR.S242903
11. Long X, Xu Q, Lou Y, Li C, Gu J, Cai H, et al. The utility of non-invasive liquid biopsy for mutational analysis and minimal residual disease assessment in extramedullary multiple myeloma. *Br J Haematol*. (2020). 189:e45–8. doi: 10.1111/bjh.16440
12. Zhao P, Qin J, Liu W, Zhu Q, Fan T, Xiao H, et al. Using circulating tumor DNA to monitor myelodysplastic syndromes status. *Hematol Oncol*. (2019) 37:531–3. doi: 10.1002/hon.2649
13. Creemers A, Krausz S, Strijker M, van der Wel MJ, Soer EC, Reinten RJ, et al. Clinical value of ctDNA in upper-GI cancers: A systematic review and meta-analysis. *Biochim Biophys Acta Rev Cancer*. (2017). (1868). 394–403. doi: 10.1016/j.bbcan.2017.08.002
14. Fontanilles M, Marguet F, Bohers É, Viailly PJ, Dubois S, Bertrand P, et al. Non-invasive detection of somatic mutations using next-generation sequencing in primary central nervous system lymphoma. *Oncotarget*. (2017) 8:48157–68. doi: 10.18632/oncotarget.18325
15. Hickmann AK, Frick M, Hadaschik D, Battke F, Bittl M, Ganslandt O, et al. Molecular tumor analysis and liquid biopsy: A feasibility investigation analyzing circulating tumor DNA in patients with central nervous system lymphomas. *BMC Cancer*. (2019) 19:192. doi: 10.1186/s12885-019-5394-x
16. Mazzotti C, Buisson L, Maheo S, Perrot A, Chretien ML, Leleu X, et al. Myeloma MRD by deep sequencing from circulating tumor DNA does not correlate with results obtained in the bone marrow. *Blood Adv*. (2018) 2:2811–3. doi: 10.1182/bloodadvances.2018025197
17. Sakata-Yanagimoto M, Nakamoto-Matsubara R, Komori D, Nguyen TB, Hattori K, Nanmoku T, et al. Detection of the circulating tumor DNAs in angioimmunoblastic T- cell lymphoma. *Ann Hematol*. (2017) 96:1471–5. doi: 10.1007/s00277-017-3038-2
18. Watanabe J, Natsumeda M, Kanemaru Y, Okada M, Oishi M, Kakita A, et al. Comparison of circulating tumor DNA between body fluids in patients with primary central nervous system lymphoma. *Leuk Lymphoma*. (2019) 60:3587–9. doi: 10.1080/10428194.2019.1639169
19. Roschewski M, Dunleavy K, Pittaluga S, Moorhead M, Pepin F, Kong K, et al. Circulating tumour DNA and CT monitoring in patients with untreated

diffuse large B-cell lymphoma: a correlative biomarker study. *Lancet Oncol*. (2015) 16:541–549. doi: 10.1016/S1470-2045(15)70106-3
20. Assouline SE, Nielsen TH, Yu S, Alcaide M, Chong L, MacDonald D, et al. Phase 2 study of panobinostat with or without rituximab in relapsed diffuse large B-cell lymphoma. *Blood*. (2016) 128:185–94. doi: 10.1182/blood-2016-02-699520
21. Kurtz DM, Scherer F, Jin MC, Soo J, Craig AFM, Esfahani MS, et al. Circulating tumor DNA measurements as early outcome predictors in diffuse large B-cell lymphoma. *J Clin Oncol*. (2018) 36:2845–53. doi: 10.1200/JCO.2018.78.5246
22. Sarkozy C, Huet S, Carlton VE, Fabiani B, Delmer A, Jardin F, et al. The prognostic value of clonal heterogeneity and quantitative assessment of plasma circulating clonal IG-VDJ sequences at diagnosis in patients with follicular lymphoma. *Oncotarget*. (2017) 8:8765–74. doi: 10.18632/oncotarget.14448
23. Hossain NM, Dahiya S, Le R, Abramian AM, Kong KA, Muffly LS, et al. Circulating tumor DNA assessment in patients with diffuse large B-cell lymphoma following CAR T-cell therapy. *Leuk Lymphoma*. (2019) 60:503–506. doi: 10.1080/10428194.2018.1474463
24. Li Q, Zhang W, Li J, Xiong J, Liu J, Chen T, et al. Plasma circulating tumor DNA assessment reveals KMT2D as a potential poor prognostic factor in extranodal NK/T-cell lymphoma. *Biomark Res*. (2020) 8:27. doi: 10.1186/s40364-020-00205-4
25. Qiu M, Wang J, Xu Y, Ding X, Li M, Jiang F, et al. Circulating tumor DNA is effective for the detection of EGFR mutation in non-small cell lung cancer: a meta-analysis. *Cancer Epidemiol Biomarkers Prev*. (2015) 24:206–12. doi: 10.1158/1055-9965.EPI-14-0895
26. Yeh P, Dickinson M, Ftouni S, Hunter T, Sinha D, Wong SQ, et al. Molecular disease monitoring using circulating tumor DNA in myelodysplastic syndromes. *Blood*. (2017) 129:1685–1690. doi: 10.1182/blood-2016-09-740308
27. Hohaus S, Giachelia M, Massini G, Mansueto G, Vannata B, Bozzoli V, et al. Cell-free circulating DNA in Hodgkin's and non-Hodgkin's lymphomas. *Ann Oncol*. (2009) 20:1408–13. doi: 10.1093/annonc/mdp006
28. Galimberti S, Luminari S, Ciabatti E, Grassi S, Guerrini F, Dondi A, et al. Minimal residual disease after conventional treatment significantly impacts on progression-free survival of patients with follicular lymphoma: the FIL FOLL05 trial. *Clin Cancer Res*. (2014) 20:6398–6405. doi: 10.1158/1078-0432.CCR-14-0407
29. Herrera AF, Kim HT, Kong KA, Faham M, Sun H, Sohani AR, et al. Next-generation sequencing-based detection of circulating tumour DNA After allogeneic stem cell transplantation for lymphoma. *Br J Haematol*. (2016) 175:841–50. doi: 10.1111/bjh.14311
30. Pott C, Hoster E, Delfau-Larue MH, Beldjord K, Böttcher S, Asnafi V, et al. Molecular remission is an independent predictor of clinical outcome in patients with mantle cell lymphoma after combined immunochemotherapy: a European MCL intergroup study. *Blood*. (2010) 115:3215–3223. doi: 10.1182/blood-2009-06-230250
31. Armand P, Oki Y, Neuberg DS, Faham M, Cummings C, Klinger M, et al. Detection of circulating tumour DNA in patients with aggressive B-cell non-Hodgkin lymphoma. *Br J Haematol*. (2013) 163:123–6. doi: 10.1111/bjh.12439
32. Scherer F, Kurtz DM, Newman AM, Stehr H, Craig AFM, Esfahani MS, et al. Distinct biological subtypes and patterns of genome evolution in lymphoma revealed by circulating tumor DNA. *Sci Transl Med*. (2016) 8:364ra155. doi: 10.1126/scitranslmed.aai8545

Conflict of Interest: The authors declare that the research was conducted in the absence of any commercial or financial relationships that could be construed as a potential conflict of interest.

frontiers in Oncology

REVIEW
published: 18 March 2021
doi: 10.3389/fonc.2021.658234

Clinical Application of Liquid Biopsy in Non-Hodgkin Lymphoma

*Liwei Lv and Yuanbo Liu**

Department of Hematology, Beijing Tiantan Hospital, Capital Medical University, Beijing, China

Non-Hodgkin lymphoma (NHL) is a common type of hematological malignant tumor, composed of multiple subtypes that originate from B lymphocytes, T lymphocytes, and natural killer cells. A diagnosis of NHL depends on the results of a pathology examination, which requires an invasive tissue biopsy. However, due to their invasive nature, tissue biopsies have many limitations in clinical applications, especially in terms of evaluating the therapeutic response and monitoring tumor progression. To overcome these limitations of traditional tissue biopsies, a technique known as "liquid biopsies" (LBs) was proposed. LBs refer to noninvasive examinations that can provide biological tumor data for analysis. Many studies have shown that LBs can be broadly applied to the diagnosis, treatment, prognosis, and monitoring of NHL. This article will briefly review various LB methods that aim to improve NHL management, including the evaluation of cell-free DNA/circulating tumor DNA, microRNA, and tumor-derived exosomes extracted from peripheral blood in NHL.

Keywords: non-Hodgkin lymphoma, diffuse large B-cell lymphoma, primary central nervous system lymphoma, liquid biopsies, cell-free DNA, circulating tumor DNA, microRNA, tumor-derived exosomes

OPEN ACCESS

Edited by:
Mina Luqing Xu,
School of Medicine Yale University,
United States

Reviewed by:
Sandra V. Fernandez,
Fox Chase Cancer Center,
United States
Antonio Giovanni Solimando,
University of Bari Aldo Moro, Italy

***Correspondence:**
Yuanbo Liu
yuanbol@ccmu.edu.cn

Specialty section:
This article was submitted to Hematologic Malignancies, a section of the journal Frontiers in Oncology

Received: *25 January 2021*
Accepted: *02 March 2021*
Published: *18 March 2021*

Citation:
Lv L and Liu Y (2021) Clinical Application of Liquid Biopsy in Non-Hodgkin Lymphoma. Front. Oncol. 11:658234. doi: 10.3389/fonc.2021.658234

INTRODUCTION

Non-Hodgkin lymphoma (NHL) is a common type of hematological malignant tumor, composed of multiple subtypes that originate from B lymphocytes, T lymphocytes, and natural killer (NK) cells, including diffuse large B cell lymphoma (DLBCL), follicular lymphoma (FL), T cell lymphoma (TCL), and NK-T cell lymphoma (NKTCL). The most common NHL subtype is DLBCL, which is a group of heterogeneous tumors (1). This heterogeneity is reflected by significant differences in the responses of these tumors to the standard first-line treatment strategy, known as R-CHOP (rituximab, cyclophosphamide, doxorubicin hydrochloride, oncovin, and prednisone). Approximately 20%–50% of patients experience relapse or develop drug-resistance after treatment (2). The 5-year survival rates for DLBCL reported for the United States and Europe are 63.8% and 55.4%, respectively (2). Primary central nervous system lymphoma (PCNSL) is a rare type of primary extranodal NHL that originates in the brain parenchyma, cranial nerves, leptomeninges, eyes, or spinal cord, without affecting other sites. In greater than 90% of PCNSL, the pathology is consistent with DLBCL. With the application of high-dose methotrexate-based combination chemotherapy, the median overall survival rate of PCNSL increased from 12.5 months in the 1970s to 26 months in the 2010s (3). Similar to systemic DLBCL, approximately 50% of PCNSL patients relapse after treatment (4), and 10% to 15% of patients are primarily refractory (5). In cases of refractory or relapsed disease, the prognosis is typically poor.

Regardless of the NHL subtype identified, the current gold standard for diagnosis remains the pathological examination of the affected tissue, which is typically obtained through surgical resection or lymph node puncture. However, tissue biopsies are invasive examinations that can only reflect the characteristics of tumors statically and locally at the biopsy location. Biopsies cannot be used for the dynamic monitoring of tumors during treatment and follow-up (6). Many disadvantages, including the risks associated with tissue biopsy (bleeding, infection, functional impairment, etc.), the complexity of obtaining biopsy samples, and difficulties associated with reproducibility, have significantly hampered the development of clinical applications for tumor evaluation and prediction. To overcome these barriers, the concept of liquid biopsies (LBs) has been introduced. LBs are characterized by being noninvasive, allowing for the convenient and continuous collection and dynamic monitoring of samples that can provide information regarding disease progression (7, 8). LBs are considered to serve as beneficial supplements to tissue biopsies. LBs can be used for screening and early detection, assessing prognosis, real-time monitoring of response to treatment, guiding treatment, identifying treatment targets, and detecting early recurrence (8). Various forms of LBs are currently widely studied, including circulating tumor cells (CTCs), circulating blood nucleic acids, tumor-derived exosomes (TDE), and tumor-educated platelets (9). Initially, studies of LB focused on CTCs, but recent research focus has shifted to circulating nucleic acids, which are easier to obtain and analyze (7). This article primarily reviews the clinical applications of various types of LBs, including cell-free DNA (cfDNA)/ circulating tumor DNA (ctDNA), microRNA (miRNA), and TDE extracted from peripheral blood, in the assessment and treatment of NHL. cfDNA/ctDNA sheds into blood from tumor cells *via* apoptosis, necrosis or through an active process (**Figure 1**). Molecular aberrations in tumor tissues, such as point mutations, insertions, deletions, and alterations in DNA methylation can be detected in cfDNA/ctDNA. Tumor cells can also shed different classes of RNA into the bloodstream. Among RNAs, miRNA is the most frequently investigated RNA species as biomarkers (**Figure 1**). The TDEs are produced by tumor cells and secreted into the bloodstream through exocytosis. TDE contents include proteins, nucleic acids, lipids and metabolites (**Figure 1**). Therefore, LBs can yield data regarding genetic, transcriptional, and proteomic changes useful for diagnosis, prognosis, and therapy of NHL (**Figure 1**). LB can be used for screening and early detection, assessing prognosis, real-time monitoring of response to treatment, guiding treatment, identifying treatment targets, and detecting early recurrence of NHL (**Figure 2**). A comprehensive understanding of the clinical application value of LBs will help clinicians better manage NHL patients, and achieve the purpose of improving treatment effects and improving prognosis.

CHARACTERISTICS AND DETECTION METHODS USED IN LBs

Following apoptosis or necrosis, both normal cells and tumor cells release nucleic acids (DNA, mRNA, and miRNA) into bodily fluids, such as the peripheral blood, cerebrospinal fluid, and urine (10, 11). Non-cell-bound DNA fragments found in the circulatory system are referred to as cfDNA, which typically consists of both normal DNA and ctDNA (12). The origins of the tumor portion of cfDNA may be apoptosis or necrosis, the lysis of CTCs, or the release of DNA from tumor cells into the circulation (13). Previous research has confirmed that cfDNA typically appears as fragments, with sizes that peak at 166–167 bp, and ctDNA is usually even shorter than normal cfDNA (14, 15). The proportion of ctDNA in cfDNA can range from 3% to 93% (16). Current methods for detecting circulating DNA include polymerase chain reaction (PCR) and next-generation sequencing (NGS, **Table 1**). The detection limit of PCR is 10^{-5}

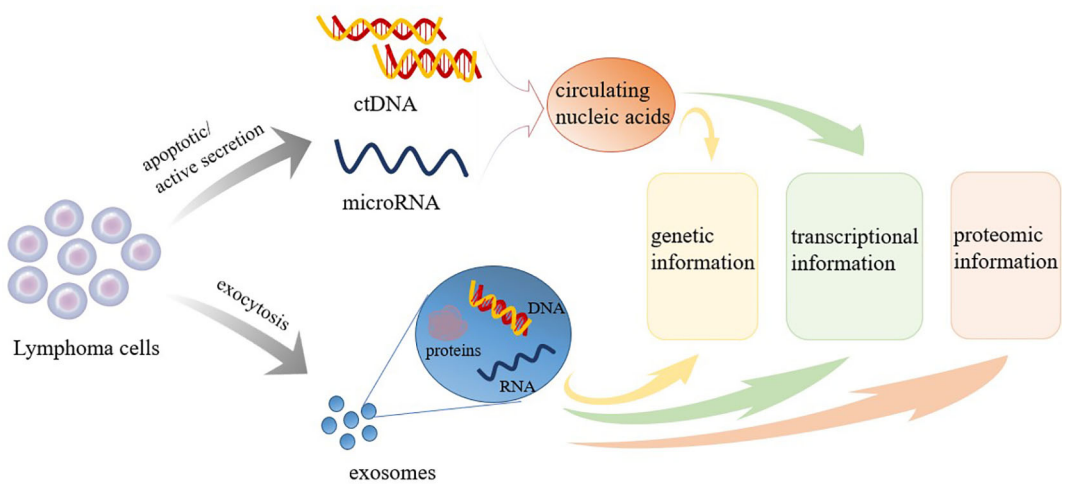

FIGURE 1 | The value of liquid biopsy. ctDNA, circulating tumor DNA.

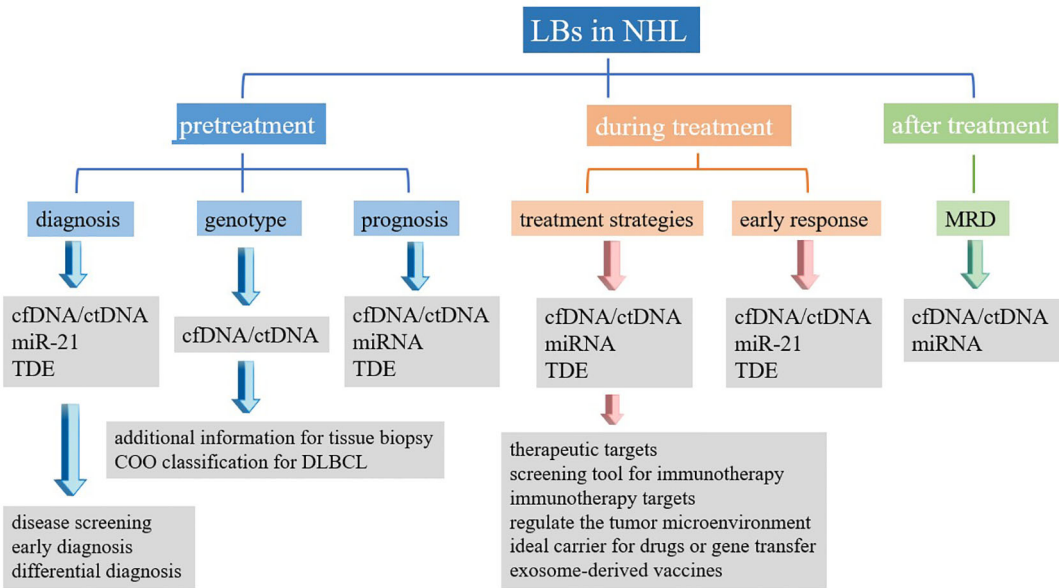

FIGURE 2 | Summary of clinical application of liquid biopsy in non-Hodgkin's lymphoma. LBs, liquid biopsies; NHL, non-Hodgkin's lymphoma; cfDNA, cell-free DNA; ctDNA, circulating tumor DNA; miRNA, microRNA; TDE, tumor-derived exosomes; MRD, minimal residual disease.

(17), and the two most commonly used PCR-based detection techniques are real-time quantitative PCR and droplet digital PCR (18, 19). Epigenetic changes can be detected by pyrosequencing (20). In contrast to PCR, which only targets specific DNA sequences, the detection range for NGS is broader because it targets the entire genome or the entire exome (17). Compared with PCR, the detection rate for NGS increase to 10^{-6} (21). The two platforms commonly used in DLBCL research are noninvasive tumor immunoglobulin gene NGS (IgNGS) and cancer personalized profiling by deep sequencing (CAPP-Seq). The cfDNA/ctDNA can be used for cancer diagnosis, prognosis, and monitoring. However, cfDNA can also be upregulated by other conditions, such as infection, trauma, inflammation, transplantation, and autoimmune disorders (22), which can introduce uncertainties to the interpretation of cfDNA results.

MicroRNAs are small, regulatory, non-coding RNAs that can negatively regulate gene expression at the post-transcriptional level by binding to target mRNA molecules, resulting in the increased degradation or translational inhibition of the targeted mRNA (23). Evidence has shown that tumor-related miRNAs can be detected in bodily fluids (such as serum or plasma) (24). As biomarkers, circulating miRNAs play an essential role in the

TABLE 1 | Detection methods used by liquid biopsy.

	Methods		Characteristics
cfDNA ctDNA	PCR	qRT-PCR ddPCR	Targets certain DNA sequences
	NGS	IgNGS CAPP-Seq	Higher sensitivity and wider coverage
miRNA	RT-PCR		High sensitivity and specificity
	NGS		Sequencing
	Microarray		High-throughput analysis Requires enough initial samples
TDE	Ultracentrifugation		Requires higher speeds and longer durations Less suitable for fluids with high viscosity
	Size-based techniques	Ultrafiltration	Faster than ultracentrifugation Protein contamination
		SEC	Pure isolates with intact physical characteristics
	PEG precipitation		Simple, low-cost, rapid Co-precipitated proteins
	Immunoaffinity enrichment		High-purity separation

cfDNA, cell-free DNA; ctDNA, circulating tumor DNA; TDE, tumor-derived exosomes; PCR, polymerase chain reaction; qRT-PCR, real-time quantitative PCR; ddPCR, droplet digital PCR; NGS, next-generation sequencing; CAPP-Seq, cancer personalized profiling by deep sequencing; RT-PCR, reverse transcription PCR; SEC, size exclusion chromatography; PEG, polyethylene glycol.

diagnosis, typing, treatment response monitoring, and prognostic prediction of NHL. The detection of miRNA can be performed by reverse transcription PCR, NGS, and microarray techniques (25). At present, in most NHL studies, miRNA expression has been evaluated in serum.

Exosomes are a type of endosome-derived extracellular vesicle with a diameter ranging from 30 to 120 nm (2). Exosomes typically contain nucleic acids, proteins, lipids, and metabolites (26). Similar to cfDNA, exosomes can also be found in a variety of bodily fluids, including peripheral blood, cerebrospinal fluid, urine, saliva, and peritoneal fluid (27). Exosomes have been shown to participate in cell-to-cell communications and can affect the phenotypes of recipient cells (28). Exosomes play important roles during both physiological and pathological conditions, including the maintenance of cell homeostasis and the regulation of gene transcription, and exosomes have been shown to participate in the immune response and tumor progression (29). Exosomes differ depending on their cellular origins, and the contents and expression of exosomes secreted by healthy cells differ from those secreted by tumor cells. Therefore, TDEs represent excellent biomarkers for the diagnosis, prognosis, and management of NHL patients at multiple stages. Many methods can be used to isolate exosomes (**Table 1**). A commonly used method for exosome separation is differential ultracentrifugation; however, this method is not suitable for processing high-viscosity fluids due to the requirement for higher speeds and longer centrifugation durations (30). Density-gradient ultracentrifugation is similar to differential ultracentrifugation and can be used to obtain purer fractions; however, density-gradient ultracentrifugation requires long processing times and expensive equipment, which are disadvantages (31). Ultrafiltration and size exclusion chromatography can be used to separate exosomes according to size. The polyethylene glycol precipitation method is a relatively simple, low-cost, and rapid method that can produce high yields while retaining the biophysical properties of isolated exosomes. However, co-precipitated proteins can contaminate exosomes in ultrafiltration and polyethylene glycol precipitation method (32). The immunoaffinity enrichment method uses antibodies against extracellular membrane markers (usually the transmembrane proteins CD9, CD63, and CD81) to isolate exosomes from biological fluids (9). The immunoaffinity method can result in high-purity separation and has been proven to be a very effective method for the separation of exosomes. These various extraction methods are each associated with advantages and disadvantages, and different methods can be selected according to the aims of the experiment.

LBs IN DIAGNOSIS

Although tissue biopsies are invasive, a pathological NHL diagnosis based on the histological examination of a tissue biopsy sample remains the "gold standard." As a noninvasive test, cfDNA assessments are safer and more reproducible than tissue biopsies and are, therefore, likely to become a standardized detection method for disease screening and early diagnosis. Several studies have shown that cfDNA is increased in DLBCL compared with the normal control group, with a sensitivity of 70%–82.5% (33–35) and a specificity of 62.8%–94% (34–36). The median cfDNA concentration has varied across studies, ranging from 11.7–845 ng/ml in DLBCL, 12.4–662 ng/ml in NKTCL, and 12.9–942 ng/ml in TCL (33, 35–37). Currently, the most commonly used methods to detect cfDNA include various types of PCR. Commonly used methods to quantify cfDNA/ctDNA are Qubit for quantification (33, 37) and quantitative PCR (34–36). Although differences in the detection methods used have resulted in heterogeneity among the cfDNA concentrations reported by different studies, all of these studies have reached the conclusion that cfDNA concentrations in NHL cases are higher than those in normal controls. This finding suggests that cfDNA might be used as a diagnostic indicator. Sun et al. compared and analyzed the cfDNA concentrations of DLBCL and NKTCL patients and found that the cfDNA concentration in NKTCL patients was significantly higher than that in DLBCL patients (19.6 ng/ml vs. 11.7 ng/ml, $p = 0.027$) (37). This result suggested that cfDNA also has the potential to identify different types of NHL. However, studies have also demonstrated that cfDNA concentration can be elevated during many non-tumor diseases, such as sepsis, severe trauma, liver damage, and immune diseases (22). Therefore, the analysis and interpretation of cfDNA data may be challenging for both diagnosis and differential diagnosis.

At present, a variety of circulating miRNAs in DLBCL have been studied, resulting in the identification of greater than 80 miRNAs, to date. Nine specific miRNAs have been examined in multiple studies, including miR-21, miR-155, miR-210, miR-15a, miR-29c, miR-494, miR-34a, miR-145, and miR-379 (38–51). However, only two miRNAs have been confirmed to be elevated in DLBCL cases compared with their levels in normal individuals: miR-21 (38–40, 44, 46, 50, 51) and miR-155 (40–42, 44, 46, 49). Moreover, the study by Chen et al. showed that the level of miR-21 in the activated B cell-like (ABC) group was higher than that of the germinal center B cell-like (GCB) group (39). A study by Eis et al. of DLBCL cell lines found that the miR-155 level in DLBCL with an ABC phenotype was higher than in cells with the GCB phenotype (42). Interestingly, Caivano et al. studied miR-155 in extracellular vesicles from 5 DLBCL patients and found that miR-155 level in extracellular vesicles in the DLBCL group did not differ from that in the normal group (52). However, the number of cases examined in this study was relatively limited. Two other miRNAs have been confirmed to be downregulated in DLBCL cases compared with normal controls, miR-145 (46, 47) and miR-379 (47, 48), but each of these has only been evaluated in two studies. Beheshti's team identified 10 related circulating miRNAs (let-7b, let-7c, miR-10b, miR-130a, miR-155, miR27a, miR-24, miR-18a, miR15a, and miR-497) in the DLBCL mouse model (53). Since then, the team has shown that 5 multi-miRNA signature (let-7b, let-7c, miR-18a, miR-24, and miR-15a) can be used to differentiate DLBC from control groups with high sensitivity and specificity (90% and 94%, respectively) (45). In addition to miRNAs that are upregulated in DLBCL, recent studies have identified some miRNAs that are downregulated in DLBCL, such as miRNA-

16-1 (54), miR-425, miR-141, miR-197, miR-345, miR-424, miR-128, and miR-122 (47). Unfortunately, none of these miRNAs has been verified repeatedly. The peripheral circulatory system of DLBCL patients is rich in miRNAs, which carry a lot of information. Currently, only miR-21 is recognized as having the potential to become a diagnostic marker for DLBCL. In addition to DLBCL, Guo et al. compared 79 NKTCL patients with 37 normal plasma samples to examine miR-221 and found that the miR-221 level in the NKTCL group was significantly higher than that in the normal group (55). However, current research on circulating miRNAs primarily focuses on DLBCL, with few studies on other NHL subtypes; therefore, many areas remain to be explored regarding circulating miRNAs.

Although exosomes can contain much information, including nucleic acids and proteins, research regarding exosomes in NHL remains scarce. Xiao et al. found that the expression level of the serum exosome miR-451a was significantly reduced in the DLBCL group compared with that in the control group, and serum exosome miR-451a levels ($p < 0.01$) had a moderate diagnostic efficiency for DLBCL (56). In PCNSL, Gállego et al. showed that RNU6-1 levels were significantly lower in serum exosomes from PCNSL patients than in those from glioblastoma patients (18.1 copies/20 μL vs. 412 copies/20 μL; $P = 0.004$) (57). The expression of RNU6-1 in serum exosomes may be used for the differential diagnosis between PCNSL and glioblastoma (57). However, so few related studies exist that the exact contribution of TDE analysis to the diagnosis of NHL is difficult to determine. The value of TDE for the diagnosis and differential diagnosis of NHL requires additional research and further exploration.

LBs IN TUMOR GENOTYPING AND CELL-OF-ORIGIN CLASSIFICATION

In 2017, Rossi et al. detected DLBCL-related mutations in cfDNA among patients with DLBCL, and the results showed that genetic variants with allele frequency ≥20% in tissue biopsies could also be detected in cfDNA, with >90% sensitivity and approximately 100% specificity (58). In contrast, Rivas et al. reported a sensitivity of detecting DLBCL mutations in cfDNA of 68% (59), whereas Liu et al. reported a sensitivity of 87.5% (60). The research by Rivas and Bohers both showed that the mutational landscape in cfDNA samples was highly consistent with that in biopsied tissue (59, 61). In a study of NHL, the genetic analysis of plasma cfDNA found that when detecting mutations that were detected at frequencies of greater than 20% in biopsy tissue, the sensitivity was 88.0%, and the specificity was greater than 99% (62). The consistencies of gene mutations detected among ctDNA and biopsied tissues from extranodal NK/T-cell lymphoma (nasal type), T-cell lymphoblastic lymphoma, and angioimmunoblastic T-cell lymphoma were 93.75%, 89.1%, and 83%, respectively (63–65). The above results indicated that cfDNA/ctDNA could be used to assess the tumor genotypes of NHL patients as alternative methods for tissue biopsy. In addition, Rossi et al. confirmed that mutations could be identified in cfDNA that were undetectable in tissue biopsies due to the spatial heterogeneity of the tumor (58). Therefore, cfDNA can be used as a supplementary test for cell-of-origin (COO) classification. Scherer et al. used NGS to detect ctDNA from pretreatment plasma for COO typing in DLBCL, and the results were 80% consistent with those derived using the Hans algorithm (66). They concluded that ctDNA genotyping could be used to classify DLBCL based on COO analysis (66). Sun et al. found that the mean concentration of cfDNA was significantly higher in non-GCB patients than that in GCB patients (15.95 ng/ml vs. 4.72ng/ml, $p = 0.015$) (37).

The above research results show that cfDNA can be used for genotyping analysis, providing a more straightforward and easier detection method for determining disease classification criteria in NHL. Although cfDNA can compensate for the heterogeneity associated with tissue biopsy and provide more supplementary information regarding genetic phenotypes, current research has indicated differences between cfDNA and tumor biopsies for the analysis of phenotypic results. No evidence has supported the use of cfDNA to completely replace biopsies for tumor genotyping.

Unfortunately, the results of studies examining PCNSL have not been as promising as those examining systemic DLBCL. Hattori et al. detected cfDNA evaluated by droplet digital PCR in 14 patients, among whom the *MYD88 L265P* mutation was identified in tumor-derived DNA. The *MYD88 L265P* mutation was detected in only eight of the 14 cfDNA samples (67). Montesinos et al. also detected *CD79b* and *MYD88* in both tumor-derived DNA and cfDNA. Among 27 PCNSL tissue biopsies, *CD79B* and *MYD88* mutations were detected in 59% and 85% of cases, respectively; however, the detection rates for the *CD79B* and *MYD88* mutations in cfDNA from the same group of patients were only 0% and 4%, respectively (68). These results showed that in PCNSL, even if the patient carries the *CD79B* or *MYD88* mutation, these mutations may not be detectable in blood-derived cfDNA (68). These studies indicate that unlike systemic DLBCL, circulating cfDNA may not be applicable for the genotyping analysis of PCNSL. Montesinos et al. proposed that the detection of genetic mutations in cfDNA may indicate the possibility of systemic DLBCL and distinguish PCNSL and second central nervous system lymphoma (68).

LBs AS BIOMARKERS FOR PROGNOSIS

A number of studies have shown that the levels of cfDNA/ctDNA may be associated with poor clinical prognosis indicators, and at least two studies have reported that the levels of cfDNA/ctDNA were significantly associated with age, B symptoms (34, 35), disease stage (34, 35, 59, 66), and the International Prognostic Index (IPI) score (34, 35, 37, 59, 61) in DLBCL. In T cell lymphoblastic lymphoma, studies have confirmed that ctDNA concentrations are associated with IPI scores (64). These indicators are highly correlated with poor prognosis. However, whether circulating DNA levels are related to lactate dehydrogenase (LDH) levels remains controversial. LDH is considered to be an indicator of tumor burden of lymphoma. Rivas et al. (59), Sun et al. (37), and Bohers et al.

(61) have shown that the detection of cfDNA/ctDNA in DLBCL is related to LDH levels. In contrast, Hur et al. (33) and Eskandari et al. (34) found no strong correlations between serum LDH and cfDNA in DLBCL. The relationship between cfDNA and Ki-67 is also unclear. Only Wu et al. have examined the relationship between cfDNA and Ki-67 in NHL, and they found that the concentration and integrity of cfDNA were significantly correlated with Ki-67 expression (69). The study also confirmed that cfDNA concentration and integrity are significantly related to the Eastern Cooperative Oncology Group (ECOG) score, LDH level, disease stage, IPI score, and B symptoms (69). In addition, higher concentrations of ctDNA have been significantly correlated with total metabolic tumor volumes, assessed by positron emission tomography/computerized tomography (PET/CT), in both DLBCL and extranodal NK/T-cell lymphoma (59, 63, 66, 70), indicating that ctDNA levels might serve as a surrogate for tumor burden. Many studies have confirmed that high levels of cfDNA/ctDNA in NHL, including DLBCL, FL, TCL, and NKTCL, are associated with shorter progression-free survival (PFS) and overall survival (OS) (33, 34, 36, 59, 71, 72), which indicates that high cfDNA/ctDNA concentrations are poor prognostic factors for NHL. Other studies have examined the DNA methylation patterns in cfDNA. Kristensen et al. analyzed 158 plasma samples from DLBCL patients and examined the DNA methylation patterns in the promoter regions for death-associated protein kinase 1 (*DAPK1*), deleted in breast cancer 1 (*DBC1*), *MIR34A*, and *MIR34B*/*C* using pyrosequencing (20). They concluded that *DAPK1* methylation was an independent prognostic factor for OS ($P < 0.0007$) (20). Chiu et al. profiled genome-wide 5-hydroxymethylcytosine (5hmC) patterns in plasma cfDNA from 48 DLBCL patients and found that the cfDNA 5hmC profiles were associated with the disease stage and IPI score (73). These results indicated that DNA methylation in cfDNA at diagnosis might also be associated with prognosis, representing a new predictive strategy for DLBCL.

A large number of favorable results have indicated that cfDNA/ctDNA have great potential for prognosis. However, no new prognostic model has been developed based on cfDNA/ctDNA. Whether cfDNA/ctDNA can serve as independent prognostic indicators of NHL and the determination of the prognostic efficacies and accuracies of cfDNA/ctDNA will require further studies.

A large number of circulating miRNAs have been associated with DLBCL; therefore, researchers are also exploring the value of miRNAs for prognosis. In 2008, Lawrie et al. found that high miR-21 expression levels were associated with longer relapse-free survival in DLBCL (40), and Chen et al. reached a similar conclusion (39). Conversely, upregulated miR-21 has been described as an independent and poor prognostic factor in another study (51), and the increased expression of miRNAs is thought to be related to poor prognosis. A high expression level of serum miR-22 in DLBCL at diagnosis is an independent prognostic factor for estimating PFS (74). DLBCL patients with upregulated miR-155 (41) and miR-125b (46) had shorter OS. Plasma high levels of miR-20a/b, miR-93, and miR-106a/b were associated with higher mortality in DLBCL (47). Although a variety of prognostic-related miRNAs have been identified, their prognostic efficacy and whether they can be applied to a prognostic model for the accurate stratification of patients remains unclear. Recently, a prognostic model for DLBCL based on four circulating miRNAs (miR21, miR130b, miR155, and miR28) was established and tested in a training cohort of 279 patients and a validation cohort of 225 patients (NCT01852435) (75). However, the potential application of this model requires additional clinical data. We also expect that any existing prognostic models for DLBCL and other NHL subtypes will likely improve as more miRNA research results become available.

Although few studies have examined the relationship between exosomes and prognosis, the results of several published studies have shown that the concentrations of TDEs and the miRNA or protein components contained in TDEs have good prognostic potential. The research by Feng et al. examining exosome miRNA in 2019 showed that the increased levels of miR-99a-5p and miR-125b-5p in serum exosomes derived from DLBCL patients were associated with shorter PFS (76). In 2020, the same team found that the increased expression level of carbonic anhydrase 1 (CA1) in serum exosomes from DLBCL patients was associated with inferior PFS and IPI scores (77). Zare et al. observed that refractory/relapsed DLBCL patients receiving R-CHOP therapy presented with higher concentrations of exosomes and exosomal miR-155 levels than responsive patients (78). Therefore, they speculated that exosome miR-155 might be used as a potential biomarker for predicting the response of DLBCL patients to treatment (78). Ryu et al. found that in extranodal NK/T-cell lymphoma, high levels of miR-4454, miR-21-5p, and miR-320e in serum exosomes were significantly related to poor OS (79). As the roles of large numbers of miRNAs are gradually being unraveled, the prognostic roles of circulating exosomes require additional exploration. With the deepening of research, the prognostic potential of TDEs will gradually become more apparent.

LBs IN TREATMENT

cfDNA can be used to detect a variety of gene mutations and abnormal pathways, and these changes can be developed as therapeutic targets. Therefore, many researchers suspect that testing cfDNA at diagnosis may be able to guide subsequent treatment. Camus et al. used digital PCR to detect *XPO1*, *MYD88*, and *EZH2* mutations in cfDNA from DLBCL patients (80). Hayashida et al. found that angioimmunoblastic T-cell lymphoma patients carried $RHOA^{G17V}$ and $IDH2^{R172}$ mutations in cfDNA (81). These related mutations may be beneficial for guiding the selection of targeted drugs. However, no studies have confirmed whether the development of treatment strategies based on cfDNA can benefit patients.

Similar to cfDNA, miRNA has been shown to be associated with some gene mutations and signaling pathways. In 2017, Beheshti et al. identified ten circulating miRNAs in a DLBCL

mouse model (let-7b, let-7c, miR-10b, miR-130a, miR-155, miR27a, miR-24, miR-18a, miR15a, and miR-497) that strongly impacted JUN and MYC oncogenic signaling (53). Khare et al. identified mRNAs that were targeted by abnormally expressed miRNAs (miR-124, miR-532-5p, miR-141, miR-145, miR-197, miR-345, miR-424, miR-128, and miR-122) in the DLBCL model mice and the biological processes in which they were involved (47). The results showed that these miRNAs might upregulate signal transducer and activator of transcription 3 (STAT3), interleukin 8 (IL8), phosphoinositide 3-kinase (PI3K)/protein kinase B (AKT), and transforming growth factor (TGF)-β signaling pathways and downregulated the phosphatase and tensin homolog (PTEN) and p53 signaling pathways (47). In addition, Cui et al. found that miR-494 was differentially upregulated in immunosuppressive monocytes and macrophages, and the levels of miR-494 and miR-21 decreased within 3–6 months after DLBCL patients initiated immunochemotherapy (38). In B lymphoma cells and DLBCL patients, miRNAs (miR-21, miR-130b, miR-155, and miR-28) were found to regulate Ras signal transduction through insulin-like growth factor (IGF1) and JUN, participating in the induction of myeloid suppressor cells and Th17 cells (75). These results suggested that miRNA expression and detection may be able to guide treatment, representing a novel treatment strategy.

Compared with circulating nucleic acids, exosomes represent a critical component of the malignant tumor microenvironment, involved in tumor progression, metastasis, immune escape, and other factors, and may have tremendous therapeutic potential. B lymphoma cell-derived exosomes contain proteins that are involved in antigen presentation, cell migration, and cell adhesion and have been shown to carry tumor surface antigens, such as CD19, CD20, and CD22 (82). These results indicated that B lymphoma cell-derived exosomes might be able to induce tumor antigen-specific anti-tumor immunity. *In vivo* experiments in a mouse model of TCL also confirmed that TDE could induce humoral and cellular immune responses (83). Therefore, TDE may serve as a potential source of lymphoma cell-related antigen immunotherapy. Chen et al. demonstrated that exosomes from DLBCL cell lines express tumor-related molecules, including c-Myc, Bcl-2, Mcl-1, CD19, and CD20 (84). TDEs from DLBCL can be captured by dendritic cells and lymphoma cells and exert an immunosuppressive effect by inducing T cell apoptosis and the upregulation of programmed cell death protein 1 (PD-1) (84). After being pulsed with TDEs, dendritic cells might stimulate the clonal expansion of T cells, increasing the secretion of IL-6 and tumor necrosis factor α (TNFα), and decreasing the production of immunosuppressive cytokine IL-4 and IL-10 (84). This study provides a theoretical basis for TDE to become a treatment for DLBCL. These results show that TDE can be used as a new immunotherapy target for NHL and the use of exosome-derived vaccines to enhance anti-tumor immune responses. Exosomes can protect cargo from nucleases and proteases during cell communication, have low immunogenicity and cytotoxicity, and have the ability to target tumor cells specifically; therefore, they are often regarded as molecular signaling factors and have been examined as carriers in applications such as drug delivery and horizontal gene transfer (85). Exosomes derived from malignant tumors can promote immune escape and directly or indirectly support tumor cells in the tumor microenvironment. Blocking the secretion of exosomes from tumor cells or removing them from the patient's body may inhibit tumor progression, suggesting that targeting TDEs may represent a novel strategy for NHL treatment.

Immunochemotherapy has achieved remarkable results in the treatment of NHL, and a variety of immunotherapies based on molecules in B-cell NHL surface provide many new possibilities for improving the prognosis of NHL (86). LBs, which can be used as a biomarker, a therapeutic target or a screening tool for immunotherapy, plays an important role in a variety of new immunotherapies such as immune checkpoints, bispecific antibodies, and antibody-drug conjugates (86).

In addition, LBs may hold great promise with tumor microenvironment. The tumor microenvironment provides protection for tumor cells and suppresses the immune response. LBs may be used to monitor and regulate the tumor microenvironment in NHL. As we all know, angiogenesis plays a key role in the progression and prognosis of NHL (87). Angiogenesis provides tumors with sufficient oxygen, nutrients and an effective metabolic waste removal system (88). Angiogenesis also provides an "escape route" for tumor cells, thereby promoting tumor spread and metastasis (88). miRNA is a regulator of tumor angiogenesis (87). It can not only play an anti-angiogenesis effect, but also act as a pro-angiogenesis factor (87). Therefore, miRNA has great potential in regulating tumor microenvironment and improving the treatment response of NHL.

LBs AS BIOMARKERS TO EVALUATE RESPONSE TO TREATMENT

Sidaway et al. used ctDNA to assess the early response of DLBCL patients to treatment (89). Within one week of starting treatment, the ctDNA levels of responders were significantly reduced, allowing the responders and non-responders to be fully distinguished before the end of the first treatment cycle (89). The 24-month event-free survival (EFS) of patients who displayed early molecular response (EMR) and major molecular response (MMR) were significantly improved compared with other patients, and EMR patients who ultimately required rescue treatment also showed higher 24-month EFS (89). Dynamic changes in cfDNA/ctDNA levels can provide early indications of clinical outcomes (89), although the results of cfDNA/ctDNA research have been controversial. A study of NHL compared cfDNA at the time of diagnosis with various time points during the treatment period (69). The results showed that the concentration and integrity of cfDNA during the diagnosis stage were significantly higher than those during the treatment stage (69). By comparing and analyzing the plasma cfDNA of DLBCL patients after R-CHOP treatment, LDBCL-related mutations were quickly cleared in patients who responded to treatment, and the basic mutations in cfDNA did not disappear from those patients who were drug-resistant (58). In addition, in

drug-resistant patients, new mutations were detected in cfDNA, and resistant clones were screened during the process of clonal evolution (58). In contrast, a recent study by Hur et al. reached a different conclusion (33). They analyzed the cfDNA from DLBCL patients before and during various chemotherapy regimens and found no significant differences in PFS and OS regardless of the cfDNA concentration (33). Changes in cfDNA levels before and after treatment may be caused not only by changes in tumor burden but also by other conditions, including infection or chemotherapy-induced inflammation (33). These discrepant findings indicated that some uncertainty exists regarding the use of cfDNA concentration to monitor treatment response. In addition, cfDNA has also been reported to be highly expressed in conditions other than malignant tumors, such as inflammation and infection. After patients receive chemotherapy, the effects of cytotoxic drugs are likely to result in inflammation-related changes in the microenvironment. Due to the small number of studies, whether cfDNA concentration can be used to monitor early treatment response remains unclear. In addition, whether any changes in cfDNA observed during treatment is related to the patient's prognosis remains controversial. The use of cfDNA concentration as an indicator of efficacy in the monitoring and guidance of treatment requires careful consideration.

A study analyzed 736 miRNAs in the serum of 20 patients with complete DLBCL remission and patients with primary refractory DLBCL (90). Five miRNAs (miR-224, miR-1236, miR-520d-3p, miR-33a, and miR-455-3p) were differentially expressed between the two groups and were verified in other 133 patients (90). The upregulation of miR-455-3p and miR-33a was associated with chemosensitivity, whereas the upregulation of miR-224, miR-1236, and miR-520d-3p was associated with chemoresistance (90). Other studies reported that miR-22, miR-494, and miR-21 were downregulated in DLBCL after immunochemotherapy (38, 74). miR-494 and miR-21 expression was reduced in patients who were PET/CT-negative but not in those who remained PET/CT-positive (38). In DLBCL patients who did not respond to treatment, plasma miR-21 and miR-197 levels were significantly upregulated (50). The circulating levels of miR-125b and miR-130a may be related to R-CHOP resistance (46). Overall, these results indicated that differences in circulating miRNA expression before and after treatment might reflect the treatment response or disease progression. Therefore, circulating miRNAs have the strong potential to serve as predictive and monitoring indicators of treatment response in DLBCL patients. However, only miR-21 has been shown to be significantly associated with treatment response in more than one study. More research remains necessary to obtain a large amount of reliable data.

With the discovery of TDEs in DLBCL patients in recent years, researchers have also explored the possibility of using exosomes to monitor tumor progression. Xiao et al. found that the expression level of exosomal miR-451a in the DLBCL group was significantly lower than that of the control group (56). After treatment with rituximab combined with chemotherapy, the level of serum exosomal miR-451a in treated patients was significantly increased, although it remained below the normal level (56). Feng et al. found that the expression level of CA1 in exosomes was significantly increased in drug-resistant DLBCL cells compared with drug-sensitive DLBCL cells, and the presence of CA1 in exosomes can boost chemotherapy resistance *via* the nuclear factor (NF)-κB and STAT3 pathways (77). These results suggested that TDE could be used to evaluate treatment response. However, additional research remains necessary to explore and verify this issue.

LBs AS BIOMARKERS IN DISEASE MONITORING

Imaging is currently the primary method used for detecting NHL. However, imaging has many limitations. CT has low sensitivity for disease detection, and although the use of PET/CT can improve sensitivity, PET/CT still has low tumor specificity and a high false-positive rate (91). More importantly, imaging cannot directly assess diseases at the molecular level or dynamically monitor or identify the biological mechanisms that drive the development of tumors, such as tumor heterogeneity and clonal evolution. In addition, imaging tests are associated with other risks, including radiation exposure, the use of invasive imaging agents, and high cost. A meta-analysis of 737 patients with DLBCL showed that a considerable number of patients relapsed during follow-up (91). The commonly used PET/CT protocols have a spatial resolution of 6–7 mm, which cannot detect minimal residual disease (MRD), which is a common origin of recurrence (18, 92).

The concept of MRD is an excellent surrogate for the evaluation of curative effects, the guidance of treatment, and the prediction of outcomes. MRD has been widely used in a variety of hematological tumors, including acute myeloid leukemia (AML) and acute lymphocytic leukemia (ALL) (93, 94). However, NHL patients typically lack leukemic involvement; therefore, the detection of MRD in NHL using current conventional methods is not currently possible. Fortunately, the discovery of circulating nucleic acids and circulating exosomes have introduced the possibility of evaluating MRD at the molecular level. MRD can be detected in the blood by studying tumor mutation using a variety of techniques, including PCR–based methods, and NGS–based techniques (21).

Scherer et al. followed up and monitored the ctDNA levels of 11 DLBCL patients and found that in 8 (73%) patients, ctDNA could be detected as an indicator of MRD before disease relapse (66). The average time from the discovery of ctDNA to clinical relapse was 188 days (66). In a National Cancer Institute (NCI) study, the ctDNA of 17 patients with DLBCL who progressed after complete remission (CR) was analyzed, and 15 were found to be positive for ctDNA before progression was detected (95). Chen et al. monitored the ctDNA of 14 T cell lymphoblastic lymphoma patients after treatment and found that in the 2 cases that relapsed during the maintenance phase, ctDNA could be detected before recurrence (64). The time from the detection of ctDNA to clinical recurrence was 83 and 84 days in these patients

(64). Shin et al. followed up the ctDNA levels of NHL patients after treatment and found that 93% (13 of 14) of patients who achieved CR presented declining ctDNA, and ctDNA disappeared in most patients. In the 2 cases in which trace ctDNA could be detected, the disease progressed after 6 months of ctDNA monitoring (62). These results indicated that ctDNA could be used as an indicator to monitor recurrence or disease progression. However, Suehare et al. suggested that the *TP53* and *DNMT3A* mutations detected in the cfDNA of DLBCL patients after the disease remission could be derived from clonal hematopoiesis of indeterminate potential (CHIP) rather than from MRD (96). The results of LBs should be analyzed more rigorously, especially for those gene mutations that are shared between lymphoma and CHIP (96). The source of cfDNA is more complicated than that of ctDNA. However, for cfDNA/ctDNA, the current research results are minimal, and more prospective research remains necessary.

Unfortunately, the results of a study conducted in PCNSL were not satisfactory. Hattori et al. detected the *MYD88 L265P* mutation in cfDNA during and after chemotherapy treatments in five patients with PCNSL, among whom the *MYD88 L265P* mutation was detected in cfDNA at diagnosis (67). However, they found that the *MYD88 L265P* mutation was not detected in cfDNA even if the disease progressed (67), which may indicate that *MYD88 L265P* may be negative in relapsed patients, or cfDNA might not circulate in the peripheral blood after chemotherapy (67). These findings indicated that cfDNA might not be applicable for the monitoring of MRD in PCNSL. However, the study only analyzed five patients, and the role of cfDNA for monitoring the MRD of PCNSL requires additional research.

Although few studies have examined the use of miRNA as a monitoring indicator, they all confirmed that miRNA has the potential for use in the monitoring of MRD or progression and recurrence. Among DLBCL patients with CR, high levels of miR-19b, miR-20a, and miR-451 were able to distinguish MRD-positive patients from patients without residual disease (50). In addition, studies have found that changes in the serum miR-130a and miR-125b levels of DLBCL patients are detectable in the clinical diagnosis of relapse or progression (46).

DISCUSSION

The evaluation of circulating DNA, cfDNA/ctDNA, as a type of LB has been increasingly studied. LBs can play vital roles in the diagnosis, classification, prognosis, and treatment of NHL. During the diagnosis and classification of NHL, tissue biopsy continues to play a decisive role; however, the evaluation of circulating DNA can be used as a complementary detection method. Tissue biopsy is difficult to use to detect recurrence or evaluate MRD because biopsy is invasive and cannot be repeated multiple times. Imaging has limited sensitivity and cannot detect changes that occur at the molecular level. The advantages of evaluating circulating DNA were discussed in-depth, and research has revealed the developmental potential for circulating DNA both during and after treatment. However, the use of cfDNA/ctDNA as a surrogate marker requires the optimization and standardization of pre-analytical steps and analysis techniques.

Researchers have similar expectations regarding the evaluation of another circulating nucleic acid: miRNA. However, although a large number of miRNAs have been studied, only miR-21 has obtained relatively consistent results in multiple studies, suggesting that it may play a role in diagnosis, prognosis, and response assessment.

Circulating exosomes contain a great deal of information, enabling a more comprehensive understanding of disordered signal transduction processes and the expression of related antigens for diagnosis and treatment. In contrast, circulating nucleic acids cannot provide information about changes in the proteome and transcriptome of lymphoma. Although few relevant studies have been published, these studies have confirmed the potential role of TDEs in the diagnosis, prognosis, treatment, and monitoring of NHL. In particular, the physiological properties of circulating exosomes make them more potential options for improved treatment.

Very few studies have examined the use of peripheral blood for the performance of LB in PCNSL. The results of several cfDNA/ctDNA studies have not been satisfactory thus far. Compared with cfDNA/ctDNA in peripheral blood, CSF ctDNA seems to have more advantages in the management of PCNSL. CSF ctDNA can better detect central nervous system lymphoma than plasma ctDNA (97). Analysis of gene mutations such as CD79B and MYD88 in CSF can be used as a molecular diagnostic method for PCNSL (10). The longitudinal analysis of CSF ctDNA revealed that sustained tumor responses were associated with the clearance of ctDNA from the CSF (98, 99). CSF ctDNA predicted central nervous system relapse in central nervous system and systemic lymphomas (97). Research on circulating exosomes in PCNSL is almost nonexistent. PCNSL is a malignant tumor that originates in the brain, making the acquisition of tissues during diagnosis or after treatment particularly difficult and enhancing the developmental prospects for LB in PCNSL. More than 90% of PCNSL pathology is DLBCL, which provides a theoretical basis for extending the LB results associated with DLBCL to PCNSL.

Although LB has been associated with positive findings in many aspects of the disease, some questions remain worth considering. (1) Thus far, no widely accepted standard protocols have been developed for the collection, processing, and storage of samples, which may lead to pre-analysis bias and varying results. (2) The best time and duration for monitoring remains undetermined. (3) cfDNA is dysregulated in many disease states, and no reliable standard has been established to distinguish normal exosomes from TDEs, which can make the interpretation of results difficult. (4) The detection cutoff levels set by different groups have been inconsistent, resulting in a lack of comparability among the results. (5) The current research primarily focuses on DLBCL, with little data and results regarding other NHL subtypes. (6) A large number of reasonably designed prospective studies remain necessary to

verify the reported findings. (7) A better understanding of the biological characteristics of circulating nucleic acids and exosomes will help optimize their use.

CONCLUSIONS

The noninvasive, easy-to-obtain, and reproducible characteristics of LB provide unique opportunities for the dynamic assessment of NHL-related changes. This method improves the diagnostic accuracy of identifying disease subtypes and prognosis and can be used to provide better-individualized treatment for patients. More importantly, LB can be used to fill the gaps in the monitoring of response to treatment and the detection of MRD in NHL. The real-time monitoring of treatment and timely adjustments to treatment plans based on identifiable characteristics will provide enhanced benefits to patients. The accurate early detection of disease recurrence can also enable clinicians to perform remedial treatments earlier. In-depth research examining the various substances in the circulatory systems of cancer patients will also help clarify the pathogenesis of NHL and promote the development of new treatment strategies.

AUTHOR CONTRIBUTIONS

LL wrote the manuscript. YL reviewed and edited the manuscript in detail. All authors contributed to the article and approved the submitted version.

FUNDING

This work was supported by Capital's Funds for Health Improvement and Research, NO.2020-2-2049.

REFERENCES

1. Sujobert P, Salles G, Bachy E. Molecular Classification of Diffuse Large B-cell Lymphoma: What Is Clinically Relevant? *Hematol Oncol Clin North Am* (2016) 30(6):1163–77. doi: 10.1016/j.hoc.2016.07.001
2. Ofori K, Bhagat G, Rai AJ. Exosomes and extracellular vesicles as liquid biopsy biomarkers in diffuse large B-cell lymphoma: Current state of the art and unmet clinical needs. *Br J Clin Pharmacol* (2021) 87(2):284–94. doi: 10.1111/bcp.14611
3. Roth P, Martus P, Kiewe P, Möhle R, Klasen H, Rauch M, et al. Outcome of elderly patients with primary CNS lymphoma in the G-PCNSL-SG-1 trial. *Neurology* (2012) 79(9):890–6. doi: 10.1212/WNL.0b013e318266fcb2
4. Ambady P, Fu R, Netto JP, Kersch C, Firkins J, Doolittle ND, et al. Patterns of relapse in primary central nervous system lymphoma: inferences regarding the role of the neuro-vascular unit and monoclonal antibodies in treating occult CNS disease. *Fluids Barriers CNS* (2017) 14(1):16. doi: 10.1186/s12987-017-0064-3
5. Jahnke K, Thiel E, Martus P, Herrlinger U, Weller M, Fischer L, et al. Relapse of primary central nervous system lymphoma: clinical features, outcome and prognostic factors. *J Neurooncol* (2006) 80(2):159–65. doi: 10.1007/s11060-006-9165-6
6. Schurch CM, Federmann B, Quintanilla-Martinez L, Fend F. Tumor Heterogeneity in Lymphomas: A Different Breed. *Pathobiology* (2018) 85(1-2):130–45. doi: 10.1159/000475530
7. Siravegna G, Marsoni S, Siena S, Bardelli A. Integrating liquid biopsies into the management of cancer. *Nat Rev Clin Oncol* (2017) 14(9):531–48. doi: 10.1038/nrclinonc.2017.14
8. Fernandez-Lazaro D, Hernandez JLG, Garcia AC, Castillo ACD, Hueso MV, Cruz-Hernandez JJ. Clinical Perspective and Translational Oncology of Liquid Biopsy. *Diagnostics (Basel)* (2020) 10(7):443–59. doi: 10.3390/diagnostics10070443
9. Maisano D, Mimmi S, Russo R, Fioravanti A, Fiume G, Vecchio E, et al. Uncovering the Exosomes Diversity: A Window of Opportunity for Tumor Progression Monitoring. *Pharmaceuticals (Basel)* (2020) 13(8):180–97. doi: 10.3390/ph13080180
10. Hiemcke-Jiwa LS, Leguit RJ, Snijders TJ, Jiwa NM, Kuiper JJW, de Weger RA, et al. Molecular analysis in liquid biopsies for diagnostics of primary central nervous system lymphoma: Review of literature and future opportunities. *Crit Rev Oncol/Hematol* (2018) 127:56–65. doi: 10.1016/j.critrevonc.2018.05.010
11. Birkenkamp-Demtroder K, Nordentoft I, Christensen E, Hoyer S, Reinert T, Vang S, et al. Genomic Alterations in Liquid Biopsies from Patients with Bladder Cancer. *Eur Urol* (2016) 70(1):75–82. doi: 10.1016/j.eururo.2016.01.007
12. Fontanilles M, Marguet F, Beaussire L, Magne N, Pepin LF, Alexandru C, et al. and circulating TERT promoter mutation for disease monitoring in newly-diagnosed glioblastoma. *Acta Neuropathol Commun* (2020) 8(1):179. doi: 10.1186/s40478-020-01057-7
13. Ray SK, Mukherjee S. Cell free DNA as an evolving liquid biopsy biomarker for initial diagnosis and therapeutic nursing in Cancer- An evolving aspect in Medical Biotechnology. *Curr Pharm Biotechnol* (2020) 21:1–13. doi: 10.2174/1389201021666201211102710
14. Snyder MW, Kircher M, Hill AJ, Daza RM, Shendure J. Cell-free DNA Comprises an In Vivo Nucleosome Footprint that Informs Its Tissues-Of-Origin. *Cell* (2016) 164(1-2):57–68. doi: 10.1016/j.cell.2015.11.050
15. Kwiatkowski DJ, Underhill HR, Kitzman JO, Hellwig S, Welker NC, Daza R, et al. Fragment Length of Circulating Tumor DNA. *PLoS Genet* (2016) 12(7):e1006162. doi: 10.1371/journal.pgen.1006162
16. Jahr S, Hentze H, Englisch S, Hardt D, Fackelmayer FO, Hesch RD, et al. DNA fragments in the blood plasma of cancer patients: quantitations and evidence for their origin from apoptotic and necrotic cells. *Cancer Res* (2001) 61(4):1659–65.
17. Corcoran RB, Chabner BA. Application of Cell-free DNA Analysis to Cancer Treatment. *N Engl J Med* (2018) 379(18):1754–65. doi: 10.1056/NEJMra1706174
18. Kwok M, Wu SP, Mo C, Summers T, Roschewski M. Circulating Tumor DNA to Monitor Therapy for Aggressive B-Cell Lymphomas. *Curr Treat options Oncol* (2016) 17(9):47. doi: 10.1007/s11864-016-0425-1
19. Darrah JM, Herrera AF. Updates on Circulating Tumor DNA Assessment in Lymphoma. *Curr Hematol Malig Rep* (2018) 13(5):348–55. doi: 10.1007/s11899-018-0468-4
20. Kristensen LS, Hansen JW, Kristensen SS, Tholstrup D, Harsløf LB, Pedersen OB, et al. Aberrant methylation of cell-free circulating DNA in plasma predicts poor outcome in diffuse large B cell lymphoma. *Clin Epigenet* (2016) 8(1):95. doi: 10.1186/s13148-016-0261-y
21. Herrera AF, Armand P. Minimal Residual Disease Assessment in Lymphoma: Methods and Applications. *J Clin Oncol* (2017) 35(34):3877–87. doi: 10.1200/jco.2017.74.5281
22. Wan JCM, Massie C, Garcia-Corbacho J, Mouliere F, Brenton JD, Caldas C, et al. Liquid biopsies come of age: towards implementation of circulating tumour DNA. *Nat Rev Cancer* (2017) 17(4):223–38. doi: 10.1038/nrc.2017.7
23. Lopez-Santillan M, Larrabeiti-Etxebarria A, Arzuaga-Mendez J, Lopez-Lopez E, Garcia-Orad A. Circulating miRNAs as biomarkers in diffuse large B-cell lymphoma: a systematic review. *Oncotarget* (2018) 9(32):22850–61. doi: 10.18632/oncotarget.25230

24. Weber JA, Baxter DH, Zhang S, Huang DY, Huang KH, Lee MJ, et al. The microRNA spectrum in 12 body fluids. *Clin Chem* (2010) 56(11):1733–41. doi: 10.1373/clinchem.2010.147405
25. Regazzo G, Marchesi F, Spagnuolo M, Díaz Méndez AB, Masi S, Mengarelli A, et al. Diffuse large B-cell lymphoma: Time to focus on circulating blood nucleic acids? *Blood Rev* (2020) 10:100776. doi: 10.1016/j.blre.2020.100776
26. Zare N, Haghjooy Javanmard SH, Mehrzad V, Eskandari N, Andalib AR. Effect of Plasma-Derived Exosomes of Refractory/Relapsed or Responsive Patients with Diffuse Large B-Cell Lymphoma on Natural Killer Cells Functions. *Cell J* (2020) 22(1):40–54. doi: 10.22074/cellj.2020.6550
27. Schorey JS, Bhatnagar S. Exosome function: from tumor immunology to pathogen biology. *Traffic (Copenhagen Denmark)* (2008) 9(6):871–81. doi: 10.1111/j.1600-0854.2008.00734.x
28. Mathieu M, Martin-Jaular L, Lavieu G, Thery C. Specificities of secretion and uptake of exosomes and other extracellular vesicles for cell-to-cell communication. *Nat Cell Biol* (2019) 21(1):9–17. doi: 10.1038/s41556-018-0250-9
29. Kalluri R, LeBleu VS. The biology, function, and biomedical applications of exosomes. *Science* (2020) 367(6478):eaau6977. doi: 10.1126/science.aau6977
30. Momen-Heravi F, Balaj L, Alian S, Trachtenberg AJ, Hochberg FH, Skog J, et al. Impact of biofluid viscosity on size and sedimentation efficiency of the isolated microvesicles. *Front Physiol* (2012) 3:162. doi: 10.3389/fphys.2012.00162
31. Shao H, Im H, Castro CM, Breakefield X, Weissleder R, Lee H. New Technologies for Analysis of Extracellular Vesicles. *Chem Rev* (2018) 118 (4):1917–50. doi: 10.1021/acs.chemrev.7b00534
32. Brennan K, Martin K, FitzGerald SP, O'Sullivan J, Wu Y, Blanco A, et al. A comparison of methods for the isolation and separation of extracellular vesicles from protein and lipid particles in human serum. *Sci Rep* (2020) 10 (1):1039. doi: 10.1038/s41598-020-57497-7
33. Hur JY, Kim YJ, Yoon SE, Son DS, Park WY, Kim SJ, et al. Plasma cell-free DNA is a prognostic biomarker for survival in patients with aggressive non-Hodgkin lymphomas. *Ann Hematol* (2020) 99(6):1293–302. doi: 10.1007/s00277-020-04008-3
34. Eskandari M, Manoochehrabadi S, Pashaiefar H, Zaimy MA, Ahmadvand M. Clinical significance of cell-free DNA as a prognostic biomarker in patients with diffuse large B-cell lymphoma. *Blood Res* (2019) 54(2):114–9. doi: 10.5045/br.2019.54.2.114
35. Hohaus S, Giachelia M, Massini G, Mansueto G, Vannata B, Bozzoli V, et al. Cell-free circulating DNA in Hodgkin's and non-Hodgkin's lymphomas. *Ann Oncol* (2009) 20(8):1408–13. doi: 10.1093/annonc/mdp006
36. Li M, Jia Y, Xu J, Cheng X, Xu C. Assessment of the circulating cell-free DNA marker association with diagnosis and prognostic prediction in patients with lymphoma: a single-center experience. *Ann Hematol* (2017) 96(8):1343–51. doi: 10.1007/s00277-017-3043-5
37. Sun P, Chen C, Xia Y, Wang Y, Liu PP, Bi XW, et al. Mutation Profiling of Malignant Lymphoma by Next-Generation Sequencing of Circulating Cell-Free DNA. *J Cancer* (2019) 10(2):323–31. doi: 10.7150/jca.27615
38. Cui Q, Vari F, Cristino AS, Salomon C, Rice GE, Sabdia MB, et al. Circulating cell-free miR-494 and miR-21 are disease response biomarkers associated with interim-positron emission tomography response in patients with diffuse large B-cell lymphoma. *Oncotarget* (2018) 9(78):34644–57. doi: 10.18632/oncotarget.26141
39. Chen W, Wang H, Chen H, Liu S, Lu H, Kong D, et al. Clinical significance and detection of microRNA-21 in serum of patients with diffuse large B-cell lymphoma in Chinese population. *Eur J Haematol* (2014) 92(5):407–12. doi: 10.1111/ejh.12263
40. Lawrie CH, Gal S, Dunlop HM, Pushkaran B, Liggins AP, Pulford K, et al. Detection of elevated levels of tumour-associated microRNAs in serum of patients with diffuse large B-cell lymphoma. *Br J Haematol* (2008) 141(5):672–5. doi: 10.1111/j.1365-2141.2008.07077.x
41. Ahmadvand M, Eskandari M, Pashaiefar H, Yaghmaie M, Manoochehrabadi S, Khakpour G, et al. Over expression of circulating miR-155 predicts prognosis in diffuse large B-cell lymphoma. *Leukemia Res* (2018) 70:45–8. doi: 10.1016/j.leukres.2018.05.006
42. Eis PS, Tam W, Sun L, Chadburn A, Li Z, Gomez MF, et al. Accumulation of miR-155 and BIC RNA in human B cell lymphomas. *Proc Natl Acad Sci U S A* (2005) 102(10):3627–32. doi: 10.1073/pnas.0500613102
43. Borges NM, do Vale Elias M, Fook-Alves VL, Andrade TA, de Conti ML, Macedo MP, et al. Angiomirs expression profiling in diffuse large B-Cell lymphoma. *Oncotarget* (2016) 7(4):4806–16. doi: 10.18632/oncotarget.6624
44. Fang C, Zhu DX, Dong HJ, Zhou ZJ, Wang YH, Liu L, et al. Serum microRNAs are promising novel biomarkers for diffuse large B cell lymphoma. *Ann Hematol* (2012) 91(4):553–9. doi: 10.1007/s00277-011-1350-9
45. Beheshti A, Stevenson K, Vanderburg C, Ravi D, McDonald JT, Christie AL, et al. Identification of Circulating Serum Multi-MicroRNA Signatures in Human DLBCL Models. *Sci Rep* (2019) 9(1):17161. doi: 10.1038/s41598-019-52985-x
46. Yuan WX, Gui YX, Na WN, Chao J, Yang X. Circulating microRNA-125b and microRNA-130a expression profiles predict chemoresistance to R-CHOP in diffuse large B-cell lymphoma patients. *Oncol Lett* (2016) 11(1):423–32. doi: 10.3892/ol.2015.3866
47. Khare D, Goldschmidt N, Bardugo A, Gur-Wahnon D, Ben-Dov IZ, Avni B. Plasma microRNA profiling: Exploring better biomarkers for lymphoma surveillance. *PLoS One* (2017) 12(11):e0187722. doi: 10.1371/journal.pone.0187722
48. Meng Y, Quan L, Liu A. Identification of key microRNAs associated with diffuse large B-cell lymphoma by analyzing serum microRNA expressions. *Gene* (2018) 642:205–11. doi: 10.1016/j.gene.2017.11.022
49. Zheng Z, Sun R, Zhao HJ, Fu D, Zhong HJ, Weng XQ, et al. MiR155 sensitized B-lymphoma cells to anti-PD-L1 antibody via PD-1/PD-L1-mediated lymphoma cell interaction with CD8+T cells. *Mol Cancer* (2019) 18(1):54. doi: 10.1186/s12943-019-0977-3
50. Bouvy C, Wannez A, George F, Graux C, Chatelain C, Dogne JM. Circulating MicroRNAs as Biomarkers in Diffuse Large B-cell Lymphoma: A Pilot Prospective Longitudinal Clinical Study. *Biomark Cancer* (2018) 10:1179299X18781095. doi: 10.1177/1179299X18781095
51. Li J, Fu R, Yang L, Tu W. miR-21 expression predicts prognosis in diffuse large B-cell lymphoma. *Int J Clin Exp Pathol* (2015) 8(11):15019–24.
52. Caivano A, La Rocca F, Simeon V, Girasole M, Dinarelli S, Laurenzana I, et al. MicroRNA-155 in serum-derived extracellular vesicles as a potential biomarker for hematologic malignancies - a short report. *Cell Oncol (Dordr)* (2017) 40(1):97–103. doi: 10.1007/s13402-016-0300-x
53. Beheshti A, Vanderburg C, McDonald JT, Ramkumar C, Kadungure T, Zhang H, et al. A Circulating microRNA Signature Predicts Age-Based Development of Lymphoma. *PLoS One* (2017) 12(1):e0170521. doi: 10.1371/journal.pone.0170521
54. Tuncer SB, Akdeniz D, Celik B, Kilic S, Sukruoglu O, Avsar M, et al. The expression levels of miRNA-15a and miRNA-16-1 in circulating tumor cells of patients with diffuse large B-cell lymphoma. *Mol Biol Rep* (2019) 46(1):975–80. doi: 10.1007/s11033-018-4554-4
55. Guo HQ, Huang GL, Guo CC, Pu XX, Lin TY. Diagnostic and prognostic value of circulating miR-221 for extranodal natural killer/T-cell lymphoma. *Dis Markers* (2010) 29(5):251–8. doi: 10.3233/DMA-2010-0755
56. Xiao XB, Gu Y, Sun DL, Ding LY, Yuan XG, Jiang HW, et al. Effect of rituximab combined with chemotherapy on the expression of serum exosome miR-451a in patients with diffuse large b-cell lymphoma. *Eur Rev Med Pharmacol Sci* (2019) 23(4):1620–5. doi: 10.26355/eurrev_201902_17121
57. Gállego Pérez-Larraya J, Alonso MM, Patiño-García A, Martínez-Vila E, Gállego-Culleré J, Díez-Valle R, et al. RNU6-1 in circulating exosomes differentiates GBM from non-neoplastic brain lesions and PCNSL but not from brain metastases. *Neuro Oncol Adv* (2020) 2(1):vdaa010. doi: 10.1093/noajnl/vdaa010
58. Rossi D, Diop F, Spaccarotella E, Monti S, Zanni M, Rasi S, et al. Diffuse large B-cell lymphoma genotyping on the liquid biopsy. *Blood* (2017) 129 (14):1947–57. doi: 10.1182/blood-2016-05-719641
59. Rivas-Delgado A, Nadeu F, Enjuanes A, Casanueva-Eliceiry S, Mozas P, Magnano L, et al. Mutational Landscape and Tumor Burden Assessed by Cell-free DNA in Diffuse Large B-Cell Lymphoma in a Population-Based Study. *Clin Cancer Res* (2021) 27(2):513–21. doi: 10.1158/1078-0432.ccr-20-2558
60. Liu H, Yang C, Zhao X, Le J, Wu G, Wei J, et al. Genotyping on ctDNA Identifies Shifts in Mutation Spectrum Between Newly Diagnosed and Relapse/Refractory DLBCL. *OncoTargets Ther* (2020) 13:10797–806. doi: 10.2147/ott.s275334
61. Bohers E, Viailly PJ, Becker S, Marchand V, Ruminy P, Maingonnat C, et al. Non-invasive monitoring of diffuse large B-cell lymphoma by cell-free DNA high-throughput targeted sequencing: analysis of a prospective cohort. *Blood Cancer J* (2018) 8(8):74. doi: 10.1038/s41408-018-0111-6
62. Shin SH, Kim YJ, Lee D, Cho D, Ko YH, Cho J, et al. Analysis of circulating tumor DNA by targeted ultra-deep sequencing across various non-Hodgkin

lymphoma subtypes. *Leuk lymphoma* (2019) 60(9):2237–46. doi: 10.1080/10428194.2019.1573998
63. Li Q, Zhang W, Li J, Xiong J, Liu J, Chen T, et al. Plasma circulating tumor DNA assessment reveals KMT2D as a potential poor prognostic factor in extranodal NK/T-cell lymphoma. *Biomarker Res* (2020) 8:27. doi: 10.1186/s40364-020-00205-4
64. Chen F, Pang D, Guo H, Jiang X, Liu S, Huang L, et al. Clinicopathological Characteristics and Mutational Profiling of Adult T-Cell Lymphoblastic Lymphoma in a Chinese Population. *Cancer Manage Res* (2020) 12:3003–12. doi: 10.2147/cmar.s242903
65. Sakata-Yanagimoto M, Nakamoto-Matsubara R, Komori D, Nguyen TB, Hattori K, Nanmoku T, et al. Detection of the circulating tumor DNAs in angioimmunoblastic T- cell lymphoma. *Ann Hematol* (2017) 96(9):1471–5. doi: 10.1007/s00277-017-3038-2
66. Scherer F, Kurtz DM, Newman AM, Stehr H, Craig AF, Esfahani MS, et al. Distinct biological subtypes and patterns of genome evolution in lymphoma revealed by circulating tumor DNA. *Sci Transl Med* (2016) 8(364):364ra155. doi: 10.1126/scitranslmed.aai8545
67. Hattori K, Sakata-Yanagimoto M, Suehara Y, Yokoyama Y, Kato T, Kurita N, et al. Clinical significance of disease-specific MYD88 mutations in circulating DNA in primary central nervous system lymphoma. *Cancer Sci* (2018) 109 (1):225–30. doi: 10.1111/cas.13450
68. Montesinos-Rongen M, Brunn A, Tuchscherer A, Borchmann P, Schorb E, Kasenda B, et al. Analysis of Driver Mutational Hot Spots in Blood-Derived Cell-Free DNA of Patients with Primary Central Nervous System Lymphoma Obtained before Intracerebral Biopsy. *J Mol Diagn* (2020) 22(10):1300–7. doi: 10.1016/j.jmoldx.2020.07.002
69. Wu J, Tang W, Huang L, Hou N, Wu J, Cheng X, et al. The analysis of cell-free DNA concentrations and integrity in serum of initial and treated of lymphoma patients. *Clin Biochem* (2019) 63:59–65. doi: 10.1016/j.clinbiochem.2018.10.002
70. Decazes P, Camus V, Bohers E, Viailly PJ, Tilly H, Ruminy P, et al. Correlations between baseline (18)F-FDG PET tumour parameters and circulating DNA in diffuse large B cell lymphoma and Hodgkin lymphoma. *EJNMMI Res* (2020) 10(1):120. doi: 10.1186/s13550-020-00717-y
71. Delfau-Larue MH, van der Gucht A, Dupuis J, Jais JP, Nel I, Beldi-Ferchiou A, et al. Total metabolic tumor volume, circulating tumor cells, cell-free DNA: distinct prognostic value in follicular lymphoma. *Blood Adv* (2018) 2(7):807–16. doi: 10.1182/bloodadvances.2017015164
72. Sarkozy C, Huet S, Carlton VE, Fabiani B, Delmer A, Jardin F, et al. The prognostic value of clonal heterogeneity and quantitative assessment of plasma circulating clonal IG-VDJ sequences at diagnosis in patients with follicular lymphoma. *Oncotarget* (2017) 8(5):8765–74. doi: 10.18632/oncotarget.14448
73. Chiu BC, Zhang Z, You Q, Zeng C, Stepniak E, Bracci PM, et al. Prognostic implications of 5-hydroxymethylcytosines from circulating cell-free DNA in diffuse large B-cell lymphoma. *Blood Adv* (2019) 3(19):2790–9. doi: 10.1182/bloodadvances.2019000175
74. Marchesi F, Regazzo G, Palombi F, Terrenato I, Sacconi A, Spagnuolo M, et al. Serum miR-22 as potential non-invasive predictor of poor clinical outcome in newly diagnosed, uniformly treated patients with diffuse large B-cell lymphoma: an explorative pilot study. *J Exp Clin Cancer Res CR* (2018) 37 (1):95. doi: 10.1186/s13046-018-0768-5
75. Sun R, Zheng Z, Wang L, Cheng S, Shi Q, Qu B, et al. A novel prognostic model based on four circulating miRNA in diffuse large B-cell lymphoma: implications for the roles of MDSC and Th17 cells in lymphoma progression. *Mol Oncol* (2021) 15(1):246–61. doi: 10.1002/1878-0261.12834
76. Feng Y, Zhong M, Zeng S, Wang L, Liu P, Xiao X, et al. Exosome-derived miRNAs as predictive biomarkers for diffuse large B-cell lymphoma chemotherapy resistance. *Epigenomics* (2019) 11(1):35–51. doi: 10.2217/epi-2018-0123
77. Feng Y, Zhong M, Tang Y, Liu X, Liu Y, Wang L, et al. The Role and Underlying Mechanism of Exosomal CA1 in Chemotherapy Resistance in Diffuse Large B Cell Lymphoma. *Mol Ther Nucleic Acids* (2020) 21:452–63. doi: 10.1016/j.omtn.2020.06.016
78. Zare N, Haghjooy Javanmard S, Mehrzad V, Eskandari N, Kefayat A. Evaluation of exosomal miR-155, let-7g and let-7i levels as a potential noninvasive biomarker among refractory/relapsed patients, responsive patients and patients receiving R-CHOP. *Leukemia lymphoma* (2019) 60 (8):1877–89. doi: 10.1080/10428194.2018.1563692
79. Ryu KJ, Lee JY, Choi ME, Yoon SE, Cho J, Ko YH, et al. Serum-Derived Exosomal MicroRNA Profiles Can Predict Poor Survival Outcomes in Patients with Extranodal Natural Killer/T-Cell Lymphoma. *Cancers* (2020) 12(12):3548–66. doi: 10.3390/cancers12123548
80. Camus V, Sarafan-Vasseur N, Bohers E, Dubois S, Mareschal S, Bertrand P, et al. Digital PCR for quantification of recurrent and potentially actionable somatic mutations in circulating free DNA from patients with diffuse large B-cell lymphoma. *Leukemia lymphoma* (2016) 57(9):2171–9. doi: 10.3109/10428194.2016.1139703
81. Hayashida M, Maekawa F, Chagi Y, Iioka F, Kobashi Y, Watanabe M, et al. Combination of multicolor flow cytometry for circulating lymphoma cells and tests for the RHOA(G17V) and IDH2(R172) hot-spot mutations in plasma cell-free DNA as liquid biopsy for the diagnosis of angioimmunoblastic T-cell lymphoma. *Leukemia lymphoma* (2020) 61(10):2389–98. doi: 10.1080/10428194.2020.1768382
82. Yao Y, Wei W, Sun J, Chen L, Deng X, Ma L, et al. Proteomic analysis of exosomes derived from human lymphoma cells. *Eur J Med Res* (2015) 20(1):8. doi: 10.1186/s40001-014-0082-4
83. Cocozza F, Menay F, Tsacalian R, Elisei A, Sampedro P, Soria I, et al. Cyclophosphamide enhances the release of tumor exosomes that elicit a specific immune response in vivo in a murine T-cell lymphoma. *Vaccine* (2019) 37(12):1565–76. doi: 10.1016/j.vaccine.2019.02.004
84. Chen Z, You L, Wang L, Huang X, Liu H, Wei JY, et al. Dual effect of DLBCL-derived EXOs in lymphoma to improve DC vaccine efficacy in vitro while favor tumorgenesis in vivo. *J Exp Clin Cancer Res CR* (2018) 37(1):190. doi: 10.1186/s13046-018-0863-7
85. Milman N, Ginini L, Gil Z. Exosomes and their role in tumorigenesis and anticancer drug resistance. *Drug Resist updates Rev Commentaries Antimicrob Anticancer Chemother* (2019) 45:1–12. doi: 10.1016/j.drup.2019.07.003
86. Solimando AG, Ribatti D, Vacca A, Einsele H. Targeting B-cell non Hodgkin lymphoma: New and old tricks. *Leukemia Res* (2016) 42:93–104. doi: 10.1016/j.leukres.2015.11.001
87. Solimando AG, Annese T, Tamma R, Ingravallo G, Maiorano E, Vacca A, et al. New Insights into Diffuse Large B-Cell Lymphoma Pathobiology. *Cancers* (2020) 12(7):1869–90. doi: 10.3390/cancers12071869
88. Leone P, Buonavoglia A, Fasano R, Solimando AG, De Re V, Cicco S, et al. Insights into the Regulation of Tumor Angiogenesis by Micro-RNAs. *J Clin Med* (2019) 8(12):2030–49. doi: 10.3390/jcm8122030
89. Sidaway P. ctDNA predicts outcomes in DLBCL. *Nat Rev Clin Oncol* (2018) 15 (11):655. doi: 10.1038/s41571-018-0091-2
90. Song G, Gu L, Li J, Tang Z, Liu H, Chen B, et al. Serum microRNA expression profiling predict response to R-CHOP treatment in diffuse large B cell lymphoma patients. *Ann Hematol* (2014) 93(10):1735–43. doi: 10.1007/s00277-014-2111-3
91. Melani C, Wilson WH, Roschewski M. Monitoring clinical outcomes in aggressive B-cell lymphoma: From imaging studies to circulating tumor DNA. *Best Pract Res Clin Haematol* (2018) 31(3):285–92. doi: 10.1016/j.beha.2018.07.004
92. Adams HJ, Nievelstein RA, Kwee TC. Prognostic value of complete remission status at end-of-treatment FDG-PET in R-CHOP-treated diffuse large B-cell lymphoma: systematic review and meta-analysis. *Br J Haematol* (2015) 170 (2):185–91. doi: 10.1111/bjh.13420
93. Dillon R, Potter N, Freeman S, Russell N. How we use molecular minimal residual disease (MRD) testing in acute myeloid leukaemia (AML). *Br J Haematol* (2020). doi: 10.1111/bjh.17185
94. Tran TH, Hunger SP. The genomic landscape of pediatric acute lymphoblastic leukemia and precision medicine opportunities. *Semin Cancer Biol* (2020) S1044-579X(20)30218-2. doi: 10.1016/j.semcancer.2020.10.013
95. Roschewski M, Dunleavy K, Pittaluga S, Moorhead M, Pepin F, Kong K, et al. Circulating tumour DNA and CT monitoring in patients with untreated diffuse large B-cell lymphoma: a correlative biomarker study. *Lancet Oncol* (2015) 16(5):541–9. doi: 10.1016/s1470-2045(15)70106-3
96. Suehara Y, Sakata-Yanagimoto M, Hattori K, Kusakabe M, Nanmoku T, Sato T, et al. Mutations found in cell-free DNAs of patients with malignant lymphoma at remission can derive from clonal hematopoiesis. *Cancer Sci* (2019) 110(10):3375–81. doi: 10.1111/cas.14176
97. Bobillo S, Crespo M, Escudero L, Mayor R, Raheja P, Carpio C, et al. Cell free circulating tumor DNA in cerebrospinal fluid detects and monitors central

nervous system involvement of B-cell lymphomas. *Haematologica* (2021) 106 (2):513–21. doi: 10.3324/haematol.2019.241208

98. Chen F, Pang D, Guo H, Ou Q, Wu X, Jiang X, et al. Clinical outcomes of newly diagnosed primary CNS lymphoma treated with ibrutinib-based combination therapy: A real-world experience of off-label ibrutinib use. *Cancer Med* (2020) 9(22):8676–84. doi: 10.1002/cam4.3499
99. Grommes C, Tang SS, Wolfe J, Kaley TJ, Daras M, Pentsova EI, et al. Phase 1b trial of an ibrutinib-based combination therapy in recurrent/refractory CNS lymphoma. *Blood* (2019) 133(5):436–45. doi: 10.1182/blood-2018-09-875732

Conflict of Interest: The authors declare that the research was conducted in the absence of any commercial or financial relationships that could be construed as a potential conflict of interest.

frontiers in Oncology

ORIGINAL RESEARCH
published: 21 April 2021
doi: 10.3389/fonc.2021.632094

Wilms Tumor 1 Mutations Are Independent Poor Prognostic Factors in Pediatric Acute Myeloid Leukemia

Yin Wang[1,2], *Wen-Jun Weng*[1,2], *Dun-Hua Zhou*[1,2], *Jian-Pei Fang*[1,2], *Srishti Mishra*[3], *Li Chai*[4*] and *Lu-Hong Xu*[1,2*]

[1] Department of Pediatrics, Sun Yat-sen Memorial Hospital, Sun Yat-sen University, Guangzhou, China, [2] Guangdong Provincial Key Laboratory of Malignant Tumor Epigenetics and Gene Regulation, Sun Yat-sen Memorial Hospital, Sun Yat-sen University, Guangzhou, China, [3] Cancer Science Institute, Yong Loo Lin School of Medicine, National University of Singapore, Singapore, Singapore, [4] Department of Pathology, Brigham & Women's Hospital, Harvard Medical School, Boston, MA, United States

OPEN ACCESS

Edited by:
Alejandro Gru,
University of Virginia Health System,
United States

Reviewed by:
Deepshi Thakral,
All India Institute of Medical Sciences, India
Michael Diamantidis,
University Hospital of Larissa, Greece

***Correspondence:**
Li Chai
lchai@bwh.harvard.edu
Lu-Hong Xu
xulhong@mail.sysu.edu.cn

Specialty section:
This article was submitted to Hematologic Malignancies, a section of the journal Frontiers in Oncology

Received: 22 November 2020
Accepted: 29 March 2021
Published: 21 April 2021

Citation:
Wang Y, Weng W-J, Zhou D-H, Fang J-P, Mishra S, Chai L and Xu L-H (2021) Wilms Tumor 1 Mutations Are Independent Poor Prognostic Factors in Pediatric Acute Myeloid Leukemia. Front. Oncol. 11:632094. doi: 10.3389/fonc.2021.632094

The prognostic impact of *Wilms tumor 1* (*WT1*) mutations remains controversial for patients with acute myeloid leukemia (AML). Here, we aimed to determine the clinical implication of *WT1* mutations in a large cohort of pediatric AML. The clinical data of 870 pediatric patients with AML were downloaded from the therapeutically applicable research to generate effective treatment (TARGET) dataset. We analyzed the prevalence, clinical profile, and prognosis of AML patients with *WT1* mutations in this cohort. Our results showed that 6.7% of total patients harbored *WT1* mutations. These *WT1* mutations were closely associated with normal cytogenetics ($P<0.001$), FMS-like tyrosine kinase 3/internal tandem duplication (*FLT3*/ITD) mutations ($P<0.001$), and low complete remission induction rates ($P<0.01$). Compared to the patients without *WT1* mutations, patients with *WT1* mutations had a worse 5-year event-free survival (21.7 ± 5.5% vs 48.9 ± 1.8%, $P<0.001$) and a worse overall survival (41.4 ± 6.6% vs 64.3 ± 1.7%, $P<0.001$). Moreover, patients with both *WT1* and *FLT3*/ITD mutations had a dismal prognosis. Compared to chemotherapy alone, hematopoietic stem cell transplantation tended to improve the prognoses of *WT1*-mutated patients. Multivariate analysis demonstrated that *WT1* mutations conferred an independent adverse impact on event-free survival (hazard ratio 1.910, $P = 0.001$) and overall survival (hazard ratio 1.709, $P = 0.020$). In conclusion, our findings have demonstrated that *WT1* mutations are independent poor prognostic factors in pediatric AML.

Keywords: acute myeloid leukemia, *WT1* mutations, pediatric patients, prognostic factors, *FLT3*/ITD mutations

INTRODUCTION

Acute myeloid leukemia (AML) is a type of blood cancer that originates in the bone marrow from immature white blood cells known as myeloblasts. About 20% of all children with leukemia have AML (1, 2). In the last few years, collaborative studies have revealed a link between the degree of genetic heterogeneity of AML and the clinical outcome, allowing risk stratification before therapy

and guiding post-induction treatment (3). The *Wilms tumor 1* (*WT1*) gene, located on chromosome 11p13, encodes a zinc-finger protein that exists in multiple isoforms. It has been implicated in the regulation of cell survival, proliferation and differentiation, and may function both as a tumor suppressor and an oncogene (4, 5). Various mutations across *WT1* gene have been reported in solid tumors and AML (6, 7). However, the prognostic impact of *WT1* mutations remains controversial for patients with AML (8).

The *WT1* mutations have been shown to be independent predictors of worse clinical outcome in some but not all adult AML studies (9–11). Recently, *WT1* mutations are proposed to be prognostic markers of risk stratification for adult AML (12). However, the prognostic implications of *WT1* mutations have not been clarified in pediatric AML. Moreover, large cohort studies on the clinical significance of *WT1* mutations in pediatric AML are scarce. A pediatric study of 298 patients with AML found that *WT1* mutations conferred an independent poor prognostic significance (13). However, another study of 842 pediatric AML revealed that the presence of *WT1* mutations had no independent prognostic significance in predicting the disease outcome (14). Recently, in a cohort of 353 pediatric patients with AML, Niktoreh et al. (15) have found that *WT1* mutations significantly increased the chance of relapse or treatment failure and reduced the probability of 3-year overall survival (OS), but had no significant impact on the 3-year probability of event-free survival (EFS). On the other hand, hematopoietic stem cell transplantation (HSCT) is an important treatment modality for patients with AML. However, the role of HSCT for patients with *WT1* mutations remains unknown.

To determine the clinical implication of *WT1* mutations, an independent large cohort study of pediatric AML is needed. Therefore, we analyzed the clinical data of 870 pediatric patients with AML from the therapeutically applicable research to generate effective treatment (TARGET) dataset. We found that *WT1* mutations are independent poor prognostic factors in pediatric AML in terms of 5-year EFS and OS. Patients with both *WT1* and FMS-like tyrosine kinase 3/internal tandem duplication (*FLT3*/ITD) mutations had a dismal prognosis. Moreover, HSCT might be an effective strategy for patients with *WT1* mutations.

MATERIALS AND METHODS

Patients

The clinical data on patients with AML were downloaded from the TARGET dataset (https://ocg.cancer.gov/programs/target/data-matrix). In total, 870 pediatric patients younger than 18 years old with the information of *WT1* mutations were included in our study. The year of diagnosis ranged from 1996 to 2010 while the year of last follow-up ranged from 1997 to 2015. The diagnosis of pediatric AML and risk stratification were defined according to the Children's Oncology Group (COG) guidelines. Subtype classifications of AML were assigned according to the French–American–British (FAB) classifications. Mutation analyses of *WT1*, *FLT3*/ITD, *NPM1*, and *CEBPA* were performed as previously described (14, 16–18). Treatment protocols for AML included AAML03P1, AAML0531 and CCG-2961. HSCT was considered for high-risk patients in the first complete remission. Detailed treatments and risk stratification of these studies have been previously described (19).

Statistical Analysis

The data were analyzed with the Statistical Package for the Social Sciences (SPSS®) version, 20.0 (IBM Corporation, Armonk, NY, USA). The $\chi 2$ test was used to compare the frequencies of mutations. Fischer's exact test was used when data were sparse. The nonparametric Mann–Whitney *U*-test was applied for continuous variables. Complete remission (CR) was defined as bone marrow aspirate with < 5% blasts by morphology. EFS was defined as the time between diagnosis and first event, including induction failure, relapse, or death of any cause. OS was defined as the time between diagnosis and death from any cause. The survival curves were estimated using the Kaplan–Meier method and compared using the log-rank test. Cox proportional hazard models were used to estimate hazard ratios (HR) for multivariate analyses. A two-sided *P*-value less than 0.05 was considered statistically significant for all statistical analyses.

RESULTS

Relationship Between *WT1* Mutations and Clinical Characteristics

The patients' clinical characteristics are shown in **Table 1**. Overall, among the 870 pediatric patients with AML, 58 patients (6.7%) were identified with *WT1* mutations. The white blood cell count (WBC) at diagnosis was significantly higher in *WT1*-mutated patients (median 56.9×10^9/L) than in *WT1* wild-type patients (median 30.8×10^9/L; *P*=0.041). In *WT1*-mutated group, the FAB subtypes were mainly M1, M2, and M4. A higher proportion of *WT1*-mutated patients had M4 morphology in comparison with *WT1* wild-type patients (41.2% vs 25.9%; *P* = 0.018). We also evaluated the associations between *WT1* mutations and cytogenetic and molecular alterations. In terms of cytogenetics, *WT1* mutations were found more frequently in the normal cytogenetics subset (44.2% of *WT1*-mutated patients had normal cytogenetics compared with 22.3% of those without *WT1* mutations; *P*<0.001). Regarding the molecular alterations, there was a substantial overlap between *WT1* mutations and *FLT3*/ITD, as shown in **Table 1**, 48.3% of those carrying a *WT1* mutation were also *FLT3*/ITD positive as opposed to 14.7% of patients without *WT1* mutations (*P*<0.001). Moreover, the *WT1*-mutated patients were classified more frequently as high risk (40.7% vs 12.6%; *P*<0.001). The treatment protocols for pediatric AML were equally distributed between these two groups (*P*=0.058). However, there were no significant differences in the median age, the median of *FLT3*/ITD allelic ratio, *NPM1*, and *CEBPA* mutations between the *WT1*-mutated group and *WT1* wild-type group.

TABLE 1 | Characteristics of pediatric patients with or without *WT1* mutations.

	All patients	*WT1*-mutated case	*WT1* wildtype case	*P*-value
Number (%)	870	58 (6.7%)	812(93.3%)	
Age, median (year)	9.6	11	9.5	0.221
<3years, n (%)	211(24.3%)	6 (10.3%)	205 (25.2%)	0.011
3≤Age<10years, n (%)	237(27.2%)	19 (32.8%)	218 (26.8%)	0.329
10≤Age<18years, n (%)	422(48.5%)	33 (56.9%)	389 (47.9%)	0.186
Sex				0.119
male, n (%)	454 (52.2%)	36 (62.1%)	418 (51.5%)	
female, n (%)	416 (47.8%)	22 (37.9%)	394 (48.5%)	
WBC, $\times10^9$/L,				
Median (range)	31.7(0.2-610)	56.9(1.1-446)	30.8(0.2-610)	0.041
FAB classification: n (%)				0.001
M0	20 (2.8%)	1 (2.0%)	19 (2.9%)	>0.999
M1	96 (13.4%)	10 (19.6%)	86 (13.0%)	0.181
M2	193 (27.0%)	11 (21.6%)	182 (27.5%)	0.362
M3	2 (0.3%)	0 (0.0%)	2 (0.3%)	>0.999
M4	193 (27.0%)	21 (41.2%)	172 (25.9%)	0.018
M5	160 (22.4%)	3 (5.9%)	157 (23.7%)	0.003
M6	11 (1.5%)	4 (7.8%)	7 (1.1%)	0.005
M7	39 (5.5%)	1 (2.0%)	38 (5.7%)	0.351
Risk group: n (%)				<0.001
Low risk	328 (39.0%)	15 (27.8%)	313 (39.8%)	0.079
Standard risk	391 (46.5%)	17 (31.5%)	374 (47.6%)	0.022
High risk	121 (14.4%)	22 (40.7%)	99 (12.6%)	<0.001
FLT3/ITD				<0.001
Positive, n (%)	147 (16.9%)	28 (48.3%)	119 (14.7%)	
Negative, n (%)	722(83.1%)	30 (51.7%)	692 (85.3%)	
FLT3/ITD allelic ratio,	0.54	0.55	0.54	0.865
Median (range)	(0.03-9.50)	(0.03-5.19)	(0.03-9.50)	
NPM1				0.794
Positive, n (%)	66(7.6%)	3(5.3%)	63(7.8%)	
Negative, n (%)	802(92.4%)	63(94.7%)	748(92.2%)	
CEBPA				0.245
Positive, n (%)	49(5.7%)	1(1.7%)	48(5.9%)	
Negative, n (%)	817(94.3%)	57(98.3)	760(94.1%)	
Cytogenetic status				
Normal (n, %)	196(23.7%)	23(44.2%)	173(22.3%)	<0.001
Abnormal (n, %)	631 (76.4%)	29 (55.8%)	602 (77.7%)	0.317
inv(16)(n, %)	106(12.8%)	9(17.3%)	97(12.5%)	0.046
t(8;21) (n, %)	128(15.5%)	3(5.8%)	125(16.1%)	
HSCT in 1st CR				0.906
No (n, %)	663 (83.8%)	38 (84.4%)	625 (83.8%)	
Yes (n, %)	128 (16.2%)	7 (15.6%)	121 (16.2%)	
Protocol				0.058
AAML03P1 (n, %)	91 (10.5%)	7 (12.1%)	84 (10.3%)	0.679
AAML0531 (n, %)	732 (84.1%)	44 (75.9%)	688 (84.7%)	0.074
CCG-2961 (n, %)	47(5.4%)	7 (12.1%)	40 (4.9%)	0.031
CR status at end of course 1				0.002
CR, n (%)	656 (76.3%)	35 (60.3%)	621 (77.4%)	0.003
Not CR, n (%)	189 (22.0%)	20 (34.5%)	169 (21.1%)	0.017
Death, n (%)	15 (1.7%)	3 (5.2%)	12 (1.5%)	0.074
CR status at end of course 2				<0.001
CR, n (%)	736 (87.2%)	38 (69.1%)	698 (88.5%)	<0.001
Not CR, n (%)	88 (10.4%)	14 (25.5%)	74 (9.4%)	<0.001
Death, n (%)	20 (2.4%)	3 (5.5%)	17 (2.2%)	0.136

CEBPA CCAAT, enhancer binding protein alpha; CR, complete remission; FAB, French–American–British morphology classification; FLT3/ITD, internal tandem duplication of the FLT3 gene; HSCT, hematopoietic stem cell transplantation; NPM1, Nucleophosmin; WBC, white blood cell count.

Clinical Outcome and Prognostic Effect of *WT1* Mutations

The CR rate was determined for all patients after the first and second course of induction therapy. At the end of the first course of therapy, patients with *WT1* mutations had a lower rate of CR (60.3%) compared to those without *WT1* mutations (77.4%), and the difference was statistically significant (P=0.002). At the end of the second course of therapy, 38(69.1%) of the 55 patients with *WT1* mutations achieved a CR compared to 698 (88.5%) of 789 patients without *WT1* mutations (P<0.001). Taken together, *WT1* mutations were significantly associated with low induction CR rates.

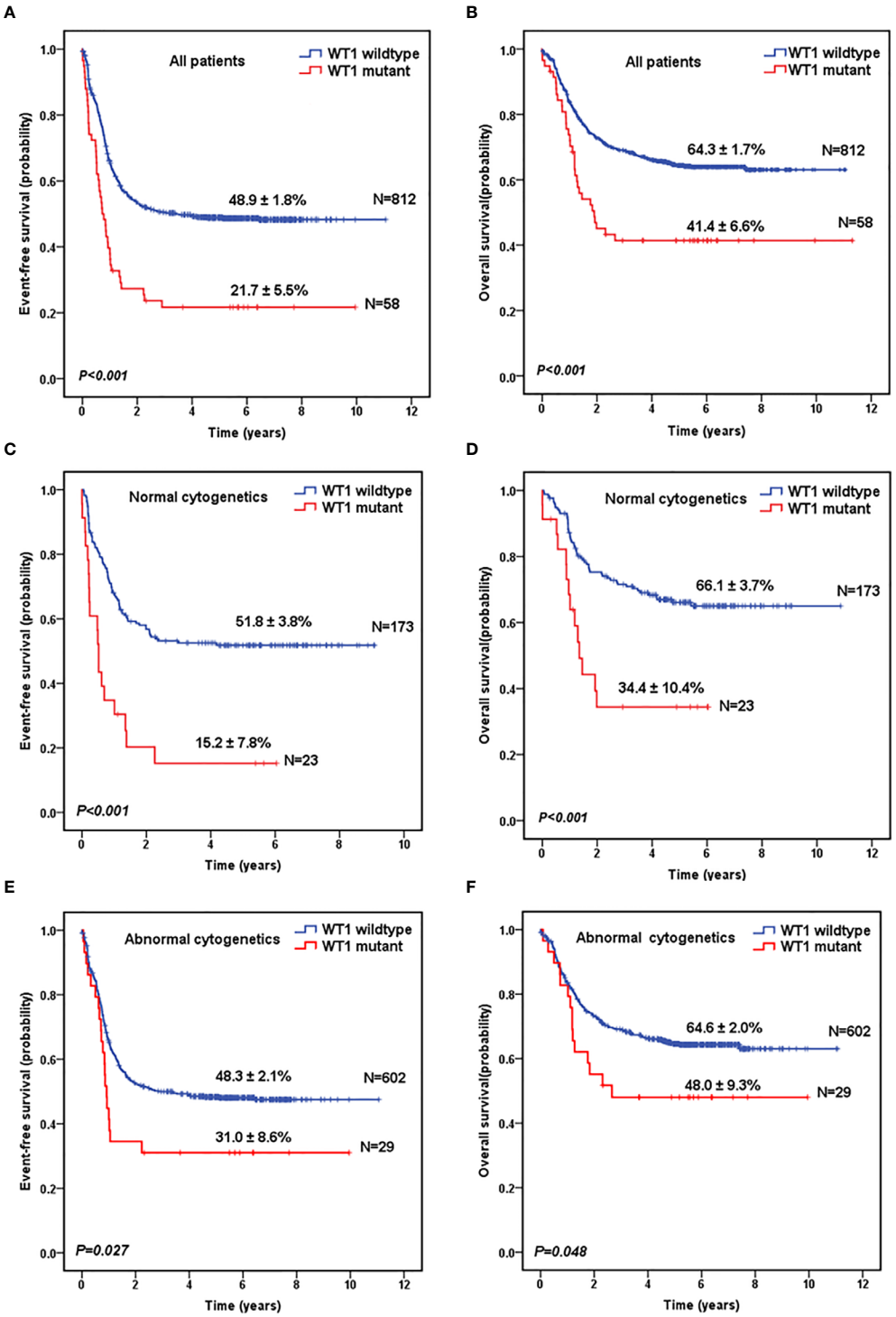

FIGURE 1 | Survival curves of pediatric AML patients with and without *WT1* mutations. Probability of EFS **(A)** and OS **(B)** for all patients with and without *WT1* mutations, respectively. Probability of EFS **(C)** and OS **(D)** for cytogenetically normal patients with and without *WT1* mutations, respectively. Probability of EFS **(E)** and OS **(F)** for cytogenetically abnormal patients with and without *WT1* mutations, respectively.

Next, we evaluated the survival data for all the 870 pediatric patients. The median follow-up time for the survivors was 5.6 years. As shown in **Figure 1A**, *WT1*-mutated patients had a significantly worse 5-year EFS (21.7 ± 5.5%) compared with *WT1* wild-type patients (48.9 ± 1.8%; *P*<0.001). Moreover, patients with *WT1* mutations had a worse 5-year OS (41.4 ± 6.6%) than those without *WT1* mutations (64.3 ± 1.7%; *P*<0.001) (**Figure 1B**). When analyses were restricted to patients having normal cytogenetics, there were significant differences in the outcome between patients with and without *WT1* mutations (**Figures 1C, D**) (5-year EFS: 15.2 ± 7.8% vs 51.8 ± 3.8%, *P*<0.001; 5-year OS: 34.4 ± 10.4% vs 66.1± 3.7%, *P*<0.001). In the subgroup of abnormal cytogenetics (**Figures 1E, F**), *WT1*-mutated patients also had a worse survival time compared with *WT1* wild-type patients in terms of 5-year EFS (31.0 ± 8.6% vs 48.3 ± 2.1%, *P*=0.027) and OS (48.0 ± 9.3% vs 64.6± 2.0%, *P*=0.048).

Prognostic Impact of *WT1* and *FLT3*/ITD Mutations

Survival data for patients with *FLT3*/ITD positive and negative were also explored. As shown in **Figure S1A**, *FLT3*/ITD positive was significantly associated with inferior EFS (5-year EFS=33.5± 4.0% vs 49.7± 1.9% for *FLT3*/ITD-negative; *P*<0.001). Moreover, the *FLT3*/ITD positive group had a worse 5-year OS (51.5 ± 4.3%) than the *FLT3*/ITD-negative group (65.0 ± 1.8%; *P*=0.003) (**Figure S1B**).

Given the overlap between *WT1* mutations and positive *FLT3*/ITD status, subset analysis was performed to assess the relative influence of *WT1* mutations and *FLT3*/ITD on the prognosis of children with AML (**Figures 2A, B**; **Table 2**). In the *FLT3*/ITD-positive subgroup, *WT1*-mutated patients had an extremely dismal prognosis (5-year EFS =12.5 ± 6.5% vs 38.4± 4.5% for *WT1* wild-type patients, HR: 2.179 [1.364-3.482], *P*=0.001; 5-year OS = 27.5± 8.8% vs 57.0 ± 4.7% for *WT*1 wild-type patients, HR: 2.225[1.305-3.796], *P*=0.003). When

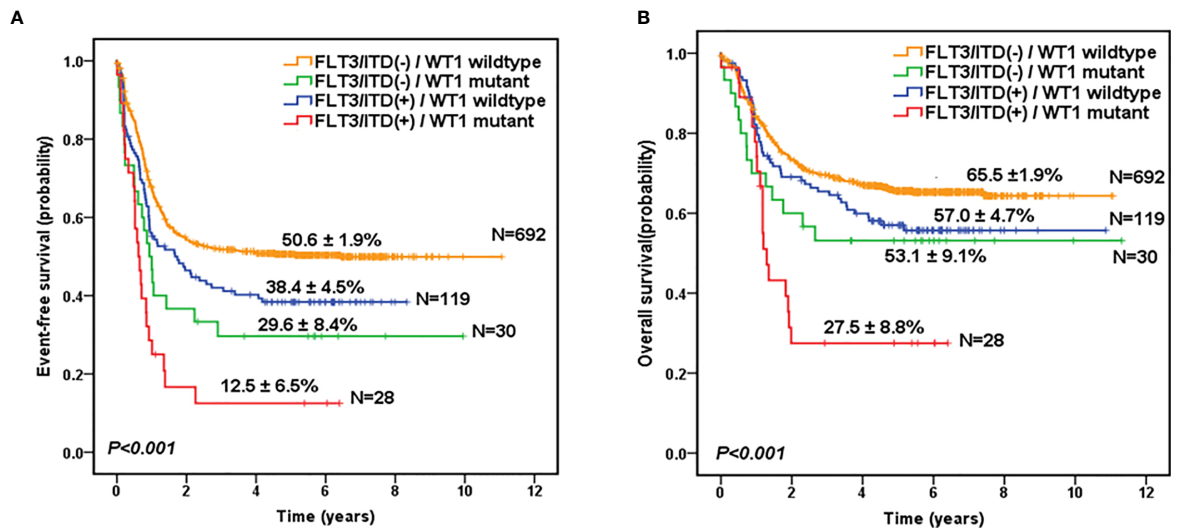

FIGURE 2 | Survival curves of all pediatric AML patients according to the combined *WT1* mutations and positive FLT3/ITD status. Probability of EFS **(A)** and OS **(B)** for patients according to the combined *WT1* mutations and positive *FLT3*/ITD status, respectively.

TABLE 2 | Statistical comparison of survival data according to both *WT1* and *FLT3*/ITD status.

Comparison	EFS hazard ratio (95% CI)	EFS *P*-value	OS hazard ratio (95% CI)	OS *P*-value
FLT3/ITD(-): *WT1* wildtype vs *WT1* mutant	1.861(1.197-2.892)	0.006	1.600(0.933-2.744)	0.088
FLT3/ITD(+): *WT1* wildtype vs *WT1* mutant	2.179(1.364-3.482)	0.001	2.225(1.305-3.796)	0.003
WT1 wildtype: *FLT3*/ITD(-)vs *FLT3*/ITD(+)	1.386(1.075-1.788)	0.012	1.305(0.961-1.771)	0.088
WT1 mutant: *FLT3*/ITD(-) vs *FLT3*/ITD(+)	1.605(0.886-2.906)	0.118	1.748(0.870-3.514)	0.117

CI, confidence interval; EFS, event-free survival; FLT3/ITD, internal tandem duplication of the FLT3 gene; OS, overall survival.

restricted to the *FLT3*/ITD-negative subgroup, *WT1* mutations had an adverse impact on 5-year EFS (HR: 1.861[1.197-2.892], *P*=0.006) instead of 5-year OS (HR: 1.600[0.933-2.744], *P*=0.088). Similarly, for the *WT1* wild-type patients, *FLT3*/ITD positive had reduced 5-year EFS (HR: 1.386[1.075-1.788], *P*=0.012) but not 5-year OS (HR: 1.305[0.961-1.771], *P*=0.088). However, *FLT3*/ITD mutations had no significantly negative influence on the outcome of *WT1*-mutated patients (EFS HR: 1.605[0.886-2.906], *P*=0.118; OS HR: 1.748[0.870-3.514], *P*=0.117).

Similar results were found in the subgroup of cytogenetically normal AML patients according to the combined *WT1* mutations and positive *FLT3*/ITD status (**Figure S2**). Of note, the survival curves showed that there were no significant differences between *WT1*-mutated patients with *FLT3*/ITD-positive (n=17) and *FLT3*/ITD negative (n=6), in terms of 5-year EFS (14.1 ± 9.0% vs 16.7 ± 15.2%; *P*=0.584) and OS (34.5 ± 12.3% vs 33.3 ± 19.2%; *P*=0.665).

The Effect of SCT in Patients With *WT1* Mutations

As shown in **Table 1**, there was no significant difference in the proportion of HSCT in *WT1*-mutated group and *WT1* wild-type group (15.6% vs 16.2%, *P*=0.906). The survival analysis, after HSCT stratification, showed that for *WT1*-mutated pediatric AML patients, HSCT conferred a favorable prognostic impact with a trend of better 5-year EFS (42.9 ± 18.7% vs 22.3 ± 7.0% for chemotherapy-only; *P*=0.316) and OS (57.1 ± 18.7% vs 43.6 ± 8.2% for chemotherapy-only; *P*=0.483) (**Figures 3A, B**).

To further evaluate the role of HSCT in the patients with co-occurring *WT1* and *FLT3*/ITD mutations, we explored the impact of HSCT on those patients. As shown in **Figures 3C, D**, for AML

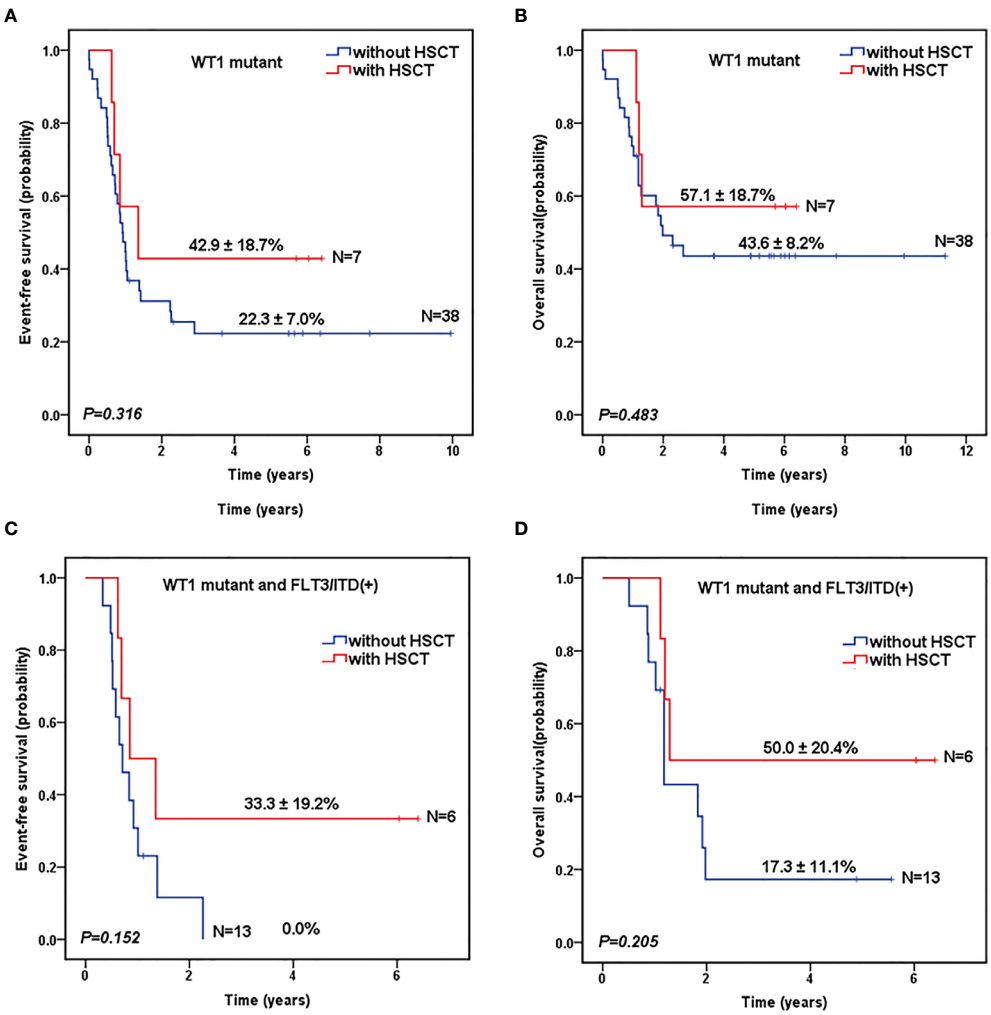

FIGURE 3 | Survival curves of pediatric AML patients according to *WT1* mutations and hematopoietic stem cell transplantation (HSCT) status. Probability of EFS **(A)** and OS **(B)** for patients with *WT1* mutations according to HSCT status, respectively. Probability of EFS **(C)** and OS **(D)** for patients with *WT1* mutations and *FLT3*/ITD positive according to HSCT status, respectively.

patients with both *WT1* mutations and positive *FLT3*/ITD, 5-year EFS (33.3 ± 19.2%) and OS (50.0 ± 20.4%) were higher in children with HSCT than those with chemotherapy-only (EFS: 0.0 ± 0.0%, *P*=0.152; OS: 17.3 ± 11.1%, *P*=0.205), respectively, although the differences between the two groups were not statistically significant.

Multivariate Analysis of Prognostic Factors

Cox regression analyses were then performed to evaluate *WT1* mutation status as a predictor of EFS and OS alongside other prognostic factors: age (utilizing 10 years of age as the cutoff value), white blood cell count at diagnosis (utilizing 50×10^{9}/L as the cutoff value), high risk, standard risk, and HSCT. We identified *WT1* mutations as an independent prognostic factor for both EFS and OS in pediatric patients with AML (**Table 3**). *WT1* mutations were significantly associated with inferior EFS (HR: 1.910, 95% CI: 1.297-2.812, *P*=0.001) and OS (HR: 1.709, 95% CI: 1.090-2.679, *P*=0.020). Additionally, age (older than 10 years), white blood cell count greater than 50×10^{9}/L at first diagnosis, high-risk and standard-risk were significantly related to poor EFS and OS, while HSCT was related to better survival prognosis (HR: 0.431, 95% CI: 0.313-0.593, *P*<0.001) and OS (HR: 0.594, 95% CI: 0.419-0.843, *P*=0.004).

DISCUSSION

The TARGET program is a collaborative COG-national cancer institute (NCI) project aiming to comprehensively characterize the mutational, transcriptional, and epigenetic landscapes of a large, well-annotated cohort of pediatric cancer (20). Using this large cohort of subjects, we were able to investigate the clinical implication of *WT1* mutations in pediatric AML. Our findings showed that the frequency of *WT1* mutations was 6.7% among these 870 pediatric AML patients. This result was similar to the adult AML studies. In a large cohort of adult AML study, the frequency of *WT1* mutations among 3157 patients was reported to be 5.5% (21). Next, we found that *WT1* mutations were significantly associated with FAB subtypes of M4, with high white blood cell counts at first diagnosis, normal cytogenetics, and *FLT3*/ITD mutations. However, no association was found between *WT1* mutations and *CEBPA* mutations. These results were different from some of the other studies. For instance, a report by Ho et al. (14) also found that *WT1* mutations were related to normal cytogenetics and *FLT3*/ITD mutations, but they found no correlation between *WT1* mutations and white blood cell counts or M4 subtype. A pediatric AML report by Hollink et al. (13) showed that *WT1* mutations clustered significantly in the subgroup with normal cytogenetics and were associated with *FLT3*/ITD and *CEBPA* mutations.

The prognostic impact of *WT1* mutations has not been clarified in pediatric AML. In our study, we found that patients with *WT1* mutations had lower CR induction rates, worse EFS and OS rates in comparison to patients without *WT1* mutations. Patients with both *WT1* and *FLT3*/ITD mutations had a dismal prognosis. The multivariate analysis showed that *WT1* mutations were an independent adverse impact factor. These results are consistent with findings by Hollink et al. (13), though they found the CR induction rates did not differ significantly between patients with *WT1*-mutated and *WT1* wild-type AML. A report from the French study group confirmed that *WT1* mutations were an independent prognostic factor for pediatric AML (22). However, a report from the Japanese study group showed that *WT1* mutations were related to a poor prognosis in patients with normal cytogenetics, excluding those with *FLT3*/ITD and those younger than 3 years (23). By contrast, a report from the Nordic Society of Pediatric Hematology and Oncology (NOPHO) revealed that no significant correlation with survival was seen for *WT1* mutations (24). Notably, they found that patients with *WT1* mutations but negative *FLT3*/ITD had a superior EFS compared with patients with *WT1* wildtype with or without concurrent *FLT3*/ITD (24). In adult studies, the presence of *WT1* mutation has been found to be associated with poor clinical outcomes of AML patients in some but not all studies. In the studies from Cancer and Leukemia Group B (9) and Hou et al. (10), *WT1* mutations were correlated with a poor prognosis in AML patients. However, in the study from the German-Austrian Study Group (11), *WT1* mutation as a single molecular marker did not seem to impact the patient outcomes. These conflicting results may be due to the differences in sample size, exon of *WT1* mutations, and variable treatment protocols across studies. It has been reported that the negative impact of *WT1* mutations may be overcome by the use of repetitive cycles of high-dose cytarabine, especially in the subgroup of patients with negative *FLT3*/ITD genotype (11).

The mechanism of *WT1* mutations in leukemogenesis remains elusive. Several different *WT1* mutations have been described in AML, which occur primarily in exons 1, 7, and 9. *WT1* mutations may result in the loss of DNA binding ability due to loss of the zinc-finger domain or result in loss of expression of the *WT1* protein altogether (25–27). *WT1* mutations fail to properly direct the ten-eleven translocation-2 to its target sites, either by disruption of the interaction itself or by failing to bind to DNA (28, 29). Recently, Pronier et al. (30)

TABLE 3 | Cox regression analysis of *WT1* mutations and other prognostic factors.

Outcome	Variable	Hazard ratio (95% CI)	P-value
EFS	*WT1*	1.910(1.297-2.812)	0.001
	High risk	3.136(2.235-4.400)	<0.001
	Standard risk	2.581(2.207-3.286)	<0.001
	HSCT	0.431(0.313-0.593)	<0.001
	Age > 10 years	1.300(1.053-1.607)	0.015
	WBC>50×10^{9}/L	1.499(1.220-1.841)	<0.001
OS	*WT1*	1.709(1.090-2.679)	0.02
	High risk	3.991(2.653-6.004)	<0.001
	Standard risk	3.413(2.494-4.670)	<0.001
	HSCT	0.594(0.419-0.843)	0.004
	Age > 10 years	1.496(1.158-1.933)	0.002
	WBC>50×10^{9}/L	1.307(1.018-1.677)	0.036

CI, confidence interval; EFS, event-free survival; HSCT, hematopoietic stem cell transplantation; OS, overall survival; WBC, white blood cell count.

have found that *WT1* heterozygous loss enhances stem cell self-renewal, *WT1* depletion cooperates with *FLT3*/ITD mutation to induce fully penetrant AML. Mutational analysis of a large cohort of AML cases revealed that *WT1* may play an important role in the epigenetic pathway (31, 32). Given the epigenetic alterations catalogued in *WT1* mutant, epigenetic-targeted therapy has been explored as a potential mechanism to deal with this subgroup of leukemia (33). Recently, Sinha et al. (34) have found that mutant *WT1* is associated with DNA hypermethylation of polycomb repressor complex 2 targets in AML, and inhibitor of enhancer of zeste homolog 2 (EZH2) may be helpful in this AML subtype.

Alternately, HSCT is one of the most effective treatments for AML. However, it is unknown whether *WT1*-mutated patients will benefit from HSCT. Our studies showed that compared to chemotherapy alone, HSCT tended to improve the prognoses of *WT1*-mutated patients, and for patients with both *WT1* and *FLT3*/ITD mutations as well. These results are in agreement with a previous pediatric AML report (14). Recently, Eisfeld et al. (12) have found that co-occurrence of *WT1* and *NPM1* mutations confers especially poor outcomes in a large cohort of 863 adult AML. They proposed that mutated *WT1* co-occurrence with mutated *NPM1* would be an adverse marker for risk stratification, indicating patients with both *WT1* and *NPM1* mutations might be considered for HSCT. However, since *NPM1* mutation is relatively rare in children, we could not draw a firm conclusion on this topic due to the small number of patients with both *WT1* and *NPM1* mutations. Thus, whether *WT1* mutation is an indication for HSCT in pediatric AML requires further investigation.

There were several limitations to our study. Firstly, since different *WT1* mutations may affect its functions on DNA binding or protein interaction differentially, the details of *WT1* mutants can be important to the clinical outcome of AML patients with these mutants. However, the information on the specific mutations of in *WT1* is not provided in the TARGET dataset, therefore, we can't perform further analysis. Secondly, though this is a large pediatric AML cohort study, the sample size is still relatively small in the subgroups of patients with *WT1* mutations. We cannot rule out the contribution of *FLT3*/ITD co-occurrence towards the prognosis. Thirdly, our findings showed that *WT1* mutations were associated with poor clinical outcomes, and *WT1*-mutated patients might benefit from HSCT. These results suggested that *WT1* mutations could be used as predictive factors and linked to a specific clinical management plan. However, due to the limitations associated with the TARGET dataset as mentioned above, and the retrospective analysis nature of our study, a large multicentric prospective future study could be of value to further address the prognostic significance of *WT1* mutations in AML.

In summary, we analyzed the clinical implication of *WT1* mutations in a large pediatric AML cohort. Our findings showed that *WT1* mutations are independent poor prognostic factors in pediatric AML. Patients with co-occurring *WT1* and *FLT3*/ITD mutations had a dismal prognosis. Moreover, HSCT might be an effective strategy for patients with *WT1* mutations. These results have important implications and might contribute to the refining risk stratification of pediatric AML.

DATA AVAILABILITY STATEMENT

The original contributions presented in the study are included in the article/**Supplementary Material**, further inquiries can be directed to the corresponding authors.

ETHICS STATEMENT

The studies involving human participants were reviewed and approved by TARGET Publications Committee. Written informed consent to participate in this study was provided by the participants' legal guardian/next of kin.

AUTHOR CONTRIBUTIONS

LC and L-HX participated in project design, data collection, analysis, interpretation and manuscript drafting. YW participated in data interpretation and manuscript drafting. W-JW participated in data collection and analysis. D-HZ and J-PF participated in project design, data interpretation and manuscript drafting. SM participated in manuscript editing. All authors contributed to the article and approved the submitted version.

FUNDING

This work was supported by the Natural Science Foundation of Guangdong Province, China (2018A030313680 to L-HX), Guangdong Basic and Applied Basic Research Foundation (2020A1515010312 to L-HX), Science and Technology Program of Guangzhou City, China (201803010032 to J-PF), Beijing Bethune Charitable Foundation (SCE111DS to J-PF), Xiu Research Fund (to LC).

ACKNOWLEDGMENTS

We would like to thank all study participants and the TARGET group for making these data publicly available.

SUPPLEMENTARY MATERIAL

The Supplementary Material for this article can be found online at: https://www.frontiersin.org/articles/10.3389/fonc.2021.632094/full#supplementary-material

REFERENCES

1. Creutzig U, van den Heuvel-Eibrink MM, Gibson B, Dworzak MN, Adachi S, de Bont E, et al. Diagnosis and management of acute myeloid leukemia in children and adolescents: recommendations from an international expert panel. *Blood* (2012) 120:3187–205. doi: 10.1182/blood-2012-03-362608
2. de Rooij JD, Zwaan CM, van den Heuvel-Eibrink M. Pediatric AML: From Biology to Clinical Management. *J Clin Med* (2015) 4:127–49. doi: 10.3390/jcm4010127
3. Conneely SE, Rau RE. The genomics of acute myeloid leukemia in children. *Cancer Metastasis Rev* (2020) 39:189–209. doi: 10.1007/s10555-020-09846-1
4. Scharnhorst V, van der Eb AJ, Jochemsen AG. WT1 proteins: functions in growth and differentiation. *Gene* (2001) 273:141–61. doi: 10.1016/s0378-1119(01)00593-5
5. Yang L, Han Y, Suarez Saiz F, Minden MD. A tumor suppressor and oncogene: the WT1 story. *Leukemia* (2007) 21:868–76. doi: 10.1038/sj.leu.2404624
6. Hohenstein P, Hastie ND. The many facets of the Wilms' tumour gene, WT1. *Hum Mol Genet* (2006) 15:R196–201. doi: 10.1093/hmg/ddl196
7. Hastie ND. Wilms' tumour 1 (WT1) in development, homeostasis and disease. *Development* (2017) 144:2862–72. doi: 10.1242/dev.153163
8. Owen C, Fitzgibbon J, Paschka P. The clinical relevance of Wilms Tumour 1 (WT1) gene mutations in acute leukaemia. *Hematol Oncol* (2010) 28:13–9. doi: 10.1002/hon.931
9. Paschka P, Marcucci G, Ruppert AS, Whitman SP, Mrozek K, Maharry K, et al. Wilms' tumor 1 gene mutations independently predict poor outcome in adults with cytogenetically normal acute myeloid leukemia: a cancer and leukemia group B study. *J Clin Oncol* (2008) 26:4595–602. doi: 10.1200/JCO.2007.15.2058
10. Hou HA, Huang TC, Lin LI, Liu CY, Chen CY, Chou WC, et al. WT1 mutation in 470 adult patients with acute myeloid leukemia: stability during disease evolution and implication of its incorporation into a survival scoring system. *Blood* (2010) 115:5222–31. doi: 10.1182/blood-2009-12-259390
11. Gaidzik VI, Schlenk RF, Moschny S, Becker A, Bullinger L, Corbacioglu A, et al. Prognostic impact of WT1 mutations in cytogenetically normal acute myeloid leukemia: a study of the German-Austrian AML Study Group. *Blood* (2009) 113:4505–11. doi: 10.1182/blood-2008-10-183392
12. Eisfeld AK, Kohlschmidt J, Mims A, Nicolet D, Walker CJ, Blachly JS, et al. Additional gene mutations may refine the 2017 European LeukemiaNet classification in adult patients with de novo acute myeloid leukemia aged <60 years. *Leukemia* (2020) 34:3215–27. doi: 10.1038/s41375-020-0872-3
13. Hollink IH, van den Heuvel-Eibrink MM, Zimmermann M, Balgobind BV, Arentsen-Peters ST, Alders M, et al. Clinical relevance of Wilms tumor 1 gene mutations in childhood acute myeloid leukemia. *Blood* (2009) 113:5951–60. doi: 10.1182/blood-2008-09-177949
14. Ho PA, Zeng R, Alonzo TA, Gerbing RB, Miller KL, Pollard JA, et al. Prevalence and prognostic implications of WT1 mutations in pediatric acute myeloid leukemia (AML): a report from the Children's Oncology Group. *Blood* (2010) 116:702–10. doi: 10.1182/blood-2010-02-268953
15. Niktoreh N, Walter C, Zimmermann M, von Neuhoff C, von Neuhoff N, Rasche M, et al. Mutated WT1, FLT3-ITD, and NUP98-NSD1 Fusion in Various Combinations Define a Poor Prognostic Group in Pediatric Acute Myeloid Leukemia. *J Oncol* (2019) 2019:1609128. doi: 10.1155/2019/1609128
16. Meshinchi S, Alonzo TA, Stirewalt DL, Zwaan M, Zimmerman M, Reinhardt D, et al. Clinical implications of FLT3 mutations in pediatric AML. *Blood* (2006) 108:3654–61. doi: 10.1182/blood-2006-03-009233
17. Brown P, McIntyre E, Rau R, Meshinchi S, Lacayo N, Dahl G, et al. The incidence and clinical significance of nucleophosmin mutations in childhood AML. *Blood* (2007) 110:979–85. doi: 10.1182/blood-2007-02-076604
18. Ho PA, Alonzo TA, Gerbing RB, Pollard J, Stirewalt DL, Hurwitz C, et al. Prevalence and prognostic implications of CEBPA mutations in pediatric acute myeloid leukemia (AML): a report from the Children's Oncology Group. *Blood* (2009) 113:6558–66. doi: 10.1182/blood-2008-10-184747
19. Vujkovic M, Attiyeh EF, Ries RE, Goodman EK, Ding Y, Kavcic M, et al. Genomic architecture and treatment outcome in pediatric acute myeloid leukemia: a Children's Oncology Group report. *Blood* (2017) 129:3051–8. doi: 10.1182/blood-2017-03-772384
20. Bolouri H, Farrar JE, Triche TJr, Ries RE, Lim EL, Alonzo TA, et al. The molecular landscape of pediatric acute myeloid leukemia reveals recurrent structural alterations and age-specific mutational interactions. *Nat Med* (2018) 24:103–12. doi: 10.1038/nm.4439
21. Krauth MT, Alpermann T, Bacher U, Eder C, Dicker F, Ulke M, et al. WT1 mutations are secondary events in AML, show varying frequencies and impact on prognosis between genetic subgroups. *Leukemia* (2015) 29:660–7. doi: 10.1038/leu.2014.243
22. Marceau-Renaut A, Duployez N, Ducourneau B, Labopin M, Petit A, Rousseau A, et al. Molecular Profiling Defines Distinct Prognostic Subgroups in Childhood AML: A Report From the French ELAM02 Study Group. *Hemasphere* (2018) 2:e31. doi: 10.1097/HS9.0000000000000031
23. Sano H, Shimada A, Tabuchi K, Taki T, Murata C, Park MJ, et al. WT1 mutation in pediatric patients with acute myeloid leukemia: a report from the Japanese Childhood AML Cooperative Study Group. *Int J Hematol* (2013) 98(4):437–45. doi: 10.1007/s12185-013-1409-6
24. Staffas A, Kanduri M, Hovland R, Rosenquist R, Ommen HB, Abrahamsson J, et al. Presence of FLT3-ITD and high BAALC expression are independent prognostic markers in childhood acute myeloid leukemia. *Blood* (2011) 118:5905–13. doi: 10.1182/blood-2011-05-353185
25. King-Underwood L, Renshaw J, Pritchard-Jones K. Mutations in the Wilms' tumor gene WT1 in leukemias. *Blood* (1996) 87:2171–9. doi: 10.1182/blood.V87.6.2171.bloodjournal8762171
26. Chen Z. The possible role and application of WT1 in human leukemia. *Int J Hematol* (2001) 73:39–46. doi: 10.1007/BF02981901
27. Bielinska E, Matiakowska K, Haus O. Heterogeneity of human WT1 gene. *Postepy Hig Med Dosw (Online)* (2017) 71:595–601. doi: 10.5604/01.3001.0010.3840
28. Wang Y, Xiao M, Chen X, Chen L, Xu Y, Lv L, et al. WT1 recruits TET2 to regulate its target gene expression and suppress leukemia cell proliferation. *Mol Cell* (2015) 57:662–73. doi: 10.1016/j.molcel.2014.12.023
29. Rampal R, Figueroa ME. Wilms tumor 1 mutations in the pathogenesis of acute myeloid leukemia. *Haematologica* (2016) 101:672–9. doi: 10.3324/haematol.2015.141796
30. Pronier E, Bowman RL, Ahn J, Glass J, Kandoth C, Merlinsky TR, et al. Genetic and epigenetic evolution as a contributor to WT1-mutant leukemogenesis. *Blood* (2018) 132:1265–78. doi: 10.1182/blood-2018-03-837468
31. Patel JP, Gonen M, Figueroa ME, Fernandez H, Sun Z, Racevskis J, et al. Prognostic relevance of integrated genetic profiling in acute myeloid leukemia. *N Engl J Med* (2012) 366:1079–89. doi: 10.1056/NEJMoa1112304
32. Fernandez HF, Sun Z, Yao X, Litzow MR, Luger SM, Paietta EM, et al. Anthracycline dose intensification in acute myeloid leukemia. *N Engl J Med* (2009) 361:1249–59. doi: 10.1056/NEJMoa0904544
33. Panuzzo C, Signorino E, Calabrese C, Ali MS, Petiti J, Bracco E, et al. Landscape of Tumor Suppressor Mutations in Acute Myeloid Leukemia. *J Clin Med* (2020) 9(3):802. doi: 10.3390/jcm9030802
34. Sinha S, Thomas D, Yu L, Gentles AJ, Jung N, Corces-Zimmerman MR, et al. Mutant WT1 is associated with DNA hypermethylation of PRC2 targets in AML and responds to EZH2 inhibition. *Blood* (2015) 125:316–26. doi: 10.1182/blood-2014-03-566018

Conflict of Interest: The authors declare that the research was conducted in the absence of any commercial or financial relationships that could be construed as a potential conflict of interest.

frontiers in Oncology

PERSPECTIVE
published: 25 May 2021
doi: 10.3389/fonc.2021.663221

Low miR-214-5p Expression Correlates With Aggressive Subtypes of Pediatric ALCL With Non-Common Histology

Piero Di Battista[1,2†], Federica Lovisa[1,2†], Enrico Gaffo[3], Ilaria Gallingani[1,2], Carlotta C. Damanti[1,2], Anna Garbin[1,2], Lavinia Ferrone[1,2], Elisa Carraro[1], Marta Pillon[1], Luca Lo Nigro[4], Rossella Mura[5], Marco Pizzi[6], Vincenza Guzzardo[6], Angelo Paolo Dei Tos[6], Alessandra Biffi[1,2], Stefania Bortoluzzi[3,7‡] and Lara Mussolin[1,2‡]*

[1] Division of Pediatric Hematology, Oncology and Stem Cell Transplant, Maternal and Child Health Department, University of Padova, Padova, Italy, [2] Istituto di Ricerca Pediatrica Città della Speranza, Padova, Italy, [3] Department of Molecular Medicine, University of Padova, Padova, Italy, [4] Center of Pediatric Hematology Oncology, Azienda Policlinico G. Rodolico – San Marco, Catania, Italy, [5] Department of Paediatric Haematology-Oncology, Ospedale Pediatrico Microcitemico, Cagliari, Italy, [6] Surgical Pathology and Cytopathology Unit, Department of Medicine - DIMED, University of Padova, Padova, Italy, [7] CRIBI Interdepartmental Research Center for Innovative Biotechnologies (CRIBI), University of Padova, Padova, Italy

The unsatisfactory cure rate of relapsing ALK-positive Anaplastic Large-Cell Lymphoma (ALCL) of childhood calls for the identification of new prognostic markers. Here, the small RNA landscape of pediatric ALK-positive ALCL was defined by RNA sequencing. Overall, 121 miRNAs were significantly dysregulated in ALCL compared to non-neoplastic lymph nodes. The most up-regulated miRNA was miR-21-5p, whereas miR-19a-3p and miR-214-5p were reduced in ALCL. Characterization of miRNA expression in cases that relapsed after first line therapy disclosed a significant association between miR-214-5p down-regulation and aggressive non-common histology. Our results suggest that miR-214-5p level may help to refine the prognostic stratification of pediatric ALK-positive ALCL.

Keywords: ALCL, childhood, miRNA, prognosis, biomarker, RNA-seq

OPEN ACCESS

Edited by:
Alejandro Gru, University of Virginia Health System, United States

Reviewed by:
Roberto Chiarle, University of Turin, Italy
Pier Paolo Piccaluga, University of Bologna, Italy

***Correspondence:**
Lara Mussolin
lara.mussolin@unipd.it

†These authors have contributed equally to this work

‡These authors share last authorship

Specialty section:
This article was submitted to Hematologic Malignancies, a section of the journal Frontiers in Oncology

Received: *02 February 2021*
Accepted: *30 April 2021*
Published: *25 May 2021*

Citation:
Di Battista P, Lovisa F, Gaffo E, Gallingani I, Damanti CC, Garbin A, Ferrone L, Carraro E, Pillon M, Lo Nigro L, Mura R, Pizzi M, Guzzardo V, Dei Tos AP, Biffi A, Bortoluzzi S and Mussolin L (2021) Low miR-214-5p Expression Correlates With Aggressive Subtypes of Pediatric ALCL With Non-Common Histology. Front. Oncol. 11:663221. doi: 10.3389/fonc.2021.663221

INTRODUCTION

Anaplastic Large-Cell Lymphoma (ALCL) accounts for 10-15% of pediatric and adolescent non-Hodgkin lymphomas. Most pediatric ALCL cases carry ALK gene fusions (ALK-positive ALCL) that constitutively activate RAS-ERK, JAK3-STAT3 and PI3K–Akt oncogenic signaling pathways, thus promoting cancer cell proliferation, differentiation, and survival (1). In pediatric ALK-positive ALCL, the current treatment regimens achieve a progression-free survival of ~70% at 10 years from diagnosis (2). The prognosis of patients with resistant or relapsing disease is still relatively poor (3), calling for an increased understanding of ALCL aggressiveness and for the development of new prognostic markers for the early identification of patients with higher risk of treatment failure, who could benefit from more intensive chemotherapy regimens. Minimal Disseminated Disease (MDD),

measured by PCR detection of NPM-ALK, and low anti-ALK antibody titer at diagnosis are significantly associated with inferior outcome (2). Recently, a large multicentric study confirmed that non-common (NC) histological patterns (e.g. small cell or lympho-histiocytic ALK-positive ALCL) are key relapse risk factors, either considered alone or in combination with MDD (2). Previous studies suggested an important role of microRNAs (miRNAs) in adult onset ALCL, and compared the ALK-positive and ALK-negative phenotypes, identifying miR-17~92 cluster up-regulation in ALK-positive ALCL and miR-155 overexpression in ALK-negative cases (4). For the first time, this study associates the risk of relapse in pediatric ALCL with miRNA signatures and identifies miRNA expression patterns specifically related to high risk NC histotypes.

THE SMALL RNA LANDSCAPE OF PEDIATRIC ALCL SHOWS DYSREGULATION OF SEVERAL MIRNAS

Small RNA (sRNA) sequencing (**Supplementary Methods**) was performed on a set of 20 pediatric ALK-positive ALCL cases. Six reactive lymph node (RLN) biopsies were also analyzed as controls. An extended cohort of 58 ALCL cases and 10 RLN, including 39 independent ALCL cases and 4 RLN, was used to validate the differential expression of selected miRNAs (**Supplementary Table 1**). All patients were treated according to the ALCL-99 protocol (2). The study was approved by the local institutional ethical committee and informed consent was obtained from the patients' legal guardians. The sRNA-seq data were analyzed with miR&moRe2 v0.2.3 (5) and DESeq2 to test for differential expression between ALCL and RLN samples (**Supplementary Methods**). Of the 1,013 miRNA-derived sRNAs detected, 449 miRNAs and 24 miRNA-offset RNAs (moRNAs) expressed in all samples of at least one group were compared. Only 51 miRNAs (5% of the detected) accounted for 95% of the observed sRNA expression (**Supplementary Figure 1B**). MiR-21-5p, miR-148a-3p and let-7i-5p were amongst the top expressed miRNAs in ALCL.

Interestingly, ALCL and RLN had different sRNA expression profiles (**Figure 1**) and 121 miRNAs resulted significantly deregulated (q-value ≤ 0.01) in ALCL (**Supplementary Table 2**). **Figure 1** shows the 60 most dysregulated (q-value ≤ 0.01 and absolute fold change ≥ 2) miRNAs, of which 37 were up-regulated and 23 were down-regulated in ALCL. Dysregulation of some of these miRNAs was previously described in adult ALCL primary tumors or cell lines (4), whereas most have not been reported before. In line with our results, miR-135b-5p is up-regulated in ALK-positive ALCL tumor biopsies compared to RLN (6) and miR-142-5p, miR-142-3p and miR-29a-3p are down-regulated compared to peripheral T cells of healthy donors (7). Quantification by qRT-PCR in the extended cohort confirmed the significant up-regulation of miR-21-5p (Mann Whitney, p-value = 0.0005; **Figure 1**), and the decreased expression of miR-19a-3p (p-value = 0.0001; **Figure 1**) and miR-214-5p (p-value = 0.02; **Figure 1**) in ALCL compared to RLN.

MiR-21-5p is a known oncomiR up-regulated in aggressive activated B cell-type diffuse large B-cell lymphomas compared to germinal center B cell-type cases (8). Previous data indicated that miR-21-5p is more expressed in ALCL than in the less mature T-cell acute lymphoblastic leukemia cell lines (9), raising the hypothesis that the up-regulation of miR-21-5p could reflect an activated T-cell phenotype of tumor cells. We examined also activated T-cells from healthy donors (**Supplementary Figure 2**), an alternative normal counterpart and putative cell-of-origin of ALCL. Quantification in activated T-cells confirmed the significant upregulation of miR-21-5p in ALCL (Mann Whitney, p-value = 0.02; **Supplementary Figure 3A**). From a pathobiological perspective, this evidence further corroborated our finding about the ectopic expression of this oncomiR in ALCL, whose role in the malignant transformation warrants further investigation.

Next, miR-19a-3p significantly downregulated in ALCL compared to RLN (**Figure 1**) was demonstrated to be significantly reduced also in comparison to activated T-cells (Mann Whitney, p-value = 0.047; **Supplementary Figure 3B**), suggesting that miR-19a-3p could play a tumor suppressor role in ALCL, in line with recent data in invasive breast cancer (10).

MIR-214-5P IS DOWN-REGULATED IN ALK-POSITIVE ALCL WITH NC HISTOLOGY AND HIGH RISK OF RELAPSE

To explore the usefulness of miRNAs in disease risk stratification, miRNA expression was assessed at diagnosis in patients that underwent relapse after first line therapy. Compared to non-relapsed (NR) cases, relapsing (REL) ALK-positive ALCL samples were characterized by the down-regulation of 26 miRNAs (**Figure 2**). These included miR-10b, miR-126-3p, miR-199a-5p, and miR-26b-5p within the most expressed in ALCL. Of note, miR-214-5p (**Figure 2**), miR-615-3p, miR-126-3p and miR-19a-3p (**Supplementary Figure 4**), which are down-regulated in ALCL, resulted significantly less expressed also in REL compared to NR patients. Since the NC histology is associated with a worse prognosis (2), we examined miR-214-5p expression in patients of the extended cohort. Compared to common type ALCL (CM), cases with NC histology disclosed significantly lower expression of miR-214-5p (Mann Whitney, p-value = 0.046; **Figure 2**). This observation was confirmed by *in situ* hybridization for miR-214-5p on representative tissue sections from ALCL cases with CM (n = 6) and NC (n = 6; 4 lympho-histiocytic and 2 small cell) histology. High positivity for miR-214-5p was observed for 5/6 CM ALCL and in none of the 6 NC variants (p-value = 0.02; **Figure 2D** and **Supplementary Table 3**). The association between miR-214-5p down-regulation and NC histology is of particular interest since NC histological patterns are currently not considered among the factors for risk-based treatment stratification. Estimating miR-214-5p expression level by qRT-PCR and miRNA *in situ* hybridization (11) could prove useful to complement the standard histopathological evaluation of pediatric ALK-positive ALCL at diagnosis.

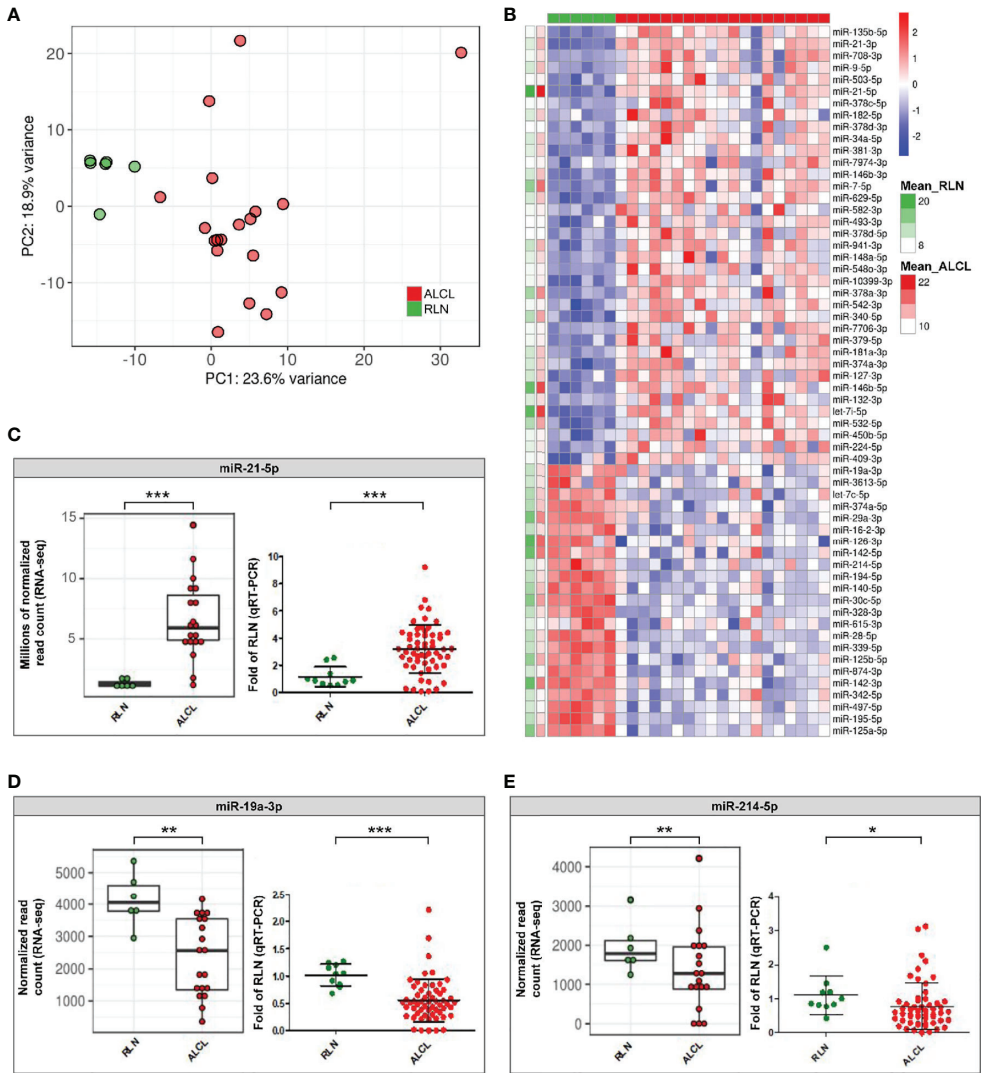

FIGURE 1 | Differentially expressed sRNAs in primary tumours of ALCL patients compared to reactive lymph nodes (RLN). **(A)** Unsupervised principal component analysis of sRNA expression profiles in ALCL (red dots) and RLN (green dots) samples. **(B)** Heatmap of the 60 miRNAs most dysregulated in ALCL compared with RLN (q-value ≤ 0.01 and absolute log2 Fold Change (LFC) ≥ 1; standardized expression; the two columns on the left indicate the mean expression in ALCL and RLN samples, for each miRNA); **(C–E)** Expression of miR-21-5p, miR-19a-3p and miR-214-5p determined by RNA-seq in the discovery cohort (left panel; ** and *** q-value < 0.01 and < 0.001) and validated by qRT-PCR in the extended cohort (right panel; * and ***, p-value < 0.05 and < 0.001; Mann-Whitney).

DISCUSSION

Low miR-214-5p expression is associated with poor prognosis in other solid tumors (12, 13), whereas high miR-214-5p expression with good outcome in diffuse large B-cell lymphoma (14). Beyond its prognostic value, the biological implications of miR-214-5p deregulation in ALK-positive ALCL with NC histology are poorly characterized and deserve further investigation. MiR-214-5p down-regulation can play a key role in ALCL lymphomagenesis, since it may lead to the de-repression of several oncogenic targets, thus driving increased cell proliferation and tumor cell migration (12, 13, 15). This is in line with previous studies in other malignancies, whereby the impairment of miR-214-5p by competitor endogen RNAs (e.g. DANCR, LINC00963 and circ-XPR1) promotes cancer cell proliferation and metastasis (12, 13, 15). These observations may be even more valid for ALK-positive ALCL, since miR-214-5p physiologically blocks key pathways for ALCL proliferation, migration and invasion. Indeed, miR-214-5p dampens Notch pathway activation by repressing the JAG1 Notch ligand (16). Notch signaling is of key importance for ALK-positive ALCL pathobiology, being constitutively activated by the NPM-ALK fusion gene through STAT3 (17). In summary, this study provides an unprecedented view of the miRNAome in pediatric ALK-positive ALCL highlighting the up-regulation of miR-21-5p, and the down-regulation of miR-19a-3p and miR-214-5p. Our results also highlight miRNAs that are particularly

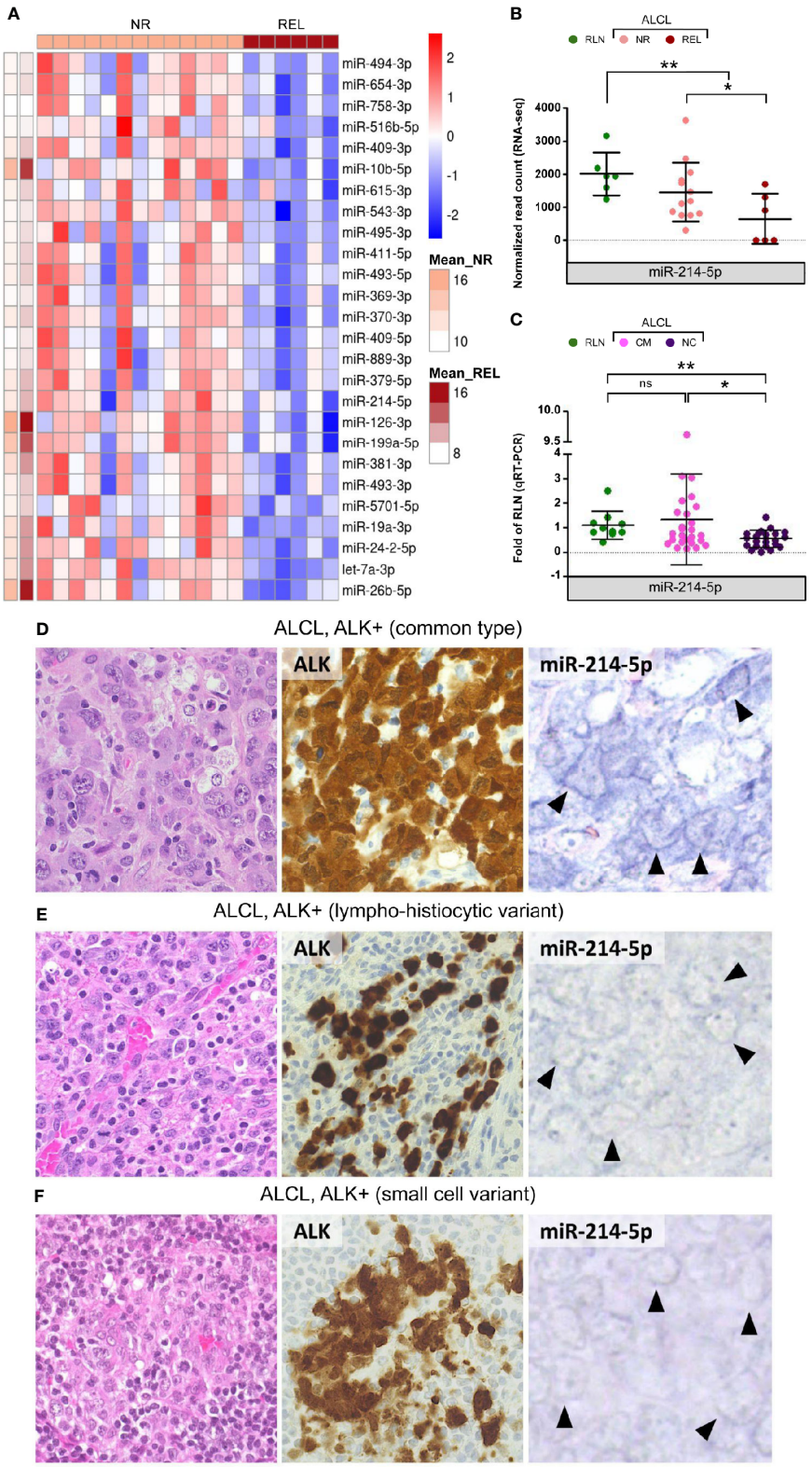

FIGURE 2 | Continued

FIGURE 2 | Differentially expressed miRNAs among relapsed and non-relapsed ALCL cases. MiR-214-5p expression is significantly reduced in ALCL of non-common histological subtypes compared to common histology. **(A)** The 26 significantly down-regulated miRNAs in relapsed (REL) compared to non-relapsed (NR) ALCL cases of the discovery cohort (Mean_REL and Mean_NR average expression (normalized read count) in REL and NR patients, respectively); **(B)** MiR-214-5p expression is significantly lower in REL compared with NR samples and in ALCL patients of the discovery cohort with respect to reactive lymph nodes (RLN), according to sRNA-seq (* and ** q-value < 0.05 and < 0.01, respectively). **(C)** MiR-214-5p expression quantification by qRT-PCR in the extended cohort of ALCL patients with common (CM) and non-common (NC) histology and in RLN from healthy donors (data relative to RLN; * and ** p-value < 0.05 and 0.01, respectively; Mann Whitney, ns, not significant). **(D)** CM ALK + ALCL (n = 6), histologically characterized by sheets of large, atypical cells with sternbergoid features, include neoplastic elements strongly and diffusely positive for ALK1 (cytoplasmic and nuclear expression), with moderate to strong positivity for miR-214-5p by *in situ* hybridization (5/6 tested cases; positive signal: blue staining in tumor cell cytoplasm - *arrowheads*). ALK+ ALCL lympho-histiocytic **(E)** and small cell **(F)** NC variants (n = 6) are instead characterized by weak to absent cytoplasmic signal for miR-214-5p (faint blue signal – *arrowheads*) (H&E and peroxidase stain; original magnification, x 40).

down-regulated in high-risk cases. Of importance, the uncovered link between miR-214-5p down-regulation and ALCL with NC histology and unfavorable prognosis suggests the use of selected miRNAs as novel biomarkers to complement the standard prognostic stratification of pediatric ALK-positive ALCL at diagnosis.

DATA AVAILABILITY STATEMENT

The datasets presented in this study can be found in online repositories. The names of the repository/repositories and accession number(s) can be found below: Gene Expression Omnibus, accession number GSE171323.

ETHICS STATEMENT

The studies involving human participants were reviewed and approved by the ethics committee for clinical experimentation of the Padova hospital CESC (Comitato Etico per la Sperimentazione Clinica Azienda Ospedaliera di Padova). Written informed consent to participate in this study was provided by the participants' legal guardian/next of kin.

AUTHOR CONTRIBUTIONS

PB, FL, SB and LM conceived the study. FL, IG, AG and CD selected and processed clinical samples and obtained sequencing data. AG and LF processed buffy coats from healthy donors and performed T-cell activation. PB and SB contributed bioinformatics methods and data analysis. PB and IG performed miRNAs quantification by qRT-PCR. EC and MPil collected clinical data and revised the manuscript. MPiz and VG collected histological samples, performed in situ hybridization analysis. LN, RM, AD and AB provided patients clinical care. PB, FL, AG, SB, EG and LM wrote the manuscript. PB, FL, AG and MPiz made the figures. LM supervised the experimental work. All authors contributed to the article and approved the submitted version.

FUNDING

This work has been supported by Associazione Italiana per la Ricerca sul Cancro, Milano, Italy (Investigator Grant – IG 2018 #21385 to LM and IG 2017 #20052 to SB); Fondazione Città della Speranza (grant 19/03 to LM); Fondazione CARIPARO, Padova, Italy (grant 17/03 to LM); Italian Ministry of Education, Universities and Research (PRIN 2017 #2017PPS2X4_003 to SB); Fondazione Roche per la Ricerca, Rome, Italy (grant to FL) and Fondazione Umberto Veronesi, Milano, Italy (fellowship to EG).

ACKNOWLEDGMENTS

The authors would like to thank all the AIEOP centers for clinical samples and data collection and Elisa Tosato for technical assistance.

SUPPLEMENTARY MATERIAL

The Supplementary Material for this article can be found online at: https://www.frontiersin.org/articles/10.3389/fonc.2021.663221/full#supplementary-material

REFERENCES

1. Turner SD, Lamant L, Kenner L, Brugières L. Anaplastic Large Cell Lymphoma in Paediatric and Young Adult Patients. *Br J Haematol* (2016) 173:560–72. doi: 10.1111/bjh.13958
2. Mussolin L, Le Deley M-C, Carraro E, Damm-Welk C, Attarbaschi A, Williams D, et al. Prognostic Factors in Childhood Anaplastic Large Cell Lymphoma: Long Term Results of the International Alcl99 Trial. *Cancers (Basel)* (2020) 12:2747. doi: 10.3390/cancers12102747
3. Woessmann W, Zimmermann M, Lenhard M, Burkhardt B, Rossig C, Kremens B, et al. Relapsed or Refractory Anaplastic Large-Cell Lymphoma in Children and Adolescents After Berlin-Frankfurt-Muenster (Bfm)–Type First-Line Therapy: A Bfm-Group Study. *JCO* (2011) 29:3065–71. doi: 10.1200/JCO.2011.34.8417
4. Hoareau-Aveilla C, Meggetto F. Crosstalk Between microRNA and DNA Methylation Offers Potential Biomarkers and Targeted Therapies in ALK-Positive Lymphomas. *Cancers (Basel)* (2017) 9:100. doi: 10.3390/cancers9080100
5. Gaffo E, Bortolomeazzi M, Bisognin A, Di Battista P, Lovisa F, Mussolin L, et al. Mir&More2: A Bioinformatics Tool to Characterize microRNAs and Microrna-Offset Rnas From Small Rna-Seq Data. *Int J Mol Sci* (2020) 21:1754. doi: 10.3390/ijms21051754

6. Matsuyama H, Suzuki HI, Nishimori H, Noguchi M, Yao T, Komatsu N, et al. Mir-135b Mediates NPM-ALK–Driven Oncogenicity and Renders IL-17–Producing Immunophenotype to Anaplastic Large Cell Lymphoma. *Blood* (2011) 118:6881–92. doi: 10.1182/blood-2011-05-354654
7. Merkel O, Hamacher F, Laimer D, Sifft E, Trajanoski Z, Scheideler M, et al. Identification of Differential and Functionally Active miRNAs in Both Anaplastic Lymphoma Kinase (ALK)+ and ALK– Anaplastic Large-Cell Lymphoma. *PNAS* (2010) 107:16228–33. doi: 10.1073/pnas.1009719107
8. Lawrie CH, Soneji S, Marafioti T, Cooper CDO, Palazzo S, Paterson JC, et al. Microrna Expression Distinguishes Between Germinal Center B Cell-Like and Activated B Cell-Like Subtypes of Diffuse Large B Cell Lymphoma. *Int J Cancer* (2007) 121:1156–61. doi: 10.1002/ijc.22800
9. Lawrie CH, Saunders NJ, Soneji S, Palazzo S, Dunlop HM, Cooper CDO, et al. Microrna Expression in Lymphocyte Development and Malignancy. *Leukemia* (2008) 22:1440–6. doi: 10.1038/sj.leu.2405083
10. Jurkovicova D, Smolkova B, Magyerkova M, Sestakova Z, Kajabova VH, Kulcsar L, et al. Down-Regulation of Traditional oncomiRs in Plasma of Breast Cancer Patients. *Oncotarget* (2017) 8:77369–84. doi: 10.18632/oncotarget.20484
11. Babapoor S, Horwich M, Wu R, Levinson S, Gandhi M, Makkar H, et al. microRNA in Situ Hybridization for Mir-211 Detection as an Ancillary Test in Melanoma Diagnosis. *Modern Pathol* (2016) 29:461–75. doi: 10.1038/modpathol.2016.44
12. Mao X, Guo S, Gao L, Li G. Circ-XPR1 Promotes Osteosarcoma Proliferation Through Regulating the miR-214-5p/DDX5 Axis. *Hum Cell* (2021) 34:122–31. doi: 10.1007/s13577-020-00412-z
13. Liu HF, Zhen Q, Fan YK. Linc00963 Predicts Poor Prognosis and Promotes Esophageal Cancer Cells Invasion Via Targeting miR-214-5p/RAB14 Axis. *Eur Rev Med Pharmacol Sci* (2020) 24:164–73. doi: 10.26355/eurrev_202001_19907
14. Lim EL, Trinh DL, Scott DW, Chu A, Krzywinski M, Zhao Y, et al. Comprehensive Mirna Sequence Analysis Reveals Survival Differences in Diffuse Large B-cell Lymphoma Patients. *Genome Biol* (2015) 16:18. doi: 10.1186/s13059-014-0568-y
15. Yao Z, Chen Q, Ni Z, Zhou L, Wang Y, Yang Y, et al. Long Non-Coding Rna Differentiation Antagonizing Nonprotein Coding RNA (Dancr) Promotes Proliferation and Invasion of Pancreatic Cancer by Sponging miR-214-5p to Regulate E2f2 Expression. *Med Sci Monit* (2019) 25:4544–52. doi: 10.12659/MSM.916960
16. Bellon M, Moles R, Chaib-Mezrag H, Pancewicz J, Nicot C. Jag1 Overexpression Contributes to Notch1 Signaling and the Migration of HTLV-1-transformed Atl Cells. *J Hematol Oncol* (2018) 11:119. doi: 10.1186/s13045-018-0665-6
17. Larose H, Prokoph N, Matthews JD, Schlederer M, Högler S, Alsulami AF, et al. Whole Exome Sequencing Reveals Notch1 Mutations in Anaplastic Large Cell Lymphoma and Points to Notch Both as a Key Pathway and a Potential Therapeutic Target. *Haematologica* (2020). doi: 10.3324/haematol.2019.238766

Conflict of Interest: The authors declare that the research was conducted in the absence of any commercial or financial relationships that could be construed as a potential conflict of interest.

frontiers in Oncology

ORIGINAL RESEARCH
published: 06 July 2021
doi: 10.3389/fonc.2021.682859

HNRNPH1 Is a Novel Regulator Of Cellular Proliferation and Disease Progression in Chronic Myeloid Leukemia

Menghan Liu, Lin Yang, Xiaojun Liu, Ziyuan Nie, Xiaoyan Zhang, Yaqiong Lu, Yuxia Pan, Xingzhe Wang and Jianmin Luo *

Department of Hematology, The Second Hospital of Hebei Medical University, Key Laboratory of Hematology, Shijiazhuang, China

RNA binding proteins act as essential modulators in cancers by regulating biological cellular processes. Heterogeneous nuclear ribonucleoprotein H1 (HNRNPH1), as a key member of the heterogeneous nuclear ribonucleoproteins family, is frequently upregulated in multiple cancer cells and involved in tumorigenesis. However, the function of HNRNPH1 in chronic myeloid leukemia (CML) remains unclear. In the present study, we revealed that HNRNPH1 expression level was upregulated in CML patients and cell lines. Moreover, the higher level of HNRNPH1 was correlated with disease progression of CML. *In vivo* and *in vitro* experiments showed that knockdown of HNRNPH1 inhibited cell proliferation and promoted cell apoptosis in CML cells. Importantly, knockdown of HNRNPH1 in CML cells enhanced sensitivity to imatinib. Mechanically, HNRNPH1 could bind to the mRNA of PTPN6 and negatively regulated its expression. PTPN6 mediated the regulation between HNRNPH1 and PI3K/AKT activation. Furthermore, the HNRNPH1–PTPN6–PI3K/AKT axis played a critical role in CML tumorigenesis and development. The present study first investigated the deregulated HNRNPH1–PTPN6–PI3K/AKT axis moderated cell growth and apoptosis in CML cells, whereby targeting this pathway may be a therapeutic CML treatment.

Keywords: CML, HNRNPH1, PTPN6, PI3K/AKT, proliferation, apoptosis

OPEN ACCESS

Edited by:
Mina Luqing Xu,
Yale University, United States

Reviewed by:
Guru Prasad Maiti,
Oklahoma Medical Research Foundation, United States
Ka Chun Cheung,
University of Adelaide, Australia

***Correspondence:**
Jianmin Luo
luojianmin1960@126.com

Specialty section:
This article was submitted to Hematologic Malignancies, a section of the journal Frontiers in Oncology

Received: *19 March 2021*
Accepted: *17 June 2021*
Published: *06 July 2021*

Citation:
Liu M, Yang L, Liu X, Nie Z, Zhang X, Lu Y, Pan Y, Wang X and Luo J (2021) HNRNPH1 Is a Novel Regulator Of Cellular Proliferation and Disease Progression in Chronic Myeloid Leukemia. Front. Oncol. 11:682859. doi: 10.3389/fonc.2021.682859

INTRODUCTION

Chronic myeloid leukemia is a malignant polyclonal disease originating from hematopoietic stem cells characterized by the Ph chromosome, which is the ectopic of t (1, 2) (q34; q11). The formation of the BCR–ABL fusion gene encodes P210 protein with constitutive tyrosine kinase activity involved in proliferation, apoptosis, and other biological functions of CML cells (3). Although the tyrosine kinase inhibitors (TKIs) chemotherapy induces a high clinical response rate in the majority

Abbreviations: CML, chronic myeloid leukemia; RBP, RNA binding protein; HNRNPH1, Heterogeneous nuclear ribonucleoprotein H1; TKI, tyrosine kinase inhibitors; AML, acute myeloid leukemia; BM-MNCs, Bone marrow mononuclear cells; NC, normal control; FBS, Fetal bovine serum; RIP, RNA immunoprecipitation; qRT-PCR, quantitative real-time reverse transcriptase-polymerase chain reaction.

of CML patients, some of them still suffered from disease progression which means poor prognosis and shorter overall survival (4, 5). While the BCR–ABL fusion gene plays an important role in the initial stages of CML, some patients were suffered from the progression of CML because of the TKI intolerance or drug resistance. As we know, the etiology of disease progression is highly complex with wide heterogeneity, involving aberrantly activated pathways driven by the gene expression abnormalities (6, 7). Thus, understanding the underlying mechanisms of CML disease progression and search novel therapeutic targets is urgently needed.

RNA-binding proteins (RBPs), which could bind to mRNA or other RNAs, play a critical role in various biological cellular processes including transcription, translation, cleavage splicing and mRNA stability. Due to structural flexibility and domain polyfunctionality, the alterations or mutations of RBPs expression may be associated with tumorgenesis in a variety of human cancers, especially in hematologic malignancies (8, 9). However, few studies have focused on the role of RBPs in the initiation and progression of CML. Therefore, investigating the intricate network of RBPs and downstream mRNA may provide a strategy for understanding the mechanism and treatment in CML progression.

HNRNPH1, as an early reported RBPs, participates in RNA editing, RNA modification, and RNA stability (10). The aberrant overexpression of HNRNPH1 was seen in many cancers, such as gliomas, esophageal cancer, rhabdomyosarcoma and hepatocarcinoma (1, 11–13). Previously studies have confirmed that high expression level of HNRNPH1 could moderate tumorigenesis not only by upregulating the expression of oncogenes but also inhibiting the expression of tumor suppressor genes, such as P53, Ron and BCL-X (14–17). Furthermore, HNRNPH1 may also contribute to the drug response in gastric cancer cells (18). Importantly, a previous study has confirmed that HNRNPH1 is frequently elevated in AML patients. Knockdown of HNRNPH1 correlated to the cell proliferation in AML cells (1). However, the role of HNRNPH1 in CML has rarely been investigated.

In the present study, we found that the HNRNPH1 level was upregulated in CML patients, especially the CML progression phase. The HNRNPH1 downregulation inhibited cell proliferation, induced cell apoptosis, and arrested the cell cycle of CML cells *in vivo* and *in vitro*. Moreover, HNRNPH1 was revealed as a member of RBPs, affecting the PI3K/AKT pathway by regulating the PTPN6 expression through binding to its mRNA. The findings of this study provide a deep insight into the metabolic dysfunctions in CML progression and a novel potential therapeutic target for CML patients in the future.

MATERIALS AND METHODS

Specimen Collection

Bone marrow mononuclear cells (BM-MNCs) were extracted from 60 newly diagnosed and untreated CML patients between 2016 and 2020 in the Department of Hematology of the Second Hospital of Hebei Medical University, Shijiazhuang, China. Full detailed information of the patient characteristics is presented in **Table 1**. Furthermore, BM-MNCs of 30 healthy donors were used as normal controls (NC). Chronic myeloid leukemia was diagnosed by molecular biology, bone marrow morphology, immunology, and cytogenetics examination (19, 20). Patients with severe cardiopulmonary, renal or liver failure or coagulation abnormality or pregnant were excluded. The BM-MNCs were extracted by lymphocyte isolation fluid following the instructions. After centrifugation, the cell layer was collected for analysis. Red blood cells were lysed using RBC lysis solution, and samples were washed twice with PBS. The ethics committee of the Second Hospital of Hebei Medical University approved this experiment.

Cell Culture

K562 and KCL22 cells were chosen as representatives of the CML cell lines. HL-60, THP-1, and U937 cells were acute leukemia cell lines. All cell types were maintained in our laboratory. All above cells were cultured in RPMI 1640-based culture medium (Gibco) or Iscoves-modified Dulbecco's medium (IMDM; Gibco) culture medium supplemented with 10% fetal bovine serum (FBS; Gibco). The aforementioned conditioned media contained 100 units/ml penicillin and 100 ug/ml streptomycin. The cells were cultivated in an incubator at 37°C, 95% air and 5% CO_2 saturated humidity (Thermo, Waltham, MA, USA).

Cell Transfection

Lentiviruses containing shRNA-HNRNPH1 or overexpression of PTPN6 plasmid were constructed by the Shanghai Genechem Co., Ltd. (Shanghai, China). The multiplicity of infection (MOI) refers to the proportion of infectious viruses per cells. K562 cells were infected with each virus at an MOI of 30. The MOI of KCL22 was 40. The virus was added into cells from the logarithmic growth stage according to the infection conditions and cultured for 12–16 h. Then the cells were incubated with culture medium containing 10% FBS. The cells were treated with puromycin at 2 μg/ml to screen for stably transfected cells lines on conditions.

Cell Viability Assay

The cell viability was measured using the CCK-8 (Beibo Biological Reagent Co., Shanghai, China) assay. Approximately

TABLE 1 | Characteristics of the patients included in the study.

Characteristic	CML-CP (n = 30)	CML-AP (n = 18)	CML-BP (n = 12)
Age (years), median (range)	51 (21–79)	49 (25–66)	57 (36–73)
Male/female (n/n)	19/11	9/9	4/8
WBC count, $\times10^9$/L, median (range)	155.4 (23.5–527.5)	72.5 (1.75–433)	78.7 (1.5–327.9)
Haemoglobin level (g/l)	105 (70–147)	85 (52–118)	92 (56–124)
Platelet count, $\times10^9$/l, median (range)	522 (3–1,476)	609 (4–3,000)	151 (11–576)

100 ul of mixed suspension cells (1×10^5 cells/ml) required for different experiments were added to the 96-well plate. Following cell culture, 10ul CCK-8 solution was added into each plate at various time points and incubated at 37°C in 5% CO_2 saturated humidity for 2 h. The optical density was read at 450 nm in a microplate reader (BioTek, Winooski, VT, USA) in different time points.

Cell Apoptosis Assay

Cell apoptosis was assayed by an Annexin V/FITC/PI Apoptosis Detection Kit (BD Biosciences, Franklin Lakes, NJ, USA). The cells required for different experiments were mixed with 5 μl Annexin V/FITC and 10 μl propidium iodide (PI) based on the manufacturer's instructions. They were analyzed with a FC500 flow cytometer (Beckman Coulter). The data was performed using Kaluza software (Beckman Coulter).

RNA Extraction and Quantitative Real-Time PCR

qRT-PCR analysis was performed with standard procedure as described previously (21). Briefly, total RNA of cells lines and BM-MNCs were extracted using Trizol (Invitrogen, Carlsad, CA, USA). The cDNA was synthesized by a SureScriptTM First-Strand cDNA Synthesis Kit (Funeng, Guangzhou, China). Quantitative real-time reverse transcriptase-polymerase chain reaction (qRT-PCR) was performed by an All-in-OneTM qPCR Mix (Funeng, Guangzhou, China). Each reaction was dependently repeated thrice. qRT-PCR was performed at 95°C for 10 min, followed by 40 cycles of 95°C (15 s), 60°C (30 s), and 72°C (30 s). Moreover, GAPDH was used as an internal reference.

Western Blot Analysis

Proteins were obtained using radioimmunoprecipitation assay (RIPA) buffer to dissolve the cells. The quantification was tested using bicinchoninic acid Protein Assay Kit (Boster Biological Company, Ltd., Wuhan, China). All protein samples were subjected to 10% sodium dodecyl sulfate-polyacrylamide gel electrophoresis. The target strip was transferred to a polyvinylidene fluoride (PVDF) membrane (Millipore, Burlington, MA, USA) *via* electrophoresis. The PVDF membrane was blocked in 5% nonfat milk. The protein bands were incubated with specific primary antibodies as follows: HNRNPH1 (1:2,000) (ab 154894, Abcam, CA, USA), PTPN6 (1:1,000) (ab 32559, Abcam, CA, USA), AKT (1:1,000) (ab 38449, Abcam, CA, USA), p-AKT (1:1,000) (ab 8805, Abcam, CA, USA), and β-ACTIN (1:8,000; Abways Technology, New York, NY, USA; AB0035). Moreover, the PVDF membrane was incubated in a goat-anti-rabbit secondary antibody (1:10,000, Boster Biological Company, Ltd., Wuhan, China) overnight. Images of protein quantification were captured by BioSpectrum Imaging System (UVP, LLC, Upland, CA, USA).

Immunofluorescence Staining

Cell samples were centrifuged, fixed, and smeared onto coverslips. The cells were fixed using 4% formaldehyde and preincubated with 10% normal goat serum (710,027, KPL, Gaithersburg, MD, USA). The cells were rinsed with PBS and incubated with anti-HNRNPH1 antibody (Abcam, ab 154894) at 37°C for 1 h. Immunofluorescence staining was enhanced using a rabbit anti-red fluorescent-labeled antibody (Rockland Immunochemicals Inc., Gilbertsville, PA, USA; 1:100). The smears were then incubated with DAPI. Furthermore, nuclear staining was observed by confocal microscopy (Zeiss LSM 700, Germany) and digitized with confocal software.

Colony-Forming Assay

The colony formation was performed with standard procedure in accordance with the method described in previous study (2, 22). The logarithmic growth phase of treated cells was added to the 1% methylcellulose for 14–18 days at 37°C with 5% CO_2 saturated humidity. The methylcellulose medium was mixed with powder culture medium with ultrapure water, 40% FBS, and 1% penicillin/streptomycin. The colonies were quantified as aggregates with greater than 50 cells by microscope (Axio-observer D1, Zeiss, Germany). Then the colonies were counted manually and photographed.

RNA Immunoprecipitation

The cells were treated with cell lysis buffer. The 10% lysis sample (named input) was stored, and 80% (named IP) was used in immunoprecipitation reactions with HNRNPH1 antibody (Abcam No 154894), and 10% (named IgG) was incubated with rabbit IgG (Cell Signaling Technology, Danvers, MA, USA) as a negative control The RNA of input and IP was extracted using TRIzol reagent (Invitrogen). The purified RNA samples were analyzed with conventional RT-PCR.

RNA-Seq

Three biological replicates in each control and knockdown HNRNPH1 groups in K562 cells were collected for microarray analysis after 14 days of infection. The total RNA was extracted using TRIzol reagent (Invitrogen) and subject to RNA sequencing. RNA seq was performed by BGI Technology Services Co., Ltd (Shenzhen, China). The differentially expressed genes were screened based on fold change (>0.5) and Student's t-test ($P < 0.05$). The RNA-sequencing raw data have been deposited into sequence read archive (SRA) database (https://www.ncbi.nlm.nih.gov/sra).

Animal Experiment

Sixteen female severe combined immunodeficient (SCID) athymic nude mice (16–20 g, 5–6 weeks' old) were purchased from SPF Biotechnology Co., Ltd. (Beijing, China). All mice were raised at an ambient temperature of 18–22°C and relative humidity of 50–60%. The stably knockdown-HNRNPH1 K562 cells and negative control K562 cells were subcutaneously injected into the left dorsal flanks of each mouse (0.5×10^6 cells per injection). Tumor size and body weight were dynamically observed. The nude mice were sacrificed on day 28 post-inoculation. All animal experiment protocols were approved by the committee on animal experimentation of Hebei Medical University and carried out following the guidelines on animal experimentation.

Immunohistochemistry

The tumor tissues of mice were fixed with 4% paraformaldehyde and routinely dehydrated, embedded in paraffin sections, and cut into 4-μm thick sections. The antigen repair was then performed with sodium citrate. Moreover, endogenous peroxidase was inactivated by 3% hydrogen peroxide. Tissue sections were incubated with the primary antibodies at 4°C overnight and with secondary antibody at room temperature for 30 min respectively. Sections were incubated with DAB chromogen at room temperature for 3–10 min after washing with phosphate-buffered saline with detergent Tween. Slices were sealed with coverslips after rinsing with running water and hematoxylin counterstain.

Statistical Analysis

The data were presented by means ± SD. Student's t-test and Chi-square test were applied to detect the significant difference by using the Statistical Package for the Social Sciences, version 13.0 (SPSS Inc., Chicago, IL, USA). P values <0.05 were considered statistically significant.

RESULTS

HNRNPH1 Is Upregulated in CML Patients and Cell Lines

The difference in the HNRNPH1 expression between the BM-MNCs of CML patients and the healthy donors was first explored to investigate the role of HNRNPH1 in CML. qRT-PCR result showed that mRNA expression of HNRNPH1 in BM-MNCs of CML patients was significantly higher compared with the normal controls (**Figure 1A**). The HNRNPH1 expression in different progressions of CML was then compared. Moreover, the HNRNPH1 expression in the progressive phase was higher compared with the chronic phase (**Figure 1B**). However, the expression level in the blast phase was the highest. HNRNPH1 protein level was then also detected in the BM-MNCs of 10 patients selected in different stages of CML and healthy donors. The Western blot analysis result showed that the HNRNPH1 protein level was significantly increased in CML patients compared with normal controls. Consistent with qRT-PCR

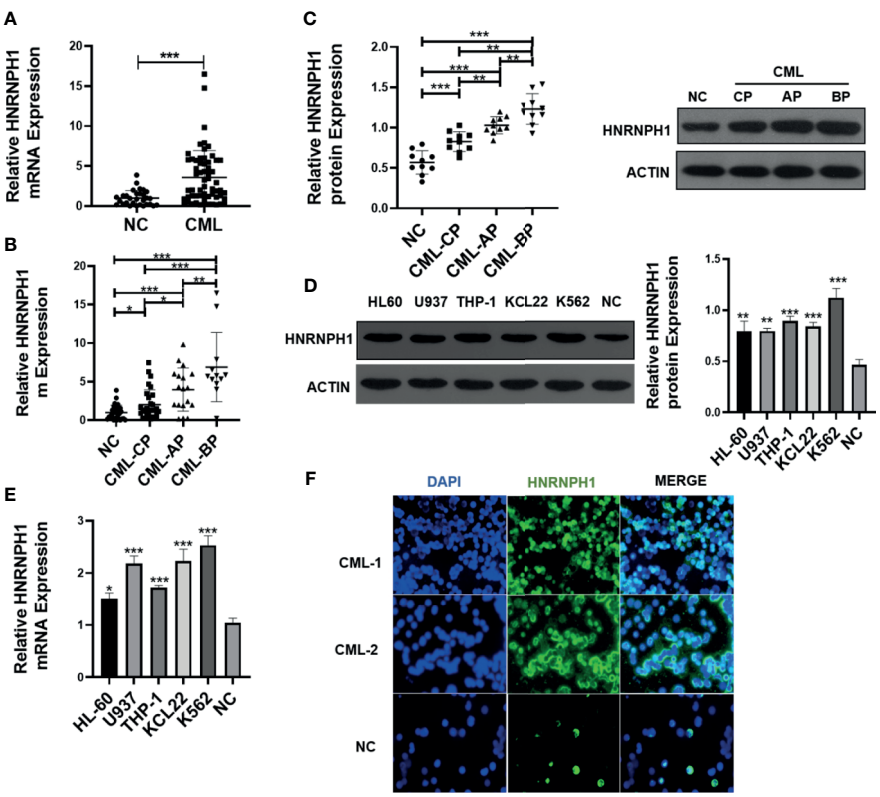

FIGURE 1 | HNRNPH1 is upregulated in CML patients and cell lines. **(A)** qRT-PCR was used to detect HNRNPH1 mRNA level in BM-MNCs of CML patients and BM-MNCs of healthy donors. Normalized to GAPDH. ***P < 0.001 *vs*. NC. **(B)** qRT-PCR was used to detect HNRNPH1 mRNA level in different phases of CML (CML-CP, CML-AP, and CML-BP) patients' BM-MNCs compared with normal controls. *P < 0.05, **P < 0.01, ***P < 0.001. **(C)** Western blot was used to detect HNRNPH1 protein levels in different phases of CML (CML-CP, CML-AP, and CML-BP) patients' BM-MNCs compared with normal controls. Left panel, scatter plots of protein densitometric analysis. **P < 0.01, ***P < 0.001. **(D)** Western blot was used to detect HNRNPH1 protein levels in leukemia cell lines (HL-60, U937, THP-1, K562, and KCL22) and BM-MNCs of normal controls. Right panel, densitometric analysis. **P < 0.01, ***P < 0.001 *vs*. NC. **(E)** qRT-PCR was used to detect HNRNPH1 mRNA levels in leukemia cell lines (HL-60, U937, THP-1, K562, and KCL22) and BM-MNCs of normal controls. *P < 0.05, ***P < 0.001 *vs*. NC. **(F)** Immunofluorescence analyzed the HNRNPH1 protein level and localization of HNRNPH1 in PBMCs of CML-CP patients and BM-MNCs of normal controls.

results, the HNRNPH1 protein level was increased in the blast and accelerated phase compared with the chronic phase (**Figure 1C**). Furthermore, mRNA and HNRNPH1 protein levels were found to be upregulated in leukemia cell lines compared with BM-MNCs of healthy donors (**Figures 1D, E**). Immunofluorescence also displayed that HNRNPH1 protein was primarily localized in the nucleus and increased in CML patients (**Figure 1F**). These results suggest that HNRNPH1 expression is abnormally elevated in CML, especially in the progressive phase.

HNRNPH1 Downregulation Promotes Apoptosis of CML Cells

HNRNPH1 was knocked by transfection of sh-RNA or empty vector (sh-Con) into CML cell lines to investigate the impact of HNRNPH1 on CML progression. The sh-RNA transfection of HNRNPH1 successfully reduced the HNRNPH1 expression level in both K562 and KCL22 cells compared with the negative controls (**Figure 2A**). Cell viabilities were then measured by CCK-8 assay. The HNRNPH1 downregulation markedly reduced cell proliferation compared with negative controls (**Figure 2B**). The cell apoptosis by flow cytometry using Annexin V-FITC/PI staining was then detected next. The result showed that HNRNPH1 knockdown in CML cells promoted cell apoptosis compared with the negative controls (**Figure 2C**). Consistently, HNRNPH1 suppression was found to inhibit the multiplication of CML cells by mainly arresting their cell cycle at G1/G0 phase(K562 44.34% *vs.* 52.35%, KCL22 43.61% *vs.* 53.60%)and caused S phase reduction(K562 48.58% *vs.* 38.86%, KCL22 52.41% *vs.* 41.9%), suggesting that HNRNPH1 knockdown played an inhibitory effect on cell arrest phase (**Figure 2D**). Furthermore, colony formation experiments also confirmed that HNRNPH1 knockdown inhibited cell proliferation (**Figure 2E**). Taken together, these results revealed that HNRNPH1 played a curtail role in CML cell survival *in vitro*.

HNRNPH1 Knockdown Increases the Sensitivity of Imatinib in CML Cells

CML cells were transfected with sh-RNA of HNRNPH1 or sh-Con and then treated with different concentrations of imatinib to investigate the effect of HNRNPH1 on imatinib sensitivity. The IC50 of imatinib was detected by the CCK-8 assay. Moreover, HNRNPH1 silencing significantly increased imatinib sensitivity compared with the negative control (**Figure 3A**). Consequently, the number of apoptotic cells induced by imatinib was increased in the knockdown group compared with the negative control (**Figure 3B**). Moreover, colony formation assay showed that HNRNPH1 knockdown in CML cells could promote cell sensibility to imatinib (**Figure 3C**). These results suggest that HNRNPH1 knockdown promotes imatinib sensitivity in CML cells.

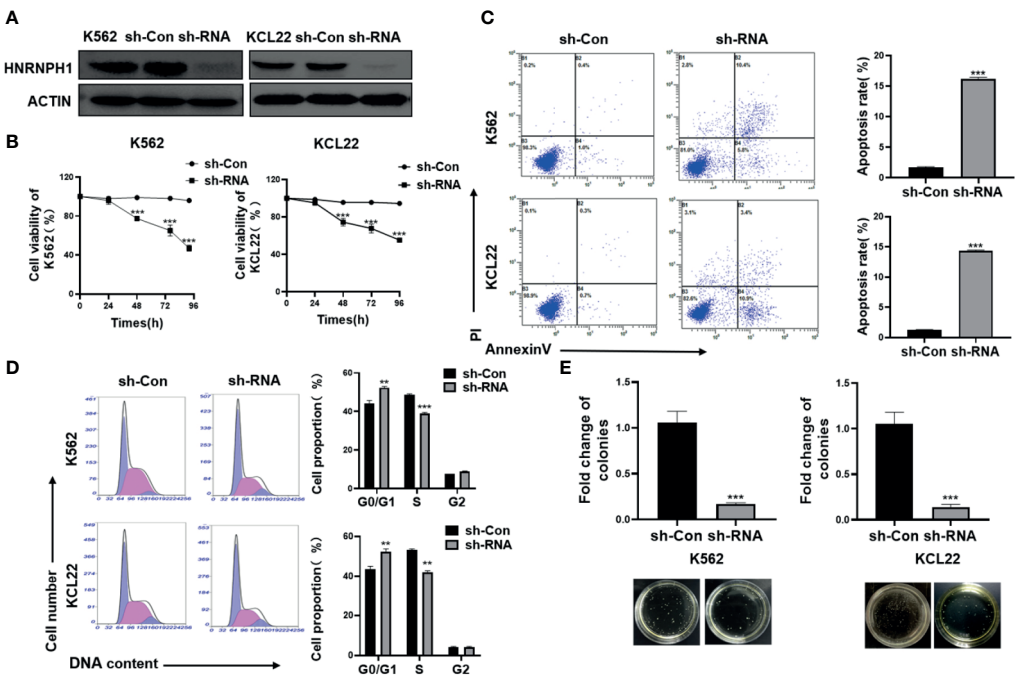

FIGURE 2 | HNRNPH1 downregulation promotes apoptosis of CML cells. **(A)** K562 and KCL22 cells were transfected with specific sh-RNA of HNRNPH1 or negative sh-RNA (sh-Con). Western blot was used to detect HNRNPH1 protein level. **(B)** CML cells were prepared as **(A)**, CCK-8 analysis was used to detect cell proliferation. ***P < 0.001 *vs.* sh-Con. **P < 0.01 *vs.* sh-Con. **(C)** CML cells were prepared as **(A)**, and cell apoptosis rate was detected by flow cytometry using Annexin V-FITC/PI staining. The right panel shows the apoptosis rate from three independent experiments. ***P < 0.001 *vs.* sh-Con. **(D)** CML cells were prepared as **(A)**, and the cell cycle was detected by flow cytometry. The right panel shows the cell proportion of three independent experiments. **P < 0.01 *vs.* sh-Con. **(E)** CML cells were prepared as **(A)**, and cell proliferation was detected by colony formation assay. ***P < 0.001 *vs.* sh-Con. The bottom panel shows an image of colonies.

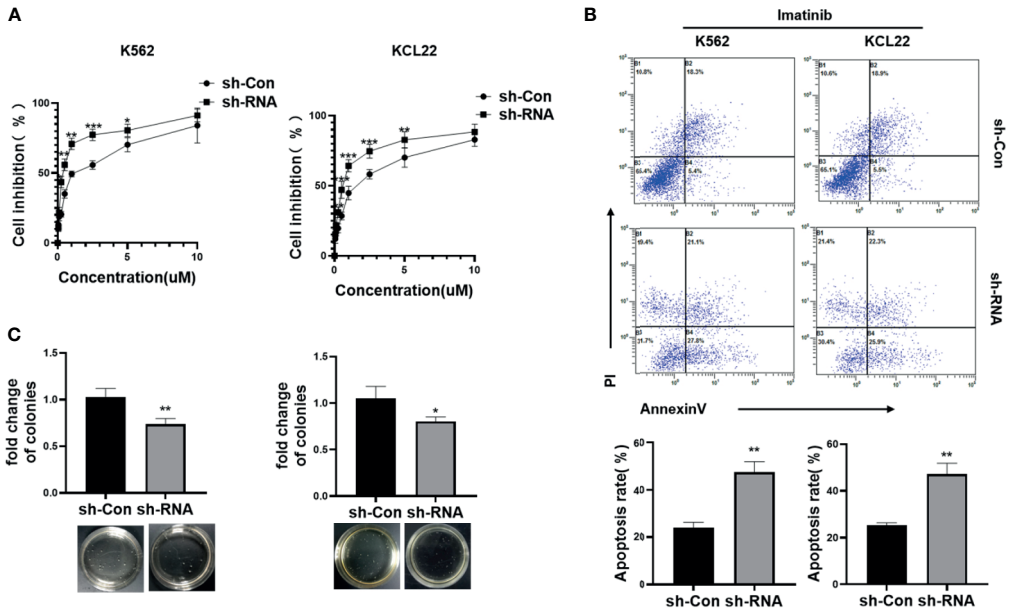

FIGURE 3 | HNRNPH1 knockdown increases imatinib sensitivity in CML cells. **(A)** K562 and KCL22 cells were transfected with specific sh-RNA of HNRNPH1 or negative sh-RNA (sh-Con) and treated with different imatinib concentrations for 48 h. CCK-8 analysis was used to detect cell inhibition. ***P < 0.001, **P < 0.01 *vs*. sh-Con. **(B)** K562 and KCL22 cells were transfected with specific sh-RNA of HNRNPH1 or negative sh-RNA (sh-Con) and treated with imatinib (3 μM) for 48 h. Cell apoptosis was detected by flow cytometry using Annexin V/FITC/PI. The right panel shows the apoptosis rate from three independent experiments. **P < 0.01 *vs*. sh-Con. **(C)** CML cells were prepared as **(B)**, and cell proliferation was detected by colony formation assay. *P < 0.05, **P < 0.01 *vs*. sh-Con. The bottom panel shows an image of colonies.

HNRNPH1 Regulates the PTPN6 Expression

HNRNPH1 was knocked down in K562 cells to identify molecular mechanisms of HNRNPH1 in regulating the growth of CML cells. RNA-seq was then performed. In addition, the differential expressed genes were displayed in the volcano plot between the sh-RNA and negative control groups (**Figure 4A**). Among those relative upregulated genes, PTPN6, which had been confirmed to play a crucial role as a cancer suppressor in leukemia, was focused on (21). The HNRNPH1 was knocked down in K562 cells to confirm the results of the RNA-seq and detect the PTPN6 expression. Consistent with the result of RNA-seq, the fold change of PTPN6 expression was upregulated in HNRNPH1 knocked down cells than control cells by qRT-PCR analysis. As shown in **Figure 4B**, the fold change of PTPN6 mRNA expression in K562 and KCL22 cell were 1.56 and 1.42, respectively. Likewise, the western blot result showed that the protein level of PTPN6 was increased in HNRNPH1-reduced cells compared with the negative control (**Figure 4C**). Additionally, the PTPN6 expression in CML patients was detected by qRT-PCR analysis. The PTPN6 expression which was reduced in CML-CP patients compared with healthy donors was related to illness aggravation (**Figure 4D**). A significant inverse correlation existed between the HNRNPH1 expression and PTPN6 in CML patients (**Figure 4E**). Taken together, these data revealed that PTPN6, which was downregulated in CML, may negatively correlate with HNRNPH1.

HNRNPH1 Regulates PI3K/AKT Pathway by Binding to PTPN6

As an RNA binding protein, HNRNPH1 is involved in gene regulation by directly assembling on its mRNA (23). Radioimmunoprecipitation (RIP) followed by RT-PCR and qRT-PCR were performed to investigate whether HNRNPH1 could bind to the mRNA of PTPN6 to regulate its expression. RIP-PCR analysis showed that PTPN6 mRNA, but not Actin, was present in the protein–RNA complex pulled down by the antibody HNRNPH1 (**Figures 5A, B**), indicating that HNRNPH1 could physically bind to the mRNA of PTPN6. The screened differential genes were enriched in the PI3K/AKT pathway (**Figure 5C**), just like a previous study reported that PTPN6 could influence the activity of the PI3K/AKT pathway (24). To further verify whether HNRNPH1 contributed to the regulation of the PI3K/AKT pathway, CML cells were transfected with sh-HNRNPH1 or PTPN6 overexpression plasmid or co-transfected them together. The western blot results showed that PTPN6 overexpression could decrease the p-AKT protein level, while this reduction effect of p-AKT could be further reduced by HNRNPH1 knockdown together in CML cells (**Figure 5D**), suggesting that PTPN6 may mediate the relationship between the HNRNPH1 and the activation of PI3K/AKT in CML cells. Interestingly, this study also found that the expression trend of P210 protein that encoded BCR–ABL1 fusion gene was surprisingly consistent which is regulated positively by HNRNPH1 but negatively by PTPN6.

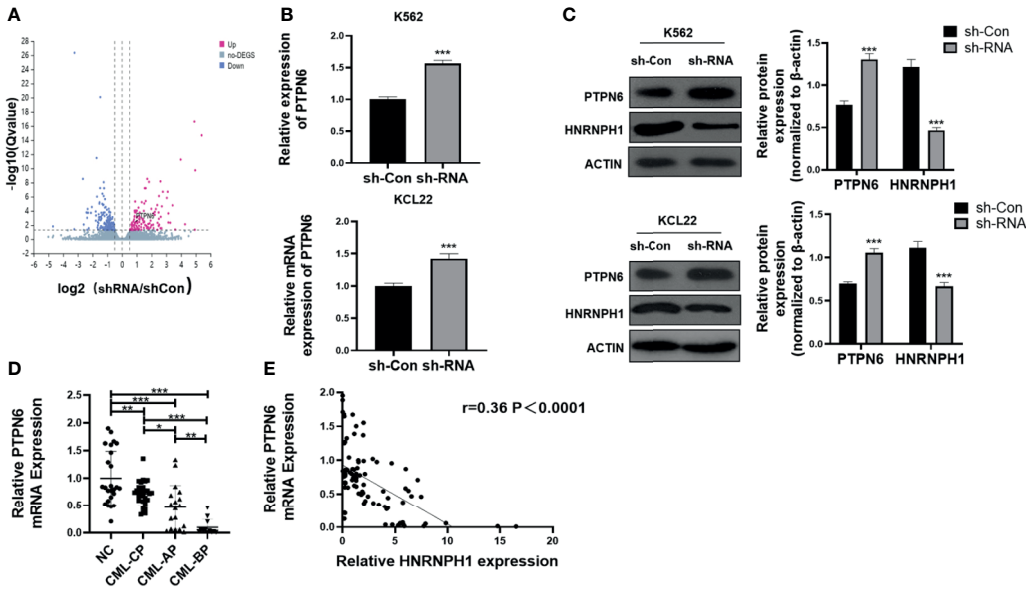

FIGURE 4 | HNRNPH1 regulates the PTPN6 expression. **(A)** Three independent HNRNPH1 reduced and control cells were prepared for RNA preparation and microarray analysis. Genes with altered expression were displayed in volcano plots. The upregulated genes are highlighted in pink and downregulated genes in blue. **(B)** K562 and KCL22 cells were transfected with specific sh-RNA of HNRNPH1 or negative sh-RNA (sh-Con). qRT-PCR was used to detect the PTPN6 mRNA level. ***P < 0.001 *vs.* sh-Con. **(C)** CML cells were prepared as **(B)**, western blot was used to detect PTPN6 protein level. Right panel, densitometric analysis. ***P < 0.001 *vs.* sh-Con. **(D)** qRT-PCR was used to detect PTPN6 mRNA level in different phases of CML (CML-CP, CML-AP, and CML-BP) patients' BM-MNCs compared with normal controls. *P < 0.05, **P < 0.01, ***P < 0.001. **(E)** Pearson correlation analysis was used to analyze the relationship between HNRNPH1 and PTPN6 in BM-MNCs of CML patients (R = 0.36, P < 0.0001).

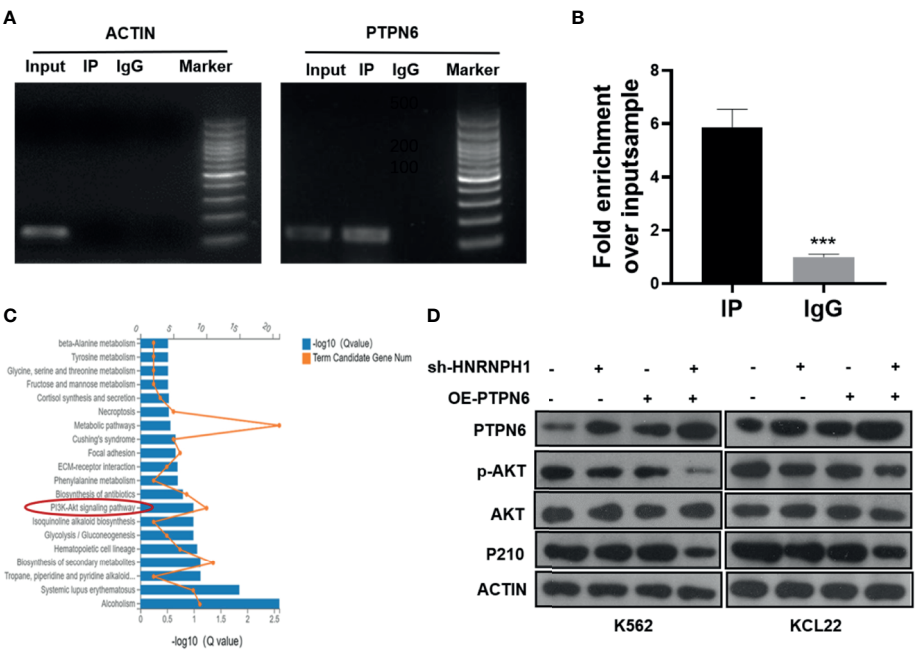

FIGURE 5 | HNRNPH1 regulates PI3K/AKT pathway by binding to PTPN6. **(A, B)** RIP-PCR and agarose gel electrophoresis were used to test the interaction between the HNRNPH1 protein and PTPN6 mRNA. ***P < 0.001 *vs.* IgG **(C)**. KEGG pathway significant enrichment was used to identify the main biochemical metabolic and signal transduction pathways involved in differentially expressed genes. **(D)** CML cells were transfected with sh-HNRNPH1 or PTPN6 overexpression plasmid or co-transfected them together. Western blot analysis was used to detect PTPN6, p-AKT, AKT, and P210BCR-ABL protein levels.

Collectively, these results revealed that HNRNPH1 contributed to CML cell progression by moderating PI3K/AKT pathway.

HNRNPH1 Downregulation Inhibits CML Cell Growth *In Vivo*

The nude mice xenograft model was applied to confirm whether the reduction of HNRNPH1 expression could inhibit the proliferation of CML cells through the PTPN6–PI3K/AKT pathway *in vivo*. The shRNA K562 cell lines stably suppressing HNRNPH1 were screened. The HNRNPH1-reduced K562 and control cells were then subcutaneously implanted into the nude mice. The HNRNPH1 reduction could inhibit the tumor size compared with the control *in vivo* (**Figures 6A, B**). Similarly, this study also found that downregulating the HNRNPH1 expression could decrease the weight of xenograft tumors (**Figure 6C**). In addition, the protein level of HNRNPH1, PTPN6, AKT, p-AKT and BCR-ABL was detected by immunohistochemical (**Figure 6D**) and western blot analysis (**Figure 6E**). The results showed that the PTPN6 protein level increased while the p-AKT and BCR-ABL dramatically decreased in the HNRNPH1 reduction group compared with the negative control. The results proved that HNRNPH1 reduction also inhibited CML cell growth *in vivo* through the PTPN6-PI3K/AKT pathway.

DISCUSSION

The pathogenesis of CML is a complex progress that is concerned with numerous mechanisms. Therefore, many studies have been dedicated to elucidate the pathogenesis of advanced CML. Our previous studies have shed light on underlying mechanisms linked to disease progression, such as epigenetic alterations, abnormal activation of coding or non-coding RNA transcripts and cancer-related pathways. For example, the PTPN6 expression is closely related to the progression of CML, which is regulated by epigenetics modifications including acetylation and methylation (21). The Long Noncoding RNA MEG3 which could sponge to miRNA inhibit the CML cell proliferation in CML cells and contributes to CML progression (25, 26). Moreover, the deubiquitinating enzyme ubiquitin-specific peptidase 15 expression level was significantly downregulated in CML patients by blocking JAK/STAT5 pathway and involved in imatinib resistance (27). However, the specific mechanisms of CML development and progression remain exclusive.

Growing evidence have proved that the post-transcription is a critical mechanism for regulating gene expression. RBPs are considered as essential modulators in RNA translation, transcription, splicing and mRNA stability, which are frequently dysregulated in tumor cells (28, 29). An increasing number of studies have indicated the critical role of RBP in hematological malignancies. For example, Wang et al. have reported that degradation of RBM39 sustains leukemia survival by altering the splicing of HOXA in AML cells (8). Gallardo et al. found that the upregulation of hnRNPK regulates MYC expression in B-cell lymphoma post-transcriptionally and translationally (9). Ge revealed that RBM25 has an impact on the AML development as a splicing factor of c-myc (30). In the present study, we found thatHNRNPH1 was upregulated in CML patients and correlated to disease progression. HNRNPH1 could function as a diagnosis related biomarker and a novel target for combination therapy for CML patients. Due to the limitations, a single-center study with a low number of patients was afforded, where subsequent research is needed to delineate the relationship with the prognosis.

Currently, some hnRNPs have been demonstrated to be involved in the oncogenesis of human hematologic malignancies.

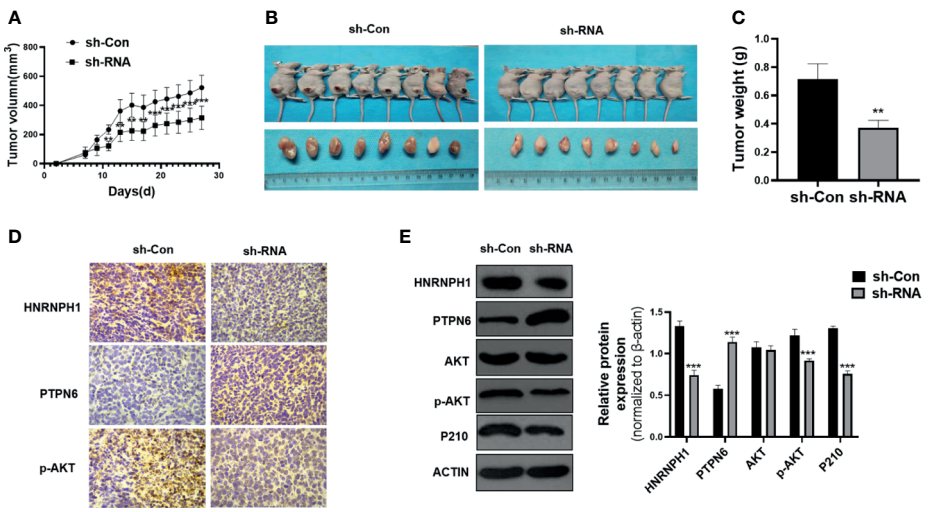

FIGURE 6 | HNRNPH1 downregulation inhibits CML cell growth *in vivo*. **(A)** K562 cells were engineered to stably knockdown HNRNPH1 and the cells were then subcutaneously injected into the nude mice to establish CML xenograft tumors. Tumor volumes were monitored by direct measurement. **P < 0.01, ***P < 0.001 *vs.* sh-Con. **(B)** Representative tumor sizes of xenograft mice in each group. **(C)** The xenograft tumor wet weight in each group of mice. **P < 0.01 *vs.* sh-Con. **(D)** Immunohistochemistry stain was used to measure the HNRNPH1, PTPN6, and P-AKT protein levels in xenograft tumors. **(E)** Western blot was used to detect the PTPN6, p-AKT, AKT, and P210BCR-ABL protein levels in xenograft tumors. Right panel, densitometric analysis. ***P < 0.001 *vs.* sh-Con.

For instance, HNRNPK was downregulated in leukemia cells. Knockdown of HNRNPK promoted tumor growth of myeloproliferative neoplasm *in vivo* (31). HNRNPD also had an effect on the proliferation of BCR-ABL-positive cell lines which were increased in hematopoietic stem cells (32). The alternative splice alterations of HNRNPA2B1 influenced the development and adverse outcome in myelodysplastic syndromes (33). Despite having some HNRNPs family members being confirmed to function as oncogenes or tumor suppressor genes in CML (32, 34–36), a few of them have clearly revealed the molecular mechanisms in CML progression. HNRNPH1, which is localized in the nucleus, has been shown aberrantly overexpressed in hematological malignancies including AML, Burkitt lymphoma, and T-acute lymphoblastic leukemia (8, 37, 38). Importantly, Yamazaki et al. also found that HNRNPH1 plays a crucial role in stem cell maintenance and hematopoietic development suggesting that HNRNPH1 may be involved in the regulation of hematopoietic stem cells (39). In the present study, we demonstrated that HNRNPH1 expression was higher in CML patients compared with healthy donors, and gradually elevated along with disease progression that blast crisis patients have significantly highly expressed HNRNPH1 (**Figures 1A–C**). The higher level of HNRNPH1 has also been observed in leukemia cell lines and was particularly prominent in CML cells. Given that some patients in the progressive phases are associated with TKIs insensitive or resistance, HNRNPH1 downregulation was found to increase imatinib sensitivity. The above results potentially indicated that HNRNPH1 was an important molecular marker for CML progression and may help improve treatment, such as early turn to more efficacious TKIs or combination chemotherapy. Our data further elaborated that the reduction of HNRNPH1 expression can promote apoptosis and inhibit proliferation in CML cells. Therefore, HNRNPH1 was shown to be an important regulator for the proliferation of CML cells. These findings further validated that HNRNPH1 may serve as therapeutic target for CML treatment as its functions as the anti-apoptotic molecule in tumor metastasis and growth. Notably, whether the downregulation of HNRNPH1 would arrest or even reverse disease progression still requires further investigations.

Besides the potential use of HNRNPH1 as a biomarker of CML disease progression, underlying mechanisms of HNRNPH1 were identified. PTPN6, possessing an SH2 domain, was a tumor suppressor by dephosphorylation in CML (21, 40). RIP-PCR revealed that HNRNPH1 could be a negative upstream regulator by regulating the mRNA expression of PTPN6 directly. Gratifyingly, HNRNPH1 motif sequence was found to be present in the PTPN6 gene, suggesting that HNRNPH1 regulated the post-transcription level of PTPN6, which supported the experimental results in our study (41). However, our experiments did not fully address the mechanism whether HNRNPH1 affects the stability or splicing of PTPN6, which still needs to be further explored. The tyrosine kinase activity of BCR-ABL activate multiple signaling pathways, including PI3K/AKT, of which is responsible for cell survival (42). It is consistent with previous studies that PTPN6 may inhibit the activation of PT3K/AKT pathway by mediating AKT dephosphorylation (43). The present study also made a promising discovery that BCR-ABL was positively regulated by HNRNPH1 downregulation mediated by PTPN6. A prior study demonstrated that PTPN6 was a binding protein of P210 BCR-ABL, which may explain the reason for this phenomenon (44). We have here provided the first piece of evidence that the HNRNPH1–PTPN6–PI3K/AKT axis mediated CML progression.

In this study, we demonstrated that downregulation of HNRNPH1 inhibits the potential tumorigenic both *in vitro* and *in vivo*, and can increase imatinib sensitivity, providing a rational drug design to prevent the expression of HNRNPH1 in BCR-ABL positive leukemia. It was confirmed that HNRNPH1 was indeed associated with PARylation with a conserved domain of pADPr-binding (45). Given that the reduction of PARG activity can significant elevate the PARylation cellular level (46), implying that PARG inhibitors may block the HNRNPH1 related tumor growth. We hypothesize that PARG inhibitor can serve as a targeted HNRNPH1 inhibitor for a combination of chemotherapies in CML patients with high level of HNRNPH1, which deserves further exploration.

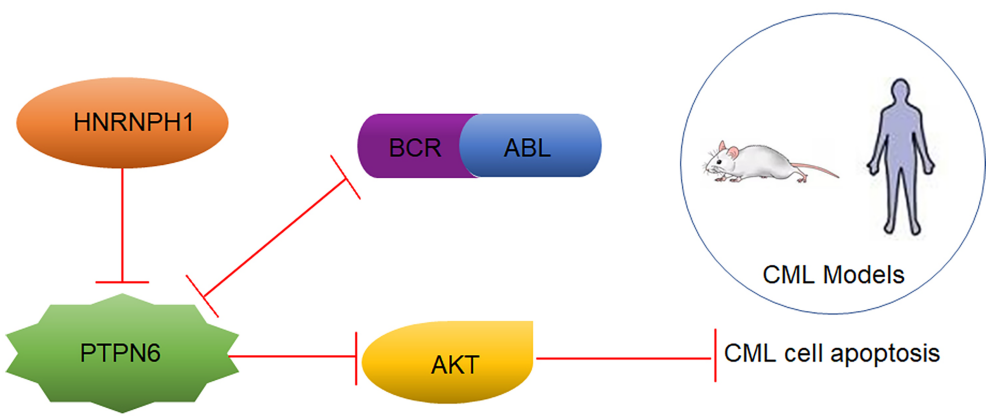

FIGURE 7 | A schematic model depicting the role of HNRNPH1–PTPN6–PI3K/AKT axis in CML.

CONCLUSION

Taken together, as displayed in **Figure 7**, HNRNPH1 was uncovered, for the first time, as a potential molecular marker in CML disease progression. In addition, HNRNPH1 was also first revealed as an upstream PTPN6 regulator that can directly bind to the PTPN6 transcript. Due to the RBP nature of HNRNPH1, which has oncogene function and multiple transcriptional factor binding sites, HNRNPH1 could be a novel CML therapeutic target that has a huge potential clinical translation value. Thus, the HNRNPH1–PTPN6–PI3K/AKT axis played an important role in the genesis and CML progression.

DATA AVAILABILITY STATEMENT

The original contributions presented in the study are included in the article/supplementary material. Further inquiries can be directed to the corresponding author.

ETHICS STATEMENT

The studies involving human participants were reviewed and approved by The second hospital of Hebei Medical University. The patients/participants provided their written informed consent to participate in this study. The animal study was reviewed and approved by Hebei Medical University.

AUTHOR CONTRIBUTIONS

ML, LY, and JL carry out the design of research study. XL and ZN contributed to solve the experimental problems. XZ and YL carry out the patient collection. XW and YP contributed to animal models. ML LY, and JL carry out acquisition and analysis of the data. ML wrote the manuscript. ML, LY, XL, and JL carry out revision of the manuscript. All authors contributed to the article and approved the submitted version.

FUNDING

This study was partially supported by the he Natural Science Foundation of Hebei Province (H2020206438).

ACKNOWLEDGMENTS

Thanks are due to Dr. Luo jianmin for his assistance with the experiment and to Dr Yang lin for valuable discussion.

REFERENCES

1. Lefave CV, Squatrito M, Vorlova S, Rocco GL, Brennan CW, Holland EC, et al. Splicing Factor hnRNPH Drives an Oncogenic Splicing Switch in Gliomas. *EMBO J* (2011) 30(19):4084–97. doi: 10.1038/emboj.2011.259
2. Pikman Y, Puissant A, Alexe G, Furman A, Chen LM, Frumm SM, et al. Targeting MTHFD2 in Acute Myeloid Leukemia. *J Exp Med* (2016) 213 (7):1285–306. doi: 10.1084/jem.20151574
3. Lugo TG, Pendergast AM, Muller AJ, Witte ON. Tyrosine Kinase Activity and Transformation Potency of Bcr-Abl Oncogene Products. *Science* (1990) 247 (4946):1079–82. doi: 10.1126/science.240814910.1126/science.2408149
4. Sherbenou DW, Druker BJ. Applying the Discovery of the Philadelphia Chromosome. *J Clin Invest* (2007) 117(8):2067–74. doi: 10.1172/JCI31988
5. Sloma I, Jiang X, Eaves AC, Eaves CJ. Insights Into the Stem Cells of Chronic Myeloid Leukemia. *Leukemia* (2010) 24(11):1823–33. doi: 10.1038/leu.2010.159
6. Chereda B, Melo JV. Natural Course and Biology of CML. *Ann Hematol* (2015) 94(Suppl 20):S107–21. doi: 10.1007/s00277-015-2325-z
7. Modi H, McDonald T, Chu S, Yee JK, Forman SJ, Bhatia R. Role of BCR/ABL Gene-Expression Levels in Determining the Phenotype and Imatinib Sensitivity of Transformed Human Hematopoietic Cells. *Blood* (2007) 109 (12):5411–21. doi: 10.1182/blood-2006-06-032490
8. Wang E, Lu SX, Pastore A, Chen X, Imig J, Chun-Wei Lee S, et al. Targeting an RNA-Binding Protein Network in Acute Myeloid Leukemia. *Cancer Cell* (2019) Mar 1835(3):369–384.e7. doi: 10.1016/j.ccell.2019.01.010
9. Gallardo M, Malaney P, Aitken MJL, Zhang X, Link TM, Shah V, et al. Uncovering the Role of RNA-Binding Protein Hnrnp K in B-Cell Lymphomas. *J Natl Cancer Inst* (2020) 112(1):95–106. doi: 10.1093/jnci/djz078
10. Han SP, Tang YH, Smith R, Biochem J. Functional Diversity of the hnRNPs: Past, Present and Perspectives. *Biochem J* (2010) 430: (3):379–92. doi: 10.1042/BJ20100396
11. Li Y, Bakke J, Finkelstein D, Zeng H, Wu J, Chen T. HNRNPH1 Is Required for Rhabdomyosarcoma Cell Growth and Survival. *Oncogenesis* (2018) 7(1):9. doi: 10.1038/s41389-017-0024-4
12. Xu H, Dong X, Chen Y, Wang X. Serum Exosomal hnRNPH1 mRNA as a Novel Marker for Hepatocellular Carcinoma. *Clin Chem Lab Med* (2018) 56 (3):479–84. doi: 10.1515/cclm-2017-0327
13. Sun YL, Liu F, Liu F, Zhao XH. Protein and Gene Expression Characteristics of Heterogeneous Nuclear Ribonucleoprotein H1 in Esophageal Squamous Cell Carcinoma. *World J Gastroenterol* (2016) 22(32):7322–31. doi: 10.3748/wjg.v22.i32.7322
14. Garneau D, Revil T, Fisette JF, Chabot B. Heterogeneous Nuclear Ribonucleoprotein F/H Proteins Modulate the Alternative Splicing of the Apoptotic Mediator Bcl-X. *J Biol Chem* (2005) 280(24):22641–50. doi: 10.1074/jbc.M501070200
15. Decorsière A, Cayrel A, Vagner S, Millevoi S. Essential Role for the Interaction Between Hnrnp H/F and a G Quadruplex in Maintaining p53 pre-mRNA 3′-End Processing and Function During DNA Damage. *Genes Dev* (2011) 25 (3):220–5. doi: 10.1101/gad.607011
16. Braun S, Enculescu M, Setty ST, Cortés-López M, de Almeida BP, Sutandy FXR, et al. Decoding a Cancer-Relevant Splicing Decision in the RON Proto-Oncogene Using High-Throughput Mutagenesis. *Nat Commun* (2018) 9 (1):3315. doi: 10.1038/s41467-018-05748-7
17. Panelli D, Lorusso FP, Papa F, Panelli P, Stella A, Caputi M. The Mechanism of Alternative Splicing of the X-Linked NDUFB11 Gene of the Respiratory Chain Complex I, Impact of Rotenone Treatment in Neuroblastoma Cells. *Biochim Biophys Acta* (2013) 1829(2):211–8. doi: 10.1016/j.bbagrm.2012.12.001
18. Zong L, Hattori N, Yasukawa Y, Kimura K, Mori A, Seto Y, et al. LINC00162 Confers Sensitivity to 5-Aza-2'-Deoxycytidine Via Modulation of an RNA Splicing Protein, HNRNPH1. *Oncogene* (2019) 38(26):5281–93. doi: 10.1038/s41388-019-0792-8
19. Quintás-Cardama A, Cortes J. Molecular Biology of bcr-abl1-positive Chronic Myeloid Leukemia. *Blood* (2009) 113(8):1619–30. doi: 10.1182/blood-2008-03-144790
20. Michael W, Neil P, Jessica K, Ellin B, Ravi B, Bhavana B, et al. Chronic Myeloid Leukemia, Version 2.2021, NCCN Clinical Practice Guidelines in Oncology. *J Natl Compr Canc Netw* (2020) 18(10):1385–415. doi: 10.6004/jnccn.2020.0047

21. Zhang X, Yang L, Liu X, Nie Z, Wang X, Pan Y. Haematology, Research on the Epigenetic Regulation Mechanism of the PTPN6 Gene in Advanced Chronic Myeloid Leukaemia. *Br J Haematol* (2017) 178(5):728–38. doi: 10.1111/bjh.14739
22. Wang LX, Wang JD, Chen JJ, Long B, Liu LL, Tu XX, et al. Aurora A Kinase Inhibitor Aki603 Induces Cellular Senescence in Chronic Myeloid Leukemia Cells Harboring T315i Mutation. *Sci Rep* (2016) 6:35533. doi: 10.1038/srep35533
23. Neckles C, Boer RE, Aboreden N, Cross AM, Walker RL, Kim B, et al. HNRNPH1-Dependent Splicing of a Fusion Oncogene Reveals a Targetable RNA G-Quadruplex Interaction. *RNA* (2019) 25(12):1731–50. doi: 10.1261/rna.072454.11920
24. Wang Y, Zhu Z, Church TD, Lugogo NL, Que LG, Francisco D, et al. SHP-1 as a Critical Regulator of Mycoplasma Pneumoniae-Induced Inflammation in Human Asthmatic Airway Epithelial Cells. *J Immunol* (2012) 188(7):3371–81. doi: 10.4049/jimmunol.1100573.I. to T Kwon HY, Zimdahl.
25. Li ZY, Yang L, Liu XJ, Wang XZ, Pan YX, Luo JM. The Long Noncoding RNA MEG3 and Its Target Mir-147 Regulate Jak/Stat Pathway in Advanced Chronic Myeloid Leukemia. *EBioMedicine* (2018) 34:61–75. doi: 10.1016/j.ebiom.2018.07.013
26. Li Z, Yang L, Liu X, Nie Z, Luo J. Long Noncoding RNA MEG3 Inhibits Proliferation of Chronic Myeloid Leukemia Cells by Sponging MicroRNA21. *BioMed Pharmacother* (2018) 104:181–92. doi: 10.1016/j.biopha.2018.05.047
27. Nie ZY, Yao M, Yang Z, Yang L, Liu XJ, Yu J, et al. De-Regulated STAT5A/miR-202-5p/USP15/Caspase-6 Regulatory Axis Suppresses CML Cell Apoptosis and Contributes to Imatinib Resistance. *J Exp Clin Cancer Res* (2020) 39(1):17. doi: 10.1186/s13046-019-1502-7
28. Kang D, Lee Y, Lee JS. Rna-Binding Proteins in Cancer: Functional and Therapeutic Perspectives. *Cancers (Basel)* (2020) 12(9):2699. doi: 10.3390/cancers12092699
29. Licatalosi DD, Darnell RB. RNA Processing and its Regulation: Global Insights Into Biological Networks. %J Nature Reviews Genetics. *Nat Rev Genet* (2010) 11(1):75–87. doi: 10.1038/nrg2673
30. Ge Y, Schuster MB, Pundhir S, Rapin N, Bagger FO, Sidiropoulos N, et al. The Splicing Factor RBM25 Controls MYC Activity in Acute Myeloid Leukemia. *Nat Commun* (2019) 10(1):172. doi: 10.1038/s41467-018-08076-y
31. Gallardo M, Lee HJ, Zhang X, Bueso-Ramos C, Pageon LR, McArthur M, et al. Hnrnp K Is a Haploinsufficient Tumor Suppressor That Regulates Proliferation and Differentiation Programs in Hematologic Malignancies. *Cancer Cell* (2015) 28(4):486–99. doi: 10.1016/j.ccell.2015.09.001
32. Ji D, Zhang P, Ma W, Fei Y, Xue W, Wang Y. Oncogenic Heterogeneous Nuclear Ribonucleoprotein D-like Modulates the Growth and Imatinib Response of Human Chronic Myeloid Leukemia CD34 Cells Via Pre-B-cell Leukemia Homeobox 1. *Oncogene* (2020) 39(2):443–53. doi: 10.1038/s41388-019-0998-9
33. Liang Y, Tebaldi T, Rejeski K, Joshi P, Stefani G, Taylor A, et al. SRSF2 Mutations Drive Oncogenesis by Activating a Global Program of Aberrant Alternative Splicing in Hematopoietic Cells. *Leukemia* (2018) 32(12):2659–71. doi: 10.1038/s41375-018-0152-710.1038/s41375-018-0152-7
34. Eiring AM, Harb JG, Neviani P, Garton C, Oaks JJ, Spizzo R, et al. miR-328 Functions as an RNA Decoy to Modulate Hnrnp E2 Regulation of mRNA Translation in Leukemic Blasts. *Cell* (2010) 140(5):652–65. doi: 10.1016/j.cell.2010.01.007
35. Du Q, Wang L, Zhu H, Zhang S, Xu L, Zheng W, et al. The Role of Heterogeneous Nuclear Ribonucleoprotein K in the Progression of Chronic Myeloid Leukemia. *Med Oncol* (2010) 27(3):673–9. doi: 10.1007/s12032-009-9267-z
36. Chang JS, Santhanam R, Trotta R, Neviani P, Eiring AM, Briercheck E, et al. High Levels of the BCR/ABL Oncoprotein Are Required for the MAPK-hnRNP-E2 Dependent Suppression of C/EBPalpha-driven Myeloid Differentiation. *Blood* (2007) 110(3):994–1003. doi: 10.1182/blood-2007-03-078303
37. Brandimarte L, Pierini V, Di Giacomo D, Borga C, Nozza F, Gorello P, et al. New MLLT10 Gene Recombinations in Pediatric T-acute Lymphoblastic Leukemia. *Blood* (2013) 121(25):5064–7. doi: 10.1182/blood-2013-02-487256
38. Yamazaki T, Liu L, Conlon E, Manley JL. TCF3Burkitt Lymphoma-Related Mutations Alter TCF3 Alternative Splicing by Disrupting hnRNPH1 Binding. *RNA Biol* (2020) 17(10):1383–90. doi: 10.1080/15476286.2020.1772559
39. Yamazaki T, Liu L, Manley JLJR. Tcf3 Mutually Exclusive Alternative Splicing Is Controlled by Long Range Cooperative Actions Between hnRNPH1 and PTBP1. *RNA* (2019) 25(11):1497–508. doi: 10.1261/rna.072298.119
40. Amin HM, Hoshino K, Yang H, Lin Q, Lai R, Garcia-Manero G. Pathology, Decreased Expression Level of SH2 Domain-Containing Protein Tyrosine Phosphatase-1 (Shp1) Is Associated With Progression of Chronic Myeloid Leukaemia. *J Pathol* (2007) 212(4):402–10. doi: 10.1002/path.2178
41. Huelga SC, Vu AQ, Arnold JD, Liang TY, Liu PP, Yan BY, et al. Integrative Genome-Wide Analysis Reveals Cooperative Regulation of Alternative Splicing by hnRNP Proteins. *Cell Rep* (2012) 1(2):167–78. doi: 10.1016/j.celrep.2012.02.001
42. Lan X, Zhao C, Chen X, Zhang P, Zang D, Wu J, et al. Nickel Pyrithione Induces Apoptosis in Chronic Myeloid Leukemia Cells Resistant to Imatinib Via Both Bcr/Abl-dependent and Bcr/Abl-independent Mechanisms. *J Hematol Oncol* (2016) 9(1):129. doi: 10.1186/s13045-016-0359-x
43. Tao T, Yang X, Zheng J, Feng D, Qin Q, Shi X, et al. PDZK1 Inhibits the Development and Progression of Renal Cell Carcinoma by Suppression of SHP-1 Phosphorylation. *Oncogene* (2017) 36(44):6119–31. doi: 10.1038/onc.2017.199
44. Jiang LC, Luo JM. Role and Mechanism of Decitabine Combined With Tyrosine Kinase Inhibitors in Advanced Chronic Myeloid Leukemia Cells. *Oncol Lett* (2017) 14(2):1295–302. doi: 10.3892/ol.2017.6318
45. Gagné JP, Hunter JM, Labrecque B, Chabot B, Poirier GG. A Proteomic Approach to the Identification of Heterogeneous Nuclear Ribonucleoproteins as a New Family of Poly(ADP-Ribose)-Binding Proteins. *Biochem J* (2003) 371(Pt 2):331–40. doi: 10.1042/BJ20021675
46. Harrision D, Gravells P, Thompson R, Bryant HE. Poly(Adp-Ribose) Glycohydrolase (PARG) *vs.* Poly(ADP-Ribose) Polymerase (Parp) - Function in Genome Maintenance and Relevance of Inhibitors for Anti-Cancer Therapy. *Front Mol Biosci* (2020) 7:191. doi: 10.3389/fmolb.2020.00191

Conflict of Interest: The authors declare that the research was conducted in the absence of any commercial or financial relationships that could be construed as a potential conflict of interest.

frontiers in Oncology

ORIGINAL RESEARCH
published: 06 July 2021
doi: 10.3389/fonc.2021.694021

Long Non-Coding RNA LINC00152 Regulates Self-Renewal of Leukemia Stem Cells and Induces Chemo-Resistance in Acute Myeloid Leukemia

Chunhong Cui[1,2], Yan Wang[3], Wenjie Gong[4], Haiju He[4], Hao Zhang[3], Wei Shi[3†] and Hui Wang[1*†]*

[1] Shanghai University of Medicine and Health Sciences Affiliated Zhoupu Hospital, Shanghai, China, [2] Laboratory of Tumor Molecular Biology, School of Basic Medical Sciences, Shanghai University of Medicine and Health Sciences, Shanghai, China, [3] Huashan Hospital, Fudan University, Shanghai, China, [4] Department of Hematology, First Affiliated Hospital of Soochow University, Suzhou, China

OPEN ACCESS

Edited by:
Mina Luqing Xu,
Yale University, United States

Reviewed by:
Deepshi Thakral,
All India Institute of Medical Sciences, India
Michael Diamantidis,
University Hospital of Larissa, Greece

***Correspondence:**
Wei Shi
shiwei@fudan.edu.cn
Hui Wang
wangh_19@sumhs.edu.cn

†These authors have contributed equally to this work

Specialty section:
This article was submitted to Hematologic Malignancies, a section of the journal Frontiers in Oncology

Received: *12 April 2021*
Accepted: *11 June 2021*
Published: *06 July 2021*

Citation:
Cui C, Wang Y, Gong W, He H, Zhang H, Shi W and Wang H (2021) Long Non-Coding RNA LINC00152 Regulates Self-Renewal of Leukemia Stem Cells and Induces Chemo-Resistance in Acute Myeloid Leukemia. Front. Oncol. 11:694021. doi: 10.3389/fonc.2021.694021

Relapse of acute myeloid leukemia (AML) has a very poor prognosis and remains a common cause of treatment failure in patients with this disease. AML relapse is partially driven by the chemoresistant nature of leukemia stem cells (LSCs), which remains poorly understood, and our study aimed at elucidating the underlying mechanism. Accumulating evidences show that long noncoding RNAs (lncRNAs) play a crucial role in AML development. Herein, the lncRNA, LINC00152, was identified to be highly expressed in $CD34^+$ LSCs and found to regulate the self-renewal of LSCs derived from AML patients. Importantly, LINC00152 upregulation was correlated with the expression of 16 genes within a 17-gene LSC biomarker panel, which contributed to the accurate prediction of initial therapy resistance in AML. Knockdown of LINC00152 markedly increased the drug sensitivity of leukemia cells. Furthermore, LINC00152 expression was found to be correlated with poly (ADP-ribose) polymerase 1 (PARP1) expression in AML, whereas LINC00152 knockdown significantly decreased the expression of PARP1. Upregulation of LINC00152 or PARP1 was associated with poor prognosis in AML patients. Collectively, these data highlight the importance and contribution of LINC00152 in the regulation of self-renewal and chemoresistance of LSCs in AML.

Keywords: leukemia stem cells, LINC00152, poly (ADP-ribose) polymerase 1, chemo-resistance, leukemia

INTRODUCTION

Acute myeloid leukemia (AML) is a heterogeneous and deadly disease characterized by aberrant myeloid lineage cell proliferation and differentiation (1). Although most AML patients achieve remission, up to 70% of adults and 30% of pediatric patients do not survive beyond 5 years after the initial clinical response due to relapse (2). Historically, the relapse of AML patients has been attributed to the pre-existence of chemoresistant leukemia stem cells (LSCs) (3, 4). Nevertheless, the mechanisms underlying LSC-mediated leukemia relapse have not been elucidated. Leukemia cells differentiate from LSCs (5), which have the capacity to initiate leukemia in immunocompromised mice. Therefore, it is warranted to investigate potential factors contributing to the self-renewal and chemoresistant nature of LSCs.

Long noncoding RNAs (lncRNAs) have been identified in whole transcriptome sequencing projects, such as gene expression profiling interactive analysis (GEPIA). The established functions of lncRNAs include cell cycle regulation, lineage differentiation, and cancer progression (6–8). Deregulated expression of lncRNAs often occurs in AML (9, 10), which has been reported to be independently associated with AML patient prognosis (9, 11, 12). Although lncRNAs have been identified to regulate leukemia progression (13–15), their detailed role in chemoresistance remains unknown. LINC00152 is an lncRNA located at chromosome 2p11.2. Recently, LINC00152 was identified as a potent oncogene in various cancers (16, 17). In particular, LINC00152 expression has been reported to be upregulated in AML samples and facilitate AML leukemogenesis (18); nevertheless, its underlying mechanism needs to be further investigated.

Considering the high expression of LINC00152 in $CD34^+$ LSCs and its regulatory role in LSC self-renewal, we hypothesized that LIN00152 could have biological significance in LSC chemoresistance, and the present study was performed with an aim to elucidate this significance. The inhibition of LINC00152 was found to increase the sensitivity of leukemia cells to doxorubicin. Furthermore, LINC00152 expression was correlated with the expression of poly [ADP-ribose] polymerase 1 (PARP1), whereas LINC00152 knockdown markedly decreased PARP1 expression. Thus, our results indicate that LINC00152 may serve as a potential prognostic marker for AML patients.

MATERIAL AND METHODS

Cell Culture

Cell lines were purchased from the American Type Culture Collection (Manassas, VA, USA) and were cultured in a humidified incubator at 37°C and 5% CO_2. 293T cells (ATCC CRL-3216) were cultured in Iscove's modified Dulbecco's medium (Thermo Fisher Scientific, Waltham, MA, USA) containing 10% fetal bovine serum (FBS) (Biochrom GmbH, Berlin, Germany) and digested with trypsin-EDTA (Sigma-Aldrich, St. Louis, MO, USA). K562 cells (ATCC CCL-243) were cultured in RPMI-1640 (Sigma-Aldrich) supplemented with 10% FBS (Biochrom GmbH). Cells were grown in log-phase (1×10^5–1×10^6 cells/ml).

Bone Marrow Cells Isolation

Bone marrow specimens were collected from 15 adult AML patients and analyzed after obtaining written informed consent in accordance with the Declaration of Helsinki.

Bone marrow cells were obtained at the diagnosis of adult patients with AML assessed at the Huashan Hospital of Fudan University, Shanghai, China. Bone marrow samples were collected in 10-ml syringes with 10.000IE/20 ml heparin after bone marrow puncture.

Flow Cytometry

Bone marrow cells were incubated with Alexa Fluor 488 anti-human CD34 antibody and phycoerythrin anti-human CD38 antibody (both from Biolegend, San Diego, CA, USA) diluted in magnetic-activated cell sorting buffer for 15 min on ice. The staining process was performed under a hood in the dark. After incubation, the cells were washed with phosphate-buffered saline (PBS). Stained cells were kept on ice before sorting. The concentration of the cells was adjusted to approximately 1×10^6 cells/ml. Sorted cells were collected and freshly filtered, with PBS containing 2% FBS used as the catch medium. Acquisition was performed using an LSR II flow cytometer (BD Biosciences, Franklin Lakes, NJ, USA). FlowJo software (BD Biosciences) was used for data analysis.

Colony Formation Assay

Methylcellulose (Stemcell Technologies, Vancouver, BC, Canada) was placed at room temperature for 30 min before usage. Each selected human LSC was adjusted to a concentration that was 10-fold higher than the final plating concentration. The cell suspension (300 µl) was mixed well with 3-ml methylcellulose at a density of 300 cells per ml of methylcellulose. After removing the air bubbles, the mixture was transferred to a 12-well plate with three replicates for each cell. Colonies (> 50 cells) were stained with trypan blue and counted under a microscope after 10 days.

Small Hairpin RNA (shRNA) and Plasmid Cloning

LINC00152 shRNAs were cloned into the pLKO.1_GFP vector with *Bam*HI and *Age*I restriction sites. The hairpin was synthesized by Sangon Biotech. The empty vector was recovered after digestion with *Bam*HI and *Age*I. The annealed hairpin and digested vector were ligated with T4 ligase (Thermo Fisher Scientific), and the ligating product was then transformed into *Escherichia coli*. The shRNA-targeting sequences were as follows: forward, CACAGCCGGAATGCAGCTGAA and reverse, CCACTGTGGACTCTGAGGCCT.

Lentivirus Package and Leukemia Cell Infection

PLKO.1_GFP vector and packaging vectors (PLP1, PLP2, and VSVG) were transfected into 293T cells using Turbofect reagent (Thermo Fisher Scientific). After 48 h, supernatants with lentivirus particles were collected by ultracentrifugation. AML cells were transduced by incubation with the viral particles in the presence of polybrene (8 µg/ml, Sigma-Aldrich). The viral titers were then determined by flow cytometry 48 h following transduction.

RNA Isolation, Reverse Transcription, and Quantitative Real-Time Polymerase Chain Reaction (qRT-PCR)

AML cells were prepared by centrifugation, and total RNA was isolated using TRIzol reagent (Thermo Fisher Scientific), followed by removal of genomic DNA. Complementary DNA was reverse transcribed using PrimeScript RT Reagent Kit (Thermo Fisher Scientific). qRT-PCR was performed with SYBR Green Master Mix (Bio-Rad, Hercules, CA, USA) on a StepOnePlus Real-Time PCR system (Thermo Fisher Scientific). The primers used for targeting *LINC00152* were (forward) TGGCACAGTCTTTTCTCTACTCA and (reverse) TCAAGA GGTTTCCAGGGGCT, whereas for *PARP1* they were (forward) ACTGACATAGAGAAAAGGCTGGAG and (reverse) GGGGAA ACCAGTAAGGCAGAC.

Drug Sensitivity Assay

K562 cells (control and LINC00152 shRNA) were seeded onto 24-well plates at a density of 2.5×10^4 viable cells/well in triplicate and treated with doxorubicin at the indicated concentrations. Cells were counted and analyzed after 3 days using a cell counting plate under a microscope.

Statistical Analyses

Statistical analyses were performed using SPSS version 22 (IBM Corp., Armonk, NY, USA) and R studio 3.5.0 (R Foundation, Vienna, Austria). Student's *t*-test or one-way analysis of variance (ANOVA) was used to identify statistical significance. For Kaplan–Meier survival analysis, the log-rank test was used to determine statistical significance. Statistical significance was set at $P < 0.05$.

RESULTS

LINC00152 Is Highly Expressed in LSCs and Correlated With Poor AML Patient Prognosis

Evidence from a previous study suggests that $CD34^+CD38^-$ stem cells are the leading cause of chemoresistance (19). To investigate the role of this stem cell population in AML, bone marrow cells from 15 paired AML patients were collected, and the $CD34^+CD38^-$ and $CD34^-CD38^+$ subpopulations were sorted using flow cytometry (**Figure 1A**). Notably, $CD34^+CD38^-$ cells possessed a markedly stronger capacity for colony formation than $CD34^-CD38^+$ cells derived from paired 15 AML patients ($P = 5.4 \times 10^{-13}$) (**Figure 1B**). qRT-PCR showed that *LINC00152* was highly expressed in $CD34^+CD38^-$ cells compared with $CD34^-CD38^+$ subpopulations ($P = 0.02$) (**Figure 1C**). Furthermore, GEPIA, based on The Cancer Genome Atlas (TCGA) data, was performed to determine the functions of LINC00152. Overall, high expression of *LINC00152* was associated with poor AML patient survival (**Figure 1D**), suggesting that LINC00152 may be a potential prognostic marker for AML.

Correlation Between LINC00152 and LSC-Associated Gene Expression

Comprehensive analysis of LSC gene expression signatures was previously performed in 78 AML patients and validated by xenotransplantation, which generated a 17-gene LSC (LSC17) biomarker panel (*ZBTB46*, *SOCS2*, *SMIM24*, *NGFRAP1*, *MMRN1*, *LAPTM4B*, *DNMT3B*, *CPXM1*, *AKR1C3*, *CDK6*, *CD34*, *ARHGAP22*, *GPR56*, *NYNR1N*, *KIAA0125*, *EMP1*, and *DPYSL3*). Moreover, Ng *et al.* reported that patients with high LSC17 scores had poor prognosis with current treatments, including allogeneic stem cell transplantation (20). To test whether *LINC00152* expression correlates with the LSC17 gene signature, GEPIA was performed, which revealed that the expression of 15 of the 17 genes was significantly associated with that of *LINC00152* (**Figure 2**). Two uncorrelated genes (*EMP1*, $P = 0.6$; and *DPYSL3*, $P = 0.69$) are not shown. These results suggest an important role of LINC00152 in leukemic stemness.

Repression of Colony Formation by LINC00152 Knockdown In $CD34^+$ AML Cells

LINC00152 upregulation in LSCs and the observed correlation between LINC00152 and the LSC17 biomarker profile suggested its possible biological contribution toward the stemness of LSCs. To explore the influence of LINC00152 on LSC stemness, knockdown of LINC00152 using targeted shRNAs (sh00152#1 and sh00152#2) was performed. qRT-PCR analysis confirmed that both shRNAs significantly decreased the expression of *LINC00152* compared with control non-targeted shRNA (**Figure 3A**). Colony formation assay is a well-characterized and validated method to assess the differentiation and proliferation ability of primitive hematopoietic cells. Herein, this assay was performed with cells lacking LINC00152. Knockdown of *LINC00152* led to a significant decrease in the colony formation capacity of $CD34^+$ cells derived from three AML patients (**Figures 3B–D**), indicating that LINC00152 regulates the self-renewal of LSCs.

LINC00152 Regulates LSC Chemoresistance Via PARP1

Chemotherapy based on doxorubicin, an anthracycline, remains the standard line of treatment for leukemia (21). As previously described, chemoresistant LSCs partially induce leukemia relapse (3, 4). Whether LINC00152 can regulate the chemoresistance of LSCs to doxorubicin was next investigated. The drug sensitivity curve indicated that *LINC00152* knockdown markedly reduced the chemoresistance of K562 cells to doxorubicin (**Figure 4A**).

PARP1 has been reported to play an important role in DNA damage repair, and its expression is correlated with poor prognosis in AML (22). Moreover, PARP1 inhibition has exhibited the potential to enhance immunotherapy efficacy in AML (23). Thus, whether LINC00152 can regulate the chemoresistance of LSCs through PARP1 was investigated. qRT-PCR analysis confirmed that *PARP1* expression in AML cells was significantly decreased upon *LINC00152* knockdown (**Figures 4B, C**). Moreover, *PARP1* was found to be highly expressed in $CD34^+CD38^-$ subpopulation compared with $CD34^-CD38^+$ cells derived from five AML patients ($P = 0.0024$) (**Figure 4D**). GEPIA further showed that the expression of *LINC00152* was highly correlated with that of *PARP1* (**Figure 4E**). Publicly available microarray data sets were also used to compare *PARP1* expression between $CD34^+$ and $CD34^-$ cells in AML patients. Overall, *PARP1* was found to be highly expressed in $CD34^+$ cells (paired $CD34^+$ vs. $CD34^-$ subpopulations from 44 AML patients; GSE30029) (**Figure 4F**), as well as in $CD34^+CD38^-$ cells, compared with $CD34^-CD38^+$ cells ($CD34^-CD38^+$ subpopulations from 54 AML patients vs. $CD34^-CD38^+$ cells from 69 AML patients; GSE76008) (**Figure 4G**). Accordingly, PARP1 overexpression was associated with poor prognosis in AML patients (**Figure 4H**). Altogether, these data suggest that LINC00152 modulates the chemoresistance of AML through PARP1.

To further explore the potential mechanism through which LINC00152 and PARP1 modulate the chemoresistance of LSCs, Gene Ontology (GO) analysis *via* gene set enrichment analysis was

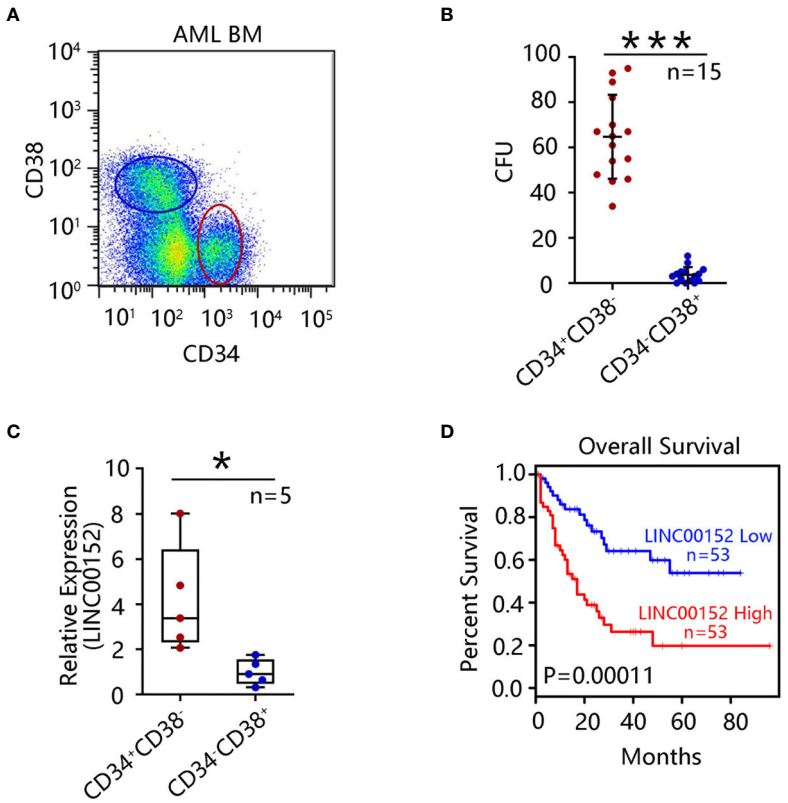

FIGURE 1 | LINC00152 expression is upregulated in leukemia stem cells (LSCs). **(A)** $CD34^+CD38^-$ and $CD34^-CD38^+$ cell subpopulations were sorted by flow cytometry from 15 acute myeloid leukemia (AML) patients. **(B)** Colony formation assay using sorted $CD34^+CD38^-$ and $CD34^-CD38^+$ cells was performed and the mean number of clone forming units was analyzed. Data are presented as the mean ± SEM of three independent experiments (***$P < 0.001$). **(C)** *LINC00152* expression in $CD34^+CD38^-$ and $CD34^-CD38^+$ cells derived from five AML patients. Data are represented as the mean ± SD of three independent experiments (*$P < 0.05$). **(D)** Correlation between overall survival of AML patients and *LINC00152* expression (based on a publicly available data set by gene expression profiling interactive analysis (***$P < 0.001$).

performed. The results of GO analysis showed that both LINC00152 and PARP1 were enriched in processes associated with DNA damage repair-related signaling, such as nucleotide-excision repair preincision complex stabilization, nucleotide-excision repair, DNA duplex unwinding, and global genome nucleotide-excision repair (GSE76009) (**Figures 5A–F** and **Table 1**).

DISCUSSION

LSCs are the most important contributors toward drug resistance and disease relapse in AML, with the proportion of LSCs in patients with AML being closely related to poor prognosis (20). A better understanding of the regulatory mechanisms of LSCs is necessary to effectively combat AML. In recent years, lncRNAs have been reported to play a key role in the growth and differentiation of cancer stem cells, in addition to being involved in cancer metastasis and drug resistance development (24, 25). Hence, the field of lncRNAs has attracted increasing attention, with drug development targeting lncRNAs emerging as a new direction. Theoretically, targeting lncRNAs can be achieved through blocking or knockdown by either antisense oligonucleotides (ASOs) or small interfering RNAs (siRNAs). However, the specific transport of ASOs or siRNAs to target cells and ensuring their stability remain considerably challenging (26).

In this study, it was confirmed that $CD34^+CD38^-$ cells from AML patients possess strong LSC characteristics and tumor formation potential. Moreover, high expression of *LINC00152* was found to be significantly correlated with the poor prognosis of AML patients. Indeed, *LINC00152* expression was significantly correlated with that of 15 genes within 17 biomarker genes, which could accurately determine the drug resistance of AML patients. Furthermore, the present experimental data revealed that *LINC00152* expression was significantly increased in $CD34^+CD38^-$ cells and that its knockdown significantly reduced the colony formation ability of LSCs obtained from three AML patients. Taken together, these data indicate that the self-renewal ability of LSCs is greatly modulated by LINC00152, but the underlying mechanism requires further clarification.

LINC00152 is a large intergenic noncoding RNA with a length of 852 bp, located on chromosome 11.2 of genome 2 (16). Recent studies have shown that LINC00152 is highly expressed in various tumors, such as glioma, non-small cell lung cancer, and gastric cancer. Upregulated LINC00152 interacts with several signaling pathways,

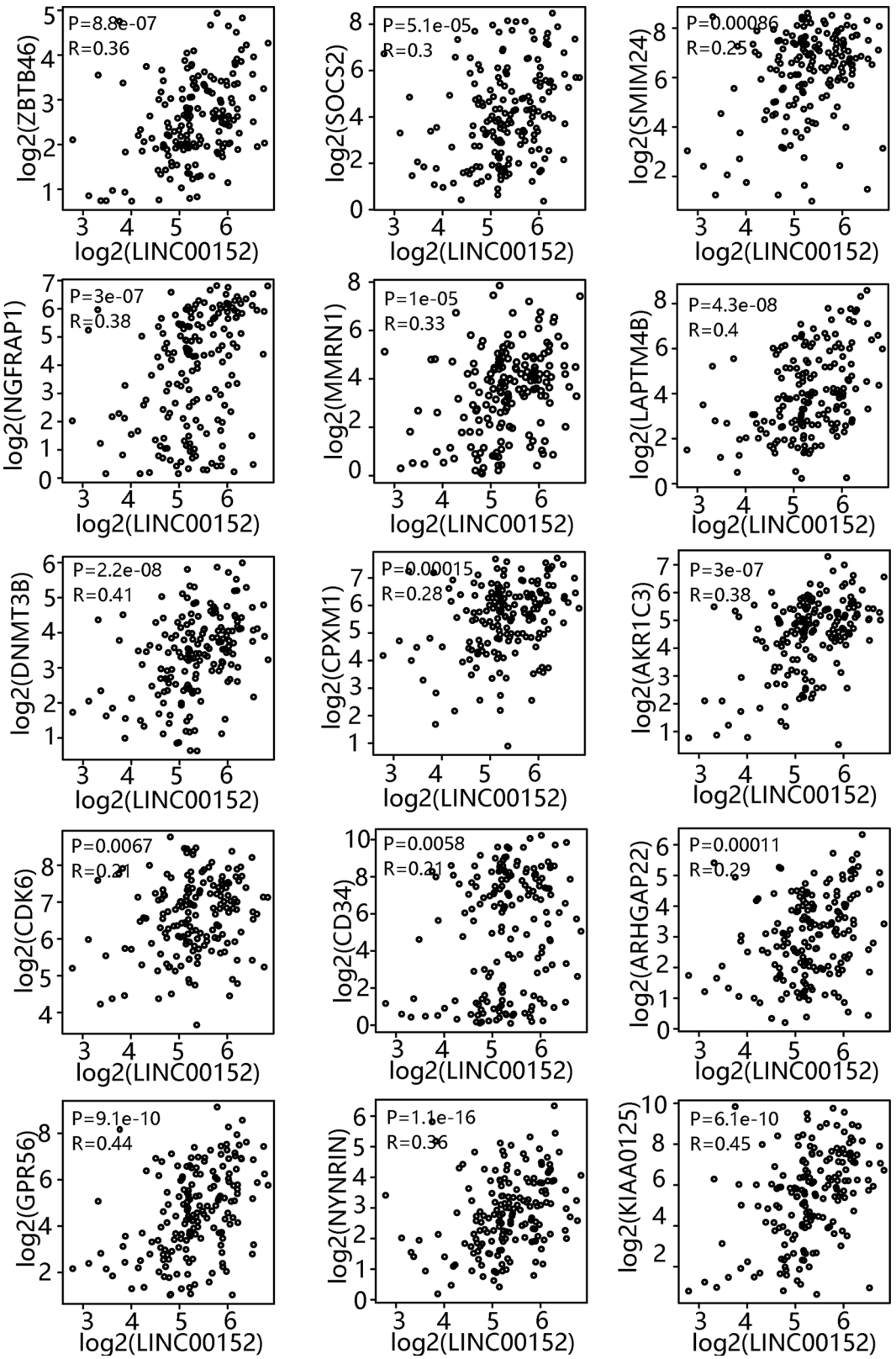

FIGURE 2 | Correlation between LINC00152 expression and leukemia stem cell (LSC)-associated gene expression. LSC17 biomarker gene profile and *LINC00152* expression were analyzed based on a publicly available data set (GSE76009) by gene expression profiling interactive analysis.

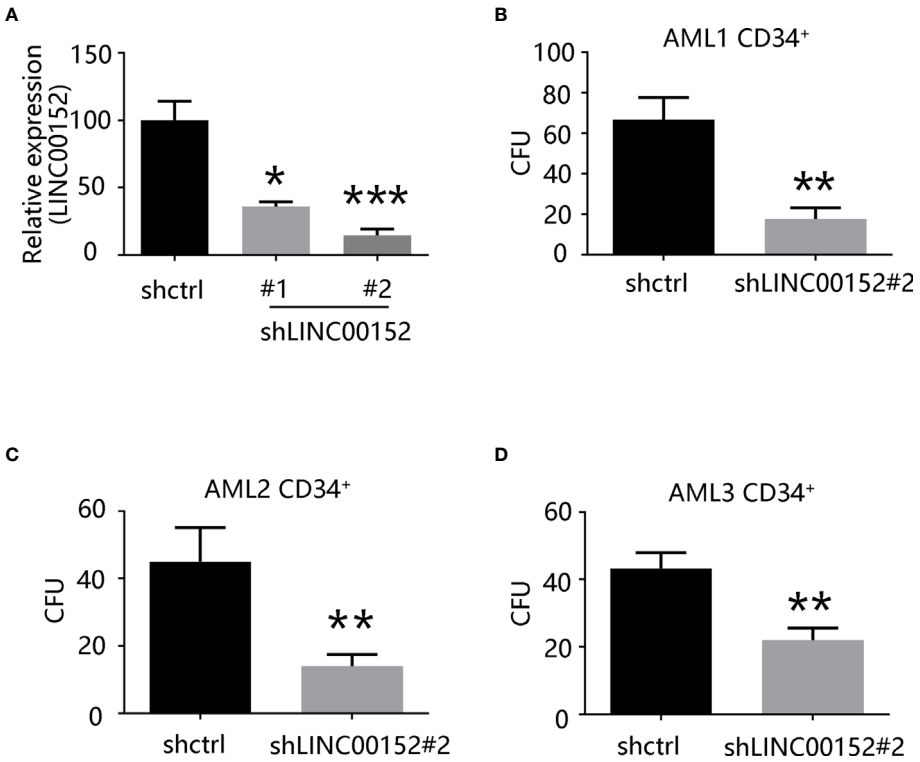

FIGURE 3 | LINC00152 knockdown decreases the capacity of colony formation of LSCs. **(A)** *LINC00152* expression in cells transfected with short hairpin RNAs (shCTRL or sh00152s) (*$P < 0.05$, ***$P < 0.001$). **(B–D)** Quantification of colony formation derived from three acute myeloid leukemia patients. Data are presented as the mean ± SEM of three independent experiments (*$P < 0.05$, **$P < 0.01$).

thereby promoting inflammatory responses as well as tumor cell proliferation, invasion, and metastasis (27–30). Recent studies have also reported that LINC00152 knockdown suppresses proliferation, accelerates apoptosis, and induces cycle arrest in AML cells (18).

Herein, the expression of *PARP1* was found to be significantly decreased when *LINC00152* was downregulated. PARP1 is mainly involved in DNA damage repair and is overexpressed in cancer stem cells. Previous studies have reported that high PARP1 expression is associated with poor AML prognosis (3) and the treatment with the PARP1 inhibitor enhances anti-AML effects (22). This is consistent with the results presented herein, which demonstrate that *PARP1* is highly expressed in LSCs and that its expression is significantly correlated with that of LINC00152 in AML. Additionally, the findings revealed that high *PARP1* expression was correlated with poor overall survival in AML. Moreover, along with the knockdown of *LINC00152*, *PARP1* expression was significantly decreased, which in turn increased the sensitivity of cancer cells to the DNA damaging agent doxorubicin. Consistently, GO analysis showed that genes of LINC00152 and PARP1 were mainly enriched in processes associated with DNA damage repair-related signaling, such as nucleotide-excision repair, preincision complex stabilization, nucleotide-excision repair, DNA duplex unwinding, and global genome nucleotide-excision repair. Chemotherapy is the standard treatment for AML; however, the prognosis of AML patients who relapse remains poor. Our study will be useful for exploring novel targets to induce DNA damage and perturb cellular DNA damage repair. However, our results contrast with data from breast cancer (31), in which lncRNA H19 overexpression promoted doxorubicin resistance by downregulating PARP1 expression. Therefore, the detailed regulatory network of LINC00152 and PARP1 in AML needs to be further explored.

lncRNAs display significant expression variability and subcellular localization diversity. Accumulating evidence shows that a novel regulatory mechanism exists between lncRNAs and microRNAs. lncRNAs can act as endogenous molecular sponges to compete for the targets of the microRNAs, thereby negatively regulating the expression of microRNAs. For example, Chen et al. reported that the lncRNA UICLM could function as a competing endogenous RNA (ceRNA) for miR-215 in colorectal cancer cells to regulate the expression of ZEB1 (32), and Li et al. demonstrated that lncRNA ZFAS1 functions as an oncogene in hepatocellular carcinoma progression by binding to miR-150 and abrogating its tumor-suppressive function (33). In particular, it has been reported that LINC00152 acts as a ceRNA for miR-185-3p and miR-632 to regulate FSCN1 expression in colorectal cancer (34) cells, and recent studies have reported that ectopically expressed LINC00152 accelerates AML proliferation and targets the miR-193a/CDK9 axis to exert its effect (18). Since PARP1 is a major downstream target of miR-181a (35), LINC00152 may also regulate PARP1 through microRNAs. Furthermore, posttranslational modifications of PARP1, such as mono (ADP-ribosyl)-ation (36, 37),

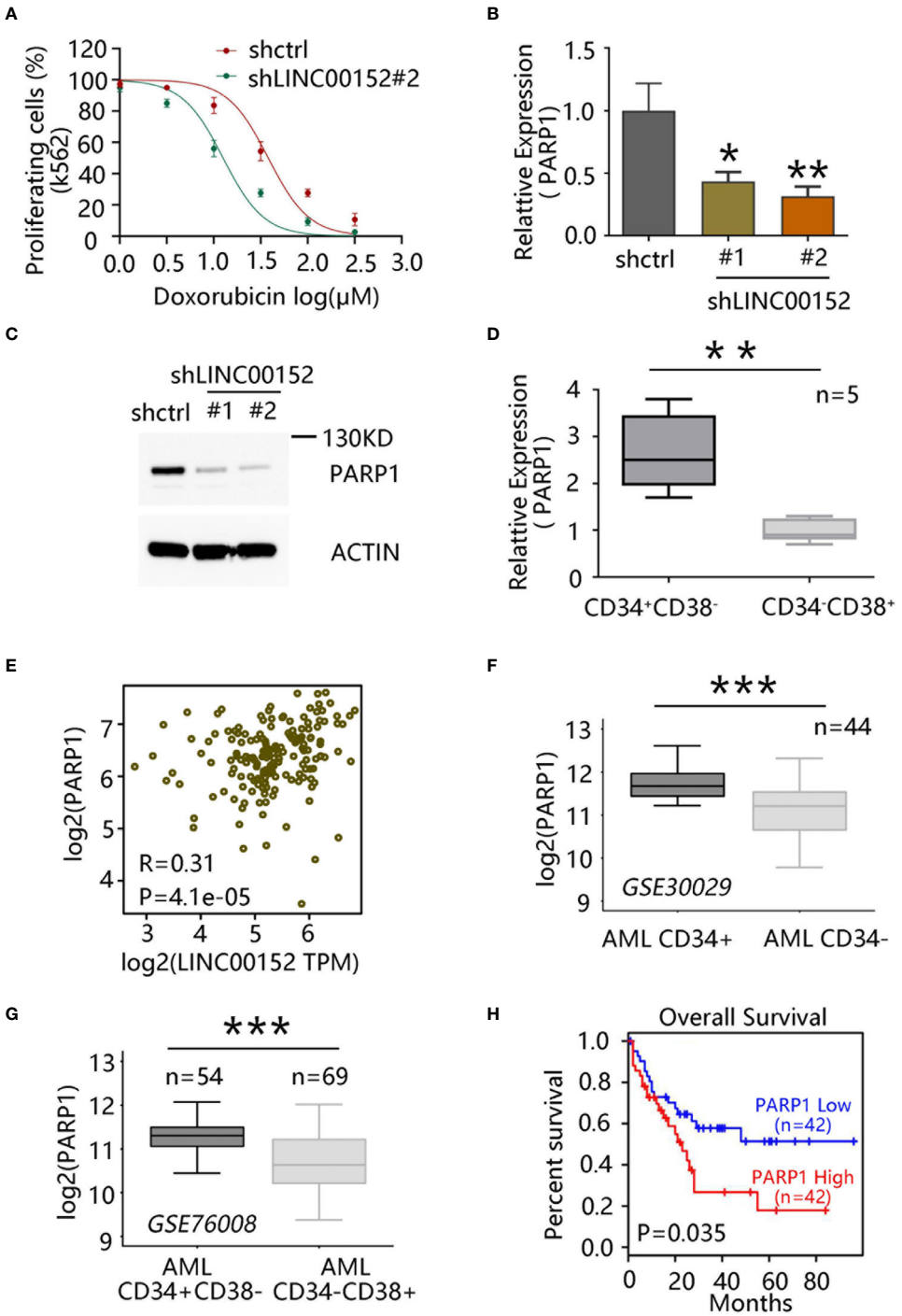

FIGURE 4 | LINC00152 regulates chemoresistance of leukemia stem cells (LSCs) *via* PARP1. **(A)** Doxorubicin sensitivity assay after *LINC00152* knockdown in K562 cells. **(B)** PARP1 mRNA level after *LINC00152* knockdown compared with control acute myeloid leukemia (AML) cells (*$P < 0.05$, **$P < 0.01$). **(C)** PARP1 expression at the protein level after *LINC00152* knockdown compared with control AML cells. **(D)** *PARP1* expression in $CD34^+CD38^-$ and $CD34^-CD38^+$ cells derived from five AML patients. Data are represented as the mean ± SD of three independent experiments (**$P < 0.01$). **(E)** Expression of *LINC00152* was correlated with that of *PARP1* in AML based on a publicly available data set by gene expression profiling interactive analysis. **(F)** *PARP1* expression in paired $CD34^+$ cells vs. $CD34^-$ cells (GSE30029, ***$P < 0.001$). **(G)** *PARP1* expression in $CD34^+CD38^-$ vs. $CD34^-CD38^+$ cells (GSE760008, ***$P < 0.001$). **(H)** Correlation between overall survival of AML patients and *PARP1* expression based on a publicly available data set (GSE76009) by gene expression profiling interactive analysis.

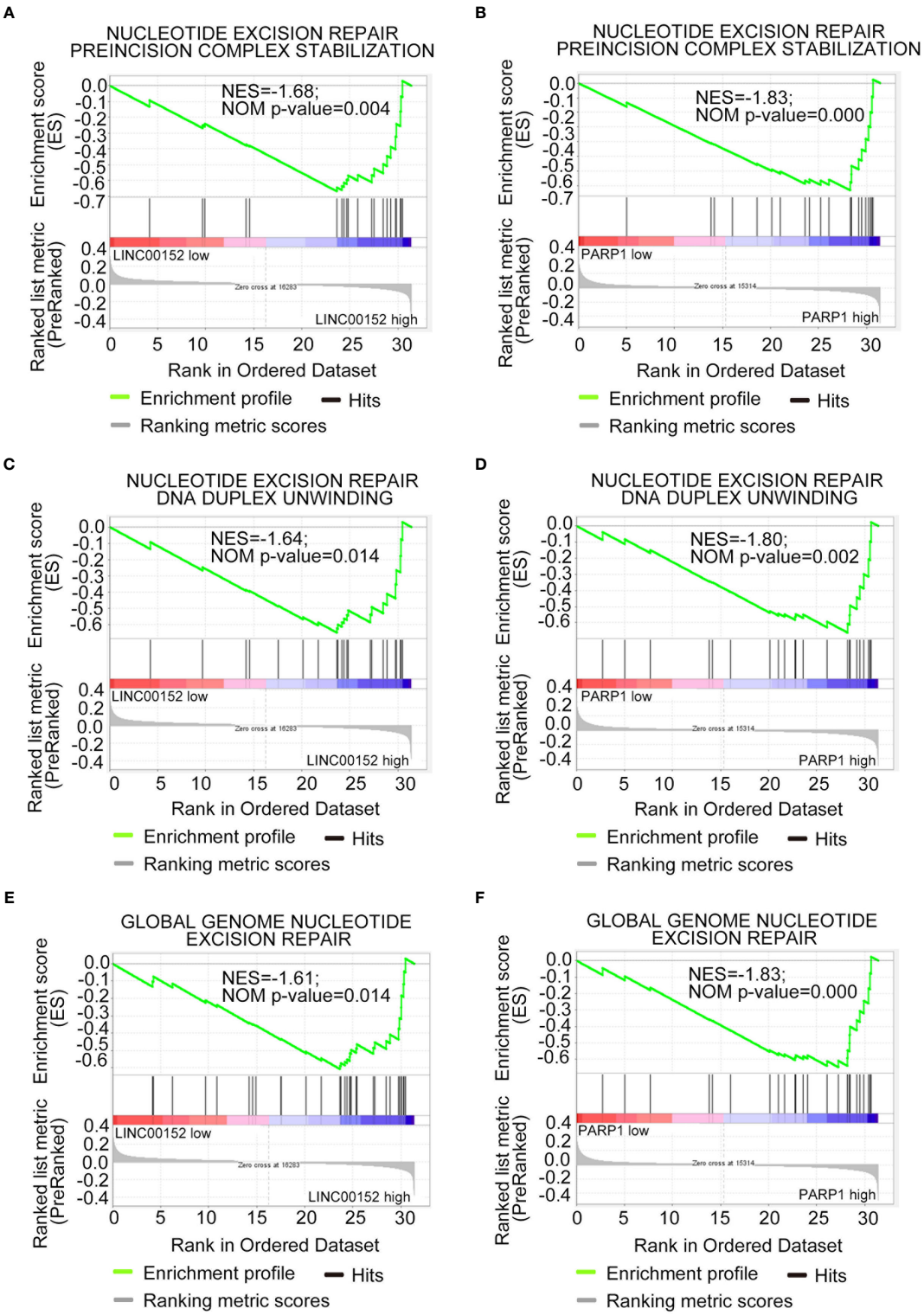

FIGURE 5 | Both *LINC00152* and *PARP1* expression correlated with DNA damage repair in acute myeloid leukemia. High expression of *LINC00152* and *PARP1* individually enriched the genes associated with nucleotide-excision repair, preincision complex stabilization **(A, B)**, nucleotide-excision repair, DNA duplex unwinding **(C, D)**, and global genome nucleotide-excision repair **(E, F)**.

TABLE 1 | Gene Ontology analysis

Gene sets enriched in phenotype (LINC00152)	P-value	Gene sets enriched in phenotype (PARP1)	P-value
NUCLEOTIDE EXCISION REPAIR PREINCISION COMPLEX ASSEMBLY	0.004	SIGNAL TRANSDUCTION INVOLVED IN REGULATION OF GENE EXPRESSION	0.004
POSITIVE REGULATION OF PROTEIN DEPOLYMERIZATION	0.002	GLOBAL GENOME NUCLEOTIDE EXCISION REPAIR	0.000
TRANSCRIPTION COUPLED NUCLEOTIDE EXCISION REPAIR	0.006	NUCLEOTIDE EXCISION REPAIR PREINCISION COMPLEX STABILIZATION	0.000
NUCLEOTIDE EXCISION REPAIR PREINCISION COMPLEX STABILIZATION	0.004	RRNA METABOLIC PROCESS	0.000
NUCLEOTIDE EXCISION REPAIR DNA INCISION	0.008	RRNA MODIFICATION	0.000
NUCLEOTIDE SUGAR METABOLIC PROCESS	0.000	EXTABLISHMENT OF PROTEIN LOCALIZATION TO TELOMERE	0.000
INTRACILIARY TRANSPORT	0.010	RIBOSOME BIOGENESIS	0.000
REGULATION OF HEMATOPOIETIC PROGENITOR CELL DIFFERENTIATION	0.000	DNA DAMAGE RESPONSE DETECTION OF DNA DAMAGE	0.000
NON RECOMBINATIONAL REPAIR	0.004	NUCLEOTIDE EXCISION REPAIR DNA DUPLEX UNWINDING	0.002
ERROR FREE TRANSLESION SYNTHESIS	0.012	TRANSLATIONAL TERMINATION	0.006
OLIGOSACCHARIDE LIPID INTERMEDIATE BIOSYNTHETIC PROCESS	0.008	MITOCHONDRIAL TRANSLATION	0.004
NUCLEOTIDE EXCISION REPAIR DNA DUPLEX UNWINDING	0.014	NCRNA PROCESSING	0.000
PURINE NUCLEOSIDE MONOPHOSPHATE METABOLIC PROCESS	0.010	GLUTAMINE METABOLIC PROCESS	0.000
HISTONE UBIQUITINATION	0.006	AMINO ACID ACTIVATION	0.006
RNA 3 END PROCESSING	0.006	NCRNA METABOLIC PROCESS	0.000
G0 TO G1 TRANSITION	0.010	PURINE NUCLEOSIDE MONOPHOSPHATE BIOSYNTHETIC PROCESS	0.000
REGULATION OF SIGNAL TRANSDUCTION BY P53 CLASS MEDIATOR	0.000	POST ANAL TAIL MORPHOGENESIS	0.004
HEMATOPOIETIC STEM CELL DIFFERENTIATION	0.004	MATURATION OF SSU RRNA FROM TRICISTRONIC RRNA TRANSCRIPT SSU RRNA 5.8S RNA LSU RRNA	0.004
MRNA 3 END PROCESSING	0.006	NEGATIVE REGULATION OF TELOMERE MAINTENANCE	0.004
GLOBAL GENOME NUCLEOTIDE EXCISION REPAIR	0.014	RIBONUCLEOPROTEIN COMPLEX BIOGENESIS	0.004

The highlights mean the same signalling enriched in LINC00152 and PARP1.

phosphorylation, methylation, and acetylation, can modulate its activity. Thus, LINC00152 may influence PARP1 posttranslational modification by binding to the enhancer of zeste homologue 2 (EZH2) (38) or participate in the phosphatidylinositol 3-kinase/AKT signaling pathway (39), which may also be important for PARP1 expression and activity.

In conclusion, our study shows that *LINC00152* is highly expressed in LSCs and correlated with *PARP1* expression, with the inhibition of LINC00152 leading to the downregulation of *PARP1*. Moreover, expression of LINC00152 or PARP1 is associated with poor prognosis in AML patients. Functionally, it can be speculated that LINC00152 regulates the self-renewal of LSCs and induces chemoresistance *via* PARP1. Therefore, these findings suggest that the LINC00152/PARP1 pathway could serve as a novel therapeutic target for AML.

DATA AVAILABILITY STATEMENT

The original contributions presented in the study are included in the article/**Supplementary Material**. Further inquiries can be directed to the corresponding authors.

ETHICS STATEMENT

The studies involving human participants were reviewed and approved by Huashan Hospital. The patients/participants provided their written informed consent to participate in this study.

AUTHOR CONTRIBUTIONS

CC participated in the concept and design experiments, collect data, analyzed and explained the data, and wrote the manuscript. YW provided the study material. WG provided the study material. HH provided study material. HZ provided study material, concept and design experiments, financial support. WS participated in the concept and design experiments, wrote the manuscript, and made final approval for the manuscript. HW participated in the concept and design experiments, financial support, write manuscript, finally approve manuscript. All authors contributed to the article and approved the submitted version.

FUNDING

This work was supported by National Natural Scientific Foundation of China Grants (81802961).

SUPPLEMENTARY MATERIAL

The Supplementary Material for this article can be found online at: https://www.frontiersin.org/articles/10.3389/fonc.2021.694021/full#supplementary-material

REFERENCES

1. Villatoro A, Konieczny J, Cuminetti V, Arranz L. Leukemia Stem Cell Release From the Stem Cell Niche to Treat Acute Myeloid Leukemia. *Front Cell Dev Biol* (2020) 8:607. doi: 10.3389/fcell.2020.00607
2. Dohner H, Estey E, Grimwade D, Amadori S, Appelbaum FR, Buchner T, et al. Diagnosis and Management of AML in Adults: 2017 ELN Recommendations From an International Expert Panel. *Blood* (2017) 129:424–47. doi: 10.1182/blood-2016-08-733196
3. Paczulla AM, Rothfelder K, Raffel S, Konantz M, Steinbacher J, Wang H, et al. Absence of NKG2D Ligands Defines Leukaemia Stem Cells and Mediates Their Immune Evasion. *Nature* (2019) 572:254–9. doi: 10.1038/s41586-019-1410-1
4. Shlush LI, Mitchell A, Heisler L, Abelson S, Ng SWK, Trotman-Grant A, et al. Tracing the Origins of Relapse in Acute Myeloid Leukaemia to Stem Cells. *Nature* (2017) 547:104–8. doi: 10.1038/nature22993
5. Laverdiere I, Boileau M, Neumann AL, Frison H, Mitchell A, Ng SWK, et al. Leukemic Stem Cell Signatures Identify Novel Therapeutics Targeting Acute Myeloid Leukemia. *Blood Cancer J* (2018) 8:52. doi: 10.1038/s41408-018-0087-2
6. Klattenhoff CA, Scheuermann JC, Surface LE, Bradley RK, Fields PA, Steinhauser ML, et al. Braveheart, a Long Noncoding RNA Required for Cardiovascular Lineage Commitment. *Cell* (2013) 152:570–83. doi: 10.1016/j.cell.2013.01.003
7. Guiducci G, Stojic L. Long Noncoding RNAs at the Crossroads of Cell Cycle and Genome Integrity. *Trends Genet* (2021) 37(6):528–46. doi: 10.1016/j.tig.2021.01.006
8. Silva-Fisher JM, Dang HX, White NM, Strand MS, Krasnick BA, Rozycki EB, et al. Long Non-Coding RNA RAMS11 Promotes Metastatic Colorectal Cancer Progression. *Nat Commun* (2020) 11:2156. doi: 10.1038/s41467-020-15547-8
9. Garzon R, Volinia S, Papaioannou D, Nicolet D, Kohlschmidt J, Yan PS, et al. Expression and Prognostic Impact of Lncrnas in Acute Myeloid Leukemia. *Proc Natl Acad Sci USA* (2014) 111:18679–84. doi: 10.1073/pnas.1422050112
10. Trimarchi T, Bilal E, Ntziachristos P, Fabbri G, Dalla-Favera R, Tsirigos A, et al. Genome-Wide Mapping and Characterization of Notch-Regulated Long Noncoding RNAs in Acute Leukemia. *Cell* (2014) 158:593–606. doi: 10.1016/j.cell.2014.05.049
11. Papaioannou D, Nicolet D, Volinia S, Mrozek K, Yan P, Bundschuh R, et al. Prognostic and Biologic Significance of Long Non-Coding RNA Profiling in Younger Adults With Cytogenetically Normal Acute Myeloid Leukemia. *Haematologica* (2017) 102:1391–400. doi: 10.3324/haematol.2017.166215
12. Beck D, Thoms JAI, Palu C, Herold T, Shah A, Olivier J, et al. A Four-Gene Lincrna Expression Signature Predicts Risk in Multiple Cohorts of Acute Myeloid Leukemia Patients. *Leukemia* (2018) 32:263–72. doi: 10.1038/leu.2017.210
13. David A, Zocchi S, Talbot A, Choisy C, Ohnona A, Lion J, et al. The Long Non-Coding RNA CRNDE Regulates Growth of Multiple Myeloma Cells *via* an Effect on IL6 Signalling. *Leukemia* (2020) 35(6):1710–21. doi: 10.1038/s41375-021-01305-2
14. Schwarzer A, Emmrich S, Schmidt F, Beck D, Ng M, Reimer C, et al. The Non-Coding RNA Landscape of Human Hematopoiesis and Leukemia. *Nat Commun* (2017) 8:218. doi: 10.1038/s41467-017-00212-4
15. Papaioannou D, Petri A, Dovey OM, Terreri S, Wang E, Collins FA, et al. The Long Non-Coding RNA HOXB-AS3 Regulates Ribosomal RNA Transcription in NPM1-Mutated Acute Myeloid Leukemia. *Nat Commun* (2019) 10:5351. doi: 10.1038/s41467-019-13259-2
16. Pang Q, Ge J, Shao Y, Sun W, Song H, Xia T, et al. Increased Expression of Long Intergenic Non-Coding RNA LINC00152 in Gastric Cancer and Its Clinical Significance. *Tumour Biol* (2014) 35:5441–7. doi: 10.1007/s13277-014-1709-3
17. Seo D, Kim D, Kim W. Long Non-Coding RNA Linc00152 Acting as a Promising Oncogene in Cancer Progression. *Genomics Inform* (2019) 17:e36. doi: 10.5808/GI.2019.17.4.e36
18. Zhang X, Tao W. Long Noncoding RNA LINC00152 Facilitates the Leukemogenesis of Acute Myeloid Leukemia by Promoting CDK9 Through miR-193a. *DNA Cell Biol* (2019) 38:236–42. doi: 10.1089/dna.2018.4482
19. Costello RT, Mallet F, Gaugler B, Sainty D, Arnoulet C, Gastaut JA, et al. Human Acute Myeloid Leukemia CD34+/CD38- Progenitor Cells Have Decreased Sensitivity to Chemotherapy and Fas-Induced Apoptosis, Reduced Immunogenicity, and Impaired Dendritic Cell Transformation Capacities. *Cancer Res* (2000) 60(16):4403–11.
20. Ng SW, Mitchell A, Kennedy JA, Chen WC, McLeod J, Ibrahimova N, et al. A 17-Gene Stemness Score for Rapid Determination of Risk in Acute Leukaemia. *Nature* (2016) 540:433–7. doi: 10.1038/nature20598
21. Gollner S, Oellerich T, Agrawal-Singh S, Schenk T, Klein HU, Rohde C, et al. Loss of the Histone Methyltransferase EZH2 Induces Resistance to Multiple Drugs in Acute Myeloid Leukemia. *Nat Med* (2017) 23:69–78. doi: 10.1038/nm.4247
22. Li X, Li C, Jin J, Wang J, Huang J, Ma Z, et al. High PARP-1 Expression Predicts Poor Survival in Acute Myeloid Leukemia and PARP-1 Inhibitor and SAHA-Bendamustine Hybrid Inhibitor Combination Treatment Synergistically Enhances Anti-Tumor Effects. *EBioMedicine* (2018) 38:47–56. doi: 10.1016/j.ebiom.2018.11.025
23. Heyman B, Jamieson C. To PARP or Not to PARP?-Toward Sensitizing Acute Myeloid Leukemia Stem Cells to Immunotherapy. *EMBO J* (2019) 38:e103479. doi: 10.15252/embj.2019103479
24. Gugnoni M, Ciarrocchi A. Long Noncoding RNA and Epithelial Mesenchymal Transition in Cancer. *Int J Mol Sci* (2019) 20:1924–48. doi: 10.3390/ijms20081924
25. Heery R, Finn SP, Cuffe S, Gray SG. Long Non-Coding RNAs: Key Regulators of Epithelial-Mesenchymal Transition, Tumour Drug Resistance and Cancer Stem Cells. *Cancers (Basel)* (2017) 9:38–5. doi: 10.3390/cancers9040038
26. Spankuch B, Strebhardt K. Combinatorial Application of Nucleic Acid-Based Agents Targeting Protein Kinases for Cancer Treatment. *Curr Pharm Des* (2008) 14:1098–112. doi: 10.2174/138161208784246243
27. Cai Q, Wang Z, Wang S, Weng M, Zhou D, Li C, et al. Long Non-Coding RNA LINC00152 Promotes Gallbladder Cancer Metastasis and Epithelial-Mesenchymal Transition by Regulating HIF-1alpha *via* Mir-138. *Open Biol* (2017) 7:160247–60. doi: 10.1098/rsob.160247
28. Chen WM, Huang MD, Sun DP, Kong R, Xu TP, Xia R, et al. Long Intergenic Non-Coding RNA 00152 Promotes Tumor Cell Cycle Progression by Binding to EZH2 and Repressing P15 and P21 in Gastric Cancer. *Oncotarget* (2016) 7:9773–87. doi: 10.18632/oncotarget.6949
29. Wu Y, Tan C, Weng WW, Deng Y, Zhang QY, Yang XQ, et al. Long Non-Coding RNA Linc00152 Is a Positive Prognostic Factor for and Demonstrates Malignant Biological Behavior in Clear Cell Renal Cell Carcinoma. *Am J Cancer Res* (2016) 6(2):285–99.
30. Wang Y, Liu J, Bai H, Dang Y, Lv P, Wu S. Long Intergenic non-Coding RNA 00152 Promotes Renal Cell Carcinoma Progression by Epigenetically Suppressing P16 and Negatively Regulates miR-205. *Am J Cancer Res* (2017) 7(2):312–22.
31. Wang Y, Zhou P, Li P, Yang F, Gao XQ. Long Non-Coding RNA H19 Regulates Proliferation and Doxorubicin Resistance in MCF-7 Cells by Targeting PARP1. *Bioengineered* (2020) 11:536–46. doi: 10.1080/21655979.2020.1761512
32. Chen DL, Lu YX, Zhang JX, Wei XL, Wang F, Zeng ZL, et al. Long Non-Coding RNA UICLM Promotes Colorectal Cancer Liver Metastasis by Acting as a ceRNA for MicroRNA-215 to Regulate ZEB2 Expression. *Theranostics* (2017) 7:4836–49. doi: 10.7150/thno.20942
33. Li T, Xie J, Shen C, Cheng D, Shi Y, Wu Z, et al. Amplification of Long Noncoding RNA ZFAS1 Promotes Metastasis in Hepatocellular Carcinoma. *Cancer Res* (2015) 75:3181–91. doi: 10.1158/0008-5472.CAN-14-3721
34. Ou C, Sun Z, He X, Li X, Fan S, Zheng X, et al. Targeting YAP1/LINC00152/FSCN1 Signaling Axis Prevents the Progression of Colorectal Cancer. *Adv Sci (Weinh)* (2020) 7:1901380. doi: 10.1002/advs.201901380
35. Zhou D, Xu P, Zhou X, Diao Z, Ouyang J, Yan G, et al. miR-181a Enhances Drug Sensitivity of Mixed Lineage Leukemia-Rearranged Acute Myeloid Leukemia by Increasing Poly(ADP-Ribose) Polymerase1 Acetylation. *Leuk Lymphoma* (2021) 62:136–46. doi: 10.1080/10428194.2020.1824067
36. Mao Z, Hine C, Tian X, Van Meter M, Au M, Vaidya A, et al. SIRT6 Promotes DNA Repair Under Stress by Activating PARP1. *Science* (2011) 332:1443–6. doi: 10.1126/science.1202723
37. Loseva O, Jemth AS, Bryant HE, Schuler H, Lehtio L, Karlberg T, et al. PARP-3 Is a Mono-ADP-Ribosylase That Activates PARP-1 in the Absence of DNA. *J Biol Chem* (2010) 285:8054–60. doi: 10.1074/jbc.M109.077834
38. Zhang S, Liao W, Wu Q, Huang X, Pan Z, Chen W, et al. LINC00152 Upregulates ZEB1 Expression and Enhances Epithelial-Mesenchymal Transition and Oxaliplatin Resistance in Esophageal Cancer by Interacting With EZH2. *Cancer Cell Int* (2020) 20:569. doi: 10.1186/s12935-020-01620-1

39. Zhang L, Wang Y, Su H. Long Non-Coding RNA LINC00152/miR-613/CD164 Axis Regulates Cell Proliferation, Apoptosis, Migration and Invasion in Glioma *via* PI3K/AKT Pathway. *Neoplasma* (2020) 67:762–72. doi: 10.4149/neo_2020_190706N598

Conflict of Interest: The authors declare that the research was conducted in the absence of any commercial or financial relationships that could be construed as a potential conflict of interest.

frontiers in Oncology

ORIGINAL RESEARCH
published: 23 July 2021
doi: 10.3389/fonc.2021.684232

PSMB7 Is a Key Gene Involved in the Development of Multiple Myeloma and Resistance to Bortezomib

Dong Wu[1†], Jiyu Miao[1†], Jinsong Hu[2], Fangmei Li[1], Dandan Gao[1], Hongli Chen[1], Yuandong Feng[1], Ying Shen[1] and Aili He[1]*

[1] Department of Hematology, The Second Affiliated Hospital of Xi'an Jiaotong University, Xi'an, China, [2] Department of Cell Biology and Genetics, Xi'an Jiaotong University Health Science Center, Xi'an, China

Multiple myeloma (MM), the second most commonly diagnosed hematologic neoplasm, is the most significant clinical manifestation in a series of plasma cell (PC) dyscrasia. Monoclonal gammopathy of undetermined significance (MGUS) and smoldering MM (SMM), approximately 1% or 10% of which, respectively, can progress to MM per year, are the premalignant stages of MM. The overall survival (OS) of MM is significantly improved by the introduction of proteasome inhibitors (PIs), but almost all MM patients eventually relapse and resist anti-MM drugs. Therefore, it is crucial to explore the progression of MM and the mechanisms related to MM drug resistance. In this study, we used weighted gene co-expression network analysis (WGCNA) to analyze the gene expression of the dynamic process from normal plasma cells (NPC) to malignant profiling PC, and found that the abnormal gene expression was mainly concentrated in the proteasome. We also found that the expression of one of the proteasomal subunits PSMB7 was capable of distinguishing the different stages of PC dyscrasia and was the highest in ISS III. In the bortezomib (BTZ) treated NDMM patients, higher PSMB7 expression was associated with shorter survival time, and the expression of PSMB7 in the BTZ treatment group was significantly higher than in the thalidomide (Thai) treatment group. In summary, we found that PSMB7 is the key gene associated with MM disease progression and drug resistance.

Keywords: multiple myeloma, proteasome inhibitor, PSMB7, WGCNA, drug resistance

OPEN ACCESS

Edited by:
Mina Luqing Xu,
Yale University, United States

Reviewed by:
Mehmet Hakan Kocoglu,
University of Maryland, Baltimore, United States
Natalia Paola Schutz,
Italian Hospital of Buenos Aires, Argentina

****Correspondence:***
Aili He
heaili@mail.xjtu.edu.cn

[†]These authors have contributed equally to this work

Specialty section:
This article was submitted to Hematologic Malignancies, a section of the journal Frontiers in Oncology

Received: *23 March 2021*
Accepted: *08 July 2021*
Published: *23 July 2021*

Citation:
Wu D, Miao J, Hu J, Li F, Gao D, Chen H, Feng Y, Shen Y and He A (2021) PSMB7 Is a Key Gene Involved in the Development of Multiple Myeloma and Resistance to Bortezomib. Front. Oncol. 11:684232. doi: 10.3389/fonc.2021.684232

INTRODUCTION

Multiple myeloma (MM), accounting for 10% of all hematological malignancies, the final stage of a continuum plasma cell (PC) dyscrasia, which is characterized by malignant profiling of monoclonal protein with increased bone marrow (BM) PC, osteolytic lesion, hypercalcemia, and anemia (1). Monoclonal gammopathy of undetermined significance (MGUS) is a premalignant stage of MM that is defined as the presence of monoclonal immunoglobulin (Ig) in blood or urine (M protein), less than 10% clonal PC in the BM, and the absence of myeloma-related end-organ damage. Approximately 1% of MGUS patients evolve to MM per year (2, 3). MGUS may progress to a more advanced stage known as smoldering multiple myeloma (SMM). SMM, the probability of

progression was 10% per years, is a transitional stage between MGUS and NDMM that is defined as M protein level of more than 3g/dl and/or >= 10% plasma cell in the BM without myeloma-related end-organ damage (4).

MM treatment has undergone many changes since the first well-documented case (5). In 1958, the introduction of melphalan was accompanied by alkylating agents and chemotherapeutic drugs, but overall survival did not significantly increase (6). In the 1980s, high-dose chemotherapy and autologous stem-cell transplantation (ASCT) were introduced, and subsequent prospective, randomized trial shown that high-dose therapy combined with ASTC could improve the response rate and overall survival in MM patients (7, 8). The introduction of immunomodulatory drugs (IMiDs) and proteasome inhibitors (PIs) expanded the therapeutic armamentarium for MM. Survival outcomes have significantly improved with the introduction of PIs, bortezomib, carfilzomib, and ixazomib, for the treatment of MM over the past decades (9). Despite an initially promising response, almost all MM patients eventually relapse and become refractory to anti-MM therapies due to drug resistance, which is the main obstacle in the treatment of MM. PIs drug resistance involves many mechanisms including increased endoplasmic reticulum (ER) stress, apoptosis failure, autophagy activation, aberrant expression of proteasomal subunits, and the bone marrow microenvironment (10–14). High-throughput genomic techniques have proved the existence of genomic instability and clonal heterogeneity during the pathogenesis of MM from the premalignant stage to the malignant proliferative stage (15). Thus, it is critical to determine the key biomolecules associated with drug resistance and related to the pathogenesis of normal PC to malignant proliferation PC.

In this study, based on WGCNA analysis of integrated dynamic progression datasets from health control (HC) to NDMM, we found that the expression of proteasome 20S subunit beta 7 (PSMB7), which could discriminate different stages of PC dyscrasia and positively correlated with the degree of the malignancy of PC dyscrasia. Additionally, the OS of NDMM patients with high expression of PSMB7 was shorter than that of patients with low expression of PSMB7 in the TT3 (total therapy 3) group and there was no statistical difference in the TT2 (total therapy 2) group and there was higher expression of PSMB7 in the TT3 than in the TT2 group.

MATERIALS AND METHODS

Microarray Dataset

The microarray dataset were downloaded from the gene expression omnibus (GEO) database (https://www.ncbi.nlm.nih.gov/geo/). The MM international staging system (ISS) prognostication analysis dataset E-MTAB-4032 was downloaded from the ArrayExpress database (https://www.ebi.ac.uk/arrayexpress/experiments/E-MTAB-4032/) (16, 17). GSE6477 (https://www.ncbi.nlm.nih.gov/geo/query/acc.cgi?acc=GSE6477) was used to construct the co-expression network and evaluate the diagnostic value in different PC dyscrasia stages (18, 19). GSE24080 (https://www.ncbi.nlm.nih.gov/geo/query/acc.cgi?acc=GSE24080) was used to validate the a prognostic signature (20).

Construction of Co-Expression Network

To construct a co-expression network by "WGCNA", the original probeids in the GSE6477 dataset were converted to genesymbol (gene name). The gene expression level was defined as the average expression level when multiple probeids correspond to a specific genesymbol. The disease progression from HC to MGUS, SMM, and finally to NDMM was treated as a continuum. The soft threshold with the argument type "signed" is selected according to the scale-free (SF) topology criterion (21). A topological overlap matrix (TOM) was used to determine modules defined as clusters of densely interconnected genes (22). In order to quantify all of the genes on the array to every module, gene significance (GS) was defined as the correlation between the individual genes and the trait, and module membership was defined as the correlation between the module eigengene and the gene expression profile (23). Next, the modules and GS was related to the different stages of PC dyscrasias.

GO and KEGG Pathway Enrichment Analysis

To identify the significant biological roles of the genes in the modules closely related to NDMM, gene ontology (GO) enrichment analysis and meaningful enrichment contained biological process (BP), molecular function (MF), and cellular component (CC) was performed using DAVID bioinformatics resources 6.8 (24). Pathway enrichment analysis was performed using the Kyoto Encyclopedia of Genes and Genomes (KEGG; http://www.Genome.Jp/kegg). KEGG pathway was selected with a cut-off of a false discovery rate (FDR) of<0.05.

Expression of PSMB7 in Different PC Dyscrasia Stages and ISS Statuses

The GSE47552 dataset, which contained 21 MGUS, 24 SMM, and 69 NDMM newly diagnosed without treatment patient samples and 15 NPC as health control (HC), was used to analyze the expression of PSMB7 in different PC dyscrasia stages. E-MTAB-4032, including 38 ISS I, 45 ISS II, and 69 ISS III, were used to analyze the expression of PSMB7 in different ISS statuses.

c-BioPortal Analysis

Mutation analysis used MM datasets (Broad, Cancer Cell 2014), containing 203 multiple myeloma paired tumor/normal sample pairs, by the cBio Cancer Genomics Portal (http://cbioportal.org) (25–27).

ROC Analysis

To measure the accuracy and specificity of PSMB7, the GSE6477 dataset was used for receiver operating characteristic (ROC) and area under the curve (AUC) analysis.

Overall Survival Analysis

345 NDMM patients were treated with TT2 (TT2 added Thai to melphalan (MEL200)-based tandem autotransplants) and 214 NDMM patients were treated with TT3 (TT3 incorporated BTZ

into a melphalan-based tandem transplant regimen) in GSE24080 was used for the OS analysis (28, 29). According to the average expression of PSMB7, the clinical and OS information of TT2 and TT3 treated NDMM patients was divided into the high or low expression group and the OS analysis was performed to calculate the correlation between the expression of PSMB7 and the survival time in TT2 or TT3.

RESULTS

Construction of WGCNA and Identification of Modules

To explore the dynamic changes associated with the PC dyscrasia process, we performed WGCNA analysis using the GSE6477 dataset, including HC, MGUS, SMM, and NDMM, showing the stepwise progression from the pre-MM stages to NDMM. The raw files were pre-processed by means of background correction and normalization, and the average gene expression was treated as the final gene expression (30, 31). A total of 13,236 genes was finally used for the WGCNA analysis. Soft threshold power β=8 was chosen for the adjacency matrix calculation and the SF topology fit index reached 0.85 (**Figures 1A, B**). Then, 12 gene modules were identified through TOM-based clustering (**Figure 1C**).

Correlation Between the Module and Different PC Dyscrasia Stages

To explore the association between each module and different PC dyscrasia stages, eigengenes, the first principal component of the expression matrix of the corresponding module, was correlated

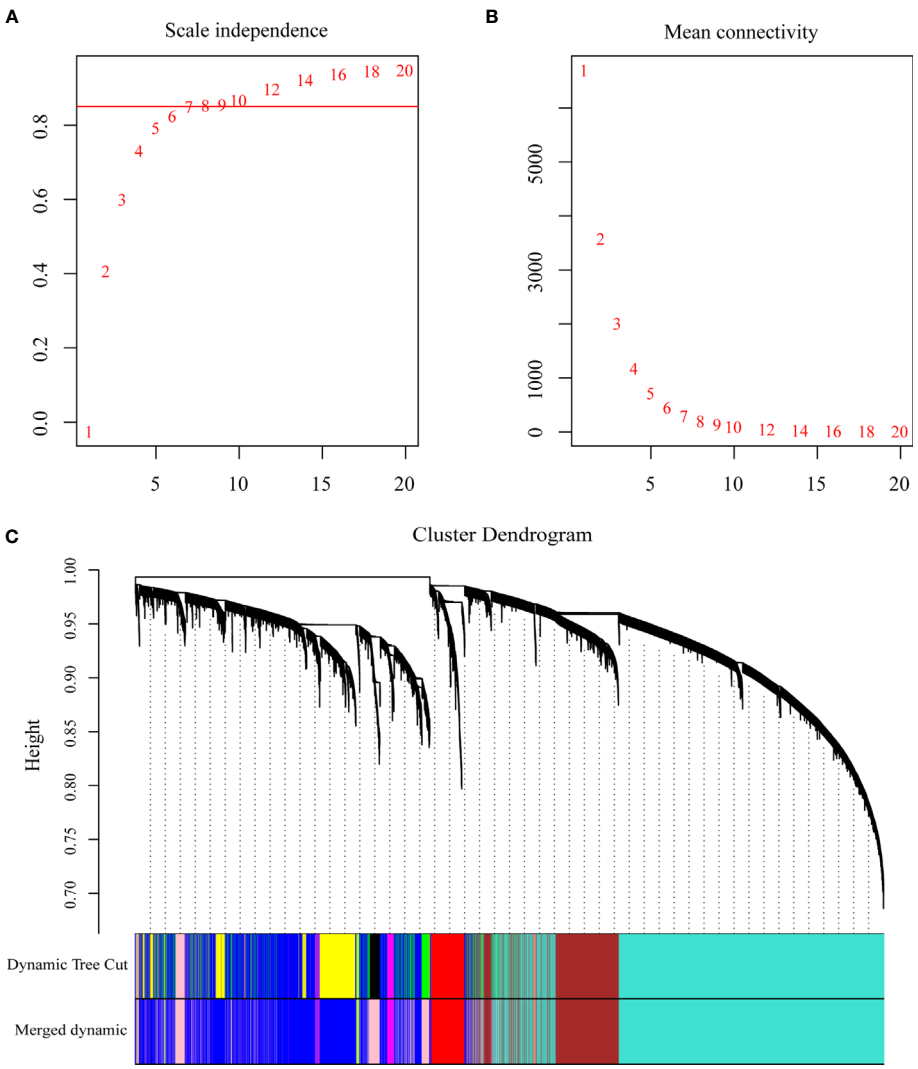

FIGURE 1 | WGCNA on the dynamic progression of MM. **(A)** Analysis of network topology for various soft threshold powers (β). **(B)** Mean connectivity with various soft threshold power. **(C)** Clustering dendrogram of all differentially expressed genes with assigned module colors. Each color block represented a module of highly co-expressed genes.

to them (23). We noticed that the module eigengene (ME) pink was closely related to NDMM (**Figure 2A**). The GS and module membership were highly correlated (cor=0.076), illustrating that genes significantly associated with NDMM were also critical elements of ME pink (**Figure 2B**).

Functional Enrichment Analysis Found That Proteasome Played a Crucial Role in the Development of MM

DAVID database were used to analyze the canonical pathway analysis and biological function of the genes contained in ME pink. As shown in **Figure 3A**, hsa03050: proteasome (red arrow) was mainly changed, suggesting that the proteasome changed significantly as the disease progressed. MF, BP, and CC enrichment analysis in ME pink was shown in **Figures 3B–D**.

PSMB7 Discriminated Different PC Dyscrasia Stages and Its Expression Was the Highest in the ISS III Status of NDMM

The GSE6477 dataset was used for explore the expression of genes in the proteasome at different PC dyscrasia stages. The results showed that PSMB7 could distinguish all stages of PC dyscrasia, from MGUS to SMM and NDMM (**Figure 4A**), HC *vs.* MGUS, P=0.112, HC *vs.* SMM, P<0.0001, HC *vs.* NDMM, P<0.0001; MGUS *vs.* SMM, P=0.019, MGUS *vs.* NDMM, P<0.0001; SMM *vs.* NDMM, P<0.0001. The E-MTAB-4032 dataset was used to explore the expression of PSMB7 in different ISS statuses of NDMM. The results showed that the expression of PSMB7 at ISS III was significantly higher than at ISS stage I (P = 0.001) and II (P = 0.038) in NDMM patients (**Figure 4B**).

No Mutation Was Found in PSMB7

Since the expression of PSMB7 is highest expressed in NDMM and ISS III, we wondered about the relationship between the high expression of PSMB7 and genomic alterations. Using cBioPortal to determine the types and frequency of PSMB7 alterations in 203 MM patients, no mutations were found, suggesting that the expression level of PSMB7 played a crucial role (**Figure 5**).

PSMB7 Has the Highest Sensitivity and Specificity for NDMM

We performed ROC analysis of MGUS, SMM, and NDMM to analyze the risk signature of PSMB7. The AUC of MGUS, SMM, and NDMM are 0.628 (P=0.1918, 95%CI: 0.4445 -0.8118), 0.9028 (P=0. 95%, 95%CI: 0.7092-0.9626), and 0.9674 (P= <0.0001, 95% CI: 0.7092-0.9626),respectively, demonstrating that PSMB7 could discriminate HC from PC and NDMM had the highest sensitivity and specificity (**Figures 6A–C**).

High Expression of PSMB7 With Shorter Overall Survival in TT3

To further explore the relationship between the expression of PSMB7 and the clinical outcome in NDMM patients, the GSE24080 dataset, containing two kinds of MM chemotherapy: TT2 and TT3, was selected for OS analysis by means of Kaplan-Meier Survival analysis. The main difference between TT2 and TT3 was that TT2 contained Thai, and TT3 contained BTZ. The

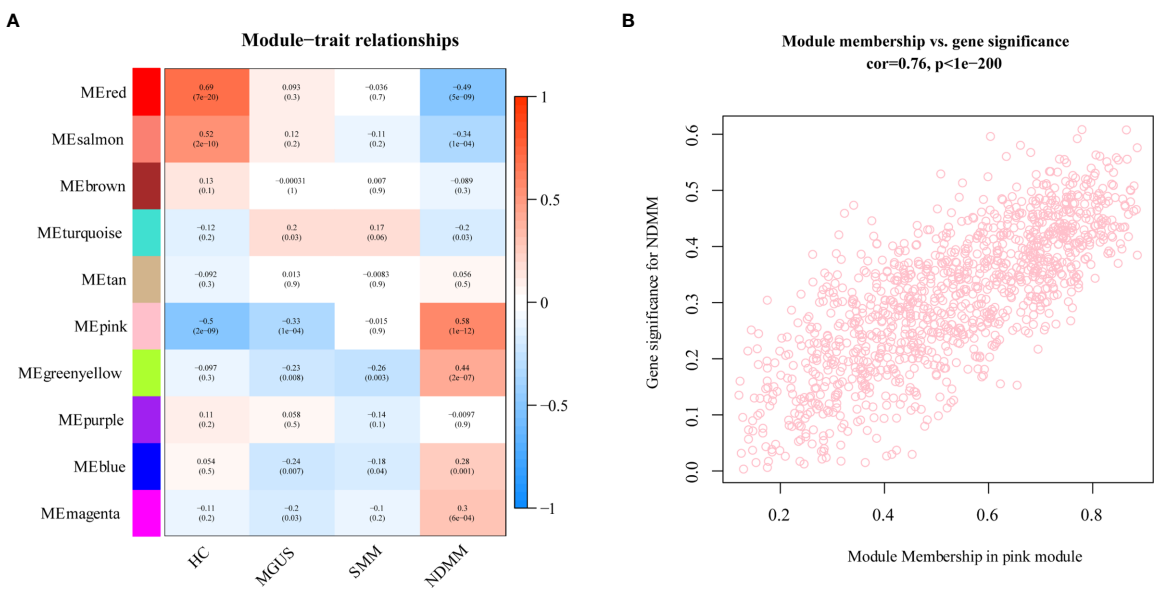

FIGURE 2 | The relationship between modules and PC dyscrasia. **(A)** Module-trait associations. Each row corresponds to a ME, each column to a stage of PC dyscrasias. The table is color-coded by the corresponding correlation according to the color legend. **(B)** A scatterplot of GS for weight *vs.* module membership in the ME pink.

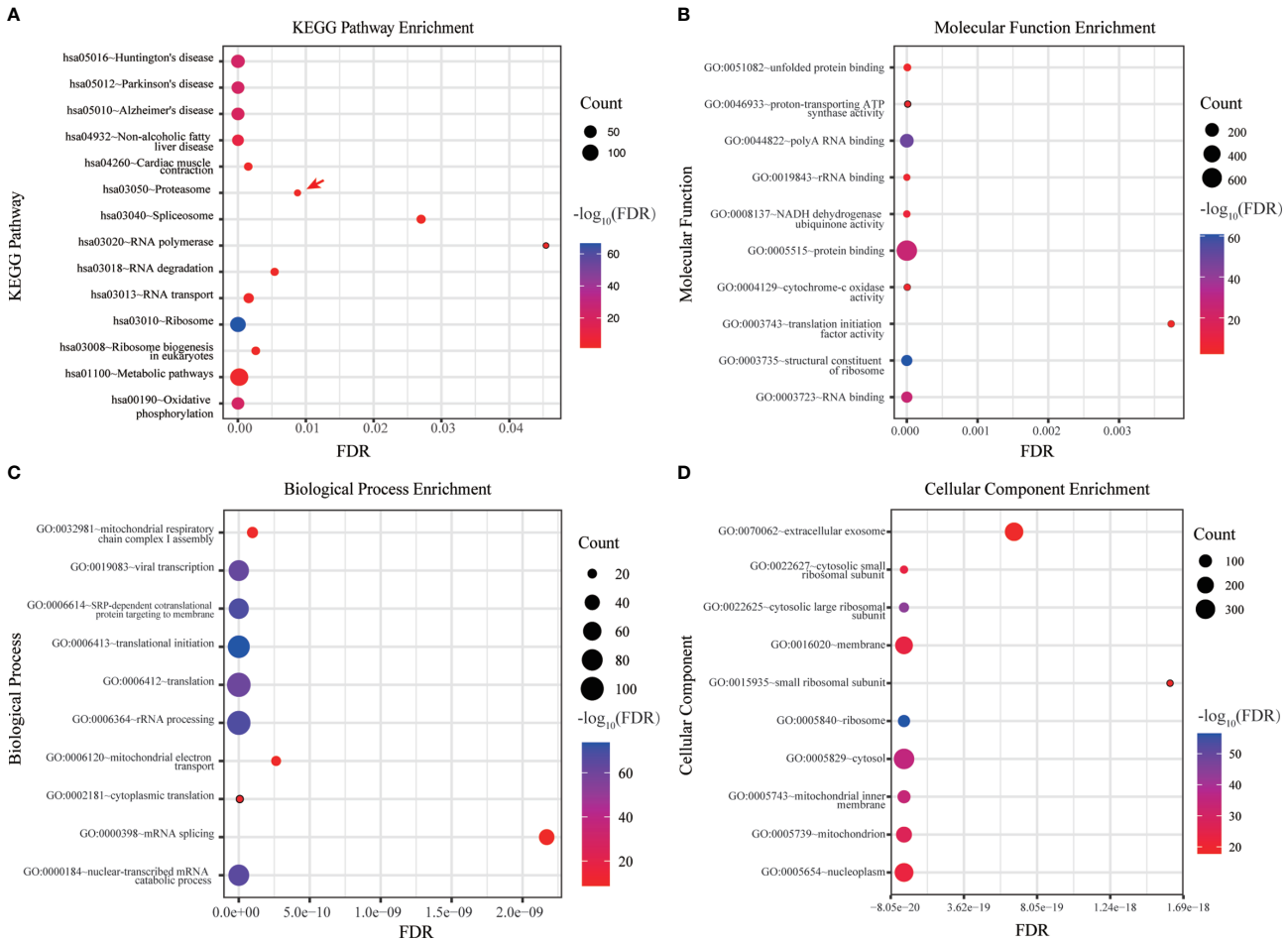

FIGURE 3 | Functional enrichment analysis of hub genes. **(A)** KEGG pathway enrichment analysis. **(B)** MF enrichment analysis. **(C)** BP enrichment analysis. **(D)** CC enrichment analysis.

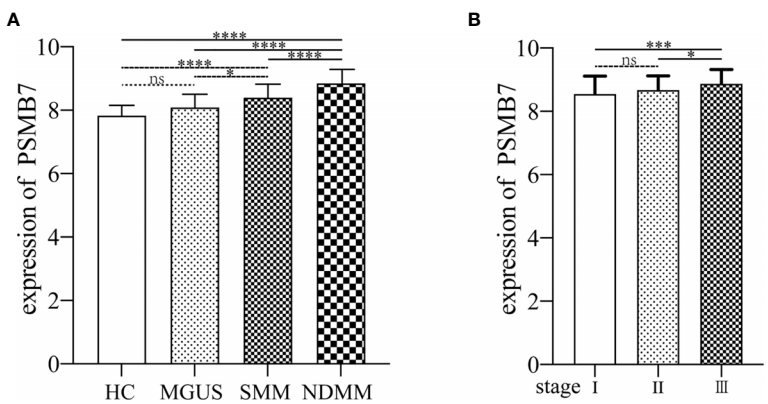

FIGURE 4 | The expression of PSMB7. **(A)** The expression of PSMB7 from HC to NDMM in GSE6477. **(B)** The expression of PSMB7 in different ISS status in E-MTAB-4032. ns, not significant, *$P < 0.05$, ***$P < 0.001$, and ****$P < 0.0001$.

FIGURE 5 | Mutation analysis of PSMB7 in NDMM. There were 0% genomic alterations of PSMB7 in MM.

result suggested that the OS of PSMB7 in the TT3 low-expression group was significantly longer than that of TT3 high-expression group, and there was no difference in the TT2 group (**Figures 7A, B**). In addition, the expression of PSMB7 in the TT3 was significantly increased compared to the TT2 group ($P < 0.001$) (**Figure 7C**).

DISCUSSION

The malignant transformation from healthy cells to cancer cells is a multi-step and multi-faceted process. Cancer biology have shown that clonal evolution drives tumor development (15). Previous studies have shown that the proportion of PC in the BM and the rate of increase of the serum M-protein level during the first years can be used to predict the possibility of MGUS/SMM progressing to NDMM[(32). Most of these studies focused on the differential gene expression in two stages of PC malignant transformation, such as comparing HC, MGUS, and SMM with NDMM, but the malignant transformation from HC to NDMM is a dynamic progression and these findings could not explain the underlying causes of the malignant progression.

In this study, by WGCNA, a systems biology algorithm can be applied to describing the correlation patterns among genes across microarray samples, finding highly related gene modules and relating modules to a particular PC dyscrasia stage (23). We analyzed the entire dynamic disease process from HC to NDMM and found that the abnormal gene expression of PC concentrated in the 26S proteasome, of which PSMB7 is positively correlated with the degree of PC malignancy and is highest expressed in NDMM. The proteasome is a large multi-catalytic protein complex that can degrade different kinds of cellular proteins (33). The 26S proteasomes is composed of 20S core particles (CP) and 19S regulatory particles (RP). 20S CP is a hollow structure in the middle, while 19S RP is located at both ends. 19S RP can recognize and bind ubiquitinated proteins and transport them to the core particle to degrade excess and abnormally folded proteins (34, 35). The proteasome and ubiquitin proteasome system (UPS) participate in the regulation of cell growth and survival. In the course of MM, abnormal UPS function can lead to excessive proteasome activation, which leads to excessive degradation of tumor suppressor p53 and the inhibition of nuclear factor-κB (NF-κB). The excessive degradation of various cancer suppressor factors and the activation of cancer-related pathways lead to the activation of NF-κB downstream effectors and form a positive feedback loop, enhancing the cell signal transmission in the BM microenvironment and the survival rate of MM cells, ultimately leading to the quick malignancy profiling of myeloma cells (36, 37).

PIs are an important new class of drugs for the treatment of multiple myeloma. The success of PIs is due to the susceptibility of myeloma cells to the inhabitation of the 26S proteasome (38). The 20S proteasome contains seven different subunits, the most important of which are PSMB6 (β1), PSMB7 (β2), and PSMB5 (β5). When stimulated by cytokine signals, the cellular stress response promotesβ1, β2, and β5 to convert into β1i, β2i, and β5i (39). The first generation of PIs, agent BTZ, is a dipeptide borate that reversibly binds to β5, β1, and β5i subunits. It prevents the formation of transcribed blood vessels and the adhesion of PC by

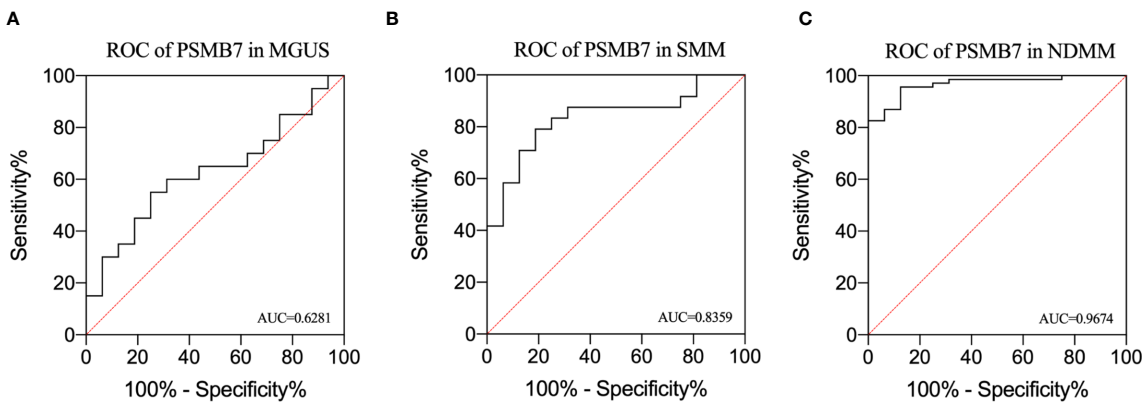

FIGURE 6 | Receiver operating characteristic curve analysis in MGUS, SMM, and NDMM. **(A)** ROC of PSMB7 in MGUS, **(B)** ROC of PSMB7 in SMM, **(C)** ROC of PSMB7 in NDMM.

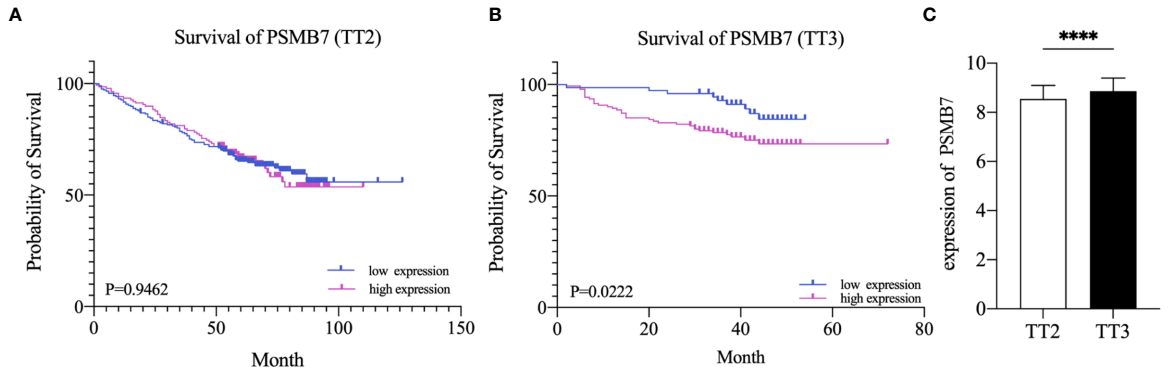

FIGURE 7 | Kaplan-Meier survival curves of NDMM patients. **(A)** Overall survival of PSMB7 in the TT2 group. **(B)** Overall survival of PSMB7 in the TT3 group. **(C)** Expression of PSMB7 in the TT2 and the TT3 group, ****P < 0.001.

inhibiting NF-κB transcription factor IκB kinase and bone marrow stromal cells from promoting MM cell apoptosis (40). Although PI agents improve the survival and prognosis of MM patients, drug resistance has become the biggest obstacle to their clinical application. In a previous study, Ruud Oerlemans et al. found that not only the PSMB5 but also PSMB6 and PSMB7 subunits increased in BTZ resistant cell lines CEM-C7 and 8226 (41). Thus, we further analyzed all of the genes contained in the proteasome, and found that the expression of PSMB7 was positively correlated with the degree of PC dyscrasia, and could distinguish the different PC dyscrasia stages.

Given the importance of the proteasome in MM biology and therapy, we further explored the relationship between PSMB7 and ISS status of NDMM and found that the expression of PSMB7 in ISS III was significantly higher than in ISS I/II, which means that PSMB7 was not only positively correlated with the malignant degree of PC dyscrasia, and it was also correlated with the ISS status of NDMM. More importantly, in the BTZ treatment group, the OS of the PSMB7 high expression group was significantly shorter than that of the low expression group with the BTZ treatment, but there was no difference in the Thai treatment group. Moreover, the expression of PSMB7 was higher in the BTZ group than in the Thai treatment group, which means increasing PSMB7 accompanies BTZ therapy. Subsequently, the ROC analysis of PSMB7 in MGUS, SMM, and NDMM was conducted. These results suggested that PSMB7 could act as a reliable diagnostic and prognostic indicator in NDMM.

PSMB7, together with PSMB5 and PSMB6 composes the 20S proteolytic of the proteasome complex 26S. It has been believed that PSMB5 played a vital role in cell viability, but other publications demonstrated that protein degradation could be inhibited only by simultaneously inhibiting PSMB5 and PSMB6 or PSMB7. Chang-Xin Shi *et al.* found that PSMB7 depletion was lethal to MM cell lines, and expression levels of PSMB5, PSMB6, and PSMB7 increased in patients after BTZ treatment, which was consistent with our findings (42).

Collectively, in this study, based on integrated bioinformatic analysis, we demonstrated that PSMB7 is a key gene in MM development and resistance to BTZ therapy. Our findings may provide clues for elucidating the mechanisms of malignant transformation in PC dyscrasia and may help identify patients at high risk of progression and point to more precise therapeutic targets.

DATA AVAILABILITY STATEMENT

Publicly available datasets were analyzed in this study. This data can be found here: https://www.ebi.ac.uk/arrayexpress/experiments/E-MTAB-4032/ https://www.ncbi.nlm.nih.gov/geo/query/acc.cgi?acc=GSE6477 https://www.ncbi.nlm.nih.gov/geo/query/acc.cgi?acc=GSE24080.

AUTHOR CONTRIBUTIONS

DW and AH conceived and designed the study. DW, JM, FL, and YF collected and processed data. DG, HC, and YS prepared tables and figures. DW and JM drafted the manuscript. AH and JH revised the manuscript. All authors contributed to the article and approved the submitted version.

FUNDING

This work was supported by National Science and Technology Major Project (2019ZX09301139).

ACKNOWLEDGMENTS

We gratefully thank Chenglong Rao from the Department of Clinical Microbiology And Immunology, the College of Pharmacy and Medical Laboratory, Army Medical University for the valuable comments on the manuscript and technical assistance. We also express our appreciation to researchers who shared their data online.

REFERENCES

1. Rajkumar SV, Dimopoulos MA, Palumbo A, Blade J, Merlini G, Mateos M, et al. International Myeloma Working Group Updated Criteria for the Diagnosis of Multiple Myeloma. *Lancet Oncol* (2014) 15(12):e538–e48. doi: 10.1016/S1470-2045(14)70442-5
2. Pawlyn C, Morgan GJ. Evolutionary Biology of High-Risk Multiple Myeloma. *Nat Rev Cancer* (2017) 17(9):543–56. doi: 10.1038/nrc.2017.63
3. Perez-Persona E, Vidriales MB, Mateo G, García-Sanz R, Mateos M-V, García de Coca A, et al. New Criteria to Identify Risk of Progression in Monoclonal Gammopathy of Uncertain Significance and Smoldering Multiple Myeloma Based on Multiparameter Flow Cytometry Analysis of Bone Marrow Plasma Cells. *Blood* (2007) 110(7):2586–92. doi: 10.1182/blood-2007-05-088443
4. Rajkumar SV, Landgren O, Mateos MV. Smoldering Multiple Myeloma. *Blood* (2015) 125(20):3069–75. doi: 10.1182/blood-2014-09-568899
5. Solly S. Remarks on the Pathology of Mollities Ossium; With Cases. *Medico-Chirurgical Trans* (1844) 27:435–98. doi: 10.1177/095952874402700129
6. Bergsagel DE, Sprague CC, Austin C, Griffith KM. Evaluation of New Chemotherapeutic Agents in the Treatment of Multiple Myeloma. IV. L-Phenylalanine Mustard (NSC-8806). *Cancer Chemother Rep* (1962) 21:87–99.
7. Mcelwain T, Powles R. High-Dose Intravenous Melphalan for Plasma-Cell Leukaemia and Myeloma. *Lancet* (1983) 322(8354):822–4. doi: 10.1016/S0140-6736(83)90739-0
8. Attal M, Harousseau J-L, Stoppa A-M, Sotto J-J, Fuzibet J-G, Rossi J-F, et al. A Prospective, Randomized Trial of Autologous Bone Marrow Transplantation and Chemotherapy in Multiple Myeloma. *N Engl J Med* (1996) 335(2):91–7. doi: 10.1056/NEJM199607113350204
9. Ito S. Proteasome Inhibitors for the Treatment of Multiple Myeloma. *Cancers (Basel)* (2020) 12(2):265. doi: 10.3390/cancers12020265
10. Zhou J, Chng WJ. Novel Mechanism of Drug Resistance to Proteasome Inhibitors in Multiple Myeloma. *World J Clin Oncol* (2019) 10(9):303–6. doi: 10.5306/wjco.v10.i9.303
11. Touzeau C, Maciag P, Amiot M, Moreau P. Targeting Bcl-2 for the Treatment of Multiple Myeloma. *Leukemia* (2018) 32(9):1899–907. doi: 10.1038/s41375-018-0223-9
12. Mishima Y, Santo L, Eda H, et al. Ricolinostat (ACY-1215) Induced Inhibition of Aggresome Formation Accelerates Carfilzomib-Induced Multiple Myeloma Cell Death. *Br J Haematol* (2015) 169(3):423–34. doi: 10.1111/bjh.13315
13. Banerjee S, Wei T, Wang J, Lee JJ, Gutierrez HL, Chapman O, et al. Inhibition of Dual-Specificity Tyrosine Phosphorylation-Regulated Kinase 2 Perturbs 26S Proteasome-Addicted Neoplastic Progression. *Proc Natl Acad Sci U S A* (2019) 116(49):24881–91. doi: 10.1073/pnas.1912033116
14. Liu Y, Liang HM, Lv YQ, Tang SM, Cheng P, et al. Blockade of SDF-1/CXCR4 Reduces Adhesion-Mediated Chemoresistance of Multiple Myeloma Cells *via* Interacting With Interleukin-6. *J Cell Physiol* (2019) 234(11):19702–14. doi: 10.1002/jcp.28570
15. Gupta RG, Somer RA. Intratumor Heterogeneity: Novel Approaches for Resolving Genomic Architecture and Clonal Evolution. *Mol Cancer Res* (2017) 15(9):1127–37. doi: 10.1158/1541-7786.MCR-17-0070
16. Kryukov F, Nemec P, Radova L, Kryukova E, Okubote S, Minarik J, et al. Centrosome Associated Genes Pattern for Risk Sub-Stratification in Multiple Myeloma. *J Transl Med* (2016) 14(1):150. doi: 10.1186/s12967-016-0906-9
17. Athar A, Fullgrabe A, George N, Iqbal H, Huerta L, Ali A, et al. ArrayExpress Update - From Bulk to Single-Cell Expression Data. *Nucleic Acids Res* (2019) 47(D1):D711–D5. doi: 10.1093/nar/gky964
18. Chng WJ, Kumar S, Vanwier S, Ahmann G, Price-Troska T, Henderson K, et al. Molecular Dissection of Hyperdiploid Multiple Myeloma by Gene Expression Profiling. *Cancer Res* (2007) 67(7):2982–9. doi: 10.1158/0008-5472.CAN-06-4046
19. Tiedemann RE, Zhu YX, Schmidt J, Yin H, Shi CX, Que Q, et al. Kinome-Wide RNAi Studies in Human Multiple Myeloma Identify Vulnerable Kinase Targets, Including a Lymphoid-Restricted Kinase, GRK6. *Blood* (2010) 115(8):1594–604. doi: 10.1182/blood-2009-09-243980
20. Shi L, Campbell G, Jones WD, Campagne F, Wen Z, Walker SJ, et al. The MicroArray Quality Control (MAQC)-II Study of Common Practices for the Development and Validation of Microarray-Based Predictive Models. *Nat Biotechnol* (2010) 28(8):827–38. doi: 10.1038/nbt.1665
21. Langfelder P. Signed vs. Unsigned Topological Overlap Matrix Technical Report. (2013). Available at: https://horvath.genetics.ucla.edu/html/Coexpression Network/Rpackages/WGCNA/Technical Reports/signedTOM.pdf (Accessed April 7, 2018).
22. Yip AM, Horvath S. "The generalized topological overlap matrix for detecting modules in gene networks," in Proceedings of the 2006 International Conference on Bioinformatics & Computational Biology, BIOCOMP'06, Las Vegas, NV 451–457.
23. Langfelder P, Horvath S. WGCNA: An R Package for Weighted Correlation Network Analysis. *BMC Bioinf* (2008) 9(1):1–13. doi: 10.1186/1471-2105-9-559
24. Huang DAW, Sherman BT, Lempicki RA. Systematic and Integrative Analysis of Large Gene Lists Using DAVID Bioinformatics Resources. *Nat Protoc* (2009) 4(1):44–57. doi: 10.1038/nprot.2008.211
25. Lohr JG, Stojanov P, Carter SL, Cruz-Gordillo P, Lawrence MS, Auclair D, et al. Widespread Genetic Heterogeneity in Multiple Myeloma: Implications for Targeted Therapy. *Cancer Cell* (2014) 25(1):91–101.
26. Cerami E, Gao J, Dogrusoz U, Gross BE, Sumer SO, Aksoy BA, et al. The Cbio Cancer Genomics Portal: An Open Platform for Exploring Multidimensional Cancer Genomics Data. *Cancer Discov* (2012) 2(5):401–4. doi: 10.1158/2159-8290.CD-12-0095
27. Gao J, Aksoy BA, Dogrusoz U, Dresdner G, Gross B, Sumer SO, et al. Integrative Analysis of Complex Cancer Genomics and Clinical Profiles Using the Cbioportal. *Sci Signal* (2013) 6(269):pl1. doi: 10.1126/scisignal.2004088
28. Barlogie B, Crowley J, Shaughnessy J, Epstein J, Jackson L, Hollmig K, et al. Total Therapy 2 (TT2) for Multiple Myeloma (MM): Thalidomide (T) Effects Superior Complete Response (CR) and Event-Free Survival (EFS); Similar Overall Survival (OS) Linked to Shorter Post-Relapse Survival. *Blood* (2005) 106(11):423–. doi: 10.1182/blood.V106.11.423.423
29. Van Rhee F, Szymonifka J, Anaissie E, Nair B, Waheed S, Alsayed Y, et al. Total Therapy 3 for Multiple Myeloma: Prognostic Implications of Cumulative Dosing and Premature Discontinuation of VTD Maintenance Components, Bortezomib, Thalidomide, and Dexamethasone, Relevant to All Phases of Therapy. *Blood* (2010) 116(8):1220–7. doi: 10.1182/blood-2010-01-264333
30. Gautier L, Cope L, Bolstad BM, Irizarry RA. Affy–Analysis of Affymetrix GeneChip Data at the Probe Level. *Bioinformatics* (2004) 20(3):307–15. doi: 10.1093/bioinformatics/btg405
31. Irizarry RA, Hobbs B, Collin F, Beazer-Barclay YD, Antonellis KJ, Scherf U, et al. Exploration, Normalization, and Summaries of High Density Oligonucleotide Array Probe Level Data. *Biostatistics* (2003) 4(2):249–64. doi: 10.1093/biostatistics/4.2.249
32. Dhodapkar MV, Sexton R, Waheed S, Usmani S, Papanikolaou X, Nair B, et al. Clinical, Genomic, and Imaging Predictors of Myeloma Progression From Asymptomatic Monoclonal Gammopathies (SWOG S0120). *Blood* (2014) 123(1):78–85. doi: 10.1182/blood-2013-07-515239
33. Fricker LD. Proteasome Inhibitor Drugs. *Annu Rev Pharmacol Toxicol* (2020) 60:(457–76). doi: 10.1146/annurev-pharmtox-010919-023603
34. Ehlinger A, Walters KJ. Structural Insights Into Proteasome Activation by the 19S Regulatory Particle. *Biochemistry* (2013) 52(21):3618–28. doi: 10.1021/bi400417a
35. Tanaka K. The Proteasome: Overview of Structure and Functions. *Proc Japan Acad Ser B* (2009) 85(1):12–36. doi: 10.2183/pjab.85.12
36. Adams J. The Proteasome: A Suitable Antineoplastic Target. *Nat Rev Cancer* (2004) 4(5):349–60. doi: 10.1038/nrc1361
37. Chauhan D, Bianchi G, Anderson KC. Targeting the UPS as Therapy in Multiple Myeloma. *BMC Biochem* (2008) 9 Suppl 1(S1):1–8. doi: 10.1186/1471-2091-9-S1-S1
38. Gandolfi S, Laubach JP, Hideshima T, Chauhan D, Anderson KC, Richardson PG, et al. The Proteasome and Proteasome Inhibitors in Multiple Myeloma. *Cancer Metastasis Rev* (2017) 36(4):561–84. doi: 10.1007/s10555-017-9707-8
39. Kuhn DJ, Orlowski RZ. The Immunoproteasome as a Target in Hematologic Malignancies. *Semin Hematol* (2012) 49(3):258–62. doi: 10.1053/j.seminhematol.2012.04.003
40. Hideshima T, Ikeda H, Chauhan D, Okawa Y, Raje N, Podar K, et al. Bortezomib Induces Canonical Nuclear Factor-κb Activation in Multiple Myeloma Cells. *Blood* (2009) 114(5):1046–52. doi: 10.1182/blood-2009-01-199604

41. Oerlemans R, Franke NE, Assaraf YG, Cloos J, van Zantwijk I, Berkers CR, et al. Molecular Basis of Bortezomib Resistance: Proteasome Subunit β5 (PSMB5) Gene Mutation and Overexpression of PSMB5 Protein. *Blood* (2008) 112(6):2489–99. doi: 10.1182/blood-2007-08-104950
42. Shi C-X, Zhu YX, Bruins LA, Bonolo de Campos C, Stewart W, Braggio E, et al. Proteasome Subunits Differentially Control Myeloma Cell Viability and Proteasome Inhibitor Sensitivity. *Mol Cancer Res* (2020) 18(10):1453–64. doi: 10.1158/1541-7786.MCR-19-1026

Conflict of Interest: The authors declare that the research was conducted in the absence of any commercial or financial relationships that could be construed as a potential conflict of interest.

Publisher's Note: All claims expressed in this article are solely those of the authors and do not necessarily represent those of their affiliated organizations, or those of the publisher, the editors and the reviewers. Any product that may be evaluated in this article, or claim that may be made by its manufacturer, is not guaranteed or endorsed by the publisher.

frontiers in Oncology

MINI REVIEW
published: 26 July 2021
doi: 10.3389/fonc.2021.704471

PHF6 Mutations in Hematologic Malignancies

Jason H. Kurzer[1] *and Olga K. Weinberg*[2*]

[1] Department of Pathology, Stanford University School of Medicine, Stanford, CA, United States, [2] Department of Pathology, UT Southwestern, Dallas, TX, United States

Next generation sequencing has uncovered several genes with associated mutations in hematologic malignancies that can serve as potential biomarkers of disease. Keeping abreast of these genes is therefore of paramount importance in the field of hematology. This review focuses on *PHF6*, a highly conserved epigenetic transcriptional regulator that is important for neurodevelopment and hematopoiesis. *PHF*6 serves as a tumor suppressor protein, with *PHF6* mutations and deletions often implicated in the development of T-lymphoblastic leukemia and less frequently in acute myeloid leukemia and other myeloid neoplasms. *PHF6* inactivation appears to be an early event in T-lymphoblastic leukemogenesis, requiring cooperating events, including *NOTCH1* mutations or overexpression of TLX1 and TLX3 for full disease development. In contrast, *PHF6* mutations tend to occur later in myeloid malignancies, are frequently accompanied by *RUNX1* mutations, and are often associated with disease progression. Moreover, *PHF*6 appears to play a role in lineage plasticity within hematopoietic malignancies, with *PHF6* mutations commonly present in mixed phenotype acute leukemias with a predilection for T-lineage marker expression. Due to conflicting data, the prognostic significance of *PHF6* mutations remains unclear, with a subset of studies showing no significant difference in outcomes compared to malignancies with wild-type *PHF6*, and other studies showing inferior outcomes in certain patients with mutated *PHF6.* Future studies are necessary to elucidate the role *PHF6* plays in development of T-lymphoblastic leukemia, progression of myeloid malignancies, and its overall prognostic significance in hematopoietic neoplasms.

Keywords: PHF6, leukemia, tumor suppressor, T-ALL, AML

OPEN ACCESS

Edited by:
Julia T. Geyer,
Weill Cornell Medical Center,
United States

Reviewed by:
Yi Miao,
Nanjing Medical University, China
Ranganatha R. Somasagara,
North Carolina Central University,
United States

***Correspondence:**
Olga K. Weinberg
Olga.Weinberg@UTSouthwestern.edu

Specialty section:
This article was submitted to Hematologic Malignancies, a section of the journal Frontiers in Oncology

Received: *03 May 2021*
Accepted: *28 June 2021*
Published: *26 July 2021*

Citation:
Kurzer JH and Weinberg OK (2021) PHF6 Mutations in Hematologic Malignancies. Front. Oncol. 11:704471. doi: 10.3389/fonc.2021.704471

INTRODUCTION

Plant homeodomain (PHD) finger proteins consist of a family of epigenetic regulators that bind to a variety of targets, including both post-translationally modified and unmodified histones (1). The PHD finger protein, homeodomain finger protein 6 (*PHF6*), is a highly conserved, 365 amino acid, 41kDa protein, that was first identified in the X-linked neurodevelopmental disorder, Börjeson-Forssman-Lehmann syndrome (BFLS) (2, 3). *PHF6* contains two imperfect PHD-like zinc finger domains, two nuclear localization signals as well as a nucleolar localization sequence (**Figure 1**) (2, 4–6). Expression of PHF6 is found in almost all tissues, with particularly high expression in the brain/developing central nervous system as well as in all hematopoietic subpopulations (high levels

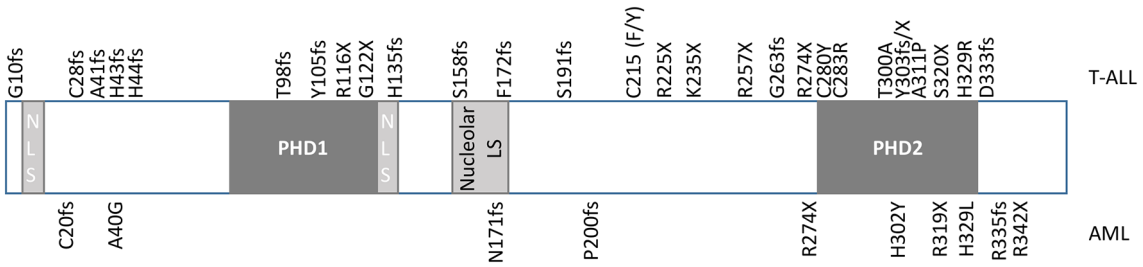

FIGURE 1 | Diagram of *PHF6*. *PHF6* has two imperfect PHD-like zinc finger domains (PHD1 and PHD2), two nuclear localization signals (NLS), and one nucleolar localization signal. Mutations originally identified in T-ALL by Van Vlierberghe et al. (4) are identified at the top of the diagram, whereas mutations originally identified in AML by Van Vliergerghe et al. (21) are identified at the bottom of the diagram.

in CD34+ precursor cells and B-cells; low levels in NK-cells and monocytes) implicating a role for *PHF6* in a variety of functions including neurogenesis and hematopoiesis (2, 7, 8).

FUNCTION OF *PHF6*

Supporting a fundamental role for *PHF6* in general development, *PHF6*-homozygous knockout mice die perinatally (9). However, scientists have also developed various knockout models in mice to explore the role of *PHF6* in hematopoiesis (8, 10–13). McRae et al. showed that germline deletion of murine *PHF6* is lethal in males whereas heterozygous females survived to adulthood (10). Using $Phf6^{lox/Y}$;$Tie\text{-}cre^{Tg/+}$ male mice with a *Phf6*-null mutation in hematopoietic and endothelial cells, McRae et al. showed an increase in $Lin^{-}c\text{-}Kit^{+}Sca\text{-}1^{+}$ (LSK) stem and progenitor cell-enriched populations, specifically the heterogeneous progenitor cell population (HPC-1), with an enrichment in cycling forms (10). Inactivation of *PHF6* at various stages of development results in increased embryologic proliferative properties of hematopoietic stem cells, but also an increased ability for *PHF6*-deficient neonatal and adult HSCs to repopulate the bone marrow in serial transplant assays (10–13). Studies suggest that this enhanced proliferative ability of *PHF6*-deleted HSCs results, at least in part, from IFN-α signaling, the inhibition of TNFα-associated growth suppressing genes, and perhaps upregulation of JAK1 signaling (10–12).

Wendorff et al. similarly showed that conditional knockout of *PHF6* displayed expansions of total immature hematopoietic LSK cells, but also showed increased multipotent MPP2, and MPP3 populations in 8-week-old mice, and no differences in the numbers of more mature myeloid progenitors, uncommitted lymphoid progenitors, or B-cell precursors (11). However, conditional knockout of *PHF6* does show a mild reduction in double-negative DN2 and DN3 thymic progenitors and decreased numbers of peripheral blood CD4 and CD8 positive T-cells in 8-week-old mice (10, 11, 13). Moreover, knockdown studies in cord blood and thymus-derived hematopoietic precursors showed that *PHF6* loss fosters a preferential differentiation of B-lymphocytes, reduced erythroid development, and accelerated T-cell development *via* downregulation of *NOTCH1* (8).

Like other PHD finger proteins, *PHF6* functions in chromatin-mediated regulation of gene expression. It is capable of binding double-stranded DNA, but not histones, *in vitro via* its atypical PHD2 domain (14). Co-immunoprecipitation experiments using antibodies to *PHF6*, reveal it interacts with constituents of the nucleosome remodeling deacetylase (NuRD) complex, including CHD_4, $HDAC_1$, and Rbb_4 (6, 15). The NuRD complex is a major ATP-dependent chromatin remodeling complex, implicated in nucleosome positioning and both repressing and activating genes involved in embryonic development (16). PHF6 has additionally been shown to bind to the PAF1 transcription elongation complex, regulating Neuroglycan C/Chondroitn sulfate proteoglycan 5 (NGC/CSPG5) and ultimately neuronal migration in murine cerebral cortex development (17). One consequence of *PHF6*-mediated transcription regulation includes the modulation of levels of the RNA Pol I preinitiation complex activator, upstream binding factor (UBF), thereby suppressing UBF-mediated rRNA transcription (5, 18).

Knockdown studies of PHF6 suggest a tumor suppressor role for the protein, as PHF6 deficiency in HeLa cell lines resulted in increased UBF protein levels, and increased DNA damage at the rDNA locus (5). Deficiency of PHF6 results in the formation of DNA-RNA hybrid (R-loops) and increased R-loop-dependent rDNA damage (5). Moreover, knockdown of *PHF6* interferes with the G2 checkpoint recovery of U2OS cells, leading to decreased DNA repair in response to ionizing radiation (19). These data implicate a tumor suppressor role for PHF6 resulting from regulating DNA damage response.

PHF6 AND HEMATOLOGIC DISEASE

Despite the discovery of *PHF6 via* its role in BFL syndrome and its prominent role in neurogenesis, mutations of *PHF6* have only been identified to date in hematologic malignancies (20). The first and most well-documented hematologic malignancy harboring mutations of *PHF6* is T-lymphoblastic leukemia (T-ALL), with fewer cases identified in acute myeloid leukemia (AML), and rarer cases identified in pre-malignant clonal hematopoiesis (4, 21–23). Mutations in hematologic malignancies include deletion, missense, frameshift, and nonsense mutations,

which span the whole coding region, with missense mutations concentrated in the PHD2 domain (**Figure 1**) (4, 21, 24). The ultimate effect of these mutations is to inhibit PHF6 function or deplete its levels, and as such, provide supporting evidence that this protein serves as a tumor suppressor. Indeed, a patient with BFLS was noted to develop T-ALL (25).

T-Lymphoblastic Leukemia

The *PHF6* locus is one of the most frequently mutated genes in T-lymphoblastic leukemia (T-ALL). Inactivating mutations of *PHF6* have been identified in 5-16% of pediatric and 19-40% of adult patients with T-ALL and ~25% of adults with T-lymphoblastic lymphoma (T-LBL) with some groups identifying an association with *NOTCH1* mutations (67%-84.6% of *PHF6* mutated/deleted T-ALL with *NOTCH1* mutations versus 39.8% *PHF6* WT) (4, 26–38). Copy number alterations of *PHF6* in pediatric T-ALL has been reported to be between 13-14% (39, 40). The location of *PHF6* on chrX26.2 lead researches to speculate that such mutations may at least partially explain the 2-3 fold increased incidence of T-ALL in males, as *PHF6* mutations were originally found predominantly in male T-ALL patients (31.5% *vs* 2.6%) (4). Subsequent studies, however, have failed to show a gender preference (26–28, 33). Recently, *PHF6* mutations have additionally been found in up to 25% (3/12) of early T-cell precursor subtype of T-ALL (ETP), a form of T-ALL that frequently expresses myeloid-associated markers (41, 42).

The role *PHF6* plays in leukemogenesis is actively under investigation. Analyzing whole exome sequencing data from diagnostic and relapse leukemias, Wendorff et al. showed that somatic mutations of *PHF6* occur early in leukeomogenesis (11). Nevertheless, animal models have revealed that while *PHF6* mutations/deletions may be initial events, they are insufficient for tumor initiation without additional driver mutations. For example, Miyagi et al. did not observe leukemia development subsequent to serial transplantation of *PHF6*-deleted HSCs in mice (12). Likewise, no T-ALL tumors developed in a $PHF6^{+/-}$ zebrafish model (43).

Studies show that *PHF6* dysfunction cooperates with several other driver mutations. For example, inactivation of *PHF6* in hematopoietic progenitors has been reported to facilitate NOTCH1-induced T-ALL, potentially through increasing leukemia-initiating cells and development of a "leukemia stem cell transcriptional program" in lymphoblasts (11, 13). A study of 102 pediatric T-ALL cases in Taiwan showed that *PHF6* mutations frequently cooperate with *HOX11L2* overexpression and/or *WT1* mutations (44). In addition, *PHF6* mutations have been shown to be associated (at times in conjunction with *DNM2*) with T-ALLs that overexpress homeobox transcription factors, *TLX1* and *TLX3* (4, 32, 45). Indeed, ectopic expression of TLX3 in *PHF6*-deleted mice facilitated early onset leukemia and a $hTLX1;PHF6^{+/-}$ zebrafish model demonstrated fully penetrant early-onset leukemia development, underscoring the role of cooperation between these mutations in leukemogenesis (10, 43). Other associations include those with mutations in X-linked genes, *USP9X* and *MED1* as well as with *IL7R-JAK* pathway genes, *WT1, PTPN2* deletions, and *HOX11L2* overexpression (33, 34, 44, 46). In the setting of ETP, *PHF6* mutations frequently occur with mutations in *EZH2*, *EED*, and *SUZ12* (41). Finally, a network of miRNAs, including miR-19b, miR-20a/93, miR-26a, miR-92, and miR-223, have been shown to target multiple PHF6 and other T-ALL-associated tumor suppressors, and thus promote leukemia (47).

PHF6 has additionally been shown to interact with LMO2 to bind DNA *via* the LMO2/TAL1/LDB/GATA2 complex in T-ALL cell lines (48). The PHF6/LMO2/TAL1/LDB/GATA2 complex was shown to bind at DNA segments associated with hematopoietic or lymphoid organ development, hematopoiesis, as well as T-cell activation and differentiation (48).

While sample sizes are small, patients with T-ALL harboring *PHF6* mutations tend to be older, have been demonstrated to have lower white blood cell counts than other T-ALL patients, as well as lower hemoglobin and platelet levels, splenomegaly/lymphadenopathy, and have blasts with a tendency to express CD13 (26, 29, 37). Genomic analysis of matched diagnosis, germline (remission) and relapse DNA samples from 46 T-ALL cases reveals that *PHF6* alterations are found commonly at diagnosis, and persist at relapse (49). While mutations in *PHF6* have been implicated in increased resistance to prednisolone in T-ALL cell lines, the majority of studies have shown no correlation with *PHF6* mutations and overall survival in patients with T-ALL, and a potential favorable prognosis associated with T-LBL (4, 26, 27, 29, 50, 51). Nevertheless, one study of pediatric T-ALL found *PHF6* mutations/deletions predict an inferior overall survival upon multivariate analysis (44). Another study of Chinese adults found that the co-existence of *PHF6* and *NOTCH1* mutations in T-ALL conferred a shorter event-free survival and a poor prognosis (37). Further study is therefore required to assess the true prognostic significance of *PHF6* mutations in T-ALL.

Myeloid Neoplasms

The largest study of *PHF6* mutations in myeloid malignancies involved targeted sequencing of 1760 cases with myeloid neoplasms (24). This study revealed 54 patients with 62 somatic mutations of *PHF6* (24). With regard to disease burden, the percentage of blasts in the bone marrow tended to be higher in patients with myeloid neoplasms harboring *PHF6* mutations (24). As for cytogenetics, abnormal karyotypes showed no significant predilection for *PHF6* mutations, although +8, t(8;21), and complex karyotypes were abnormalities most often identified (24). At the molecular level, co-mutated genes associated with *PHF6* mutations included *RUNX1*, *U2AF1*, *SMC1A*, *ZRSR2*, *EZH2*, and *ASXL1*, whereas *PHF6* was found to be mutually exclusive with *SF3B1* (24). In contrast to T-ALL, mutations of *PHF6* tend to occur later in disease evolution, sometimes with different mutations in parallel clones (24).

Acute Myeloid Leukemia

Inactivating somatic *PHF6* mutations have been found in ~2-3% of AMLs (20, 21, 24, 28, 52, 53). Similar to T-ALL, a male predominance was initially reported but not further substantiated

for AML identified with *PHF6* mutations (21, 24, 53). With respect to AML subtypes, *PHF6* mutations are found in 15% of AML with inv(3)(q21q26.2)/t(3;3)(q21;q26.2) and 15.4% of cases of AML with myelodysplasia related changes (MRC) (24, 54). Interestingly, a case report of AML with MRC harboring a *P2RY8-CRLF2* fusion was found to have gained a *PHF6* mutation upon transformation to AML, suggesting a potential role for *PHF6* in the transition of MDS to AML (55). Further evidence for *PHF6* mutations acquired secondarily and leading to progression of myeloid neoplasms was found in patients with germline mutations of *RUNX1*, where *PHF6* mutations were implicated in the transition to MDS in one patient and the transition to AML in the other (56, 57). Interestingly, *PHF6* has been shown to frequently co-occur with *RUNX1* in AML (58).

Despite *PHF6* mutations leading to inactivation of the protein, an analysis of *PHF6* expression levels in AML regardless of mutation status revealed that PHF6 protein levels are higher in patients with AML than normal controls, a finding seemingly at odds with its role as a tumor suppressor (59). Moreover, increased PHF6 levels correlated with an increased percentage of blasts, with a possible correlation with CD34 positivity (59). Decreased PHF6 protein expression correlated with longer overall survival than those with high expression levels (2 years versus 6 months) (59).

A study of 318 pediatric patients with *de novo* AML identified *PHF6* mutations in 6 (2%) cases with FAB subtypes of M0, M1, and M2 (53). The median age for this group was 12.6 years (versus 9.5 in wild type *PHF6 AML*), with 4 of 6 succumbing to the disease. Co-genetic abnormalities included *RUNX1/RUNX1T1* translocations, *NUP98/KDM5A* translocations, and mutations in *WT1*, *RAS*, *ETV6*, *TET2*, *IDH1*, and *BCORL1* (53). Measuring the expression level of PHF6 showed decreased PHF6 levels in patients with mutations compared to M0, M1, and M2 AML subtypes with wild-type *PHF6*, again supporting a tumor suppressor role for *PHF6* and providing at least some genetic context to the results found by Mousa et al. above (53, 59).

A study of 398 patients with AML younger than 60 years of age revealed *PHF6* to be associated with decreased overall survival in patients with intermediate-risk AML with wild-type FLT3-ITD (60). This implicates *PHF6* mutations as a potential prognostic marker to be used in intermediate-risk AML, although it should be noted that this finding has not been replicated by others (24). Interestingly, subdividing AML with MRC cases that are associated with complex karyotypes into typical (those harboring 5q, 7q and/or 17p abnormalities) and atypical (those without these abnormalities) shows that AML with atypical complex karyotypes tend to have *PHF6* mutations more frequently, *TP53* mutations less frequently, be younger, have a higher WBC and blast percentage, and higher complete remission and overall survival rates (61).

Myelodysplastic Syndrome

Animal models suggest a possible role for *PHF6* mutations in myelodysplastic syndrome (MDS), as aged mice with knocked-out *PHF6* exhibit megakaryocytic dysplasia and associated decreased platelet counts as well as extramedullary hematopoiesis (13). Nevertheless, *PHF6* mutations are relatively rare (~3%) in MDS (24, 62–64). The limited data indicate that *PHF6* mutations are found most frequently (5.3% of MDS cases) in the high-grade subtypes (MDS with excess blasts) (24). *PHF6* mutations tended to show low variant allele frequencies and acquisition in sub-clonal populations (24). The most frequent co-mutations were seen in ASXL1, RUNX1, TET2, and DNMT3A (64). A study of 21 MDS patients harboring *PHF6* mutations revealed 61.9% had normal karyotypes and no patients had complex karyotypes (64).

Myeloproliferative Neoplasms

PHF6 mutations are rarely identified in myeloproliferative neoplasms (MPN) (0.7%), occurring in only 1.6% of chronic myelogenous leukemia (24). A screen of 81patients with CML in myeloid blast crisis identified 2 male patients with *PHF6* mutations, with at least one patient showing no *PHF6* mutations in the preceding chronic phase (65). This finding raises the possibility that, similar to MDS, the accumulation of *PHF6* mutations might mediate progression of the disease. Relatedly, a review of 22 patients with *PHF6* mutations in myeloproliferative neoplasms at three institutions revealed an enrichment in cases with increased fibrosis and/or blast crisis (66). Other than JAK2, the most common co-mutations in these MPNs were *ASXL1*, and *TET2* with a median of 2.5 non JAK2 co-mutated genes (66).

With respect to mixed myelodysplastic syndrome/myeloproliferative neoplasm cases, *PHF6* mutations were seen in 4.7% of CMML patients (24). To date, no effect on survival has been seen in *PHF6*-mutation associated CMML patients (64).

B-Lymphoblastic Leukemia

Despite their prevalence in T-ALL, *PHF6* mutations have only rarely been identified in B-lymphoblastic leukemia (4, 41, 67). 50% of the rare *MEF2D*-rearranged B-ALL was found to have *PHF6* mutations (67). Intriguingly, use of a retrovirally-expressed shRNA screening library into a B-lymphobastic leukemia cell line revealed that knockdown of PHF6 levels inhibited cell growth and leukemia growth in transplanted models (68). Indeed, CRISPR-Cas9-mediated deletion of *PHF6* in a murine *BCR-ABL1*$^{+}$*; p19*$^{-/-}$*; mCherry*$^{+}$ B-ALL cell line resulted in delayed tumor formation after injection in immunocompetent mice compared to wild-type B-ALL cells (69). Moreover, *PHF6* KO B-ALL cells induced a malignancy closer in presentation to lymphoma than leukemia, with tumor cells showing reduced expression of CD19 and B220 and B-cell development genes (e.g., *Cd74*, *IL4ra*, *Lyn*, *Ly86*, and *BLK*), and upregulation of CD4 and T-cell signal transduction genes (69). These data therefore implicate PHF6 mutations as lineage specific with respect to tumorigenesis, and even implicate mutation of *PHF6* as a potential mediator of lineage plasticity in hematopoietic neoplasms.

Acute Leukemia of Ambiguous Lineage

The association of *PHF6* mutations with leukemias of ambiguous lineage further supports a role for these mutations in lineage plasticity. An analysis of 29 mixed phenotype acute leukemia cases at Memorial Sloan Kettering Cancer Center revealed *PHF6*

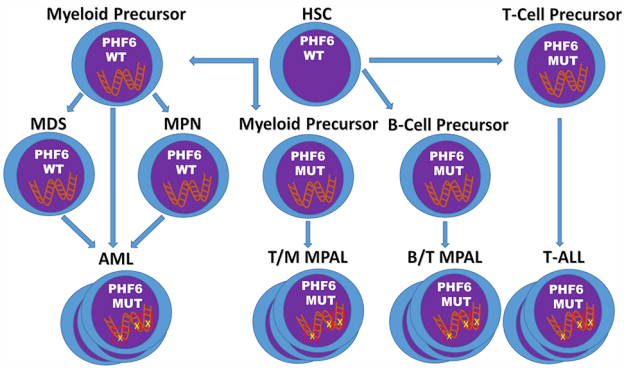

FIGURE 2 | Model of *PHF6* in Hematopoietic Malignancies. The timing and context of the acquisition of *PHF6* deletions/mutations appear to determine the fate of the resulting malignancy. In T-ALL, *PHF6* deletions/mutations arise early, but are insufficient for transformation into leukemia. In contrast, in myeloid neoplasms, *PHF6* deletions/mutations tend to develop later possibly leading to disease progression. Finally, acquisition of inactivating mutations of *PHF6* in myeloid or B-cell precursors may promote T-cell gene expression and eventual development of mixed phenotype acute leukemias.

(23%) and *DNMT3A* (23%) as the most common recurrent mutations (70). Mutations in *PHF6* and *DNMT3A* are mutually exclusive in MPAL, correlate with T-lineage marker expression (83% and 100%, respectively), and have higher relapse at 2 years (58% and 79%, respectively) compared to MPAL lacking these mutations (70).

In addition to T/M cases, Xiao et al. identified *PHF6* mutations in patients with T/B/M and T/B phenotypes (70). Similarly, Getta et al. found *PHF6* mutations in 3 of 16 MPAL patients with at least 2 of 3 patients of the MPAL, NOS subtype (B/T or B/T/M) (71). Furthermore, a review of 9 patients from multiple institutions identified *PHF6* mutations in 5 patients with B/T MPAL (56%) (72).

Similar to T-ALL, *PHF6* mutations are believed to be early events in MPAL, as Xiao et al. found every blast population isolated from selected cases showed nearly 100% VAF (70). Interestingly, *PHF6*-associated MPAL correlates with younger patients, higher hemoglobin and higher platelet values (70, 72).

Bond et al. performed an analysis of the transcriptional program of AMLs and T-ALLs and identified an expression program at the interface of these two diseases (73). Comparing T-ALL to T-ALL-like AMLs and AML-like T-ALLs, it was found that all T-ALLs with *PHF6* mutations were accompanied by *NOTCH1* mutations, whereas 3/5 *PHF6* mutated interface cases lacked *NOTCH1* mutations (73).

Interestingly, a study of acute undifferentiated leukemias found *PHF6* mutations in 7/16 cases of AUL, whereas only 1/25 cases of minimally differentiated AML harbored these mutations (74). Nevertheless, in the limited study, no clinical outcome differences were seen between the two groups (74).

DISCUSSION

The last two decades have elucidated a role for *PHF6* in neurodevelopment and hematopoiesis, and revealed it as a potent tumor suppressor with an exclusive tendency for hematologic malignancies (**Figure 2**). *PHF6* mutations are most common in T-ALL, and appear early in the disease course yet appear insufficient for leukemia development. Given the conflicting data regarding the prognostic significance of *PHF6* mutations in T-ALL, additional studies are necessary to clarify the role of *PHF6* inactivation in the disease course. It is likely that appropriately powered studies will need to assess its significance in specific patient cohorts.

In contrast to T-ALL, *PHF6* mutations are less frequent in myeloid malignancies. Of interest, these mutations are more frequently found later in the disease course at points of disease progression. Further work is therefore required to determine the mechanism by which *PHF6* pushes these neoplasms to a more aggressive disease, as well as to determine the overall prognostic significance of *PHF6* mutations in myeloid malignancies in general. If additional studies continue to show a role for *PHF6* mutations in disease progression, laboratories may wish to offer specific targeted analysis of *PHF6* for the monitoring of myeloid disease.

Finally, it is becoming clear that *PHF6* plays a role in lineage plasticity of hematopoietic malignancies, as *PHF6* mutations exist in T/Myeloid MPAL as well as MPAL, NOS (particularly B/T MPAL) and is frequently associated with early T-ALL which frequently shows myeloid marker expression. The underlying contextual factors, including cell of origin and cooperative gene mutations, remain to be elucidated to understand what drives a *PHF6*-associated malignancy to be T-lineage, myeloid lineage, or a combination of both.

AUTHOR CONTRIBUTIONS

OW conceived of the review subject matter and provided editorial review while JK primarily composed the manuscript. All authors contributed to the article and approved the submitted version.

REFERENCES

1. Musselman CA, Kutateladze TG. Handpicking Epigenetic Marks With PHD Fingers. *Nucleic Acids Res* (2011) 39:9061–71. doi: 10.1093/nar/gkr613
2. Lower KM, Turner G, Kerr BA, Mathews KD, Shaw MA, Gedeon AK, et al. Mutations in PHF6 Are Associated With Börjeson-Forssman-Lehmann Syndrome. *Nat Genet* (2002) 32:661–5. doi: 10.1038/ng1040
3. Todd MAM, Ivanochko D, Picketts DJ. PHF6 Degrees of Separation: the Multifaceted Roles of a Chromatin Adaptor Protein. *Genes* (2015) 6:325–52. doi: 10.3390/genes6020325
4. Van Vlierberghe P, Palomero T, Khiabanian H, Van der Meulen J, Castillo M, Van Roy N, et al. PHF6 Mutations in T-Cell Acute Lymphoblastic Leukemia. *Nat Genet* (2010) 42:338–42. doi: 10.1038/ng.542
5. Wang J, Leung JW, Gong Z, Feng L, Shi X, Chen J. PHF6 Regulates Cell Cycle Progression by Suppressing Ribosomal RNA Synthesis. *J Biol Chem* (2013) 288:3174–83. doi: 10.1074/jbc.M112.414839
6. Todd MAM, Picketts DJ. PHF6 Interacts With the Nucleosome Remodeling and Deacetylation (Nurd) Complex. *J Proteome Res* (2012) 11:4326–37. doi: 10.1021/pr3004369
7. Voss AK, Gamble R, Collin C, Shoubridge C, Corbett M, Gécz J, et al. Protein and Gene Expression Analysis of Phf6, the Gene Mutated in the Börjeson-Forssman-Lehmann Syndrome of Intellectual Disability and Obesity. *Gene Expr. Patterns GEP* (2007) 7:858–71. doi: 10.1016/j.modgep.2007.06.007
8. Loontiens S, Dolens A-C, Strubbe S, Van de Walle I, Moore FE, Depestel L, et al. Phf6 Expression Levels Impact Human Hematopoietic Stem Cell Differentiation. *Front Cell Dev Biol* (2020) 8:599472. doi: 10.3389/fcell.2020.599472
9. Cheng C, Deng P-Y, Ikeuchi Y, Yuede C, Li D, Rensing N, et al. Characterization of a Mouse Model of Börjeson-Forssman-Lehmann Syndrome. *Cell Rep* (2018) 25:1404–14.e6. doi: 10.1016/j.celrep.2018.10.043
10. McRae HM, Garnham AL, Hu Y, Witkowski MT, Corbett MA, Dixon MP, et al. PHF6 Regulates Hematopoietic Stem and Progenitor Cells and its Loss Synergizes With Expression of TLX3 to Cause Leukemia. *Blood* (2019) 133:1729–41. doi: 10.1182/blood-2018-07-860726
11. Wendorff AA, Quinn SA, Rashkovan M, Madubata CJ, Ambesi-Impiombato A, Litzow MR, et al. Phf6 Loss Enhances HSC Self-Renewal Driving Tumor Initiation and Leukemia Stem Cell Activity in T-ALL. *Cancer Discov* (2019) 9:436–51. doi: 10.1158/2159-8290.CD-18-1005
12. Miyagi S, Sroczynska P, Kato Y, Nakajima-Takagi Y, Oshima M, Rizq O, et al. The Chromatin-Binding Protein Phf6 Restricts the Self-Renewal of Hematopoietic Stem Cells. *Blood* (2019) 133:2495–506. doi: 10.1182/blood.2019000468
13. Hsu Y-C, Chen T-C, Lin C-C, Yuan C-T, Hsu C-L, Hou H-A, et al. Phf6-Null Hematopoietic Stem Cells Have Enhanced Self-Renewal Capacity and Oncogenic Potentials. *Blood Adv* (2019) 3:2355–67. doi: 10.1182/bloodadvances.2019000391
14. Liu Z, Li F, Ruan K, Zhang J, Mei Y, Wu J, et al. Structural and Functional Insights Into the Human Börjeson-Forssman-Lehmann Syndrome-Associated Protein PHF6 *. *J Biol Chem* (2014) 289:10069–83. doi: 10.1074/jbc.M113.535351
15. Liu Z, Li F, Zhang B, Li S, Wu J, Shi Y. Structural Basis of Plant Homeodomain Finger 6 (PHF6) Recognition by the Retinoblastoma Binding Protein 4 (RBBP4) Component of the Nucleosome Remodeling and Deacetylase (Nurd) Complex. *J Biol Chem* (2015) 290:6630–8. doi: 10.1074/jbc.M114.610196
16. Basta J, Rauchman M. The Nucleosome Remodeling and Deacetylase (Nurd) Complex in Development and Disease. *Transl Res J Lab Clin Med* (2015) 165:36–47. doi: 10.1016/j.trsl.2014.05.003
17. Zhang C, Mejia LA, Huang J, Valnegri P, Bennett EJ, Anckar J, et al. The X-Linked Intellectual Disability Protein PHF6 Associates With the PAF1 Complex and Regulates Neuronal Migration in the Mammalian Brain. *Neuron* (2013) 78:986–93. doi: 10.1016/j.neuron.2013.04.021
18. Todd MAM, Huh MS, Picketts DJ. The Sub-Nucleolar Localization of PHF6 Defines its Role in Rdna Transcription and Early Processing Events. *Eur J Hum Genet EJHG* (2016) 24:1453–9. doi: 10.1038/ejhg.2016.40
19. Warmerdam DO, Alonso-de Vega I, Wiegant WW, van den Broek B, Rother MB, Wolthuis RM, et al. PHF6 Promotes non-Homologous End Joining and G2 Checkpoint Recovery. *EMBO Rep* (2020) 21:e48460. doi: 10.15252/embr.201948460
20. Huether R, Dong L, Chen X, Wu G, Parker M, Wei L, et al. The Landscape of Somatic Mutations in Epigenetic Regulators Across 1,000 Paediatric Cancer Genomes. *Nat Commun* (2014) 5:3630. doi: 10.1038/ncomms4630
21. Van Vlierberghe P, Patel J, Abdel-Wahab O, Lobry C, Hedvat CV, Balbin M, et al. PHF6 Mutations in Adult Acute Myeloid Leukemia. *Leukemia* (2011) 25:130–4. doi: 10.1038/leu.2010.247
22. Yoshizato T, Dumitriu B, Hosokawa K, Makishima H, Yoshida K, Townsley D, et al. Somatic Mutations and Clonal Hematopoiesis in Aplastic Anemia. *N Engl J Med* (2015) 373:35–47. doi: 10.1056/NEJMoa1414799
23. Abelson S, Collord G, Ng SWK, Weissbrod O, Mendelson Cohen N, Niemeyer E, Barda N, et al. Prediction of Acute Myeloid Leukaemia Risk in Healthy Individuals. *Nature* (2018) 559:400–4. doi: 10.1038/s41586-018-0317-6
24. Mori T, Nagata Y, Makishima H, Sanada M, Shiozawa Y, Kon A, et al. Somatic PHF6 Mutations in 1760 Cases With Various Myeloid Neoplasms. *Leukemia* (2016) 30:2270–3. doi: 10.1038/leu.2016.212
25. Chao MM, Todd MA, Kontny U, Neas K, Sullivan MJ, Hunter AG, et al. T-Cell Acute Lymphoblastic Leukemia in Association With Börjeson-Forssman-Lehmann Syndrome Due to a Mutation in PHF6. *Pediatr Blood Cancer* (2010) 55:722–4. doi: 10.1002/pbc.22574
26. Grossmann V, Haferlach C, Weissmann S, Roller A, Schindela S, Poetzinger F, et al. The Molecular Profile of Adult T-Cell Acute Lymphoblastic Leukemia: Mutations in RUNX1 and DNMT3A Are Associated With Poor Prognosis in T-ALL. *Genes Chromosomes Cancer* (2013) 52:410–22. doi: 10.1002/gcc.22039
27. Wang Q, Qiu H, Jiang H, Wu L, Dong S, Pan J, et al. Mutations of PHF6 are Associated With Mutations of NOTCH1, JAK1 and Rearrangement of SET-NUP214 in T-Cell Acute Lymphoblastic Leukemia. *Haematologica* (2011) 96:1808–14. doi: 10.3324/haematol.2011.043083
28. Yoo NJ, Kim YR, Lee SH. Somatic Mutation of PHF6 Gene in T-Cell Acute Lymphoblatic Leukemia, Acute Myelogenous Leukemia and Hepatocellular Carcinoma. *Acta Oncol Stockh Swed* (2012) 51:107–11. doi: 10.3109/0284186X.2011.592148
29. Huh HJ, Lee SH, Yoo KH, Sung KW, Koo HH, Jang JH, et al. Gene Mutation Profiles and Prognostic Implications in Korean Patients With T-Lymphoblastic Leukemia. *Ann Hematol* (2013) 92:635–44. doi: 10.1007/s00277-012-1664-2
30. Chang Y-H, Yu C-H, Jou S-T, Lin C-Y, Lin K-H, Lu M-Y, et al. Targeted Sequencing to Identify Genetic Alterations and Prognostic Markers in Pediatric T-Cell Acute Lymphoblastic Leukemia. *Sci Rep* (2021) 11:769. doi: 10.1038/s41598-020-80613-6
31. Sentís I, Gonzalez S, Genescà E, García-Hernández V, Muiños F, Gonzalez C, et al. The Evolution of Relapse of Adult T Cell Acute Lymphoblastic Leukemia. *Genome Biol* (2020) 21:284. doi: 10.1186/s13059-020-02192-z
32. Liu Y, Easton J, Shao Y, Maciaszek J, Wang Z, Wilkinson MR, et al. The Genomic Landscape of Pediatric and Young Adult T-Lineage Acute Lymphoblastic Leukemia. *Nat Genet* (2017) 49:1211–8. doi: 10.1038/ng.3909
33. Spinella J-F, Cassart P, Richer C, Saillour V, Ouimet M, Langlois S, et al. Genomic Characterization of Pediatric T-Cell Acute Lymphoblastic Leukemia Reveals Novel Recurrent Driver Mutations. *Oncotarget* (2016) 7:65485–503. doi: 10.18632/oncotarget.11796
34. Vicente C, Schwab C, Broux M, Geerdens E, Degryse S, Demeyer S, et al. Targeted Sequencing Identifies Associations Between IL7R-JAK Mutations and Epigenetic Modulators in T-Cell Acute Lymphoblastic Leukemia. *Haematologica* (2015) 100:1301–10. doi: 10.3324/haematol.2015.130179
35. Zhang H-H, Wang H-S, Qian X-W, Fan C-Q, Li J, Miao H, et al. Genetic Variants and Clinical Significance of Pediatric Acute Lymphoblastic Leukemia. *Ann Transl Med* (2019) 7:296. doi: 10.21037/atm.2019.04.80
36. Richter-Pechańska P, Kunz JB, Hof J, Zimmermann M, Rausch T, Bandapalli OR, et al. Identification of a Genetically Defined Ultra-High-Risk Group in Relapsed Pediatric T-Lymphoblastic Leukemia. *Blood Cancer J* (2017) 7:e523. doi: 10.1038/bcj.2017.3
37. Li M, Xiao L, Xu J, Zhang R, Guo J, Olson J, et al. Co-Existence of PHF6 and NOTCH1 Mutations in Adult T-Cell Acute Lymphoblastic Leukemia. *Oncol Lett* (2016) 12:16–22. doi: 10.3892/ol.2016.4581
38. De Keersmaecker K, Atak ZK, Li N, Vicente C, Patchett S, Girardi T, et al. Exome Sequencing Identifies Mutation in CNOT3 and Ribosomal Genes

RPL5 and RPL10 in T-Cell Acute Lymphoblastic Leukemia. *Nat Genet* (2013) 45:186–90. doi: 10.1038/ng.2508
39. Teachey DT, Pui C-H. Comparative Features and Outcomes Between Paediatric T-Cell and B-Cell Acute Lymphoblastic Leukaemia. *Lancet Oncol* (2019) 20:e142–54. doi: 10.1016/S1470-2045(19)30031-2
40. Lejman M, Włodarczyk M, Styka B, Pastorczak A, Zawitkowska J, Taha J, et al. Advantages and Limitations of SNP Array in the Molecular Characterization of Pediatric T-Cell Acute Lymphoblastic Leukemia. *Front Oncol* (2020) 10:1184. doi: 10.3389/fonc.2020.01184
41. Zhang J, Ding L, Holmfeldt L, Wu G, Heatley SL, Payne-Turner D, et al. The Genetic Basis of Early T-Cell Precursor Acute Lymphoblastic Leukaemia. *Nature* (2012) 481:157–63. doi: 10.1038/nature10725
42. Noronha EP, Marques LVC, Andrade FG, Thuler LCS, Terra-Granado E, Pombo-de-Oliveira MS, et al. The Profile of Immunophenotype and Genotype Aberrations in Subsets of Pediatric T-Cell Acute Lymphoblastic Leukemia. *Front Oncol* (2019) 9:316. doi: 10.3389/fonc.2019.00316
43. Loontiens S, Vanhauwaert S, Depestel L, Dewyn G, Van Loocke W, Moore FE, et al. A Novel TLX1-Driven T-ALL Zebrafish Model: Comparative Genomic Analysis With Other Leukemia Models. *Leukemia* (2020) 34:3398–403. doi: 10.1038/s41375-020-0938-2
44. Yeh T-C, Liang D-C, Liu H-C, Jaing T-H, Chen S-H, Hou J-Y, et al. Clinical and Biological Relevance of Genetic Alterations in Pediatric T-Cell Acute Lymphoblastic Leukemia in Taiwan. *Pediatr Blood Cancer* (2019) 66:e27496. doi: 10.1002/pbc.27496
45. Seki M, Kimura S, Isobe T, Yoshida K, Ueno H, Nakajima-Takagi Y, et al. Recurrent SPI1 (PU.1) Fusions in High-Risk Pediatric T Cell Acute Lymphoblastic Leukemia. *Nat Genet* (2017) 49:1274–81. doi: 10.1038/ng.3900
46. Alcantara M, Simonin M, Lhermitte L, Touzart A, Dourthe ME, Latiri M, et al. Clinical and Biological Features of PTPN2-Deleted Adult and Pediatric T-Cell Acute Lymphoblastic Leukemia. *Blood Adv* (2019) 3:1981–8. doi: 10.1182/bloodadvances.2018028993
47. Mavrakis KJ, Van Der Meulen J, Wolfe AL, Liu X, Mets E, Taghon T, et al. A Cooperative Microrna-Tumor Suppressor Gene Network in Acute T-Cell Lymphoblastic Leukemia (T-ALL). *Nat Genet* (2011) 43:673–8. doi: 10.1038/ng.858
48. Stanulović VS, Binhassan S, Dorrington I, Ward DG, Hoogenkamp M. PHF6 Interacts With LMO2 During Normal Haematopoiesis and in Leukaemia and Regulates Gene Expression and Genome Integrity. *bioRxiv* (2020), 2020.08.18.255471. doi: 10.1101/2020.08.18.255471
49. Oshima K, Zhao J, Pérez-Durán P, Brown JA, Patiño-Galindo JA, Chu T, et al. Mutational and Functional Genetics Mapping of Chemotherapy Resistance Mechanisms in Relapsed Acute Lymphoblastic Leukemia. *Nat Cancer* (2020) 1:1113–27. doi: 10.1038/s43018-020-00124-1
50. Xiang J, Wang G, Xia T, Chen Z. The Depletion of PHF6 Decreases the Drug Sensitivity of T-Cell Acute Lymphoblastic Leukemia to Prednisolone. *Biomed Pharmacother Biomed Pharmacother* (2019) 109:2210–7. doi: 10.1016/j.biopha.2018.11.083
51. Kroeze E, Loeffen JLC, Poort VM, Meijerink JPP. T-Cell Lymphoblastic Lymphoma and Leukemia: Different Diseases From a Common Premalignant Progenitor? *Blood Adv* (2020) 4:3466–73. doi: 10.1182/bloodadvances.2020001822
52. Ding L, Ley TJ, Larson DE, Miller CA, Koboldt DC, Welch JS, et al. Clonal Evolution in Relapsed Acute Myeloid Leukaemia Revealed by Whole-Genome Sequencing. *Nature* (2012) 481:506–10. doi: 10.1038/nature10738
53. Rooij JDE de, van den Heuvel-Eibrink MM, van de Rijdt NKAM, Verboon LJ, de Haas V, Trka J, et al. PHF6 Mutations in Paediatric Acute Myeloid Leukaemia. *Br J Haematol* (2016) 175:967–71. doi: 10.1111/bjh.13891
54. Papaemmanuil E, Gerstung M, Bullinger L, Gaidzik VI, Paschka P, Roberts ND, et al. Genomic Classification and Prognosis in Acute Myeloid Leukemia. *N Engl J Med* (2016) 374:2209–21. doi: 10.1056/NEJMoa1516192
55. Aypar U, Taylor J, Garcia JS, Momeni-Boroujeni A, Gao Q, Baik J, et al. P2RY8-CRLF2Fusion-Positive Acute Myeloid Leukemia With Myelodysplasia-Related Changes: Response to Novel Therapy. *JCO Precis Oncol* (2020) 4:152–60. doi: 10.1200/PO.19.00294
56. Ng IK, Lee J, Ng C, Kosmo B, Chiu L, Seah E, et al. Preleukemic and Second-Hit Mutational Events in an Acute Myeloid Leukemia Patient With a Novel Germline RUNX1 Mutation. *Biomark Res* (2018) 6:16. doi: 10.1186/s40364-018-0130-2
57. Staňo Kozubík K, Radová L, Pešová M, Réblová K, Trizuljak J, Plevová K, et al. C-Terminal RUNX1 Mutation in Familial Platelet Disorder With Predisposition to Myeloid Malignancies. *Int J Hematol* (2018) 108:652–7. doi: 10.1007/s12185-018-2514-3
58. Desai P, Mencia-Trinchant N, Savenkov O, Simon MS, Cheang G, Lee S, et al. Somatic Mutations Precede Acute Myeloid Leukemia Years Before Diagnosis. *Nat Med* (2018) 24:1015–23. doi: 10.1038/s41591-018-0081-z
59. Mousa NO, Gado M, Assem MM, Dawood KM, Osman A, Mousa NO, et al. Expression Profiling of Some Acute Myeloid Leukemia - Associated Markers to Assess Their Diagnostic/Prognostic Potential. *Genet Mol Biol* (2021) 44(1). doi: 10.1590/1678-4685-gmb-2019-0268
60. Patel JP, Gado M, Assem MM, Dawood KM, Osman A, Mousa NO, et al. Prognostic Relevance of Integrated Genetic Profiling in Acute Myeloid Leukemia. *N Engl J Med* (2012) 366:1079–89. doi: 10.1016/j.yonc.2012.07.030
61. Mrózek K, Eisfeld A-K, Kohlschmidt J, Carroll AJ, Walker CJ, Nicolet D, et al. Complex Karyotype in *De Novo* Acute Myeloid Leukemia: Typical and Atypical Subtypes Differ Molecularly and Clinically. *Leukemia* (2019) 33:1620–34. doi: 10.1038/s41375-019-0390-3
62. Haferlach T, Nagata Y, Grossmann V, Okuno Y, Bacher U, Nagae G, et al. Landscape of Genetic Lesions in 944 Patients With Myelodysplastic Syndromes. *Leukemia* (2014) 28:241–7. doi: 10.1038/leu.2013.336
63. Yoshida K, Sanada M, Shiraishi Y, Nowak D, Nagata Y, Yamamoto R, et al. Frequent Pathway Mutations of Splicing Machinery in Myelodysplasia. *Nature* (2011) 478:64–9. doi: 10.1038/nature10496
64. Chien KS, Kanagal-Shamanna R, Naqvi K, Sasaki K, Alvarado Y, Takahashi K, et al. The Impact of PHF6 Mutations in Myelodysplastic Syndromes, Chronic Myelomonocytic Leukemia, and Acute Myeloid Leukemia. *Blood* (2019) 134:1436–6. doi: 10.1182/blood-2019-131188
65. Li X, Yao H, Chen Z, Wang Q, Zhao Y, Chen S. Somatic Mutations of PHF6 in Patients With Chronic Myeloid Leukemia in Blast Crisis. *Leuk Lymphoma* (2013) 54:671–2. doi: 10.3109/10428194.2012.725203
66. Kurzer JH, Nardi V, Ouseph M, Weinberg OK. Clinical and Genomic Characterization of Myeloproliferative Neoplasms Harboring PHF6 Mutations, Abstract 1411. *Abstr USCAP 2020 Hematop 1316-1502 Mod Pathol* (2020) 33:1328–9. doi: 10.1038/s41379-020-0475-6
67. Ohki K, Kiyokawa N, Saito Y, Hirabayashi S, Nakabayashi K, Ichikawa H, et al. Clinical and Molecular Characteristics of MEF2D Fusion-Positive B-Cell Precursor Acute Lymphoblastic Leukemia in Childhood, Including a Novel Translocation Resulting in MEF2D-HNRNPH1 Gene Fusion. *Haematologica* (2019) 104:128–37. doi: 10.3324/haematol.2017.186320
68. Meacham CE, Lawton LN, Soto-Feliciano YM, Pritchard JR, Joughin BA, Ehrenberger T, et al. A Genome-Scale *In Vivo* Loss-of-Function Screen Identifies Phf6 as a Lineage-Specific Regulator of Leukemia Cell Growth. *Genes Dev* (2015) 29:483–8. doi: 10.1101/gad.254151.114
69. Soto-Feliciano YM, Bartlebaugh JME, Liu Y, Sánchez-Rivera FJ, Bhutkar A, Weintraub AS, et al. PHF6 Regulates Phenotypic Plasticity Through Chromatin Organization Within Lineage-Specific Genes. *Genes Dev* (2017) 31:973–89. doi: 10.1101/gad.295857.117
70. Xiao W, Bharadwaj M, Levine M, Farnhoud N, Pastore F, Getta BM, et al. PHF6 and DNMT3A Mutations Are Enriched in Distinct Subgroups of Mixed Phenotype Acute Leukemia With T-Lineage Differentiation. *Blood Adv* (2018) 2:3526–39. doi: 10.1182/bloodadvances.2018023531
71. Getta BM, Roshal M, Zheng J, Park JH, Stein EM, Levine R, et al. Allogeneic Hematopoietic Stem Cell Transplantation With Myeloablative Conditioning Is Associated With Favorable Outcomes in Mixed Phenotype Acute Leukemia. *Biol Blood Marrow Transplant J Am Soc Blood Marrow Transplant* (2017) 23:1879–86. doi: 10.1016/j.bbmt.2017.06.026
72. Mi X, Griffin G, Lee W, Patel S, Ohgami R, Ok CY, et al. Genomic and Clinical Characterization of B/T Mixed Phenotype Acute Leukemia Reveals Recurrent Features and T-ALL Like Mutations. *Am J Hematol* (2018) 93:1358–67. doi: 10.1002/ajh.25256
73. Bond J, Krzywon A, Lhermitte L, Roumier C, Roggy A, Belhocine M, et al. A Transcriptomic Continuum of Differentiation Arrest Identifies Myeloid Interface Acute Leukemias With Poor Prognosis. *Leukemia* (2021) 35:724–36. doi: 10.1038/s41375-020-0965-z
74. Weinberg OK, Hasserjian RP, Baraban E, Ok CY, Geyer JT, Philip JKSS, et al. Clinical, Immunophenotypic, and Genomic Findings of Acute Undifferentiated Leukemia and Comparison to Acute Myeloid Leukemia

With Minimal Differentiation: a Study From the Bone Marrow Pathology Group. *Mod Pathol Off J U S Can Acad Pathol Inc* (2019) 32:1373–85. doi: 10.1038/s41379-019-0263-3

Conflict of Interest: The authors declare that the research was conducted in the absence of any commercial or financial relationships that could be construed as a potential conflict of interest.

Publisher's Note: All claims expressed in this article are solely those of the authors and do not necessarily represent those of their affiliated organizations, or those of the publisher, the editors and the reviewers. Any product that may be evaluated in this article, or claim that may be made by its manufacturer, is not guaranteed or endorsed by the publisher.

frontiers in Oncology

ORIGINAL RESEARCH
published: 17 August 2021
doi: 10.3389/fonc.2021.706935

Risk Stratification of Cytogenetically Normal Acute Myeloid Leukemia With Biallelic *CEBPA* Mutations Based on a Multi-Gene Panel and Nomogram Model

Li-Xin Wu[1†], Hao Jiang[1†], Ying-Jun Chang[1], Ya-Lan Zhou[1], Jing Wang[1], Zi-Long Wang[1], Lei-Ming Cao[1], Jin-Lan Li[1], Qiu-Yu Sun[1], Shan-Bo Cao[2], Feng Lou[2], Tao Zhou[2], Li-Xia Liu[2], Cheng-Cheng Wang[2], Yu Wang[1], Qian Jiang[1], Lan-Ping Xu[1], Xiao-Hui Zhang[1], Kai-Yan Liu[1], Xiao-Jun Huang[1,3,4] and Guo-Rui Ruan[1*]*

[1] Beijing Key Laboratory of Hematopoietic Stem Cell Transplantation, Peking University People's Hospital, Peking University Institute of Hematology, National Clinical Research Center for Hematologic Disease, Beijing, China, [2] Department of Bioinformatics, AcornMed Biotechnology Co., Ltd., Beijing, China, [3] Peking-Tsinghua Center for Life Sciences, Academy for Advanced Interdisciplinary Studies, Peking University, Beijing, China, [4] Research Unit of Key Technique for Diagnosis and Treatments of Hematologic Malignancies, Chinese Academy of Medical Sciences, Beijing, China

Background: Approximately 30% of Chinese individuals with cytogenetically normal acute myeloid leukemia (CN-AML) have biallelic *CEBPA* (bi*CEBPA*) mutations. The prognosis and optimal therapy for these patients are controversial in clinical practice.

Methods: In this study, we performed targeted region sequencing of 236 genes in 158 individuals with this genotype and constructed a nomogram model based on leukemia-free survival (LFS). Patients were randomly assigned to a training cohort (N =111) and a validation cohort (N =47) at a ratio of 7:3. Risk stratification was performed by the prognostic factors to investigate the risk-adapted post-remission therapy by Kaplan–Meier method.

Results: At least 1 mutated gene other than *CEBPA* was identified in patients and mutation number was associated with LFS (61.6% *vs.* 39.0%, P =0.033), survival (85.6% *vs.* 62.9%, P =0.030) and cumulative incidence of relapse (CIR) (38.4% *vs.* 59.5%, P =0.0496). White blood cell count, mutations in *CFS3R*, *KMT2A* and DNA methylation related genes were weighted to construct a nomogram model and differentiate two risk subgroups. Regarding LFS, low-risk patients were superior to the high-risk (89.3% *vs.* 33.8%, P <0.001 in training cohort; 87.5% *vs.* 18.2%, P =0.009 in validation cohort). Compared with chemotherapy, allogenic hematopoietic stem cell transplantation (allo-HSCT) improved 5-year LFS (89.6% *vs.* 32.6%, P <0.001), survival (96.9% *vs.* 63.6%, P =0.001) and CIR (7.2% *vs.* 65.8%, P <0.001) in high-risk patients but not low-risk patients (LFS, 77.4% *vs.* 88.9%, P =0.424; survival, 83.9% *vs.* 95.5%, P =0.173; CIR, 11.7% *vs.* 11.1%, P =0.901).

Conclusions: Our study indicated that bi*CEBPA* mutant-positive CN-AML patients could be further classified into two risk subgroups by four factors and allo-HSCT should be recommended for high-risk patients as post-remission therapy. These data will

OPEN ACCESS

Edited by:
Julia T. Geyer, Weill Cornell Medical Center, United States

Reviewed by:
Eduardo Rego, São Paulo State University, Brazil
Runqing Lu, First Affiliated Hospital of Zhengzhou University, China

***Correspondence:**
Guo-Rui Ruan
ruanguorui@pkuph.edu.cn
Xiao-Jun Huang
huangxiaojun@bjmu.edu.cn

[†]These authors have contributed equally to this work

Specialty section:
This article was submitted to Hematologic Malignancies, a section of the journal Frontiers in Oncology

Received: *08 May 2021*
Accepted: *14 July 2021*
Published: *17 August 2021*

Citation:
Wu L-X, Jiang H, Chang Y-J, Zhou Y-L, Wang J, Wang Z-L, Cao L-M, Li J-L, Sun Q-Y, Cao S-B, Lou F, Zhou T, Liu L-X, Wang C-C, Wang Y, Jiang Q, Xu L-P, Zhang X-H, Liu K-Y, Huang X-J and Ruan G-R (2021) Risk Stratification of Cytogenetically Normal Acute Myeloid Leukemia With Biallelic CEBPA Mutations Based on a Multi-Gene Panel and Nomogram Model. Front. Oncol. 11:706935. doi: 10.3389/fonc.2021.706935

help physicians refine treatment decision-making in bi*CEBPA* mutant-positive CN-AML patients.

Keywords: acute myeloid leukemia, targeted region sequencing (TRS), bi*CEBPA* mutations, risk stratification, therapy

INTRODUCTION

Acute myeloid leukemia (AML) is one of the adult malignancies bearing the fewest mutations (1, 2). However, this disorder still comprises heterogeneous subgroups with variable responses to therapy stratified by identified leukemia driver events such as abnormalities in *FLT3*-ITD, *NPM1*, and *BCR-ABL1* fusion. Patients without adverse or favorable genetic alterations were classified into the intermediate-risk subgroup and allogenic hematopoietic stem cell transplantation (allo-HSCT) was recommended to improve survival (3). Some of the intermediate-risk patients with normal karyotype were refined as the favorable risk ones in the revised 2016 WHO classification of AML because they had the prognostically favorable alteration, biallelic *CEBPA* (bi*CEBPA*) mutations, compared with patients with wild-type or monoallelically mutated *CEBPA* (4, 5). However, this subgroup is still not homogeneous with relapse rate reaching approximately 40% (4, 6) and thus the best post-remission therapy remains controversial. Elucidation of cooperating events in this subgroup is urgently required.

Approximately 86% of AML patients have two or more driver mutations and such gene-gene interactions significantly alter the prognosis (5). To clarify the potential risk factors in bi*CEBPA* mutated AML patients, next-generation sequencing has been adopted in many studies for the detection of co-mutated genes with sensitivity reaching 1 in 10^7 cells (7). *GATA2*, *CSF3R* and other tyrosine kinase genes (*KIT*, *JAK3* and *FLT3*-ITD), *WT1* and genes involved in chromatin/DNA modification, cohesin complex, and splicing were identified as hotspots in recent studies to decipher prognostic stratification in bi*CEBPA* mutated AML (6, 8–12). Despite promising results, the true status of these concomitant mutations and their prognostic impact on bi*CEBPA* mutated AML remain to be fully defined (13). This discordance may be attributed to two reasons. First, the sample size of bi*CEBPA* mutated AML patients was small (<100 in most studies), thus limiting the statistical significance of the conclusions to some extent. Second, dozens of genes, or just the hotspot genes, were detected, hindering analysis of the relationships among different mutations.

In addition to mutational information, clinical data are also of significance. In our previous study, we established the prognostic value of pretreatment parameter, such as higher white blood cell (WBC) count, and posttreatment parameter, such as minimal residual disease detected by multiparameter flow cytometry (MFC-MRD) in bi*CEBPA* mutated AML (14, 15). Patients with positive MFC-MRD after consolidation therapy showed a high risk of relapse and benefited from transplantation (15). Therefore, chemotherapy would no longer be appropriate as the first-line treatment for some bi*CEBPA* mutated AML patients and identification of additional risk factors is required to refine treatment decision-making. However, a comprehensive and risk-adapted estimation of the most appropriate post-remission therapy based on clinical and molecular data at diagnosis (pretreatment parameters) in this population remains to be established.

In this study, we conducted high-depth (≥1 000×) targeted region sequencing (TRS) in a large panel with 236 known and potential driver genes to investigate the mutational context in 158 newly diagnosed patients with cytogenetically normal AML (CN-AML) and bi*CEBPA* mutations. Mutational and clinical data at diagnosis were combined and weighted in a nomogram model for refined risk stratification. This study will provide practical prognosis information for bi*CEBPA* mutated CN-AML patients and pave the way for precision treatment.

PATIENTS AND METHODS

Patients

A total of 1 255 patients with newly diagnosed AML were enrolled from February 2010 to December 2019 at Peking University People's Hospital. All participants included in our study met the following criteria: (1) age ≥15 years; (2) normal cytogenetics; (3) achieved complete remission (CR); (4) bi*CEBPA* mutant-positive (**Figure 1**). In total, 158 participants qualified for subsequent analyses. The protocols for induction therapy and post-remission therapy are described in our previous study (14, 16–18). Induction treatment included 1–2 cycles of IA10 (idarubicin 10 mg/m^2 for 3 days and cytarabine 100 mg/m^2 for 7 days), HAA (homoharringtonine 2 mg/m^2 for 7 days, aclarubicin 20 mg/day for 7 days and cytarabine 100 mg/m^2 for 7 days) or CAG (cytarabine 10 mg/m^2 every 12 hours for 14 days, aclarubicin 20 mg/day for 4 days and granulocyte-colony stimulating factor 300μg/day for 14 days). When CR was achieved, patients were recommended to receive at least 6 cycles of consolidation chemotherapy, including 4 cycles of intermediate-dose cytarabine (2 g/m^2 every 12 hours for 3 days) and 2 or more cycles of anthracycline (daunorubicin 45 mg/m^2 or idarubicin 10 mg/m^2 for 3 days or mitoxantrone 8 mg/m^2 for 3 days) in combination with cytarabine (100 mg/m^2 for 7 days). Patients proceeded to undergo an allo-HSCT received at least 2 cycles of consolidation chemotherapy. Donors were selected from human leukocyte antigen (HLA) matched siblings, HLA matched unrelated donors or HLA haploidentical related donors. MFC-MRD monitoring was described as previously reported (15). The sensitivity was 0.01% and any measurable level of MRD was considered positive (19). For patients with positive MRD after allo-HSCT, preemptive antileukemic chemotherapy in combination with donor lymphocyte infusion (DLI) or interferon-α was given (20). For patients with

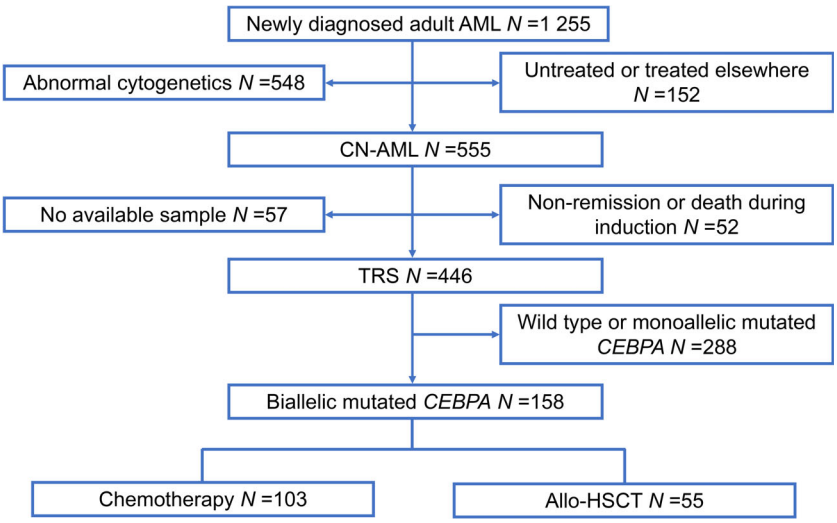

FIGURE 1 | Patient recruitment and cohort assignment. AML, acute myeloid leukemia; CN, cytogenetically normal; TRS, targeted region sequencing; Allo-HSCT, allogenic hematopoietic stem cell transplantation.

hematologic relapse, chemotherapy followed by DLI was given as the first-line strategy. And for relapse prophylaxis, only DLI was used. Details of DLI were described previously (21, 22).

High-Depth TRS and Analysis

We designed a panel of 236 known and potential driver genes for TRS (**Supplementary Table 1**). DNA was extracted from bone marrow samples using DNAzol® kits (Invitrogen, Carlsbad, CA, USA) according to the manufacturer's instructions. The sequencing process was performed according to our previous report (23). The average sequencing depth on target *per* sample was ≥1 000×. Typical mutations in *NPM1* (type A/B/D) were validated by real-time quantitative polymerase chain reaction and atypical mutations were validated by Sanger sequencing (24). Mutations in *FLT3*-ITD were validated by Sanger sequencing.

Nomogram Model and Risk Stratification

Participants were assigned to a training cohort (N =111) and a validation cohort (N =47) at a ratio of 7:3 randomly. A nomogram was constructed based on the variables selected from the Cox regression model. The discrimination ability of the prediction model was measured by the concordance index (C-index) and the calibration was evaluated graphically by the calibration plots. Risk stratification was performed based on the nomogram model.

Endpoints and Statistical Analyses

The primary endpoint in this study was leukemia-free survival (LFS), which was calculated from the date of CR to relapse, death from any cause, last contact, or June 30th, 2020. The secondary endpoints included survival, cumulative incidence of relapse (CIR) and non-relapse mortality (NRM). Survival was calculated from the date of diagnosis to death from any cause, last contact, or June 30th, 2020. CIR and NRM were used in a competing risk setting and death without disease progression or relapse was treated as a competing event. Continuous variables were analyzed by Mann-Whitney U test. Categorized variables were analyzed by Pearson Chi-square test. Survival functions were estimated using the Kaplan-Meier method and compared by the log-rank test. Variables were selected by univariate Cox regression model and those with P <0.15 were subsequently enrolled in the multivariate Cox regression model. Receiving an allo-HSCT was recorded as a censored event to identify the prognostic factors before an allo-HSCT. Landmark analysis was performed to revise bias from early relapse or death when comparing the outcomes of post-remission therapies. Analyses were performed using SPSS software version 22.0 (Chicago, IL, USA), GraphPad Prism 7.04® (San Diego, CA, USA) and R software version 4.0.2 (http://www.Rproject.org). P <0.05 was considered to indicate statistical significance.

RESULTS

Patient Characteristics

Among the 158 patients with bi*CEBPA* mutations, 103 received chemotherapy only, while 55 received an allo-HSCT. Rate of patients receiving an allo-HSCT was significantly decreased after 2016 than before (22.5% *vs.* 44.8%, P =0.003). The median time from the first CR (CR1) to receiving an allo-HSCT was 4.77 months. According to the landmark analysis, 10 patients with LFS ≤4.77 months would be excluded from the subsequent analyses unless receiving an allo-HSCT was treated as a censored event. As shown in **Table 1**, there were no significant differences between the consolidation chemotherapy and allo-HSCT cohorts in terms of sex, WBC, hemoglobin, platelets, French-American-British (FAB) type and MRD after induction (MRDint) (all P >0.05). Age and CR rate after first induction were significantly greater in the consolidation chemotherapy

TABLE 1 | Patient characteristics categorized by post-remission therapy.

Variables	Consolidation Chemotherapy (*N*=94)	Allo-HSCT (CR1) (*N*=54)	*P*-value
Sex, *N* (%)			
Male	55 (58.5)	38 (70.4)	0.151
Age, y			
Median (range)	41 (17–74)	33 (15–59)	<0.001
WBC, $\times10^9$/L			
Median (range)	17.27 (1.15–315.62)	18.30 (3.52–266.00)	0.164
Hemoglobin, g/L			
Median (range)	102 (47–157)	100 (58–157)	0.707
Platelets, $\times10^9$/L			
Median (range)	27 (5–184)	35 (2–172)	0.363
FAB type, *N* (%)			
M2	88 (93.6)	48 (88.9)	0.483
CR after first induction, *N* (%)			
Yes	87 (92.6)	43 (79.6)	0.021
MRDint positivity, *N/N* (%)			
Yes	48/88 (54.5)	35/51 (68.6)	0.103

Allo-HSCT, allogenic hematopoietic stem cell transplantation; CR, complete remission; WBC, white blood cell; FAB, French–American–British; MRDint, minimal residual disease after induction.

cohort than that in the allo-HSCT cohort (age, median, 41 y *vs.* 33 y, P <0.001; CR rate, 92.6% *vs.* 79.6%, P =0.021). The allo-HSCT cohort had better 5-year LFS (84.8% *vs.* 51.2%, P <0.001) and 5-year survival (91.9% *vs.* 74.1%, P =0.018), lower 5-year CIR (9.1% *vs.* 47.7%, P <0.001) but comparable NRM (6.1% *vs.* 1.1%, P =0.125) (**Supplementary Figure 1**).

Genomic Analysis of bi*CEBPA* Mutated CN-AML

Of the 158 bi*CEBPA* mutated ones, two patients carried two frameshift deletion mutations respectively and one carried two frameshift insertion mutations (**Figure 2**). We identified 1 306 mutations in 203 genes other than *CEBPA*. The median mutation number was 8 (1–20). Interestingly, additional mutations of ≤5, 6–7, 8, 9–10, >10 were identified uniformly with ~20% of patients (**Supplementary Figure 2**). Missense mutations were the predominant type (N =1 024; 78.4%), followed by frame-shift (N =103; 7.9%), in-frame (N =98; 7.5%), nonsense (N =55; 4.2%) and splice-site (N =26; 2.0%) mutations. These genes (mutated in ≥10 patients) were classified into 9 genetic subgroups: transcription factors (*GATA2* and *MYC*), tumor suppressors (*WT1* and *MPL*), activated signaling (*NRAS*, *CSF3R*, *LILRB3*, *JAK3*, *MACF1*, *MST1*, *FLT3*-ITD, *KIT*, *NCOR2* and *LAMA5*), chromatin modifiers (*EP300*, *SRCAP*, *DPF2*, *ASXL2* and *ALK*), cell metabolism (*HERC2*), DNA methylation (*TET2*), cohesin complex (*RAD21*), histone methylation (*KMT2A* and *KMT2D*) and others (*AHNAK2*, *PCLO*, *EPPK1*, *POTEG*, *TRIO*, *POTEH*, *LOXHD1*, *AHNAK*, *HMCN1* and *PLEC*). Two genetic subgroups (spliceosome and adhesion) were not listed because of the low frequency of their mutated genes. *GATA2* was the most frequently affected gene in 48 patients (30.4%), followed by *WT1* (N =42, 26.6%), *NRAS* (N =31, 19.6%), *AHNAK2* (N =31, 19.6%), *PCLO* (N =28, 17.7%) and *CSF3R* (N =24, 15.2%). *FLT3*-ITD represented 10.1% (N =16) in this population and 14 of

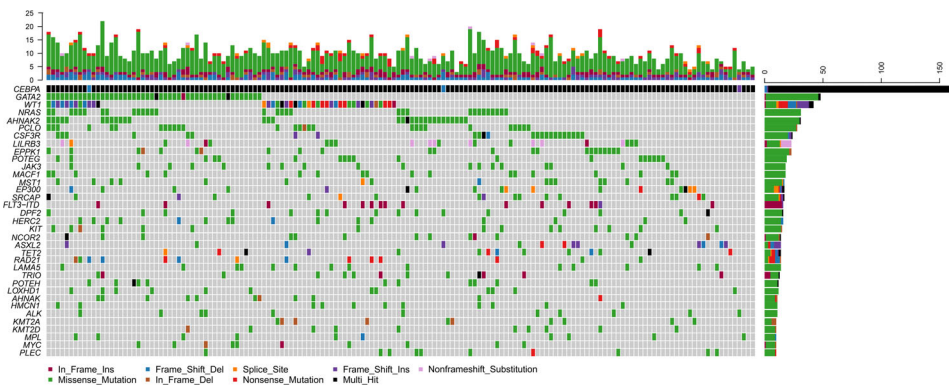

FIGURE 2 | Genomic landscape of 158 CN-AML patients with bi*CEBPA* mutations. Genes mutated in ≥10 patients are shown. Boxes are colored according to the mutation type. Black box indicates multi-hit of mutation type. Non-black box of *CEBPA* indicates the same mutation type in one patient. The top bar indicates mutation load (mutation/Mb DNA) and the right bar indicates mutation frequency.

them were identified by Sanger sequencing. The missed two variants were attributed to the low mutational burden (7.7% and 7.9% respectively). Only 1 patient had *NPM1* mutation and this variant was further validated by real-time quantitative polymerase chain reaction.

We further identified 21 pairs of genes with co-occurrence and 1 pair with mutual exclusivity with significance (P<0.05, **Figure 3A**). Both *NRAS* and *NCOR2* had 4 pairwise associated genes. Mutations in *NRAS*, *JAK3* and *KIT* showed significant associations with each other. Positive pairwise associations were also found in *TET2* and *POTEG*, *GATA2* and *AHNAK*, and *CSF3R* and *ASXL2*. Only *GATA2* showed significant mutual exclusivity with *KMT2A*. KEGG pathway enrichment analysis revealed that the mutated genes, including *CEBPA*, were mainly involved in cancer (**Figure 3B**). These genes represent pan-cancer biomarkers not only in myelogenous leukemia (acute and chronic myeloid leukemia) but also in many solid tumors. Apart from several pivotal cancer-related pathways in signal transduction, we also enriched pathways in central carbon metabolism in cancer, microRNAs in cancer and EGFR tyrosine kinase inhibitor resistance.

Mutational Context and Clinical Relevance

The general relapse rate was 32.3% (51/158) in our cohort. We further explored the correlation of mutational complexity with disease progression. A higher median mutation number was seen in ones with events (9 [2–18] *vs.* 8 [1–20]; P =0.050) for the patients receiving consolidation chemotherapy only. According to the median mutation number (N =8), patients were simply divided into two subgroups: patients with low mutational burden (mutation number <8, N=66) and high mutational burden (mutation number ≥8, N =92). Patients with low mutational burden showed significantly higher 5-year LFS (61.6% *vs.* 39.0%, P =0.033), higher 5-year survival (85.6% *vs.* 62.9%, P =0.030), lower 5-year CIR (38.4% *vs.* 59.5%, P =0.0496) and comparable 5-year NRM (0 *vs.* 1.5%, P =0.407) compared with those with high (**Supplementary Figure 3**).

Nomogram for LFS Analysis

Clinical variables, genes, and genetic groups with mutations in ≥10 patients were enrolled for univariate analysis of LFS (allo-HSCT was recorded as a censored event). Eight variables were eligible for subsequent analysis with P <0.15 in the training cohort (**Supplementary Table 2**) and 4 of them eventually entered the nomogram model after multivariate Cox analysis: WBC (high *vs.* low, represents >18.30×10^9/L *vs.* ≤18.30×10^9/L), *CSF3R* mutation (+ *vs.* -), *KMT2A* mutation (+ *vs.* -) and DNA methylation related mutation (mutations in *TET2*, *DNMT3A*, *BAZ2A*, *IDH2* and *IDH1*, mutated in 14, 9, 5, 5 and 3 patients respectively) (+ *vs.* -) (**Figure 4A**). All points corresponding to the 4 variables were summed to predict individual probabilities of 1-, 3- and 5-year LFS. The model showed good discrimination with C-index value of 0.750 (95% confidence interval, 0.670–0.830) as well as good calibration (**Supplementary Figure 4A**). In validation cohort, the model also had good discrimination (C-index, 0.771; 95% confidence interval, 0.661–0.881) and calibration (**Supplementary Figure 4B**).

Risk Stratification Based on Nomogram Model

According to the variables in nomogram model, patients with no identified risk factor were assigned to the low-risk subgroup (N =50) and the remaining to the high-risk (N =108). In training cohort, low-risk patients (N =35) showed better 5-year LFS compared with the high-risk (N =76, 89.3% *vs.* 33.8%, P <0.001) (**Figure 4B**). In the validation cohort, there were 15 patients assigned to low-risk subgroup and 32 to high-risk. The validation cohort also differentiated the two risk subgroups (low risk *vs.* high risk, 87.5% *vs.* 18.2%, P =0.009) (**Figure 4C**). MRDint was available in 148 patients and 59 (39.9%) ones were positive. The positive rate was significantly lower in low-risk subgroup (9/45, 20.0%) compared with high-risk (50/103, 48.5%) (P =0.001).

Allo-HSCT Was Superior to Chemotherapy in High-Risk Subgroup

We then interrogated the effect of consolidation chemotherapy and allo-HSCT as post-remission therapies in the two risk subgroups. In the low-risk subgroup (N =49), there was no significant difference in the 5-year LFS (allo-HSCT *vs.* consolidation chemotherapy, 77.4% *vs.* 88.9%, P =0.424), 5-year survival (83.9% *vs.* 95.5%, P =0.173), 5-year CIR (11.7% *vs.* 11.1%, P =0.901) and 5-year NRM (10.9% *vs.* 0, P =0.099) (**Figures 5A–D**). However, in the high-risk subgroup (N =99), allo-HSCT was superior to consolidation chemotherapy alone (5-year LFS, 89.6% *vs.* 32.6%, P <0.001; 5-year survival, 96.9% *vs.* 63.6%, P =0.001; 5-year CIR, 7.2% *vs.* 65.8%, P <0.001) with comparable 5-year NRM (3.1% *vs.* 1.6%, P =0.685) (**Figures 5E–H**).

DISCUSSION

Our study presents comprehensive information on mutational context and detailed risk stratification of bi*CEBPA* mutated CN-AML patients. A significant reduction in the rate of transplantation in recent years was seen in our study. This was attributed to the important insights into bi*CEBPA* mutations in AML and recommendation for consolidation chemotherapy as the first-line post-remission therapy (25). However, in accordance with other studies (4, 6), we observed a considerable relapse rate in the CN-AML patients with bi*CEBPA* mutations. Furthermore, although not limited to CN-AML, our previous study with 36 patients identical to the current study, also supported the heterogeneity of bi*CEBPA* mutations in patients with similar relapse rate (15). It has been found that HSCT reduced the relapse rate in this population; however, the survival benefit is still controversial (26, 27). Our study indicated that allo-HSCT improved the prognosis (**Supplementary Figure 1**), demonstrating that the first-line post-remission treatment should be tailored according to an individualized risk assessment. Risk factors alone cannot represent the actual status of a patient and a comprehensive and quantitative method such as a nomogram model may

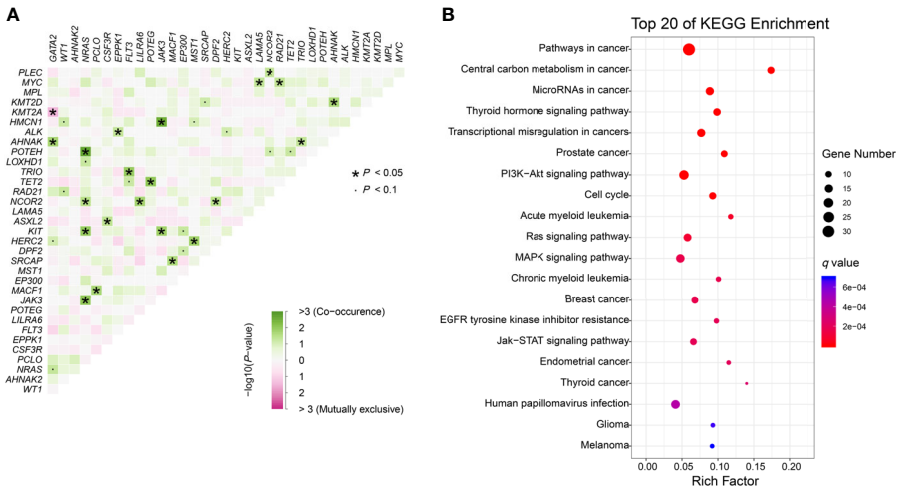

FIGURE 3 | Genomic analyses. **(A)** Pairwise association between genes mutated in ≥10 patients. Green colors indicate positive association and pink colors indicate negative association. **(B)** KEGG enrichment analysis. The top 20 pathways are shown. Dot size depends on the mutation number and color depends on the *q* value (adjust *P* value).

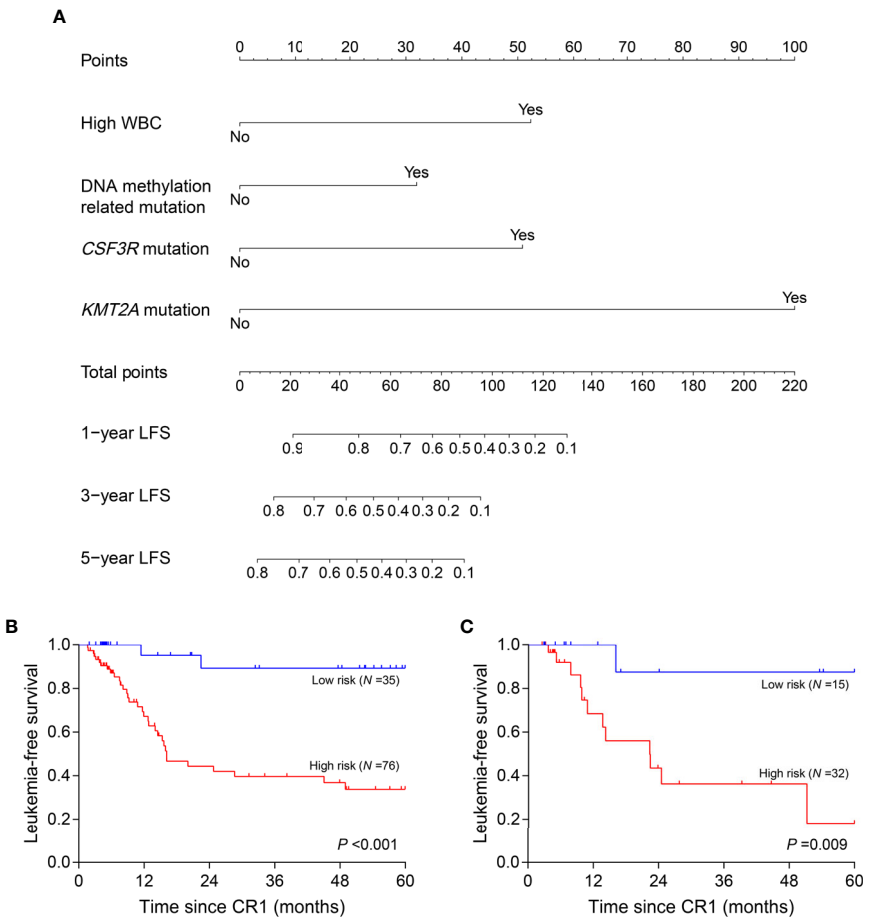

FIGURE 4 | Nomogram model and risk stratification. **(A)** For WBC, "Yes" represents WBC >18.30×10^9/L at diagnosis; for genes or genetic group, "Yes" represents mutation. **(B, C)** Leukemia-free survival analyses by risk stratification in training **(B)** and validation **(C)** cohort. WBC, white blood cell.

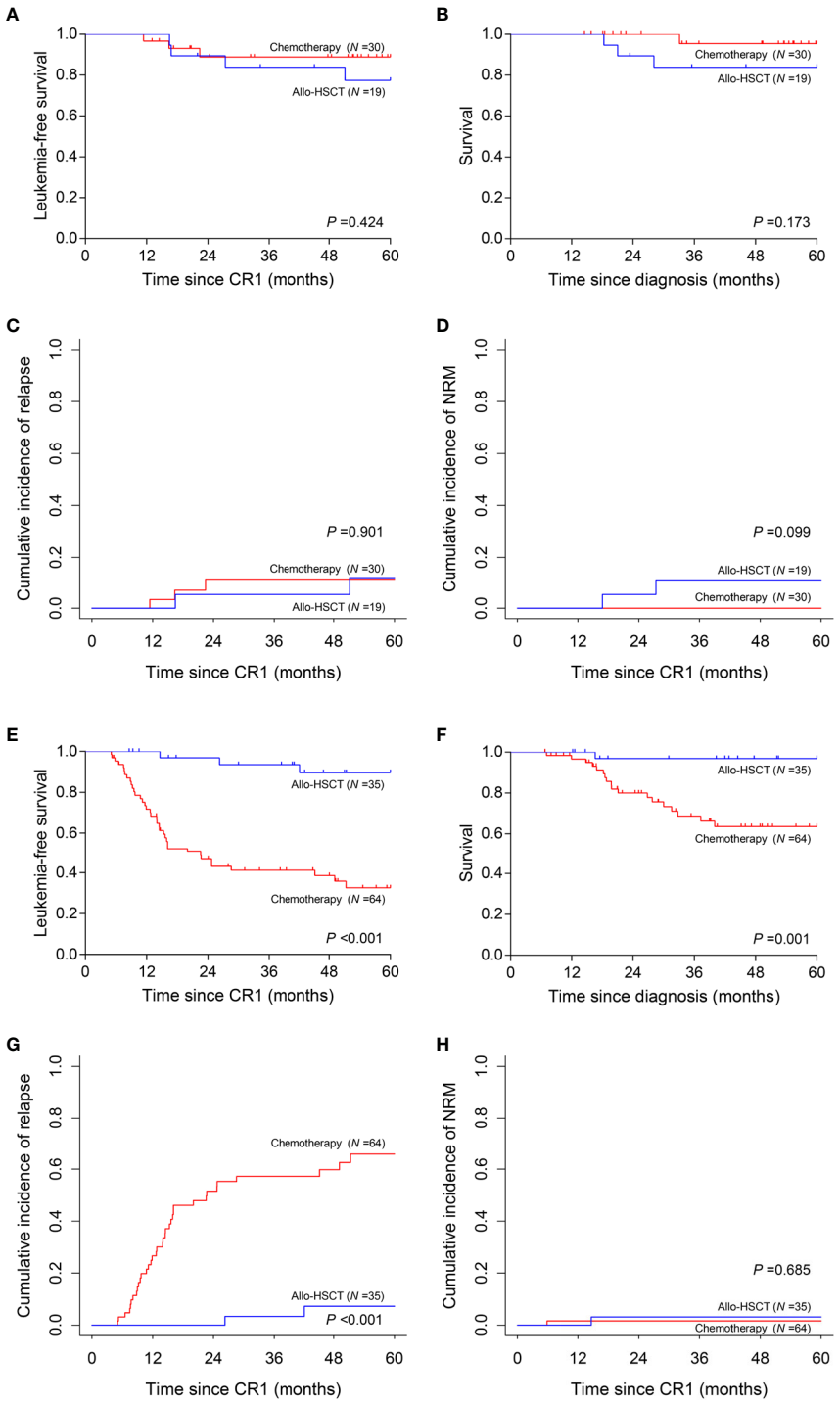

FIGURE 5 | Prognosis of two post-remission therapies by risk stratification. **(A–D)** Leukemia-free survival, survival, cumulative incidence of relapse and non-relapse mortality analyses in low-risk subgroup. **(E–H)** Leukemia-free survival, survival, cumulative incidence of relapse and non-relapse mortality analyses in high-risk subgroup.

provide a refined stratification. We thus sought to elucidate the heterogeneity by a large panel and develop a new prognostic model based on clinical and molecular data in this population.

As expected, higher WBC (median as the cutoff) was identified as the clinical prognostic factor. We found that at least 1 mutation cooccurred with mutated bi*CEBPA* and

mutation complexity did confer higher relapse risk, which further verified the heterogeneity of bi*CEBPA* mutated CN-AML. *GATA2* mutation was the most frequent co-activated event with bi*CEBPA* mutations (6, 8, 11). Study showed that *GATA2* activity affected the mutational dynamics of leukemia in Cbfb-MYH11 knockin mice (28). The prognostic value of this gene is not well established. Several studies have revealed a trend of improvement in *GATA2* mutated CN-AML patients with bi*CEBPA* mutations (8, 29), especially when mutations disrupted the zinc finger 1 domain. In our study, *GATA2* mutation showed no correlation with prognosis (data not shown). We further identified two mutated genes (*CSF3R* and *KMT2A*) and a genetic group (DNA methylation) which conferred prognostic significance in our cohort. Braun et al. (30) confirmed that *CEBPA* mutations must be the initial event prior to mutant *CSF3R* since otherwise, AML did not develop and *CSF3R* and *CEBPA* mutations cooperated to promote leukemogenesis. *CSF3R*, which is involved in the JAK-STAT signaling pathway, is a common tyrosine kinase mutated gene in bi*CEBPA* mutated AML patients who were sensitive to JAK inhibition (9, 11, 31). The EGFR tyrosine kinase inhibitor resistance is also a pathway related to tyrosine kinase. Reports of the role of EGFR and its inhibitors (gefitinib and erlotinib) in the origination, progression and treatment of AML were discordant (32–34). Mahmud et al. (35) reported elevated protein levels of EGFR and its activation in a subset of AML and attributed the discordance in other studies to patient selection because the EGFR levels in more than 80% of AML patients did not differ from those in normal individuals. Although *EGFR* mutations were not identified in this study and its expression was not evaluated, the downstream mutated genes which were enriched in the EGFR tyrosine kinase inhibitor resistance pathway may confer drug resistance in bi*CEBPA* mutated CN-AML patients. Genes involved in DNA methylation (such as *TET2* and *DNMT3A*) were frequently mutated in bi*CEBPA* mutated AML, especially in the older participants and mutated *TET2* was not significantly different from wild type in relapse/event-free survival (6, 36). We further studied these genes as a genetic group and found that mutations in this group conferred a worse outcome. However, reports of other epigenetic modifiers involved in histone methylation are rare (13). We identified that *KMT2A*, as well as *KMT2D* and *EP300* mutations, were mutually exclusive with the most frequent *GATA2* mutation (**Figure 3A**). The infrequent mutation in KMT2 gene family members represents an obstacle to interpretation. In our study, we revealed that mutated *KMT2A* was also an independent risk factor in bi*CEBPA* mutated CN-AML patients.

Combined with sequencing data, we developed a nomogram model and further stratified the patients by the risk factors. According to our stratification, approximately one third of the patients were categorized into the low-risk subgroup, which had only bi*CEBPA* mutations and no other detrimental clinical or genetic factors. Low-risk patients were more sensitive to induction chemotherapy with lower MRD level after induction therapy. The 5-year LFS and CIR in this subgroup were not significantly improved by allo-HSCT and chemotherapy alone seemed to have better 5-year survival. That was because of the high rate of transplant-related mortality counterbalancing the graft-versus-leukemia effect in allo-HSCT. These data strongly indicated that this subgroup represented the patients with a real favorable prognosis in those with bi*CEBPA* mutated CN-AML. However, allo-HSCT was shown to be a powerful therapy to reverse the high mortality resulting from relapse in the high-risk subgroup.

One limitation of our study was the analysis of *FLT3*-ITD. The prognostic impact of *FLT3*-ITD in bi*CEBPA* mutated AML patients was controversial. Grossmann et al. (36) indicated that *FLT3*-ITD had no impact, while Zhang et al. (11) revealed that *FLT3*-ITD had worse outcome in bi*CEBPA* mutated CN-AML patients. In our study, 13 *FLT3*-ITD patients with bi*CEBPA* mutations received allo-HSCT during the CR1 (median time from CR1 to allo-HSCT, 4.53 months). The prognostic value could not be estimated because these patients were censored at the date of allo-HSCT. Although *FLT3*-ITD was more frequently observed in non-bi*CEBPA* mutated AML patients (6), the contribution of *FLT3*-ITD to risk stratification warrants further investigation because two of the *FLT3*-ITD patients receiving the consolidation chemotherapy relapsed (LFS, 20.0 months and 16.1 months respectively) eventually. Other prognostically associated genes in our study, like *CSF3R* and *KMT2A*, still need a larger and prospective study to validate.

In summary, we validated the heterogeneity of CN-AML patients with bi*CEBPA* mutations and developed a new system of risk stratification based on a nomogram model. Only one third of these patients represented the low-risk subgroup, and consolidation chemotherapy should be the first-line post-remission therapy. While in the high-risk subgroup, allo-HSCT is recommended. These data, if validated, will be greatly beneficial in translating commercial sequencing into clinical testing and directing decision-making during treatment of CN-AML patients with bi*CEBPA* mutations.

DATA AVAILABILITY STATEMENT

The sequencing data presented in the study are deposited in the NCBI Sequence Read Archive (SRA) repository, accession number PRJNA749620.

ETHICS STATEMENT

The studies involving human participants were reviewed and approved by the Ethics Committee of Peking University People's Hospital. Written informed consent to participate in this study was provided by the participants' legal guardian/next of kin.

AUTHOR CONTRIBUTIONS

G-RR and X-JH designed the project and prepared the manuscript. L-XW, Y-LZ, Z-LW, L-MC, S-BC, FL, TZ, L-XL, and C-CW performed the experiments and statistical analyses. HJ, Y-JC, JW, J-LL, Q-YS, YW, QJ, L-PX, X-HZ, and K-YL provided the clinical data. All authors contributed to the article and approved the submitted version.

FUNDING

This work was supported by grants from National Key Research and Development Program of China [Grant 2017YFA0104500], National Natural Science Foundation of China [Grant 81770156], Innovative Research Groups of the National Natural Science Foundation of China [Grant 81621001], Beijing Municipal Science and Technology Commission [Grant Z181100009618032] and Beijing Municipal Natural Science Foundation [Grant 7192213].

ACKNOWLEDGMENTS

We would like to thank all our colleagues at Peking University Institute of Hematology for their cooperation in sample collection.

SUPPLEMENTARY MATERIAL

The Supplementary Material for this article can be found online at: https://www.frontiersin.org/articles/10.3389/fonc.2021.706935/full#supplementary-material

REFERENCES

1. Ley TJ, Miller C, Ding L, Raphael BJ, Mungall AJ, Robertson A, et al. Genomic and Epigenomic Landscapes of Adult De Novo Acute Myeloid Leukemia. *N Engl J Med* (2013) 368(22):2059–74. doi: 10.1056/NEJMoa1301689
2. Lawrence MS, Stojanov P, Polak P, Kryukov GV, Cibulskis K, Sivachenko A, et al. Mutational Heterogeneity in Cancer and the Search for New Cancer-Associated Genes. *Nature* (2013) 499(7457):214–8. doi: 10.1038/nature12213
3. Huang XJ, Zhu HH, Chang YJ, Xu LP, Liu DH, Zhang XH, et al. The Superiority of Haploidentical Related Stem Cell Transplantation Over Chemotherapy Alone as Postremission Treatment for Patients With Intermediate- or High-Risk Acute Myeloid Leukemia in First Complete Remission. *Blood* (2012) 119(23):5584–90. doi: 10.1182/blood-2011-11-389809
4. Dufour A, Schneider F, Metzeler KH, Hoster E, Schneider S, Zellmeier E, et al. Acute Myeloid Leukemia With Biallelic CEBPA Gene Mutations and Normal Karyotype Represents a Distinct Genetic Entity Associated With a Favorable Clinical Outcome. *J Clin Oncol Off J Am Soc Clin Oncol* (2010) 28(4):570–7. doi: 10.1200/jco.2008.21.6010
5. Papaemmanuil E, Gerstung M, Bullinger L, Gaidzik VI, Paschka P, Roberts ND, et al. Genomic Classification and Prognosis in Acute Myeloid Leukemia. *N Engl J Med* (2016) 374(23):2209–21. doi: 10.1056/NEJMoa1516192
6. Konstandin NP, Pastore F, Herold T, Dufour A, Rothenberg-Thurley M, Hinrichsen T, et al. Genetic Heterogeneity of Cytogenetically Normal AML With Mutations of CEBPA. *Blood Adv* (2018) 2(20):2724–31. doi: 10.1182/bloodadvances.2018016840
7. Pulsipher MA, Carlson C, Langholz B, Wall DA, Schultz KR, Bunin N, et al. Igh-V(D)J NGS-MRD Measurement Pre- and Early Post-Allotransplant Defines Very Low- and Very High-Risk ALL Patients. *Blood* (2015) 125 (22):3501–8. doi: 10.1182/blood-2014-12-615757
8. Greif PA, Dufour A, Konstandin NP, Ksienzyk B, Zellmeier E, Tizazu B, et al. GATA2 Zinc Finger 1 Mutations Associated With Biallelic CEBPA Mutations Define a Unique Genetic Entity of Acute Myeloid Leukemia. *Blood* (2012) 120 (2):395–403. doi: 10.1182/blood-2012-01-403220
9. Lavallee VP, Krosl J, Lemieux S, Boucher G, Gendron P, Pabst C, et al. Chemo-Genomic Interrogation of CEBPA Mutated AML Reveals Recurrent CSF3R Mutations and Subgroup Sensitivity to JAK Inhibitors. *Blood* (2016) 127(24):3054–61. doi: 10.1182/blood-2016-03-705053
10. Zhang Y, Wang F, Chen X, Zhang Y, Wang M, Liu H, et al. Csf3r Mutations are Frequently Associated With Abnormalities of RUNX1, Cbfb, CEBPA, and NPM1 Genes in Acute Myeloid Leukemia. *Cancer* (2018) 124(16):3329–38. doi: 10.1002/cncr.31586
11. Zhang Y, Wang F, Chen X, Zhang Y, Wang M, Liu H, et al. Companion Gene Mutations and Their Clinical Significance in AML With Double Mutant CEBPA. *Cancer Gene Ther* (2020) 27(7-8):599–606. doi: 10.1038/s41417-019-0133-7
12. Tien FM, Hou HA, Tang JL, Kuo YY, Chen CY, Tsai CH, et al. Concomitant WT1 Mutations Predict Poor Prognosis in Acute Myeloid Leukemia Patients With Double Mutant CEBPA. *Haematologica* (2018) 103(11):e510–3. doi: 10.3324/haematol.2018.189043
13. Wilhelmson AS, Porse BT. CCAAT Enhancer Binding Protein Alpha (CEBPA) Biallelic Acute Myeloid Leukaemia: Cooperating Lesions, Molecular Mechanisms and Clinical Relevance. *Br J Haematol* (2020) 190 (4):495–507. doi: 10.1111/bjh.16534
14. Deng DX, Zhu HH, Liu YR, Chang YJ, Ruan GR, Jia JS, et al. Minimal Residual Disease Detected by Multiparameter Flow Cytometry Is Complementary to Genetics for Risk Stratification Treatment in Acute Myeloid Leukemia With Biallelic CEBPA Mutations. *Leukemia Lymphoma* (2019) 60(9):2181–9. doi: 10.1080/10428194.2019.1576868
15. Wang J, Lu R, Wu Y, Jia J, Gong L, Liu X, et al. Detection of Measurable Residual Disease May Better Predict Outcomes Than Mutations Based on Next-Generation Sequencing in Acute Myeloid Leukaemia With Biallelic Mutations of CEBPA. *Br J Haematol* (2020) 190(4):533–44. doi: 10.1111/bjh.16535
16. Lv M, Wang Y, Chang YJ, Zhang XH, Xu LP, Jiang Q, et al. Myeloablative Haploidentical Transplantation Is Superior to Chemotherapy for Patients With Intermediate-risk Acute Myelogenous Leukemia in First Complete Remission. *Clin Cancer Res An Off J Am Assoc Cancer Res* (2019) 25 (6):1737–48. doi: 10.1158/1078-0432.ccr-18-1637
17. Xu L, Chen H, Chen J, Han M, Huang H, Lai Y, et al. The Consensus on Indications, Conditioning Regimen, and Donor Selection of Allogeneic Hematopoietic Cell Transplantation for Hematological Diseases in China-recommendations From the Chinese Society of Hematology. *J Hematol Oncol* (2018) 11(1):33. doi: 10.1186/s13045-018-0564-x
18. Wang Y, Chen H, Chen J, Han M, Hu J, Jiong H, et al. The Consensus on the Monitoring, Treatment, and Prevention of Leukemia Relapse After Allogeneic Hematopoietic Stem Cell Transplantation in China. *Cancer Lett* (2018) 438:63–75. doi: 10.1016/j.canlet.2018.08.030
19. Chang YJ, Wang Y, Liu YR, Xu LP, Zhang XH, Chen H, et al. Haploidentical Allograft Is Superior to Matched Sibling Donor Allograft in Eradicating Pre-Transplantation Minimal Residual Disease of AML Patients as Determined by Multiparameter Flow Cytometry: A Retrospective and Prospective Analysis. *J Hematol Oncol* (2017) 10(1):134. doi: 10.1186/s13045-017-0502-3
20. Mo XD, Zhang XH, Xu LP, Wang Y, Yan CH, Chen H, et al. Interferon-α: A Potentially Effective Treatment for Minimal Residual Disease in Acute Leukemia/Myelodysplastic Syndrome After Allogeneic Hematopoietic Stem Cell Transplantation. *Biol Blood Marrow Transplant J Am Soc Blood Marrow Transplant* (2015) 21(11):1939–47. doi: 10.1016/j.bbmt.2015.06.014
21. Chang YJ, Xu LP, Wang Y, Zhang XH, Chen H, Chen YH, et al. Controlled, Randomized, Open-Label Trial of Risk-Stratified Corticosteroid Prevention of Acute Graft-Versus-Host Disease After Haploidentical Transplantation. *J Clin*

Oncol Off J Am Soc Clin Oncol (2016) 34(16):1855–63. doi: 10.1200/jco.2015.63.8817
22. Huang XJ, Liu DH, Liu KY, Xu LP, Chen H, Han W. Donor Lymphocyte Infusion for the Treatment of Leukemia Relapse After HLA-Mismatched/Haploidentical T-Cell-Replete Hematopoietic Stem Cell Transplantation. *Haematologica* (2007) 92(3):414–7. doi: 10.3324/haematol.10570
23. Zhou YL, Wu LX, Peter Gale R, Wang ZL, Li JL, Jiang H, et al. Mutation Topography and Risk Stratification for De Novo Acute Myeloid Leukaemia With Normal Cytogenetics and No Nucleophosmin 1 (NPM1) Mutation or Fms-like Tyrosine Kinase 3 Internal Tandem Duplication (FLT3-ITD). *Br J Haematol* (2020) 190(2):274–83. doi: 10.1111/bjh.16526
24. Ruan GR, Li JL, Qin YZ, Li LD, Xie M, Chang Y, et al. Nucleophosmin Mutations in Chinese Adults With Acute Myelogenous Leukemia. *Ann Hematol* (2009) 88(2):159–66. doi: 10.1007/s00277-008-0591-8
25. Dohner H, Estey E, Grimwade D, Amadori S, Appelbaum FR, Buchner T, et al. Diagnosis and Management of AML in Adults: 2017 ELN Recommendations From an International Expert Panel. *Blood* (2017) 129(4):424–47. doi: 10.1182/blood-2016-08-733196
26. Ahn JS, Kim JY, Kim HJ, Kim YK, Lee SS, Jung SH, et al. Normal Karyotype Acute Myeloid Leukemia Patients With CEBPA Double Mutation Have a Favorable Prognosis But No Survival Benefit From Allogeneic Stem Cell Transplant. *Ann Hematol* (2016) 95(2):301–10. doi: 10.1007/s00277-015-2540-7
27. Schlenk RF, Taskesen E, van Norden Y, Krauter J, Ganser A, Bullinger L, et al. The Value of Allogeneic and Autologous Hematopoietic Stem Cell Transplantation in Prognostically Favorable Acute Myeloid Leukemia With Double Mutant CEBPA. *Blood* (2013) 122(9):1576–82. doi: 10.1182/blood-2013-05-503847
28. Saida S, Zhen T, Kim E, Yu K, Lopez G, McReynolds LJ, et al. Gata2 Deficiency Delays Leukemogenesis While Contributing to Aggressive Leukemia Phenotype in Cbfb-MYH11 Knockin Mice. *Leukemia* (2020) 34(3):759–70. doi: 10.1038/s41375-019-0605-7
29. Tien FM, Hou HA, Tsai CH, Tang JL, Chiu YC, Chen CY, et al. GATA2 Zinc Finger 1 Mutations Are Associated With Distinct Clinico-Biological Features and Outcomes Different From GATA2 Zinc Finger 2 Mutations in Adult Acute Myeloid Leukemia. *Blood Cancer J* (2018) 8(9):87. doi: 10.1038/s41408-018-0123-2
30. Braun TP, Okhovat M, Coblentz C, Carratt SA, Foley A, Schonrock Z, et al. Myeloid Lineage Enhancers Drive Oncogene Synergy in CEBPA/CSF3R Mutant Acute Myeloid Leukemia. *Nat Commun* (2019) 10(1):5455. doi: 10.1038/s41467-019-13364-2
31. Braun TP, Coblentz C, Smith BM, Coleman DJ, Schonrock Z, Carratt SA, et al. Combined Inhibition of JAK/STAT Pathway and Lysine-Specific Demethylase 1 as a Therapeutic Strategy in CSF3R/CEBPA Mutant Acute Myeloid Leukemia. *Proc Natl Acad Sci USA* (2020) 117(24):13670–9. doi: 10.1073/pnas.1918307117
32. Sun JZ, Lu Y, Xu Y, Liu F, Li FQ, Wang QL, et al. Epidermal Growth Factor Receptor Expression in Acute Myelogenous Leukaemia Is Associated With Clinical Prognosis. *Hematol Oncol* (2012) 30(2):89–97. doi: 10.1002/hon.1002
33. Deangelo DJ, Neuberg D, Amrein PC, Berchuck J, Wadleigh M, Sirulnik LA, et al. A Phase II Study of the EGFR Inhibitor Gefitinib in Patients With Acute Myeloid Leukemia. *Leukemia Res* (2014) 38(4):430–4. doi: 10.1016/j.leukres.2013.10.026
34. Boehrer S, Ades L, Braun T, Galluzzi L, Grosjean J, Fabre C, et al. Erlotinib Exhibits Antineoplastic Off-Target Effects in AML and MDS: A Preclinical Study. *Blood* (2008) 111(4):2170–80. doi: 10.1182/blood-2007-07-100362
35. Mahmud H, Kornblau SM, Ter Elst A, Scherpen FJ, Qiu YH, Coombes KR, et al. Epidermal Growth Factor Receptor Is Expressed and Active in a Subset of Acute Myeloid Leukemia. *J Hematol Oncol* (2016) 9(1):64. doi: 10.1186/s13045-016-0294-x
36. Grossmann V, Haferlach C, Nadarajah N, Fasan A, Weissmann S, Roller A, et al. CEBPA Double-Mutated Acute Myeloid Leukaemia Harbours Concomitant Molecular Mutations in 76.8% of Cases With TET2 and GATA2 Alterations Impacting Prognosis. *Br J Haematol* (2013) 161(5):649–58. doi: 10.1111/bjh.12297

Conflict of Interest: Authors S-BC, FL, TZ, L-XL, and C-CW are employed by Acornmed Biotechnology Co., Ltd.

The remaining authors declare that the research was conducted in the absence of any commercial or financial relationships that could be construed as a potential conflict of interest.

The reviewer RL declared a past co-authorship with the authors to the handling editor.

Publisher's Note: All claims expressed in this article are solely those of the authors and do not necessarily represent those of their affiliated organizations, or those of the publisher, the editors and the reviewers. Any product that may be evaluated in this article, or claim that may be made by its manufacturer, is not guaranteed or endorsed by the publisher.

frontiers in Oncology

ORIGINAL RESEARCH
published: 30 August 2021
doi: 10.3389/fonc.2021.701318

Comparison of Multiple Clinical Testing Modalities for Assessment of NPM1-Mutant AML

*Amanda Lopez[1], Sanjay Patel[1], Julia T. Geyer[1], Joelle Racchumi[1], Amy Chadburn[1], Paul Simonson[1], Madhu M. Ouseph[1], Giorgio Inghirami[1], Nuria Mencia-Trinchant[2], Monica L. Guzman[2], Alexandra Gomez-Arteaga[2,3], Sangmin Lee[2], Pinkal Desai[2], Ellen K. Ritchie[2], Gail J. Roboz[2], Wayne Tam[1] and Michael J. Kluk[1]**

[1] Department of Pathology and Laboratory Medicine, Weill Cornell Medicine, New York, NY, United States, [2] Clinical and Translational Leukemia Program, Division of Hematology and Oncology, Department of Medicine, Weill Cornell Medicine, New York, NY, United States, [3] Stem Cell Transplant Program, Division of Hematology and Oncology, Department of Medicine, Weill Cornell Medicine, New York, NY, United States

OPEN ACCESS

Edited by:
Alessandro Isidori,
AORMN Hospital, Italy

Reviewed by:
Sangeetha Venugopal,
University of Texas MD Anderson Cancer Center, United States
Brunangelo Falini,
Università degli Studi di Perugia, Italy

***Correspondence:**
Michael J. Kluk
mik9095@med.cornell.edu

Specialty section:
This article was submitted to Hematologic Malignancies, a section of the journal Frontiers in Oncology

Received: 27 April 2021
Accepted: 12 August 2021
Published: 30 August 2021

Citation:
Lopez A, Patel S, Geyer JT, Racchumi J, Chadburn A, Simonson P, Ouseph MM, Inghirami G, Mencia-Trinchant N, Guzman ML, Gomez-Arteaga A, Lee S, Desai P, Ritchie EK, Roboz GJ, Tam W and Kluk MJ (2021) Comparison of Multiple Clinical Testing Modalities for Assessment of NPM1-Mutant AML. Front. Oncol. 11:701318. doi: 10.3389/fonc.2021.701318

Background: *NPM1* mutation status can influence prognosis and management in AML. Accordingly, clinical testing (i.e., RT-PCR, NGS and IHC) for mutant *NPM1* is increasing in order to detect residual disease in AML, alongside flow cytometry (FC). However, the relationship of the results from RT-PCR to traditional NGS, IHC and FC is not widely known among many practitioners. Herein, we aim to: i) describe the performance of RT-PCR compared to traditional NGS and IHC for the detection of mutant *NPM1* in clinical practice, and also compare it to FC, and ii) provide our observations regarding the advantages and disadvantages of each approach in order to inform future clinical testing algorithms.

Methods: Peripheral blood and bone marrow samples collected for clinical testing at variable time points during patient management were tested by quantitative, real-time, RT-PCR and results were compared to findings from a Myeloid NGS panel, mutant NPM1 IHC and FC.

Results: RT-PCR showed superior sensitivity compared to NGS, IHC and FC with the main challenge of NGS, IHC and FC being the ability to identify a low disease burden (<0.5% NCN by RT-PCR). Nevertheless, the positive predictive value of NGS, IHC and FC were each ≥ 80% indicating that positive results by those assays are typically associated with RT-PCR positivity. IHC, unlike bulk methods (RT-PCR, NGS and FC), is able provide information regarding cellular/architectural context of disease in biopsies. FC did not identify any *NPM1*-mutated residual disease not already detected by RT-PCR, NGS or IHC.

Conclusion: Overall, our findings demonstrate that RT-PCR shows superior sensitivity compared to a traditional Myeloid NGS, suggesting the need for "deep-sequencing" NGS panels for NGS-based monitoring of residual disease in *NPM1*-mutant AML. IHC provides

complementary cytomorphologic information to RT-PCR. Lastly, FC may not be necessary in the setting of post-therapy follow up for *NPM1*-mutated AML. Together, these findings can help inform future clinical testing algorithms.

Keywords: NPM1, AML, MRD, RT-PCR, NGS, IHC, Flow Cytometry

INTRODUCTION

Nucleophosmin (*NPM1*) is a highly expressed nucleolar protein, which has been implicated in diverse cellular functions in many cell types (1). Genetic alterations including translocations and mutations of *NPM1* have been reported in a variety of myeloid disorders (1, 2). More specifically, mutations in *NPM1* have been reported in approximately 50% of acute myeloid leukemia (AML) with a normal karyotype and represents a distinct subset of AML according to the World Health Organization classification (2, 3). *NPM1* mutations in AML are frameshift variants (i.e., small insertion/deletions) in the terminal exon, frequently involving codons Trp288 or Trp290 (3). The most common variant is the Type A mutation (c.860_863dupTCTG; p.W288Cfs*12), which constitutes approximately 80% of all *NPM1* mutations in AML (3). As a result of the Type A frameshift variant (as well as other less common frameshift variants), the amino acid sequence of the C-terminus of the NPM1 protein is altered, leading to abnormal cytoplasmic localization of mutant NPM1 in leukemic cells (3, 4).

The presence of *NPM1* mutations in AML has prognostic significance which is modified with co-mutations in *FLT3* (internal tandem duplications, ITD) and *DNMT3A*. For example, *NPM1* mutation without *FLT3* ITD or *DNMT3A* co-mutation tends to be associated with a better prognosis, than when co-existing with *FLT3* ITD and/or *DNMT3A* mutations (2, 5–8). Thus, the mutation status of *NPM1* (as well as other genes such as *FLT3*) can help direct clinical management decisions related to bone marrow transplantation (2, 9, 10) as well as specific chemotherapy regimens, including the use of BH3-mimetics (e.g., venetoclax) (11–13). Additionally, *NPM1* has been shown to be a reliable molecular biomarker of disease, which is retained in > 90% of relapsed patients who initially had mutated *NPM1* at AML diagnosis (9, 14, 15); thus, interrogation of mutant *NPM1* can be used to identify minimal/measurable residual disease (MRD) and/or early relapse, post-therapy. According to Ivey et al., after the second cycle of chemotherapy, AML patients with mutated *NPM1* transcripts detectable in the blood had a greater relapse rate and shorter survival than patients without detectable mutated *NPM1* transcripts (9). Other studies have suggested a relationship between high *NPM1* mutant allele burden at diagnosis and inferior clinical outcome in *de novo* *NPM1*-mutated AML (16–18). Additionally, recent preliminary studies suggest that therapy response (i.e., post-therapy fold-reduction of mutant *NPM1* transcripts from baseline levels at diagnosis) may affect risk of disease progression (19). Thus, the need to assess and track mutant *NPM1* is growing, as part of an overall effort to harness molecular and immunophenotypic approaches to evaluate residual disease and identify early relapse in AML (20, 21).

Molecular testing for *NPM1* mutation has been described using both RNA and/or genomic DNA (15, 22). RNA has been suggested to provide greater analytical sensitivity than genomic DNA, and consequently, RNA input has been used in most follow-up monitoring studies (9, 22). Typically, RNA is used in a quantitative, real-time, reverse transcription PCR (RT-PCR) assay using mutant-*NPM1* specific primers with the *NPM1*-mutant transcript signal normalized by *ABL1* transcripts (% Normalized Copy Number: (mutant *NPM1* copy number/ *ABL1* copy number) x 100). Other methods to detect mutant *NPM1* including next generation sequencing (NGS)-based (23, 24) and immunohistochemical (IHC)-based (17, 25, 26) approaches have been described. A recent European LeukemiaNet consensus document has begun to raise awareness of the clinical and technical challenges for the application of molecular (i.e., RT-PCR, NGS) and flow cytometric (FC) methods to assess MRD in AML, including the assessment of mutant *NPM1* (21). Thus, as these assays become more broadly implemented in the clinical setting, continued improvement in the understanding of the relative performance of these assays is needed by practitioners in pathology, oncology and other disciplines who perform, interpret and use the results for clinical management. Currently, RT-PCR is considered by most to be the "gold standard" for the detection of MRD in *NPM1*-mutant AML; thus, at our center, we have implemented RT-PCR, alongside other testing methods, to assess mutant *NPM1* as a part of prospective testing used in real-time, during routine clinical practice. Herein, we aim to: *i*) compare the performance of our RT-PCR assay to our NGS and IHC (i.e., to compare the detection of mutant *NPM1* RNA transcript, mutant *NPM1* genomic DNA sequence, and mutant NPM1 protein, respectively) as well as compare RT-PCR to routine FC, *ii*) provide information regarding the advantages and disadvantages experienced with each approach.

MATERIALS AND METHODS

Cases

The samples comprise individual, consecutively received peripheral blood (PB) and/or bone marrow (BM) specimens from patients undergoing routine clinical work up for diagnosis and/or follow up of acute myeloid leukemia [94 samples from 37 unique patients: 17 men, 20 women, average age at diagnosis: 60y (range 30-93y)]. Patients had a prior history of *NPM1* mutation

(Type A) and corresponded to follow up samples, except for 7 samples (#21, #28, #62, #63, #66, #84, #93) which were tested at initial diagnosis (of note, all of these 7 initial diagnostic samples showed concordant results for *NPM1* mutation status by RT-PCR, NGS and IHC (pan-negative: #21, #28, #62, #63, #66, #93; or pan-positive: #84). Appropriately, the 6 samples that were negative for *NPM1*-mutation at diagnosis (#21, #28, #62, #63, #66, #93) were not used in the comparison of FC to RT-PCR since, as expected, FC would be positive for leukemia at diagnosis and RT-PCR would be negative. Overall, all samples with *NPM1* RT-PCR data available and data from at least one other testing modality (NGS, IHC or FC) were included (see **Supplementary Table 1** for data available for each sample). Specimen types available for RT-PCR and NGS included both PB and BM, while specimen type available for IHC and FC included only BM samples (**Supplementary Figure 1**). In standard clinical practice, all laboratory tests are not performed on both PB and BM simultaneously. Thus, for PB specimens with RT-PCR data or with RT-PCR and NGS data available, comparison was made to the results of the other testing modalities (e.g., IHC, FC) from a recent BM biopsy (within 2 weeks of the PB sample). In addition, separate comparison of the results from the various testing modalities was performed after restricting samples to the same specimen type and the same collection date (**Supplementary Table 2**), in order to rule out any potential confounding effect of time and sample for the assay results being compared. Lastly, a separate group of diagnostic AML samples which did not have RT-PCR data were used to compare mutant NPM1 IHC *versus* NGS (**Supplementary Table 3**).

Real-Time, Reverse Transcription PCR (RT-PCR) Assay for Type A Mutant *NPM1* Transcripts

Patients' PB and/or BM aspirate samples collected in EDTA tubes underwent RNA extraction (QIAamp RNA Blood Mini Kit, #52304) according to standard protocol. Reverse transcription was performed with RNA (≥ 1μg) in 20 μL final volume (SuperScript III RT, Life Technologies, #18080085; RNaseOUT, Life Technologies, #10777019; Random Primers, Life Technologies, #48190011; dNTP mix (10 mM), Promega, #U151B; First Strand Buffer (5x) and DTT (0.1 M)) at 65°C for 5 minutes, then placed on ice or left at 4°C for at least 1 minute; cycling conditions: 25°C (10 min), 50°C (50 min), 85°C (5 min), 4°C (Hold) (Applied Biosystems, GeneAmp 9700 thermocycler or ProFlex PCR systems). cDNA was diluted by adding 30 μL of nuclease-free water (50 μL total volume). Five μL of the diluted cDNA (corresponding to ≥ 100 ng RNA equivalent) was input into real-time PCR (*NPM1* mutA MutaQuant primers and probes, Ipsogen, Qiagen, #677513) using ABI 7500 Fast Real-Time PCR system (Applied Biosystems), TaqMan Universal PCR Master Mix, Life Technologies, #4304437; with cycling conditions: 50°C (2 min); 95°C (10 min); [95°C (15 sec), 60°C (60 sec)] x 50 cycles. Analysis was performed with a threshold of approximately 0.1 set for both *NPM1* and *ABL*. RT-PCR results were reported as % Normalized Copy Number (%NCN): (*NPM1* Mutant A Copy Number/ABL Copy Number) x 100. All samples and controls were run in duplicate reactions. We have previously validated the performance characteristics of the RT-PCR assay to detect *NPM1* Type A mutant transcripts in patient PB and BM aspirate specimens (27); the RT-PCR assay showed the expected analytical sensitivity (limit of detection approximately 0.01% NCN).

Myeloid NGS Panel

A custom 45 gene NGS panel [Thunderstorm system, RainDance Technologies, Billerica, MA, USA, Illumina MiSeq (v3 chemistry)] interrogating single nucleotide variants (SNV) and insertion/deletions (InDels) was used. Samples were run in duplicate. The NGS detection sensitivity was approximately 2% for SNV and 1% for INDEL. In addition, every NGS case was manually reviewed in IGV for the presence of any mutant *NPM1* sequencing reads (limit of detection approximately 0.1%-1% variant allele frequency (VAF)). The mean and median sequencing read depth at the *NPM1* mutation locus (chr5:170,837,530-170,837,570) were 3036 and 2905 reads, respectively.

Immunohistochemistry

IHC for mutant NPM1 was performed on 5um Bouin or formalin fixed paraffin embedded BM core biopsy or clot sections using anti-mutant NPM1 antibody (Thermo Fisher/PA1-46356, Polyclonal, 1:1500 dilution) with ER2 antigen retrieval for 30 mins [H2 (30 mins) on the Leica Bond III automated immunostainer using alkaline phosphatase Refine Red detection (Leica Biosystems Inc., Buffalo Grove, IL.]. The antibody is directed against the epitope of Type A mutation (c.863_864insTCTG) of *NPM1* and it targets the c-terminus region (including amino acids within the final exon of *NPM1*). Differences in immunostaining were not observed for Bouin or formalin fixed samples. Immunostaining results were reviewed by the original hematopathologist and also reviewed by a separate hematopathologist (MK) blinded to results from other testing modalities. Immunostaining for mutant NPM1 protein was considered positive if there was homogenous, cytoplasmic staining in >3 hematopoietic cells, with the positive cells often forming clusters. Cases were considered negative if there was no such staining in hematopoietic cells. Cases were considered borderline positive when there were very rare (i.e., 1-3 cells), scattered hematopoietic cells with variable cytoplasmic staining, such that the result could not be easily distinguished from background signal, due to the very low number and variable intensity staining of suspected cells. If there was discordance such that one pathologist considered the case to be borderline positive by IHC, but the other pathologist considered it negative, then the case was assigned to the borderline positive IHC category, since the presence of any potential mutant NPM1 protein staining (above background) in hematopoietic cells could be significant (given that the mutant protein is not expressed in normal tissues).

Flow Cytometry

Flow cytometry (8-color) was performed using the EuroFlow AML panels (28), which include many markers (e.g. CD45,

HLA-DR, CD117, CD34, CD13, CD33, CD56, CD7, etc). FC does not include analysis of NPM1 protein. FC results were analyzed with BD FACSDiva software (BD Biosciences, San Jose, CA). Gating was performed using FSC-A/FSC-H to identify singlets, CD45/Viability Dye to identify viable cells, and FSC/SSC, CD45/SSC to identify blast, lymphocyte, monocyte and granulocyte subpopulations. In follow up samples, identification of leukemic blasts was performed by assessment for the abnormal immunophenotypic profile which was recorded at diagnosis. Approximately 500,000 cells were collected in samples if FC appeared negative and an adequate number of cells were available. FC was reported as positive when there was diagnostic evidence of the patient's prior leukemic blast population. FC was reported as borderline when there was an atypical blast population with a dissimilar phenotype of uncertain significance. FC was considered negative when diagnostic evidence of acute leukemia was not seen.

Statistical Analysis

Sensitivity, specificity, positive predictive value (PPV), negative predictive value (NPV) and concordance (i.e., the number of cases which were positive (and negative) by the 2 respective testing modalities, divided by total number of cases tested) were calculated for each modality (NGS, IHC and FC) in comparison to RT-PCR. Fisher's Exact Test was used for statistical comparison (**Table 2**, **Supplementary Table 2**). PPV and NPV indicate the performance of NGS, IHC and FC compared to RT-PCR (which is considered the "gold standard" test). Statistical analysis was performed using the base R package; graphics were generated with GGPLOT2.

This work is covered under the IRB Protocol #: 1007011151.

RESULTS

Samples were acquired from patients undergoing routine clinical workup for diagnosis and/or follow up of AML. A total of 94 PB or BM specimens were received for *NPM1* quantitative RT-PCR testing, for which data were also available from other testing modalities (e.g., NGS, IHC, FC) (**Supplementary Figure 1**). A small subset of patients in the current cohort had both PB and BM available from the same date of collection; RT-PCR of these samples showed %NCN scores for BM which were similar to, or greater than, the % NCN score seen in the concomitant PB (**Supplementary Figure 2**), consistent with the pattern of potentially greater sensitivity of bone marrow samples reported previously (9).

TABLE 1 | Summary of Results: NPM1 Type A Mutation Status.

	RT-PCR+ (*n* = 54)	RT-PCR- (*n* = 40)	Total (*N* = 94)
NGS, *n* (%)			
NGS+	12 (31%)	2 (6%)	14 (19%)
NGS-	27 (69%)	31 (94%)	58 (81%)
Total	39 (100%)	33 (100%)	72 (100%)
NPM1 IHC, *n* (%)			
IHC+	21 (45%)	0 (0%)	21 (26%)
IHC Borderline+	16 (34%)	7 (21%)	23 (28%)
IHC-	10 (21%)	27 (79%)	37 (46%)
Total	47 (100%)	34 (100%)	81 (100%)
FC, *n* (%)			
Flow+	6 (13%)	5 (14%)	11 (14%)
Flow Borderline+	11 (24%)	4 (12%)	15 (18%)
Flow-	29 (63%)	26 (74%)	55 (68%)
Total	46 (100%)	35 (100%)	81 (100%)

NPM1 Type A mutant RT-PCR results were compared to NGS, IHC and FC results (**Table 1**). Overall, there were 94 samples with RT-PCR data including 54 (57%) positive and 40 (43%) negative samples. Among these 94 samples, NGS data was available for 72 (77%), IHC data for 81 (86%) and FC data for 81 (86%) samples (see **Supplementary Table 1** for additional details regarding data available from each modality for each sample). Among the RT-PCR positive samples, 12 of 39 (31%) samples with NGS data were NGS positive, 37 of 47 (79%) samples with IHC data were IHC positive (including borderline positive samples), and 17 of 46 (37%) FC samples were FC positive (including borderline positive samples) (**Table 1**).

In order to better understand the relationship between RT-PCR results compared to Myeloid NGS, Mutant NPM1 IHC and FC, contingency tables were generated (**Table 2**).

Myeloid NGS

As noted above, the Myeloid NGS panel showed a sensitivity of 31% (12/39) compared to RT-PCR; the RT-PCR positive samples which were negative by NGS had RT-PCR values of ≤ 0.5% NCN in 22 of 27 samples (**Supplementary Table 1**, **Figure 1**) indicating a low disease burden that was detectable by RT-PCR but not NGS. The remaining 5 samples had >0.5% NCN by RT-PCR and 4 of these samples had IHC data available; each of the 4 samples were positive by IHC, compatible with the positive RT-PCR result. These 27 NGS-negative cases accounted for the negative predictive value of approximately 53% for NGS compared to the RT-PCR assay. On the other hand, the Myeloid NGS panel showed a specificity of 94% (**Table 2**); the 2 samples which were positive for NGS, but negative by RT-PCR (samples 27 and 79, **Supplementary Table 1**, both with known history of NPM1 Type A mutation) showed very low/borderline NGS VAF values (approximately 0.08% VAF), borderline IHC results and negative FC results. These 2 cases resulted in the NGS assay showing a positive predictive value 86% compared to RT-PCR. For sample 27, RT-PCR and NGS were both performed on the BM specimen at 100 days post-transplant; additional follow up over the subsequent 10 months for this patient has shown persistent negativity for *NPM1* by both RT-PCR (x2) and NGS (x2) (samples 36 and 75). The underlying reason for the difference in the RT-PCR and NGS results for sample 27 is uncertain but, may have resulted from sampling variability at a low level of disease, that subsequently was associated with more complete clearance of disease further out from transplant. For sample 79, NGS was performed on BM (at 28 days post-transplant) and subsequently (i.e., 6 days later) RT-PCR was performed on PB (as a follow up for the NGS finding); subsequent follow up on this patient 2 months later has

TABLE 2 | *NPM1* status: RT-PCR v. NGS.

	PCR+	PCR-	Total	Predictive Value
NGS+	12	2	14	Positive: 86%
NGS-	27	31	58	Negative: 53%
Total	39	33	72	
	Sensitivity: 31%	Specificity: 94%		Concordance: 60%

P Value: 0.01473.

NPM1 status: RT-PCR v. IHC.

	PCR+	PCR-	Total	Predictive Value
IHC+	37	7	44	Positive: 84%
IHC-	10	27	37	Negative: 73%
Total	47	34	81	
	Sensitivity: 79%	Specificity: 79%		Concordance: 79%

P Value: 0.0000003.

RT-PCR v. Flow Cytometry.

	PCR+	PCR-	Total	Predictive Value
Flow+	17	3	20	Positive: 85%
Flow-	29	26	55	Negative: 47%
Total	46	29	75	
	Sensitivity: 37%	Specificity: 90%		Concordance: 57%

P Value: 0.01512.

revealed BM positivity for a very low level of disease by RT-PCR (0.014% NCN, sample 92) and borderline staining by IHC.

Taken together, these findings indicate that the genomic DNA-based, standard Myeloid NGS panel used herein (with limit of detection 0.1%-1% VAF) is less sensitive than RNA-based RT-PCR, due primarily to the challenge of detecting mutant *NPM1* in samples with a low burden of disease (<0.5% NCN by RT-PCR). Nevertheless, NGS may provide some helpful information in BM cases with borderline IHC and negative RT-PCR of PB. These findings support the need for further development and implementation of "deep-sequencing" NGS-based approaches in order to improve the sensitivity of NGS-based assays for the assessment of *NPM1*.

Mutant NPM1 IHC

Representative images of immunostaining are shown in **Figure 2**. Comparison of IHC results to RT-PCR, reveals a sensitivity of 79% (37/47) was observed for the IHC (including borderline IHC positive samples)(**Table 2**); the RT-PCR positive cases which were negative by IHC (10 samples) had a very low disease burden as evidenced by the %NCN RT-PCR values (≤0.05% NCN in 8 of 10 samples and <0.5% in the remaining 2 samples (**Supplementary Table 1**, **Figure 1**); in 7 of these 10 samples NGS data was available (**Supplementary Table 1**) and no mutant *NPM1* alleles were detected in the 7 samples, consistent with the above NGS findings for cases with a low burden of disease by RT-PCR. Given the findings in these 10 samples, the negative predictive value of the IHC was 73% compared to the RT-PCR assay. In terms of other performance variables, the specificity of the IHC was 79% compared to RT-PCR (**Table 2**) and the positive predictive value of IHC was 84% compared to RT-PCR. The 7 samples (sample #s: 16, 17, 27, 37, 65, 67, 79) (**Supplementary Table 1**) which were positive by IHC but negative by RT-PCR showed only borderline IHC results, were negative by FC results, and were negative by NGS except for two cases (samples 27 and 79 which showed very low/borderline 0.08% VAF for *NPM1* Type A mutation by NGS, as described in preceding section). Overall, the underlying reasons for the difference in the RT-PCR and IHC results for these 7 samples likely includes sampling variability at a low level of disease and/or difficulty discerning background IHC staining from true, rare positive cells. Sample 79 highlights a situation where borderline IHC results (when associated with even minimal evidence of mutant NPM1 by NGS) may be relevant, since RT-PCR on a subsequent BM sample from this patient (sample 92) has revealed very low persistent levels of mutant *NPM1* by RT-PCR(0.014% NCN) as well as borderline IHC staining. Furthermore, the findings from another patient (corresponding to samples 16, 17, 37) also illustrate the potential utility of IHC in some BM samples to prompt appropriate follow up studies; more specifically, sample 16 (PB) and sample 17 (BM) collected at the same time were both negative for mutant *NPM1* by RT-PCR and NGS; FC was also negative in the BM, however, IHC showed borderline staining. A subsequent PB specimen (sample 24) was negative by RT-PCR and NGS. Continued follow up of the patient over time revealed a very low level of mutant *NPM1* transcripts (0.05% NCN) in PB (sample 33) by RT-PCR. During further follow up, BM biopsy was done and showed mutant NPM1 staining in rare, scattered cells (**Figure 2**, bottom left panel); NGS on the BM was negative and concomitant RT-PCR on a limited PB specimen (sample 37) appeared negative. Further follow up PB samples (sample 41, 42) confirmed low level of mutant NPM1 transcripts by RT-PCR. Taken together, the scenarios from these two patients highlight how mutant NPM1 IHC can be helpful in some cases to prompt appropriate follow up monitoring by RT-PCR and other studies.

A related useful aspect of mutant NPM1 immunostaining is that it can provide helpful information when the cellularity of BM aspirate and PB specimens used for bulk studies (i.e., RT-PCR, NGS and FC) may be variable (e.g., due to a "packed-marrow") and may underestimate tumor cell number (Sample 64, **Figure 2**, bottom right panel). Again, in this situation also, the presence of mutant NPM1 staining can prompt appropriate follow up studies (RT-PCR, NGS, etc).

Lastly, IHC can provide information regarding the cytomorphologic details of mutant NPM1-positive cell types; it was observed that in addition to hematopoietic precursor-like cells (i.e., blast forms) being positive by mutant NPM1 IHC, occasional megakaryocytes were also positive. For example, a case with a subset of the megakaryocytes positive for mutant NPM1 is shown (**Figure 2**, top right panel). Subsequent biopsies from this patient (data not shown) revealed persistent mutant NPM1 staining predominantly in immature hematopoietic cells, as well as scattered megakaryocytes.

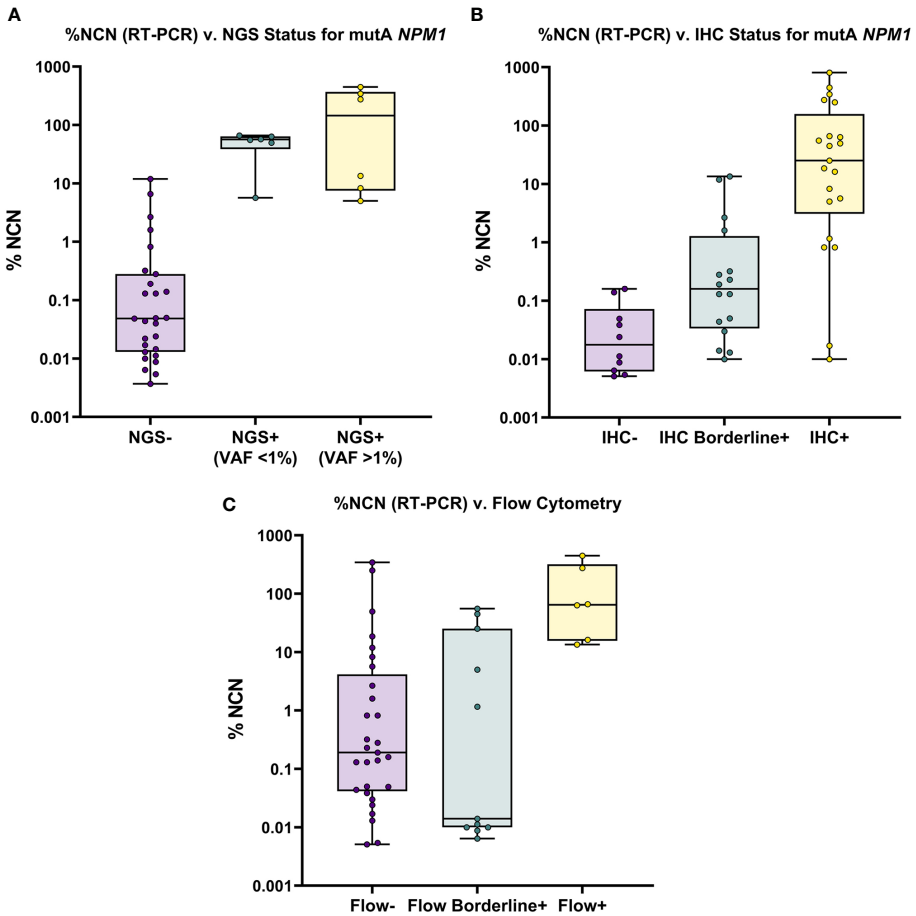

FIGURE 1 | Overview of NGS, IHC and FC Results for All RT-PCR Positive Samples. **(A)** Mutant (Type A) *NPM1* RT-PCR (%NCN) (*plotted on Log_{10} scale*) is shown compared to NGS results; samples are grouped by NGS status (i.e., Negative, <1% VAF and >1% VAF). Samples are noted to be detectable by NGS only when RT-PCR % NCN values are ≥5%. **(B)** Mutant (Type A) *NPM1* RT-PCR (%NCN) is shown compared to IHC results; samples are grouped by IHC status (i.e., Negative, Borderline Positive and Positive). In general, mutant NPM1 protein is detectable (i.e., Positive) by IHC when RT-PCR % NCN values are ≥1% (although occasional samples may show detectable mutant NPM1 protein by IHC at lower % NCN values (i.e., 0.01-1% NCN). **(C)** Mutant (Type A) *NPM1* RT-PCR (%NCN) is shown compared to FC results; samples are grouped by FC status (i.e., Negative, Borderline Positive and Positive). In general, samples are Positive by FC only when RT-PCR % NCN values are >10% (although occasional samples may show borderline FC positivity at lower % NCN values).

Taken together, these findings indicate that, compared to RT-PCR, mutant NPM1 IHC demonstrates sensitivity and specificity approaching 80%, and provides cytomorphologic insight into mutant NPM1-positive cell populations in biopsies, but that interpretation of IHC in samples with a low burden of disease can be challenging and thus requires correlation with molecular studies (e.g., RT-PCR).

Flow Cytometry

In comparison to RT-PCR, FC showed a sensitivity of 37% (17/46) (including borderline FC positive samples) (**Table 2**). The RT-PCR positive cases which were negative by FC had a variable disease burden as evidenced by the %NCN RT-PCR values of ≤ 0.5% NCN in 18 of 29 cases, 0.5%-5% NCN in 4 samples, 5%-15% NCN in 3 samples and >15% NCN in 4 samples (**Supplementary Table 1**, **Figure 1**). In 7 of the 11 samples with disease burden >0.5% NCN by RT-PCR which were negative by FC, the samples available for FC were limited due to hypocellularity (mean +/- SD = 260,000 +/- 58,000 cells). Given the negative FC findings in the RT-PCR positive samples, the negative predictive value of the FC was 47% compared to the RT-PCR assay. In terms of other performance variables, the specificity of the FC was 90% (26/29) compared to RT-PCR (**Table 2**) when considering cases which had a known history of mutant *NPM1*. As shown in **Table 2** and **Supplementary Table 1**, only 3 samples with a history of mutant *NPM1* were positive by FC and negative by RT-PCR (samples # 36, 43 and 55); these samples were also negative by NGS and IHC, and, not surprisingly showed only borderline FC results (0.3%-0.7% abnormal cells by FC). These 3 cases resulted in the overall FC positive predictive value being 85%. The atypical flow cytometric findings in these 3 cases likely represented immunophenotypic variability resulting from therapy and/or presence of clonal (non-leukemic) populations; indeed, as mentioned above, NGS

in each of these 3 cases was negative for *NPM1* mutation but, interestingly, 2 of these 3 samples did show variants associated with clonal hematopoiesis (i.e., *DNMT3A* and/or *TET2*). FC did not detect residual disease in any cases which was not identified by RT-PCR, NGS or IHC. Taken together, the FC findings indicated that FC is less sensitive than RT-PCR, and phenotypic variations post-therapy related to clonal hematopoiesis may confound assessment for residual disease by FC. Thus, in the setting of monitoring for residual disease in *NPM1*-mutant AML, FC appears to provide no additional benefit beyond RT-PCR, NGS and IHC.

In addition to the above findings regarding RT-PCR, NGS, IHC and FC results, a similar pattern of findings was observed when comparing the available RT-PCR, NGS, IHC and FC results for samples restricted to the same specimen type and the same collection date (i.e., PB samples with RT-PCR and NGS from same date, or BM samples with RT-PCR, NGS, IHC and/or FC from same date) (See (**Supplementary Tables 1** and **2**).

Clinical Application

Lastly, to provide a specific example of the sensitivity of RT-PCR and its suitability for quantitative, serial monitoring on PB specimens, a time course of RT-PCR data from a patient is shown (**Figure 3**). The patient presented as a 58-year-old woman with an incidental finding of circulating blasts in PB. She had a history of prior gynecological tumor treated with surgical resection (no chemotherapy and no radiation therapy). Work-up lead to a diagnosis of AML with normal karyotype; molecular studies (Myeloid NGS) revealed variants in *NPM1* (Type A mutation, p.Trp299Cysfs*12, 40% VAF), *NRAS* (p.Gly13Asp, 42% VAF) and *IDH2* (p.Arg140Gln, 45% VAF). The patient was treated with induction and consolidation chemotherapy

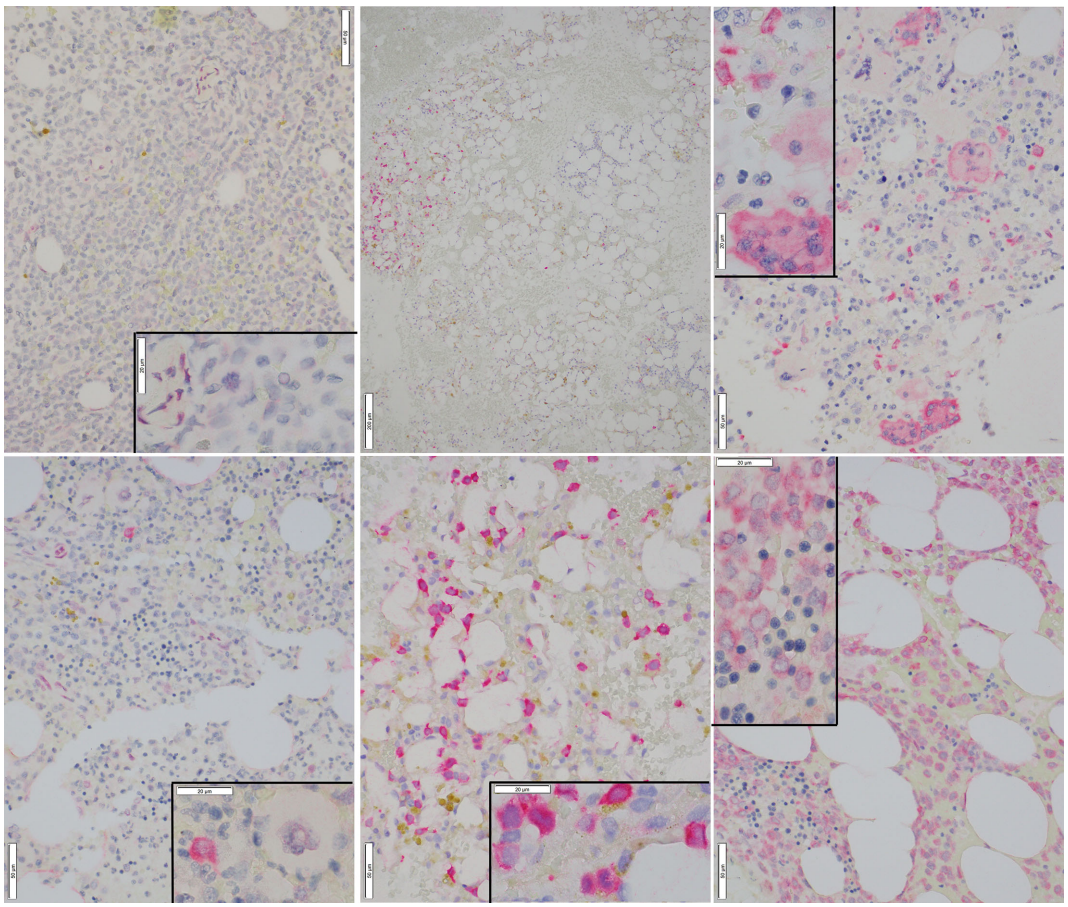

FIGURE 2 | Representative Images of Mutant NPM1 IHC. *Top Left:* Bone marrow negative for mutant NPM1 immunostaining (40x); inset (100x) shows lack of staining in hematopoietic cells; occasional background staining in vascular cells is noted. *Bottom Left:* Bone marrow borderline positive for mutant NPM1 immunostaining (40x); inset (100x) shows an immature hematopoietic cell which is positive for red, homogeneous cytoplasmic, mutant NPM1 immunostaining. Adjacent megakaryocyte is negative. *Top Center:* Bone marrow positive for mutant NPM1 immunostaining; this low power view (10x) shows patchy nature of staining; the cluster of red (positive) cells is noted on the left side of field. *Bottom Center:* Bone marrow positive for red, homogeneous cytoplasmic mutant NPM1 immunostaining in hematopoietic cells(40x); inset(100x). *Top Right*: Bone marrow positive for mutant NPM1 immunostaining; scattered positive hematopoietic cells are seen admixed with scattered positive megakaryocytes (40x); inset (100x). *Bottom Right:* Bone marrow positive for mutant NPM1 immunostaining in a sample with a very high tumor cell burden; frequent positive hematopoietic cells are seen (40x); inset (100x): focally admixed mature erythroid elements (i.e., cells with small, round, hyperchromatic (i.e., dark blue) nuclei) are negative.

(4 cycles) and achieved complete remission. RT-PCR testing of PB for mutant *NPM1* was negative through 10 months post diagnosis, except for one borderline finding at 5 months post diagnosis (before starting final cycle of consolidation therapy), which was followed by several negative RT-PCR PB samples (as well as a BM biopsy (sample 17) at 7 months post diagnosis which was negative by RT-PCR, NGS and FC). 13 months post diagnosis, a PB sample (Sample 33) showed a low level of mutant *NPM1* transcripts by RT-PCR (0.05% NCN) and a BM biopsy was performed and was negative by NGS and FC assessment; mutant NPM1 staining revealed rare, single, scattered positive cells consistent with a borderline positive IHC result (**Figure 2**, bottom left panel)(i.e., very rare mutant NPM1 positive cells seen). Close interval monitoring of PB by RT-PCR was initiated and confirmed the presence and increase in mutant *NPM1* transcripts over the following 4 weeks. Azacitidine was started, and although the RT-PCR-detected mutant NPM1 transcripts in PB continued to rise 2 weeks after starting the azacitidine, the mutant transcript level began decreasing by day 29 after initiation. Azacitidine therapy was continued and venetoclax therapy was added. By RT-PCR, mutant *NPM1* transcript levels in the PB continued to decrease and have remained undetectable during continued azacytidine/venetoclax therapy. Taken together, this patient's time course illustrates the potential significance of very low level (i.e., 0.05%-0.5% NCN) of mutant *NPM1* transcripts detected in PB by RT-PCR in some cases, and highlights the utility of serial, quantitative RT-PCR testing of the PB for mutant *NPM1* during patient management. Recent findings by other authors have also demonstrated the utility of quantitative RT-PCR and IHC in clinical management (29).

DISCUSSION

The detection and monitoring of mutant *NPM1* in AML is becoming increasingly implemented in the clinical setting. Thus, clinical practitioners in oncology and pathology need to be familiar with the various issues related to the application and interpretation of the assays used to detect mutant *NPM1* in clinical practice. Several methods are available to detect mutant *NPM1* including: RT-PCR for mutant *NPM1* transcripts (15, 21, 22), NGS for *NPM1* mutation (16, 23) and IHC for mutant NPM1 protein (17, 25). Having implemented RT-PCR for Type A mutant *NPM1* transcripts, IHC for mutant NPM1 protein and a myeloid NGS panel at our academic center, we set out to: *i*) assess the relative performance of these assays and, *ii*) provide information regarding the advantages and disadvantages of each approach.

We have found that RT-PCR for Type A mutant *NPM1* transcripts showed superior sensitivity compared to NGS, IHC and FC. Nevertheless, the positive predictive value of NGS, IHC and FC were each > 80% indicating that positive results by those

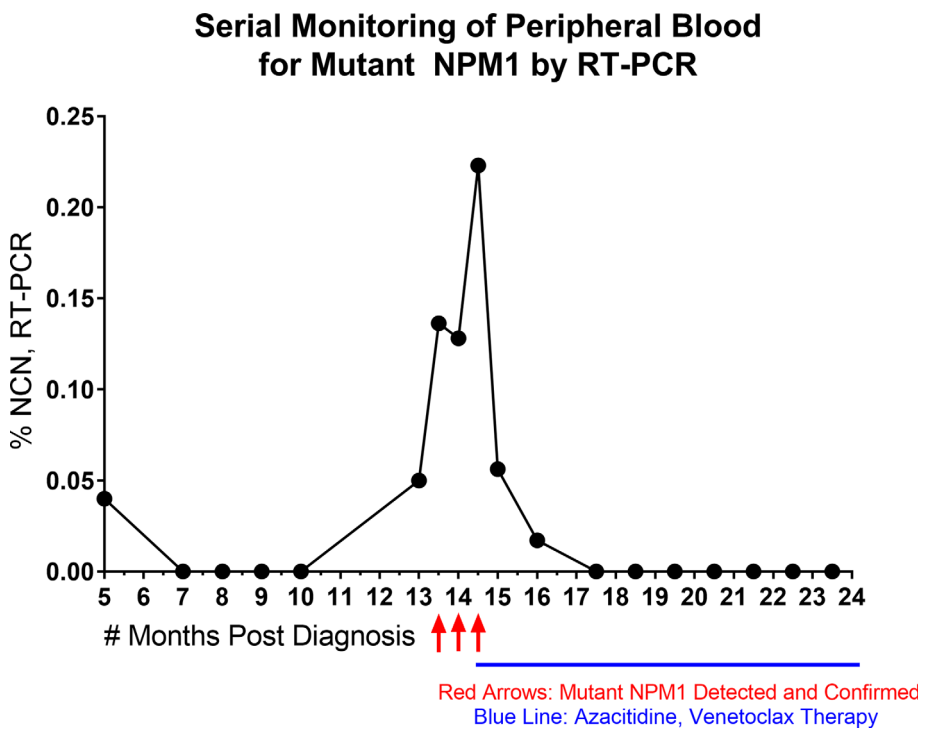

FIGURE 3 | Time Course of Serial, Quantitative RT-PCR of Peripheral Blood. *NPM1* (Type A) mutant transcript monitoring by RT-PCR (%NCN) from peripheral blood is shown over time for a patient. Red arrows indicate detection and confirmation of unexpected increase in *NPM1* mutant transcripts. Blue line indicates initiation and duration of azacitidine/venetoclax therapy. Shortly after the initiation of azacitidine therapy, the *NPM1* mutant transcripts continued to rise, but then decreased during further into azacitidine treatment and remained undetectable with continuation of azacitidine/venetoclax therapy.

assays are typically associated with RT-PCR positivity. The NGS and FC were limited in their ability to detect a low disease burden (i.e., <0.5% NCN by RT-PCR). For NGS, although manual review of the relevant NPM1 sequencing reads permitted the detection of 0.1%-1% VAF in this study, the myeloid NGS assay used herein does not incorporate molecular barcoding and is not a so-called "deep-sequencing" NGS panel. The superior analytical sensitivity of RT-PCR may also be derived from the fact that *NPM1* transcripts are known to be expressed at high levels (30, 31), and that skewed expression of *NPM1* transcripts from the mutant allele (32), lead to a technical advantage of approaches using RNA-based input. Other studies of mutant *NPM1* have also suggested that RNA-based input provides greater sensitivity than genomic DNA input (22). For FC, analytical sensitivity was impaired when the total number of cells available for analysis was limited due to sample hypocellularity. Also, for FC, the lack of an aberrant immunophenotype of the blasts in some cases can render their identification difficult by FC (21). IHC (79%) was more sensitive than NGS (31%) and FC (37%), however, samples which were negative by IHC showed a low burden of disease by RT-PCR (i.e., < 0.5% NCN). A technical limitation of IHC is that samples with low %NCN by RT-PCR often show rare, if any, scattered mutant NPM1 positive cells. Thus, a challenge with IHC can be differentiating background staining from rare, scattered mutant NPM1-positive cells. Indeed, similar findings have been recently reported by Falini et al. (29) who described rare NPM1 cytoplasmic positive cells (likely post-mitotic cells) even in occasional normal bone marrow samples. Nevertheless, in occasional cases with low burden of disease by RT-PCR (<0.5% NCN), it is possible to identify mutant NPM1 staining in rare single hematopoietic cells. Overall, IHC for mutant NPM1 alone is not suitable as a stand-alone assay for assessment of residual disease, but, in combination with RT-PCR, IHC can help visualize the tumor cell burden and provide information regarding neoplastic cell distribution and cell type; along these lines, mutant NPM1 staining was noted in occasional megakaryocytes, which has been previously described, indicating multilineage involvement of mutant NPM1 (25).

With regards to the advantages and disadvantages of each approach:

RT-PCR, in addition to its superior sensitivity, has the advantages that it is quantitative and can be performed on PB, without BM biopsy, providing non-invasive serial testing during follow up to monitor disease dynamics. However, a disadvantage of RT-PCR for *NPM1* is that mutation-specific assays are required, and up to 20% of *NPM1* mutations in AML can be non-Type A mutations (i.e., so called Type B, Type D mutations, etc.). Recently a multiplex digital droplet RT-PCR assay has been reported which permits the detection of several types of *NPM1* mutations (e.g., Type A, B, D, etc) in one reaction (33); although the specific type of *NPM1* variant present is not identifiable with that assay and confirmation of reliable performance in the clinical setting is needed. A disadvantage of all RT-PCR approaches is that the input RNA may be degraded if not handled properly during collection, transport and processing.

NGS has the advantages that it uses genomic DNA (i.e., a stable substrate), it is quantitative and can detect various *NPM1* mutation types as well as co-mutated genes (e.g., *DNMT3A*, *FLT3*, etc). However, myeloid NGS approaches in routine clinical practice often have limited analytical sensitivity, with limits of detection in the 1-5% VAF range. RT-PCR may show 1-2 orders of magnitude greater signal than NGS assays with genomic DNA input [see **Supplementary Table 1** and (22)]. More recent so-called "deep sequencing" NGS approaches (23, 24, 34) demonstrate limits of detection of approximately 0.001%-0.01% VAF. However, they typically interrogate a limited panel of genes, require higher DNA input, use increased replicates, and incur greater cost to acquire and to analyze the deeper sequencing (i.e., 200,000-450,000 reads); therefore, these "deep-sequencing" NGS approaches will likely take more time before they are widely implemented for clinical testing.

FC has the potential advantages of quantitation and cell-sorting, but its main disadvantage is the challenge of phenotypic variability in AML due to disease heterogeneity (21), therapy-induced changes in protein expression, and phenotypic aberrations associated with background clonal hematopoiesis, which can confound the identification of residual disease, as we, and others (35) have observed. Thus, in the setting of post-therapy follow up for NPM1-mutated disease, priority can be given to RT-PCR, NGS and IHC testing.

IHC has unique advantages including its capacity to visualize tumor cell burden *in situ*, and to detect architectural and cytologic features that are not apparent by bulk methods (i.e., RT-PCR, NGS, FC). In addition, IHC is inexpensive and rapid compared to the other techniques. IHC may be helpful in cases where fibrosis, a "packed-marrow" with high disease burden, or other technical factors compromise the BM aspirate material for RT-PCR, NGS and FC. However, the disadvantages of IHC include the need for a BM biopsy, its qualitative nature, and the potential difficulty to discern rare mutant NPM1-positive cells from background staining [a similar challenge has been recently reported by other authors (29)]. An additional caveat is that mutant NPM1 IHC may rarely detect cytoplasmic NPM1 in AML cases with a negative molecular assay; this may occur if the mutation involving NPM1 is not covered by a "type-specific" RT-PCR assay or occurs in an exon not covered by NGS (36). Taken together, the advantages and disadvantages mentioned above for each assay highlight how the various methods provide complementary information during the analysis of patient samples.

Our findings have prompted us to consider further optimizing our testing algorithms. Currently, we perform Myeloid NGS (along with ancillary *FLT3*, *IDH1/2* molecular testing) and FC on BM biopsies at the time of initial diagnosis of AML. We are not routinely performing RT-PCR for *NPM1* mutation status at initial diagnosis. However, given the evolving role to monitor mutant *NPM1* levels to check response to initial chemotherapy (19), and given the usual 2 week turn-around time of NGS reporting, IHC staining at initial AML diagnosis could aid in the rapid identification of *NPM1*-mutated AML cases needing baseline RT-PCR. In the follow up setting for *NPM1*-mutated AML, currently we receive PB samples for mutant *NPM1* RT-PCR monitoring. When a BM biopsy is collected, the BM is tested by NGS (for mutation status of *NPM1*

and co-mutations in other genes), RT-PCR, mutant-NPM1 IHC and FC. Given the FC findings herein, we have considered eliminating FC assessment in follow up BM samples of known *NPM1*-mutated AML, if there is no other clear indication to perform FC. An additional point for further study in the setting of follow-up testing includes performance of RT-PCR on PB and/or BM samples; we (see **Supplementary Figure 2**) and others (9) have found BM samples appear to provide the potential for greater sensitivity for RT-PCR than PB.

In sum, our findings indicate that each method (RT-PCR, NGS, IHC and FC) provides complementary information and thus, while cognizant of the strengths and limitations of each assay, a multimodal assessment of mutant *NPM1* can improve our understanding of mutant *NPM1* status in patient samples.

DATA AVAILABILITY STATEMENT

The original contributions presented in the study are included in the article/**Supplementary Material**. Further inquiries can be directed to the corresponding author.

ETHICS STATEMENT

The studies involving human participants were reviewed and approved by Weill Cornell Medicine, Internal Review Board. Written informed consent for participation was not required for this study in accordance with the national legislation and the institutional requirements. Written informed consent was not obtained from the individual(s) for the publication of any potentially identifiable images or data included in this article.

AUTHOR CONTRIBUTIONS

AL and MK contributed to the conception and design of the study, organized the database, performed the statistical analysis, created the figures and tables and wrote the first draft of the manuscript. SP, JG, AC, PS, GI, MG, AG-A, SL, ER, GR and WT reviewed the manuscript and provided input for edits of the initial draft. All authors contributed to the article and approved the submitted version.

FUNDING

This work was performed with support from the Department of Pathology and Laboratory Medicine, Weill Cornell Medicine.

SUPPLEMENTARY MATERIAL

The Supplementary Material for this article can be found online at: https://www.frontiersin.org/articles/10.3389/fonc.2021.701318/full#supplementary-material

Supplementary Figure 1 | Specimen Information. **(A)** Overview of specimen types available for each assay. **(B)** For each sample number, the details of specimen types available for each assay are shown.

Supplementary Figure 2 | Mutant (Type A) *NPM1* RT-PCR (Peripheral Blood *vs.* Bone Marrow). Comparison of RT-PCR %NCN values obtained with paired peripheral blood and bone marrow samples collected on the same day. Overall, bone marrow specimens were noted to show similar or higher %NCN values compared to peripheral blood. Specific sample numbers are shown. %NCN = (*NPM1* Type A mutant transcript copy number/ABL copy number) x 100.

Supplementary Table 1 | RT-PCR (%NCN), NGS (%VAF), IHC (% mutant NPM1 positive cells) and FC (% abnormal cells) are shown (when available) for each sample.

Supplementary Table 3 | IHC for Mutant-NPM1 was performed in Diagnostic AML cases and the IHC results were compared to the results of NGS. Mutant-NPM1 IHC showed 100% concordance with NGS studies for NPM1 mutation status. IHC detected pathogenic mutations in NPM1 including Type A, Type B and pathogenic Non-Type A/Non-Type B/Non-Type D frameshift variants occurring at the known mutational hotspot region. RNA for RT-PCR was not available for these Diagnostic AML samples.

REFERENCES

1. Grisendi S, Mecucci C, Falini B, Pandolfi PP. Nucleophosmin and Cancer. *Nat Rev Cancer* (2006) 6:493–505. doi: 10.1038/nrc1885
2. Swerdlow SH, Campo E, Harris NL, Jaffe ES, Pileri SA, Stein H, et al eds. *WHO Classification of Tumours of Haematopoietic and Lymphoid Tissues. Revised 4th Edition*. Lyon: International Agency for Research on Cancer (2017). p. 585.
3. Falini B, Mecucci C, Tiacci E, Alcalay M, Rosati R, Pasqualucci L, et al. Cytoplasmic Nucleophosmin in Acute Myelogenous Leukemia With a Normal Karyotype. *N. Engl J Med* (2005) 352:254–66. doi: 10.1056/NEJMoa041974
4. Falini B, Bolli N, Shan J, Martelli MP, Liso A, Pucciarini A, et al. Both Carboxy-Terminus NES Motif and Mutated Tryptophan(s) Are Crucial for Aberrant Nuclear Export of Nucleophosmin Leukemic Mutants in NPMc+ AML. *Blood* (2006) 107:4514–23. doi: 10.1182/blood-2005-11-4745
5. Suzuki T, Kiyoi H, Ozeki K, Tomita A, Yamaji S, Suzuki R, et al. Clinical Characteristics and Prognostic Implications of NPM1 Mutations in Acute Myeloid Leukemia. *Blood* (2005) 106:2854–61. doi: 10.1182/blood-2005-04-1733
6. Dohner K, Schlenk RF, Habdank M, Scholl C, Rucker FG, Corbacioglu A, et al. Mutant Nucleophosmin (NPM1) Predicts Favorable Prognosis in Younger Adults With Acute Myeloid Leukemia and Normal Cytogenetics: Interaction With Other Gene Mutations. *Blood* (2005) 106:3740–6. doi: 10.1182/blood-2005-05-2164
7. Schnittger S, Schoch C, Kern W, Mecucci C, Tschulik C, Martelli MF, et al. Nucleophosmin Gene Mutations Are Predictors of Favorable Prognosis in Acute Myelogenous Leukemia With a Normal Karyotype. *Blood* (2005) 106:3733–9. doi: 10.1182/blood-2005-06-2248
8. Loghavi S, Zuo Z, Ravandi F, Kantarjian HM, Bueso-Ramos C, Zhang L, et al. Clinical Features of De Novo Acute Myeloid Leukemia With Concurrent DNMT3A, FLT3 and NPM1 Mutations. *J Hematol Oncol* (2014) 7:74. doi: 10.1186/s13045-014-0074-4
9. Ivey A, Hills RK, Simpson MA, Jovanovic JV, Gilkes A, Grech A, et al. Assessment of Minimal Residual Disease in Standard-Risk AML. *N. Engl J Med* (2016) 374:422–33. doi: 10.1056/NEJMoa1507471
10. Dillon R, Hills R, Freeman S, Potter N, Jovanovic J, Ivey A, et al. Molecular MRD Status and Outcome After Transplantation in NPM1-Mutated AML. *Blood* (2020) 135:680–8. doi: 10.1182/blood.2019002959
11. Lachowiez CA, Loghavi S, Kadia TM, Daver N, Borthakur G, Pemmaraju N, et al. Outcomes of Older Patients With NPM1-Mutated AML: Current Treatments and the Promise of Venetoclax-Based Regimens. *Blood Adv* (2020) 4:1311–20. doi: 10.1182/bloodadvances.2019001267

12. Wei AH, Montesinos P, Ivanov V, DiNardo CD, Novak J, Laribi K, et al. Venetoclax Plus LDAC for Newly Diagnosed AML Ineligible for Intensive Chemotherapy: A Phase 3 Randomized Placebo-Controlled Trial. *Blood* (2020) 135:2137–45. doi: 10.1182/blood.2020004856
13. Tiong IS, Dillon R, Ivey A, Teh TC, Nguyen P, Cummings N, et al. Venetoclax Induces Rapid Elimination of NPM1 Mutant Measurable Residual Disease in Combination With Low-Intensity Chemotherapy in Acute Myeloid Leukaemia. *Br J Haematol.* (2021) 192:1026–30. doi: 10.1111/bjh.16722
14. Cocciardi S, Dolnik A, Kapp-Schwoerer S, Rucker FG, Lux S, Blatte TJ, et al. Clonal Evolution Patterns in Acute Myeloid Leukemia With NPM1 Mutation. *Nat Commun* (2019) 10:2031. doi: 10.1038/s41467-019-09745-2
15. Schnittger S, Kern W, Tschulik C, Weiss T, Dicker F, Falini B, et al. Minimal Residual Disease Levels Assessed by NPM1 Mutation-Specific RQ-PCR Provide Important Prognostic Information in AML. *Blood* (2009) 114:2220–31. doi: 10.1182/blood-2009-03-213389
16. Patel SS, Kuo FC, Gibson CJ, Steensma DP, Soiffer RJ, Alyea EP. 3rd, Et alHigh NPM1-Mutant Allele Burden at Diagnosis Predicts Unfavorable Outcomes in De Novo AML. *Blood* (2018) 131:2816–25. doi: 10.1182/blood-2018-01-828467
17. Patel SS, Pinkus GS, Ritterhouse LL, Segal JP, Dal Cin P, Restrepo T, et al. High NPM1 Mutant Allele Burden at Diagnosis Correlates With Minimal Residual Disease at First Remission in De Novo Acute Myeloid Leukemia. *Am J Hematol* (2019) 94:921–8. doi: 10.1002/ajh.25544
18. Linch DC, Hills RK, Burnett AK, Russell N, Gale RE. Analysis of the Clinical Impact of NPM1 Mutant Allele Burden in a Large Cohort of Younger Adult Patients With Acute Myeloid Leukaemia. *Br J Haematol.* (2020) 188:852–9. doi: 10.1111/bjh.16239
19. Tiong IS, Dillon R, Ivey A, Kok CH, Kuzich JA, Thiagarajah N, et al. The Natural History of NPM1MUT Measurable Residual Disease (MRD) Positivity After Completion of Chemotherapy in Acute Myeloid Leukemia (AML). *Blood* (2020) 136(Supplement 1):25–7. doi: 10.1182/blood-2020-140296
20. Forghieri F, Comoli P, Marasca R, Potenza L, Luppi M. Minimal/Measurable Residual Disease Monitoring in NPM1-Mutated Acute Myeloid Leukemia: A Clinical Viewpoint and Perspectives. *Int J Mol Sci* (2018) 19:3492. doi: 10.3390/ijms19113492
21. Schuurhuis GJ, Heuser M, Freeman S, Bene MC, Buccisano F, Cloos J, et al. Minimal/measurable Residual Disease in AML: A Consensus Document From the European LeukemiaNet MRD Working Party. *Blood* (2018) 131:1275–91. doi: 10.1182/blood-2017-09-801498
22. Gorello P, Cazzaniga G, Alberti F, Dell'Oro MG, Gottardi E, Specchia G, et al. Quantitative Assessment of Minimal Residual Disease in Acute Myeloid Leukemia Carrying Nucleophosmin (NPM1) Gene Mutations. *Leukemia* (2006) 20:1103–8. doi: 10.1038/sj.leu.2404149
23. Blombery P, Jones K, Doig K, Ryland G, McBean M, Thompson E, et al. Sensitive NPM1 Mutation Quantitation in Acute Myeloid Leukemia Using Ultradeep Next-Generation Sequencing in the Diagnostic Laboratory. *Arch Pathol Lab Med* (2018) 142:606–12. doi: 10.5858/arpa.2017-0229-OA
24. Ritterhouse LL, Parilla M, Zhen CJ, Wurst MN, Puranik R, Henderson CM, et al. Clinical Validation and Implementation of a Measurable Residual Disease Assay for NPM1 in Acute Myeloid Leukemia by Error-Corrected Next-Generation Sequencing. *Mol Diagn Ther* (2019) 23:791–802. doi: 10.1007/s40291-019-00436-8
25. Pasqualucci L, Liso A, Martelli MP, Bolli N, Pacini R, Tabarrini A, et al. Mutated Nucleophosmin Detects Clonal Multilineage Involvement in Acute Myeloid Leukemia: Impact on WHO Classification. *Blood* (2006) 108:4146–55. doi: 10.1182/blood-2006-06-026716
26. Patel SS, Lipschitz M, Pinkus GS, Weirather JL, Pozdnyakova O, Mason EF, et al. Multiparametric in Situ Imaging of NPM1-Mutated Acute Myeloid Leukemia Reveals Prognostically-Relevant Features of the Marrow Microenvironment. *Mod. Pathol* (2020) 33:1380–8. doi: 10.1038/s41379-020-0498-z
27. Racchumi J, Tam W, Kluk MJ. Clinical Laboratory Validation and Implementation of Quantitative, Real-Time PCR-Based Detection of NPM1 Type A Mutation. *Clin Lab* (2020) 66:2413–21. doi: 10.7754/Clin.Lab.2020.200104
28. van Dongen JJ, Lhermitte L, Bottcher S, Almeida J, van der Velden VH, Flores-Montero J, et al. EuroFlow Antibody Panels for Standardized N-Dimensional Flow Cytometric Immunophenotyping of Normal, Reactive and Malignant Leukocytes. *Leukemia* (2012) 26:1908–75. doi: 10.1038/leu.2012.120
29. Falini B, Brunetti L, Martelli MP. How I Diagnose and Treat NPM1-Mutated AML. *Blood* (2021) 137:589–99. doi: 10.1182/blood.2020008211
30. *Human Protein Atlas*. Available at: https://www.proteinatlas.org/ENSG00000181163-NPM1/tissue.
31. Uhlen M, Fagerberg L, Hallstrom BM, Lindskog C, Oksvold P, Mardinoglu A, et al. Proteomics. Tissue-Based Map of the Human Proteome. *Science* (2015) 347:394–403. doi: 10.1126/science.1260419
32. Bailey GD, Doolan L, Baskar A, Smith LC, Seedhouse CH. Preferential Transcription of the Mutated Allele in NPM1 Mutated Acute Myeloid Leukaemia. *Sci Rep* (2020) 10:17695. doi: 10.1038/s41598-020-73782-x
33. Mencia-Trinchant N, Hu Y, Alas MA, Ali F, Wouters BJ, Lee S, et al. Minimal Residual Disease Monitoring of Acute Myeloid Leukemia by Massively Multiplex Digital PCR in Patients With NPM1 Mutations. *J Mol Diagn* (2017) 19:537–48. doi: 10.1016/j.jmoldx.2017.03.005
34. Delsing Malmberg E, Johansson Alm S, Nicklasson M, Lazarevic V, Stahlman S, Samuelsson T, et al. Minimal Residual Disease Assessed With Deep Sequencing of NPM1 Mutations Predicts Relapse After Allogeneic Stem Cell Transplant in AML. *Leuk. Lymphoma* (2019) 60:409–17. doi: 10.1080/10428194.2018.1485910
35. Loghavi S, DiNardo CD, Furudate K, Takahashi K, Tanaka T, Short NJ, et al. Flow Cytometric Immunophenotypic Alterations of Persistent Clonal Haematopoiesis in Remission Bone Marrows of Patients With NPM1-Mutated Acute Myeloid Leukaemia. *Br J Haematol.* (2021) 192:1054–63. doi: 10.1111/bjh.17347
36. Falini B, Brunetti L, Sportoletti P, Martelli MP. NPM1-Mutated Acute Myeloid Leukemia: From Bench to Bedside. *Blood* (2020) 136:1707–21. doi: 10.1182/blood.2019004226

Conflict of Interest: The authors declare that the research was conducted in the absence of any commercial or financial relationships that could be construed as a potential conflict of interest.

Publisher's Note: All claims expressed in this article are solely those of the authors and do not necessarily represent those of their affiliated organizations, or those of the publisher, the editors and the reviewers. Any product that may be evaluated in this article, or claim that may be made by its manufacturer, is not guaranteed or endorsed by the publisher.

frontiers in Oncology

ORIGINAL RESEARCH
published: 30 August 2021
doi: 10.3389/fonc.2021.701492

High Counts of CD68+ and CD163+ Macrophages in Mantle Cell Lymphoma Are Associated With Inferior Prognosis

Philippa Li[1†], Ji Yuan[2,3†], Fahad Shabbir Ahmed[1,4], Austin McHenry[1], Kai Fu[3,5], Guohua Yu[3,6], Hongxia Cheng[3,7], Mina L. Xu[1], David L. Rimm[1] and Zenggang Pan[1]*

[1] Department of Pathology, Yale University School of Medicine, New Haven, CT, United States, [2] Department of Laboratory Medicine and Pathology, Mayo Clinic, Rochester, MN, United States, [3] Department of Pathology and Microbiology, University of Nebraska Medical Center, Omaha, NE, United States, [4] Department of Pathology, Wayne State University, Detroit, MI, United States, [5] Department of Pathology and Laboratory Medicine, Roswell Park Cancer Center, Buffalo, NY, United States, [6] Department of Pathology, Yantai Yuhuangding Hospital, Yantai, China, [7] Department of Pathology, Shandong Provincial Hospital Affiliated to Shandong First Medical University, Jinan, China

OPEN ACCESS

Edited by:
Shimin Hu,
University of Texas MD Anderson Cancer Center, United States

Reviewed by:
Shaoying Li,
University of Texas MD Anderson Cancer Center, United States
Madhu M. Ouseph,
Cornell University, United States

***Correspondence:**
Zenggang Pan
zenggang.pan@yale.edu

[†]These authors have contributed equally to this work

Specialty section:
This article was submitted to Hematologic Malignancies, a section of the journal Frontiers in Oncology

Received: *28 April 2021*
Accepted: *12 August 2021*
Published: *30 August 2021*

Citation:
Li P, Yuan J, Ahmed FS, McHenry A, Fu K, Yu G, Cheng H, Xu ML, Rimm DL and Pan Z (2021) High Counts of CD68+ and CD163+ Macrophages in Mantle Cell Lymphoma Are Associated With Inferior Prognosis. Front. Oncol. 11:701492. doi: 10.3389/fonc.2021.701492

Background: Lymphoma-associated macrophages (LAMs) are key components in the lymphoma microenvironment, which may impact disease progression and response to therapy. There are two major subtypes of LAMs, CD68+ M1 and CD163+ M2. M2 LAMs can be transformed from M1 LAMs, particularly in certain diffuse large B-cell lymphomas (DLBCL). While mantle cell lymphoma (MCL) is well-known to contain frequent epithelioid macrophages, LAM characterization within MCL has not been fully described. Herein we evaluate the immunophenotypic subclassification, the expression of immune checkpoint molecule PD-L1, and the prognostic impact of LAMs in MCL.

Materials and Methods: A total of 82 MCL cases were collected and a tissue microarray block was constructed. Immunohistochemical staining was performed using CD68 and CD163, and the positive cells were recorded manually in four representative 400× fields for each case. Multiplexed quantitative immunofluorescence assays were carried out to determine PD-L1 expression on CD68+ M1 LAMs and CD163+ M2 LAMs. In addition, we assessed Ki67 proliferation rate of MCL by an automated method using the QuPath digital imaging analysis. The cut-off points of optimal separation of overall survival (OS) were analyzed using the X-Tile software, the SPSS version 26 was used to construct survival curves, and the log-rank test was performed to calculate the *p*-values.

Results: MCL had a much higher count of M1 LAMs than M2 LAMs with a CD68:CD163 ratio of 3:1. Both M1 and M2 LAMs were increased in MCL cases with high Ki67 proliferation rates (>30%), in contrast to those with low Ki67 (<30%). Increased number of M1 or M2 LAMs in MCL was associated with an inferior OS. Moreover, high expression of PD-L1 on M1 LAMs had a slightly better OS than the cases with low PD-L1 expression, whereas low expression of PD-L1 on M2 LAMs had a slightly improved OS, although both were not statistically significant.

Conclusions: In contrast to DLBCL, MCL had a significantly lower rate of M1 to M2 polarization, and the high levels of M1 and M2 LAMs were associated with poor OS. Furthermore, differential PD-L1 expressions on LAMs may partially explain the different functions of tumor-suppressing or tumor-promoting of M1 and M2 LAMs, respectively.

Keywords: mantle cell lymphoma, lymphoma microenvironment, lymphoma associated macrophage, PD-L1, quantitative immunofluorescence analysis

INTRODUCTION

Mantle cell lymphoma (MCL) accounts for 5-6% of non-Hodgkin lymphomas, with characteristic expression of cyclin D1 due to *CCND1-IGH* gene rearrangement. MCL has a broad morphologic spectrum with variable architectural patterns and cytologic features, which are associated with heterogeneous clinical behaviors (1–3). Patients with MCL usually present at advanced stages with an aggressive clinical course. The long-term prognosis remains poor with a median overall survival of 3-5 years despite significant improvement in the management (4). On the other hand, ~15% cases of MCL demonstrate indolent clinical course with an overall survival of 7-10 years (5–7). Therefore, it is necessary to identify the different prognostic subgroups of MCL and allow for risk-adjusted therapeutic approaches.

In recent years, studies focusing on tumor microenvironment and associated immunotherapies have been increasingly pursued, particularly in solid tumors including breast cancer, lung cancer and melanoma. Some of the most widely studied biomarkers for immunotherapy are the programmed death-1 receptor (PD-1, CD279) and its ligands PD-L1 (CD274, B7-H1) and PD-L2 (CD273, PDCD1LG2, B7-DC), which are essential in many autoimmune and neoplastic conditions (8–11). Interactions between PD-1 and PD-L1/PD-L2 induce immune evasion of tumor cells, which can be reversed by restoring effector T-cell functions through targeted therapy against PD-1 or its ligands (12, 13). In the hematopoietic system, PD-L1 is expressed in antigen-presenting cells and activated T-cells (12). Certain types of B-cell lymphomas may express PD-L1, including classic Hodgkin lymphoma (CHL), nodular lymphocyte-predominant Hodgkin lymphoma (NLPHL), and some diffuse large B-cell lymphoma (DLBCL) subtypes (14). Immunotherapies with PD-1 or PD-L1 blockade have shown clinical responses in these lymphomas (15).

Relatively few studies have assessed MCL immune microenvironment. In MCL, the lymphoma cells and microenvironment are thought to have low expression of PD-L1 (14, 16); however, it is not certain whether PD-L1 expression has any significance in clinical therapy and survival. In addition, immunotherapy in MCL has not provided desirable results. PD-L1 expression on MCL cells may induce suppression of anti-tumor immune responses. Therefore targeting PD-L1 on tumor cells may represent a novel approach to improve the efficacy of immunotherapy (17). Consequently, immunotherapy may be feasible in treating MCL and preventing lymphoma relapse.

Macrophages represent an essential component of tumor microenvironment, and a variable number of macrophages have been found in association with nearly all lymphoma types, which are referred as lymphoma-associated macrophages (LAMs) (18, 19). MCL is well-known for the presence of epithelioid histiocytes without phagocytic activities, so called "pink histiocytes" by many pathologists. LAMs have been divided into two major subtypes based on their immunophenotype, M1 and M2. Their functions are thought to be variable among different lymphoma types. M1 LAMs are considered to prevent the growth of tumors, whereas M2 LAMs are associated with angiogenesis and tumor progression (20). The presence of a high number of LAMs has been associated with aggressive clinical course in CHL, DLBCL, follicular lymphoma (FL) and angioimmunoblastic T-cell lymphoma (AITL) (18, 19, 21, 22). However, the significance of LAMs in MCL has not been fully characterized (18). Only a few studies have linked macrophage number with the prognosis of MCL, and the data on functional roles for LAMs in MCL are limited. Therefore, further studies are necessary to explore the characteristics and biological functions of LAMs in MCL. In this study, we investigated the number, subtype, and PD-L1 expression of LAMs in MCL and assessed their prognostic impact.

MATERIALS AND METHODS

Case Selection and Data Collection

The pathology archives from two institutions (Yale University and University of Nebraska Medical Center) were retrospectively searched to identify cases of MCL from 2000 to 2019 after approval from local institutional review board (IRB# 2000023891). No individual patient consent was required. Diagnosis of MCL was based on the following major criteria: 1) Morphology: small cell, classic, and blastoid variants (blastic and pleomorphic); diffuse and nodular growth patterns; 2) Immunophenotype, particularly expression of CD5, cyclin D1, and SOX11; and 3) Molecular genetic studies for *CCND1* rearrangement if necessary. The major inclusion criteria of case selection included: 1) All *de novo* cases without prior treatment; 2) Locations: lymph node, gastrointestinal tract, spleen, and other solid organs; 3) Sufficient clinical data availability, including clinical information at diagnosis, treatment plans, follow-up, and survival data; and 4) Excisional or large biopsies. The exclusion criteria included: 1) *In-situ* mantle cell neoplasm, and MCL with mantle zone growth pattern; 2) Core biopsy, bone marrow biopsy, and decalcified specimens; 3) Suboptimal specimens with inadequate fixation, poor processing, or marked crush artifacts; 4) Inadequate remaining tissue in paraffin blocks; and 5) Insufficient clinical or pathology data.

The essential clinical information of each patient was collected, including age, gender, biopsy site(s), extent of disease by imaging studies, bone marrow biopsy results, clinical stage and status (ECOG and sMIPI), treatment regimens, responses, and outcomes. For all eligible cases, the pathology reports, H&E slides, and immunohistochemical slides were reviewed to confirm the diagnosis, in conjunction with flow cytometric results, molecular assays, and cytogenetic studies. The detailed clinical and pathologic characteristics are summarized in **Supplementary Tables 1, 2**.

Construction of Tissue Microarray

A total of 82 eligible MCL cases were included in the study, and the formalin-fixed paraffin embedded (FFPE) tissue from each case was collected for tissue microarray (TMA). The H&E slides were reviewed to select the paraffin blocks with adequate tumor tissue for TMA construction. For each case, the lymphoma tissue was punched in duplicate (1.0 mm in diameter) and separately plated into one TMA block.

Immunohistochemical Stains and Manual Evaluation

The TMA block was sectioned at 4.0 um thick. Immunohistochemical staining was performed on the sections according to the manufacture's manual. The antibodies used in this study included CD68 (Clone PG-M1; DAKO, Carpinteria, CA, USA), CD163 (Clone 10D6; Abcam, Cambridge, MA, USA), cyclin D1 (Clone SP4; Cell Marque, Rocklin, California), and SOX11 (Clone MRQ-58; Cell Marque). The immunostains were performed on a Ventana Benchmark Ultra immunostainer (Ventana Medical Systems, Tucson, AZ, USA), with appropriate positive and negative controls. Immunohistochemical stains for CD68 and CD163 were evaluated in a quantitative method by recording positive cells manually in four representative 400× fields on the two 1.0 mm cores of each case.

QuPath Digital Image Analysis

The immunostained slide for Ki67 (Clone MIB1; DAKO) was scanned using the Aperio ScanScope CS2 platform (Leica Biosystems, Inc., Buffalo Grove, IL, USA). The slide was scanned at 200× with a pixel size of 0.4986 μm × 0.4986 μm, which was analyzed using the QuPath software (https://qupath.github.io) to quantitatively calculate the Ki67 proliferative rate of the positive cells over all nucleated cells.

Multiplexed Quantitative Immunofluorescence Assays

The TMA sections were briefly deparaffinized, followed by antigen retrieval at 97°C with pH 8.0 EDTA buffer for 20 minutes using PT module epitope retrieval solutions (Lab Vision, Waltham, MA, USA). Subsequently, a 30-minute incubation in 2.5% hydrogen peroxide was performed to block endogenous peroxidases and then unspecific antigens were blocked using a 0.3% BSA for 30 minutes. A multiplexed immunofluorescence staining was performed with three primary antibodies, including CD68 (Clone PG-M1; 1:200; DAKO), CD163 (Clone 10D6; 1:7500; Abcam), and PD-L1 (Clone SP142; 1:800; Abcam) on the same tissue section. Horseradish peroxidases (HRP)-conjugated secondary antibodies specific to each primary antibody isotype were used sequentially (anti-mouse IgG1, 1:100, eBioscience; anti-rabbit EnVision, DAKO; anti-mouse IgG3, 1:1,000, Abcam). Tyramide-bound fluorophores were added after each secondary antibody to bind to the HRPs. Specifically, Cyanine 7 tyramide (Cy7), cyanine 3 tyramide (CY3) tyramide, and cyanine 5 tyramide (Cy5) were used for CD68, CD163 and PD-L1, respectively. Finally, the nuclei were stained with 4,6-diamidino-2-phenylin-dole (DAPI). Quantitative immunofluorescence assays were performed on the Vectra Polaris (Perkin Elmer, Inc., Waltham, MA, USA) automated fluorescence microscopy platforms. The resultant images were analyzed and quantified using the InForm Software (Perkin Elmer) on all tumor spots as described previously (23).

Statistical Analysis

The cut-off points of optimal separation of overall survival were analyzed using the X-Tile software (24), the SPSS version 26 (IBM, Armonk, New York, USA) was used to construct survival curves, and the log-rank test was performed to calculate the *p*-values.

RESULTS

Clinical and Pathology Characteristics

The clinical and pathology data of the 82 patients with MCL are briefly summarized in **Table 1**, and the detailed clinicopathologic characteristics are depicted in **Supplementary Tables 1, 2**. There was a male predominance with a male to female ratio of ~3:1, and the median age at diagnosis was 67 years (range, 37 to 92 years). Thirty percent (22/74) of patients had documented systemic

TABLE 1 | Summary of the clinicopathologic data of the 82 patients with MCL.

Total case number	**82**
Median Age (Years)	67 (37-92)
Male/Female	61/21
B-Symptoms	22/74 (30%)
BM Involvement	48/59 (81%)
Advanced Clinical Stages (III/IV)	67/70 (96%)
sMIPI Risk	
Low	18/50 (36%)
Intermediate	22/50 (44%)
High	10/50 (20%)
Immunohistochemical Stains	
CD20	53/53 (100%)
CD5	45/50 (90%)
CD23	0/14 (0%)
Cyclin D1	79/80 (99%)
SOX11	69/79 (87%)
CD10	2/29 (7%)
BCL6	0/21 (0%)
CCND1 FISH	28/32 (88%)
Treatment	
Chemo- and/or Radio-Therapy	67/75 (87%)
Watchful Waiting	8/75 (13%)
Reponses to Treatment	
Complete Remission	38/63 (60%)
Partial Response	13/63 (21%)
Persistent or Progressive	12/63 (19%)
Stem Cell Transplant	24/68 (35%)
Follow Up (Median, Months)	36 (1-221)
Outcome (Deceased)	46/81 (57%)

symptoms, including fatigue, fever, and weight loss. Bone marrow involvement was detected in 81% (48/59) of patients. The majority (67/70; 96%) of patients presented at high clinical stages (III/IV). Fifty cases had sufficient data to calculate the sMIPI score, of which 18 (36%) cases were classified as low risk, 22 (44%) intermediate risk, and 10 (20%) high risk.

Of the 75 patients with clinical treatment information, 67 (87%) received chemotherapy and/or radiotherapy, and the remaining eight (13%) were under observation with no therapy. Sixty-three patients had treatment responses available; 38 patients (60%) achieved a complete remission, 13 (21%) yielded a partial response, and 12 (19%) had persistent or progressive disease. Following chemotherapy, 24/68 (35%) of patients received allogeneic hematopoietic stem cell transplant. Eight-one patients were followed up clinically with a median duration of 36 months (range 1-221 months), and 46 (57%) had died.

On the TMA block, each MCL case had two separate 1.0 mm cores with representative lymphoma tissue (**Figure 1A**). A variable number of epithelioid histiocytes were present admixed with tumor cells (**Figure 1B**). The vast majority of the MCL cases were positive for CD5 (45/50, 90%), cyclin D1 (79/80, 99%), and SOX11 (69/79, 87%); one case (case #60) was negative for both cyclin D1 and SOX11 without *CCND1* FISH data, which was excluded from further assays. Only two of 29 cases (7%) expressed CD10. BCL6 and CD23 were negative in 21 and 14 cases tested, respectively. FISH studies for *CCND1* rearrangement were performed in 32 cases, of which 28 (88%) cases were positive.

Manual Counts of CD68+ and CD163+ Macrophages and Overall Survival

Immunohistochemical stains for CD68 and CD163 were performed on the TMA sections (**Figures 1C, D**), and the number of positive cells were recorded manually by a pathologist on four representative 400× fields for each case. A total of 73 MCLs were included in this assay after excluding nine cases with suboptimal staining or insufficient tissue. The average count for CD68+ cells was 170 (range 29-493) and CD163+ cells was 57 (range 0-519) (**Figures 2A, B**). The CD68+ macrophages were present in higher numbers than the CD163+ macrophages with an overall CD68:CD163 ratio of 3:1. In addition, CD163+ macrophages had a broader range and more frequent low counts.

The overall survival (OS) of the 73 MCL patients was calculated based on the CD68+ or CD163+ macrophages using the Kaplan-Meier analysis. The CD68+ macrophage cut-off was set to the median (50%) by X-Tile. The 50% of cases with lower CD68+ counts (n=36) had a significantly better OS than those 50% with higher counts (n=37) (**Figure 2C**). The CD163+ macrophage optimal cut-off was set to 90% by X-Tile, and the 90% of cases with lower (n=66) CD163+ macrophages had a better OS than the higher 10% (n=7) (**Figure 2D**).

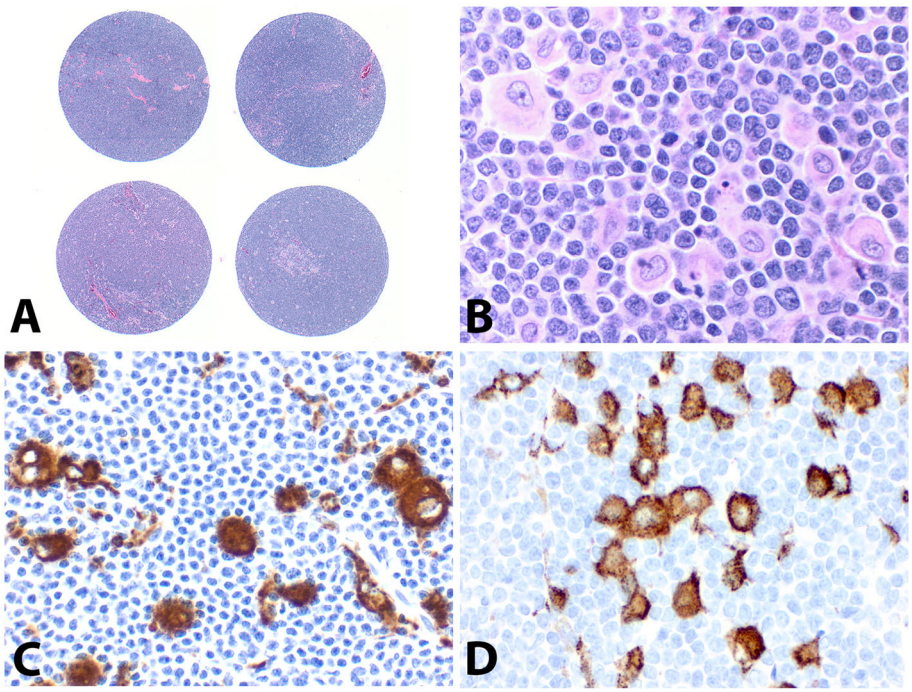

FIGURE 1 | Construction of tissue microarray (TMA) and immunostains of CD68 and CD163. **(A)** Each MCL case had two separate 1.0 mm cores on the TMA (H&E, original magnification ×20). **(B)** Scattered epithelioid histiocytes admixed with abundant lymphoma cells (H&E, ×400), which were highlighted by immunostains with CD68 (**C**, ×400) and CD163 (**D**, ×400).

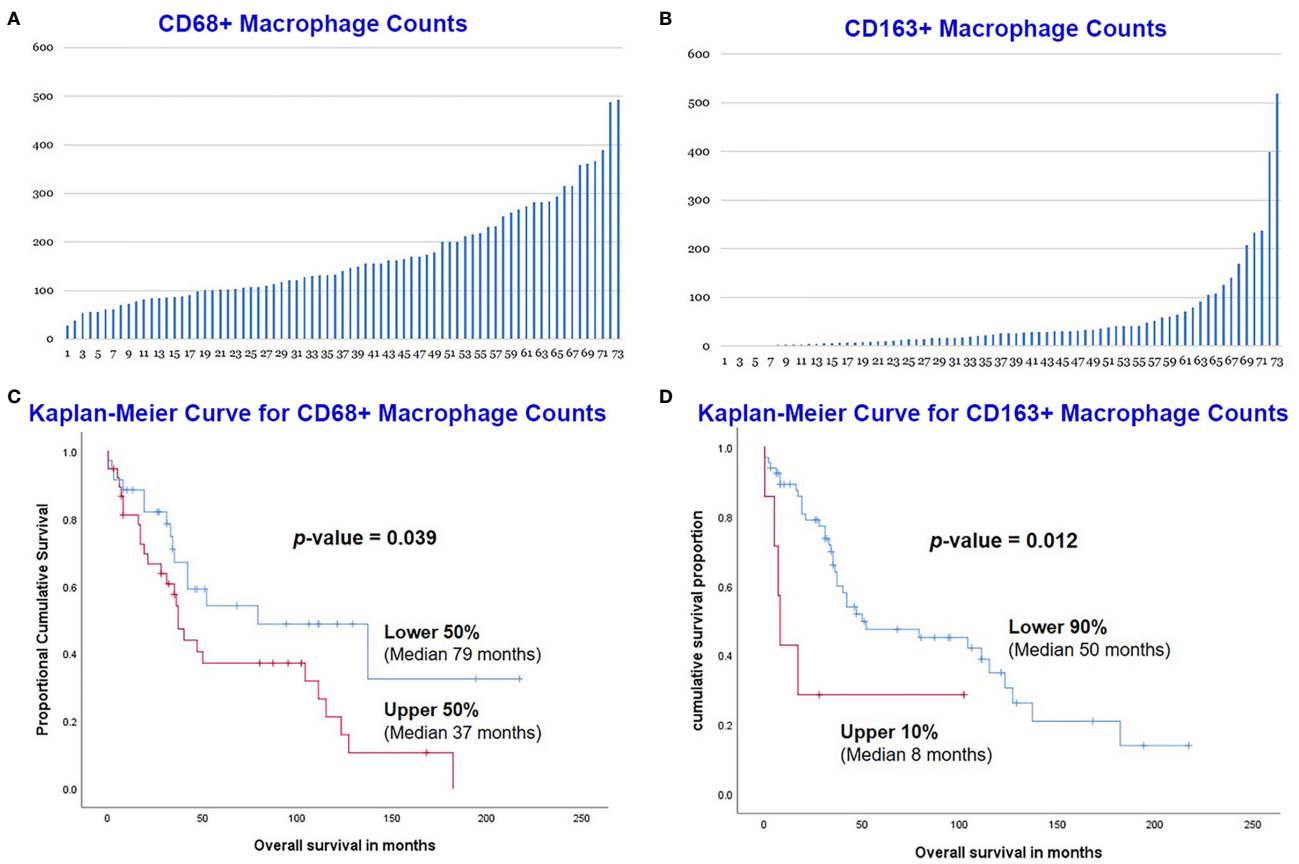

FIGURE 2 | Manual count of CD68+ macrophages **(A)** and CD163+ macrophages **(B)** in the 73 MCL cases. MCL with lower CD68+ counts had a better overall survival (OS) than those with higher counts **(C)**. The lower count of CD163+ macrophage also predicted an improved OS **(D)**.

CD68, CD163, and PD-L1 Expression With Multiplexed Quantitative Immunofluorescence Analysis and Overall Survival

Expression of CD68, CD163, and PD-L1 was assessed on the TMA section with multiplexed quantitative immunofluorescence analysis, and the PD-L1 expression was co-localized with either CD68 or CD163 (**Figures 3A–J**). A total of 73 MCLs were included in this assay after excluding nine cases with poor staining or insufficient tissue.

The optimal cut-off for survival curve of CD68 expression was set to 90% by X-Tile, and the 90% of cases with lower expression of CD68 (n=66) had a significantly better OS than the higher 10% (n=7) (p=0.002) (**Figure 4A**). Similarly, the optimal cut-off of CD163 expression was set to 80% by X-Tile, and the 80% of cases with lower expression of CD163 (n=57) had a significantly better OS than the higher 20% (n=16) (p=0.001) (**Figure 4B**).

For PD-L1 expression on CD68+ macrophages, the optimal cut-off for survival curve was set to 65% by X-Tile, and the 65% of cases (n=47) with higher expression of PD-L1 on CD68+ cells had a slightly better OS than the lower 35% (n=26) but it did not reach statistical significance (p=0.097) (**Figure 4C**). Expression of PD-L1 on CD163+ macrophages was measured and the optimal cut-off for survival curve was set to 80% by X-Tile; the 80% of cases (n=57) with lower expression of PD-L1 on CD163+ cells had a slightly better OS than the higher 20% (n=16) but it was not statistically significant (p=0.120) (**Figure 4D**).

Assessment of Ki67 Proliferation Index With Digital Image Analysis

A total of 69 MCLs had adequate tissue on the Ki67 stained TMA slide. These 69 patients included 52 males and 17 females, with a median age of 68 years (range 37-92). The median survival was 35 months (range 1-213). The TMA slide stained with Ki67 was scanned using the Aperio scanner and then analyzed using the QuPath program to count the positive cells (**Figures 5A–D**). For each case, the Ki67 proliferation index was assessed using the Ki67-positive cells over all cells in the cores, and an average percentage was calculated from the two cores (**Figure 5E**).

The optimal cut-off point for the Ki67 proliferation index was 31.9% using X-Tile, which was very close to the 30% cut-off in the clinical practice. Therefore, we adopted the same cutoff of 30% for comparison of OS. Most of the cases (61/69, 88%) had a Ki67 proliferation rate of <30%, while the remain 8 cases (12%)

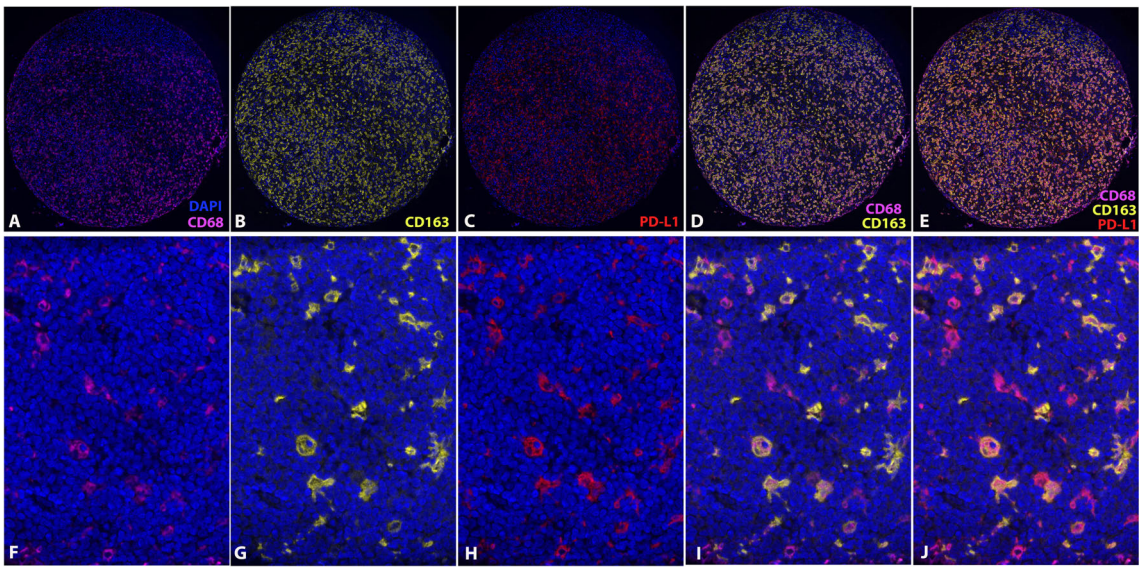

FIGURE 3 | Multiplexed quantitative immunofluorescence analysis. Immunofluorescence stains of CD68 **(A, F)**, CD163 **(B, G)**, and PD-L1 **(C, H)**. Overlying of CD68 and CD163 **(D, I)**. Overlying of CD68, CD163 and PD-L1 **(E, J)**. (DAPI, counterstaining of nuclei; CD68, Cy7; CD163, Cy3; PD-L1, Cy5).

>30%. In our study, the patients with lower Ki67 proliferation index of <30% had a median survival of 52 months, which was significantly better than those >30% (median survival 8 months; p=0.021) (**Figure 5F**).

The MCL cases with high Ki67 (>30%) had a significantly higher count of CD68+ M1 LAMs than the cases with low Ki67 (<30%) (p=0.018). CD163+ M2 LAMs were also increased in the high Ki67 cases than in the low Ki67 group albeit it was not statistically significant (p=0.17).

DISCUSSION

The studies on lymphoma microenvironment (LME) have been markedly increased in recently years, which provided better understanding of the interactions between the neoplastic cells and the supporting cells. In particular, immunotherapies to modulate the signals between the tumor cells and the microenvironmental components have shown promising results in treating lymphomas. This study utilized quantitative imaging analysis on TMA sections to evaluate LAMs and Ki67 proliferation index in MCL. Our findings demonstrated that an increase in CD68+ M1 LAMs or CD163+ M2 LAMs was associated with inferior prognosis in MCL. In addition, M1 LAMs were present in higher numbers than M2 LAMs, indicating that MCL had a lower rate of M1 to M2 polarization in contrast to DLBCL. Both M1 and M2 LAMs were increased in the MCL cases with high Ki67 (>30%), compared to the Ki67 low group (<30%). Furthermore, the M2 LAM counts had a broader range and more frequent low counts, suggesting increased heterogeneity of the M2 microenvironment.

Using multiplexed quantitative immunofluorescence assays, we found that high expression of PD-L1 on M1 LAMs was associated with a slightly improved OS, whereas increased PD-L1 expression on M2 LAMs predicted a slightly inferior OS, although both did not reach statistical significance. Finally, our studies also showed that QuPath DIA is a very promising tool to measure Ki67 proliferation index in MCL, and it accurately separated the patient groups with significantly different OS, which is very close to the 30% cut-off in the clinical practice. Further studies are necessary with large cohorts to validate this assay.

LME consists of variable numbers of immune cells (reactive B-cells, T-cells, macrophages, natural killer cells, and granulocytes), stromal cells, blood vessels, and extracellular matrix (19, 21, 21, 25, 26). The LME influences the behavior of lymphoma, providing a protective niche for neoplastic cells and facilitating tumor cell proliferation and survival. Meanwhile, lymphoma cells recruit and activate the LME cells. The collaborative interactions between lymphoma cells and LME cells enable and sustain tumor cell growth, anti-apoptosis, immunosuppression, angiogenesis, chemoresistance, cell homing and metastasis, and disease progression.

Exploration of the LME has escalated in recent years, particularly with regard to CHL and DLBCL. Similar to other B-cell lymphomas, extrinsic signaling is believed to favor MCL growth, survival, and migration. CD3+, CD8+, and particularly CD4+ T-cells are increased in indolent MCL but decrease with more aggressive histology. A high CD4:CD8 ratio correlates independently from other high-risk prognostic factors with longer OS, suggesting a prognostic role for T-cells in MCL (27). However, studies on the LME cells, soluble factors, intercellular interactions, and intracellular regulations in MCL are limited (18). Therefore, further studies are necessary to integrate the key roles of the LME cells, uncover the mechanisms of the interactions between lymphoma cells and LME, provide more effective treatment, and predict response to therapy and overall survival.

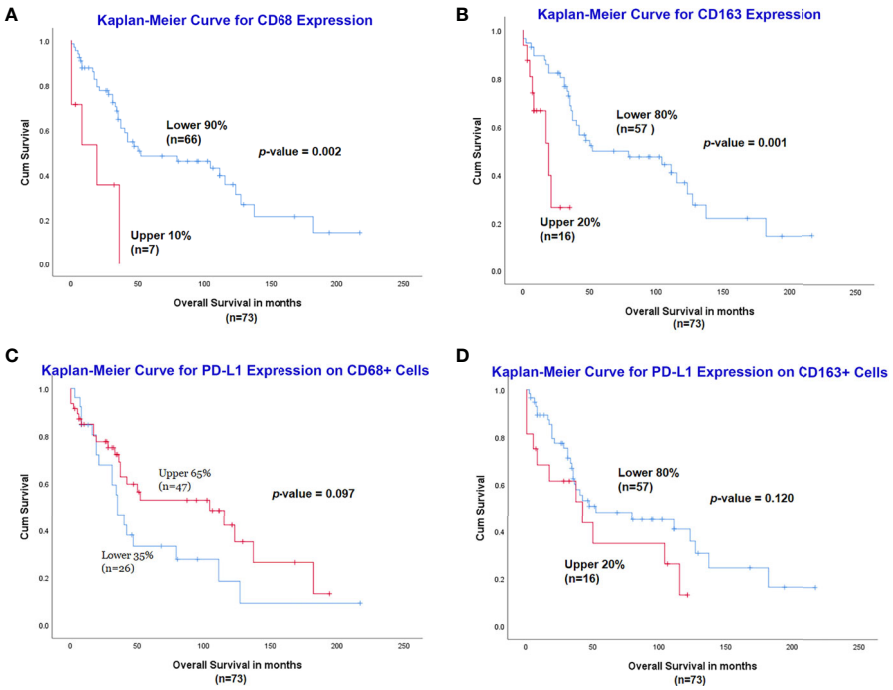

FIGURE 4 | Assessment of CD68, CD163 and PD-L1 expression with multiplexed quantitative immunofluorescence analysis. Lower expression of CD68 **(A)** and CD163 **(B)** was associated with a significantly better outcome. Increased expression of PD-L1 on CD68+ cells had a slightly better OS **(C)**, while the high expression of PD-L1 on CD163+ cells was related to inferior prognosis **(D)**, although both were not statistically significant.

Variable numbers of macrophages are present in nearly all lymphoma types, including CHL, NLPHL, T-cell lymphoma, and low-grade or high-grade B-cell non-Hodgkin lymphoma. These macrophages can be sparsely distributed, form small loose clusters, or become so abundant as to form granulomas and even obscure lymphoma cells. They are referred to as lymphoma associated macrophages (LAMs), which are composed of different biologic subtypes. Furthermore, they can shift their functional phenotypes depending on signals generated from lymphoma and stromal cells, a process known as polarization of LAMs (18, 22, 28). Currently, there are two major subtypes of LAMs, CD68+ M1 and CD163+ M2 LAMs (18, 20, 22, 29–31). M1 LAMs are considered to be tumor-suppressing or classically activated macrophages, and they are mainly involved in inflammatory responses and antitumoral defense by producing various activated lytic enzymes, reactive oxygen species, and inflammation-promoting chemokines. M2 LAMs are known as tumor-promoting, polarized, or alternatively activated macrophages. M2 LAMs secrete key chemokines, cytokines, and bioactive proteases, which can stimulate lymphoma cell growth, angiogenesis, metastasis, chemoresistance, and immunosuppression. In particular, M2 LAMs express checkpoint molecules, including PD1 and PD-L1, which are key immunotherapeutic targets for specific checkpoint-blocking immunotherapies (anti-PD-1/PDL-1). The tumor-promoting M2 LAMs can be induced under the influence of the cytokines (IL-4, IL-13, IL-10 and M-CSF) produced by the lymphoma cells and the microenvironment. Lymphomas may be able to escape the immune surveillance by recruiting and polarizing M1 LAMs to M2 LAMs that highly express immune checkpoint molecules, such as PD-L1 and PD-L2 (20, 22, 30–32).

The presence of LAMs in different lymphoma types may be associated with different outcomes. A high level of macrophages in CHL correlated with EBV-positivity, advanced stage, and inferior prognosis (33). However, in primary testicular DLBCL, high PD-L1+ LAM content predicted favorable survival (34). Primary cutaneous DLBCL, leg type, and nodal DLBCL had a significantly higher level of M2 LAMs than M1 LAMs, which contributed to the poor prognosis (35, 36). According to the studies from Poles et al., EBV-positive DLBCL showed a significant elevated M2 polarization with a higher CD163/CD68 ratio (median value 1.24), compared to EBV-negative DLBCL cohort (median value 0.14) (37). Furthermore, in EBV-negative DLBCL, the CD163/CD68 ratio was higher among advanced-staged/high-tumor burden disease (37). In our study, the overall ratio of CD163:CD68 is 1:3, indicating a lower M2 polarization, in contrast to DLBCL. In addition, the MCL cases with high Ki67 proliferation rates (>30%) contained increased M1 and M2 LAMs, compared to the Ki67 low group (<30%).

One of the most widely studied pathways for immunotherapy is the PD-l and its ligands PD-L1 and PD-L2, which play a critical role in a variety of autoimmune and neoplastic conditions (8–11). PD-1 is expressed on the activated T-cells and B-cells, follicular helper T-cells, dendritic cells, and monocytes/macrophages, while PD-L1 is detected on monocytes/macrophages, dendritic cells, and regulatory T-cells. Many solid tumors (carcinoma and melanoma) and Hodgkin lymphomas express PD-L1. In contrast,

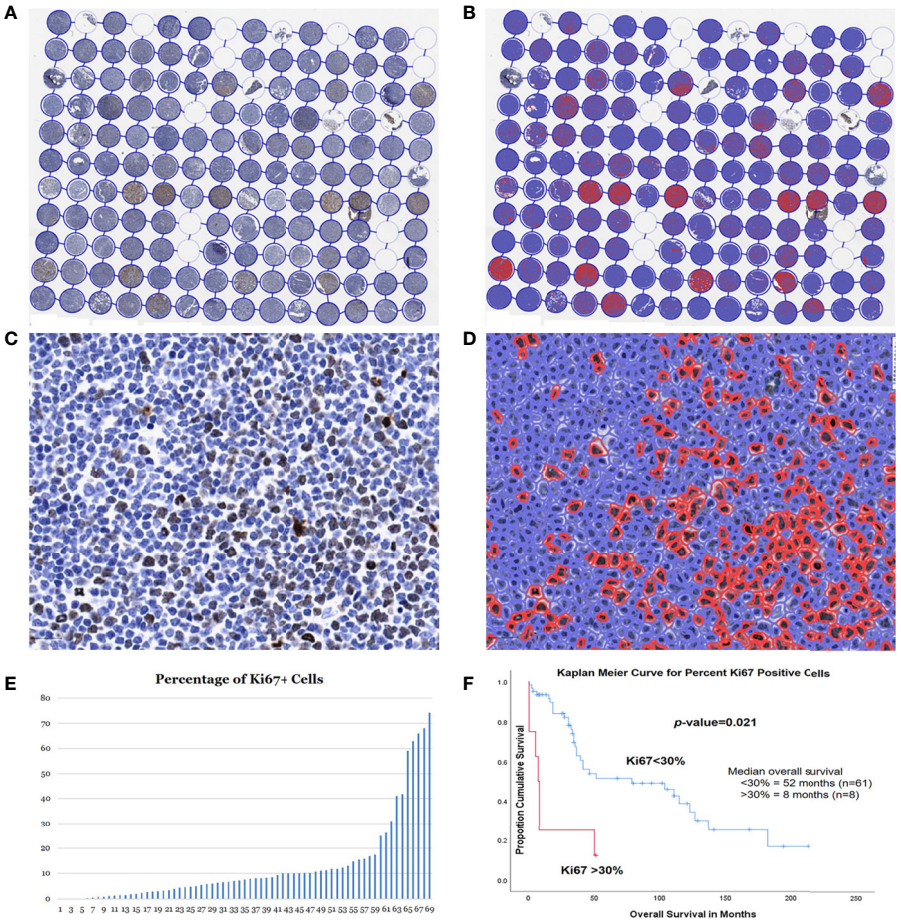

FIGURE 5 | Assessment of Ki67 proliferation rates using QuPath DIA. Whole TMA image with Ki67 immunostain before **(A)** and after **(B)** cell detection and positive cell detection. High magnification of a case before **(C)** and after **(D)** cell detection and positive cell detection. **(E)** Dynamic percentage range of Ki67 proliferation rates of the 73 MCL cases. **(F)** Kaplan-Meier curves for optimal cut-point for patients with high (>30%) *vs*. low (<30%) Ki67 proliferation rates.

PD-L1 is only rarely expressed by non-Hodgkin lymphomas, except some DLBCLs and virus-associated lymphomas. The interaction between PD-1 and PD-L1 reduces T-cell proliferation and cytokine release, inhibits survival proteins, and therefore results in apoptosis. Immune checkpoint inhibitors, such as anti-PD-1 antibody, bind to the PD-1 on activated cytotoxic T-cells, thus stimulating their proliferative capacity and enabling the immune system to resume recognizing, attacking, and destroying tumor cells. This may be one reason that PD-1 inhibition in DLBCL has been effective when directed at specific subtypes, including primary mediastinal large B-cell lymphoma, T-cell/histiocyte-rich large B-cell lymphoma, and EBV-positive lymphoma (15, 16, 36, 38–41). Especially, PD-1 blockade with nivolumab in relapsed and/or refractory CHL has revealed robust response rates as high as 87% (42).

Through multiplex quantitative immunofluorescence analysis, we demonstrated that higher expression of PD-L1 in CD163+ M2 LAMs had a slightly worse OS, whereas higher expression of PD-L1 in CD68+ M1 LAMs was associated with a slightly better OS, although both did not reach statistical significance. These findings suggested that the tumor-suppressing functions in M1 LAMs and tumor-promoting functions in M2 LAMs are at least partially attributed to the expression of PD-L1 in these two subtypes. Studies have shown that PD-L1 expressed on MCL was able to inhibit T-cell proliferation induced by the tumor cells, impair the generation of antigen-specific T-cell responses, and render MCL cells resistant to T-cell-mediated cytolysis (17). In addition, blocking or knocking down PD-L1 on MCL cells enhanced T-cell responses and restored tumor-cell sensitivity to T-cell-mediated killing *in vitro* and *in vivo* (17). Moreover, knocking down PD-L1 on MCL cells primed more CD4+ or CD8+ memory effector T cells. Therefore, it might be beneficial to include checkpoint-blocking immunotherapies for aggressive, relapsed or chemo-resistant MCLs, particularly in those cases with high PD-L1 expression on neoplastic cells and M2 LAMs.

In a recently published study using syngeneic MCL cells and xenografted human MCL cell lines in the mouse models, Le et al. confirmed the presence of polarized M1 and M2 TAMs in the MCL tumors *in vivo*. They also demonstrated that MCL cells can differentiate TAM toward a M2-like phenotype and particularly M2 but not M1 TAMs favor MCL cell growth and tumorigenesis *via*

STAT1 signaling by secretion of IL-10 (43). In another study, through coculture of MCL cells and monocytes, Papin et al. showed that MCL polarized monocytes into M2-like macrophages through secretion of CSF1 and, to a lesser extent, IL-10, which in turn promoted lymphoma survival and proliferation (44). These studies explored molecular level of the dynamic interactions between MCL cells and TAMs in the lymphoma microenvironment.

In our study, we also assessed the Ki67 proliferation rates of MCL by an automated method using the QuPath DIA. The Ki67 immunostaining is commonly utilized to assess the proliferation index of MCL (cut-off at 30%). The Ki67 proliferation index is a prognostic biomarker independent of sMIPI score and predicts survival in patients receiving chemotherapy and autologous stem cell transplant; a low Ki67 correlates with a more indolent form of MCL. However, it may be difficult to accurately assess the Ki67 proliferation rate, since the current "eyeballing" method has a high inter-observer variability and often results in over-estimation.

Automated immunohistochemical scoring by computerized image analysis (CIA) enables accurate and reproducible scores by circumventing the poor reproducibility of manual scoring. The automated scoring system also provides extensive evaluation of relevant cutoff points, taking advantage of the continuous scale quantification compared to the categorical measurement of manual scoring. In our study, the QuPath DIA accurately separated the patient groups with significantly different OS, and the optimal cut-off point for the Ki67 proliferation index was 31.9%, which was very close to the 30% cut-off in the clinical practice. Therefore, QuPath DIA is a very promising tool to measure Ki67 proliferation index in MCL. Further studies may be necessary with large cohorts to validate this assay, which may potentially be applied for future practice.

Taken together, we utilized the complexed quantitative fluorescence imaging analysis with automated whole-slide imaging and integrated whole-slide image analysis in our studies. These techniques enabled simultaneous detection and automatic quantification of multiple markers on TMA sections constructed from formalin-fixed paraffin-embedded tissues. However, our studies are limited by the small number of MCL cases in the different cohorts and the heterogeneity of treatments.

CONCLUSIONS

M1 and M2 LAM counts may serve as a fast and affordable tool to stratify MCL patients into risk groups. MCL had a significantly lower rate of M1 to M2 polarization, and the high levels of M1 and M2 LAMs were associated with poor OS. However, high expression of PD-L1 on M1 and M2 LAMs may have different impacts on MCL outcomes, which requires further studies with larger cohorts and more in-depth assessment of LAMs.

AUTHOR'S NOTE

The content of this manuscript has been presented in part as abstracts at the United States and Canadian Academy of Pathology (USCAP) Annual Meetings, 02/28/2020-03/05/2020, Los Angeles, CA. (Abstracts #1319 and #1415) [Abstracts from USCAP 2020: Hematopathology. Mod Pathol 33, 1409–1586 (2020)].

DATA AVAILABILITY STATEMENT

The original contributions presented in the study are included in the article/**Supplementary Material**. Further inquiries can be directed to the corresponding author.

AUTHOR CONTRIBUTIONS

ZP designed the study, collected and analyzed the data, and wrote the paper. PL collected and analyzed the data, performed the assays, and revised the manuscript. JY designed the study, collected and analyzed the data, and revised the manuscript. FA performed the assays and analyzed the data. AM analyzed the data and revised the manuscript. KF, GY, and HC collected the data. MX designed the study and revised the manuscript. DR designed the study. All authors contributed to the article and approved the submitted version.

ACKNOWLEDGMENTS

The authors would like to thank Dr. Rimm's lab for providing reagents, equipment, and technical supports for this study. The authors also acknowledge Yale Pathology Tissue Services for assistance in tissue retrieval, handling and staining as well as all researchers and study participants for their contributions.

SUPPLEMENTARY MATERIAL

The Supplementary Material for this article can be found online at: https://www.frontiersin.org/articles/10.3389/fonc.2021.701492/full#supplementary-material

REFERENCES

1. Ott G, Kalla J, Hanke A, Muller JG, Rosenwald A, Katzenberger T, et al. The Cytomorphological Spectrum of Mantle Cell Lymphoma Is Reflected by Distinct Biological Features. *Leuk Lymphoma* (1998) 32:55–63. doi: 10.3109/10428199809059246
2. Tiemann M, Schrader C, Klapper W, Dreyling MH, Campo E, Norton A, et al. Histopathology, Cell Proliferation Indices and Clinical Outcome in 304 Patients With Mantle Cell Lymphoma (MCL): A Clinicopathological Study From the European MCL Network. *Br J Haematol* (2005) 131:29–38. doi: 10.1111/j.1365-2141.2005.05716.x
3. Klapper W. Histopathology of Mantle Cell Lymphoma. *Semin Hematol* (2011) 48:148–54. doi: 10.1053/j.seminhematol.2011.03.006
4. Abrahamsson A, Albertsson-Lindblad A, Brown PN, Baumgartner-Wennerholm S, Pedersen LM, D'Amore F, et al. Real World Data on Primary Treatment for Mantle Cell Lymphoma: A Nordic Lymphoma

Group Observational Study. *Blood* (2014) 124:1288–95. doi: 10.1182/blood-2014-03-559930
5. Carvajal-Cuenca A, Sua LF, Silva NM, Pittaluga S, Royo C, Song JY, et al. *In Situ* Mantle Cell Lymphoma: Clinical Implications of an Incidental Finding With Indolent Clinical Behavior. *Haematologica* (2012) 97:270–8. doi: 10.3324/haematol.2011.052621
6. Hsi ED, Martin P. Indolent Mantle Cell Lymphoma. *Leuk Lymphoma* (2014) 55:761–7. doi: 10.3109/10428194.2013.815353
7. Hsu P, Yang T, Sheikh-Fayyaz S, Brody J, Bandovic J, Roy S, et al. Mantle Cell Lymphoma With *In Situ* or Mantle Zone Growth Pattern: A Study of Five Cases and Review of Literature. *Int J Clin Exp Pathol* (2014) 7:1042–50.
8. Butte MJ, Keir ME, Phamduy TB, Sharpe AH, Freeman GJ. Programmed Death-1 Ligand 1 Interacts Specifically With the B7-1 Costimulatory Molecule to Inhibit T Cell Responses. *Immunity* (2007) 27:111–22. doi: 10.1016/j.immuni.2007.05.016
9. Francisco LM, Sage PT, Sharpe AH. The PD-1 Pathway in Tolerance and Autoimmunity. *Immunol Rev* (2010) 236:219–42. doi: 10.1111/j.1600-065X.2010.00923.x
10. Keir ME, Butte MJ, Freeman GJ, Sharpe AH. PD-1 and Its Ligands in Tolerance and Immunity. *Annu Rev Immunol* (2008) 26:677–704. doi: 10.1146/annurev.immunol.26.021607.090331
11. Sharpe AH, Wherry EJ, Ahmed R, Freeman GJ. The Function of Programmed Cell Death 1 and Its Ligands in Regulating Autoimmunity and Infection. *Nat Immunol* (2007) 8:239–45. doi: 10.1038/ni1443
12. Chen L. Co-Inhibitory Molecules of the B7-CD28 Family in the Control of T-Cell Immunity. *Nat Rev Immunol* (2004) 4:336–47. doi: 10.1038/nri1349
13. Latchman Y, Wood CR, Chernova T, Chaudhary D, Borde M, Chernova I, et al. PD-L2 Is a Second Ligand for PD-1 and Inhibits T Cell Activation. *Nat Immunol* (2001) 2:261–8. doi: 10.1038/85330
14. Panjwani PK, Charu V, DeLisser M, Molina-Kirsch H, Natkunam Y, Zhao S. Programmed Death-1 Ligands PD-L1 and PD-L2 Show Distinctive and Restricted Patterns of Expression in Lymphoma Subtypes. *Hum Pathol* (2018) 71:91–9. doi: 10.1016/j.humpath.2017.10.029
15. Xu-Monette ZY, Zhou J, Young KH. PD-1 Expression and Clinical PD-1 Blockade in B-Cell Lymphomas. *Blood* (2018) 131:68–83. doi: 10.1182/blood-2017-07-740993
16. Vranic S, Ghosh N, Kimbrough J, Bilalovic N, Bender R, Arguello D, et al. PD-L1 Status in Refractory Lymphomas. *PloS One* (2016) 11:e0166266. doi: 10.1371/journal.pone.0166266
17. Wang L, Qian J, Lu Y, Li H, Bao H, He D, et al. Immune Evasion of Mantle Cell Lymphoma: Expression of B7-H1 Leads to Inhibited T-Cell Response to and Killing of Tumor Cells. *Haematologica* (2013) 98:1458–66. doi: 10.3324/haematol.2012.071340
18. Pham LV, Pogue E, Ford RJ. The Role of Macrophage/B-Cell Interactions in the Pathophysiology of B-Cell Lymphomas. *Front Oncol* (2018) 8:147. doi: 10.3389/fonc.2018.00147
19. Scott DW, Gascoyne RD. The Tumour Microenvironment in B Cell Lymphomas. *Nat Rev Cancer* (2014) 14:517–34. doi: 10.1038/nrc3774
20. Murray PJ, Allen JE, Biswas SK, Fisher EA, Gilroy DW, Goerdt S, et al. Macrophage Activation and Polarization: Nomenclature and Experimental Guidelines. *Immunity* (2014) 41:14–20. doi: 10.1016/j.immuni.2014.06.008
21. Blonska M, Agarwal NK, Vega F. Shaping of the Tumor Microenvironment: Stromal Cells and Vessels. *Semin Cancer Biol* (2015) 34:3–13. doi: 10.1016/j.semcancer.2015.03.002
22. Roussel M, Irish JM, Menard C, Lhomme F, Tarte K, Fest T. Regulatory Myeloid Cells: An Underexplored Continent in B-Cell Lymphomas. *Cancer Immunol Immunother* (2017) 66:1103–11. doi: 10.1007/s00262-017-2036-5
23. Schalper KA, Brown J, Carvajal-Hausdorf D, McLaughlin J, Velcheti V, Syrigos KN, et al. Objective Measurement and Clinical Significance of Tils in Non-Small Cell Lung Cancer. *J Natl Cancer Inst* (2015) 107. doi: 10.1093/jnci/dju435
24. Camp RL, Dolled-Filhart M, Rimm DL. X-Tile: A New Bio-Informatics Tool for Biomarker Assessment and Outcome-Based Cut-Point Optimization. *Clin Cancer Res* (2004) 10:7252–9. doi: 10.1158/1078-0432.CCR-04-0713
25. Kumar D, Xu ML. Microenvironment Cell Contribution to Lymphoma Immunity. *Front Oncol* (2018) 8:288. doi: 10.3389/fonc.2018.00288
26. Shain KH, Dalton WS, Tao J. The Tumor Microenvironment Shapes Hallmarks of Mature B-Cell Malignancies. *Oncogene* (2015) 34:4673–82. doi: 10.1038/onc.2014.403
27. Nygren L, Wasik AM, Baumgartner-Wennerholm S, Jeppsson-Ahlberg A, Klimkowska M, Andersson P, et al. T-Cell Levels Are Prognostic in Mantle Cell Lymphoma. *Clin Cancer Res* (2014) 20:6096–104. doi: 10.1158/1078-0432.CCR-14-0889
28. Xu B, Wang T. Intimate Cross-Talk Between Cancer Cells and the Tumor Microenvironment of B-Cell Lymphomas: The Key Role of Exosomes. *Tumour Biol* (2017) 39:1010428317706227. doi: 10.1177/1010428317706227
29. Tamura R, Tanaka T, Yamamoto Y, Akasaki Y, Sasaki H. Dual Role of Macrophage in Tumor Immunity. *Immunotherapy* (2018) 10:899–909. doi: 10.2217/imt-2018-0006
30. Funes SC, Rios M, Escobar-Vera J, Kalergis AM. Implications of Macrophage Polarization in Autoimmunity. *Immunology* (2018) 154:186–95. doi: 10.1111/imm.12910
31. Mantovani A, Sozzani S, Locati M, Allavena P, Sica A. Macrophage Polarization: Tumor-Associated Macrophages as a Paradigm for Polarized M2 Mononuclear Phagocytes. *Trends Immunol* (2002) 23:549–55. doi: 10.1016/S1471-4906(02)02302-5
32. Alvarado-Vazquez PA, Bernal L, Paige CA, Grosick RL, Moracho Vilrriales C, Ferreira DW, et al. Macrophage-Specific Nanotechnology-Driven CD163 Overexpression in Human Macrophages Results in an M2 Phenotype Under Inflammatory Conditions. *Immunobiology* (2017) 222:900–12. doi: 10.1016/j.imbio.2017.05.011
33. Hollander P, Rostgaard K, Smedby KE, Molin D, Loskog A, de Nully Brown P, et al. An Anergic Immune Signature in the Tumor Microenvironment of Classical Hodgkin Lymphoma Is Associated With Inferior Outcome. *Eur J Haematol* (2018) 100:88–97. doi: 10.1111/ejh.12987
34. Pollari M, Bruck O, Pellinen T, Vahamurto P, Karjalainen-Lindsberg ML, Mannisto S, et al. PD-L1+ Tumor-Associated Macrophages and PD-1+ Tumor Infiltrating Lymphocytes Predict Survival in Primary Testicular Lymphoma. *Haematologica* (2018) 103(11):1908–14. doi: 10.3324/haematol.2018.197194
35. Mitteldorf C, Berisha A, Pfaltz MC, Broekaert SMC, Schon MP, Kerl K, et al. Tumor Microenvironment and Checkpoint Molecules in Primary Cutaneous Diffuse Large B-Cell Lymphoma-New Therapeutic Targets. *Am J Surg Pathol* (2017) 41:998–1004. doi: 10.1097/PAS.0000000000000851
36. Menguy S, Prochazkova-Carlotti M, Beylot-Barry M, Saltel F, Vergier B, Merlio JP, et al. PD-L1 and PD-L2 Are Differentially Expressed by Macrophages or Tumor Cells in Primary Cutaneous Diffuse Large B-Cell Lymphoma, Leg Type. *Am J Surg Pathol* (2018) 42:326–34. doi: 10.1097/PAS.0000000000000983
37. Poles WA, Nishi EE, de Oliveira MB, Eugenio AIP, de Andrade TA, Campos AHFM, et al. Targeting the Polarization of Tumor-Associated Macrophages and Modulating Mir-155 Expression Might be a New Approach to Treat Diffuse Large B-Cell Lymphoma of the Elderly. *Cancer Immunol Immunother* (2019) 68:269–82. doi: 10.1007/s00262-018-2273-2
38. Goodman A, Patel SP, Kurzrock R. PD-1-PD-L1 Immune-Checkpoint Blockade in B-Cell Lymphomas. *Nat Rev Clin Oncol* (2017) 14:203–20. doi: 10.1038/nrclinonc.2016.168
39. Chen BJ, Dashnamoorthy R, Galera P, Makarenko V, Chang H, Ghosh S, et al. The Immune Checkpoint Molecules PD-1, PD-L1, TIM-3 and LAG-3 in Diffuse Large B-Cell Lymphoma. *Oncotarget* (2019) 10:2030–40. doi: 10.18632/oncotarget.26771
40. Miyoshi H, Kiyasu J, Kato T, Yoshida N, Shimono J, Yokoyama S, et al. PD-L1 Expression on Neoplastic or Stromal Cells Is Respectively a Poor or Good Prognostic Factor for Adult T-Cell Leukemia/Lymphoma. *Blood* (2016) 128:1374–81. doi: 10.1182/blood-2016-02-698936
41. Pascual M, Mena-Varas M, Robles EF, Garcia-Barchino MJ, Panizo C, Hervas-Stubbs S, et al. PD-1/PD-L1 Immune Checkpoint and P53 Loss Facilitate Tumor Progression in Activated B Cell Diffuse Large B-Cell Lymphomas. *Blood* (2019) 133(22):2401–12. doi: 10.1182/blood.2018889931
42. Ansell SM, Lesokhin AM, Borrello I, Halwani A, Scott EC, Gutierrez M, et al. PD-1 Blockade With Nivolumab in Relapsed or Refractory Hodgkin's Lymphoma. *N Engl J Med* (2015) 372:311–9. doi: 10.1056/NEJMoa1411087
43. Le K, Sun J, Khawaja H, Shibata M, Maggirwar SB, Smith MR, et al. Mantle Cell Lymphoma Polarizes Tumor-Associated Macrophages Into M2-Like Macrophages, Which in Turn Promote Tumorigenesis. *Blood Adv* (2021) 5(14):2863–78. doi: 10.1182/bloodadvances.2020003871
44. Papin A, Tessoulin B, Bellanger C, Moreau A, Le Bris Y, Maisonneuve H, et al. CSF1R and BTK Inhibitions as Novel Strategies to Disrupt the Dialog Between

Mantle Cell Lymphoma and Macrophages. *Leukemia* (2019) 33(10):2442–53. doi: 10.1038/s41375-019-0463-3

Conflict of Interest: MX has served in the Seattle Genetics lymphoma advisory board and as a Pure Marrow consultant. DR has served as a consultant, advisor or served on a Scientific Advisory Board for Amgen, Astra Zeneca, Agendia, Biocept, BMS, Cell Signaling Technology, Cepheid, Daiichi Sankyo, GSK, Merck, NanoString, Perkin Elmer, PAIGE, and Ultivue. He has received research funding from Astra Zeneca, Cepheid, Nanostring, Navigate/Novartis, NextCure, Lilly, Ultivue, and Perkin Elmer.

The remaining authors declare that the research was conducted in the absence of any commercial or financial relationships that could be construed as a potential conflict of interest.

Publisher's Note: All claims expressed in this article are solely those of the authors and do not necessarily represent those of their affiliated organizations, or those of the publisher, the editors and the reviewers. Any product that may be evaluated in this article, or claim that may be made by its manufacturer, is not guaranteed or endorsed by the publisher.

frontiers in Oncology

ORIGINAL RESEARCH
published: 06 September 2021
doi: 10.3389/fonc.2021.724435

Downregulation of GNA15 Inhibits Cell Proliferation *via* P38 MAPK Pathway and Correlates with Prognosis of Adult Acute Myeloid Leukemia With Normal Karyotype

Mengya Li[1], *Yu Liu*[1], *Yajun Liu*[2], *Lu Yang*[1], *Yan Xu*[1], *Weiqiong Wang*[1], *Zhongxing Jiang*[1], *Yanfang Liu*[1], *Shujuan Wang*[1*] *and Chong Wang*[1*]

[1] *Department of Hematology, The First Affiliated Hospital of Zhengzhou University, Zhengzhou, China,* [2] *Department of Orthopaedics, Rhode Island Hospital, Warren Alpert Medical School, Brown University, Providence, RI, United States*

OPEN ACCESS

Edited by:
Mina Luqing Xu,
Yale University,
United States

Reviewed by:
Tomasz Stoklosa,
Medical University of Warsaw, Poland
Daniele Sorcini,
University of Perugia, Italy

***Correspondence:**
Chong Wang
fccwangc@zzu.edu.cn
Shujuan Wang
fccwangsj1@zzu.edu.cn

Specialty section:
This article was submitted to Hematologic Malignancies, a section of the journal Frontiers in Oncology

Received: *13 June 2021*
Accepted: *17 August 2021*
Published: *06 September 2021*

Citation:
Li M, Liu Y, Liu Y, Yang L, Xu Y, Wang W, Jiang Z, Liu Y, Wang S and Wang C (2021) Downregulation of GNA15 Inhibits Cell Proliferation via P38 MAPK Pathway and Correlates with Prognosis of Adult Acute Myeloid Leukemia With Normal Karyotype. Front. Oncol. 11:724435. doi: 10.3389/fonc.2021.724435

Background: The prognosis of acute myeloid leukemia (AML) with a normal karyotype is highly heterogonous, and the current risk stratification is still insufficient to differentiate patients from high-risk to standard-risk. Changes in some genetic profiles may contribute to the poor prognosis of AML. Although the prognostic value of G protein subunit alpha 15 (*GNA15*) in AML has been reported based on the GEO (Gene Expression Omnibus) database, the prognostic significance of *GNA15* has not been verified in clinical samples. The biological functions of *GNA15* in AML development remain open to investigation. This study explored the clinical significance, biological effects and molecular mechanism of *GNA15* in AML.

Methods: Reverse transcription-quantitative polymerase chain reaction (RT-qPCR) was used to detect the mRNA expression level of *GNA15* in blasts of bone marrow specimens from 154 newly diagnosed adult AML patients and 26 healthy volunteers. AML cell lines, Kasumi-1 and SKNO-1, were used for lentiviral transfection. Cell Counting Kit-8 (CCK8) and colony formation assays were used to determine cell proliferation. Cell cycle and apoptosis were analyzed by flow cytometry. The relevant signaling pathways were evaluated by Western blot. The Log-Rank test and Kaplan-Meier were used to evaluate survival rate, and the Cox regression model was used to analyze multivariate analysis. Xenograft tumor mouse model was used for *in vivo* experiments.

Results: The expression of *GNA15* in adult AML was significantly higher than that in healthy individuals. Subjects with high *GNA15* expression showed lower overall survival and relapse-free survival in adult AML with normal karyotype. High *GNA15* expression was independently correlated with a worse prognosis in multivariate analysis. Knockdown of *GNA15* inhibited cell proliferation and cell cycle progression, and induced cell apoptosis in AML cells. *GNA15*-knockdown induced down-regulation of p-P38 MAPK and its downstream p-MAPKAPK2 and p-CREB. Rescue assays confirmed that

P38 MAPK signaling pathway was involved in the inhibition of proliferation mediated by GNA15 knockdown.

Conclusions: In summary, *GNA15* was highly expressed in adult AML, and high *GNA15* expression was independently correlated with a worse prognosis in adult AML with normal karyotype. Knockdown of *GNA15* inhibited the proliferation of AML regulated by the P38 MAPK signaling pathway. Therefore, *GNA15* may serve as a potential prognostic marker and a therapeutic target for AML in the future.

Keywords: acute myeloid leukemia, GNA15, cell proliferation, P38 MAPK, prognosis

INTRODUCTION

Acute myeloid leukemia (AML) is a group of heterogeneous clonal hematopoietic progenitor cell neoplasm and the adverse-risk subjects experience poor prognosis (1, 2). Advances in the therapy of AML, such as risk stratification, concurrent chemotherapy, novel drugs and hematopoietic stem cell transplantation, have improved the treatment outcomes of patients (3). Cytogenetic analysis has proved to be crucial for the risk stratification of AML patients (4). However, nearly half of AML patients have a normal karyotype (NK) (4). Identification of the changes in genetic profiles such as mutations of *NPM1*, *FLT3-ITD* and *CEBPA* has further improved the risk stratification of NK-AML. However, most NK-AML still belongs to the intermediate prognostic subgroup in which the most appropriate treatment remains to be defined (4). It is urgent to identify novel prognostic biomarkers and update the risk stratification for NK-AML.

Our group screened and verified 7 new biomarkers of B cell acute lymphoblastic leukemia (B-ALL) based on the ImmuSort database and clinical specimens. G protein subunit alpha 15 (*GNA15*) is one of the prominent candidates (5). In the process of verification, we found that the expression level of *GNA15* in AML was significantly higher than that in B-ALL and normal controls, suggesting that *GNA15* may play an important biological role in AML.

The *GNA15* gene is located on chromosome 19p13.3, spans approximately 27.7 kb, and encodes a 44 KDa GNA15 protein (6). *GNA15* is a member of the *GNA* gene family (including *GNAq*, *GNA11* and *GNA14*) (7). The protein encoded by the *GNA15* gene is the alpha subunit of the G protein, which participates in the regulation of cell proliferation and apoptosis (8). The GNA15 protein, or Gα15, belongs to the Gαq subfamily and is highly expressed in some cell types, such as hematopoietic stem cells and epithelial cells during specific stages of differentiation. It is up-regulated in $CD34^+$ hematopoietic stem cells and decreases with cell maturation (9, 10). G protein-coupled receptors (GPCRs) are the largest cell surface molecule family involved in signal transmission. It accounts for more than 2% of genes encoded in the human genome (11). Abnormal activation of GPCRs is related to tumor occurrence and metastasis (12). By coupling to GPCRs, *GNA15* promotes cell proliferation and inhibits cell apoptosis by regulating downstream signaling pathways (10). *GNA15* is known to play as an oncogene in several tumors, such as gastroenteropancreatic neuroendocrine neoplasia (GEP-NEN) (8), liver cancer (13, 14), pancreatic ductal adenocarcinoma (15) and ovarian cancer (16). These biological functions are mediated by ERK, NFκB and Akt signaling pathways in GEP-NEN (8, 13–16). Nevertheless, the clinical value and biological function of *GNA15* in AML remain unknown.

Therefore, in this study, we examined the expression and prognostic value of *GNA15* in AML and its effects on cellular proliferation, cell cycle and apoptosis. The underlying mechanism of *GNA15* regulation was also explored.

Abbreviations: AML, acute myeloid leukemia; BM, bone marrow; CCK8, Cell Counting Kit-8; CREB, cAMP-response element binding protein; DEG, differentially expressed gene; DAVID, The Database for Annotation, Visualization and Integrated Discovery; FLT3-ITD, FMS-like tyrosine kinase-3 internal tandem duplications; GNA15, guanine nucleotide binding protein subunit alpha-15; GEO, Gene Expression Omnibus; GO, gene ontology; HSC, hematopoietic stem cell; IST, in silico transcriptomics database; KEGG, Kyoto Encyclopedia of Genes and Genomes; LSC, leukemia stem cell; MAPK, mitogen-activated protein kinase; MAPKAPK2, MAPK-activated protein kinase 2; OS, overall survival; PBMC, peripheral blood mononuclear cell; RFS, relapse-free survival; RT-qPCR, reverse transcription-quantitative polymerase chain reaction.

MATERIALS AND METHODS

Database Analyses

We collected the expression data of 263 hematopoietic stem cell (HSC) samples and 113 leukemia stem cell (LSC) in the ImmuCo database (http://immuco.bjmu.edu.cn), 74 peripheral blood mononuclear cell (PBMC) samples, 542 AML samples in the ONCOMINE database (https://www.oncomine.org) and 173 AML samples in the Gene Expression Profiling Interactive Analysis (GEPIA2) database (http://gepia2.cancer-pku.cn), and compared the expression level of *GNA15*. One publicly available cytogenetically normal AML data sets (GSE12417 of GEO database) were used to perform survival analysis.

Subjects

Bone marrow samples from 154 newly diagnosed AML patients (patients with acute promyelocytic leukemia were excluded) and 26 healthy controls were obtained following informed consent at the First Affiliated Hospital of Zhengzhou University between February 2017 and April 2019. Details of treatment regimens were reported (17). Subjects were followed up until death, loss to

follow-up or April 2021. Complete remission, relapse, risk stratification, overall survival (OS) and relapse-free survival (RFS) were defined as described (17). The study was approved by the Ethics Committee of the First Affiliated Hospital of Zhengzhou University and informed consent was obtained according to the Declaration of Helsinki.

Next-Generation Sequencing

The mutational hotspots of genes were assessed by next-generation sequencing. The detection was performed utilizing a Rightongene AML/MDS/MPN Sequencing Panel (Rightongene, Shanghai, China) on an Illumina MiSeq System (Illumina, San Diego, CA) high-throughput sequencing platform. The original data after sequencing was analyzed by bioinformatics using NCBI, CCDS, dbSNP (v138), COSMIC, human genome database (HG19) and other databases to determine the pathogenic mutation site. The average depth of the sequencing was 4837.978Kb, detection sensitivity was ~ 5%.

Cell Lines and Reagents

The human AML cell lines (Kasumi-1, SKNO-1, and HL-60), were purchased from American Type Culture Collection (Manassas, VA, USA). The human ALL cell lines (Sup-B15, BV173, NALM-6, and BALL-1) were obtained from Guangzhou Jennio Biotech Co. Ltd (Guangzhou, China). The human AML cell line HEL, chronic myeloid leukemia cell line K562, the human lymphoma cell line Ramos and the human myeloma cell line KM-3 were kind gifts from Professor K. Y. Liu of Peking University People's Hospital. These cell lines were maintained in RPMI 1640 medium containing 10% fetal bovine serum (FBS), 1% streptomycin and penicillin (all from Gibco, Billings, MT, USA) at 37 °C with 5% CO_2. Cell viability was observed daily with a microscope (Olympus, Ckx53sf, Tokyo, Japan), cell lines (except SKNO-1 cell line) were passaged every 2–3 days and SKNO-1 cells were passaged every 3-4 days. Asiatic Acid (Selleck Chemicals, Houston, TX, USA), was used as a P38 MAPK activator.

Lentiviral Transduction

Kasumi-1 and SKNO-1 (*FLT3*-wildtype) cells were infected with human GNA15 shRNA lentiviral particles (Genechem, Shanghai, China) or empty control lentiviral particles (Genechem) at a 100 multiplicity of infection (MOI). Media containing lentiviral particles were replaced with a complete medium 12 hours post-infection. Stably transfected Kasumi-1 and SKNO-1 cells were selected with 2 μg/ml and 5 μg/ml puromycin dihydrochloride (Genechem, Shanghai, China) respectively at 72 h post-infection. After 3 weeks of antibiotic selection, stable GNA15-knockdown cells and control cells were obtained. GNA15 expression levels were confirmed by real-time quantitative PCR (RT-qPCR) and Western blot analyses.

RNA Extraction and RT-qPCR

Bone marrow was collected by Ethylene Diamine Tetraacetic Acid (EDTA) anticoagulant tube and mononuclear cells were isolated from bone marrow by density gradient centrifugation. TRIzol® (Invitrogen, Carlsbad, CA, USA) was used to extract total RNA following the manufacturer's instructions. The cDNA templates were synthesized with a High Capacity cDNA Reverse Transcription Kit (Applied Biosystems, Foster City, CA, USA) (18). Gene transcript levels were determined by the Taqman method as previously reported (19). Serial dilutions of plasmids expressing *GNA15* and *ABL1* (Genechem) were amplified to construct standard quantification curves. Copy numbers of *GNA15* and *ABL1* were calculated from standard curves using Ct values. Samples were assayed in duplicates to evaluate data reproducibility. The primers and probe sequences of *GNA15* and *ABL1* are shown in **Supplementary Table 1.**

Western Blot Analyses

RIPA lysis buffer (Solarbio, Beijing, China) with Protein phosphatase inhibitor (Biomed, Beijing, China) and phenylmethylsulfonyl fluoride (PMSF, Biomed) was used to extract total protein lysate. Lysates were run on 10% SDS-PAGE gels, and protein bands were transferred to 0.45μm polyvinylidene difluoride (PVDF) membrane (Millipore, Billerica, MA, USA), then blocked with 5% skim milk at room temperature for 1 hour. The membrane was incubated with primary antibodies (GNA15, Novus Biologicals, Centennial, USA, 1:1000; GAPDH, Solarbio, 1:1000; p-P38 MAPK, P38 MAPK, p-CREB, CREB, p-MAPKAPK2^{Thr222}, MAPKAPK2^{Thr222}, p53, cleaved-PARP, cleaved-Caspase3, p27 Kip1, Cyclin D1, CDK4, p-p44/42 MAPK, p-AMPKα, p-Akt, p-Smad3, LC3A/B, Cell Signaling Technology [CST], MA, USA, 1:1000) overnight at 4°C and probed with secondary antibodies (goat anti-rabbit IgG, goat anti-mouse IgG, Solarbio, 1:1000) at room temperature for 1 hour. The immunoreactive bands were defined using Super ECL Prime (US EVERBRIGHT, Suzhou, China).

Cell Proliferation and Colony-Forming Assay

The stably transfected cells were seeded in 96-well plates at a density of 1×10^5 cells/ml. Then 10 μl of Cell Counting Kit-8 (CCK8, Dojin Laboratories, Kumamoto, Japan) was added into each well after 0, 24, 48, 72 hours. Cell proliferation was detected by a full-wavelength microplate reader at 450 nm 3 hours later. To analyze the colony formation, cells were seeded into 35 mm dishes (6×10^3 cells/well) in methylcellulose-based MethoCult medium (STEMCELLTM TECHNOLOGIES, Vancouver, British Columbia, Canada). The colonies with ≥50 cells were counted with an inverted microscope after 10 days of growing in a humid incubator. The experiments were performed three times to show the repeatability of the data.

Cell cycle and Apoptosis Analyses

Cells were seeded into 6-well plates (1×10^5 cells/ml) and starved by adding serum-free medium for 24 hours to research synchronization, and a complete medium was then added for an additional 48 hours. The Cell Cycle and Apoptosis Kit (US EVERBRIGHT, Suzhou, China) was used for cell cycle analyses and the Annexin V-APC/PI Apoptosis Kit (US EVERBRIGHT) was used as the apoptosis assay. The cell cycle and apoptosis were determined by flow cytometry according to the manufacturer's instructions.

Xenograft Tumor Mouse Model

Male 6-week-old BALB/c nude mice (Beijing HFK Bioscience Co., Ltd.; Beijing, China) were prepared for generating xenograft models. All mice were divided into two groups (CTRL and KD, 5 mice/group) with intraperitoneal injections of cyclophosphamide (100mg/kg/d × 2d). After two days, the cells (1.5×10^7 cells suspended in 100 µl PBS) with lentiviral particles were syringed in the right flank. We measured the diameters (the longest and shortest diameters) and calculated the volume ($L \times I^2 \times 0.5$; L: the longest diameter, I: the shortest diameter) of tumor every other day for 12 days, after that all mice were euthanized and tumor tissues obtained for the following assay. All studies were approved by the Ethics Committee of the First Affiliated Hospital of Zhengzhou University.

Statistical Analyses

Differences across groups were compared using the Pearson Chi-square test or Fisher exact analysis for categorical data and Mann-Whitney *U*-test or Student's *t*-test for continuous variables. The Kaplan-Meier method and Log-Rank test were used for survival analysis. A Cox proportional hazard regression model was used to determine associations between *GNA15* transcript levels and OS and RFS. Variables with $P < 0.1$ in the single variable analysis were included in the model. A two-sided $P < 0.05$ was considered significant. Analyses were performed by SPSS software version 26.0 (Chicago, IL, USA) and Graphpad Prism™ 8.01 (San Diego, California, USA).

RESULTS

The *GNA15* Gene Is Highly Expressed in Subjects With AML

Firstly, we surveyed the expression level of *GNA15* in AML based on the database. As shown in **Figure 1**, the gene expression level of *GNA15* was higher in leukemic stem cells than in hematopoietic

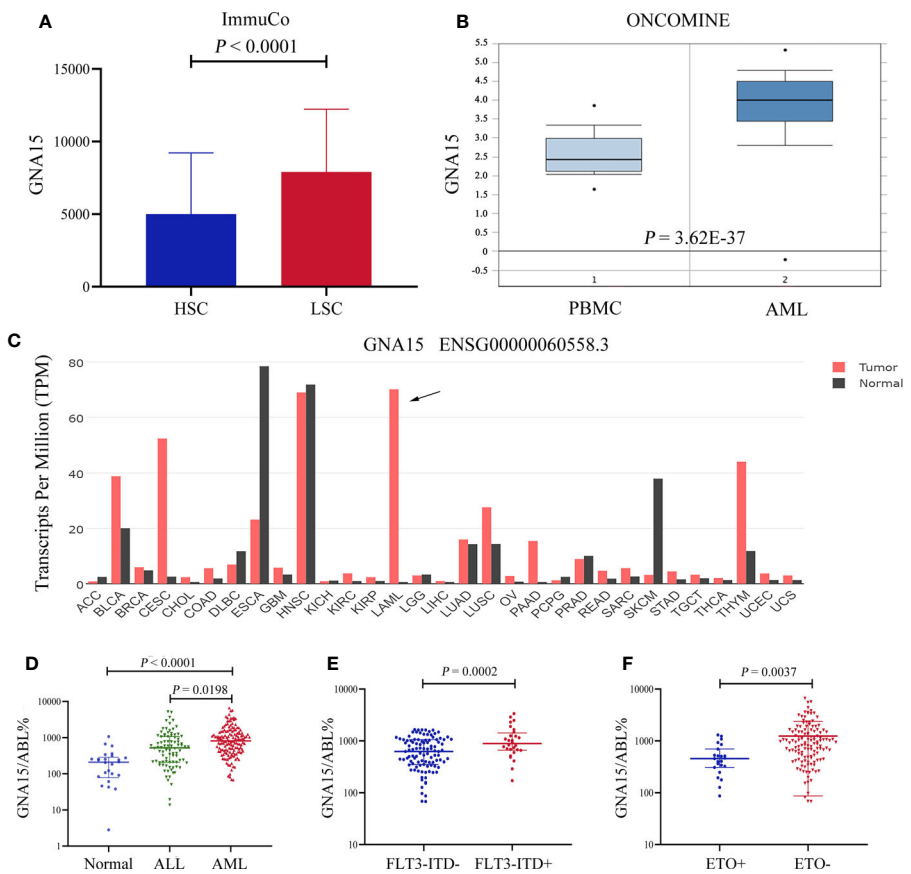

FIGURE 1 | The *GNA15* gene was highly expressed in subjects with acute myeloid leukemia (AML). **(A)** In the ImmuCo database, the gene expression level of *GNA15* was higher in leukemic stem cells (LSC, n=113) than in hematopoietic stem cells (HSC, n=263). **(B)** In the ONCOMINE database, *GNA15* showed significantly higher expression in AML patients (n=542) than in normal peripheral blood mononuclear samples (PBMC, n=74). **(C)**The expression of *GNA15* in various cancers and normal tissues was significantly different and *GNA15* was overexpressed in AML in the GEPIA2 database. The height of the bar represents the median expression of *GNA15* of a certain tumor or normal tissue. **(D)** *GNA15* transcript levels in normal volunteers, acute lymphoblastic leukemia (ALL) and AML. **(E)** *GNA15* transcript levels in AML with or without *FLT3-ITD* mutation. **(F)** *GNA15* transcript levels in AML with or without *AML1-ETO* fusion gene. Error bars indicate median with interquartile range **(D–F)**.

stem cells based on the ImmuCo database (P<0.0001, **Figure 1A**). *GNA15* expression in AML patients from the Oncomine database was also compared, and similarly, *GNA15* showed significantly higher expression in AML patients than normal peripheral blood mononuclear samples (PBMC, $P=3.62\times10^{-37}$, **Figure 1B**). Furthermore, by using the public GEPIA2 database, we also observed elevated GNA15 expression levels in AML (**Figure 1C**). Thus, we surveyed the transcript levels of *GNA15* in the bone marrow of newly diagnosed subjects with AML and normal healthy volunteers. The expression of *GNA15* in AML was significantly higher than healthy volunteers and ALL in our cohort (median 810.00%, range [67.87%-6630.48%] *vs* 209.15% range [0-1073.74%], P<0.0001; 810.00%, range [67.87%-6630.48%] *vs* 520.55% range [13.64%-5205.27%], P=0.0003; **Figure 1D**). AML with *FLT3-ITD* mutation had higher *GNA15* transcript levels than those without *FLT3-ITD* mutation (889.85% [171.59%-3351.42%] *vs* 625.16% [67.87%-1656.21%], P=0.0002, **Figure 1E**). AML with *AML1-ETO* fusion gene had lower transcript levels than those without *AML1-ETO* fusion gene (456.58% [86.78%-1306.69%] *vs* 941.28% [67.87%-6630.48%], P=0.0037; **Figure 1F**). The transcript levels of *GNA15* showed no difference in AML with different French-American-British (FAB) classification or cytogenetic risk stratifications (**Supplementary Figure 1**).

GNA15 Transcript Levels Are Independently Associated With OS and RFS in AML With Normal Karyotype

Subjects in the GSE12417 database (AML with normal karyotype) were divided into the high expression group and the low expression group according to the median expression value of *GNA15*. Subjects with high expression of *GNA15* showed a relatively worse 3-year OS than the subjects with low expression of *GNA15* (20.3% [10.1%-30.5%] *vs* 43.1% [31.5%-54.7%], P=0.0009, **Figure 2A**) in the GSE12417 database. In our AML cohort, AML patients were classified into the high expression group and the low expression group according to the median value of *GNA15* (810.00%). The median follow-up of these 154 patients was 410 days (range 14–1057 days). In the whole cohort, the 2-year OS between low expression group and high expression group showed no significant difference (40.4%, 95% confidence interval (CI) [28.8%-52.0%] *vs* 38.2% [26.2%-50.2%], P=0.564, **Figure 2B**). Then we analyzed the prognostic value of *GNA15* in the

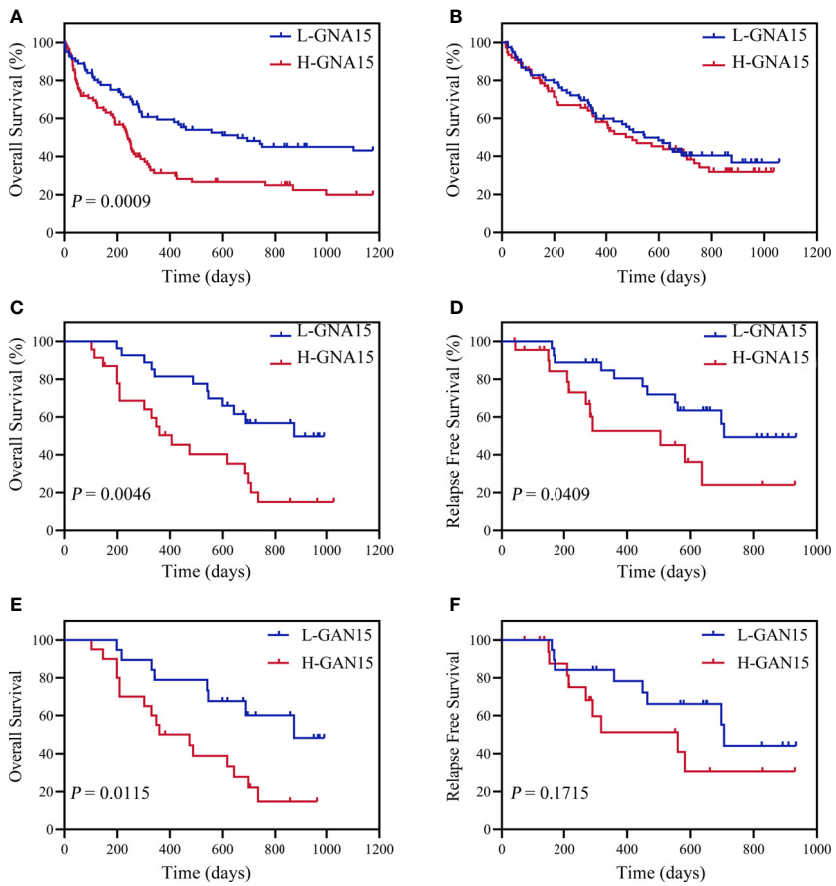

FIGURE 2 | Overall survival (OS) and relapse free survival (RFS) of adult subjects with AML according to *GNA15*. **(A)** OS of 163 AML subjects with normal karyotype in GSE12417. **(B)** OS of 154 AML subjects in our cohort. **(C, D)** OS **(C)** and RFS **(D)** of 50 AML subjects with normal karyotype in our cohort. **(E, F)** OS **(E)** and RFS **(F)** of 39 *FLT3-ITD*-negative subjects in NK-AML cohort according to *GNA15*. H-*GNA15*, high *GNA15* expression; L-*GNA15*, low *GNA15* expression.

subgroup with normal karyotype (NK, n=50). In the NK-AML subgroup, subjects in the high expression group were older,had higher expression of Wilms tumor gene 1 (*WT1*) at diagnosis and higher minimal residual disease (MRD) levels after a course of induction chemotherapy (**Table 1**). However, there was no significant correlation between the level of *GNA15* expression and other clinical characteristics, including risk groups, gender, platelets, hemoglobin level, gene mutations and transplant (**Table 1**). In the NK-AML subgroup, subjects with high *GNA15* expression showed a worse 2-year OS and RFS than subjects with low *GNA15* expression (OS: 15.1% [0%-30.8%] *vs* 49.7% [28.1%-71.3%], *P*=0.0046; RFS: 24.1% [0%-49.8%] *vs* 49.4% [26.7%-72.1%], *P*=0.0409; **Figures 2C, D**). Moreover, in the NK-AML without *FLT3-ITD* mutations, subjects with high *GNA15* expression showed a worse 2-year OS (13.7% [0%-50.7%] vs 44.5% [18.2%-70.8%], *P*=0.0115; **Figure 2E**) and a similar 2-year RFS (32.3% [0%-65.0%] vs 40.6% [13.6%-67.6%], *P*=0.1715; **Figure 2F**). In multivariate analysis, high *GNA15* expression was independently associated with a worse OS and RFS (**Table 2**). Female was independently associated with a better OS and RFS (**Table 2**). Other factors, such as age, risk group, *WT1* expression, *FLT3-ITD* mutation and other gene mutations did not show any significant correlation with OS or RFS.

Down-Regulation of *GNA15* Inhibits Cell Proliferation and Colony Formation in AML Cells

We quantified the transcriptional level and protein level of GNA15 in cell lines of hematological malignancies. RT-qPCR and Western blot analysis revealed that GNA15 is highly expressed in nearly all acute leukemia cell lines tested while lowly expressed in lymphoma and myeloma cell lines and normal controls (**Supplementary Table 2** and **Supplementary Figure 2**). Cell lines with stable *GNA15* knockdown and control cell lines using lentiviral small hairpin RNAs were constructed in Kasumi-1 and SKNO-1, and the knockdown efficiency was assessed by RT-qPCR (**Figures 3A, B**) and Western blot (**Figures 3C, F**). CCK8 analysis revealed a significant reduction in cell viability in both Kasumi-1 and SKNO-1 following *GNA15* knockdown (**Figures 3D, E**). Moreover, the knockdown of *GNA15* dramatically inhibited the cell colony formation ability in Kasumi-1 (**Figures 3G–I**). SKNO-1 control and knockdown cells failed to complete the colony formation test.

Knockdown of *GNA15* Promotes Cell Cycle Arrest and Induces Apoptosis of AML Cells

Flow cytometry analysis showed that knockdown of *GNA15* significantly increased the apoptosis rate in both Kasumi-1 and SKNO-1 cells (**Figures 4A, B**). In addition, compared to the control group, knockdown of *GNA15* significantly increased cell counts in the G0/G1 phase in both Kasumi-1 and SKNO-1 and decreased cell counts in the G2/M phase in Kasumi-1 (**Figures 4C–E**). To further explore the effect of *GNA15* knockdown on cell apoptosis and cell cycle, Western blot was used to evaluate proteins related to cell cycle and apoptosis. Knockdown of *GNA15* resulted in an increase in cleaved-PARP, cleaved-Caspase3, p53 and p27 and a significant decrease in Cyclin D1 but no change in CDK4 (**Figure 4F**).

P38 MAPK Pathway Is Critical for *GNA15*-mediated Changes

To understand the mechanism behind the reduction in cell proliferation of *GNA15* knockdown, we examined the expression levels of phosphorylated proteins related to

TABLE 1 | Relationship between Transcription Level of GNA15 and Clinical Characteristics in Normal Karyotype AML.

Variables	Total N = 50	L-*GNA15* N = 27	H-*GNA15* N = 23	*P*-value
Age,years				
Mean ± SD	43.9 ± 15.8	39.4 ± 15.5	49.3 ± 14.7	0.024
≥60, n (%)	7 (14)	2 (7.4)	5 (21.7)	0.295
Female, n (%)	28 (56.0)	16 (59.3)	12 (52.2)	0.615
Risk group, n (%)				0.868
Low	10 (20)	6 (22.2)	4 (17.4)	
Medium	20 (40)	10 (37.0)	10 (43.5)	
High	20 (40)	11 (40.7)	9 (39.1)	
PLT, $\times 10^9$/l	38 (4-260)	29 (6-260)	45 (4-218)	0.453
Hb, g/l	85.3 ± 21.7	82.5 ± 19.4	88.5 ± 24.2	0.339
Blast of BM (%)	75.0 (0-99)	75.0 (0-99)	75.5 (0-94)	0.016
MRD of flow cytometry (%)	0.7 (0-75.5)	0.9 (0-26.9)	0.9 (0-75.5)	0.003
Mutations, n (%)				
FLT3-ITD	11 (22)	5 (18.5)	6 (26.1)	0.520
NPM1	6 (12)	3 (11.1)	3 (13.0)	1.000
CEBPA	5 (10)	3 (11.1)	2 (8.7)	1.000
DNMT3A	5 (10)	4 (80)	1 (20)	0.449
WT1	6.2 (0-86.9)	0.5 (0-12.9)	6.2 (5-86.9)	0.000
TET2	19 (38)	12 (63.2)	7 (36.8)	0.309
IDH1/2	8 (16)	7 (87.5)	1 (12.5)	0.092
RUNX1	2 (4)	1 (50)	1 (50)	1.000
Transplant, n (%)	11 (22)	8 (29.6)	3 (13.0)	0.285

H-GNA15, high GNA15 expression; L-GNA15, low GNA15 expression; SD, standard deviation; PLT, platelet; Hb, hemoglobin; BM, bone marrow; MRD, minimal residual disease.

TABLE 2 | Univariate and Multivariate Analysis of OS and RFS in AML with Normal Karyotype.

End point	Variables	Univariate		Multivariate	
		HR (95% *CI*)	*P*-value	HR (95% *CI*)	*P*-value
OS					
	H-*GNA15*	2.77 (1.33-5.79)	0.007	2.62 (1.25-5.51)	0.011
	Age≥60 years	1.74 (0.74-4.07)	0.205		
	Female	0.43 (0.21-0.89)	0.024	0.46 (0.22-0.96)	0.039
	Risk group				
	Low *vs* High	0.62 (0.20-1.90)	0.400		
	Medium *vs* High	0.86 (0.40-1.85)	0.694		
	MRD	1.00 (0.99-1.03)	0.676		
	FLT3-ITD+	0.76 (0.31-1.87)	0.553		
	WT1	1.00 (0.99-1.02)	0.660		
	NPM1	0.96 (0.33-2.74)	0.933		
	DNMT3A	0.86 (0.26-2.86)	0.810		
	IDH1/2	0.82 (0.32-2.16)	0.693		
	TET2	1.36 (0.66-2.81)	0.399		
	RUNX1	3.71 (0.83-16.62)	0.087	2.89 (0.63-13.28)	0.174
RFS					
	H-*GNA15*	2.36 (1.01-5.52)	0.047	2.45 (1.04-5.73)	0.040
	Age≥60 years	1,51 (0.50-4.53)	0.466		
	Female	0.39 (0.17-0.90)	0.028	0.37 (0.16-0.88)	0.024
	Risk group				
	Low *vs* High	0.92 (0.28-3.03)	0.889		
	Medium *vs* High	1.12 (0.44-2.85)	0.811		
	MRD	1.01 (0.99-1.03)	0.412		
	FLT3-ITD+	0.90 (0.33-2.45)	0.838		
	WT1	1.01 (0.99-1.03)	0.555		
	NPM1	0.96 (0.28-3.24)	0.940		
	DNMT3A	0.73 (0.17-3.13)	0.670		
	IDH1/2	1.10 (0.40-2.97)	0.864		
	TET2	1.25 (0.54-2.92)	0.603		
	RUNX1	2.23 (0.28-17.47)	0.446		

OS, overall survival; RFS, relapse free survival; H-GNA15, high GNA15 expression; L-GNA15, low GNA15 expression; HR, hazard ratio; CI, confidence interval; MRD, minimal residual disease.

proliferation, metabolism, and autophagy. As shown in **Figure 5**, phosphorylation of P38 MAPK, MAPKAPK2^{Thr222} and CREB were notably decreased in *GNA15*-KD cells whereas phosphorylation of AMPK, Akt, Smad3, ERK and LC3 A/B were not significantly different (**Figures 5A, B**). To confirm the role of the P38 MAPK pathway in *GNA15*-mediated effects, we used Asiatic Acid, a P38 MAPK activator in *GNA15*-KD cells of Kasumi-1. As shown in **Figure 5C**, the addition of the P38 MAPK activator (2.5μM, 5μM, 10μM for 48 hours) could visibly increase the protein level of p-P38MAPK and the downstream p-MAPKAPK2^{Thr222}. Phosphorylation of P38 MAPK after adding Asiatic Acid reversed the inhibitory effect of *GNA15* knockdown on the proliferation of AML cells (**Figures 5D–G**).

Knockdown of *GNA15* Inhibits the Growth of Tumor Tissues *In Vivo*

Xenograft tumor model was used to verify the results of functional experiments and changes in signaling pathways *in vitro*. Our study showed that in Kasumi-1 cells, *GNA15* knockdown significantly inhibited the growth of tumors compared to controls (**Figures 6A, C**). The inhibitory effect was also verified in SKNO-1 cells (**Figures 6B, D**). Western blot was performed to investigate the mechanism of change, GNA15, p-P38 MAPK, p-MAPKAPK2^{Thr222} were significantly decreased (**Figure 6E**). These changes in the signaling pathway were the same as the results *in vitro*.

DISCUSSION

In this study, we evaluated the role of *GNA15* in predicting the prognosis of adult AML patients and investigated its molecular mechanism. Based on the bioinformatics analyses and our data, we found that the expression level of *GNA15* in AML was significantly higher than that of normal controls. The high expression of *GNA15* was independently associated with worse survival in AML with normal karyotype. *GNA15* knockdown inhibited cell proliferation and colony formation, induced cell apoptosis, and promoted cell cycle arrest in AML cell lines, and decreased cell proliferation through inhibiting the P38 MAPK pathway.

There are few studies on *GNA15*, and its effect on cancer was reported even less frequently. A study based on bioinformatics analysis suggested that *GNA15* may be related to ovarian cancer, but it has not been clinically and experimentally verified (16). The high expression of *GNA15* was associated with poor survival in small intestinal neuroendocrine neoplasia (8). de Jonge et al. reported that *GNA15* may be a specific marker of AML leukemia

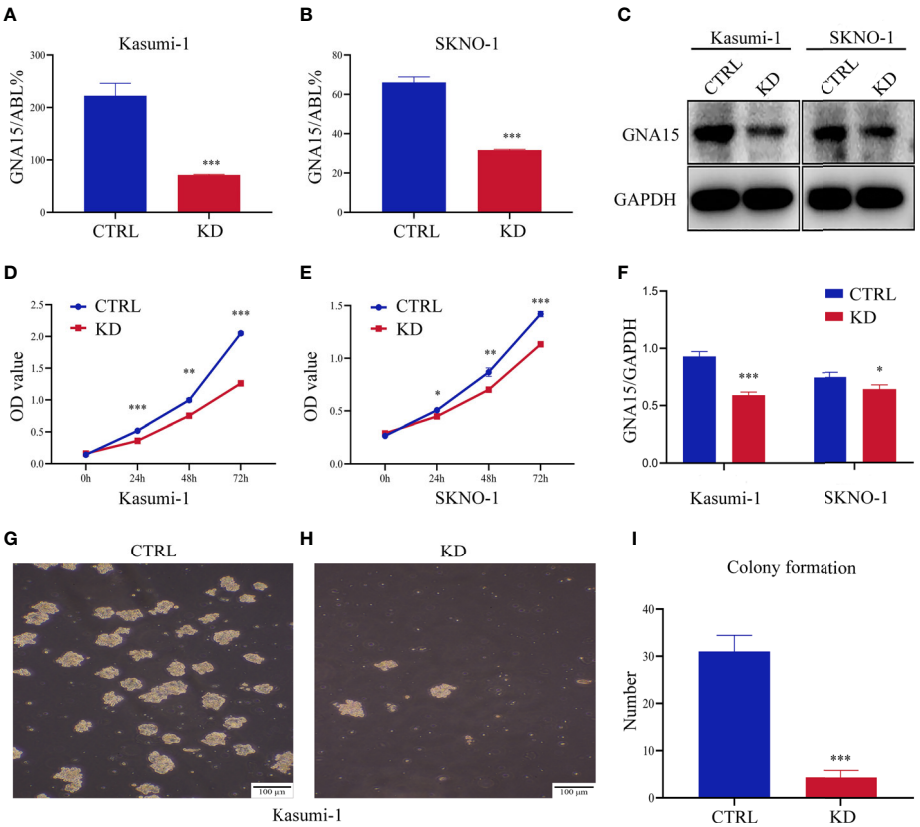

FIGURE 3 | Down-regulation of *GNA15* inhibited cell proliferation and colony formation in AML cells. The efficiency of *GNA15* knockdown in the Kasumi-1 and SKNO-1 cell lines was verified by **(A, B)** real-time quantitative polymerase chain reaction and **(C, F)** Western blot, respectively. **(D, E)** Cell proliferation was detected by the CCK-8 assay in Kasumi-1 and SKNO-1**. (G–I)** The colony formation of *GNA15*-CTRL and *GNA15*-KD in Kasumi-1. CTRL, control; KD, knockdown; $^{*}P < 0.05$ compared with CTRL cells; $^{**}P < 0.01$ compared with CTRL cells; $^{***}P < 0.001$ compared with CTRL cells; Error bars indicate the standard deviation.

stem cells based on gene expression profile analysis of bone marrow CD34(+) and CD34(-) cells of AML patients and normal bone marrow CD34(+) cells (9). Their study suggested that *GNA15* can be used as a new marker for prognostic evaluation of AML with normal karyotype. However, the prognostic study of this study was based solely on the GEO database. Thus the prognostic significance of *GNA15* has not been verified in clinical samples, and the function and mechanism of *GNA15* in AML have not yet been studied.

In our study, we found that the expression of *GNA15* in acute leukemia was significantly higher than that in controls, and the expression of *GNA15* in AML was significantly higher than that in ALL. In addition, we found that the expression of *GNA15* in AML patients with *FLT3-ITD* (FMS-like tyrosine kinase-3 internal tandem duplications) was significantly higher than those without *FLT3-ITD*. Patients with *FLT3-ITD* account for 20% to 30% of AML (20), and often have a poor prognosis (21–23). Therefore, patients with high *GNA15* expression are more likely to have *FLT3-ITD* mutation, which may be one of the reasons for the adverse outcomes. There was no significant difference in the survival analysis of *GNA15* expression in the entire cohort, which may be caused by the complicated prognostic analysis of AML. For example, the application of hematopoietic stem cell transplantation, targeted drugs and immunotherapy could greatly improve the prognosis of high-risk patients (24, 25). Therefore, we further performed the prognostic analysis in adult AML with normal karyotype and found that high *GNA15* expression was independently associated with poor OS and RFS in this subgroup, which was consistent with the survival analysis results of the GEO database. It is worth noting that *FLT3-ITD* mutations, which constitute well-established negative prognostic factor, did not show significant correlation with OS and RFS. In our NK-AML cohort, there are 11 cases with *FLT3-ITD*, 4 of them had *NPM1* co-mutation and 2 of them received an allo-transplant. That may partially explain why *FLT3-ITD* mutations did not show significant correlation with OS and RFS. In order to solve the possible confounding factor of *FLT3-ITD mutations*, we performed a subgroup analysis of NK-AML without *FLT3-ITD* mutations and found that subjects with high *GNA15* expression also showed a worse OS in NK-AML without *FLT3-ITD* mutations. These results indicate that *GNA15* may be used as a potential marker for predicting survival and recurrence of AML patients, especially for patients with normal karyotype.

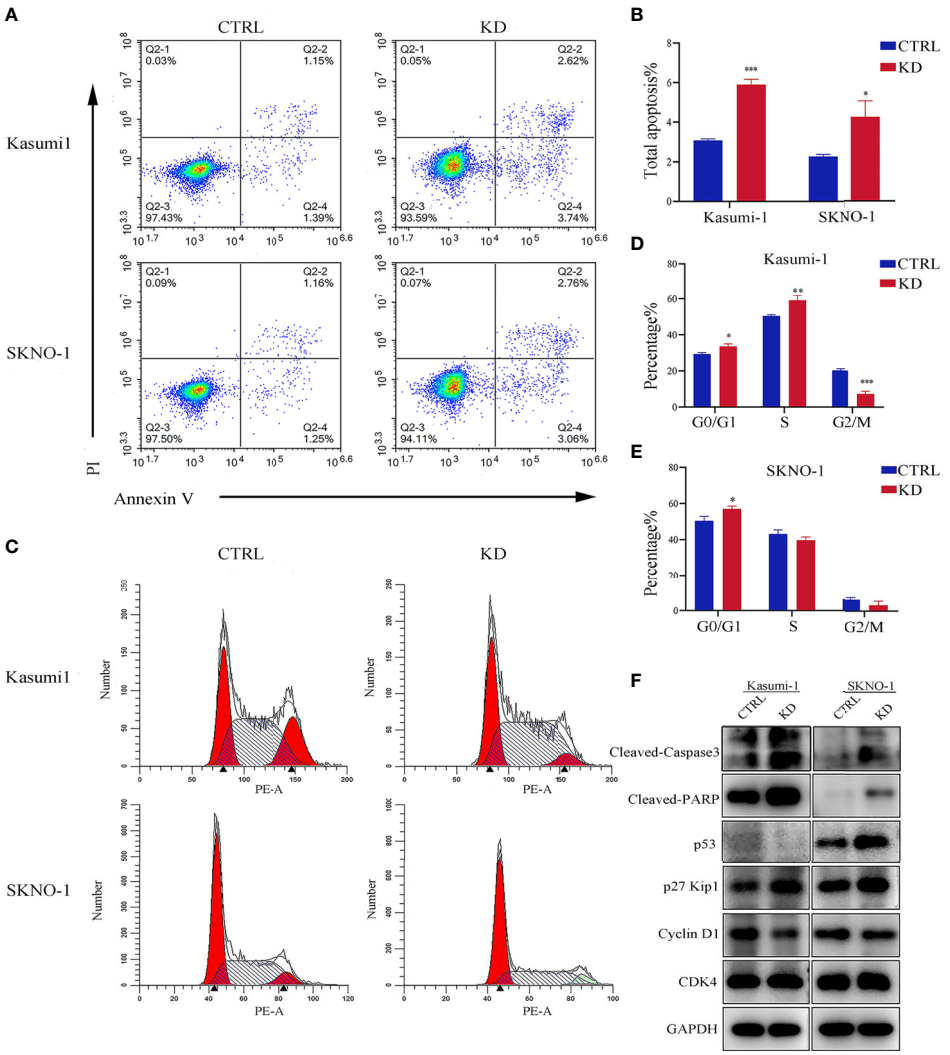

FIGURE 4 | Apoptosis and cell cycle analysis in AML cell lines. **(A, B)** The flow cytometry was utilized to analyze apoptosis in *GNA15* knockdown cells compared with control. **(C–E)** Cell cycle was determined with propidium iodide (PI) staining in CTRL and KD cells. **(F)** Alterations in apoptosis and cell cycle-related protein assay in *GNA15*-KD cells compared to those of their vector controls. CTRL, control; KD, knockdown; *$P < 0.05$ compared with CTRL cells; **$P < 0.01$ compared with CTRL cells; ***$P < 0.001$ compared with CTRL cells.

GNA15 participates in a variety of biological processes through interactions with a diverse set of cellular targets (26). Zanini et al. showed that down-regulation of *GNA15* significantly inhibited cell proliferation in small intestinal neuroendocrine neoplasia, and the expression levels of cell cycle-dependent kinase inhibitors p16 and p21 were significantly reduced (8). In this study, we also found that the down-regulation of *GNA15* significantly inhibited proliferation and colony formation of AML cell lines, an increased proportion of apoptotic cells, and inhibited cell cycle progression. These results indicate that *GNA15* plays an oncogene role in AML and is likely to become the potential therapeutic target of AML.

To further explore the mechanism of the biological function, we studied the changes in important signaling pathways related to proliferation, metabolism and autophagy in AML cell lines. Mitogen-activated protein kinase (MAPK) is one of the main signaling pathways mediating the growth and survival of tumor cells and plays important roles in regulating cell proliferation, cell cycle, apoptosis, migration and invasion (27–29). Our results revealed that the phosphorylated P38 MAPK was significantly reduced in the *GNA15*-KD cells, while the phosphorylated ERK, AMPKα, Smad3, Akt and LC3 A/B showed no change. The results indicated that the P38 MAPK pathway was involved in inhibiting the proliferation of AML mediated by *GNA15* knockdown. MAPK-activated protein kinase (MAPKAPK2) is a target of P38 MAPK and acts directly after phosphorylation of P38 MAPK, under stress conditions (30, 31). cAMP-response element binding protein (CREB) is a bZIP transcription factor

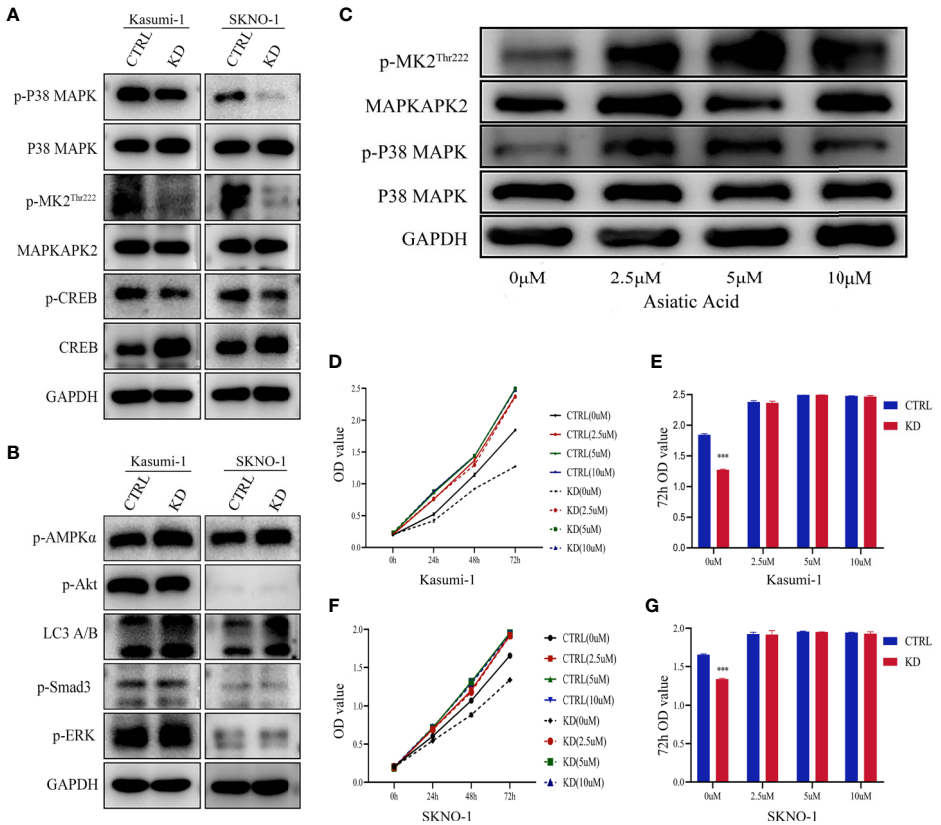

FIGURE 5 | P38 MAPK pathway is critical for GNA15-mediated alterations. **(A)** Western blot analysis of P38 MAPK pathway in GNA15-KD cells and controls. **(B)** Western blot analysis of other proliferation- and metabolism-related proteins in GNA15-KD cells and controls. **(C)** The upregulation of P38 MAPK signaling pathway by Asiatic Acid (P38 MAPK activator) in GNA15-KD cells of Kasumi-1. **(D, F)** Asiatic Acid (2.5μM, 5μM, 10μM) reversed the inhibitory effect of GNA15 knockdown on the proliferation of Kasumi-1 **(D)** and SKNO-1 **(F)**. **(E, G)** Asiatic Acid (2.5μM, 5μM, 10μM) reversed the inhibitory effect of GNA15 knockdown on the proliferation of Kasumi-1 **(E)** and SKNO-1 **(G)** at 72h. CTRL, control; KD, knockdown; p-MK2^{Thr222}: p-MAPKAPK2^{Thr222}; ***$P < 0.001$ compared with CTRL cells; Error bars indicate the standard deviation.

that can be activated by phosphorylated kinases such as MAPKAPK2, and then it activates the target gene through cAMP response elements to further mediate many physiological signaling transmission and regulate various cellular responses (32–34). Our research found that *GNA15* knockdown inhibited the expression of p-P38 MAPK and its downstream p- MAPKAPK2 and p-CREB, confirming that *GNA15* knockdown inhibits the activation of the p38 MAPK pathway. Moreover, a MAPK activator, Asiatic Acid, increased the protein level of p-P38MAPK and the downstream p-MAPKAPK2^{Thr222}, which in turn ameliorated the suppressed proliferation caused by *GNA15* knockdown. The xenograft tumor mouse model also showed that *GAN15* affects the growth of tumor tissues *in vivo* by regulating the P38 MAPK pathway. These results suggest that *GNA15* could modulate the growth and survival of AML cells by regulating the P38 MAPK pathway.

There are several limitations to our study. Firstly, our study was retrospective, and the inherent biases should not be neglected. The second limitation is the small sample size, especially in the subgroup analysis. Also, there is the potential for an interaction between *GNA15* transcript levels and gene mutation including *FLT3-ITD*. Due to these limitations, our present conclusions need to be further validated in prospectively randomized studies with large samples.

CONCLUSIONS

In summary, our research indicated that *GNA15* was highly expressed in adult AML, and the high expression of *GNA15* was independently correlated with worse OS and RFS in adult AML with normal karyotype. In addition, *GNA15* knockdown inhibited cell proliferation, promoted cell cycle arrest, and induced apoptosis of AML cells. Moreover, GNA15 modulated the growth of AML cells by regulating the P38 MAPK signaling pathway. Although the detailed mechanisms still require further investigation, our current research suggests *GNA15* may serve as a potential prognostic marker and a therapeutic target for AML in the future.

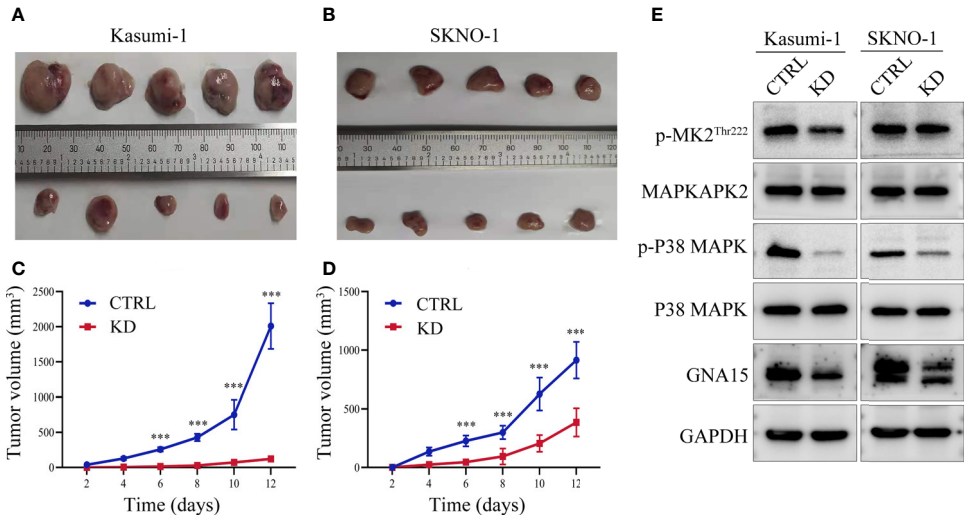

FIGURE 6 | *GNA15* knockdown reduces the proliferation ability of AML cells in nude mice by inhibiting the P38 MAPK signaling pathway. **(A–D)** *GNA15*-KD inhibits tumor growth in Kasumi-1 and SKNO-1 cells. **(E)** The expression of P38 MAPK signaling pathway proteins in tumor tissues by Western blot. CTRL, control; KD, knockdown; ***$P < 0.001$ compared with CTRL cells. Error bars indicate the standard deviation.

DATA AVAILABILITY STATEMENT

Publicly available datasets were analyzed in this study. This data can be found here: http://immuco.bjmu.edu.cn https://www.oncomine.org.

ETHICS STATEMENT

The studies involving human participants were reviewed and approved by the Ethics Committee of the First Affiliated Hospital of Zhengzhou University. Written informed consent for participation was not required for this study in accordance with the national legislation and the institutional requirements. The animal study was reviewed and approved by the Ethics Committee of the Zhengzhou University Animal Center.

AUTHOR CONTRIBUTIONS

Conceptualization and design: CW, SW, and YFL. Data acquisition: ML, YL, LY, YX, and WW. Methodology: SW and LY. Data analysis and interpretation: ML, CW, and SW; Writing (original draft): ML. Writing (review and editing): SW, CW, and YJL. Project administration: CW, SW, and ZJ.

FUNDING

This work was supported by the National Natural Science Foundation of China [grant number 81800137 and U1804191] and Henan Medical Science and Technique Foundation (grant number 2018020068).

ACKNOWLEDGMENTS

We thank all the treating physicians for allowing us to enroll their patients and the patients for allowing us to analyze their data.

SUPPLEMENTARY MATERIAL

The Supplementary Material for this article can be found online at: https://www.frontiersin.org/articles/10.3389/fonc.2021.724435/full#supplementary-material

REFERENCES

1. Chen Y, Cortes J, Estrov Z, Faderl S, Qiao W, Abruzzo L, et al. Persistence of Cytogenetic Abnormalities at Complete Remission After Induction in Patients With Acute Myeloid Leukemia: Prognostic Significance and the Potential Role of Allogeneic Stem-Cell Transplantation. *J Clin Oncol Off J Am Soc Clin Oncol* (2011) 29:2507–13. doi: 10.1200/JCO.2010.34.2873
2. Vandewalle V, Essaghir A, Bollaert E, Lenglez S, Graux C, Schoemans H, et al. miR-15a-5p and miR-21-5p Contribute to Chemoresistance in Cytogenetically Normal Acute Myeloid Leukaemia by Targeting PDCD4, ARL2 and BTG2. *J Cell Mol Med* (2021) 25:575–85. doi: 10.1111/jcmm.16110
3. Fehniger TA, Uy GL, Trinkaus K, Nelson AD, Demland J, Abboud CN, et al. A Phase 2 Study of High-Dose Lenalidomide as Initial Therapy for Older Patients With Acute Myeloid Leukemia. *Blood* (2011) 117:1828–33. doi: 10.1182/blood-2010-07-297143

4. Salmoiraghi S, Cavagna R, Zanghì P, Pavoni C, Michelato A, Buklijas K, et al. High Throughput Molecular Characterization of Normal Karyotype Acute Myeloid Leukemia in the Context of the Prospective Trial 02/06 of the Northern Italy Leukemia Group (NILG). *Cancers (Basel)* (2020) 12:2242. doi: 10.3390/cancers12082242
5. Wang SJ, Wang PZ, Gale RP, Qin YZ, Liu YR, Lai YY, et al. Cysteine and Glycine-Rich Protein 2 (CSRP2) Transcript Levels Correlate With Leukemia Relapse and Leukemia-Free Survival in Adults With B-Cell Acute Lymphoblastic Leukemia and Normal Cytogenetics. *Oncotarget* (2017) 8:35984–6000. doi: 10.18632/oncotarget.16416
6. Amatruda TT3rd, Steele DA, Slepak VZ, Simon MI. G Alpha 16, a G Protein Alpha Subunit Specifically Expressed in Hematopoietic Cells. *Proc Natl Acad Sci U S A* (1991) 88:5587–91. doi: 10.1073/pnas.88.13.5587
7. Chen H, Yao W, Jin D, Xia T, Chen X, Lei T, et al. Cloning, Expression Pattern, Chromosomal Localization, and Evolution Analysis of Porcine Gnaq, Gna11, and Gna14. *Biochem Genet* (2008) 46:398–405. doi: 10.1007/s10528-008-9158-6
8. Zanini S, Giovinazzo F, Alaimo D, Lawrence B, Pfragner R, Bassi C, et al. GNA15 Expression in Small Intestinal Neuroendocrine Neoplasia: Functional and Signalling Pathway Analyses. *Cell Signal* (2015) 27:899–907. doi: 10.1016/j.cellsig.2015.02.001
9. de Jonge HJ, Woolthuis CM, Vos AZ, Mulder A, van den Berg E, Kluin PM, et al. Gene Expression Profiling in the Leukemic Stem Cell-Enriched CD34+ Fraction Identifies Target Genes That Predict Prognosis in Normal Karyotype AML. *Leukemia* (2011) 25:1825–33. doi: 10.1038/leu.2011.172
10. Giannone F, Malpeli G, Lisi V, Grasso S, Shukla P, Ramarli D, et al. The Puzzling Uniqueness of the Heterotrimeric G15 Protein and its Potential Beyond Hematopoiesis. *J Mol Endocrinol* (2010) 44:259–69. doi: 10.1677/JME-09-0134
11. Dorsam RT, Gutkind JS. G-Protein-Coupled Receptors and Cancer. *Nat Rev Cancer* (2007) 7:79–94. doi: 10.1038/nrc2069
12. Wu J, Xie N, Zhao X, Nice EC, Huang C. Dissection of Aberrant GPCR Signaling in Tumorigenesis–a Systems Biology Approach. *Cancer Genomics Proteomics* (2012) 9:37–50.
13. Nguyen L, Masouminia M, Mendoza A, Samadzadeh S, Tillman B, Morgan T, et al. Alcoholic Hepatitis Versus non-Alcoholic Steatohepatitis: Levels of Expression of Some Proteins Involved in Tumorigenesis. *Exp Mol Pathol* (2018) 104:45–9. doi: 10.1016/j.yexmp.2017.12.007
14. Wu J, Qu J, Cao H, Jing C, Wang Z, Xu H, et al. Monoclonal Antibody AC10364 Inhibits Cell Proliferation in 5-Fluorouracil Resistant Hepatocellular Carcinoma via Apoptotic Pathways. *Onco Targets Ther* (2019) 12:5053–67. doi: 10.2147/ott.S206517
15. Gu Y, Feng Q, Liu H, Zhou Q, Hu A, Yamaguchi T, et al. Bioinformatic Evidences and Analysis of Putative Biomarkers in Pancreatic Ductal Adenocarcinoma. *Heliyon* (2019) 5:e02378. doi: 10.1016/j.heliyon.2019.e02378
16. Lu X, Lu J, Liao B, Li X, Qian X, Li K. Driver Pattern Identification Over the Gene Co-Expression of Drug Response in Ovarian Cancer by Integrating High Throughput Genomics Data. *Sci Rep* (2017) 7:16188. doi: 10.1038/s41598-017-16286-5
17. Wang S, Zhang Y, Liu Y, Zheng R, Wu Z, Fan Y, et al. Inhibition of CSRP2 Promotes Leukemia Cell Proliferation and Correlates With Relapse in Adults With Acute Myeloid Leukemia. *Onco Targets Ther* (2020) 13:12549–60. doi: 10.2147/ott.S281802
18. Ruan GR, Qin YZ, Chen SS, Li JL, Ma X, Chang Y, et al. Abnormal Expression of the Programmed Cell Death 5 Gene in Acute and Chronic Myeloid Leukemia. *Leuk Res* (2006) 30:1159–65. doi: 10.1016/j.leukres.2005.12.028
19. Wang S, Wang C, Wang W, Hao Q, Liu Y. High RASD1 Transcript Levels at Diagnosis Predicted Poor Survival in Adult B-Cell Acute Lymphoblastic Leukemia Patients. *Leuk Res* (2019) 80:26–32. doi: 10.1016/j.leukres.2019.03.005
20. Hospital MA, Jacquel A, Mazed F, Saland E, Larrue C, Mondesir J, et al. RSK2 is a New Pim2 Target With Pro-Survival Functions in FLT3-ITD-Positive Acute Myeloid Leukemia. *Leukemia* (2018) 32:597–605. doi: 10.1038/leu.2017.284
21. Döhner H, Estey E, Grimwade D, Amadori S, Appelbaum FR, Büchner T, et al. Diagnosis and Management of AML in Adults: 2017 ELN Recommendations From an International Expert Panel. *Blood* (2017) 129:424–47. doi: 10.1182/blood-2016-08-733196
22. Papaemmanuil E, Gerstung M, Bullinger L, Gaidzik VI, Paschka P, Roberts ND, et al. Genomic Classification and Prognosis in Acute Myeloid Leukemia. *N Engl J Med* (2016) 374:2209–21. doi: 10.1056/NEJMoa1516192
23. Tallman MS, Wang ES, Altman JK, Appelbaum FR, Bhatt VR, Bixby D, et al. Acute Myeloid Leukemia, Version 3.2019, NCCN Clinical Practice Guidelines in Oncology. *J Natl Compr Canc Netw* (2019) 17:721–49. doi: 10.6004/jnccn.2019.0028
24. Daher-Reyes G, Kim T, Novitzky-Basso I, Kim KH, Smith A, Stockley T, et al. Prognostic Impact of the Adverse Molecular-Genetic Profile on Long-Term Outcomes Following Allogeneic Hematopoietic Stem Cell Transplantation in Acute Myeloid Leukemia. *Bone Marrow Transplant* (2021) 56:1908–18. doi: 10.1038/s41409-021-01255-4
25. Stanchina M, Soong D, Zheng-Lin B, Watts JM, Taylor J. Advances in Acute Myeloid Leukemia: Recently Approved Therapies and Drugs in Development. *Cancers (Basel)* (2020) 12:3225. doi: 10.3390/cancers12113225
26. Yeung WW, Wong YH. Galpha16 Interacts With Class IA Phosphatidylinositol 3-Kinases and Inhibits Akt Signaling. *Cell Signal* (2010) 22:1379–87. doi: 10.1016/j.cellsig.2010.05.008
27. Liu K, Hu H, Jiang H, Zhang H, Gong S, Wei D, et al. RUNX1 Promotes MAPK Signaling to Increase Tumor Progression and Metastasis via OPN in Head and Neck Cancer. *Carcinogenesis* (2021) 42:414–22. doi: 10.1093/carcin/bgaa116
28. Asl ER, Amini M, Najafi S, Mansoori B, Mokhtarzadeh A, Mohammadi A, et al. Interplay Between MAPK/ERK Signaling Pathway and MicroRNAs: A Crucial Mechanism Regulating Cancer Cell Metabolism and Tumor Progression. *Life Sci* (2021) 278:119499. doi: 10.1016/j.lfs.2021.119499
29. Zhou XR, Li X, Liao LP, Han J, Huang J, Li JC, et al. P300/CBP Inhibition Sensitizes Mantle Cell Lymphoma to PI3Kδ Inhibitor Idelalisib. *Acta Pharmacol Sin* (2021) 0:1–13. doi: 10.1038/s41401-021-00643-2
30. Rouse J, Cohen P, Trigon S, Morange M, Alonso-Llamazares A, Zamanillo D, et al. A Novel Kinase Cascade Triggered by Stress and Heat Shock That Stimulates MAPKAP Kinase-2 and Phosphorylation of the Small Heat Shock Proteins. *Cell* (1994) 78:1027–37. doi: 10.1016/0092-8674(94)90277-1
31. Ben-Levy R, Leighton IA, Doza YN, Attwood P, Morrice N, Marshall CJ, et al. Identification of Novel Phosphorylation Sites Required for Activation of MAPKAP Kinase-2. *EMBO J* (1995) 14:5920–30. doi: 10.1002/j.1460-2075.1995.tb00280.x
32. Lonze BE, Riccio A, Cohen S, Ginty DD. Apoptosis, Axonal Growth Defects, and Degeneration of Peripheral Neurons in Mice Lacking CREB. *Neuron* (2002) 34:371–85. doi: 10.1016/s0896-6273(02)00686-4
33. Lee MM, Badache A, DeVries GH. Phosphorylation of CREB in Axon-Induced Schwann Cell Proliferation. *J Neurosci Res* (1999) 55:702–12. doi: 10.1002/(sici)1097-4547(19990315)55:6<702::Aid-jnr5>3.0.Co;2-n
34. Xing J, Kornhauser JM, Xia Z, Thiele EA, Greenberg ME. Nerve Growth Factor Activates Extracellular Signal-Regulated Kinase and P38 Mitogen-Activated Protein Kinase Pathways to Stimulate CREB Serine 133 Phosphorylation. *Mol Cell Biol* (1998) 18:1946–55. doi: 10.1128/mcb.18.4.1946

Conflict of Interest: The authors declare that the research was conducted in the absence of any commercial or financial relationships that could be construed as a potential conflict of interest.

Publisher's Note: All claims expressed in this article are solely those of the authors and do not necessarily represent those of their affiliated organizations, or those of the publisher, the editors and the reviewers. Any product that may be evaluated in this article, or claim that may be made by its manufacturer, is not guaranteed or endorsed by the publisher.

frontiers in Oncology

CASE REPORT
published: 13 September 2021
doi: 10.3389/fonc.2021.730503

Comprehensive Clinicopathologic and Molecular Analysis of Mast Cell Leukemia With Associated Hematologic Neoplasm: A Report and In-Depth Study of 5 Cases

Philippa Li[1†], *Giulia Biancon*[2†], *Timil Patel*[2], *Zenggang Pan*[1], *Shalin Kothari*[2], *Stephanie Halene*[2], *Thomas Prebet*[2] *and Mina L. Xu*[1*]

[1] Department of Pathology, Yale School of Medicine, New Haven, CT, United States, [2] Section of Hematology, Department of Internal Medicine and Yale Comprehensive Cancer Center, Yale School of Medicine, New Haven, CT, United States

OPEN ACCESS

Edited by:
Robert Ohgami,
University of California, San Francisco,
United States

Reviewed by:
Sanjay Patel,
Cornell University, United States
Michael Kluk,
Weill Cornell Medical Center,
United States

***Correspondence:**
Mina L. Xu
mina.xu@yale.edu

[†]These authors have contributed equally to this work

Specialty section:
This article was submitted to Hematologic Malignancies, a section of the journal Frontiers in Oncology

Received: 25 June 2021
Accepted: 17 August 2021
Published: 13 September 2021

Citation:
Li P, Biancon G, Patel T, Pan Z, Kothari S, Halene S, Prebet T and Xu ML (2021) Comprehensive Clinicopathologic and Molecular Analysis of Mast Cell Leukemia With Associated Hematologic Neoplasm: A Report and In-Depth Study of 5 Cases. Front. Oncol. 11:730503. doi: 10.3389/fonc.2021.730503

Mast cell leukemia with associated hematologic neoplasm (MCL-AHN) is a rare and highly aggressive entity that remains understudied due to the paucity of cases. We present a case of a 45-year-old man who was concurrently diagnosed with mast cell leukemia and acute myeloid leukemia. We identified four additional patients who had MCL-AHN in our institution and performed whole-exome sequencing of all available tumors. Our series revealed a novel and identical *NR2F6* variant shared among two of the patients. This case series and sequencing results demonstrate the importance of fully characterizing rare tumors that are resistant to treatment.

Keywords: mast cell leukemia, associated hematologic neoplasm, whole-exome sequencing, acute myeloid leukemia, systemic mastocytosis (SM)

INTRODUCTION

Mast cell leukemia (MCL) is an exceedingly rare and aggressive form of systemic mastocytosis (SM), carrying a poor prognosis with median survival time of less than 6 months (1, 2). The diagnostic criteria of MCL require mast cell (MC) involvement of >20% of the bone marrow aspirate and can be further classified into typical/classic MCL (≥10% MCs in peripheral blood) or aleukemic variant (<10% MCs in peripheral blood) (1). MCL can arise *de novo* or by transformation from other SM subtypes (1). Furthermore, it can be diagnosed with an associated hematologic neoplasm, so-called MCL-AHN.

Somatic gain-of-function mutations in the coding region of *KIT* are identified in >80% of SM, most frequently *KIT* D816V (1). Unfortunately, despite this frequently identified targetable mutation, SM is often refractory to medical treatment. Given the advancements in molecular studies, more complex genetic profiles have been described in SM. We present comprehensive clinicopathologic features of five cases of MCL-AHN coupled with results from in-depth targeted DNA sequencing and whole-exome

Abbreviations: MCL, mast cell leukemia; SM, systemic mastocytosis; MC, mast cell; MCL-AHN, mast cell leukemia with associated hematologic neoplasm; AML, acute myeloid leukemia; ETP-ALL, early T-cell precursor acute lymphoblastic leukemia; WES, whole-exome sequencing; BM, bone marrow; PB, peripheral blood.

sequencing (WES). In addition to mutations in *KIT* and other genes associated with hematologic malignancies, our series revealed a novel and identical *NR2F6* variant shared among two of the patients. This advocates for the integration of high-throughput genomic profiling to better understand the molecular landscape of this disease process.

CASE DESCRIPTION

Patient 1 is a 45-year-old man with no significant past medical history. He presented to the hospital with abdominal pain and malaise of 2 weeks. Laboratory studies were notable for macrocytic anemia (10.6 g/dl, reference range 12.0–18.0 g/dl; 102.0 fl, reference range 78.0–94.0 fl) and profound thrombocytopenia (19,000/µl, reference range 140,000–440,000/µl). Initial bloodwork also identified 33% blasts in the peripheral blood. Physical exam was notable for a palpable spleen to the left umbilicus with mild tenderness to palpation. An ultrasound examination demonstrated an enlarged spleen measuring 22.2 × 21.0 cm without focal lesions or perisplenic collections. The patient was subsequently admitted to the hematology service for further workup.

Bone marrow biopsy (**Figure 1**) demonstrated markedly hypercellular marrow (90% cellular), with approximately 50% of the cellularity composed of pale, round, degranulated mast cells scattered and in clusters, aberrantly expressing CD25. Aspirate smears revealed approximately 48% abnormal degranulated mast cells and 23% myeloblasts. The patient was diagnosed with mast cell leukemia, aleukemic variant, with concurrent acute myeloid leukemia (MCL-AML). His serum tryptase level was 614 µg/l (reference range <11.0 µg/l) at the time of diagnosis.

The patient received chemotherapy with 7 + 3 regimen (cytarabine 100 mg/m^2/day and idarubicin 12 mg/m^2) with midostaurin (50 mg daily). After salvage cladribine (0.13 mg/kg daily for 5 days) with high-dose midostaurin, his recovery marrow showed persistent mast cell leukemia with no increase in blasts. The patient was subsequently switched to avapritinib, and his tryptase levels decreased from 391 to 22 UI/l after 6 months. The patient's bone marrow at 8 months following initial diagnosis showed 15% mast cells without evidence of AML, compared to 50% mast cells at initiation of avapritinib. He received a matched unrelated donor peripheral blood stem cell transplant 10 months after initial diagnosis, which was complicated by severe gastrointestinal graft-versus-host-disease. Currently, the patient is 17 months from his initial diagnosis; he remains on avapritinib with regular follow-up.

Four additional patients with MCL-AHN were identified within our institution, and all available records were reviewed (**Table 1**). Patient 2 was a 71-year-old man who presented for evaluation of extreme fatigue. Workup revealed early T-cell precursor acute lymphoblastic leukemia (ETP-ALL), and the patient was started on combination chemotherapy consisting of 6-mercaptopurine, vincristine, methotrexate, and prednisone (POMP) with low-intensity intrathecal methotrexate. A posttreatment bone marrow biopsy/aspirate 3 months later demonstrated no evidence of residual leukemia but marked mastocytosis (63%) with aberrant positive expression of CD25 and CD2, consistent with MCL. Flow cytometry revealed recurrent ETP-ALL 19 months after the first diagnosis of malignancy despite maintenance chemotherapy. He died of disease 2 months later.

Patient 3 was a 74-year-old man who was evaluated 14 years prior for chronic anemia. His bone marrow biopsy at that time revealed myelodysplastic syndrome with ringed sideroblasts, and he

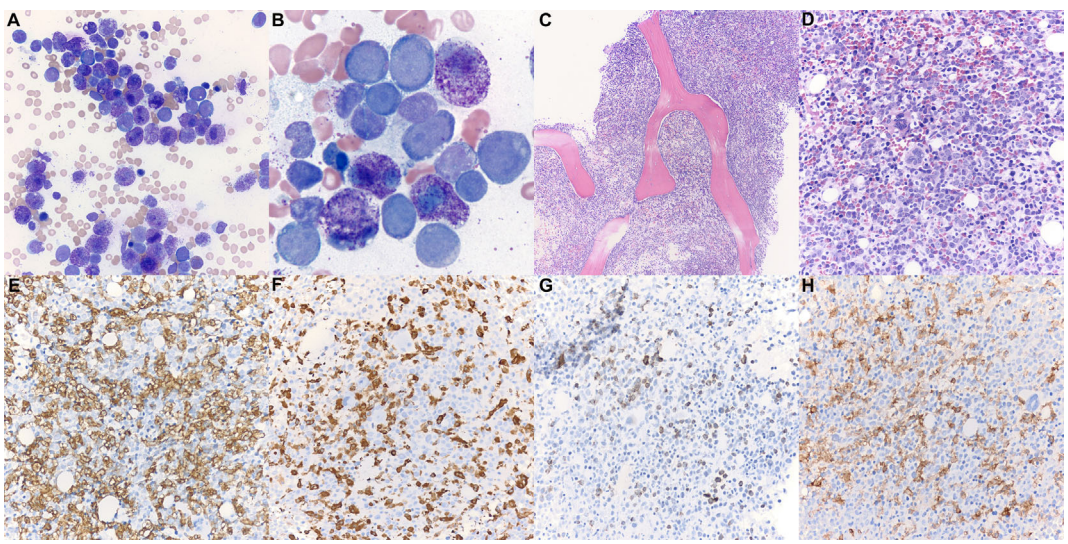

FIGURE 1 | Patient 1 bone marrow aspirate and trephine biopsy. **(A, B)** Bone marrow aspirate smear (Wright-Giemsa, ×400, ×1,000) is notable for numerous mast cells intermixed with myeloblasts. Degranulated mast cells are interspersed throughout the bone marrow aspirate smear. **(C)** The bone marrow biopsy (H&E, ×100) demonstrates hypercellular marrow for age (90% cellularity). **(D)** Approximately 50% of the cellularity is composed of mast cells with oval nuclei, and hypogranulated cytoplasm (H&E, ×400). Blast elements and other marrow elements are scattered throughout. **(E)** CD117 immunostain (×400) highlights abundant mast cells. **(F)** Mast cell tryptase immunostain (×400). **(G)** CD34 immunostain (×400) highlights blast elements, comprising >20% of non-mast cell cellularity. **(H)** CD25 immunostain (×400) is positive in the neoplastic mast cells.

TABLE 1 | Summary of MCL-AHN cases.

	Patient 1	Patient 2	Patient 3	Patient 4	Patient 5
Age (at diagnosis of first hematologic malignancy), race, and gender	45 yo Caucasian male	71 yo Caucasian male	74 yo Caucasian male	60 yo Caucasian male	68 yo Caucasian female
MCL type	Aleukemic *de novo* MCL	Aleukemic *de novo* MCL, subsequent diagnosis	Aleukemic secondary MCL, subsequent diagnosis	Aleukemic secondary MCL, subsequent diagnosis	Aleukemic *de novo* MCL, subsequent diagnosis
AHN type	AML without maturation	ETP-ALL	MDS with ringed sideroblasts	AML NOS	AML with t(8;21)
Aspirate findings at diagnosis	23% blasts and 48% mast cells	31% lymphoblasts on initial aspirate, 63% mast cells on aspirate	3% myeloblasts on initial aspirate, 20% mast cells on subsequent aspirate	78% myeloblasts and <5% mast cells on initial aspirate, 37% mast cells on subsequent aspirate	72% myeloblasts on initial aspirate, 34% mast cells on subsequent aspirate
Cytogenetics	Trisomy 8q, trisomy 21	Normal 46, *XY* male karyotype	Normal 46, *XY* male karyotype	Failed cytogenetics	Positive *RUNX1T1/RUNX1* fusion
S/A/R status[‡]	S/A/R^{pos}	Unknown	S/A/R^{neg}	Unknown	S/A/R^{neg}
Outcome	Alive	Deceased	Deceased	Deceased	Deceased
Interval time between MCL and AHN	Concurrent diagnoses	3 months	9 years 10 months	10 months	2 months
Survival time from first diagnosed malignancy	17 months	21 months	14 years 3 months	21 months	47 months

MCL, mast cell leukemia; AHN, associated hematologic neoplasm; AML, acute myeloid leukemia; ETP-ALL, early T-cell precursor acute lymphoblastic leukemia; MDS, myelodysplastic syndrome; [‡] *S/A/R status indicates any mutation present in panel of SRSF2, ASXL1, and RUNX1.*

was managed on observation. Eight years later, a repeat marrow biopsy was performed for worsening anemia, demonstrating persistent myelodysplastic syndrome and 3% mast cells. He was started on Aranesep and red blood cell transfusions. Repeat bone marrow 2 years later revealed persistent myeloid neoplasm with mast cell aspirate count of 20%, consistent with MCL-AHN. He began midostaurin and received darbepoetin every other week. The patient died 4 years after the diagnosis of MCL-AHN from pneumonia with persistent mastocytosis at time of death.

Patient 4 was a 60-year-old man who presented to the hospital with a suspected cardiovascular accident. His initial bone marrow biopsy demonstrated AML with abnormal mast cells (positive for CD25 and CD2) involving <5% marrow cellularity. He was treated with standard induction chemotherapy followed by consolidation. A repeat marrow biopsy 10 months later demonstrated no evidence of AML but 37% mast cells consistent with MCL. He received cladribine, then switched to midostaurin for persistent disease. The patient failed to respond significantly to any MCL therapy, and subsequent bone marrow biopsies continued to show persistent MCL without evidence of AML. He died of disease less than 2 years after his initial diagnosis.

Patient 5 was a 68-year-old female who was diagnosed with AML after presenting with fatigue and increased peripheral blood myeloblasts. The patient was started on standard induction chemotherapy and achieved morphologic remission on day 14. One month later, a bone marrow aspirate revealed 11% myeloblasts with 34% mast cells, which aberrantly expressed CD25. The patient underwent consolidation therapy with a matched unrelated donor stem cell transplant. Unfortunately, the patient demonstrated AML relapse and persistent low-level mastocytosis. She died of disease 47 months after her initial diagnosis of AML.

METHODOLOGY

Available specimens from all five MCL-AHN patients were subjected to molecular profiling: allele-specific PCR for *KIT* mutation on residue 816, targeted DNA-sequencing for genes relevant in myeloid neoplasms, and/or whole-exome sequencing (WES) combined with a high-coverage spike-in panel for known cancer-associated genes (see **Supplementary Methodology**). Patient 1 specimens were pretreatment bone marrow (BM), with involvement by MCL-AML, and buccal swab as matched normal sample. Patient 2 specimen was peripheral blood (PB) with involvement by ETP-ALL 1 month prior to the diagnosis of MCL, and PB at MCL diagnosis. Patient 3 and 4 specimens were PB at the time of MCL diagnosis. Patient 5 pretreatment PB was drawn at diagnosis of AML, while her subsequent BM sampled 3 months later was remission AML, with involvement by MCL only (**Tables 1**, **2**).

Targeted Sequencing Panel

Tumor specimens from patients 1 (BM), 3 (PB), and 5 (PB, BM) underwent high-throughput genotyping analysis by the Tumor Profiling Laboratory at Yale New Haven Hospital. Genomic DNA was extracted from the specimens and amplified using 1,298 primer pairs, designed with Ion Torrent AmpliSeq

TABLE 2 | Molecular profiling results.

Patient 1		
Timepoint	MCL-AHN	
Source	BM	
Molecular Method	targeted DNA-seq, WES	
Variants:		
KIT c.2447A>T p.D816V, COSMIC: COSV55386424, dbSNP: rs121913507	32.6	
PHF6 c.1024C>T p.R342X, COSMIC: COSV59699091, dbSNP: rs132630297	13.7	
RUNX1 c.319C>T p.R107C, COSMIC: COSV55866866	45.6	
Patient 2		
Timepoint	ETP-ALL	MCL-AHN
Source	PB	PB
Molecular Method	WES	PCR
Variants:		
KIT c.2447A>T p.D816V, COSMIC: COSV55386424, dbSNP: rs121913507	n/d	present
DHRS4L2 c.236A>G p.E79G, COSMIC: COSV58730199	2.4	
DNMT3A c.2656C>G p.Q886E, COSMIC: COSV53044466, dbSNP: rs752280049	15.9	
EXOC7 c.1826G>A p.R609Q, COSMIC: COSV58035445, dbSNP: rs768692750	50.0	
JAK2 c.1849G>T p.V617F, COSMIC: COSV67569051, dbSNP: rs77375493	4.3	
NR2F6 c.394C>G p.P132A, COSMIC: COSV52244108, dbSNP: rs202200760	47.8	
PTPN11 c.179G>T p.G60V, COSMIC: COSV61005028, dbSNP: rs397507509	5.9	
Patient 3		
Timepoint	MCL-AHN	
Source	PB	
Molecular Method	targeted DNA-seq	
Variants:		
KIT c.2447A>T p.D816V, COSMIC: COSV55386424, dbSNP: rs121913507	7.0	
CBL c.1228-2A>G splice acceptor variant, COSMIC: COSV50629953, dbSNP: rs727504426	10.0	
SF3B1 c.2098A>G p.K700E, COSMIC: COSV59205318, dbSNP: rs559063155	36.0	
Patient 4		
Timepoint	MCL-AHN	
Source	PB	
Molecular Method	PCR	
Variants:		
KIT c.2447A>T p.D816V, COSMIC: COSV55386424, dbSNP: rs121913507	present	
Patient 5		
Timepoint	AML	MCL-AHN
Source	PB	BM
Molecular Method	targeted DNA-seq, WES	targeted DNA-seq, WES
Variants:		
KIT c.2447A>T p.D816V, COSMIC: COSV55386424, dbSNP: rs121913507	33.8	n/d
ANO4 c.2747G>A p.R916Q, COSMIC: COSV54611712, dbSNP: rs267603265	50.6	39.4
CACNA1C c.5737G>A p.E1913K, COSMIC: COSV59697224, dbSNP: rs200231105	7.3	10.2
DNM2 c.1072G>A p.G358R, COSMIC: COSV58965871, dbSNP: rs267606772	4.1	n/d
GNB1 c.169A>G p.K57E, COSMIC: COSV66100005, dbSNP: rs141326438	n/d	13.6
JAK2 c.1849G>T p.V617F, COSMIC: COSV67569051, dbSNP: rs77375493	4.2	n/d
NR2F6 c.394C>G p.P132A, COSMIC: COSV52244108, dbSNP: rs202200760	43.4	35.3
WFIKKN2 c.244G>A p.V82I, COSMIC: COSV60958856, dbSNP: rs562819910	54.0	47.6

Variants are defined by: gene, coding sequece change, amino acid chage, COSMIC ID, dbSNP ID if available, variant allele frequency (color-coded according to the values; lowest value in blue, highest value in orange).

For samples with targeted DNA-seq and WES profiling, only the WES frequency is reported.

After KIT variant, the other variants are reported in alphabetical order. Variants identified in more than one sample are underlined.

MCL-AHN, mast cell leukemia with associated hematologic neoplasm; AML, acute myeloid leukemia; BM, bone marrow; WES, whole exome sequencing; ETP-ALL, early T-cell precursor acute lymphoblastic leukemia; PB, peripheral blood; PCR, polymerase chain reaction.

software, covering full exonic regions or hotspot regions of selected genes (see **Supplementary Methodology**). Next-generation sequencing was performed on the Ion Torrent S5 Sequencer.

Whole-Exome Sequencing

Additional tumor specimens from patients 1 (BM), 2 (PB), and 5 (PB, BM) underwent WES with a high-coverage spike-in panel for known cancer-associated genes developed at the Yale Center for Genome Analysis in collaboration with Integrated DNA technologies (IDT) and the Yale Cancer Center. Tumor DNA was extracted from bone marrow cells or peripheral blood cells after Ficoll separation. Normal DNA for Patient 1 was extracted from buccal swab. DNA extraction was performed using the QIAGEN DNeasy Blood & Tissue Kit according to the manufacturer's instructions. WES libraries were prepared adding spike-ins for cancer genes and sequenced on the Illumina NovaSeq sequencer (paired-end, 100bp).

DISCUSSION

To date, the most significant prognostic indicator for MCL patients is mutational status in any of the *SRSF2*, *ASXL1*, or *RUNX1* genes, collectively referred to as S/A/R gene panel (3). In a study cohort of 25 MCL patients, approximately half demonstrated S/A/R^{pos} status (1), which correlated with more aggressive phenotypes, more (intrinsic) resistance to disparate treatment modalities, and worse treatment response in comparison to S/A/R^{neg} patients (1). In our cohort, only patient 1 was S/A/R^{pos} due to a *RUNX1* mutation (**Table 1**). The S/A/R status of patients 2 and 4 is unknown due to limited molecular study results.

The PB sample of Patient 5 was taken at the diagnosis of AML without known evidence of MC disease and contained the following variants: *KIT* p.D816V, *ANO4* p.R916Q, *CACNA1C* p.E1913K, *DNM2* p.G358R, *JAK2* p.V617F, *WFIKKN2* p.V82I, and *NR2F6* p.P132A. Her BM specimen following treatment showed no evidence of leukemia but did contain MCL. This subsequent specimen demonstrated the following variants: *GNB1* p.K57E, *ANO4* p.R916Q, *CACNA1C* p.E1913K, *WFIKKN2* p.V82I, and *NR2F6* p.P132A. Peripheral blood sequencing identified the *KIT* p.D816V mutation, which may have hinted at early/evolving MCL disease. Interestingly, the *KIT* mutation is not identified on the later BM specimen, possibly indicating treatment effect on *KIT*+ mast cells (**Table 2** and **Supplementary Figure 1**).

We also identified identical missense *NR2F6* variants in patients 2 and 5, previously undescribed in SM. *NR2F6* (nuclear receptor subfamily 2, group F, member 6) is an orphan member of the nuclear receptor superfamily (4). This variant is clinically interesting due to studies demonstrating that *NR2F6-/-* mice had enhanced IL-2 and IFN-gamma secretion, favoring T cell-mediated cancer cell elimination (4). *NR2F6*-deficient tumor-bearing mice have enhanced survival *via* T cell-dependent antitumor immunity (4). This is a possible means to potentiate established PD-L1 and CTLA-4 blockade therapies (4, 5). Further studies will be necessary to determine the function of the *NR2F6* p.P132A missense variant observed in these cases, exploring the somatic pathogenicity or the germline predisposition for MCL.

In MCL, *KIT* p.D816V is found in approximately 55% of cases, which is lower in frequency than in other forms of advanced SM (2). Even though all our patients demonstrated the *KIT* p.D816V mutation in at least one specimen (**Table 2**), none of them demonstrated durable response to targeted therapy. The average survival time was 32 months following the diagnosis of MCL. The only patient to have considerable survival time after the first hematologic diagnosis was patient 3, who had a less aggressive AHN with a long interval time prior to the development of MCL.

Avapritinib, a new tyrosine-kinase inhibitor targeting *KIT* and its mutants, is the most recent addition to our drug armamentarium and has shown some remarkable activity in less aggressive presentations (6). Its use in advanced forms of mast cell disease such as MCL is scarce, but the treatment response presented in patient 1 is encouraging.

The direction of hematologic malignancies has increasingly leaned toward molecular profiling, which would aid in the diagnosis, prognosis, and identification of potential novel treatment options. We conducted a pilot study on five patients affected by MCL-AHN. Despite the small size of the patient cohort due to the rarity of the disease and the limited specimen availability given the nature of retrospective studies, the application of a boosted whole-exome sequencing allowed us to detect somatic variants at the whole-exome level without losing depth in regions frequently affected by cancer-associated mutations, resulting in a comprehensive and deep characterization of MCL-AHN molecular features. MCL has proven to be largely resistant to treatment, despite frequently identified *KIT* mutations. The molecular aberrations of MCL-AHN identified presently are not well understood but could be of potential value in treatment guidance.

DATA AVAILABILITY STATEMENT

The original contributions presented in the study are included in the article/**Supplementary Material**. Further inquiries can be directed to the corresponding author.

ETHICS STATEMENT

The studies involving human participants were reviewed and approved by Yale University IRB. The patients/participants provided their written informed consent to participate in this study.

AUTHOR CONTRIBUTIONS

PL, GB, and MX designed and performed the research as well as wrote the manuscript. PL and MX collected patient samples. GB analyzed next-generation sequencing data. TPa, ZP, SK, SH, and TPr revised the clinical data and edited the manuscript. All authors contributed to the article and approved the submitted version.

FUNDING

This work was in part supported by the DeLuca Center for Innovation in Hematology Research at Yale Cancer Center and The Frederick A. Deluca Foundation.

ACKNOWLEDGMENTS

We would like to thank Allen Bale, Daniel Dykas, Preti Jain, Irina Tikhonova, and Kaya Bilguvar for contributing to the whole-exome/cancer-exome sequencing.

SUPPLEMENTARY MATERIAL

The Supplementary Material for this article can be found online at: https://www.frontiersin.org/articles/10.3389/fonc.2021.730503/full#supplementary-material

REFERENCES

1. Jawhar M, Schwaab J, Meggendorfer M, Naumann N, Horny HP, Sotlar K, et al. The Clinical and Molecular Diversity of Mast Cell Leukemia With or Without Associated Hematologic Neoplasm. *Haematologica* (2017) 102(6):1035–43. doi: 10.3324/haematol.2017.163964
2. Georgin-Lavialle S, Lhermitte L, Dubreuil P, Chandesris MO, Hermine O, Damaj G. Mast Cell Leukemia. *Blood* (2013) 121(8):1285–95. doi: 10.1182/blood-2012-07-442400
3. Jawhar M, Schwaab J, Schnittger S, Meggendorfer M, Pfirrmann M, Sotlar K, et al. Additional Mutations in SRSF2, ASXL1 and/or RUNX1 Identify a High-Risk Group of Patients With KIT D816V+ Advanced Systemic Mastocytosis. *Leukemia* (2016) 30(1):136–43. doi: 10.1038/leu.2015.284
4. Hermann-Kleiter N, Klepsch V, Wallner S, Siegmund K, Klepsch S, Tuzlak S, et al. The Nuclear Orphan Receptor NR2F6 Is a Central Checkpoint for Cancer Immune Surveillance. *Cell Rep* (2015) 12(12):2072–85. doi: 10.1016/j.celrep.2015.08.035
5. Klepsch V, Hermann-Kleiter N, Do-Dinh P, Jakic B, Offermann A, Efremova M, et al. Nuclear Receptor NR2F6 Inhibition Potentiates Responses to PD-L1/PD-1 Cancer Immune Checkpoint Blockade. *Nat Commun* (2018) 9(1):1538. doi: 10.1038/s41467-018-04004-2
6. Rossignol J, Polivka L, Maouche-Chrétien L, Frenzel L, Dubreuil P, Hermine O. Recent Advances in the Understanding and Therapeutic Management of Mastocytosis. *F1000Res* (2019) 8:8. doi: 10.12688/f1000research.19463.1

Conflict of Interest: MX serves as a consultant (advisory board) for Blueprint Medicines and for Seattle Genetics.

The remaining authors declare that the research was conducted in the absence of any commercial or financial relationships that could be construed as a potential conflict of interest.

frontiers in Oncology

REVIEW
published: 23 September 2021
doi: 10.3389/fonc.2021.729550

A Different View for an Old Disease: NEDDylation and Other Ubiquitin-Like Post-Translational Modifications in Chronic Lymphocytic Leukemia

Víctor Arenas[†], *Jose Luis Castaño*[†], *Juan José Domínguez-García*, *Lucrecia Yáñez and Carlos Pipaón*[*]

Laboratorio de Hematología Molecular, Servicio de Hematología, Hospital Universitario Marqués de Valdecilla-Instituto de Investigación Marqués de Valdecilla (IDIVAL), Santander, Spain

OPEN ACCESS

Edited by:
Mina Luqing Xu,
Yale University, United States

Reviewed by:
Filomena De Falco,
University of Perugia, Italy
Dimitris Xirodimas,
Délégation Ile-de-France Sud (CNRS), France

***Correspondence:**
Carlos Pipaón
carlos.pipaon@scsalud.es
orcid.org/0000-0002-3851-6710

[†]*These authors have contributed equally to this work and share first authorship*

Specialty section:
This article was submitted to Hematologic Malignancies, a section of the journal Frontiers in Oncology

Received: *23 June 2021*
Accepted: *07 September 2021*
Published: *23 September 2021*

Citation:
Arenas V, Castaño JL, Domínguez-García JJ, Yáñez L and Pipaón C (2021) A Different View for an Old Disease: NEDDylation and Other Ubiquitin-Like Post-Translational Modifications in Chronic Lymphocytic Leukemia. Front. Oncol. 11:729550. doi: 10.3389/fonc.2021.729550

Despite the enormous amount of molecular data obtained over the years, the molecular etiology of chronic lymphocytic leukemia (CLL) is still largely unknown. All that information has enabled the development of new therapeutic approaches that have improved life expectancy of the patients but are still not curative. We must increase our knowledge of the molecular alterations responsible for the characteristics common to all CLL patients. One of such characteristics is the poor correlation between mRNA and protein expression, that suggests a role of post-translational mechanisms in CLL physiopathology. Drugs targeting these processes have indeed demonstrated an effect either alone or in combination with other aimed at specific pathways. A recent article unveiled an increment in ubiquitin-like modifications in CLL, with many protein members of relevant pathways affected. Interestingly, the inhibition of the NEDD8-activating protein NAE reverted a substantial number of those modifications. The present review gets the scarce data published about the role of NEDDylation in CLL together and establishes connections to what is known from other neoplasias, thus providing a new perspective to the underlying mechanisms in CLL.

Keywords: chronic lymphocytic leukemia, post-translational modifications, ubiquitin, NEDD8, MLN4924-pevonedistat

CHRONIC LYMPHOCYTIC LEUKEMIA

Chronic lymphocytic leukemia (CLL) is the most frequent lymphoid malignancy in the Western world and appears typically in the elderly. The diagnosis of this disease requires the presence of ≥5 x10^9/L monoclonal mature CD19+ CD5+ B cells with a characteristic phenotype that usually infiltrates the blood, bone marrow and lymphoid tissues (1). CLL has a very heterogeneous clinical course: some patients show a stable course without the requirement for therapy, while others show a more aggressive disease requiring early treatment and, in some cases, turning into an aggressive lymphoma (Richter transformation) (1). In the last 30 years, many aspects on its biology have been unraveled. The discovery of the dysregulation of several survival pathways or the importance of BCR signaling in the maintenance of the tumoral cells (2), has uncovered new therapeutic targets. Nevertheless, our knowledge about the causes of this chronic disease is still quite poor.

PHYSIOPATHOLOGY OF CLL

The physiopathology of CLL is a complex process that can be explained in part by a sequence of events that lead to the transformation of a normal B CD5+ cell into a neoplastic cell. The starting point of the disease is not well known. The fact that CLL develops in the adult population suggests that aging-related factors, unknown at present, play an essential role in the pathogenesis of the disease. In approximately 10% of the patients, a genetic predisposition may explain the development of CLL (3). Other initiation factors such as a dysfunction on the immune system related to some infections or the exposition to certain toxics have been speculated, but to date none of them has been reliably verified.

In cancer, the neoplastic transformation usually starts with an alteration of the chromosomal material and in approximately 80% of patients with CLL at least one of four common chromosomal abnormalities (Chromosome 13q deletion, chromosome 12 trisomy, chromosome 11q deletion and chromosome 17p deletion) can be detected by interphase fluorescence *in situ* hybridization (FISH) at the moment of diagnosis or in their evolution. A model of sequential chromosomal abnormalities and genetic mutations has been proposed, defining early, intermediate and late drivers that allow CLL cells to develop and evolve. Chromosome 13q deletion, chromosome 12 trisomy and mutations in MYD88 or NOTCH1 are considered early drivers of the disease while the acquisition of chromosome 11q or chromosome 17p deletions as well as mutations in genes frequently mutated in cancer (TP53, ATM, SF3B1 or NRAS) appear during CLL progression (4).

The microenvironment has also been related to the proliferation, survival, and drug resistance in B cell neoplasms like multiple myeloma, mantle cell lymphoma and specifically CLL. Mesenchymal cells, nurse-like and lymphoma-associated macrophagic cells, natural killer and other T cells, interact with CLL neoplastic cells engaging some receptors like BCMA, TACI, BAFF-R or VLA-4, thus activating anti-apoptotic pathways and promoting the secretion of cytokines, chemokines, growth factors and adhesion molecules allowing the extended survival of the malignant B cell (5).

GENOMIC STUDIES IN CLL

Over the last years, a great effort has been put in trying to identify the genomic causes of CLL. As a result of these studies, several genes have been identified as involved in the pathogenesis of the disease. Among those are TP53, NOTCH1, BIRC3, SF3B1 or ATM (2, 6, 7). Nevertheless, the mutations affecting them do not exceed a 15% of penetration, so there are still many issues to be solved. Taking into account the somatic mutations, the cytogenetic alterations and the mutations in non-coding regions, they conclude CLL relates to alterations in eight signaling pathways: B cell receptor, cell cycle regulation, apoptosis, response to DNA damage, chromatin remodeling, RNA metabolism and Notch and NF-kB pathways (7).

CURRENT THERAPIES

For many years, chemotherapy was the treatment of choice for patients with CLL. However, the improvement in the knowledge of the molecular processes involved in CLL pathogenesis has marked current therapeutic strategies. The discovery of the importance of B-cell antigen receptor (BCR) signaling in CLL cells completely changed the landscape in the treatment of this disease. BCR engagement leads to a massive recruitment of kinases to the plasma membrane that transduce the signal to many effector pathways and transcription factors essential for B lymphocyte survival and proliferation. To date, drugs against phosphoinositide 3-kinase (PI3K) (idelalisib, duvelisib, copanlisib, umbralisib) and Bruton´s Tyrosine Kinase (BTK) (ibrutinib, acalabrutinib, zanubrutinib, pirtobrutinib) have been studied, and some approved, for the therapy of patients with CLL with excellent results, not only in progression free survival but also in overall survival, in comparison to standard chemoimmunotherapy (8).

The involvement of Bcl-2 in the prolonged survival of B-CLL cells is long known (9). However, the toxicity related to the first in class Bcl-2 inhibitor, navitoclax, prevented this drug from being used in the past. Recently, a new Bcl-2 specific inhibitor, venetoclax, has demonstrated a huge activity against B-CLL cell survival with an excellent toxicity profile and nowadays is broadly used to achieve a deep response that allow to stop the treatment (10).

NEDDylation

NEDDylation is a post-translational modification consisting in the covalent conjugation of a NEDD8 peptide with target proteins at lysine residues. NEDD8 is one of the ubiquitin-like peptides (UBLs), with 80% homology to ubiquitin and an activation and conjugation mechanism absolutely analogous (**Figure 1**). This occurs through the sequential action of three enzymes generally termed as E1, E2 and E3. NAE is the specific E1 that activates NEDD8 and is the target of an investigational inhibitor named MLN4924-Pevonedistat. Activated NEDD8 is then transferred to the E2s UBE2M or UBE2F. Different target-specific E3 proteins adapt the system for the modification of many different proteins, thus affecting a wide array of cellular processes. The majority of NEDD8 E3 ligases contain a RING domain, including RBX1, RBX2, c-CBL, FBXO11, IAP, MDM2, TRIM40, RNF111 and TFB3. Noteworthy, the existence of isopeptidases that remove NEDD8 from target proteins underlines the regulatory essence of this process. Among them, only NEDP1 and the COP9 signalosome are NEDD8-specific (11). There is a close connection between the ubiquitination and NEDDylation processes, since the major group of E3 ubiquitin ligases, the Cullin-RING ligases (CRLs), must have their Cullin component NEDDylated to be functional (12, 13). Although Cullins are the main target of NEDDylation, many cellular processes have been reported to be regulated by the conjugation of NEDD8 to some of their effector proteins (14).

ROLE OF NEDDylation IN CLL

NEDDylation is a post-translational modification that affects many critical aspects of cancer (15, 16). Due to this, MLN4924-

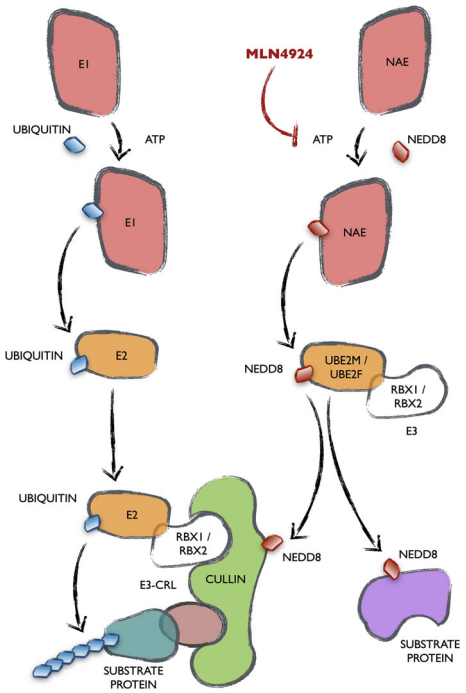

FIGURE 1 | Mechanism and connection of the ubiquitination and the NEDDylation cascades. All UBLs are conjugated to their target proteins following a completely homologous cascade in three steps catalyzed by enzymes generally termed as E1, E2 and E3. The names of the enzymes specific of the NEDDylation cascade are stated (NAE, UBE2M/UBE2F as well as its best characterized E3s RBX1/RBX2). The main NEDDylation target proteins are Cullins, that form part of one of the biggest groups of E3 ubiquitin ligases, the Cullin-RING ligases (CRLs).

pevonedistat is being tested in clinical trials for the treatment of different types of tumors (https://clinicaltrials.gov/ct2/results?term=MLN4924&Search=Search). Our knowledge of the role of NEDDylation in the physiopathology of CLL comes from the reported action of MLN4924 in ex-vivo experiments, as well as in other types of cancer. These studies have identified several target pathways in CLL.

As already mentioned, B-CLL cells are highly dependent on cell to cell interactions in bone marrow and lymphoid organs. In these niches, nuclear factor-κB (NF-κB) signaling gets activated in B-CLL cells, ensuring apoptosis evasion (17). It has been shown that MLN4924 successfully truncates NF-κB pathway activity, B-CLL cell survival and chemoresistance in an *in vitro* co-culture model that mimics the lymph node microenvironment. MLN4924 extends the half-life of the inhibitor of NF-κB (IκB), a negative modulator of the pathway, by preventing its polyubiquitination and degradation (18, 19).

Earlier findings suggested that CLL cells possess DNA damage repair ability that is highly variable between individual samples (20, 21). Contrarily, others reported a defect in the repair of UVC-induced lesions in CLL cells (22), suggesting an affection of specific DNA repair pathways in CLL. Treatment with MLN4924 leads to an accumulation of the licensing factor Cdt1 and sensitization to alkylating agents in B-CLL cells (23). Overexpression of Cdt1 has been shown to induce DNA re-replication followed by head-to-tail collision of replication forks (24).

DISTRIBUTION OF THE UBIQUITIN-LIKE MODIFICATIONS IN CLL

As already mentioned, several groups have shown a cytostatic effect of MLN4924 over B-CLL cells ex vivo, potentiating the action of alkylating agents and drugs commonly used in the treatment of this neoplasia, like ibrutinib and idelalisib (18, 23, 25). Nevertheless, the extension and relevance of NEDDylation in these cells is unknown. To shed some light on this respect, we recently used the Ubiscan platform, that utilizes an antibody against the di-glycine remnants left over the modified lysines when proteins are digested with trypsin (26). The peptides thus enriched were then identified by mass spectroscopy. However, the homology between ubiquitin, NEDD8 and ISG15 in their N terminus makes it impossible to distinguish each of these types of modifications using this methodology. Akimov et al. developed a ubiquitination-specific antibody for the profiling of whole cell samples treated with the endopeptidase Lys-C and reported a ubiquitination profile of Jurkat and Hep2 cell lines (27). Although some reports have tried to establish a consensus NEDDylation target sequence that would allow to discriminate exclusive NEDDylation sites (28), this is still largely unknown, so we could not use Akimov's work as a reference to exclude ubiquitination sites from our screening. On the other hand, two different groups have recently developed strategies to identify proteome-wide NEDD8 modification sites in HEK293T and HCT116 human cell lines (29, 30). Unfortunately, the genetic alteration methods needed make them not suitable for the profiling of primary samples from patients.

In an attempt to circumvent those drawbacks, we analyzed matched samples treated or not with MLN4924, to distinguish NEDDylation-sensitive sites in CLL. The fact that cullins and other previously identified NEDDylated sites reverted their modification level with the treatment, validated the approach. Even so, as the NEDDylation of Cullins regulates CRL function, the modifications found could still be NEDDylation-sensitive ubiquitinations. In concordance with those works reporting a somehow correcting effect of MLN4924 over B-CLL cells, our screening identified a preponderance of peptides with an increased rather than decreased MLN4924-sensitive modification, supporting the idea that NEDDylation is elevated in chronic lymphocytic leukemia. We identified 353 lysines with a significant increment in their di-Gly remnant modification (2.5 fold threshold) that was reverted with MLN4924, thus making them candidates to be direct NEDDylations. We compared those NEDDylation candidate sites to the bona fide NEDDylation sites obtained in the screenings of Vogl et al. and Lobato-Gil et al. (29, 30) in search for some kind of confirmation. 23 and 14 sites coincide with each of the screenings, respectively. Only 5 lysines were common to all three screenings: NEDD8 K22, PPIA K125,

PARP1 K97, UBA3 K409 and HMGB1 K114. When comparing the proteins target of the modifications, we found 20 coincidences between the three studies: 34 and 62 common target proteins between our study and each of those screenings, respectively. These data, emphasizes the cell-type specific profiles of NEDDylation but does not exclude other nature for the UBL modifications found in CLL. Interestingly, 5 of the NEDD8 lysines found in B-CLL cells showed a discreet increment in their modification, that was clearly reverted upon incubation with MLN4924 (31), indicating the generation of poly-NEDD8 chains in CLL. Only lysine 11 and, to a lesser extent, lysine 5 of SUMO2, but no ubiquitin residue, were represented in our screening, indicating putative alterations in the NEDD8-SUMO2 but not in the NEDD8-ubiquitin chains in CLL. These data are in concordance with those pointing at K11 of SUMO2 as a key residue in the generation of NEDD8-SUMO2 hybrid chains (30).

Deletion 2q37 is the genomic alteration that confers the highest augmented overall survival-hazard ratio in CLL (7). Interestingly, this region harbors the loci for three members of the COP9 signalosome complex: COPS8, COPS7B and COPS9. Additionally, COPS5P1 locus maps in 6q16.1, a region which deletion is also related to an increase in survival hazard (7). Theoretically, deletion of these members of the COP9 signalosome, involved in the deNEDDylation of Cullins, may result in the overall increase in protein post-translational modifications that we observed in the scan, supporting a key role of NEDDylation in the cellular phenotype of CLL. In addition, although the mononuclear fraction of patients and controls is not completely comparable, the data showed an over-expression of the genes coding for the E1 and E2 proteins specific of the NEDD8 activation pathway (NAE1, UBE2F and UBE2M) in CLL patients (31).

The analysis of the UBL-PTM data by intracellular pathways fits very well with the mutational studies and the cellular manifestations of the disease. However, a detailed characterization of the nature and effects of the modifications found in the harboring proteins is needed to determine their contribution to the CLL phenotype. For some of those pathways there was reported evidence of the role of NEDDylation in their regulation. This is the case of the non-homologous end joining DNA repair mechanism of double strand breaks (DSB), involved in some resistances of CLL cells (32), where NEDDylation is needed for the release of Ku70 and Ku80 from DNA (33) (**Figure 2A**). These two proteins are profusely over-modified in CLL and MLN4924 reverts in part those modifications. Ku70 and Ku80 stabilize the DNA ends generated when double strand breaks occur and recruit ligase IV (XRCC4) to rejoin them. This mechanism is error prone, and it might be behind the cytogenetic alterations selected in CLL. By contrast, proteins involved in the repair of DSB by homologous recombination are scarcely represented in the screening of UBL-PTM in CLL, being lysine 765 of FANCB an exception. FANCB participates in the E3 complex that monoubiquitinates FANCD2 and FANCI as part of the detection and signaling of DSB, but none of those proteins showed variations in their modifications, maybe suggesting a role of FANCB in CLL aside of the FANCcore

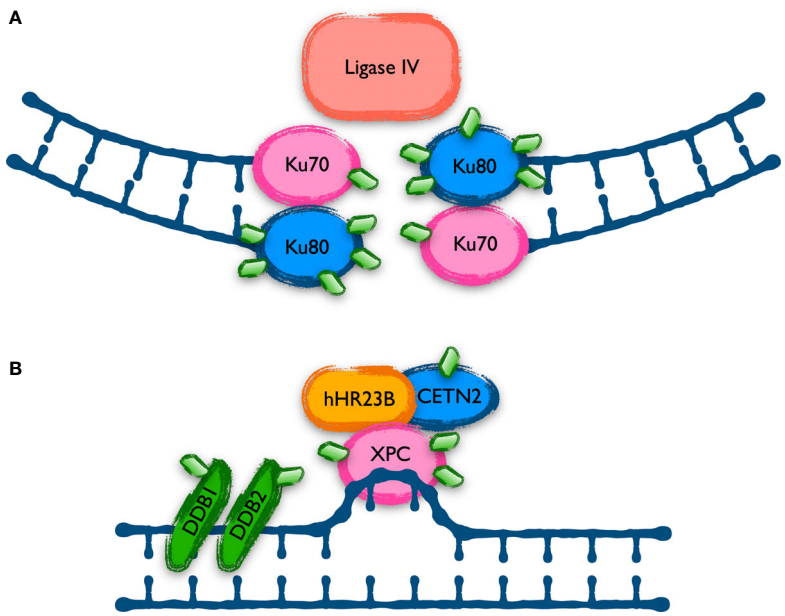

FIGURE 2 | Proteins involved in DNA repair mechanisms with UBL-PTM affected in CLL. Cells repair different types of DNA damage using specific mechanisms. Proteins involved in two of these mechanisms show an altered UBL modification level in CLL. **(A)** The Non-Homologous End Joining (NHEJ) is the main mechanism to repair double strand breaks in human cells but is prone to introduce mutations. Ku70 and Ku80 play a key role in the re-joining of the broken ends, and they are aberrantly modified in CLL, as shown with green diamonds in the scheme. **(B)** The Nucleotide Excision Repair (NER) system is in charge of repairing lesions generating mismatches in the DNA, like those induced by UV irradiation. Previous data indicated a defect in NER in CLL and the recent data shows alterations in the level of UBL modification of some of the proteins involved, as represented in the figure with green diamonds.

complex. In that direction, overexpression of FANCA have been found as a bad prognosis factor in CLL, since it collaborates with MDM2 in the destabilization of p53 (34). Moreover, FANCA is necessary in the NEDDylation of several CLL markers like CXCR5, beta-2-microglobulin and CD44 (35). Apart from the repair of DSB, several members of the nucleotide excision repair (NER) machinery, specialized in the repair of mismatched DNA bases like those produced by UV radiation, were found to be highly modified with MLN4924-sensitive UBLs in CLL (**Figure 2B**). Distortions in the DNA helix are directly recognized by XPC, complexed with hRAD23B and centrin 2 (CETN2). Lesions that do not destabilize DNA duplexes are first recognized by DDB2 (XPE) in complex with DDB1, creating a kink that is then recognized by XPC. DDB1 and DDB2 are part of the CUL4-ROC1 ubiquitin ligase complex that ubiquitinates DDB2, XPC and several histones upon DNA damage. The XPC-hRAND23b-CETN2 complex melts the DNA around the lesion and attracts the rest of the NER repair proteins. The UBL modification of these proteins involved in the recognition of DNA lesions might be related to the hypersensitivity of B-CLL cells to UVC radiation (22, 36). Whether these modifications collaborate in the generation of mutations or cytogenetic aberrations leading to the progression of CLL is still to be determined.

The NF-kB pathway is a well stablished target of the action of MLN4924, supporting a key role of NEDDylation in its regulation (19, 37). The group of Doctor Danilov have found that MLN4924 thwarts the survival support provided over B-CLL cells by the stroma of lymphoid organs through its negative regulation of the NF-kB pathway (18, 38). NF-kB signaling inhibition in T cells also seems to play a role in the immunologic anergy of CLL (39). Since activation of the NF-kB pathway by the canonical way involves the degradation of the inhibitor IkB by the Skp1-Cul1-F-box (SCF^{Fbw1}) complex, and given the regulation exerted by NEDDylation over this later, IkB stabilization has been assumed as the interaction level of MLN4924 over the pathway. Of note, several works have demonstrated the association of the COP9 signalosome and the IKK complexes, facilitating the coupled phosphorylation and degradation of IkB, central in the activation of the pathway (40, 41). However, the MLN4924-sensitive modifications found in the UBL-PTM profile of CLL reveals other putative points where the drug may be exerting its action. Thus, the upstream proteins TANK, TRAF2, CD40, NEMO and IKKß are aberrantly modified in B-CLL cells, suggesting other levels of regulation of this pathway by NEDDylation (**Figure 3**). Interestingly, NEDDylation of NEMO by the RING E3 ligase TRIM40 in the gastrointestinal tract inhibits NF-kB activity and TRIM40 is down regulated in gastrointestinal carcinomas (42). In addition, MLN4924 induces phosphorylation of IkB as well as p65 by itself, keeping total p65 levels unchanged (43).

As previously mentioned, current therapies to fight CLL target the pathways downstream of the B cell receptor (BCR), as well as the anti-apoptotic protein Bcl-2. BCR drives the B-cell response to the presentation of antigens, triggering a bunch of survival pathways that lead to the expansion of the clone to fight infection. Due to reasons still not fully understood, BCR signaling is elevated

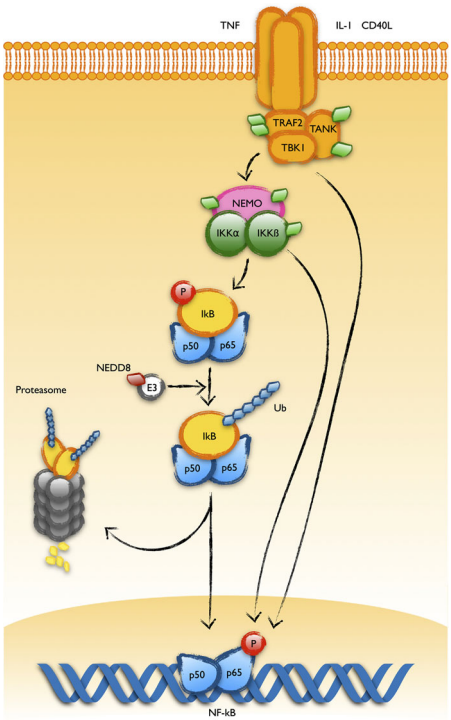

FIGURE 3 | UBL-PTMs of the NF-kB pathway altered in CLL. Schematic representation of the main components of the NF-kB pathway showing the ubiquitin-like post-translational modifications found in B cells from patients of CLL. It was long known that activation of the pathway involves the polyubiquitination of the inhibitor IkBa and its degradation at the proteasome. This process is regulated by NEDDylation of the Cullin component of the E3 ubiquitin ligase targeting IkB for its polyubiquitination. Recent observations in B-CLL cells have revealed alterations in the post-translational pattern of proteins working upstream in the pathway, like TRAF2, TANK, NEMO or IKKß (represented as green diamonds in the figure).

in CLL. Upon binding to an antigen, BCR recruits a great amount of kinases to the cytoplasmic membrane, thus promoting their mutual inter-activation. This is the case of the kinases SYK and LYN. In addition, BCR signaling receives positive and negative reinforces from other membrane proteins (44): CD19 activates PI3K, which in turn phosphorylates phosphatidylinositol (4, 5)-bisphosphate that recruits BTK to the membrane where it is activated by phosphorylation (45, 46). On the other hand, membrane proteins like CD22 recruit phosphatases like SHIP, reverting the previous process (47). The recruitment of this protein complex to the membrane results in the activation of downstream survival and proliferation pathways like NF-kB or MAPK in CLL. SYK, LYN, BTK or the adaptor protein BLNK are highly modified with UBL molecules in CLL (**Figure 4**). More interestingly, these modifications coordinately increase in response to MLN4924, which discards their direct NEDD8 modification but suggests a common NEDDylation-dependent regulation. This might be an exploitable mechanism to strongly interfere with the activation of the pathway and avoid resistances based on individual mutations.

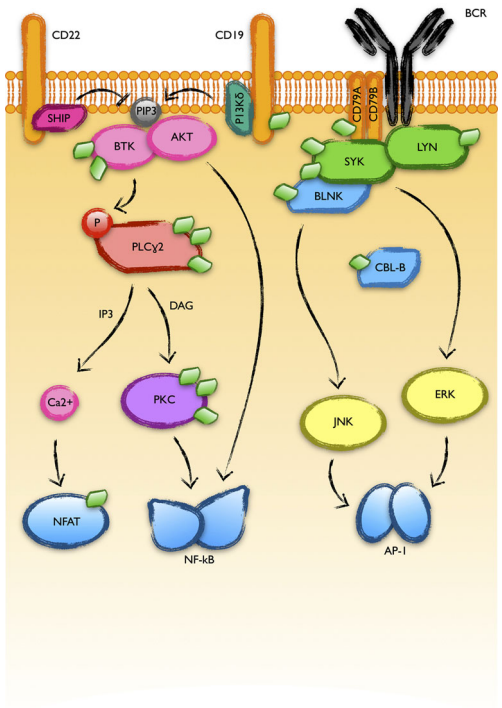

FIGURE 4 | BCR-activated pathways with UBL-PTMs altered in CLL. B cell receptor (BCR) engagement triggers a massive recruitment of protein kinases to the plasma membrane where they get activated and transduce the signal to final transcription factor effectors like NFAT, NF-kB or AP-1. The good response of B-CLL cells to inhibitors of BTK or PI3K-delta supports a relevant role of these pathways in the physiopathology of CLL. The recent screening of the UBL-PTM in CLL showed alterations in the modifications of many proteins involved in these pathways (represented as green diamonds in the figure).

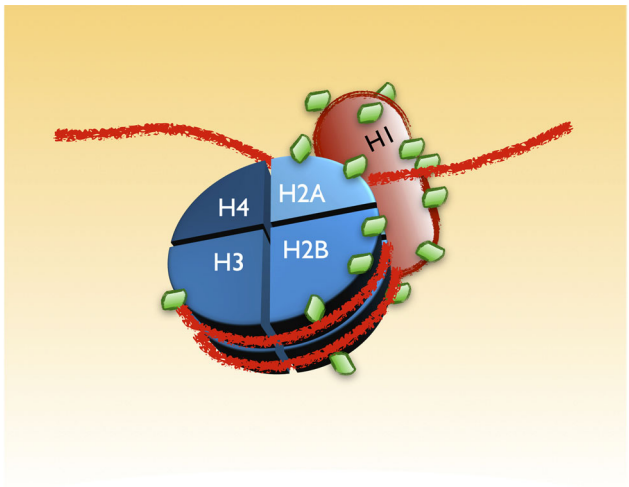

FIGURE 5 | UBL-PTMs of components of the chromatin altered in CLL. B-CLL cells are characterized by a distinctive appearance of their chromatin. The recent screening revealed an extensive alteration in the pattern of UBL-PTMs of the histones that may account for the particular chromatin dynamics in these cells. The figure is a scheme of those modifications, depicted as green diamonds. As in the other figures, the amount of green diamonds on each protein represents the approximated proportion of lysines with altered modifications in CLL.

Proteins involved in many other cellular processes associated with the development or prognosis of CLL were also revealed as aberrantly modified in CLL in the screening. This is the case of proteins of the cytoskeleton, the chromatin or the RNA processing machinery, as described next.

One of the most largely known alterations of B-CLL cells, still used in its diagnosis, is the condensation of the chromatin in clonal cells (48). For that reason, it was interesting to realize that the largest group of proteins with K-GG remnants sensitive to MLN4924 identified in our screening were histones and other chromatin associated proteins. As schematically seen in **Figure 5**, several histones conforming the core of the nucleosomes (H2B, H2A, H3 and specially H1) receive a higher amount of modifications in CLL (31). Interestingly, all of these modifications are reverted at different extent with 0.25μM of the NAE inhibitor, suggesting a role of NEDDylation in the characteristic chromatin dynamics of CLL.

Similarly, fragility of the B-CLL cells when smeared in microscopy preparations is another distinctive characteristic of this pathology, giving rise to broken cells named smudge cells or Gumprecht shadows. The manifestation of smudge cells in smear peripheral blood preparations of CLL patients has been associated with low vimentin levels (49, 50) and, intriguingly, with a better prognosis (51). Vimentin and other cytoskeleton proteins showed an increase in post-translational modifications in CLL and treatment with MLN4924 reverted those modifications along with a reduction in the amount of smudge cells (31). Although the study of a larger amount of samples is needed to get solid conclusions, these results suggest a negative effect of NEDDylation over vimentin and other components of the cytoskeleton, posing a role of post-translational modifications in a characteristic cellular manifestation of CLL.

Mutations in the splicing factor SF3B1 have been found in around 15% of CLL patients, suggesting an alteration of RNA splicing (52). Our screening found alterations in the modification state of many proteins involved in this mechanism. Eukaryotic genes include non-coding sequences called introns that are removed by a complex array of proteins known as the spliceosome. Introns are marked by sequence elements in the mRNA. These cis elements include conserved sequences at the 5' and 3' ends of exons as well as two other elements called the branch point sequence (BPS or BS) and the polypyrimidine (PY) tract. In addition, pre-mRNAs include exonic and intronic splicing enhancers (ESEs or ISEs) and silencers (ESSs or ISSs) that modulate constitutive and alternative splicing by binding regulatory proteins that either stimulate or repress the splicing at an adjacent site (53). Many proteins binding to these cis elements, responsible for the initial steps of spliceosome assembly, received an elevated and MLN4924-sensitive level of UBL post-translational modifications in CLL, indicating a putative NEDDylation. Among them are the BPS binding

protein SF1, the U2 small nuclear ribonucleoprotein (snRNP)-associated protein SF3A1, several members of the serine/arginine (SR)-rich protein family (SFRS2, SFRS3 and SRFS7) or the ESE-binding SF2 factor (**Figure 6**). In addition, the UBL modifications of a bulky list of proteins that include PY tract binding proteins, ESE or ESS binding factors, RNA helicases or small nuclear ribonucleoproteins, among others, are altered in CLL with different sensitivities to NAE inhibition. NEDDylation of SRSF3 at lysines 11 and 85 has already been related to processes like the progression of liver disease and the assembly of stress granules in response to arsenite-induced oxidative stress, respectively (54). On the other hand, SUMOylation plays a well-known role in the regulation of the RNA processing machinery (55). Together with the presence of alterations in the modification of SUMO in lysine 11 (see above), our data may indicate a cross-talk between these two post-translational modifications in the regulation of splicing in CLL.

Constitutive activation of NOTCH is considered one of the main drivers of CLL, since it has been found in at least, but not only, the 4-13% of CLL cases carrying NOTCH1 mutations (2, 56, 57). Somehow surprisingly, no alteration in the modifications of proteins directly involved in this pathway were found in CLL. However, some modulators of this pathway are represented in our study like MIB1 (highly modified in two adjacent lysines in CLL according to our screening) that positively regulates NOTCH signaling by ubiquitinating and facilitating the endocytosis of NOTCH ligands by epsin (58), a protein also over-modified in CLL. In addition, IKAROS (that shows a reduction in its K-GG remnant modification in B-CLL cells compared to control CD19+ peripheral cells) has been shown to antagonize NOTCH signaling (59, 60). These observations may be quite relevant, contributing to the nonmutational NOTCH1 activation found in many CLL patients (61). Further studies are necessary to discern how those modifications contribute to the activation of the NOTCH pathway in CLL.

WNT signaling is nowadays considered as a network of interacting pathways that affect many cellular processes like micro-environment interactions, cytoskeleton rearrangements, cell cycle regulation, proliferation and apoptosis among others. B-CLL cell survival is greatly dependent on stroma and cell to cell interactions, suggesting a key role of WNT signaling in its pathogenesis (62). Indeed, early studies found high expression of genes encoding ligands able to activate the Wnt/ß-catenin pathway (63), although this could not be related to an aggressive form of the disease (64). However, the Wnt/PCP signaling branch, that do not require ß-catenin stabilization, show several of its members up-regulated in B-CLL cells (65). The Wnt/PCP pathway controls the chemotactic response and cell homing in CLL (66) and represents a very promising therapeutic target (62). Indirect data support a role of NEDDylation in the regulation of Wnt signaling, since knockdown of the catalytic subunit of COP9 signalosome, CSN5, leads to decreased ß-catenin levels and to an up-regulation of DKK1 in colorectal carcinoma cell lines (67). Moreover, the NAE inhibitor MLN4924 induces a reduction in DKK1 expression. However, our screening did not identify alterations in the UBL-PTM of any member of this pathway.

Mutations or alterations in the function of p53 are virtually behind all types of tumors. In CLL, deletion of 17p (del17p) or mutation of p53 are the main markers of bad prognosis. Post-translational modifications of p53 play a key role in its function as tumor suppressor and many of them have been described (68). It was somehow surprising to find that only the modification of lysine 120 of p53 was altered in CLL. Lysine 120 is located within de DNA binding domain of p53, and its acetylation has been related to the stabilization of p53 and the increase of its affinity to the promoters of proapoptotic genes (69, 70). Acetylation of lysine 120 has also been related to the induction of apoptosis by p53 through transcriptional-independent mechanisms (71). Either NEDDylation or ubiquitination of p53 impaired its transactivation capacity in luciferase experiments, in concordance with previous reports (72). However, while ubiquitination mediated p53 destabilization, NEDDylation did not. Moreover, we could demonstrate for the first time that NEDDylation of lysine 120 of p53 greatly abolished the acetylation in this residue, along with a loss in the transactivation capacity of p53 and an

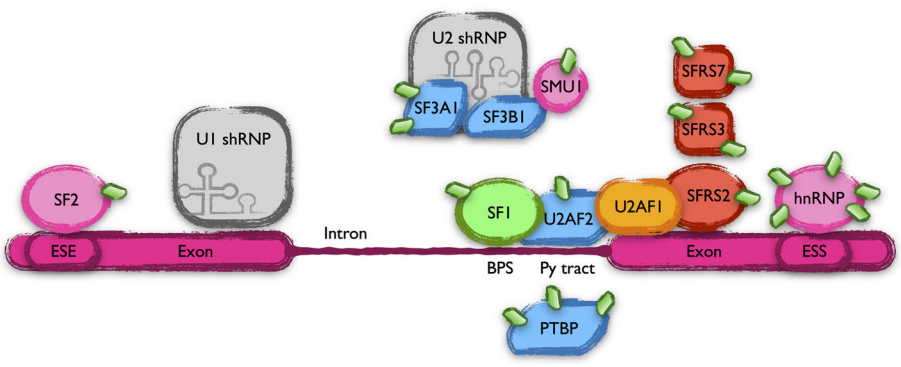

FIGURE 6 | Scheme of the members of the spliceosome that harbor UBL-PTMs altered in CLL. Schematic representation of part of the spliceosome complex, focusing on the proteins with altered UBL-PTM in CLL. Introns are marked in nascent mRNAs by cis elements (BPS, Py tract, ESE, ESS, *etc*, see text) bound by an array of proteins that collaborate in their elimination.

impairment of its interaction with Bcl-2 (31). These alterations in p53 function support a role of lysine 120 over-NEDDylation in the etiology and prognosis of CLL patients.

SUMMARY AND FUTURE DIRECTIONS

The recently published UBL-PTM profile of chronic lymphocytic leukemia has placed these transversal processes in a central position between the different intrinsic, genetic and environmental factors that explain the CLL phenotype. Among them, NEDDylation is recently receiving special attention, due to the promising results obtained with its inhibitor, MLN4924, in preclinical assays. MLN4924 blocks the micro environmental activation of NF-kB and induces cell death or senescence in B-CLL cells. However, the UBL-PTM profile of these cells has extended the putative role of NEDDylation over the regulation of many other different pathways, key in the physiopathology of CLL and target of the new therapies used to fight it. However, the limitations of the tools available to date to specifically profile NEDDylation in different pathologies makes mandatory a detailed study of the nature of each of the modifications found as altered. These studies will help us understand the role of these kind of post-translational modifications in the physiopathology of CLL and will surely uncover new therapeutic targets.

AUTHOR CONTRIBUTIONS

VA and JC contributed equally to the writing of the introduction to the molecular aspects. JD-G wrote the introduction to the clinical aspects of the disease. LY and CP defined the conception and design of the manuscript, revised and wrote parts of it. All authors contributed to the article and approved the submitted version.

FUNDING

This work has been funded by: Project PI17/01688 from Instituto de Salud Carlos III co-financed by European Development Regional Fund (FEDER); Project CI20/30 from Asociación Luchamos por la Vida.

REFERENCES

1. Hallek M, Cheson BD, Catovsky D, Caligaris-Cappio F, Dighiero G, Döhner H, et al. iwCLL Guidelines for Diagnosis, Indications for Treatment, Response Assessment, and Supportive Management of CLL. *Blood* (2018) 131:2745–60. doi: 10.1182/blood-2017-09-806398
2. Puente XS, Pinyol M, Quesada V, Conde L, Ordóñez GR, Villamor N, et al. Whole-Genome Sequencing Identifies Recurrent Mutations in Chronic Lymphocytic Leukaemia. *Nature* (2011) 475:101–5. doi: 10.1038/nature10113
3. Speedy HE, Beekman R, Chapaprieta V, Orlando G, Law PJ, Martín-García D, et al. Insight Into Genetic Predisposition to Chronic Lymphocytic Leukemia From Integrative Epigenomics. *Nat Commun* (2019) 10(1):3615. doi: 10.1038/s41467-019-11582-2
4. Landau DA, Tausch E, Taylor-Weiner AN, Stewart C, Reiter JG, Bahlo J, et al. Mutations Driving CLL and Their Evolution in Progression and Relapse. *Nature* (2015) 526:525–30. doi: 10.1038/nature15395
5. Burger JA, Gribben JG. The Microenvironment in Chronic Lymphocytic Leukemia (CLL) and Other B Cell Malignancies: Insight Into Disease Biology and New Targeted Therapies. *Semin Cancer Biol* (2014) 24:71–81. doi: 10.1016/j.semcancer.2013.08.011
6. Nadeu F, Delgado J, Royo C, Bauman T, Stankovic T, Pinyol M, et al. Clinical Impact of Clonal and Subclonal TP53, SF3B1, BIRC3, and ATM Mutations in Chronic Lymphocytic Leukemia. *Blood* (2015) 126:4138–8. doi: 10.1182/blood.V126.23.4138.4138
7. Puente XS, Beà S, Valdés-Mas R, Villamor N, Gutiérrez-Abril J, Martín-Subero JI, et al. Non-Coding Recurrent Mutations in Chronic Lymphocytic Leukaemia. *Nature* (2015) 526:519–24. doi: 10.1038/nature14666
8. Shanafelt TD, Wang XV, Kay NE, Hanson CA, O'Brien S, Barrientos J, et al. Ibrutinib–Rituximab or Chemoimmunotherapy for Chronic Lymphocytic Leukemia. *New Engl J Med* (2019) 381:432–43. doi: 10.1056/NEJMoa1817073
9. McConkey D, Chandra J, Wright S, Plunkett W, McDonnell T, Reed J, et al. Apoptosis Sensitivity in Chronic Lymphocytic Leukemia Is Determined by Endogenous Endonuclease Content and Relative Expression of BCL-2 and BAX. *J Immunol (Baltimore Md: 1950)* (1996) 156(7):2624–30.
10. Roberts AW, Davids MS, Pagel JM, Kahl BS, Puvvada SD, Gerecitano JF, et al. Targeting BCL2 With Venetoclax in Relapsed Chronic Lymphocytic Leukemia. *New Engl J Med* (2016) 374:311–22. doi: 10.1056/NEJMoa1513257
11. Chung D, Dellaire G. The Role of the COP9 Signalosome and Neddylation in DNA Damage Signaling and Repair. *Biomolecules* (2015) 5:2388–416. doi: 10.3390/biom5042388
12. Pan Z-Q, Kentsis A, Dias DC, Yamoah K, Wu K. Nedd8 on Cullin: Building an Expressway to Protein Destruction. *Oncogene* (2004) 23:1985–97. doi: 10.1038/sj.onc.1207414
13. Chiba T, Tanaka K. Cullin-Based Ubiquitin Ligase and Its Control by NEDD8-Conjugating System. *Curr Protein Pept Sci* (2004) 5:177–84. doi: 10.2174/1389203043379783
14. Enchev RI, Schulman BA, Peter M. Protein Neddylation: Beyond Cullin–RING Ligases. *Nat Rev Mol Cell Biol* (2014) 16:30–44. doi: 10.1038/nrm3919
15. Abidi N, Xirodimas DP. Regulation of Cancer-Related Pathways by Protein NEDDylation and Strategies for the Use of NEDD8 Inhibitors in the Clinic. *Endocrine-Related Cancer* (2014) 22(1):T55-70. doi: 10.1530/erc-14-0315
16. Ying J, Zhang M, Qiu X, Lu Y. Targeting the Neddylation Pathway in Cells as a Potential Therapeutic Approach for Diseases. *Cancer Chemother Pharmacol* (2018) 81:797–808. doi: 10.1007/s00280-018-3541-8
17. Herishanu Y, Pérez-Galán P, Liu D, Biancotto A, Pittaluga S, Vire B, et al. The Lymph Node Microenvironment Promotes B-Cell Receptor Signaling, NF-κb Activation, and Tumor Proliferation in Chronic Lymphocytic Leukemia. *Blood* (2011) 117:563–74. doi: 10.1182/blood-2010-05-284984
18. Godbersen JC, Humphries LA, Danilova OV, Kebbekus PE, Brown JR, Eastman A, et al. The Nedd8-Activating Enzyme Inhibitor MLN4924 Thwarts Microenvironment-Driven NF-κb Activation and Induces Apoptosis in Chronic Lymphocytic Leukemia B Cells. *Clin Cancer Res* (2014) 20:1576–89. doi: 10.1158/1078-0432.CCR-13-0987
19. Milhollen MA, Traore T, Adams-Duffy J, Thomas MP, Berger AJ, Dang L, et al. MLN4924, a NEDD8-Activating Enzyme Inhibitor, Is Active in Diffuse Large B-Cell Lymphoma Models: Rationale for Treatment of NF-κb–Dependent Lymphoma. *Blood* (2010) 116:1515–23. doi: 10.1182/blood-2010-03-272567
20. Buschfort C, Müller MR, Seeber S, Rajewsky MF, Thomale J. DNA Excision Repair Profiles of Normal and Leukemic Human Lymphocytes: Functional Analysis at the Single-Cell Level. *Cancer Res* (1997) 57:651.
21. Müller MR, Buschfort C, Thomale J, Lensing C, Rajewsky MF, Seeber S. DNA Repair and Cellular Resistance to Alkylating Agents in Chronic Lymphocytic Leukemia. *Clin Cancer Res* (1997) 3:2055.
22. Tuck A, Smith S, Larcom L. Chronic Lymphocytic Leukemia Lymphocytes Lack the Capacity to Repair UVC-Induced Lesions. *Mutat Res/DNA Repair* (2000) 459:73–80. doi: 10.1016/S0921-8777(99)00060-9
23. Paiva C, Godbersen JC, Berger A, Brown JR, Danilov AV. Targeting Neddylation Induces DNA Damage and Checkpoint Activation and Sensitizes Chronic Lymphocytic Leukemia B Cells to Alkylating Agents. *Cell Death Dis* (2015) 6:e1807. doi: 10.1038/cddis.2015.161

24. Davidson IF, Li A, Blow JJ. Deregulated Replication Licensing Causes DNA Fragmentation Consistent With Head-To-Tail Fork Collision. *Mol Cell* (2006) 24:433–43. doi: 10.1016/j.molcel.2006.09.010
25. Godbersen C, Paiva C, Berger AJ, Brown JR, Danilov AV. Targeting Nedd8 Activating Enzyme Induces DNA Damage and Cell Cycle Arrest and Sensitizes Chronic Lymphocytic Leukemia (CLL) B-Cells to Alkylating Agents. *Blood* (2014) 124:4690–0. doi: 10.1182/blood.V124.21.4690.4690
26. Xu G, Paige JS, Jaffrey SR. Global Analysis of Lysine Ubiquitination by Ubiquitin Remnant Immunoaffinity Profiling. *Nat Biotechnol* (2010) 28:868–73. doi: 10.1038/nbt.1654
27. Akimov V, Barrio-Hernandez I, Hansen SVF, Hallenborg P, Pedersen A-K, Bekker-Jensen DB, et al. UbiSite Approach for Comprehensive Mapping of Lysine and N-Terminal Ubiquitination Sites. *Nat Struct Mol Biol* (2018) 25:631–40. doi: 10.1038/s41594-018-0084-y
28. Yavuz A, Sözer N, Sezerman O. Prediction of Neddylation Sites From Protein Sequences and Sequence-Derived Properties. *BMC Bioinf* (2015) 16(Suppl 18):S9. doi: 10.1186/1471-2105-16-S18-S9
29. Vogl AM, Phu L, Becerra R, Giusti SA, Verschueren E, Hinkle TB, et al. Global Site-Specific Neddylation Profiling Reveals That NEDDylated Cofilin Regulates Actin Dynamics. *Nat Struct Mol Biol* (2020) 27:210–20. doi: 10.1038/s41594-019-0370-3
30. Lobato-Gil S, Heidelberger JB, Maghames C, Bailly A, Brunello L, Rodriguez MS, et al. Proteome-Wide Identification of NEDD8 Modification Sites Reveals Distinct Proteomes for Canonical and Atypical NEDDylation. *Cell Rep* (2021) 34:108635. doi: 10.1016/j.celrep.2020.108635
31. Bravo-Navas S, Yáñez L, Romón Í, Briz M, Domínguez-García JJ, Pipaón C. Map of Ubiquitin-Like Post-Translational Modifications in Chronic Lymphocytic Leukemia. Role of P53 Lysine 120 NEDDylation. *Leukemia* (2021). doi: 10.1038/s41375-021-01184-7
32. Deriano L. Human Chronic Lymphocytic Leukemia B Cells can Escape DNA Damage-Induced Apoptosis Through the Nonhomologous End-Joining DNA Repair Pathway. *Blood* (2005) 105:4776–83. doi: 10.1182/blood-2004-07-2888
33. Brown Jessica S, Lukashchuk N, Sczaniecka-Clift M, Britton S, le Sage C, Calsou P, et al. Neddylation Promotes Ubiquitylation and Release of Ku From DNA-Damage Sites. *Cell Rep* (2015) 11:704–14. doi: 10.1016/j.celrep.2015.03.058
34. Bravo-Navas S, Yáñez L, Romón Í, Pipaón AC. Elevated FANCA Expression Determines a Worse Prognosis in Chronic Lymphocytic Leukemia and Interferes With P53 Function. *FASEB J* (2019) 33:10477–89. doi: 10.1096/fj.201802439RR
35. Renaudin X, Guervilly J-H, Aoufouchi S, Rosselli F. Proteomic Analysis Reveals a FANCA-Modulated Neddylation Pathway Involved in CXCR5 Membrane Targeting and Cell Mobility. *J Cell Sci* (2014) 127:3546–54. doi: 10.1242/jcs.150706
36. Tuck A, Smith S, Whitesides JF, Larcom L. Hypersensitivity of Lymphocytes From Chronic Lymphocytic Leukemia Patients to Ultraviolet Light-C Radiation. *Leukemia Lymphoma* (1999) 36:169–77. doi: 10.3109/10428199909145961
37. Barth MJ, Mavis C, Hernandez-Ilizaliturri FJ, Czuczman MS. MLN4924, an Investigational Small Molecule Inhibitor of NEDD8-Activating Enzyme (NAE), Inhibits NF-κb Activity and Induces G1 Cell Cycle Arrest and Apoptosis in Pre-Clinical Models of Hodgkin Lymphoma (Hl). *Blood* (2012) 120:3717–7. doi: 10.1182/blood.V120.21.3717.3717
38. Godbersen JC, Paiva C, Danilova OV, Berger A, Brown JR, Danilov AV. Targeting Neddylation Effectively Antagonizes Nuclear Factor-κb in Chronic Lymphocytic Leukemia B-Cells. *Leukemia Lymphoma* (2015) 56:1566–9. doi: 10.3109/10428194.2014.990901
39. Best S, Lam V, Liu T, Bruss N, Kittai A, Danilova OV, et al. Immunomodulatory Effects of Pevonedistat, a NEDD8-Activating Enzyme Inhibitor, in Chronic Lymphocytic Leukemia-Derived T Cells. *Leukemia* (2020) 35:156–68. doi: 10.1038/s41375-020-0794-0
40. Orel L, Neumeier H, Hochrainer K, Binder BR, Schmid JA. Crosstalk Between the NF-κb Activating IKK-Complex and the CSN Signalosome. *J Cell Mol Med* (2009) 14:1555–68. doi: 10.1111/j.1582-4934.2009.00866.x
41. Schweitzer K, Bozko PM, Dubiel W, Naumann M. CSN Controls NF-κb by Deubiquitinylation of Iκbα. *EMBO J* (2007) 26:1532–41. doi: 10.1038/sj.emboj.7601600
42. Noguchi K, Okumura F, Takahashi N, Kataoka A, Kamiyama T, Todo S, et al. TRIM40 Promotes Neddylation of IKK and Is Downregulated in Gastrointestinal Cancers. *Carcinogenesis* (2011) 32:995–1004. doi: 10.1093/carcin/bgr068
43. Hryniewicz-Jankowska A, Wierzbicki J, Tabola R, Stach K, Sossey-Alaoui K, Augoff K. The Effect of Neddylation Inhibition on Inflammation-Induced MMP9 Gene Expression in Esophageal Squamous Cell Carcinoma. *Int J Mol Sci* (2021) 22:1716. doi: 10.3390/ijms22041716
44. Sato S, Jansen PJ, Tedder TF. CD19 and CD22 Expression Reciprocally Regulates Tyrosine Phosphorylation of Vav Protein During B Lymphocyte Signaling. *Proc Natl Acad Sci* (1997) 94:13158–62. doi: 10.1073/pnas.94.24.13158
45. Okkenhaug K, Vanhaesebroeck B. PI3K in Lymphocyte Development, Differentiation and Activation. *Nat Rev Immunol* (2003) 3:317–30. doi: 10.1038/nri1056
46. Tuveson D, Carter R, Soltoff S, Fearon D. CD19 of B Cells as a Surrogate Kinase Insert Region to Bind Phosphatidylinositol 3-Kinase. *Science* (1993) 260:986–9. doi: 10.1126/science.7684160
47. Doody G, Justement L, Delibrias C, Matthews R, Lin J, Thomas M, et al. A Role in B Cell Activation for CD22 and the Protein Tyrosine Phosphatase SHP. *Science* (1995) 269:242–4. doi: 10.1126/science.7618087
48. Seidel T, Garbes A. Cellules Grumelées: Old Terminology Revisited. Regarding the Cytologic Diagnosis of Chronic Lymphocytic Leukemia and Well-Differentiated Lymphocytic Lymphoma in Pleural Effusions. *Acta Cytol* (1985) 29(5):775–80.
49. Nowakowski GS, Hoyer JD, Shanafelt TD, Jelinek DF, Rassenti LZ, Kipps TJ, et al. Percentage of Smudge Cells on Blood Smear Predicts Prognosis in Chronic Lymphocytic Leukemia: A Multicenter Study. *Blood* (2007) 110:745–5. doi: 10.1182/blood.V110.11.745.745
50. Nowakowski GS, Lee YK, Bone ND, Morice WG, Barnidge D, Jelinek DF, et al. Proteomic Analysis of Chronic Lymphocytic Leukemia Cells Identifies Vimentin as a Novel Prognostic Factor for Aggressive Disease. *Blood* (2005) 106:707–7. doi: 10.1182/blood.V106.11.707.707
51. Nowakowski GS, Hoyer JD, Shanafelt TD, Geyer SM, LaPlant B, Call TG, et al. Smudge Cells on Routine Blood Smear Predict Clinical Outcome in Chronic Lymphocytic Leukemia: A Universally Available Prognostic Test. *Blood* (2006) 108:2785–5. doi: 10.1182/blood.V108.11.2785.2785
52. Wan Y, Wu CJ. SF3B1 Mutations in Chronic Lymphocytic Leukemia. *Blood* (2013) 121:4627–34. doi: 10.1182/blood-2013-02-427641
53. Will CL, Luhrmann R. Spliceosome Structure and Function. *Cold Spring Harbor Perspect Biol* (2010) 3(7). doi: 10.1101/cshperspect.a003707
54. Jayabalan AK, Sanchez A, Park RY, Yoon SP, Kang G-Y, Baek J-H, et al. NEDDylation Promotes Stress Granule Assembly. *Nat Commun* (2016) 7:12125. doi: 10.1038/ncomms12125
55. Nuro-Gyina PK, Parvin JD. Roles for SUMO in pre-mRNA Processing. *Wiley Interdiscip Rev: RNA* (2015) 7:105–12. doi: 10.1002/wrna.1318
56. Maleki Y, Alahbakhshi Z, Heidari Z, Moradi M, Rahimi Z, Yari K, et al. NOTCH1, SF3B1, MDM2 and MYD88 Mutations in Patients With Chronic Lymphocytic Leukemia. *Oncol Lett* (2019) 17(4):4016–23. doi: 10.3892/ol.2019.10048
57. Rosati E, Sabatini R, Rampino G, Tabilio A, Di Ianni M, Fettucciari K, et al. Constitutively Activated Notch Signaling Is Involved in Survival and Apoptosis Resistance of B-CLL Cells. *Blood* (2009) 113:856–65. doi: 10.1182/blood-2008-02-139725
58. Meloty-Kapella L, Shergill B, Kuon J, Botvinick E, Weinmaster G. Notch Ligand Endocytosis Generates Mechanical Pulling Force Dependent on Dynamin, Epsins, and Actin. *Dev Cell* (2012) 22:1299–312. doi: 10.1016/j.devcel.2012.04.005
59. Kleinmann E, Geimer Le Lay A-S, Sellars M, Kastner P, Chan S. Ikaros Represses the Transcriptional Response to Notch Signaling in T-Cell Development. *Mol Cell Biol* (2008) 28:7465–75. doi: 10.1128/MCB.00715-08
60. Lemarié M, Bottardi S, Mavoungou L, Pak H, Milot E. IKAROS Is Required for the Measured Response of NOTCH Target Genes Upon External NOTCH Signaling. *PloS Genet* (2021) 17(3):e1009478. doi: 10.1371/journal.pgen.1009478
61. Fabbri G, Holmes AB, Viganotti M, Scuoppo C, Belver L, Herranz D, et al. Common Nonmutational NOTCH1 Activation in Chronic Lymphocytic Leukemia. *Proc Natl Acad Sci* (2017) 114(14):E2911–9. doi: 10.1073/pnas.1702564114
62. Janovská P, Bryja V. Wnt Signalling Pathways in Chronic Lymphocytic Leukaemia and B-Cell Lymphomas. *Br J Pharmacol* (2017) 174:4701–15. doi: 10.1111/bph.13949
63. Lu D, Zhao Y, Tawatao R, Cottam HB, Sen M, Leoni LM, et al. Activation of the Wnt Signaling Pathway in Chronic Lymphocytic Leukemia. *Proc Natl Acad Sci* (2004) 101:3118–23. doi: 10.1073/pnas.0308648100

64. Poppova L, Janovska P, Plevova K, Radova L, Plesingerova H, Borsky M, et al. DecreasedWNT3expression in Chronic Lymphocytic Leukaemia Is a Hallmark of Disease Progression and Identifies Patients With Worse Prognosis in the Subgroup With mutatedIGHV. *Br J Haematol* (2016) 175:851–9. doi: 10.1111/bjh.14312
65. Kotašková J, Pavlová Š, Greif I, Stehlíková O, Plevová K, Janovská P, et al. ROR1-Based Immunomagnetic Protocol Allows Efficient Separation of CLL and Healthy B Cells. *Br J Haematol* (2015) 175:339–42. doi: 10.1111/bjh.13848
66. Kaucká M, Plevová K, Pavlová Š, Janovská P, Mishra A, Verner J, et al. The Planar Cell Polarity Pathway Drives Pathogenesis of Chronic Lymphocytic Leukemia by the Regulation of B-Lymphocyte Migration. *Cancer Res* (2013) 73:1491–501. doi: 10.1158/0008-5472.CAN-12-1752
67. Jumpertz S, Hennes T, Asare Y, Schütz AK, Bernhagen J. CSN5/JAB1 Suppresses the WNT Inhibitor DKK1 in Colorectal Cancer Cells. *Cell Signalling* (2017) 34:38–46. doi: 10.1016/j.cellsig.2017.02.013
68. Liu Y, Tavana O, Gu W. P53 Modifications: Exquisite Decorations of the Powerful Guardian. *J Mol Cell Biol* (2019) 11:564–77. doi: 10.1093/jmcb/mjz060
69. Sykes SM, Mellert HS, Holbert MA, Li K, Marmorstein R, Lane WS, et al. Acetylation of the P53 DNA-Binding Domain Regulates Apoptosis Induction. *Mol Cell* (2006) 24:841–51. doi: 10.1016/j.molcel.2006.11.026
70. Liu X, Tan Y, Zhang C, Zhang Y, Zhang L, Ren P, et al. NAT 10 Regulates P53 Activation Through Acetylating P53 at K120 and Ubiquitinating Mdm2. *EMBO Rep* (2016) 17:349–66. doi: 10.15252/embr.201540505
71. Sykes SM, Stanek TJ, Frank A, Murphy ME, McMahon SB. Acetylation of the DNA Binding Domain Regulates Transcription-Independent Apoptosis by P53. *J Biol Chem* (2009) 284:20197–205. doi: 10.1074/jbc.M109.026096
72. Xirodimas DP, Saville MK, Bourdon J-C, Hay RT, Lane DP. Mdm2-Mediated NEDD8 Conjugation of P53 Inhibits Its Transcriptional Activity. *Cell* (2004) 118:83–97. doi: 10.1016/j.cell.2004.06.016

Conflict of Interest: The authors declare that the research was conducted in the absence of any commercial or financial relationships that could be construed as a potential conflict of interest.

Publisher's Note: All claims expressed in this article are solely those of the authors and do not necessarily represent those of their affiliated organizations, or those of the publisher, the editors and the reviewers. Any product that may be evaluated in this article, or claim that may be made by its manufacturer, is not guaranteed or endorsed by the publisher.

frontiers in Oncology

REVIEW
published: 30 September 2021
doi: 10.3389/fonc.2021.748250

Biomarkers in Acute Myeloid Leukemia: Leveraging Next Generation Sequencing Data for Optimal Therapeutic Strategies

Hanadi El Achi and Rashmi Kanagal-Shamanna *

Department of Hematopathology, The University of Texas MD Anderson Cancer Center, Houston, TX, United States

Next generation sequencing (NGS) is routinely used for mutation profiling of acute myeloid leukemia. The extensive application of NGS in hematologic malignancies, and its significant association with the outcomes in multiple large cohorts constituted a proof of concept that AML phenotype is driven by underlying mutational signature and is amenable for targeted therapies. These findings urged incorporation of molecular results into the latest World Health Organization (WHO) sub-classification and integration into risk-stratification and treatment guidelines by the European Leukemia Net. NGS mutation profiling provides a large amount of information that guides diagnosis and management, dependent on the type and number of gene mutations, variant allele frequency and amenability to targeted therapeutics. Hence, molecular mutational profiling is an integral component for work-up of AML and multiple leukemic entities. In addition, there is a vast amount of informative data that can be obtained from routine clinical NGS sequencing beyond diagnosis, prognostication and therapeutic targeting. These include identification of evidence regarding the ontogeny of the disease, underlying germline predisposition and clonal hematopoiesis, serial monitoring to assess the effectiveness of therapy and resistance mutations, which have broader implications for management. In this review, using a few prototypic genes in AML, we will summarize the clinical applications of NGS generated data for optimal AML management, with emphasis on the recently described entities and Food and Drug Administration approved target therapies.

Keywords: AML, acute myeloid leukemia, next generation sequencing, actionable mutations, targeted therapy, FDA

OPEN ACCESS

Edited by:
Julia T. Geyer,
Weill Cornell Medical Center, United States

Reviewed by:
Gang Zheng,
Mayo Clinic, United States
Deepshi Thakral,
All India Institute of Medical Sciences, India

***Correspondence:**
Rashmi Kanagal-Shamanna
RKanagal@mdanderson.org

Specialty section:
This article was submitted to Hematologic Malignancies, a section of the journal Frontiers in Oncology

Received: *27 July 2021*
Accepted: *14 September 2021*
Published: *30 September 2021*

Citation:
El Achi H and Kanagal-Shamanna R (2021) Biomarkers in Acute Myeloid Leukemia: Leveraging Next Generation Sequencing Data for Optimal Therapeutic Strategies. Front. Oncol. 11:748250. doi: 10.3389/fonc.2021.748250

INTRODUCTION

Acute myeloid leukemia (1) is a clonal malignant expansion of immature myeloid precursors due to block in differentiation. Mutation profiling is standard for routine baseline clinical evaluation of AML. Prior to 2008, there were two functional genetic groups for leukemic pathogenesis: class I (activated signaling genes such as *FLT3*, *KIT* and *RAS* mutations) that conferred the proliferative potential, and class II genes involved in transcription and differentiation such as *CEBPA* and *RUNX1* (2). The development of high-throughput NGS sequencing platforms uncovered many somatic mutations in AML. In 2013, the Cancer Genome Atlas (TCGA) project expanded the

functional genetic classes to nine families involved in the pathogenesis of the myeloid neoplasms. An average of 14 mutations were identified in the AML genome, ranging between five to 23 genetic mutations in each case (3). In 2016, a large cohort that enrolled 1540 AML patients described 11 subgroups of genomic alterations with different clinical outcomes using NGS. The additional separate categories included AML with mutations in genes encoding chromatin and RNA-splicing regulators, AML with *TP53* mutations and/or chromosomal aneuploidies, and AML with *IDH2* R172 mutations (4). Taken together, these findings supported the fact that AML phenotype is driven by underlying mutational signature (**Figure 1**).

Accordingly, both the 2016 revisions to the WHO and 2017 European LeukemiaNet (5) incorporated gene mutations into the sub-classification and risk-stratification of AML (6, 7). Molecular testing plays a major role in the current World Health Organization (WHO) classification of myeloid neoplasms. Specific genetic abnormalities are regarded as disease-defining mutations and others have important prognostic and therapeutic implications. The WHO recognizes 3 distinct sub-categories of AML based on somatic mutations: AML with *NPM1* mutation, AML with bi-allelic mutations of *CEBPA*, and AML with mutated *RUNX1* (provisional entity). Genes such as *TP53, RUNX1, IDH1/2* and FMS-related tyrosine kinase 3 (8), among others, are found to be altered in the different subcategories of AML with prognostic and/or therapeutic implications of utmost importance. The latest 2017 European Leukemia Net (ENL) guidelines for AML recommends molecular profiling for mutations in *NPM1, CEBPA, FLT3-ITD, TP53, RUNX1, ASXL1*, and *BCR-ABL1*. Therefore, the complete cytogenetic and molecular work-up is essential at the time of initial AML

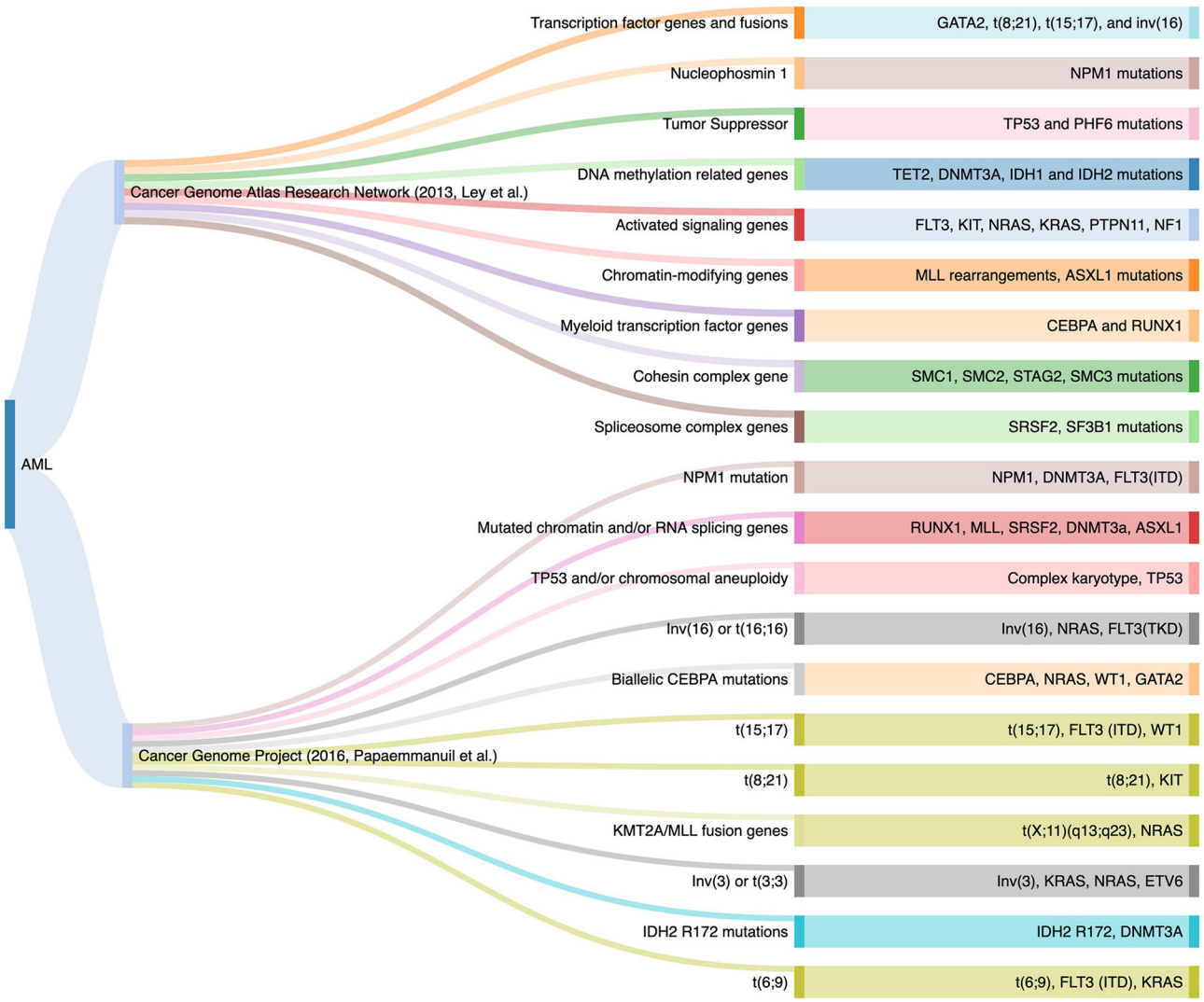

FIGURE 1 | Genomic Classifications of Acute Myeloid Leukemia as Proposed by the TCGA Project and the 2016 Study.

evaluation. The main goal of genome sequencing is the identification of actionable gene mutations and risk-stratification. Hence, multi-gene panel next-generation sequencing (NGS) based mutation analysis is the primary mode for assessment for multiple AML associated genes (9).

In this review, we will provide an overview of the diagnostic, prognostic and therapeutic data that can be obtained from routine clinical NGS data in AML. In addition, we will describe the implications of the vast amount of additional data that can be obtained from routine clinical NGS beyond prognostication and management, such as the ontogeny of AML, clues regarding underlying germline predisposition and clonal hematopoiesis, serial monitoring to assess the effectiveness of therapy and resistance mutations. We will use a few prototypic genes for each section, with emphasis on the recently described entities and actionable mutations, specifically pertaining to the Food and Drug Administration (10) approved target therapies and the ongoing clinical trials. AML-defining translocations are beyond the scope of this review.

GENETIC ALTERATIONS WITH FDA-APPROVED TARGETED THERAPIES

AML With Mutated *FLT3*

Category: activated signaling genes.

Clinicopathologic and morphologic features: Leukocytosis.

Recommended method of testing: NGS for tyrosine kinase domain (TKD) mutations (25) and small internal tandem duplications (8), Polymerase Chain Reaction (PCR) followed by capillary electrophoresis (CE) for medium and large internal tandem duplications (8, 31).

FLT3 is a receptor with tyrosine kinase (TK) activity, involved in proliferation and differentiation of hematopoietic progenitors. The associated mutations generally affect the juxta-membrane and the TK domain of the receptor. Broadly, mutations in *FLT3* are of two types: *FLT3*-ITD which is the most frequent alteration, and *FLT3*-TKD which consists of a point mutation in the TK domain (25).

FLT3-ITD

FLT3-ITD are in-frame mutations which consist of duplication of small sequences, ranging from 3 to larger than 400 base pairs resulting in a receptor with an elongated juxta-membrane domain. This leads to constitutive activation of the receptor and activation of intracellular pathways resulting in cellular proliferation (25, 32). The frequency of *FLT3*-ITD mutations in AML ranges from 20-50% (30). *FLT3*-ITD is associated with proliferative AML with a high WBC count (25). The prognostic implication of the mutation is dependent on the allelic burden (33). The allele burden of *FLT3*-ITD can be measured using one of the two parameters (10): allele ratio (AR), defined as the ratio of the area under the curve of mutant to wild-type and (2) allele frequency (AF) which is defined as the ratio of the area under the curve of mutant to total (mutant + wild-type). The 2017 ELN adopts a cut-off of 0.5 to differentiate between low *versus* high AR (34). AML patients with high AR *FLT3*-ITD had significantly low complete remission (CR) rates, with poor survival and relapse; only high *FLT3*-ITD AR patients (≥0.5) benefited from allogeneic stem cell transplantation (32). Per ELN, *NPM1* mutated AML with *FLT3*-ITD AR <0.5 is considered as a favorable prognostic subgroup, similar to AML with absent *FLT3*-ITD mutation, and stem cell transplant is not recommended (34).

FLT3-TKD

FLT3-TKD mutations are less common than the *FLT3*-ITD; they consist mainly of missense point mutations, deletions or insertions within the TK domain. The most frequent alteration is a point mutation involving nucleotide substitution on codon 835. NGS can identify numerous mutations outside of D835, including deletions. The definitive implications of these various *FLT3*-TKD in prognostic stratification are still under review (25).

FLT3 mutations can be targeted using tyrosine kinase inhibitor drugs in combination with standard chemotherapy. The addition of tyrosine kinase inhibitor (TKI), Midostaurin, to standard chemotherapy protocol for AML led to significantly longer overall survival (OS) and event-free survival (EFS) in three *FLT3* subgroups: *FLT3*-TKD, *FLT3*-ITD low and *FLT3*-ITD high AR (RATIFY-NCT00651261) (12). Midostaurin, the first FDA approved targeted therapy in AML, is a non-selective first generation TKI that targets multiple other pathways including c-KIT, PKC, PDGFR, VEGFR, resulting in higher toxicity (13). In 2018, a more selective "second-generation" *FLT3* inhibitor, Gilteritinib, with fewer side-effects received FDA approval for relapsed or refractory *FLT3*-ITD or *FLT3*-TKD mutations-positive AML (14) based on the results of ADMIRAL (NCT02421939) and CHRYSALIS (NCT02014558) clinical trials, both of which demonstrated significantly improved outcomes in the Gilteritinib group (15, 16). Other first and second generation of inhibitors for *FLT3* such as Sorafenib (NCT01398501) (31) and Quizartinib (NCT02668653) (in newly diagnosed AML) (8), have currently reached late stages of clinical testing.

While NGS is ideal for identification of mutations across the entire coding region, specifically FLT3 TKD mutations and small FLT3 ITDs, amplicon-based targeted NGS is unable to pick up majority of the medium to larger ITDs. Hence, ITD mutations are always tested concurrently by PCR followed by fragment analysis using capillary electrophoresis (CE). Alternate computational algorithms, such as Pindel to analyze NGS data have shown promising results with 100% sensitivity and specificity in detecting medium and large insertions at 1% VAF (35). Pindel is a pattern growth algorithm to detect breakpoints of medium and large alterations from paired-end short reads (36).

Resistance mutations to *FLT3* inhibitors can emerge over the course of therapy *via* activation of alternative alternate intracellular pathways. Certain type II (second generation) *FLT3* inhibitors do not have activity against TKD mutations, therefore the emergence of a *FLT3*-TKD mutation during treatment, particularly *FLT3* D835 mutation would confer resistance to TKI (16). Crenolanib is a second generation inhibitor with activity against ITD and TKD mutations, hence,

able to overcome the treatment resistance resulting from *FLT3*-TKD alteration (25). Other mechanisms of resistance to *FLT3* inhibitors include the emergence of leukemia clones harboring mutations that activate RAS/MAPK pathway signaling, or *BCR-ABL1* fusions (37). Hence, sequential mutation analysis is important for early detection of these resistant clone to modulate the therapy accordingly, prior to overt morphologic relapse (**Tables 1**, **2** and **Figure 2**).

AML With Mutated *IDH1* and *IDH2*

Category: DNA methylation related.

Clinicopathologic and morphologic features: AML without maturation [French-American-British classification (FAB) M1], AML with maturation (FAB M2), and acute monocytic leukemia (FAB M5).

Recommended method of testing: NGS, droplet digital PCR (ddPCR) for MRD (38).

IDH1 and *IDH2* are DNA methylation genes; the mutations in *IDH* induce dysregulation of epigenetic methylation particularly the function of the *TET* family of methylators. These aberrations will ultimately result in muting the pathways involved in differentiation of hematopoietic progenitors leading to maturation arrest (5). Moreover, *IDH* mutations diminish the DNA repair mechanism and result in the accumulation of secondary mutations (39). *IDH1* and *IDH2* mutations are associated with AML in 4–9% and 8–19% of the cases respectively; they are generally a founding clone sufficient to cause overt leukemia without additional genetic alterations (23). The hotspot mutations involve amino-acid substitutions at codon 132 in exon 4 of the *IDH1* gene and codons 140 or 172 in exon 4 of *IDH2*. *IDH2*-R172 is mutually exclusive with *NPM1* mutation and is regarded as an independent sub-category by genomic analysis, but not currently recognized by the WHO (40).

Similar to *FLT3*, mutations in *IDH1*/2 are a prototypic example of targeted therapy in AML. Enasidenib is an oral selective inhibitor of mutant *IDH2* enzyme variants R140Q, R172S, and R172K (11); it was FDA approved in 2017 for the treatment of relapsed/refractory AML patients (11). Ivosidenib targets mutant IDH1enzyme leading to normal differentiation and maturation of malignant cells, and was FDA approved in 2019 for treatment of relapsed/refractory AML cases (10).

Despite the presence of hotspot mutations, NGS is ideally suited for baseline identification, serial monitoring of response to therapy and relapse emergence. Droplet digital PCR for specific mutations during serial monitoring can provide a higher sensitivity than standard NGS, however, can miss detection new emerging mutations (**Tables 1**, **2** and **Figure 2**).

AML With Mutated *KIT*

Category: Kinase signaling pathway.

Clinicopathologic and morphologic features:

Seen mostly in core-binding factor (CBF) leukemias that encompass AML with inv(16) and t(8;21). In the absence of either translocations, detection of KIT mutation is a helpful clue to search for underlying mastocytosis.

Recommended method of testing: 1-(10) Allele-specific PCR to detect exon 17 D816V specifically (41); 2- NGS (preferred) or other sequencing techniques covering for exons 17 and 8.

Activating mutations of *KIT* (encoding a transmembrane glycoprotein) leading to constitutional activation of receptor tyrosine kinase pathway, similar to systemic mastocytosis, GIST and germ cell tumors, are most commonly observed in "core binding factor" (CBF) leukemias which encompass AML with t(8;21) and AML with inv(16). Gain of function mutations in *KIT* have been found in 2% of AML overall and in a 33% of the CBF leukemias. These mutations tend to occur within exon 17,

TABLE 1 | Summary of key FDA approved targeted therapy for acute myeloid leukemia treatment.

	Drug	Targeted gene/ protein	Year of approval	Study/Clinical trial	Indication	Response Rate (RR) Complete Remission (CR) Overall Survival (OS)	Refs
1	**Enasidenib**	*IDH2*	2017	NCT01915498	Relapsed/refractory AML patients	40.3% RR 19.3% CR 5.8 months OS	11
2	**Ivosidenib**	*IDH1*	2019	NCT02074839	Relapsed/refractory AML	41.6% RR 21.6% CR 9.3 months OS	10
3	**Midostaurin**	*FLT3*	2017	RATIFY (NCT00651261)	Newly diagnosed AML with *FLT3*-TKD or *FLT3*-ITD mutations	58.9% CR 74.7 months OS	12, 13
4	**Gilteritinib**	*FLT3*	2018	ADMIRAL (NCT02421939) CHRYSALIS (NCT02014558)	Relapsed/refractory AML showing *FLT3*-TKD or *FLT3*-ITD mutations	34% CR 9.3 months OS 52% RR 41% CR 31 months OS	14–16
5	**Quizartinib**	*FLT3*	2019	Approved only in Japan Study: NCT02668653	Relapsed/refractory AML showing *FLT3*-ITD mutations	48% CR 6.2 months OS	8
6	**Venetoclax**	BCL2 protein	2018	NCT02203773 NCT02287233	Newly diagnosed AML in patients > 75 years old or who have severe comorbidities	37% CR with azacitidine 54% CR with decitabine 21% CR with cytarabine	14, 17, 18

TABLE 2 | Summary of distribution of frequencies of genes mutations in Acute Myeloid Leukemia.

Genetic Mutation	Frequency in AML (%)	Refs
ETV6	1	19
KIT	2	20
DDX41	3	21
TERT	3	22
IDH1	4-9	23
Biallelic *CEBPA*	4-9	24
FLT3-TKD	7-10	25
IDH2	8-19	23
TP53 in *de novo* AML	8-14	26–28
TP53 in therapy related AML	60	
GATA2	9	29
RUNX1 (somatic)	4-16	24
NPM1	27	4
FLT3-ITD	20-50	30

most importantly the hotspot D816, and exon 8 of the *KIT* gene (42).

Although CBF-AML has a favorable overall prognosis, most reports indicate that co-occurrence of *KIT* mutations confer an adverse prognosis in AML with both inv(16) and t (8;21), and a higher incidence of relapse in AML with inv(16) (41–44).

Therefore, CBF-AML with *KIT* mutations has been reclassified into intermediate-risk group in the National Comprehensive Cancer Network recommendations (43). Nevertheless, data is still unclear since some authors attributed the negative prognostic effect of KIT alterations to only those present at an allelic burden higher than 25% or 35% (43, 45, 46).

Moreover, the prognostic effect of *KIT* mutation in pediatric CBF AML patients is still uncertain (47).

Given the prognostic implication of the gain-of-function *KIT* mutations, and over-expression of KIT observed in most CBF-AML including those with *KIT* mutations (48), studies have explored the addition of *KIT* inhibitors such as dasatinib and avapritinib to frontline therapy (49) to improve the outcome. Results are promising in terms of reducing relapse rates of *KIT* mutated CBF-AML to levels comparable to non-KIT mutated CBF AML (49) (**Tables 1**, **2** and **Figure 2**).

WHO CLASSIFICATION DEFINING GENETIC MUTATIONS

AML With Mutated *NPM1*

Category: DNA replication and cell cycle.

Clinicopathologic and morphologic features: monocytic/myelomonocytic phenotype; blasts with classical fish-mouth morphology.

Recommended method of testing: NGS, PCR followed by CE (50), ddPCR for serial monitoring (51).

NPM1 is a molecular chaperone involved in cell cycle progression with multiple critical functions including ribosome biogenesis and transport, apoptotic response to stress stimuli, maintenance of genomic stability, and DNA repair (52). *NPM1* mutations are the most common genetic alteration in AML occurring in 25% to 41% of cases (53). These alterations affect exclusively the C-terminal region, leading to cytoplasmic mis-localization of the *NPM1* and leukemogenesis induction by inhibition of p53 activity (54). The most frequent mutation is a 4 base pair insertion of TCTG at position 956–959 (55). Multiple gene variants of NPM1 have been identified, all engendering the

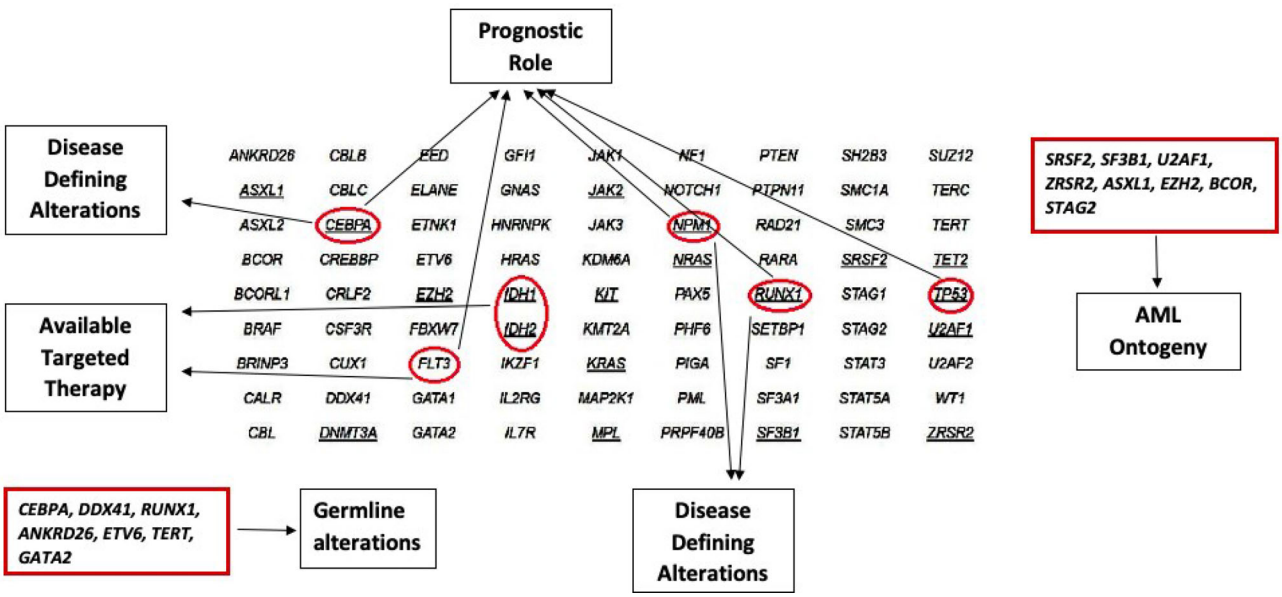

FIGURE 2 | Role of different Genetic Alterations as Diagnostic, and Prognostic markers, as well as the Availability of Targeted Therapy.

same biological effect. They are mostly associated with normal karyotype, and they are mutually exclusive with other known recurrent genetic abnormalities including *RUNX1* and *CEBPA*. Interestingly, *NPM1* mutations co-occur with mutations in epigenetic modifiers including DNMT3A, TET2 and IDH1/2 in 73% of the cases (55); these epigenetic alterations, unlike *NPM1*, are usually identified in pre-leukemic cells, and *NPM1* mutations are believed to be a later occurrence (56). *NPM1* mutated AML is considered a distinct biological subtype of AML in the latest (2016) WHO classification (57). In the settings of myelodysplastic syndrome (MDS) or myelodysplastic syndrome/myeloproliferative neoplasms (MDS/MPN), independent studies have suggested that the presence of *NPM1* mutation should be an AML-defining mutation, irrespective of the blast percentage, since these patients benefit from AML-type treatment with intensive chemotherapy (58, 59).

NPM1 mutated AML is generally considered a favorable prognostic marker with good response to induction therapy (60). The prognosis is influenced by concurrent mutations in other genes particularly FLT3 allele ratio. AML patients with *NPM1* mutation with absent or low FLT3-ITD AR (<0.5) have similar OS, and are classified as favorable risk by 2017 ELN, whereas AML patients with mutated NPM1 and high FLT3 ITD AR are classified as intermediate-risk along with wild-type *NPM1* with absent or low FLT3 ITD AR. *NPM1* mutations in AML disappear with CR. However, the persistence of the mutation during follow-up is a sign of adverse prognosis (1). Unfortunately, residual leukemia is not always apparent by morphology or flow cytometry. Cocciardi et al. described the loss of *NPM1* mutation at relapse in 9% of *NPM1* mutated AML, a finding that alters the prognosis through the selection of clones that harbor FLT3 or DNMT3A mutations exclusively (61). Both of the above findings highlight the importance of serial NGS as a follow up tool for AML to identify the clonal evolution of the disease.

A significant improvement of OS was observed in *NPM1* mutated AML with Venetoclax, a BCL2 inhibitor, in combination with hypomethylating agents in patients > 65 years old (17). Venetoclax was approved by the FDA in combination with azacitidine or decitabine for the treatment of newly diagnosed AML in patients older than 75 years old or who have severe comorbidities (14, 18). Multiple other targeted therapeutic options for *NPM1* mutated AML are ongoing; these include: 1- Deguelin, a selective silencer of the *NPM1* mutation that stimulates apoptosis and induces differentiation in AML cells (62); 2- NSC34884 a molecula that disrupts the hydrophobic region that induce *NPM1* oligomerization leading to apoptosis; 3- CIGB-300 a molecule that binds *NPM1* to prevent the phosphorylation process resulting in induction of apoptosis (63); 4- Selinexor (KPT 330), an inhibitor of exportin 1 responsible of the cytoplasmic mis-localization of mutated *NPM1* (64); 6- EAPB0503, a molecule that promotes *NPM1* degradation and corrects the *NPM1* mis-localization causing an inhibition of the leukemia cell growth (65) (**Table 2**).

AML With Mutated RUNX1

Category: myeloid transcription factor (22).

Clinicopathologic and morphologic features: minimally differentiated AML (AML-M0).

Recommended method of testing: NGS that includes the whole coding region (66).

RUNX1 is a TF located on chromosome 21q22.12 recurrently involved in leukemia due to multiple types of alterations including chromosomal translocations, mutations, and copy number changes. Somatic mutations occur in up to 15% of the AML, and the frequency is higher in secondary AML arising from MDS (67). De novo AML with mutated *RUNX1* have characteristic clinicopathologic features that include male predominance, higher frequency of *SRSF2* and *ASXL1* mutations, normal karyotype, and absent NPM1 mutations (68).

Per 2017 ELN guidelines, mutated *RUNX1* is considered as an adverse prognostic factor. You et al. reported the results of a study on 219 patients with AML, those with *RUNX1* mutations had shorter relapse-free survival than patients with wild type-*RUNX1* (69). In a meta-analysis of four studies, *RUNX1* mutation was associated with dismal prognosis in AML (70). Stengel et al. reported a better outcome when *RUNX1* mutation was associated with IDH2 mutation, but worse when associated with ASXL1, SF3B1, SRSF2 and PHF6 mutations (71). Based on the poor outcome observed in studies that evaluated AML with *RUNX1* mutations, the 2016 revised WHO AML classification system regards de novo AML with mutated *RUNX1* as a provisional entity (57, 69, 70). However, when only de novo AML cases are evaluated, the outcome is similar to AML with wild-type *RUNX1* cases (68).

Notably, as *RUNX1* is a gene implicated in germline predisposition disorders, attention should be given to specific findings in *RUNX1* alterations. The presence of double mutations or mutations with near heterozygous or homozygous VAF, presence of mutation in familial clusters and history of thrombocytopenia should prompt investigation for an underlying familial platelet disorder with predisposition to myeloid malignancy (72).

While there are no direct targeted therapies at this time, enhancer suppression using bromodomain and extra-terminal motif (BET) inhibitor prevents aberrant *RUNX1* and *ERG* signal-induced transcription in pre-clinical studies (73). Using CRISPR/Cas9, the BET protein antagonist induced inhibition of *RUNX1* resulting in more apoptosis of leukemic cells expressing mutated *RUNX1* compared to wild-type cells, inducing an improvement of the survival of mice (74) (**Table 2**).

AML With Mutated CEBPA

Category: myeloid TF.

Clinicopathologic and morphologic features: AML with or without maturation.

Recommended method of testing: NGS and PCR followed by direct sequencing (sanger-sequencing) (75).

CCAAT enhancer binding protein (*CEBPA)* is a TF located on chromosome 9q13.11 expressed in myeloid lineage. It plays a major role in proliferation and differentiation of the myeloid precursors to granulocytes or monocytes (76).

CEBPA mutations are found in 10–15% of patients (77). AML with biallelic *CEBPA* mutations in a heterozygous or

homozygous pattern are significantly associated with better overall prognosis and outcomes independently of other molecular markers (77, 78). AML with single *CEBPA* mutations are uncommon, and more studies are needed to elucidate the clinical significance. Detection of biallelic *CEBPA* alterations should also prompt investigation for an underlying germline mutation on constitutional DNA with skin fibroblast culture and investigation of underlying familial predisposition (57, 79).

Due to the high GC content, *CEBPA* is a notoriously difficult gene to sequence. There are reports of successful CEBPA sequencing by NGS. This requires extensive modifications and tweaking of the PCR conditions and probe sequences (75).

Jakobsen et al. identified *NT5E* that encodes CD73 to be up-regulated in bi-allelic *CEBPA* mutant leukemia (80). The efficacy of CD73 inhibitors, including synergy with immune checkpoint inhibitors such as PD-1/PD-L1 are being evaluated as targeted therapy in bi-allelic *CEBPA* mutant AML (NCT03454451) (**Table 2**).

GENES INVOLVED IN PROGNOSTIC RISK-STRATIFICATION OF AML

Tumor Protein p53 (*TP53*)

Category: tumor suppressor.

Clinicopathologic and morphologic features: associated with complex karyotype and shorter OS.

Recommended method of testing: NGS for detections mutations across the whole coding region and low mutant burden (81).

TP53 is mutated in 8-14% of *de novo* AML cases, but as high as 73% in AML in older patients and therapy-related AML (26–28). The mutations induce loss-of-function, dominant negative and gain-of-function phenotypes (82). The presence of a *TP53* mutation is an independent predictor of poor survival and is associated with a high risk of recurrence and treatment resistance. The 2017 ELN classification regards the presence of *TP53* mutation as an adverse risk category (7).

One important additional information obtained from NGS for prognostication, beyond just the presence of a *TP53* mutation, is the variant allele frequency (VAF). In MDS, there is significant difference in prognosis between MDS with *TP53* VAF >40% *vs.* <20% (median OS of 124 months *vs.* OS not reached) (83). Prochazka et al. categorized 98 *de novo* AML cases using similar cut-offs: VAF >40%, VAF 20% - 40% and VAF <20%; sub-clonal *TP53* mutation (VAF <20%) showed a negative prognostic effect in terms of CR rate, OS and EFS (81). These findings highlight the importance of a sensitive molecular assay that detects minute sub-clones of TP53 mutation, and the importance of the genetic data provided by NGS, including accurate VAF.

The development of targeted therapy in *TP53* mutated cases should take into consideration multiple factors such as alterations affecting related pathways as well as other therapeutic options such as BCL2 inhibitors' in the latter, the *TP53* activation may overcome resistance to BCL-2 inhibitors (84). Idasanutlin, an *MDM2* inhibitor (85) and Cobimetinib a MEK inhibitor (86), both affecting *TP53* expression, are being evaluated in combination with Venetoclax (BCL2 inhibitor) in phase I and phase II trials. Also, clinical trials exploring APR-246, a mutant P53 activator, are underway (NCT03931291); recently, in 2020, FDA granted breakthrough therapy designation for APR-246 in Combination with Azacitidine for the treatment of MDS with a *TP53* Mutation (87). The different roles of *TP53* in chemotherapy response and particularly the work of Zuber et al. on the activation of *TP53* gene in mice provide supportive data of the significant role of exogenous activation of *TP53* pathway in regard to treatment response (79) (**Table 2**).

GENE MUTATION SIGNATURES FOR IDENTIFICATION OF AML ONTOGENY

Lindsley et al. evaluated the differences in gene mutation patterns between secondary AML, therapy-related AML, and *de novo* AML to decode the ontogeny of different subsets of AML. The authors identified a set of gene mutations that can provide an objective evidence of AML ontogeny irrespective of clinical information. The presence of a mutations in any of these genes: *SRSF2, SF3B1, U2AF1, ZRSR2, ASXL1, EZH2, BCOR*, or *STAG2* was >95% specific for the diagnosis of secondary AML (88). Majority of these genes, *SRSF2, SF3B1, U2AF1, ZRSR2*, are genes encoding proteins that belong to the spliceosomal complex that encompasses a large number of members including small nuclear ribonucleoproteins and protein factors responsible for removing introns from a transcribed pre-mRNA (89). *EZH2* and *BCOR* mutations are associated with worse OS in AML (55, 90, 91) while *STAG2* is a part of the cohesion complex.

The findings have major clinical and diagnostic implications. When detected in "*de novo*" setting, the presence of secondary AML mutations can identify a subset of patients with worse outcome (88). The "secondary-type" mutations, as expected, are frequently present in MDS (92) and chronic myelomonocytic leukemia (CMML) (93). These findings imply these mutations are unlikely to promote the development of acute leukemia without a co-operating event. It is also to be noted that these mutations occur early in the disease course and persist during follow-up despite morphologic CR, hence should not be used for MRD follow up purposes (**Figure 2** and **Table 2**).

UNCOVERING UNDERLYING GERMLINE MUTATIONS IN AML AND FAMILIAL PREDISPOSITION

Somatic NGS sequencing in AML can potentially uncover incidental germline mutations. The latest WHO recognizes myeloid neoplasms with germline predisposition syndromes as a distinct diagnostic category (57). Recognition of these

conditions has major therapeutic implications (94) and different diagnostic and monitoring strategies for the patient himself, as well as the family members. When clinically suspicious, germline mutations testing and proper family screening are important, especially when an allogeneic bone marrow transplant is under consideration.

The new WHO classification introduced four broad categories of AML with germline predisposition: 1-nMyeloid neoplasms with germline predisposition without a pre-existing disorder or organ dysfunction, it includes AML with *CEBPA* and *DDX41* mutations 2- Myeloid neoplasms with germline predisposition and pre-existing platelet disorders, which encompass *RUNX1*, *ANKRD26* and *ETV6* mutations 3- Myeloid neoplasms with germline *GATA2* mutation and 4- Myeloid neoplasms with germline predisposition associated with inherited bone failure syndromes and telomere biology disorders. Hence, it is recommended to include these genes, *CEBPA, DDX41, RUNX1, ANKRD26, ETV6, TERT* and *GATA2*, within the standard NGS panel.

Since most of the mutated genes associated with germline predisposition disorders are also recurrently mutated in sporadic leukemia cases, attention should be given when interpreting the results of sequencing to identify clues suggesting a germline origin, such as double mutations, one with a near heterozygous or homozygous VAF (95). The presence of any of these mutations in a newly diagnosed leukemia is not sufficient to diagnose an AML with germline predisposition. Germline origin by testing constitutional DNA (skin fibroblast culture in most patients with active hematological malignancies) should be performed for confirmation (72, 88). It is important to highlight that targeted sequencing will not detect all the germline alterations such as intronic regions and large deletions spanning multiple exons; additional tests should be done to further investigate when clinically suspicious, such as array comparative hybridization for deletions and whole exome sequencing for novel mutations (96, 97). The confirmation of germline origin requires a prior genetic counseling since the results may cause significant disturbance of the affected individuals and families if not properly interpreted and handled (**Figure 2** and **Table 2**).

VARIANT ALLELE FREQUENCY OF GENE MUTATIONS ESTIMATED BY NGS IS IMPORTANT FOR TREATMENT DECISIONS

NGS is a quantitative assay that provides information on mutant allele burden, which is critical for management decisions and predict outcome. VAF is defined as the ratio of reads with mutation against total (mutant + wild-type) reads. Hence, current NGS reports are generally not limited to presence or absence of mutations but include the VAF of each alteration. VAF is important for management decisions and outcome prediction in AML and MDS. This was previously elaborated in the context of TP53 mutations in AML and MDS (81, 83). A high mutant allele burden at diagnosis can be a negative prognostic factor. Patel et al. demonstrated a negative prognostic effect of high *NPM1* mutant allele burden at diagnosis in *de novo* AML cases (98). Sasaki et al. investigated the effect of the VAF of clonal hematopoiesis associated genes *ASXL1, DNMT3A, JAK2, TET2*, and *TP53* mutations on survival in 421 newly diagnosed AML using NGS. Higher VAF (cut-off of 30%) was associated with worse survival in AML patients within intermediate-risk cytogenetic group (99).

SEQUENTIAL NGS ASSESSMENT FOR MRD CHEMORESISTANCE AND EARLY RELAPSE DETECTION

Serial NGS is ideal for monitoring AML patients for mutational clearance and/or clonal evolution and relapse. Clearance of somatic mutations in non-preleukemia genes at the time of CR was associated with better OS and decreased risk for relapse (100). Sequential analysis for persistent mutations is particularly helpful to evaluate residual disease in patients treated using novel targeted therapeutic agents, such as *IDH* inhibitors, as these can pose diagnostic challenges on morphology and/flow cytometry. Therefore, NGS is particularly useful to objectively evaluate evidence of residual disease in these circumstances.

The implications of NGS include assessment of effectiveness of therapy and detection of resistance mutations which can have implications on management and therapeutic regimen choices. Most importantly, sequencing of blast cells can detect *TP53* mutations which are independent predictors of poor survival and treatment resistance (7). Moreover, mutations that trigger resistance to *FLT3* inhibitors can be identified in AML cases including emergence of leukemic clones harboring mutations that activate RAS/MAPK pathway signaling (37). On the other hand, emergence of *FLT3*-TKD mutation during treatment can engender resistance to TKI; therefore, sequential mutational analysis is mandatory for early detection of potential treatment resistance and the choice of alternative drugs. Finally, the acquisition of *IDH1, WT1, ASXL1* variants in certain AML clones, either present at diagnosis or gained at relapse confer chemotherapy resistance (101).

While NGS facilitates identification of disease evolution and treatment resistance mutations, there are several caveats. First, the sensitivity of standard NGS panels used in clinical laboratories, currently limited to 2-5% VAF (102) is less or comparable to standard flow cytometry techniques for detection of residual disease at the time of morphologic remission. Yet, NGS results are more helpful than latter in settings where blasts show monocytic differentiation or in settings with limited sample quality. The identification of the mutations is partly limited by the intrinsic error rates (0.1% to 1%), that can be potentially overcome using the error correction methodologies such as molecular barcoding (103). Alternately, ultra-deep sequencing NGS with an ultra-high depth of coverage or individual gene assays such as ddPCR assays can be helpful (104). In one study, a high-throughput deep sequencing NGS

method showed a detection sensitivity of 10^{-4} for SNVs and 10^{-5} for insertions/deletions (105).

Second, persistence of "pre-leukemia" mutation signature cannot be used for MRD detection. NGS enables the identification of background clonal hematopoiesis. Clonal hematopoiesis of indeterminate potential (CHIP), defined as the presence of a somatic alterations (either a somatic mutation associated with myeloid malignancy present at least 2% VAF or cytogenetic abnormality) in apparently healthy individuals. These patients have an increased risk of developing a hematologic malignancy, higher risk of developing therapy related myeloid neoplasms following chemotherapy for a solid tumor and increased frequency of adverse cardiovascular events (106).

Most of the CHIP alterations belong to genes *DNMT3A, TET2* and *ASXL1* (DTA) (106, 107). All three genes are involved in epigenetic regulation of myeloid differentiation and are considered to be within preleukemic hematopoetic stem cells (108). DTA gene mutations cannot induce leukemia without a co-operating second hits (109). The mutations in either one of the DTA genes impart negative prognostic outcomes in AML (110–112). The 2017 ELN classifies *ASXL1* mutations as adverse risk category (7), and its presence was >95% specific for AML of secondary origin (88).

Mutations in all three genes can be seen within the entire coding region, and include missense, frameshift, nonsense and splice-site mutations leading to a non-functional protein. The only exception being *DNMT3A*, which has a hotspot point mutation in codon R882 (113, 114). Loss of *TET2* function can also occur *via* mutations in *IDH1*, *IDH2* and *WT1* (115, 116), that explain the mutual exclusivity between *IDH1/2-TET2-WT1* mutations in AML (116). Hence, NGS is an ideal technique for detection of all these mutations.

Importantly, DTA gene mutations likely persist at the time of remission of AML in pre-leukemic clones, hence they cannot be used to detect MRD (109). *DNMT3A* R882 mutation persists in 75% of AML patients during remission without any negative impact on outcomes (117). Interestingly, ascorbate supplementation can restore methylation patterns and minimize proliferation of blasts (118). A clinical trial evaluating the efficacy of azacitidine and high dose ascorbic acid in AML with mutated *TET2* is ongoing (NCT03397173).

9- Subclonal evolution in AML using single-cell technology:

All malignancies are genetically heterogeneous, composed of mutationally-defined subclonal cell populations characterized by distinct phenotypes. Precise identification of clonal and sub-clonal architecture is mandatory to understand the temporal evolution of tumor and the emergence of treatment resistance. Bulk sequencing cannot definitively resolve the actual complex clonal composition of neoplasms generally and AML specifically. Therefore, there is great interest in understanding the genetic alterations at a single-cell level using the newly designed sequencing platforms. Multiple reports published recently highlighted the subclonal selection during the treatment journey. Morita et al. reported the sub-clonal complexity in 37, clonal architecture and mutational histories of 123 AML patients. The authors explored single cell-level mutation co-occurrence and mutual exclusivity revealing novel clonal relationships; and emergence and selection of resistant subclones under therapies by longitudinal analysis (119). Interestingly, current emerging single-cell multi-omics technology, aid in profiling simultaneously single-cell mutations and cell surface proteins in AML cases, allowing correlation of genetic and phenotypic heterogeneity (120). Using the novel features of this technology, Petti et al., using a high-throughput platform to distinguish tumor and non-tumor cells in AML, identified tumor cells showing phenotypic aberrancies and lineage infidelity, evaluated the sub-clonal progression of tumor samples with time with a molecular signature for each sample, and cell-surface markers that could be used to isolate specific cells for downstream studies (121). Another study showed that *FLT3*-ITD mutation was present in the primitive cells, whereas *FLT3*-TKD mutation was present in the more differentiated cells within the same tumor. The study demonstrated that *FLT3* variants differentially affected AML differentiation that explained the worse prognosis associated with certain alleles (122).

DISCUSSION

We believe that NGS is an exciting tool that has helped pathologists and oncologists tremendously to improve their understanding of AML pathogenesis and clonal evolution of the disease. It has played a major role in designing therapies targeting the disease and control relapse. Genomic analysis of cases at diagnosis and relapse have uncovered the alterations and clonal evolution of the genetic profile of the tumor cells during disease progression. The cited studies and clinical trial results highlight the unique genetic signature of every patient's disease, not only with respect to different combinations of mutations, but also in terms of clonal burden of different mutations, sequence of mutations, and concurrent chromosomal gain and losses. As a consequence of this, 1- the prognostic outcome of each patient can be unique and cannot be simply generalized based on the presence or absence of mutations; 2- the therapeutic molecules should be targeted to attack both the primary clone and emerging sub-clones with potential resistance mechanisms. Hence, a better understanding of each patient's AML genome by NGS is mandatory to make decisions related to appropriate personalized therapy.

Nevertheless, a lot more standardization is needed for implementing NGS in daily clinical practice; for instance, so far there is no universal consensus, yet on which target genes should be included in the sequencing panels. Moreover, the sequencing depth of coverage is still a subjective number chosen by each laboratory for the validation of their sequencer. Furthermore, there is no consistent practice for quality assessment of sequencing data; the accuracy of results is compromised at genome locations with highly repetitive sequences, or in GC-rich locations, common problems encountered during sequencing and data analysis. Finally, results interpretation can be time-consuming and requires specific expertise from

bioinformatics and pathology (or equivalent degree). Further standardizations are needed when NGS is used for serial follow-up to assess measurable residual disease. It is important to keep in mind that bulk NGS represents the "average" findings per cell, and hence the data on genomic complexity is only inferred. On the other hand, single-cell NGS can accurately provide concrete information on sub-clonal architecture, but it has not reached the mainstream clinical work-flow yet (123).

At the same time, while NGS is an important component of AML workup, other testing needs to be performed to accurately sub-classify the disease, specify the prognosis, and determine the best targeted therapy. A comprehensive workup for AML should include a karyotype to identify the disease defining chromosomal translocations including t(8;21), t(15;17), t(16;16) and the new WHO entity AML with *BCR/ABL* (57); however, some fusions can be cryptic (57), and other testing is required to highlight these aberrations including Fluorescence in situ hybridization (FISH), RT-PCR, RNAseq, and other targeted fusions assays. Moreover copy-neutral loss of heterozygosity (cnLOH) has prognostic significance in patients with acute leukemia (124); Walker et al. showed that LOH mediated by uniparental disomy (UPD) is a common finding in cytogenetically normal AML. Also, UPD involving 13q and 11p are important for genetic risk stratification in these cases (125). FISH and karyotyping can be used to depict copy number aberrations; however, they are limited by low resolution or restriction to targeted assessment. The alternative method of testing is Chromosomal microarray which can characterize chromosomal copy number changes and cnLOH in myeloid malignancies (126).

Overall, NGS has enabled phenomenal advances in understanding of molecular genetics of AML and opened up new horizons for development of highly effective therapeutic molecules and protocols for individualized treatment and monitoring that are completely reshaping the management of the different subtypes of AML.

AUTHOR CONTRIBUTIONS

All authors contributed to writing the manuscript, reviewing the final version and preparing the figures and tables. All authors contributed to the article and approved the submitted version.

REFERENCES

1. Ivey A, Hills RK, Simpson MA, Jovanovic JV, Gilkes A, Grech A, et al. Assessment of Minimal Residual Disease in Standard-Risk AML. *N Engl J Med* (2016) 374(5):422–33. doi: 10.1056/NEJMoa1507471
2. DG Gilliland ed. Molecular Genetics of Human Leukemias: New Insights Into Therapy. *Semin Hematol*. (2002) 39(4 Suppl 3):6–11. doi: 10.1053/shem.2002.36921
3. Cancer Genome Atlas Research N, Ley TJ, Miller C, Ding L, Raphael BJ, Mungall AJ, et al. Genomic and Epigenomic Landscapes of Adult *De Novo* Acute Myeloid Leukemia. *N Engl J Med* (2013) 368(22):2059–74. doi: 10.1056/NEJMoa1301689
4. Papaemmanuil E, Gerstung M, Bullinger L, Gaidzik VI, Paschka P, Roberts ND, et al. Genomic Classification and Prognosis in Acute Myeloid Leukemia. *N Engl J Med* (2016) 374(23):2209–21. doi: 10.1056/NEJMoa1516192
5. Figueroa ME, Abdel-Wahab O, Lu C, Ward PS, Patel J, Shih A, et al. Leukemic IDH1 and IDH2 Mutations Result in a Hypermethylation Phenotype, Disrupt TET2 Function, and Impair Hematopoietic Differentiation. *Cancer Cell* (2010) 18(6):553–67. doi: 10.1016/j.ccr.2010.11.015
6. Arber DA, Orazi A, Hasserjian R, Thiele J, Borowitz MJ, Le Beau MM, et al. The 2016 Revision to the World Health Organization Classification of Myeloid Neoplasms and Acute Leukemia. *Blood* (2016) 127(20):2391–405. doi: 10.1182/blood-2016-06-721662
7. Dohner H, Estey E, Grimwade D, Amadori S, Appelbaum FR, Buchner T, et al. Diagnosis and Management of AML in Adults: 2017 ELN Recommendations From an International Expert Panel. *Blood* (2017) 129(4):424–47. doi: 10.1182/blood-2016-08-733196
8. *Quizartinib With Standard of Care Chemotherapy and as Continuation Therapy in Patients With Newly Diagnosed FLT3-ITD (+) Acute Myeloid Leukemia (AML) (QuANTUM-First)* . Available at: https://clinicaltrials.gov/ct2/show/NCT02668653 (Accessed September 2020).
9. Luthra R, Patel KP, Reddy NG, Haghshenas V, Routbort MJ, Harmon MA, et al. Next-Generation Sequencing-Based Multigene Mutational Screening for Acute Myeloid Leukemia Using MiSeq: Applicability for Diagnostics and Disease Monitoring. *Haematologica* (2014) 99(3):465–73. doi: 10.3324/haematol.2013.093765
10. Available at: https://www.fda.gov/drugs/resources-information-approved-drugs/fda-approves-ivosidenib-first-line-treatment-aml-idh1-mutation (Accessed September 2020).
11. Stein EM, DiNardo CD, Fathi AT, Pollyea DA, Stone RM, Altman JK, et al. Molecular Remission and Response Patterns in Patients With Mutant-IDH2 Acute Myeloid Leukemia Treated With Enasidenib. *Blood* (2019) 133(7):676–87. doi: 10.1182/blood-2018-08-869008
12. Sakaguchi M, Yamaguchi H, Najima Y, Usuki K, Ueki T, Oh I, et al. Prognostic Impact of Low Allelic Ratio FLT3-ITD and NPM1 Mutation in Acute Myeloid Leukemia. *Blood Adv* (2018) 2(20):2744–54. doi: 10.1182/bloodadvances.2018020305
13. Stone RM, Mandrekar SJ, Sanford BL, Laumann K, Geyer S, Bloomfield CD, et al. Midostaurin Plus Chemotherapy for Acute Myeloid Leukemia With a FLT3 Mutation. *N Engl J Med* (2017) 377(5):454–64. doi: 10.1056/NEJMoa1614359
14. Administration USFaD. Available at: https://www.fda.gov/drugs/fda-approves-gilteritinib-relapsed-or-refractory-acute-myeloid-leukemia-aml-flt3-mutatation (Accessed September 2020).
15. Perl AE, Altman JK, Cortes J, Smith C, Litzow M, Baer MR, et al. Selective Inhibition of FLT3 by Gilteritinib in Relapsed or Refractory Acute Myeloid Leukaemia: A Multicentre, First-in-Human, Open-Label, Phase 1-2 Study. *Lancet Oncol* (2017) 18(8):1061–75. doi: 10.1016/S1470-2045(17)30416-3
16. Perl AE, Martinelli G, Cortes JE, Neubauer A, Berman E, Paolini S, et al. Gilteritinib or Chemotherapy for Relapsed or Refractory FLT3-Mutated AML. *N Engl J Med* (2019) 381(18):1728–40. doi: 10.1056/NEJMoa1902688
17. Lachowiez CA, Loghavi S, Kadia TM, Daver N, Borthakur G, Pemmaraju N, et al. Outcomes of Older Patients With NPM1-Mutated AML: Current Treatments and the Promise of Venetoclax-Based Regimens. *Blood Adv* (2020) 4(7):1311–20. doi: 10.1182/bloodadvances.2019001267
18. *FDA Approves Venetoclax in Combination for AML in Adults*. Available at: https://www.fda.gov/drugs/fda-approves-venetoclax-combination-aml-adults.
19. Zhou F, Chen B. Acute Myeloid Leukemia Carrying ETV6 Mutations: Biologic and Clinical Features. *Hematology* (2018) 23(9):608–12. doi: 10.1080/10245332.2018.1482051
20. Zaker F, Mohammadzadeh M, Mohammadi M. Detection of KIT and FLT3 Mutations in Acute Myeloid Leukemia With Different Subtypes. *Arch Iran Med* (2010) 13(1):21–5.
21. Sébert M, Passet M, Raimbault A, Rahmé R, Raffoux E, Sicre de Fontbrune F, et al. Germline DDX41 Mutations Define a Significant Entity Within Adult MDS/AML Patients. *Blood* (2019) 134(17):1441–4. doi: 10.1182/blood.2019000909

22. Mosrati MA, Willander K, Falk IJ, Hermanson M, Höglund M, Stockelberg D, et al. Association Between TERT Promoter Polymorphisms and Acute Myeloid Leukemia Risk and Prognosis. *Oncotarget* (2015) 6(28):25109–20. doi: 10.18632/oncotarget.4668
23. Dohner H, Weisdorf DJ, Bloomfield CD. Acute Myeloid Leukemia. *N Engl J Med* (2015) 373(12):1136–52. doi: 10.1056/NEJMra1406184
24. SH Swerdlow, E Campo, NL Harris, ES Jaffe, SA Pileri, H Stein, J Thiele eds. *WHO Classif Ication of Tumours of Haematopoietic and Lymphoid Tissues. Revised 4th edition*. Lyon: IARC (2017).
25. Daver N, Schlenk RF, Russell NH, Levis MJ. Targeting FLT3 Mutations in AML: Review of Current Knowledge and Evidence. *Leukemia* (2019) 33 (2):299–312. doi: 10.1038/s41375-018-0357-9
26. Barbosa K, Li S, Adams PD, Deshpande AJ. The Role of TP53 in Acute Myeloid Leukemia: Challenges and Opportunities. *Genes Chromosomes Cancer* (2019) 58(12):875–88. doi: 10.1002/gcc.22796
27. Kadia TM, Jain P, Ravandi F, Garcia-Manero G, Andreef M, Takahashi K, et al. TP53 Mutations in Newly Diagnosed Acute Myeloid Leukemia: Clinicomolecular Characteristics, Response to Therapy, and Outcomes. *Cancer* (2016) 122(22):3484–91. doi: 10.1002/cncr.30203
28. Boddu P, Kantarjian H, Ravandi F, Garcia-Manero G, Borthakur G, Andreeff M, et al. Outcomes With Lower Intensity Therapy in TP53-Mutated Acute Myeloid Leukemia. *Leuk Lymphoma* (2018) 59(9):2238–41. doi: 10.1080/10428194.2017.1422864
29. Fasan A, Eder C, Haferlach C, Grossmann V, Kohlmann A, Dicker F, et al. GATA2 Mutations are Frequent in Intermediate-Risk Karyotype AML With Biallelic CEBPA Mutations and are Associated With Favorable Prognosis. *Leukemia* (2013) 27(2):482–5. doi: 10.1038/leu.2012.174
30. Schneider F, Hoster E, Schneider S, Dufour A, Benthaus T, Kakadia PM, et al. Age-Dependent Frequencies of NPM1 Mutations and FLT3-ITD in Patients With Normal Karyotype AML (NK-AML). *Ann Hematol* (2012) 91 (1):9–18. doi: 10.1007/s00277-011-1280-6
31. Levis M. FLT3 Mutations in Acute Myeloid Leukemia: What is the Best Approach in 2013? *Hematol Am Soc Hematol Educ Program* (2013) 2013:220–6. doi: 10.1182/asheducation-2013.1.220
32. Gale RE, Green C, Allen C, Mead AJ, Burnett AK, Hills RK, et al. The Impact of FLT3 Internal Tandem Duplication Mutant Level, Number, Size, and Interaction With NPM1 Mutations in a Large Cohort of Young Adult Patients With Acute Myeloid Leukemia. *Blood* (2008) 111(5):2776–84. doi: 10.1182/blood-2007-08-109090
33. Schlenk RF, Kayser S, Bullinger L, Kobbe G, Casper J, Ringhoffer M, et al. Differential Impact of Allelic Ratio and Insertion Site in FLT3-ITD-Positive AML With Respect to Allogeneic Transplantation. *Blood* (2014) 124 (23):3441–9. doi: 10.1182/blood-2014-05-578070
34. Boddu PC, Kadia TM, Garcia-Manero G, Cortes J, Alfayez M, Borthakur G, et al. Validation of the 2017 European LeukemiaNet Classification for Acute Myeloid Leukemia With NPM1 and FLT3-Internal Tandem Duplication Genotypes. *Cancer* (2019) 125(7):1091–100. doi: 10.1002/cncr.31885
35. Spencer DH, Abel HJ, Lockwood CM, Payton JE, Szankasi P, Kelley TW, et al. Detection of FLT3 Internal Tandem Duplication in Targeted, Short-Read-Length, Next-Generation Sequencing Data. *J Mol Diagn* (2013) 15 (1):81–93. doi: 10.1016/j.jmoldx.2012.08.001
36. Ye K, Schulz MH, Long Q, Apweiler R, Ning Z. Pindel: A Pattern Growth Approach to Detect Break Points of Large Deletions and Medium Sized Insertions From Paired-End Short Reads. *Bioinformatics* (2009) 25 (21):2865–71. doi: 10.1093/bioinformatics/btp394
37. McMahon CM, Ferng T, Canaani J, Wang ES, Morrissette JJD, Eastburn DJ, et al. Clonal Selection With RAS Pathway Activation Mediates Secondary Clinical Resistance to Selective FLT3 Inhibition in Acute Myeloid Leukemia. *Cancer Discovery* (2019) 9(8):1050–63. doi: 10.1158/2159-8290.CD-18-1453
38. Petrova L, Vrbacky F, Lanska M, Zavrelova A, Zak P, Hrochova K. IDH1 and IDH2 Mutations in Patients With Acute Myeloid Leukemia: Suitable Targets for Minimal Residual Disease Monitoring? *Clin Biochem* (2018) 61:34–9. doi: 10.1016/j.clinbiochem.2018.08.012
39. Aref S, Kamel Areida el S, Abdel Aaal MF, Adam OM, El-Ghonemy MS, El-Baiomy MA, et al. Prevalence and Clinical Effect of IDH1 and IDH2 Mutations Among Cytogenetically Normal Acute Myeloid Leukemia Patients. *Clin Lymphoma Myeloma Leuk* (2015) 15(9):550–5. doi: 10.1016/j.clml.2015.05.009
40. Marcucci G, Maharry K, Wu YZ, Radmacher MD, Mrozek K, Margeson D, et al. IDH1 and IDH2 Gene Mutations Identify Novel Molecular Subsets Within *De Novo* Cytogenetically Normal Acute Myeloid Leukemia: A Cancer and Leukemia Group B Study. *J Clin Oncol* (2010) 28(14):2348–55. doi: 10.1200/JCO.2009.27.3730
41. Gulley ML, Shea TC, Fedoriw Y. Genetic Tests to Evaluate Prognosis and Predict Therapeutic Response in Acute Myeloid Leukemia. *J Mol Diagn: JMD* (2010) 12(1):3–16. doi: 10.2353/jmoldx.2010.090054
42. Paschka P, Marcucci G, Ruppert AS, Mrózek K, Chen H, Kittles RA, et al. Adverse Prognostic Significance of KIT Mutations in Adult Acute Myeloid Leukemia With inv(16) and t(8;21): A Cancer and Leukemia Group B Study. *J Clin Oncol* (2006) 24(24):3904–11. doi: 10.1200/jco.2006.06.9500
43. Kuykendall A, Duployez N, Boissel N, Lancet JE, Welch JS. Acute Myeloid Leukemia: The Good, the Bad, and the Ugly. *Am Soc Clin Oncol Educ Book* (2018) 38):555–73. doi: 10.1200/edbk_199519
44. Jin H, Zhu Y, Hong M, Wu Y, Qiu H, Wang R, et al. Co-Occurrence of KIT and NRAS Mutations Defines an Adverse Prognostic Core-Binding Factor Acute Myeloid Leukemia. *Leuk Lymphoma* (2021) 1–10. doi: 10.1080/10428194.2021.1919660
45. Allen C, Hills RK, Lamb K, Evans C, Tinsley S, Sellar R, et al. The Importance of Relative Mutant Level for Evaluating Impact on Outcome of KIT, FLT3 and CBL Mutations in Core-Binding Factor Acute Myeloid Leukemia. *Leukemia* (2013) 27(9):1891–901. doi: 10.1038/leu.2013.186
46. Duployez N, Marceau-Renaut A, Boissel N, Petit A, Bucci M, Geffroy S, et al. Comprehensive Mutational Profiling of Core Binding Factor Acute Myeloid Leukemia. *Blood* (2016) 127(20):2451–9. doi: 10.1182/blood-2015-12-688705
47. Pollard JA, Alonzo TA, Gerbing RB, Ho PA, Zeng R, Ravindranath Y, et al. Prevalence and Prognostic Significance of KIT Mutations in Pediatric Patients With Core Binding Factor AML Enrolled on Serial Pediatric Cooperative Trials for *De Novo* AML. *Blood* (2010) 115(12):2372–9. doi: 10.1182/blood-2009-09-241075
48. Lück SC, Russ AC, Du J, Gaidzik V, Schlenk RF, Pollack JR, et al. KIT Mutations Confer a Distinct Gene Expression Signature in Core Binding Factor Leukaemia. *Br J Haematol* (2010) 148(6):925–37. doi: 10.1111/j.1365-2141.2009.08035.x
49. Borthakur G, Kantarjian H. Core Binding Factor Acute Myelogenous Leukemia-2021 Treatment Algorithm. *Blood Cancer J* (2021) 11(6):114. doi: 10.1038/s41408-021-00503-6
50. Szankasi P, Jama M, Bahler DW. A New DNA-Based Test for Detection of Nucleophosmin Exon 12 Mutations by Capillary Electrophoresis. *J Mol Diagn* (2008) 10(3):236–41. doi: 10.2353/jmoldx.2008.070167
51. Wertheim GBW, Bagg A. NPM1 for MRD? Droplet Like It's Hot! *J Mol Diagn* (2017) 19(4):498–501. doi: 10.1016/j.jmoldx.2017.04.008
52. Zarka J, Short NJ, Kanagal-Shamanna R, Issa GC. Nucleophosmin 1 Mutations in Acute Myeloid Leukemia. *Genes (Basel)* (2020) 11(6):649. doi: 10.3390/genes11060649
53. Rau R, Brown P. Nucleophosmin (NPM1) Mutations in Adult and Childhood Acute Myeloid Leukaemia: Towards Definition of a New Leukaemia Entity. *Hematol Oncol* (2009) 27(4):171–81. doi: 10.1002/hon.904
54. Colombo E, Marine JC, Danovi D, Falini B, Pelicci PG. Nucleophosmin Regulates the Stability and Transcriptional Activity of P53. *Nat Cell Biol* (2002) 4(7):529–33. doi: 10.1038/ncb814
55. Damiani D, Tiribelli M. Molecular Landscape in Adult Acute Myeloid Leukemia: Where We are Where We Going? *J Lab Prec Med* (2019) 4 (0):17. doi: 10.21037/jlpm.2018.09.08
56. Villanueva MT. Genetics: Acute Myeloid Leukaemia: Driving the Driver. *Nat Rev Cancer* (2016) 16(8):479. doi: 10.1038/nrc.2016.75
57. Swerdlow SHCE, Harris NL, Jaffe ES, Pileri SA, Stein H, et al. *WHO Classification of Tumours of Haematopoietic and Lymphoid Tissues, Revised 4th edition.* (2017).
58. Montalban-Bravo G, Kanagal-Shamanna R, Sasaki K, Patel K, Ganan-Gomez I, Jabbour E, et al. NPM1 Mutations Define a Specific Subgroup of MDS and MDS/MPN Patients With Favorable Outcomes With Intensive Chemotherapy. *Blood Adv* (2019) 3(6):922–33. doi: 10.1182/bloodadvances.2018026989
59. Patel SS, Ho C, Ptashkin RN, Sadigh S, Bagg A, Geyer JT, et al. Clinicopathologic and Genetic Characterization of Nonacute NPM1-

Mutated Myeloid Neoplasms. *Blood Adv* (2019) 3(9):1540–5. doi: 10.1182/bloodadvances.2019000090
60. DiNardo CD, Cortes JE. Mutations in AML: Prognostic and Therapeutic Implications. *Hematol Am Soc Hematol Educ Program* (2016) 2016(1):348–55. doi: 10.1182/asheducation-2016.1.348
61. Cocciardi S, Dolnik A, Kapp-Schwoerer S, Rucker FG, Lux S, Blatte TJ, et al. Clonal Evolution Patterns in Acute Myeloid Leukemia With NPM1 Mutation. *Nat Commun* (2019) 10(1):2031. doi: 10.1038/s41467-019-09745-2
62. Yi S, Wen L, He J, Wang Y, Zhao F, Zhao J, et al. Deguelin, a Selective Silencer of the NPM1 Mutant, Potentiates Apoptosis and Induces Differentiation in AML Cells Carrying the NPM1 Mutation. *Ann Hematol* (2015) 94(2):201–10. doi: 10.1007/s00277-014-2206-x
63. Di Matteo A, Franceschini M, Chiarella S, Rocchio S, Travaglini-Allocatelli C, Federici L. Molecules That Target Nucleophosmin for Cancer Treatment: An Update. *Oncotarget* (2016) 7(28):44821–40. doi: 10.18632/oncotarget.8599
64. Talati C, Sweet KL. Nuclear Transport Inhibition in Acute Myeloid Leukemia: Recent Advances and Future Perspectives. *Int J Hematol Oncol* (2018) 7(3):IJH04. doi: 10.2217/ijh-2018-0001
65. Nabbouh AI, Hleihel RS, Saliba JL, Karam MM, Hamie MH, Wu HJM, et al. Imidazoquinoxaline Derivative EAPB0503: A Promising Drug Targeting Mutant Nucleophosmin 1 in Acute Myeloid Leukemia. *Cancer* (2017) 123(9):1662–73. doi: 10.1002/cncr.30515
66. Kohlmann A, Nadarajah N, Alpermann T, Grossmann V, Schindela S, Dicker F, et al. Monitoring of Residual Disease by Next-Generation Deep-Sequencing of RUNX1 Mutations Can Identify Acute Myeloid Leukemia Patients With Resistant Disease. *Leukemia* (2014) 28(1):129–37. doi: 10.1038/leu.2013.239
67. Dicker F, Haferlach C, Sundermann J, Wendland N, Weiss T, Kern W, et al. Mutation Analysis for RUNX1, MLL-PTD, FLT3-ITD, NPM1 and NRAS in 269 Patients With MDS or Secondary AML. *Leukemia* (2010) 24(8):1528–32. doi: 10.1038/leu.2010.124
68. Quesada AE, Montalban-Bravo G, Luthra R, Patel KP, Sasaki K, Bueso-Ramos CE, et al. Clinico-Pathologic Characteristics and Outcomes of the World Health Organization (WHO) Provisional Entity *De Novo* Acute Myeloid Leukemia With Mutated RUNX1. *Modern Pathol* (2020) 33(9):1678–89. doi: 10.1038/s41379-020-0531-2
69. You E, Cho YU, Jang S, Seo EJ, Lee JH, Lee JH, et al. Frequency and Clinicopathologic Features of RUNX1 Mutations in Patients With Acute Myeloid Leukemia Not Otherwise Specified. *Am J Clin Pathol* (2017) 148(1):64–72. doi: 10.1093/ajcp/aqx046
70. Jalili M, Yaghmaie M, Ahmadvand M, Alimoghaddam K, Mousavi SA, Vaezi M, et al. Prognostic Value of RUNX1 Mutations in AML: A Meta-Analysis. *Asian Pac J Cancer Prev* (2018) 19(2):325–9. doi: 10.22034/APJCP.2018.19.2.325
71. Stengel A, Kern W, Meggendorfer M, Nadarajah N, Perglerova K, Haferlach T, et al. Number of RUNX1 Mutations, Wild-Type Allele Loss and Additional Mutations Impact on Prognosis in Adult RUNX1-Mutated AML. *Leukemia* (2018) 32(2):295–302. doi: 10.1038/leu.2017.239
72. Kanagal-Shamanna R, Loghavi S, DiNardo CD, Medeiros LJ, Garcia-Manero G, Jabbour E, et al. Bone Marrow Pathologic Abnormalities in Familial Platelet Disorder With Propensity for Myeloid Malignancy and Germline RUNX1 Mutation. *Haematologica* (2017) 102(10):1661–70. doi: 10.3324/haematol.2017.167726
73. Antony J, Gimenez G, Taylor T, Khatoon U, Day R, Morison IM, et al. BET Inhibition Prevents Aberrant RUNX1 and ERG Transcription in STAG2 Mutant Leukaemia Cells. *J Mol Cell Biol* (2020) 12(5):397–9. doi: 10.1093/jmcb/mjz114
74. Mill CP, Fiskus W, DiNardo CD, Qian Y, Raina K, Rajapakshe K, et al. RUNX1-Targeted Therapy for AML Expressing Somatic or Germline Mutation in RUNX1. *Blood* (2019) 134(1):59–73. doi: 10.1182/blood.2018893982
75. Grossmann V, Schnittger S, Schindela S, Klein HU, Eder C, Dugas M, et al. Strategy for Robust Detection of Insertions, Deletions, and Point Mutations in CEBPA, a GC-Rich Content Gene, Using 454 Next-Generation Deep-Sequencing Technology. *J Mol Diagn* (2011) 13(2):129–36. doi: 10.1016/j.jmoldx.2010.09.001
76. Song G, Wang L, Bi K, Jiang G. Regulation of the C/EBPalpha Signaling Pathway in Acute Myeloid Leukemia (Review). *Oncol Rep* (2015) 33(5):2099–106. doi: 10.3892/or.2015.3848
77. Walker A, Marcucci G. Molecular Prognostic Factors in Cytogenetically Normal Acute Myeloid Leukemia. *Expert Rev Hematol* (2012) 5(5):547–58. doi: 10.1586/ehm.12.45
78. Li HY, Deng DH, Huang Y, Ye FH, Huang LL, Xiao Q, et al. Favorable Prognosis of Biallelic CEBPA Gene Mutations in Acute Myeloid Leukemia Patients: A Meta-Analysis. *Eur J Haematol* (2015) 94(5):439–48. doi: 10.1111/ejh.12450
79. Zuber J, Radtke I, Pardee TS, Zhao Z, Rappaport AR, Luo W, et al. Mouse Models of Human AML Accurately Predict Chemotherapy Response. *Genes Dev* (2009) 23(7):877–89. doi: 10.1101/gad.1771409
80. Jakobsen JS, Laursen LG, Schuster MB, Pundhir S, Schoof E, Ge Y, et al. Mutant CEBPA Directly Drives the Expression of the Targetable Tumor-Promoting Factor CD73 in AML. *Sci Adv* (2019) 5(7):eaaw4304. doi: 10.1126/sciadv.aaw4304
81. Prochazka KT, Pregartner G, Rucker FG, Heitzer E, Pabst G, Wolfler A, et al. Clinical Implications of Subclonal TP53 Mutations in Acute Myeloid Leukemia. *Haematologica* (2019) 104(3):516–23. doi: 10.3324/haematol.2018.205013
82. Oren M, Rotter V. Mutant P53 Gain-of-Function in Cancer. *Cold Spring Harb Perspect Biol* (2010) 2(2):a001107. doi: 10.1101/cshperspect.a001107
83. Sallman DA, Komrokji R, Vaupel C, Cluzeau T, Geyer SM, McGraw KL, et al. Impact of TP53 Mutation Variant Allele Frequency on Phenotype and Outcomes in Myelodysplastic Syndromes. *Leukemia* (2016) 30(3):666–73. doi: 10.1038/leu.2015.304
84. Pan R, Ruvolo V, Mu H, Leverson JD, Nichols G, Reed JC, et al. Synthetic Lethality of Combined Bcl-2 Inhibition and P53 Activation in AML: Mechanisms and Superior Antileukemic Efficacy. *Cancer Cell* (2017) 32(6):748–60 e6. doi: 10.1016/j.ccell.2017.11.003
85. Khurana A, Shafer DA. MDM2 Antagonists as a Novel Treatment Option for Acute Myeloid Leukemia: Perspectives on the Therapeutic Potential of Idasanutlin (RG7388). *Onco Targets Ther* (2019) 12:2903–10. doi: 10.2147/OTT.S172315
86. Han L, Zhang Q, Dail M, Shi C, Cavazos A, Ruvolo VR, et al. Concomitant Targeting of BCL2 With Venetoclax and MAPK Signaling With Cobimetinib in Acute Myeloid Leukemia Models. *Haematologica* (2020) 105(3):697–707. doi: 10.3324/haematol.2018.205534
87. *PatentScope* . Available at: https://patentscope.wipo.int/search/en/detail.jsf?docId=WO2019134070&docAn=CN2018070051 (Accessed September 2020).
88. Lindsley RC, Mar BG, Mazzola E, Grauman PV, Shareef S, Allen SL, et al. Acute Myeloid Leukemia Ontogeny is Defined by Distinct Somatic Mutations. *Blood* (2015) 125(9):1367–76. doi: 10.1182/blood-2014-11-610543
89. Taylor J, Lee SC. Mutations in Spliceosome Genes and Therapeutic Opportunities in Myeloid Malignancies. *Genes Chromosomes Cancer* (2019) 58(12):889–902. doi: 10.1002/gcc.22784
90. Mechaal A, Menif S, Abbes S, Safra I. EZH2, New Diagnosis and Prognosis Marker in Acute Myeloid Leukemia Patients. *Adv Med Sci* (2019) 64(2):395–401. doi: 10.1016/j.advms.2019.07.002
91. Zhang Q, Han Q, Zi J, Ma J, Song H, Tian Y, et al. Mutations in EZH2 are Associated With Poor Prognosis for Patients With Myeloid Neoplasms. *Genes Dis* (2019) 6(3):276–81. doi: 10.1016/j.gendis.2019.05.001
92. Walter MJ, Shen D, Shao J, Ding L, White BS, Kandoth C, et al. Clonal Diversity of Recurrently Mutated Genes in Myelodysplastic Syndromes. *Leukemia* (2013) 27(6):1275–82. doi: 10.1038/leu.2013.58
93. Itzykson R, Kosmider O, Renneville A, Morabito M, Preudhomme C, Berthon C, et al. Clonal Architecture of Chronic Myelomonocytic Leukemias. *Blood* (2013) 121(12):2186–98. doi: 10.1182/blood-2012-06-440347
94. University of Chicago Hematopoietic Malignancies Cancer Risk T. How I Diagnose and Manage Individuals at Risk for Inherited Myeloid Malignancies. *Blood* (2016) 128(14):1800–13. doi: 10.1182/blood-2016-05-670240
95. Kanagal-Shamanna R. The Emerging Role of Hematopathologists and Molecular Pathologists in Detection, Monitoring, and Management of Myeloid Neoplasms With Germline Predisposition. *Curr Hematol Malig Rep* (2021) 24:1–9. doi: 10.1007/s11899-021-00636-2

96. Wlodarski MW, Hirabayashi S, Pastor V, Stary J, Hasle H, Masetti R, et al. Prevalence, Clinical Characteristics, and Prognosis of GATA2-Related Myelodysplastic Syndromes in Children and Adolescents. *Blood* (2016) 127(11):1387–97. doi: 10.1182/blood-2015-09-669937
97. Jongmans MC, Kuiper RP, Carmichael CL, Wilkins EJ, Dors N, Carmagnac A, et al. Novel RUNX1 Mutations in Familial Platelet Disorder With Enhanced Risk for Acute Myeloid Leukemia: Clues for Improved Identification of the FPD/AML Syndrome. *Leukemia* (2010) 24(1):242–6. doi: 10.1038/leu.2009.210
98. Patel SS, Pinkus GS, Ritterhouse LL, Segal JP, Dal Cin P, Restrepo T, et al. High NPM1 Mutant Allele Burden at Diagnosis Correlates With Minimal Residual Disease at First Remission in *De Novo* Acute Myeloid Leukemia. *Am J Hematol* (2019) 94(8):921–8. doi: 10.1002/ajh.25544
99. Sasaki K, Kanagal-Shamanna R, Montalban-Bravo G, Assi R, Jabbour E, Ravandi F, et al. Impact of the Variant Allele Frequency of ASXL1, DNMT3A, JAK2, TET2, TP53, and NPM1 on the Outcomes of Patients With Newly Diagnosed Acute Myeloid Leukemia. *Cancer* (2020) 126 (4):765–74. doi: 10.1002/cncr.32566
100. Jongen-Lavrencic M, Grob T, Hanekamp D, Kavelaars FG, Al Hinai A, Zeilemaker A, et al. Molecular Minimal Residual Disease in Acute Myeloid Leukemia. *N Engl J Med* (2018) 378(13):1189–99. doi: 10.1056/NEJMoa1716863
101. Ding L, Ley TJ, Larson DE, Miller CA, Koboldt DC, Welch JS, et al. Clonal Evolution in Relapsed Acute Myeloid Leukaemia Revealed by Whole-Genome Sequencing. *Nature* (2012) 481(7382):506–10. doi: 10.1038/nature10738
102. Petrackova A, Vasinek M, Sedlarikova L, Dyskova T, Schneiderova P, Novosad T, et al. Standardization of Sequencing Coverage Depth in NGS: Recommendation for Detection of Clonal and Subclonal Mutations in Cancer Diagnostics. *Front Oncol* (2019) 9:851. doi: 10.3389/fonc.2019.00851
103. Levine RL, Valk PJM. Next-Generation Sequencing in the Diagnosis and Minimal Residual Disease Assessment of Acute Myeloid Leukemia. *Haematologica* (2019) 104(5):868–71. doi: 10.3324/haematol.2018.205955
104. Kanagal-Shamanna R. Digital PCR: Principles and Applications. *Methods Mol Biol* (2016) 1392:43–50. doi: 10.1007/978-1-4939-3360-0_5
105. Onecha E, Linares M, Rapado I, Ruiz-Heredia Y, Martinez-Sanchez P, Cedena T, et al. A Novel Deep Targeted Sequencing Method for Minimal Residual Disease Monitoring in Acute Myeloid Leukemia. *Haematologica* (2019) 104(2):288–96. doi: 10.3324/haematol.2018.194712
106. Jaiswal S, Fontanillas P, Flannick J, Manning A, Grauman PV, Mar BG, et al. Age-Related Clonal Hematopoiesis Associated With Adverse Outcomes. *N Engl J Med* (2014) 371(26):2488–98. doi: 10.1056/NEJMoa1408617
107. Young AL, Challen GA, Birmann BM, Druley TE. Clonal Haematopoiesis Harbouring AML-Associated Mutations is Ubiquitous in Healthy Adults. *Nat Commun* (2016) 7:12484. doi: 10.1038/ncomms12484
108. Jan M, Snyder TM, Corces-Zimmerman MR, Vyas P, Weissman IL, Quake SR, et al. Clonal Evolution of Preleukemic Hematopoietic Stem Cells Precedes Human Acute Myeloid Leukemia. *Sci Transl Med* (2012) 4 (149):149ra18. doi: 10.1126/scitranslmed.3004315
109. Voso MT, Ottone T, Lavorgna S, Venditti A, Maurillo L, Lo-Coco F, et al. MRD in AML: The Role of New Techniques. *Front Oncol* (2019) 9:655. doi: 10.3389/fonc.2019.00655
110. Kumar D, Mehta A, Panigrahi MK, Nath S, Saikia KK. DNMT3A (R882) Mutation Features and Prognostic Effect in Acute Myeloid Leukemia in Coexistent With NPM1 and FLT3 Mutations. *Hematol Oncol Stem Cell Ther* (2018) 11(2):82–9. doi: 10.1016/j.hemonc.2017.09.004
111. Wang R, Gao X, Yu L. The Prognostic Impact of Tet Oncogene Family Member 2 Mutations in Patients With Acute Myeloid Leukemia: A Systematic-Review and Meta-Analysis. *BMC Cancer* (2019) 19(1):389. doi: 10.1186/s12885-019-5602-8
112. Khan M, Cortes J, Kadia T, Naqvi K, Brandt M, Pierce S, et al. Clinical Outcomes and Co-Occurring Mutations in Patients With RUNX1-Mutated Acute Myeloid Leukemia. *Int J Mol Sci* (2017) 18(8):1618. doi: 10.3390/ijms18081618
113. Gale RE, Lamb K, Allen C, El-Sharkawi D, Stowe C, Jenkinson S, et al. Simpson's Paradox and the Impact of Different DNMT3A Mutations on Outcome in Younger Adults With Acute Myeloid Leukemia. *J Clin Oncol* (2015) 33(18):2072–83. doi: 10.1200/JCO.2014.59.2022
114. Gowher H, Loutchanwoot P, Vorobjeva O, Handa V, Jurkowska RZ, Jurkowski TP, et al. Mutational Analysis of the Catalytic Domain of the Murine Dnmt3a DNA-(Cytosine C5)-Methyltransferase. *J Mol Biol* (2006) 357(3):928–41. doi: 10.1016/j.jmb.2006.01.035
115. Solary E, Bernard OA, Tefferi A, Fuks F, Vainchenker W. The Ten-Eleven Translocation-2 (TET2) Gene in Hematopoiesis and Hematopoietic Diseases. *Leukemia* (2014) 28(3):485–96. doi: 10.1038/leu.2013.337
116. Pan F, Weeks O, Yang FC, Xu M. The TET2 Interactors and Their Links to Hematological Malignancies. *IUBMB Life* (2015) 67(6):438–45. doi: 10.1002/iub.1389
117. Bhatnagar B, Eisfeld AK, Nicolet D, Mrozek K, Blachly JS, Orwick S, et al. Persistence of DNMT3A R882 Mutations During Remission Does Not Adversely Affect Outcomes of Patients With Acute Myeloid Leukaemia. *Br J Haematol* (2016) 175(2):226–36. doi: 10.1111/bjh.14254
118. Cimmino L, Dolgalev I, Wang Y, Yoshimi A, Martin GH, Wang J, et al. Restoration of TET2 Function Blocks Aberrant Self-Renewal and Leukemia Progression. *Cell* (2017) 170(6):1079–95 e20. doi: 10.1016/j.cell.2017.07.032
119. Kiyomi Morita FW, Jahn K, Hu T, Tanaka T, Sasaki Y. Author Correction: Clonal Evolution of Acute Myeloid Leukemia Revealed by High-Throughput Single-Cell Genomics. *Nat Commun* (2021) 12(1):2823. doi: 10.1038/s41467-021-23280-z
120. Hu Y, An Q, Sheu K, Trejo B, Fan S, Guo Y. Single Cell Multi-Omics Technology: Methodology and Application. *Front Cell Dev Biol* (2018) 6:28 (28). doi: 10.3389/fcell.2018.00028
121. Petti AA, Williams SR, Miller CA, Fiddes IT, Srivatsan SN, Chen DY, et al. A General Approach for Detecting Expressed Mutations in AML Cells Using Single Cell RNA-Sequencing. *Nat Commun* (2019) 10(1):3660. doi: 10.1038/s41467-019-11591-1
122. van Galen P, Hovestadt V, Wadsworth Ii MH, Hughes TK, Griffin GK, Battaglia S, et al. Single-Cell RNA-Seq Reveals AML Hierarchies Relevant to Disease Progression and Immunity. *Cell* (2019) 176(6):1265–81.e24. doi: 10.1016/j.cell.2019.01.031
123. Miles LA, Bowman RL, Merlinsky TR, Csete IS, Ooi AT, Durruthy-Durruthy R, et al. Single-Cell Mutation Analysis of Clonal Evolution in Myeloid Malignancies. *Nature* (2020) 587(7834):477–82. doi: 10.1038/s41586-020-2864-x
124. Gronseth CM, McElhone SE, Storer BE, Kroeger KA, Sandhu V, Fero ML, et al. Prognostic Significance of Acquired Copy-Neutral Loss of Heterozygosity in Acute Myeloid Leukemia. *Cancer* (2015) 121(17):2900–8. doi: 10.1002/cncr.29475
125. Walker CJ, Kohlschmidt J, Eisfeld AK, Mrozek K, Liyanarachchi S, Song C, et al. Genetic Characterization and Prognostic Relevance of Acquired Uniparental Disomies in Cytogenetically Normal Acute Myeloid Leukemia. *Clin Cancer Res* (2019) 25(21):6524–31. doi: 10.1158/1078-0432.CCR-19-0725
126. Ronaghy A, Yang RK, Khoury JD, Kanagal-Shamanna R. Clinical Applications of Chromosomal Microarray Testing in Myeloid Malignancies. *Curr Hematol Malig Rep* (2020) 15(3):194–202. doi: 10.1007/s11899-020-00578-1

Conflict of Interest: The authors declare that the research was conducted in the absence of any commercial or financial relationships that could be construed as a potential conflict of interest.

Publisher's Note: All claims expressed in this article are solely those of the authors and do not necessarily represent those of their affiliated organizations, or those of the publisher, the editors and the reviewers. Any product that may be evaluated in this article, or claim that may be made by its manufacturer, is not guaranteed or endorsed by the publisher.

frontiers in Oncology

REVIEW
published: 01 October 2021
doi: 10.3389/fonc.2021.741376

The Role of the Gut Microbiome in Pathogenesis, Biology, and Treatment of Plasma Cell Dyscrasias

Marcin Jasiński[1], *Jarosław Biliński*[1,2*] *and Grzegorz W. Basak*[1,2]

[1] *Department of Hematology, Transplantation and Internal Medicine, Medical University of Warsaw, Warsaw, Poland,*
[2] *Human Biome Institute, Gdansk, Poland*

In response to emerging discoveries, questions are mounting as to what factors are responsible for the progression of plasma cell dyscrasias and what determines responsiveness to treatment in individual patients. Recent findings have shown close interaction between the gut microbiota and multiple myeloma cells. For instance, that malignant cells shape the composition of the gut microbiota. We discuss the role of the gut microbiota in (i) the development and progression of plasma cell dyscrasias, and (ii) the response to treatment of multiple myeloma and highlight faecal microbiota transplantation as a procedure that could modify the risk of progression or sensitize refractory malignancy to immunotherapy.

Keywords: plasma cell dyscrasias, gut microbiome, multiple myeloma, microbiota, short-chain fatty acids

OPEN ACCESS

Edited by:
Mina Luqing Xu,
Yale University, United States

Reviewed by:
Muhammad Bilal Abid,
Medical College of Wisconsin, United States
Somsubhra Nath,
Saroj Gupta Cancer Centre and Research Institute, India

****Correspondence:***
Jarosław Biliński
jbilinski@wum.edu.pl

Specialty section:
This article was submitted to Hematologic Malignancies, a section of the journal Frontiers in Oncology

Received: *14 July 2021*
Accepted: *13 September 2021*
Published: *01 October 2021*

Citation:
Jasiński M, Biliński J and Basak GW (2021) The Role of the Gut Microbiome in Pathogenesis, Biology, and Treatment of Plasma Cell Dyscrasias. Front. Oncol. 11:741376. doi: 10.3389/fonc.2021.741376

INTRODUCTION – PATHOGENESIS OF PLASMA CELL DYSCRASIAS

Typical genetic alterations in plasma cell dyscrasias are IgH translocations, hyperdiploidy, and cyclin D dysregulation. These are responsible for initiating changes in B-cell postgerminal centres, which result in the transformation of normal cells into benign tumour cells that cause monoclonal gammopathy of undetermined significance (MGUS) (1). This condition is the preclinical stage of multiple myeloma (MM) and occurs in ~3.2% of the population aged over 50 years (2). MGUS is an asymptomatic condition with elevated serum concentration of M protein. Only rarely does it progress to symptomatic MM (1% of patients/year) (3), which can be associated with symptoms that manifest as a result of hypercalcaemia, renal failure, anaemia, and bone lesions. Smouldering MM (SMM) is an asymptomatic, intermediate stage between MGUS and MM, that carries a 10% risk of progression to symptomatic MM per year during the first five years after diagnosis (4). If it is to be possible to screen intensively, perform prophylactic investigations on, and treat in the early stages only those patients who are most at risk of disease progression, accurate prognostic markers of progression of MGUS or SMM to MM are needed.

During the past few years, evidence has emerged that human gut microbiota play an important role in the progression of MM (5–7). The gut microbiota influence the course of MM and the disease shapes the composition of the bacteria in the intestines (6). These interactions, as described below, are based on the strong reliance of MM cells on proinflammatory cytokines [interleukin (IL)-6, tumour necrosis factor (TNF)-α, IL-13] and the ability of bacteria to recycle nitrogen (8).

Recent studies have yielded plenty of information on the differences in microbiota among MM patients and about longitudinal changes acquired during the treatment as well (9). Some recently identified gut microbes are responsible for inducing an inflammatory environment, both within the gut layer and throughout the whole body. These proinflammatory microbes might contribute to the progression of MGUS to MM (5). If they do, the microbiome composition could be used as a prognostic factor for assessing the risk of MGUS transformation or MM progression.

GUT MICROBIOTA AND IMMUNE SYSTEM IN HEALTH AND DISEASE, SPECIFICALLY INFECTIONS

The colonization of the intestine by microbes plays a key role in the maturation of the host's immune system (10). Current knowledge about crosstalk between gut microbiota and immune cells derives mainly from experiments conducted on germ-free animals (11). For instance, in germ-free mice the population of αβ and γδ intra-epithelial lymphocytes is significantly reduced (12), there is no production of IgA antibodies (13) and Th17 cells are absent (14). One example of a complicated interplay between gut microbiota and immune cells is the following. Polysaccharide A produced by *Bacteroides fragilis* binds to TLR2/TLR1 (Toll-like receptor) heterodimer connected with Dectin-1 (15). Then, the phosphoinositide 3-kinase (PI3K) pathway is activated, glycogen synthase kinase 3β inactivated, which eventually induces cAMP response element-binding protein expression of anti-inflammatory genes (15). Finally, the secretion of polysaccharide A by *Bacteroides fragilis* leads to the differentiation of Treg cells and influences the balance between Th1 and Th2 populations. On the other hand, butyrate produced by the gut microbiota can promote macrophage differentiation from monocytes through histone deacetylase 3 (HDAC3) inhibition that leads to enhanced antimicrobial host defense (16). These are only a few examples of how intricate the crosstalk on the line gut microbiota - immune cells is.

Gut microbiota can also predict responses to therapies administered in oncology. Chaput et al. showed that the presence of *Faecalibacterium* spp. increases the efficacy of anti-CTLA-4 immunotherapy while probably the *Bacteroides* spp. is associated with inferior responses in metastatic melanoma (17). Moreover, it is recently hypothesized that gut microbiota composition can influence the responses to the CAR-T therapy (18), and bearing in mind recent papers about the efficacy of such therapy in multiple myeloma the discussion about gut microbiota as a predictive marker of response is warranted (19).

The impact of the interplay between the immune system and gut microbiota in the context of infections cannot be forgotten as patients with multiple myeloma are far more prone to infections than the healthy population (20). The ability of microbes to release signaling molecules into the bloodstream can modulate the host's response to infections *via* the regulation of immune cell development (21). For instance, butyrate secreted by bacteria promotes the differentiation of monocytes in the bone marrow to a tolerogenic phenotype (22). Moreover, it was recently showed that some bacterial species could decrease the level of corticosterone in the blood which could improve the function of the immune system during the infection (23).

GUT MICROBIOTA AND TUMOURIGENESIS

The available data show that the gut microbiota are more numerous than genes, cells, and enzymatic reactions in the host organism, which suggest their importance for its health. In healthy persons, microorganisms are responsible for production of vitamins K, B_2 (riboflavin), B_{12} (cobalamin), folates, and biotin (24), metabolism of indigestible compounds, and protection from colonisation by opportunistic bacteria (25), and are necessary for the development of the humoral and cellular mucosal immune systems (26) (**Figure 1**). Along with these advantages of the gut microbiome, there are also some disadvantages. It is well established that dysbiosis, which is an imbalance in the proportion of microbes compared to a healthy state, plays a role in the pathogenesis of colorectal cancer (CRC) (27). Wang et al. showed that there is a difference in the composition of gut microbiota between patients with CRC and healthy individuals (28). A similar influence of microbial dysbiosis, *via* proinflammatory microbe-associated molecular patterns (MAMPs) and bacterial metabolites, has been shown in liver (29) and pancreatic (30) cancer.

The gut microbiota are accompanied by gut-associated lymphoid tissue (GALT), which is the largest peripheral immune organ (31). As many as 60–70% of peripheral lymphocytes are localised within the gut mucosa, so it is not surprising that the number of interactions between immune cells and the gut microbiota is high (32). There are numerous examples of how the gut microbiota and immune system influence each other within the gut mucosa. Brandsma et al. showed that the transplantation of proinflammatory faecal microbiota from *Casp1*$^{-/-}$ mice to *Ldlr*$^{-/-}$ mice resulted in systemic inflammation and promoted atherogenesis (33). In contrast, Mason et al. reported that reduced anti-inflammatory gut microbiota was correlated positively with depression. This correlation could be explained by inflammation playing a role in the pathogenesis of depression (34). The crosstalk from microbes to immune cells can be forwarded directly through their metabolites used as messengers, such as MAMPs or damage-associated molecular patterns (DAMPs), or through activation of Toll-like receptors (TLRs) that in turn cause the activation of immune cells (35, 36). Some metabolites, such as short-chain fatty acids (SCFAs), can directly promote the generation of T regulatory (Treg) cells (37) or are responsible for transforming growth factor-β production in epithelial cells within the gut. This in turn promotes Treg-cell confluence in the gut mucosa, which inhibits the activation of immune cells (38). Germ-free (GF) mice that are deprived completely of gut microbiota comprise excellent examples of the importance of gut bacteria for efficient immune function (26). In GF mice, Treg cell function is impaired, which suggests that gut microflora are necessary for the development of a fully functional

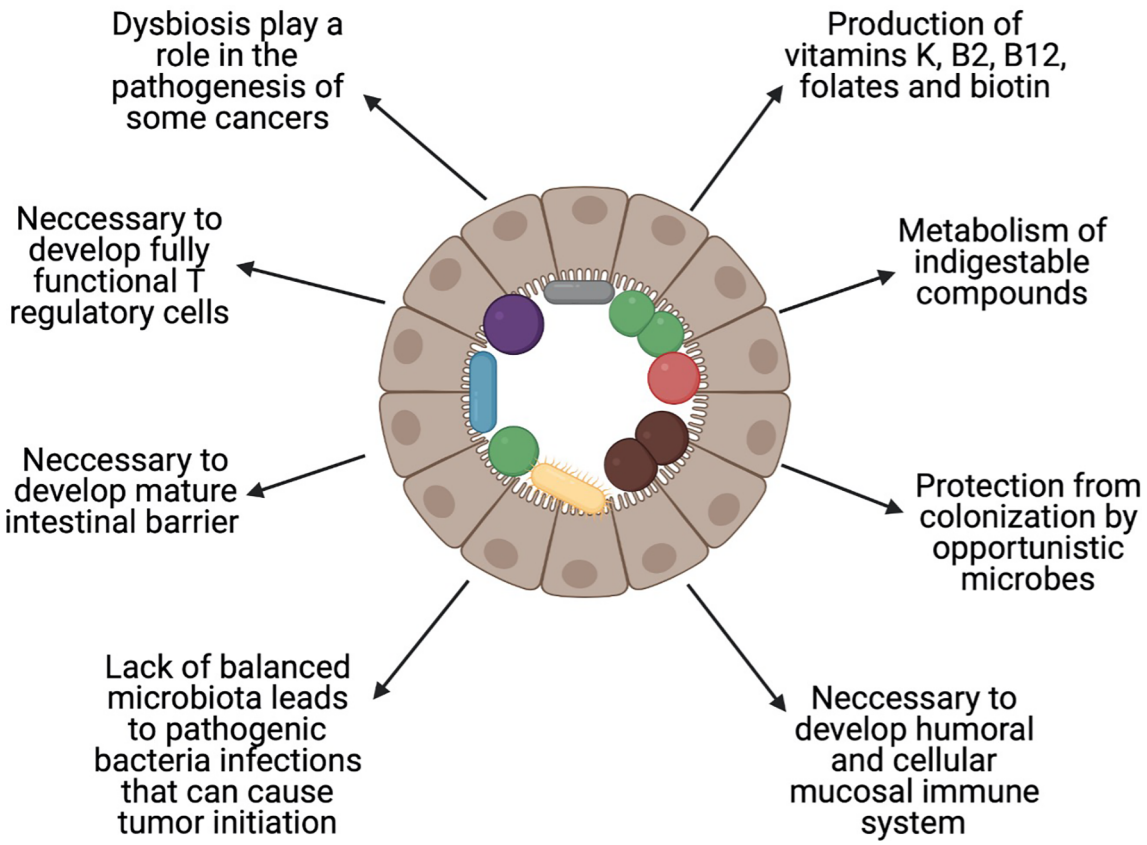

FIGURE 1 | Role of the balanced gut microbiota. Healthy gut microbiota are important in maintaining health. The figure shows the most important roles that are played by the human gut microbiota. Created with BioRender.com.

Treg cell population (39). In GF mice, the intestinal barrier is immature, which results in increased mucosal permeability (40). This is a key mechanism that leads to the development of inflammatory bowel disease or enteric infections (40). Colonisation of GF animals with normal gut microbiota leads to increased systemic immunological capacity, different patterns of migration of immune cells, significant changes in the production of specific antibodies, a general increase of immunoglobulin production, and changes in mucosal-associated lymphocyte tissues and cell populations (41–43).

In summary, in general, the micro-organisms in the gut are beneficial, but under certain conditions can have a damaging effect, in severe cases promoting the growth of cancer cells.

COMPARISON OF THE GUT MICROBIOME IN PATIENTS WITH PLASMA CELL DYSCRASIAS AND HEALTHY INDIVIDUALS

In recent years, scientists have confirmed the link between certain kinds of tumours and the composition of gut microbiota. For example, in CRC, many changes in the composition of bacterial species that colonise the gut have been identified and their contribution to tumourigenesis confirmed. Specific bacterial species colonizing the gut have even been indicated as possible markers of early diagnosis of CRC (44).

Regarding plasma cell dyscrasias and the gut microbiome, recent evidence shows metagenomic changes in the composition of commensal bacteria and frequent colonisation by opportunistic bacteria. Jian et al. performed a study on samples collected from 19 patients who had been newly diagnosed with MM and 18 healthy controls (6). They observed significant differences in the composition of bacteria in the gut between these two groups. One of the main changes was the increase of nitrogen-recycling bacteria, such as *Klebsiella* and *Streptococcus*, which are opportunistic pathogens that are responsible for infections associated with high mortality in this immunocompromised population. It has been suggested that this change might be due to the high serum concentration of urea in patients with MM, which results from increased production of NH_4^+ by tumour cells and restricted secretion of urea due to impaired renal function (45). The mechanism presented above is responsible attracting nitrogen-recycling bacteria to the gut. Changes in diversity in gut

microbiota have been reported, which indicates that samples from MM patients are characterised by increased diversity and poorer interactions between genera (6), although other studies have produced results that indicate contrary phenomena (46, 47). Furthermore, samples from MM patients included a reduced number of SCFA-producing bacteria, which affect tumourigenesis in plasma cell dyscrasias (see below) (6). Other changes in the composition of commensal bacteria, and colonisation with opportunistic pathogens, occur because of the treatment of MM. Unfortunately, research in this field is limited to the study of bacterial composition only. Further research, which studies differences in the balance and numbers, etc., of fungi, viruses, and eukaryotic organisms are needed (**Table 1**).

INFLUENCE OF THE GUT MICROBIOME ON THE DEVELOPMENT AND PROGRESSION OF PLASMA CELL DYSCRASIAS

As mentioned previously, MGUS is an asymptomatic state that occurs in ~3.2% of people aged over 50 (1). Only a small percentage of patients progress to symptomatic MM. For many years, researchers have wanted to identify the factors responsible for the development of plasma cell dyscrasias, and the reasons why some patients progress to MM whereas others do not.

Researchers have shown that there are no significant genetic differences between MGUS and MM cells. This suggests that environmental conditions could be an important factor in determining the risk for progression, although such factors are not necessarily present at the time at which MGUS develops. Therefore, tumour microenvironment seems to be a strong predictor of MGUS progression. Given the high degree of heterogeneity between clones in plasma cell dyscrasias, it is probable that only clones that are developing in a favourable niche will become an initiation point for further progression. As mentioned previously, proinflammatory TME in the bone marrow is needed for successful progression from MGUS to symptomatic MM, but it is a further issue how the gut microbiota can influence this microenvironment and contribute to tumour progression.

Short-Chain Fatty Acids

SCFAs are bacterial products that are responsible for ion absorption, gut motility, and modulation of immune responses (48). SCFAs can inhibit the nuclear factor kappa-light-chain enhancer of activated B cells (NF-κB) and such proinflammatory cytokines as IL-6 and TNF-α which are playing the role in activating osteoclasts to create niches for myeloma cells and additionally promote differentiation of Th17 cell (49). In contrast, SCFAs may also increase the level of IL-10 and induce expression of FoxP3 which in turn leads to differentiation of immunosuppressive $CD4^+$ T cell subset (Treg) (48). Eventually, both Treg (IL-10 and TGF-β) and Th17 (IL-17) cells secrete cytokines that promote MM cell proliferation *via* positive feedback loop (50). One SCFA, butyrate, is reported to increase T-cell apoptosis by HDAC-dependent Fas upregulation and consequent Fas-mediated apoptosis of T cells. That in turn inhibit T-cell accumulation within inflamed colonic mucosa which could prevent antigenic stimulation known for its role in multiple myeloma development (51). Furthermore, Jian et al. showed that SCFA-producing bacteria such as *Anaerostipes hadrus, Clostridium butyricum, and Clostridium saccharobutylicum* were reduced in patients with MM, and that the addition of *Clostridium butyricum* in a mouse model of MM resulted in mitigation of tumour progression (6). SCFAs are also involved in the response to treatment. Small, uncontrolled studies have indicated that SCFA-producing bacteria play a significant role in reducing the level of proinflammatory cytokines, thereby protecting the host from tumour progression. Loss of SCFA-producing bacteria can result in a higher risk of tumour progression. Bearing in mind that specific diets can increase the population of SCFA-producing bacteria, studies are needed to investigate whether changes in diet in patients with MGUS can influence the risk of tumour progression.

L-Glutamine

Jian et al. showed that stool samples from MM patients had higher concentrations than in healthy patients of bacteria that are involved in nitrogen utilisation and recycling, such as *Klebsiella* and *Streptococcus* (6). The following mechanism has been proposed to explain this phenomenon (6). MM cells are known producers of NH_4^+ (52), which results from uptake of glutamine (53). This NH_4^+ then accumulates in the bone marrow and is released into the blood. In a healthy organism, the liver successfully converts NH_4^+ into urea in the urea cycle. However, MM patients experience a high increase in blood NH_4^+ level that exceeds the capacity of the liver to convert it to urea and can even result occasionally in hyperammonaemic encephalopathy (54). In addition, monoclonal protein renal deposition and consequent reduction in renal function mean that the process of urea excretion is impaired severely (55). Taken together, these factors lead to an increased concentration of urea in the blood, such that excessive amounts of urea reach the intestinal lumen. The presence of urea in the gut layer causes the selection of nitrogen-recycling bacteria, such as *Klebsiella* and *Streptococcus.* These bacteria are involved in the hydrolysis of urea and synthesis of L-glutamine that is taken up by MM cells, which promotes tumour progression. It is probable that MM cells harness the gut microbiota of the host as a recycler of $NH4^+$ to deliver the necessary L-glutamine. In light of this, we speculate that targeting human microbiota with natural methods, or

TABLE 1 | Summary of the alterations of the gut microbiota in MM patients.

Gut microbiota of MM patients
Frequently colonised with opportunistic bacteria (6)
Increase in the number of bacteria involved in nitrogen recycling, such as *K. pneumoniae* or *S, pneumoniae* (6)
Increased diversity and poorer interactions between genera (6)
Reduced number of SCFA-producing bacteria (6)
Changes resulting from applied treatments especially antibiotics

antibiotics, if necessary, could be an attractive strategy to stop this vicious cycle.

Th17 Cells

The differentiation of Th17 in GF mice is inhibited (14). Microbial colonization, especially with segmented filamentous bacteria (SFB) promotes induction of Th17 cells (56). Furthermore, it is already known that Th17 elicited by SFB are of non-inflammatory phenotype while Th17 cells induced by other bacteria *Citrobacter* are secreting plenty of proinflammatory cytokines (57).

Plasma cells express IL-17 receptors on their surface and are stimulated *in vitro* and *in vivo via* IL-17 produced by Th17 cells (58). Of note, IL-6-STAT3 signalling pathway activated by IL-17 is relevant both for tumour (59) and plasma cell (60) growth which suggests the role of IL-17 during different stages of MM. IL-17 causes the upregulation of the receptor activator of the NF-κB ligand, which results in the activation of osteoclasts (61) and eosinophils that are producing IL-6 and TNF-α (5). Hence, IL-17 is the cytokine that bears the principal responsibility for bone lesions in plasma cell dyscrasias. Stromal cells respond to IL-17 as well by producing IL-6 (62). Moreover, the interplay between IL-6 and TGF-β, that are highly expressed in the bone marrow of patients with MM, is influencing the generation of Th17 cells (49).

Prevotella heparinolytica is responsible for the differentiation of Th17 cells and their migration to the bone marrow in the Vk*MYC mouse model of MM (5). In mice that lacked IL-17, the progression of plasma cell dyscrasias was delayed. Inhibition of IL-17, IL-17 receptor A, and IL-5 in a Vk*MYC model with monoclonal antibodies results in reduced accumulation of Th17 cells and eosinophils in the bone marrow, which results in delayed tumour progression (5).

Patients with MM have elevated serum level of IL-17 but interestingly after therapy with bis-phosphonate level of that cytokine is reduced (63). A higher level of IL-17 is also seen in the blood of patients with SMM and is a predictor of rapid progression of tumour growth. Therefore the level of IL-17 could be used as a potential marker of high-risk SMM patients (64). Similar to the Vk*MYC model, it would be useful to initiate studies on patients to determine which bacteria are involved in Th17 differentiation. Using this approach, bacteria that are involved indirectly in the development of bone lytic lesions, which is one of the main causes of morbidity in MM patients, could be eradicated (**Figure 2**).

THE LINK BETWEEN THE GUT MICROBIOME AND TREATMENT IN PLASMA CELL DYSCRASIAS

It is known that different results of treatment and toxicity profiles are associated with the gut microbiome (65, 66). For instance, a specific composition of gut microbiota is required for an optimal response to treatment with immune checkpoint inhibitors (67). Baruch et al. conducted a phase I study on faecal microbiota transplantation from complete responders to treatment for metastatic melanoma to 10 non-responders, which resulted in

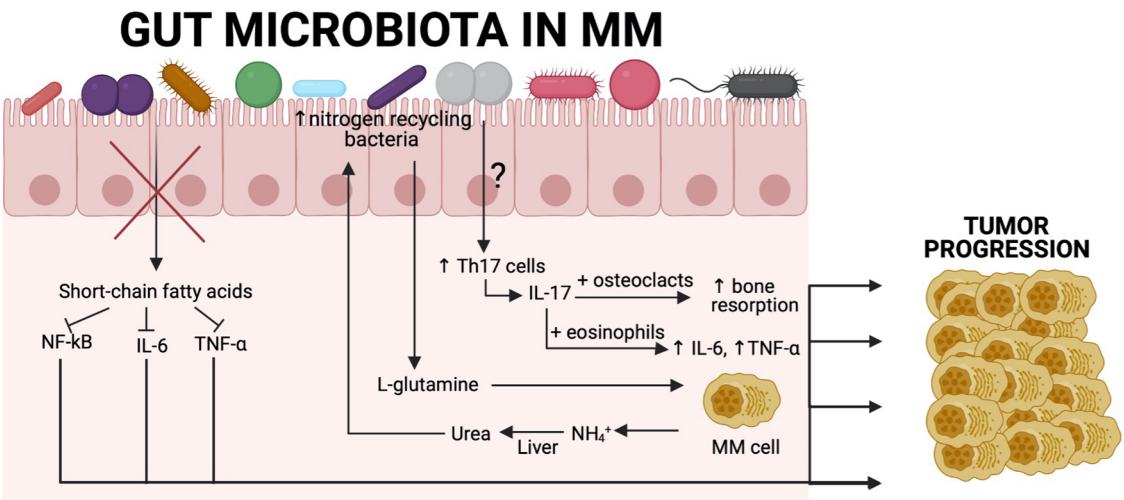

FIGURE 2 | Association between the gut microbiota and tumour progression in MM patients. Recent findings show a close relationship between gut commensal microbiota and MM cells. SCFA-producing bacteria are significantly reduced, resulting in increased levels of NF-κB, IL-6, and TNF-α, which are known to contribute to tumor progression in MM. Another example derives from the fact that MM patients have increased nitrogen-recycling bacteria. These bacteria are involved in L-glutamine production, which is an essential amino acid for MM cells. MM cells produce high amounts of $NH4^+$, which is transformed in the liver into urea and reaches high concentrations in the blood and can select nitrogen-recycling bacteria such as *K. pneumoniae* or *S. pneumoniae*. The influence of the gut microbiota on Th17 cell differentiation in MM patients remains to be characterised, although we know that in a Vk*MYC mouse model, *P. heparinolytica* was responsible for that. Patients with MM have significantly higher level of IL-17 in the blood, which is produced by Th17 cells and causes bone resorption, resulting in bone lesions that are the main symptom of this malignancy. Additionally, IL-17 activates eosinophils that are consequently producing proinflammatory cytokines (IL-6 and TNF-α) that are involved in tumor progression. Created with BioRender.com.

partial responses in three patients and a complete response in one (68). The gut microbiome can influence the results of treatment, especially in respect of adverse events, and treatment can modulate the gut microbiome.

During the last decade, new treatments for plasma cell dyscrasias have been introduced, including immunomodulatory drugs (thalidomide, lenalidomide, and pomalidomide), proteasome inhibitors, and monoclonal antibodies. These have improved the length and quality of life of patients with MM (69). To emphasise the role of the gut microbiome in plasma cell dyscrasias, we describe how microbes can affect the outcomes of treatment in plasma cell malignancies. Their role is particularly visible in respect of possible infectious complications after treatment that are due to infection. It was recently confirmed that treatment of MM changes the composition of the gut microbiome in respect of diversity (70).

Pianko et al. showed that MM patients with no minimal residual disease (MRD) after completion of upfront therapy had greater numbers of butyrate-producing *Eubacterium halii* than MRD-positive patients (71). Similarly, another butyrate producer, *Faecalibacterium prausnitzii*, was associated with an absence of MRD (71). Moreover, Peled et al. showed that intestinal *Eubacterium limosum* was associated with decreased risk of MM relapse after allogeneic haematopoietic cell transplantation (72). These observations suggest that changes in commensal microbiota caused by MM treatment could influence the entire process of therapy or be a predictor of a better response. Gopalakrishnan et al. showed how significant the impact of the changes in the gut microflora on the response to treatment can be. They showed that melanoma patients who responded well to immunotherapy with anti-PD-1 agents had a relative abundance of *Ruminococcaceae* family and higher alpha diversity (diversity within one sample) in faecal microbiome samples (73). Thus, it is possible that the composition of gut microbiota in MM patients has a major influence on the outcomes of immunotherapy, especially taking into account that MM, similarly to melanoma, is closely related to immune response.

Proteasome Inhibitors

PIs, such as bortezomib or carfilzomib are commonly used in primary and relapsed MM. One common adverse effect is gastrointestinal (GI) toxicity that results in diarrhoea. First, it was thought that PIs alter gut motility or cause neurotoxicity, resulting in autonomic neuropathy. The molecular reason for GI toxicity is now established as an increase in TNF-α receptor 1 expression on intestinal cells and higher concentrations of IL-6, TNF-α and IL-1β (74). However, there is a lack of evidence that PIs influence composition of the gut microbiota. It might be that inhibition of the NF-κB pathway is responsible for GI toxicity of PIs (75). SCFAs can suppress the NF-κB pathway, which could augment GI toxicity of PIs (76).

Steroids

Steroids are among the most commonly used anti-inflammatory drugs. They are used in chemotherapy regimens for MM, as well as in the treatment of a wide range of rheumatoid diseases. Huang et al. showed that mice that had been subjected to chronic exposure to steroids differed in the composition of their gut microbiota compared with their healthy counterparts (77). Steroid-treated mice had an increase in *Bifidobacterium* and *Lactobacillus*, which are both associated with anti-inflammatory effects, whereas they noted an absence of *Mucospirillum*, which is responsible for degradation of colonic mucin. This effect might be explained by the decrease of mucin production in mice treated chronically with steroids. Dexamethasone exerts its anti-inflammatory effects by blocking the NF-κB pathway (78). Furthermore, mice that were treated with dexamethasone produced less IL-17 than healthy mice (77). This may be another case in which steroids reshape the intestinal flora, since IL-17 production depends on Th17 cell differentiation, which is associated with specific gut microbiota. However, not only chronic exposure to, but also acute treatment with, steroids affected gut microbiota in mice (77). Ünsal et al. showed that rodents that were injected with a single, strong dose of dexamethasone underwent an increase in the number of ileal anaerobic bacteria. Moreover, a single injection of a low dose of dexamethasone resulted in an increase in the population of coliform bacteria (79). However, the long-term effect of these changes remains to be determined.

Antimicrobials

The link between antibiotics and the gut microbiome seems to be the most examined and the influence of this group of drugs on commensal bacteria is well established. However, although this link has been studied intensively in healthy volunteers, there remains a lack of wider studies with many groups of antibiotics in MM patients. Ziegler et al. showed that levofloxacin, which is the most commonly prescribed drug for bloodstream infections and neutropenic fever prophylaxis, had a less damaging effect on intestinal microbiota than broad-spectrum β-lactam (BSBL) antibiotics (80). The latter group reduced alpha diversity. The former was not associated with specific changes in the gut microbiome that had been found to be associated with poor clinical results (decrease in populations responsible for protection against *C. difficile*; increase in non-Bacteroidetes taxa, and reduction of alpha diversity). In light of their results, the authors emphasised that fluoroquinolone antibiotics protected patients from the negative effects of BSBLs (80). In MM patients who had been newly diagnosed and who were at particular risk of infection, the effect of prophylactic antibiotics was small and there was no decrease in early mortality (81). However, Valkovic et al. reported that MM diagnosis or progression was frequently preceded by infection (82). That could have been because bacterial infections are associated with robust production of proinflammatory cytokines and TLR activation on MM cells (83, 84). This is why prophylactic broad-spectrum antibiotics can result in a delay in disease progression. In respect of allogeneic stem-cell transplantation (alloSCT), Weber et al. showed that early use of broad-spectrum antibiotics that are active against commensal organisms, such as *Clostridiales* was associated with increased transplant-related mortality and decreased overall survival (85). Administration of imipenem–cilastatin or piperacillin–tazobactam for neutropenic

fever resulted in gut microbial perturbation and increased graft-*versus*-host disease-related mortality compared with aztreonam or cefepime, both of which decreased activity against commensal, anaerobic bacteria (86). Such observations of antibiotic effects on the response to treatment of MM need to be investigated in patients who are treated with autologous stem-cell transplantation (ASCT). There is also a recently published systematic review of infections associated with selinexor in patients with relapsed/refractory MM that also compares the risk of infections with other novel agents. It is already known that selinexor could prevent viral infections through blocking of XPO1 - mediated nuclear transport which facilitates the export of viral proteins. The authors state that randomized clinical trials are needed to fully understand the risk of infections associated with selinexor (87).

Autologous Stem-Cell Transplantation

D'Angelo showed that after ASCT, patients showed significantly decreased diversity of the microbial gut population (88). El Jurdi et al. showed an association between baseline microbiota of patients undergoing ASCT with further regimen-related toxicities and with the rate of neutrophil engraftment (89). They found that bacterial diversity after ASCT recovered within 1 month after the procedure, but that fungal populations constantly decreased, which suggests that a longer time is needed for the reconstitution of the mycobiome. Although the prospective study included only 15 patients, the results were encouraging for further studies. This group recognised several links between the composition of the microbiota and effects on ASCT-related toxicity and outcomes. One of the links relied on identifying an increased population of *Bacteroides* at day +7 in patients with less severe diarrhoea, while more severe diarrhoea, nausea, and vomiting occurred in patients with a higher prevalence of the stool populations of *Blautia* and *Ruminococcus*. They also identified a negative correlation between fungal phyla *Glomerella* presence in stools and neutrophil engraftment (89). Similar conclusions were drawn from the results of the small pilot study with 15 patients, showing that baseline microbiota were associated with subsequent incidence and severity of nausea, vomiting, neutropenic fever, and rate of neutrophil engraftment (90). Khan et al. showed recently that 534 adult recipients of high-dose chemotherapy with ASCT had significantly decreased alpha diversity at early pretransplant stages than healthy individuals and that this reduction in diversity tended to be more marked in the course of the procedure (9). The pattern of this loss of diversity and dominance of specific taxa were similar to those seen in patients after alloSCT. In addition, they showed that the greater the diversity of the gut microbiota, the lower risk of progression or death. Our group showed in a retrospective, single-centre study that colonisation with antibiotic-resistant bacteria had a significant influence on the outcomes of alloSCT (91). The main finding was that the overall survival of patients who were colonised by antibiotic-resistant bacteria was estimated to be half that of the noncolonised group. A similar conclusion was reached by Scheich et al. concerning the effect of colonisation by multidrug-resistant organisms on the results of ASCT (92).

Other Treatments

There is little information on the possible influence of other treatments, such as immunomodulatory drugs and monoclonal antibodies, on plasma cell dyscrasias (**Table 2**).

CONCLUSIONS

Despite some progress in the outcomes of treatment of MM, it remains a disease that cannot currently be cured, due to relapse or refractoriness to any available therapy. An emerging factor that could influence not only the refractoriness of MM but also a progression from asymptomatic MGUS to MM is the gut microbiota. We see that changes in the composition of

TABLE 2 | Relationship between the gut microbiota and treatment of plasma cell dyscrasias.

Treatment	How it affects the gut microbiota in plasma cell dyscrasias?
PIs	• There is no evidence proving the influence of PIs on gut microbiota
Steroids	• Mice treated with steroids had increased *Bifidobacterium* and *Lactobacillus* population and the absence of *Mucospirillum* bacteria (77)
	• Mice treated with dexamethasone had decreased production of IL-17 compared with an untreated group. IL-17 production is strictly related to the presence of Th17 cells, whose differentiation in the gut was recently proved in the Vk*MYC mouse model. This indicates some relationship (77)
	• Not only chronic exposure but also acute treatment resulted in alteration of the gut microbiota in rodents (79)
Antimicrobials	• Levofloxacin had no significant impact on the human gut microbiota, while BSBL antibiotics caused a reduction of alpha diversity (80)
	• Administration of broad-spectrum antibiotics efficient against commensal microbiota resulted in higher transplant-related mortality and decreased overall survival (85)
	• Patients treated with imipenem–cilastatin or piperacillin–tazobactam had increased risk of GVHD-related mortality compared with aztreonam or cefepime (86)
ASCT	• Patients after ASCT had decreased diversity of microbial populations in the gut and the normal composition was rebuilt within 1 month after the procedure (89)
	• There is a strong relationship between baseline microbiota of MM patients and severity of toxicity related to the procedure and with the rate of neutrophil engraftment (89)
	• Patients after high-dose chemotherapy before ASCT had significantly decreased alpha diversity of the gut microbiota compared with healthy individuals (9)
Other treatments	• Little is known about possible influence of gut microbiome on treatment outcomes with immunomodulatory drugs or monoclonal antibodies

commensal bacteria can affect the process of transforming MGUS to MM. Further, these changes are associated with colonisation with opportunistic pathogens that can become an aetiological agent of complications due to infection that are associated with treatment. Probably, in the future, it will be possible to identify patients who have an especially high risk of progression to MM, or even to modulate intestinal microflora to reduce the risk of progression of MGUS. It is also possible that the gut microbiota will be modulated to reduce complications that are due to treatment and disease, or to improve treatment outcomes. However, the field of microbiota in MM is still in its infancy and further work is required to gain a fuller understanding of the phenomena.

AUTHOR CONTRIBUTIONS

All authors contributed to the article and approved the submitted version.

REFERENCES

1. Agarwal A, Ghobrial IM. Monoclonal Gammopathy of Undetermined Significance and Smoldering Multiple Myeloma: A Review of the Current Understanding of Epidemiology, Biology, Risk Stratification, and Management of Myeloma Precursor Disease. *Clin Cancer Res* (2013) 19 (5):985–94. doi: 10.1158/1078-0432.CCR-12-2922
2. Kyle RA, Therneau TM, Rajkumar SV, Larson DR, Plevak MF, Offord JR, et al. Prevalence of Monoclonal Gammopathy of Undetermined Significance. *N Engl J Med* (2006) 354(13):1362–9. doi: 10.1056/NEJMoa054494
3. Kyle RA, Therneau TM, Rajkumar SV, Offord JR, Larson DR, Plevak MF, et al. A Long-Term Study of Prognosis in Monoclonal Gammopathy of Undetermined Significance. *N Engl J Med* (2002) 346(8):564–9. doi: 10.1056/NEJMoa01133202
4. Kyle RA, Remstein ED, Therneau TM, Dispenzieri A, Kurtin PJ, Hodnefield JM, et al. Clinical Course and Prognosis of Smoldering (Asymptomatic) Multiple Myeloma. *N Engl J Med* (2007) 356(25):2582–90. doi: 10.1056/NEJMoa070389
5. Calcinotto A, Brevi A, Chesi M, Ferrarese R, Garcia Perez L, Grioni M, et al. Microbiota-Driven Interleukin-17-Producing Cells and Eosinophils Synergize to Accelerate Multiple Myeloma Progression. *Nat Commun* (2018) 9(1):4832. doi: 10.1038/s41467-018-07305-8
6. Jian X, Zhu Y, Ouyang J, Wang Y, Lei Q, Xia J, et al. Alterations of Gut Microbiome Accelerate Multiple Myeloma Progression by Increasing the Relative Abundances of Nitrogen-Recycling Bacteria. *Microbiome* (2020) 8 (1):74. doi: 10.1186/s40168-020-00854-5
7. D'Angelo CR, Sudakaran S, Callander NS. Clinical Effects and Applications of the Gut Microbiome in Hematologic Malignancies. *Cancer* (2021) 127 (5):679–87. doi: 10.1002/cncr.33400
8. Ahmed N, Ghannoum M, Gallogly M, de Lima M, Malek E. Influence of Gut Microbiome on Multiple Myeloma: Friend or Foe? *J Immunother Cancer* (2020) 8(1):1–3. doi: 10.1136/jitc-2020-000576
9. Khan N, Lindner S, Gomes ALC, Devlin SM, Shah G, Sung AD, et al. Fecal Microbiota Diversity Disruption and Clinical Outcomes After Auto-HCT: A Multicenter Observational Study. *Blood* (2020) 137:13–5. doi: 10.1182/blood.2020006923
10. Gensollen T, Iyer SS, Kasper DL, Blumberg RS. How Colonization by Microbiota in Early Life Shapes the Immune System. *Science* (2016) 352 (6285):539–44. doi: 10.1126/science.aad9378
11. Bauer H, Horowitz RE, Levenson SM, Popper H. The Response of the Lymphatic Tissue to the Microbial Flora. Studies on Germfree Mice. *Am J Pathol* (1963) 42:471–83.
12. Umesaki Y, Setoyama H, Matsumoto S, Okada Y . Expansion of Alpha Beta T-Cell Receptor-Bearing Intestinal Intraepithelial Lymphocytes After Microbial Colonization in Germ-Free Mice and its Independence From Thymus. *Immunology* (1993) 79(1):32–7.
13. Hapfelmeier S, Lawson MA, Slack E, Kirundi JK, Stoel M, Heikenwalder M, et al. Reversible Microbial Colonization of Germ-Free Mice Reveals the Dynamics of Iga Immune Responses. *Science* (2010) 328(5986):1705–9. doi: 10.1126/science.1188454
14. Ivanov II, Frutos Rde L, Manel N, Yoshinaga K, Rifkin DB, Sartor RB, et al. Specific Microbiota Direct the Differentiation of IL-17-Producing T-Helper Cells in the Mucosa of the Small Intestine. *Cell Host Microbe* (2008) 4(4):337–49. doi: 10.1016/j.chom.2008.09.009
15. Erturk-Hasdemir D, Oh SF, Okan NA, Stefanetti G, Gazzaniga FS, Seeberger PH, et al. Symbionts Exploit Complex Signaling to Educate the Immune System. *Proc Natl Acad Sci USA* (2019) 116:26157–66. doi: 10.2139/ssrn.3362573
16. Schulthess J, Pandey S, Capitani M, Rue-Albrecht KC, Arnold I, Franchini F, et al. The Short Chain Fatty Acid Butyrate Imprints an Antimicrobial Program in Macrophages. *Immunity* (2019) 50(2):432–445 e7. doi: 10.1016/j.immuni.2018.12.018
17. Chaput N, Lepage P, Coutzac C, Soularue E, Le Roux K, Monot C, et al. Baseline Gut Microbiota Predicts Clinical Response and Colitis in Metastatic Melanoma Patients Treated With Ipilimumab. *Ann Oncol* (2017) 28(6):1368–79. doi: 10.1093/annonc/mdx108
18. Abid MB, Shah NN, Maatman TC, Hari PN. Gut Microbiome and CAR-T Therapy. *Exp Hematol Oncol* (2019) 8:31. doi: 10.1186/s40164-019-0155-8
19. Jasinski M, Basak GW, Jedrzejczak WW. Perspectives for the Use of CAR-T Cells for the Treatment of Multiple Myeloma. *Front Immunol* (2021) 12:632937. doi: 10.3389/fimmu.2021.632937
20. Blimark C, Holmberg E, Mellqvist UH, Landgren O, Bjorkholm M, Hultcrantz M, et al. Multiple Myeloma and Infections: A Population-Based Study on 9253 Multiple Myeloma Patients. *Haematologica* (2015) 100(1):107–13. doi: 10.3324/haematol.2014.107714
21. Khosravi A, Yanez A, Price JG, Chow A, Merad M, Goodridge HS, et al. Gut Microbiota Promote Hematopoiesis to Control Bacterial Infection. *Cell Host Microbe* (2014) 15(3):374–81. doi: 10.1016/j.chom.2014.02.006
22. Gao Y, Zhou J, Qi H, Wei J, Yang Y, Yue J, et al. Lncrna Lncly6c Induced by Microbiota Metabolite Butyrate Promotes Differentiation of Ly6C(High) to Ly6C(Int/Neg) Macrophages Through Lncly6c/C/Ebpbeta/Nr4A1 Axis. *Cell Discov* (2020) 6(1):87. doi: 10.1038/s41421-020-00211-8
23. Menezes-Garcia Z, Do Nascimento Arifa RD, Acurcio L, Brito CB, Gouvea JO, Lima RL, et al. Colonization by Enterobacteriaceae is Crucial for Acute Inflammatory Responses in Murine Small Intestine via Regulation of Corticosterone Production. *Gut Microbes* (2020) 11(6):1531–46. doi: 10.1080/19490976.2020.1765946
24. Hill MJ. Intestinal Flora and Endogenous Vitamin Synthesis. *Eur J Cancer Prev* (1997) 6(Suppl 1):S43–5. doi: 10.1097/00008469-199703001-00009
25. Round JL, Mazmanian SK. The Gut Microbiota Shapes Intestinal Immune Responses During Health and Disease. *Nat Rev Immunol* (2009) 9(5):313–23. doi: 10.1038/nri2515
26. Cebra JJ. Influences of Microbiota on Intestinal Immune System Development. *Am J Clin Nutr* (1999) 69(5):1046S–51S. doi: 10.1093/ajcn/69.5.1046s
27. Zackular JP, Baxter NT, Iverson KD, Sadler WD, Petrosino JF, Chen GY, et al. The Gut Microbiome Modulates Colon Tumorigenesis. *mBio* (2013) 4(6): e00692–13. doi: 10.1128/mBio.00692-13
28. Wang T, Cai G, Qiu Y, Fei N, Zhang M, Pang X, et al. Structural Segregation of Gut Microbiota Between Colorectal Cancer Patients and Healthy Volunteers. *ISME J* (2012) 6(2):320–9. doi: 10.1038/ismej.2011.109
29. Dapito DH, Mencin A, Gwak GY, Pradere JP, Jang MK, Mederacke I, et al. Promotion of Hepatocellular Carcinoma by the Intestinal Microbiota and TLR4. *Cancer Cell* (2012) 21(4):504–16. doi: 10.1016/j.ccr.2012.02.007
30. Ochi A, Nguyen AH, Bedrosian AS, Mushlin HM, Zarbakhsh S, Barilla R, et al. Myd88 Inhibition Amplifies Dendritic Cell Capacity to Promote Pancreatic Carcinogenesis via Th2 Cells. *J Exp Med* (2012) 209(9):1671–87. doi: 10.1084/jem.20111706

31. Ohno H. Intestinal M Cells. *J Biochem* (2016) 159(2):151–60. doi: 10.1093/jb/mvv121
32. Macpherson AJ, McCoy KD, Johansen FE, Brandtzaeg P. The Immune Geography of Iga Induction and Function. *Mucosal Immunol* (2008) 1 (1):11–22. doi: 10.1038/mi.2007.6
33. Brandsma E, Kloosterhuis NJ, Koster M, Dekker DC, Gijbels MJJ, van der Velden S, et al. A Proinflammatory Gut Microbiota Increases Systemic Inflammation and Accelerates Atherosclerosis. *Circ Res* (2019) 124(1):94–100. doi: 10.1161/CIRCRESAHA.118.313234
34. Mason BL, Li Q, Minhajuddin A, Czysz AH, Coughlin LA, Hussain SK, et al. Reduced Anti-Inflammatory Gut Microbiota are Associated With Depression and Anhedonia. *J Affect Disord* (2020) 266:394–401. doi: 10.1016/j.jad.2020.01.137
35. Chassaing B, Ley RE, Gewirtz AT. Intestinal Epithelial Cell Toll-Like Receptor 5 Regulates the Intestinal Microbiota to Prevent Low-Grade Inflammation and Metabolic Syndrome in Mice. *Gastroenterology* (2014) 147(6):1363–77 e17. doi: 10.1053/j.gastro.2014.08.033
36. Sanchez JMS, Doty DJ, DePaula-Silva AB, Brown DG, Bell R, Klag KA, et al. Molecular Patterns From a Human Gut-Derived Lactobacillus Strain Suppress Pathogenic Infiltration of Leukocytes Into the Central Nervous System. *J Neuroinflamm* (2020) 17(1):291. doi: 10.1186/s12974-020-01959-2
37. Furusawa Y, Obata Y, Fukuda S, Endo TA, Nakato G, Takahashi D, et al. Commensal Microbe-Derived Butyrate Induces the Differentiation of Colonic Regulatory T Cells. *Nature* (2013) 504(7480):446–50. doi: 10.1038/nature12721
38. Martin-Gallausiaux C, Beguet-Crespel F, Marinelli L, Jamet A, Ledue F, Blottiere HM, et al. Butyrate Produced by Gut Commensal Bacteria Activates TGF-Beta1 Expression Through the Transcription Factor SP1 in Human Intestinal Epithelial Cells. *Sci Rep* (2018) 8(1):9742. doi: 10.1038/s41598-018-28048-y
39. Ostman S, Rask C, Wold AE, Hultkrantz S, Telemo E. Impaired Regulatory T Cell Function in Germ-Free Mice. *Eur J Immunol* (2006) 36(9):2336–46. doi: 10.1002/eji.200535244
40. Ukena SN, Singh A, Dringenberg U, Engelhardt R, Seidler U, Hansen W, et al. Probiotic Escherichia Coli Nissle 1917 Inhibits Leaky Gut by Enhancing Mucosal Integrity. *PloS One* (2007) 2(12):e1308. doi: 10.1371/journal.pone.0001308
41. Stepankova R, Sinkora J, Hudcovic T, Kozakova H, Tlaskalova-Hogenova H. Differences in Development of Lymphocyte Subpopulations From Gut-Associated Lymphatic Tissue (GALT) of Germfree and Conventional Rats: Effect of Aging. *Folia Microbiol (Praha)* (1998) 43(5):531–4. doi: 10.1007/BF02820814
42. Tlaskalova-Hogenova H, Sterzl J, Stepankova R, Dlabac V, Veticka V, Rossmann P, et al. Development of Immunological Capacity Under Germfree and Conventional Conditions. *Ann N Y Acad Sci* (1983) 409:96–113. doi: 10.1111/j.1749-6632.1983.tb26862.x
43. Tlaskalova-Hogenova H, Cerna J, Mandel L. Peroral Immunization of Germfree Piglets: Appearance of Antibody-Forming Cells and Antibodies of Different Isotypes. *Scand J Immunol* (1981) 13(5):467–72. doi: 10.1111/j.1365-3083.1981.tb00158.x
44. Dai Z, Coker OO, Nakatsu G, Wu WKK, Zhao L, Chen Z, et al. Multi-Cohort Analysis of Colorectal Cancer Metagenome Identified Altered Bacteria Across Populations and Universal Bacterial Markers. *Microbiome* (2018) 6(1):70. doi: 10.1186/s40168-018-0451-2
45. Howman R, Thakerer A, Pitman M, Ding N, Thompson PA, Khot A, et al. Bortezomib, Cyclophosphamide, and Dexamethasone: Highly Effective for Rapid Reversal of Myeloma-Associated Hyperammonemic Encephalopathy. *Leuk Lymphoma* (2010) 51(12):2299–302. doi: 10.3109/10428194.2010.518654
46. Antoine Pepeljugoski C, Morgan G, Braunstein M. Analysis of Intestinal Microbiome in Multiple Myeloma Reveals Progressive Dysbiosis Compared to MGUS and Healthy Individuals. *Blood* (2019) 134(Supplement_1):3076–6. doi: 10.1182/blood-2019-130643
47. Zhang B, Gu J, Liu J, Huang B, Li J. Fecal Microbiota Taxonomic Shifts in Chinese Multiple Myeloma Patients Analyzed by Quantitative Polimerase Chain Reaction (QPCR) and 16S Rrna High-Throughput Sequencing. *Med Sci Monit* (2019) 25:8269–80. doi: 10.12659/MSM.919988
48. Kim CH, Park J, Kim M. Gut Microbiota-Derived Short-Chain Fatty Acids, T Cells, and Inflammation. *Immune Netw* (2014) 14(6):277–88. doi: 10.4110/in.2014.14.6.277
49. Hideshima T, Mitsiades C, Tonon G, Richardson PG, Anderson KC, et al. Understanding Multiple Myeloma Pathogenesis in the Bone Marrow to Identify New Therapeutic Targets. *Nat Rev Cancer* (2007) 7(8):585–98. doi: 10.1038/nrc2189
50. Manzo VE, Bhatt AS. The Human Microbiome in Hematopoiesis and Hematologic Disorders. *Blood* (2015) 126(3):311–8. doi: 10.1182/blood-2015-04-574392
51. Zimmerman MA, Singh N, Martin PM, Thangaraju M, Ganapathy V, Waller JL, et al. Butyrate Suppresses Colonic Inflammation Through HDAC1-Dependent Fas Upregulation and Fas-Mediated Apoptosis of T Cells. *Am J Physiol Gastrointest Liver Physiol* (2012) 302(12):G1405–15. doi: 10.1152/ajpgi.00543.2011
52. Otsuki T, Yamada O, Sakaguchi H, Ichiki T, Kouguchi K, Wada H, et al. In Vitro Excess Ammonia Production in Human Myeloma Cell Lines. *Leukemia* (1998) 12(7):1149–58. doi: 10.1038/sj.leu.2401077
53. Bolzoni M, Chiu M, Accardi F, Vescovini R, Airoldi I, Storti P, et al. Dependence on Glutamine Uptake and Glutamine Addiction Characterize Myeloma Cells: A New Attractive Target. *Blood* (2016) 128(5):667–79. doi: 10.1182/blood-2016-01-690743
54. Pham A, Reagan JL, Castillo JJ. Multiple Myeloma-Induced Hyperammonemic Encephalopathy: An Entity Associated With High in-Patient Mortality. *Leuk Res* (2013) 37(10):1229–32. doi: 10.1016/j.leukres.2013.07.014
55. Kourelis TV, Nasr SH, Dispenzieri A, Kumar SK, Gertz MA, Fervenza FC, et al. Outcomes of Patients With Renal Monoclonal Immunoglobulin Deposition Disease. *Am J Hematol* (2016) 91(11):1123–8. doi: 10.1002/ajh.24528
56. Ivanov II, Atarashi K, Manel N, Brodie EL, Shima T, Karaoz U, et al. Induction of Intestinal Th17 Cells by Segmented Filamentous Bacteria. *Cell* (2009) 139 (3):485–98. doi: 10.1016/j.cell.2009.09.033
57. Omenetti S, Bussi C, Metidji A, Iseppon A, Lee S, Tolaini M, et al. The Intestine Harbors Functionally Distinct Homeostatic Tissue-Resident and Inflammatory Th17 Cells. *Immunity* (2019) 51(1):77–89 e6. doi: 10.1016/j.immuni.2019.05.004
58. Prabhala RH, Pelluru D, Fulciniti M, Prabhala HK, Nanjappa P, Song W, et al. Elevated IL-17 Produced by TH17 Cells Promotes Myeloma Cell Growth and Inhibits Immune Function in Multiple Myeloma. *Blood* (2010) 115(26):5385–92. doi: 10.1182/blood-2009-10-246660
59. Wang L, Yi T, Kortylewski M, Pardoll DM, Zeng D, Yu H. IL-17 can Promote Tumor Growth Through an IL-6-Stat3 Signaling Pathway. *J Exp Med* (2009) 206(7):1457–64. doi: 10.1084/jem.20090207
60. Palumbo A, Anderson K. Multiple Myeloma. *N Engl J Med* (2011) 364 (11):1046–60. doi: 10.1056/NEJMra1011442
61. Noonan K, Marchionni L, Anderson J, Pardoll D, Roodman GD, Borrello I. A Novel Role of IL-17-Producing Lymphocytes in Mediating Lytic Bone Disease in Multiple Myeloma. *Blood* (2010) 116(18):3554–63. doi: 10.1182/blood-2010-05-283895
62. Prabhala RH, Fulciniti M, Pelluru D, Rashid N, Nigroiu A, Nanjappa P, et al. Targeting IL-17A in Multiple Myeloma: A Potential Novel Therapeutic Approach in Myeloma. *Leukemia* (2016) 30(2):379–89. doi: 10.1038/leu.2015.228
63. Oteri G, Allegra A, Bellomo G, Alonci A, Nastro E, Penna G, et al. Reduced Serum Levels of Interleukin 17 in Patients With Osteonecrosis of the Jaw and in Multiple Myeloma Subjects After Bisphosphonates Administration. *Cytokine* (2008) 43(2):103–4. doi: 10.1016/j.cyto.2008.05.010
64. Rajkumar SV, Landgren O, Mateos MV. Smoldering Multiple Myeloma. *Blood* (2015) 125(20):3069–75. doi: 10.1182/blood-2014-09-568899
65. Hooper LV, Littman DR, Macpherson AJ. Interactions Between the Microbiota and the Immune System. *Science* (2012) 336(6086):1268–73. doi: 10.1126/science.1223490
66. Ivanov II, Honda K. Intestinal Commensal Microbes as Immune Modulators. *Cell Host Microbe* (2012) 12(4):496–508. doi: 10.1016/j.chom.2012.09.009
67. Matson V, Fessler J, Bao R, Chongsuwat T, Zha Y, Alegre ML, et al. The Commensal Microbiome is Associated With Anti-PD-1 Efficacy in Metastatic Melanoma Patients. *Science* (2018) 359(6371):104–8. doi: 10.1126/science.aao3290
68. Baruch EN, Youngster I, Ben-Betzalel G, Ortenberg R, Lahat A, Katz L, et al. Fecal Microbiota Transplant Promotes Response in Immunotherapy-Refractory Melanoma Patients. *Science* (2021) 371(6529):602–9. doi: 10.1126/science.abb5920

69. Naymagon L, Abdul-Hay M. Novel Agents in the Treatment of Multiple Myeloma: A Review About the Future. *J Hematol Oncol* (2016) 9(1):52. doi: 10.1186/s13045-016-0282-1
70. Ashraf A, Shaha N, Zahoor A, Arafat AF, Saif UR, Syeda SB, et al. Intestinal Microbiome Diversity and Clinical Outcomes With Multiple Myeloma: A Systematic Review. *J Clin Oncol* (2020) 38(15_suppl):e20542–2. doi: 10.1200/JCO.2020.38.15_suppl.e20542
71. Pianko MJ, Devlin SM, Littmann ER, Chansakul A, Mastey D, Salcedo M, et al. Minimal Residual Disease Negativity in Multiple Myeloma is Associated With Intestinal Microbiota Composition. *Blood Adv* (2019) 3(13):2040–4. doi: 10.1182/bloodadvances.2019032276
72. Peled JU, Devlin SM, Staffas A, Lumish M, Khanin R, Littmann ER, et al. Intestinal Microbiota and Relapse After Hematopoietic-Cell Transplantation. *J Clin Oncol* (2017) 35(15):1650–9. doi: 10.1200/JCO.2016.70.3348
73. Gopalakrishnan V, Spencer CN, Nezi L, Reuben A, Andrews MC, Karpinets TV, et al. Gut Microbiome Modulates Response to Anti-PD-1 Immunotherapy in Melanoma Patients. *Science* (2018) 359(6371):97–103. doi: 10.1126/science.aan4236
74. Stansborough RL, Gibson RJ. Proteasome Inhibitor-Induced Gastrointestinal Toxicity. *Curr Opin Support Palliat Care* (2017) 11(2):133–7. doi: 10.1097/SPC.0000000000000266
75. Al-Homsi AS, Feng Y, Duffner U, Al Malki MM, Goodyke A, Cole K, et al. Bortezomib for the Prevention and Treatment of Graft-*Versus*-Host Disease After Allogeneic Hematopoietic Stem Cell Transplantation. *Exp Hematol* (2016) 44(9):771–7. doi: 10.1016/j.exphem.2016.05.005
76. Alkharabsheh O, Sidiqi MH, Aljama MA, Gertz MA, Frankel AE. The Human Microbiota in Multiple Myeloma and Proteasome Inhibitors. *Acta Haematol* (2020) 143(2):118–23. doi: 10.1159/000500976
77. Huang EY, Inoue T, Leone VA, Dalal S, Touw K, Wang Y, et al. Using Corticosteroids to Reshape the Gut Microbiome: Implications for Inflammatory Bowel Diseases. *Inflamm Bowel Dis* (2015) 21(5):963–72. doi: 10.1097/MIB.0000000000000332
78. Scheinman RI, Gualberto A, Jewell CM, Cidlowski JA, Baldwin AS Jr. Characterization of Mechanisms Involved in Transrepression of NF-Kappa B by Activated Glucocorticoid Receptors. *Mol Cell Biol* (1995) 15(2):943–53. doi: 10.1128/MCB.15.2.943
79. Unsal H, Balkaya M, Unsal C, Biyik H, Basbulbul G, Poyrazoglu E. The Short-Term Effects of Different Doses of Dexamethasone on the Numbers of Some Bacteria in the Ileum. *Dig Dis Sci* (2008) 53(7):1842–5. doi: 10.1007/s10620-007-0089-6
80. Ziegler M, Han JH, Landsburg D, Pegues D, Reesey E, Gilmar C, et al. Impact of Levofloxacin for the Prophylaxis of Bloodstream Infection on the Gut Microbiome in Patients With Hematologic Malignancy. *Open Forum Infect Dis* (2019) 6(7):ofz252. doi: 10.1093/ofid/ofz252
81. Mohyuddin GR, Aziz M, McClune B, Abdallah AO, Qazilbash M. Antibiotic Prophylaxis for Patients With Newly Diagnosed Multiple Myeloma: Systematic Review and Meta-Analysis. *Eur J Haematol* (2020) 104(5):420–6. doi: 10.1111/ejh.13374
82. Valkovic T, Nacinovic AD, Petranovic D. Prophylactic Broad Spectrum Antibiotics as a New Anti-Myeloma Therapy. *Med Hypotheses* (2013) 81(6):1137–40. doi: 10.1016/j.mehy.2013.10.021
83. Jego G, Bataille R, Geffroy-Luseau A, Descamps G, Pellat-Deceunynck C. Pathogen-Associated Molecular Patterns are Growth and Survival Factors for Human Myeloma Cells Through Toll-Like Receptors. *Leukemia* (2006) 20(6):1130–7. doi: 10.1038/sj.leu.2404226
84. Bohnhorst J, Rasmussen T, Moen SH, Flottum M, Knudsen L, Borset M, et al. Toll-Like Receptors Mediate Proliferation and Survival of Multiple Myeloma Cells. *Leukemia* (2006) 20(6):1138–44. doi: 10.1038/sj.leu.2404225
85. Weber D, Jenq RR, Peled JU, Taur Y, Hiergeist A, Koestler J, et al. Microbiota Disruption Induced by Early Use of Broad-Spectrum Antibiotics is an Independent Risk Factor of Outcome After Allogeneic Stem Cell Transplantation. *Biol Blood Marrow Transplant* (2017) 23(5):845–52. doi: 10.1016/j.bbmt.2017.02.006
86. Shono Y, Docampo MD, Peled JU, Perobelli SM, Velardi E, Tsai JJ, et al. Increased GVHD-Related Mortality With Broad-Spectrum Antibiotic Use After Allogeneic Hematopoietic Stem Cell Transplantation in Human Patients and Mice. *Sci Transl Med* (2016) 8(339):339ra71. doi: 10.1126/scitranslmed.aaf2311
87. Abid H, Wu JF, Abid MB. Risk for Infections With Selinexor in Patients With Relapsed/Refractory Multiple Myeloma: A Systematic Review of Clinical Trials. *Eur J Cancer* (2021) 154:7–10.
88. D'Angelo C, Sudakaran S, Hematti P, Asimakopoulos F, Augustine C, Safdar N, et al. Impact of Antibiotics on Gut Microbiota Diversity and the Results of a Prospective Dietary Assessment in Patients With Multiple Myeloma Undergoing Autologous Hematopoietic Stem Cell Transplantation. *Blood* (2019) 134(Supplement_1):4653–3. doi: 10.1182/blood-2019-123530
89. El Jurdi N, Filali-Mouhim A, Salem I, Retuerto M, Dambrosio NM, Baer L, et al. Gastrointestinal Microbiome and Mycobiome Changes During Autologous Transplantation for Multiple Myeloma: Results of a Prospective Pilot Study. *Biol Blood Marrow Transplant* (2019) 25(8):1511–9. doi: 10.1016/j.bbmt.2019.04.007
90. Kusakabe S, Fukushima K, Maeda T, Motooka D, Nakamura S, Fujita J, et al. Pre- and Post-Serial Metagenomic Analysis of Gut Microbiota as a Prognostic Factor in Patients Undergoing Haematopoietic Stem Cell Transplantation. *Br J Haematol* (2020) 188(3):438–49. doi: 10.1111/bjh.16205
91. Bilinski J, Robak K, Peric Z, Marchel H, Karakulska-Prystupiuk E, Halaburda K, et al. Impact of Gut Colonization by Antibiotic-Resistant Bacteria on the Outcomes of Allogeneic Hematopoietic Stem Cell Transplantation: A Retrospective, Single-Center Study. *Biol Blood Marrow Transplant* (2016) 22(6):1087–93. doi: 10.1016/j.bbmt.2016.02.009
92. Scheich S, Reinheimer C, Brandt C, Wichelhaus TA, Hogardt M, Kempf VAJ, et al. Clinical Impact of Colonization With Multidrug-Resistant Organisms on Outcome After Autologous Stem Cell Transplantation: A Retrospective Single-Center Study. *Biol Blood Marrow Transplant* (2017) 23(9):1455–62. doi: 10.1016/j.bbmt.2017.05.016

Conflict of Interest: JB and GWB are the founders of the faecal microbiota bank and laboratory named the Human Biome Institute.

The remaining authors declare that the research was conducted in the absence of any commercial or financial relationships that could be construed as a potential conflict of interest.

Publisher's Note: All claims expressed in this article are solely those of the authors and do not necessarily represent those of their affiliated organizations, or those of the publisher, the editors and the reviewers. Any product that may be evaluated in this article, or claim that may be made by its manufacturer, is not guaranteed or endorsed by the publisher.

frontiers in Oncology

ORIGINAL RESEARCH
published: 25 October 2021
doi: 10.3389/fonc.2021.757664

Prevalence of the GFI1-36N SNP in Multiple Myeloma Patients and Its Impact on the Prognosis

Cyrus Khandanpour[1], Christine Eisfeld[1], Subbaiah Chary Nimmagadda[1], Marc S. Raab[2], Niels Weinhold[2], Anja Seckinger[3], Dirk Hose[3], Anna Jauch[4], Asta Försti[5,6,7], Kari Hemminki[8,9], Thomas Hielscher[10], Manuela Hummel[10,11], Georg Lenz[1], Hartmut Goldschmidt[2,12] and Stefanie Huhn[2]**

[1] Department of Medicine A, Hematology, Oncology and Pneumology, University Hospital Münster, Münster, Germany, [2] Department of Hematology, Oncology and Rheumatology, University Hospital Heidelberg, Heidelberg, Germany, [3] Department of Hematology and Immunology, Myeloma Center Brussels & Laboratory for Myeloma research, Vrije Universiteit Brussel (VUB), Jette, Belgium, [4] Institute of Human Genetics, University Heidelberg, Heidelberg, Germany, [5] Hopp Children's Cancer Center (KiTZ), Heidelberg, Germany, [6] Division of Pediatric Neurooncology, German Cancer Research Center (DKFZ), German Cancer Consortium (DKTK), Heidelberg, Germany, [7] Division of Molecular Genetic Epidemiology, German Cancer Research Center (DKFZ), Heidelberg, Germany, [8] Division of Cancer Epidemiology, German Cancer Research Center (DKFZ), Heidelberg, Germany, [9] Faculty of Medicine and Biomedical Center in Pilsen, Charles University in Prague, Pilsen, Czechia, [10] Division of Biostatistics, German Cancer Research Center (DKFZ), Heidelberg, Germany, [11] Roche Diagnostics GmbH, Penzberg, Germany, [12] National Centre of Tumor Diseases, Heidelberg, Germany

Transcription factor Growth Factor Independence 1 (GFI1) regulates the expression of genes important for survival, proliferation and differentiation of hematopoietic cells. A single nucleotide polymorphism (SNP) variant of GFI1 (GFI1-36N: serine replaced by asparagine at position 36), has a prevalence of 5-7% among healthy Caucasians and 10-15% in patients with myelodysplastic syndrome (MDS) and acute myeloid leukaemia (AML) predisposing GFI-36N carriers to these diseases. Since GFI1 is implicated in B cell maturation and plasma cell (PC) development, we examined its prevalence in patients with multiple myeloma (MM), a haematological malignancy characterized by expansion of clonal PCs. Strikingly, as in MDS and AML, we found that the GFI1-36N had a higher prevalence among MM patients compared to the controls. In subgroup analyses, GFI1-36N correlates to a shorter overall survival of MM patients characterized by the presence of t(4;14) translocation and gain of 1q21 (≤3 copies). MM patients carrying gain of 1q21 (≥3 copies) demonstrated poor progression free survival. Furthermore, gene expression

OPEN ACCESS

Edited by:
Andrew G. Evans, University of Rochester, United States

Reviewed by:
Cosimo Cumbo, University of Bari Aldo Moro, Italy
Chandraditya Chakraborty, Jerome Lipper Multiple Myeloma Center, Dana-Farber Cancer Institute and Harvard Medical School, United States

***Correspondence:**
Stefanie Huhn
Stefanie.Huhn@med.uni-heidelberg.de
Cyrus Khandanpour
cyrus.khandanpour@ukmuenster.de

Specialty section:
This article was submitted to Hematologic Malignancies, a section of the journal Frontiers in Oncology

Received: *12 August 2021*
Accepted: *01 October 2021*
Published: *25 October 2021*

Citation:
Khandanpour C, Eisfeld C, Nimmagadda SC, Raab MS, Weinhold N, Seckinger A, Hose D, Jauch A, Försti A, Hemminki K, Hielscher T, Hummel M, Lenz G, Goldschmidt H and Huhn S (2021) Prevalence of the GFI1-36N SNP in Multiple Myeloma Patients and Its Impact on the Prognosis. Front. Oncol. 11:757664. doi: 10.3389/fonc.2021.757664

analysis implicated a role for GFI1-36N in epigenetic regulation and metabolism, potentially promoting the initiation and progression of MM.

Keywords: Gfi1, SNP variant, prevalance, prognosis, multiple myeloma

INTRODUCTION

GFI1 is a zinc-finger transcriptional repressor with an essential role in controlling hematopoietic stem cell biology, myeloid and lymphoid differentiation and lymphocyte effector functions. The establishment of murine models with constitutive and conditional loss of Gfi1 expression enabled visualization of their cell-specific expression and understanding of Gfi1 function in hematopoietic lineages (1). GFI1 exerts its function as a transcriptional repressor by recruiting histone-modifying enzymes to its target genes (2). GFI1 binds histone deacetylases (HDAC1-3), histone methyltransferases (G9A) or histone demethylases (LSD1) and recruits them to their target genes. In a stepwise process, it induces deacetylation of lysine 9 of histone 3 (H3K9) followed by dimethylation of H3K9 or de-methylation of histone 3, lysine 4 (H3K4), resulting in gene silencing (1).

We previously reported that a coding single nucleotide polymorphism (SNP) in the human GFI1 (rs34631763, denominated as *GFI1-36N*) predisposes carriers to myelodysplastic syndrome (MDS) and acute myeloid leukaemia (AML) and influenced their prognosis (3, 4). On the molecular level, the GFI1-36N protein differs from the more common GFI1-36S with regards to its ability in inducing epigenetic changes as deacetylation of H3K9 at the HOXA9 locus (3, 4). However, genome-wide H3K9-acetylation level of GFI1 target genes was increased in hematopoietic progenitor cells of GFI1-36N mice and primary murine and human GFI1-36N leukemic cells (3). Higher H3K9-acetylation of the genes in GFI1-36N-expressing cells correlated with higher expression and activation of genes facilitating AML development (3).

Several publications previously reported the association of at least 24 independent loci carrying germline variants associated with increased risk of development of multiple myeloma (MM) (2, 5–8). MM is a B cell malignancy characterized by a multistep accumulation of genetic and epigenetic changes leading to malignant transformation and proliferation of plasma cells (PCs) (9, 10). MM prognosis depends on age, stage, overall performance status and chromosomal aberrations and gene mutations (10). Since GFI1 plays an important role in B-cell development and subsequent PC differentiation (11, 12) we investigated whether the presence of GFI1-36N might predispose carriers to MM and affect their prognosis. Several genetic aberrations are strongly associated with MM treatment response and patient survival (13). Of these, translocation (4, 14) and gain of 1q21 are associated with poor prognosis (13, 14). In this study, we investigated the frequency of the germline *GFI1-36N* and its impact on overall survival (OS) and progression-free survival (PFS) of MM patients. We finally investigated how the GFI1-36N SNP variant potentially altered the overall gene expression pattern of GFI1-36N homo or heterozygous PCs.

MATERIALS AND METHODS

Patients

We determined the frequency of germline *GFI1-36N* homo- or heterozygous carriers among a cohort of 1229 newly diagnosed MM patients and 2005 unaffected control persons based on published genome-wide association study (GWAS) data of patients treated within the German-Speaking Myeloma Multicenter Group (GMMG), HD3, HD4 and MM5 trials. The characteristics of the patient and control groups have been described earlier (2, 6, 15).

Gene Expression Analysis

Gene expression profiling using U133 2.0 plus arrays (Affymetrix, Santa Clara, CA, USA) was performed as published in MM patients (n=716, 637 were homozygous for *GFI1-36S*, 79 hetero- or homozygous for *GFI1-36N*) (16). Gene set enrichment analysis of Gene Ontology pathways between *GFI1-36S* and *GFI1-36N* was performed as published before (17). The analysed data-set have been published at the following link: https://www.ebi.ac.uk/arrayexpress/experiments/E-MTAB-2299/.

Statistics

Fisher's exact test and Wilcoxon test were used to assess the association of the genotypes with categorical and continuous parameters, respectively. Logistic regression was used to estimate the odds ratio and corresponding 95% confidence interval. No adjustment for multiples testing was required since the GFI1-36N locus was selected a priori. Cox regression and log-rank test were used to assess the prognostic impact. Kaplan-Meier estimates were used to estimate distribution of PFS and OS times.

RESULTS

Prevalence of the GFI1-36N Variant Allele and Its Association With Key Characteristics of MM Patients

The overall prevalence of the *GFI1-36N* allele was 7.9% among healthy controls and 10.4% among MM patients indicating an association of the GFI1-36N allele with the risk of developing

MM (OR 1.35, 95%CI 1.06-1.72, p-value 0.016; corrected for population stratification; **Table 1**). There was no significant difference between *GFI1-36S* homozygous and *GFI1-36N* homo-or heterozygous MM patients concerning age, sex, ISS stage or GFI1-RNA expression level (**Tables 2**, **3**). To evaluate the effect of the GFI1-36N allele on disease progression, overall survival (OS) and progression-free survival (PFS) of MM patients treated within the MM5 trial was examined (**Figure 1A**). The MM5 phase III trial examined the impact of induction therapy with doxorubicin, bortezomib and dexamethasone versus cyclophosphamide in combination with bortezomib and dexamethasone (15). Log-rank test and Cox regression were used to compare PFS and OS between groups. The presence of the *GFI1-36N* allele did not influence OS and PFS (**Figures 1A**, **2** and **3**). Of note, in a subset of MM patients characterized by the presence of t(4,14) translocation, *GFI1-36N* demonstrated a negative impact on OS (Log-rank: p= 0.02) but not on PFS (**Figures 1B**, **2** and **3**). Furthermore, in MM patients characterized by the gain of 1q21 (≤3 copies), GFI1-36N demonstrated a negative impact with a borderline statistical significance on OS and with significance on PFS (Log-rank: p= 0.052 and 0.008, respectively (**Figures 1C**, **2** and **3**). Of note, Gain of 1q21 (>3 copies) was associated with negative PFS (p=0.034, **Figures 1D**, **2** and **3**). It has been previously shown that gain of 1q21 involves genes such as *BCL9, MCL1, CKS1B* and *ANP32E*, which contribute either to inhibition of apoptosis or enhancement of cell cycling or epigenetic modification (18, 19).

We next determined potential pathways by which presence of GFI1-36N might alter gene expression pattern in PC. Analysing the gene expression profile between *GFI1-36S* and *-36N* patient groups, we found that pathways responsible for epigenetic regulation were upregulated and those regulating metabolism were down-regulated in plasma cells of heterozygous *GFI1-36S* and homozygous *-36N* MM patients (**Table 4**). This is again in line with earlier reports that GFI1 is implicated in metabolic regulation and this might contribute to the malignant transformation (20). This corresponds to our previous observations in GFI1-36N myeloid malignancies, whereby GFI1-36N failed to induce epigenetic changes to the same extent as the GFI1-36S protein (3, 21).

DISCUSSION

Our previous investigations and observations have underscored a role for *GFI1*-36S and -36N SNP variants in myeloid malignancies. We had reported that the presence of the GFI1-36N protein was associated with an increased incidence of mutations in genes encoding epigenetic modifiers such as *DNMT3a* and could be therapeutically exploited in AML therapy (2, 15). One of the physiological functions of GFI1 is to recruit histone-modifying genes to its target genes and induce repressive epigenetic changes. GFI1 also regulates lymphoid development in general and B-cell development in particular. Hence it would be conceivable that the presence of GFI1-36N might not only disturb myeloid development but also B-cell development and predispose to myeloma development.

TABLE 1 | The frequency of the GFI1-36N allele was determined within a population of newly diagnosed MM patients and a respective control population. OR 1.35, 95%CI 1.06-1.72.

	Controls (n = 2005)		MM cases (n = 1229)		p-value
	n	%	n	%	
GFI1-36N allele homozygous	5	0.2	2	0.2	
GFI1-36N allele heterozygous	154	7.7	126	10.2	
GFI1-36N allele homozygous + heterozygous	159	7.9	128	10.4	P=0.02
GFI1-36S allele homozygous	1846	92.1	1101	89.6	

TABLE 2 | Clinical factors and their association with GFI136N. No significant association between the presence of the GFI1-36N allele and gender or ISS was observed.

	GFI1-36N Homo or heterozygous					
Prognostic factor	**n**	**%**	**n**	**%**	**p-value**	**OR**
						95%CI
Gender					0.51	0.88 (0.621-1.28
Male	72	56.2	653	59.3		
Female	56	43.8	448	40.7		
ISS stage					0.37	
I	40	36.4	397	41.4		
II	44	40	319	33.2		(II vs I) 1.37 (0.87-2.16)
III	26	23.6	244	25.4		(III vs I) 1.06 (0.62-1.77)

TABLE 3 | Correlation between presence of GFI1-36N allele and age or GFI1-RNA expression level.

Variable	Group	n	Min	Q1	Median	Mean	Q3	Max
Age	*GFI1-36N* homo or heterozygous	128	37	51	57	56.4	62.5	70
P=0.33	*GFI1-36S* homozygous	1101	24.8	52	58	56.9	63	73.4
OR (per 10 year) 0.93 (0.75-1.16)	All	1229	24.8	51.8	58	56.8	63	73.4
GFI1 expression	*GFI1-36N* homo or heterozygous	79	3.4	7.6	8.3	8	8.8	10.2
P=0.71								
OR (per FC increase)								
1.02 (0.87-1.22)								
	GFI1-36S homozygous	637	3.4	7.4	8.2	8	8.9	11.1
	All	716	3.4	7.4	8.2	8	8.9	11.1

No significant difference was seen between GFI1-36N homo or heterozygous MM patients on one hand and GFI1-36S homozygous patients on the other hand concerning age or GFI1expression. FC, Fold change.

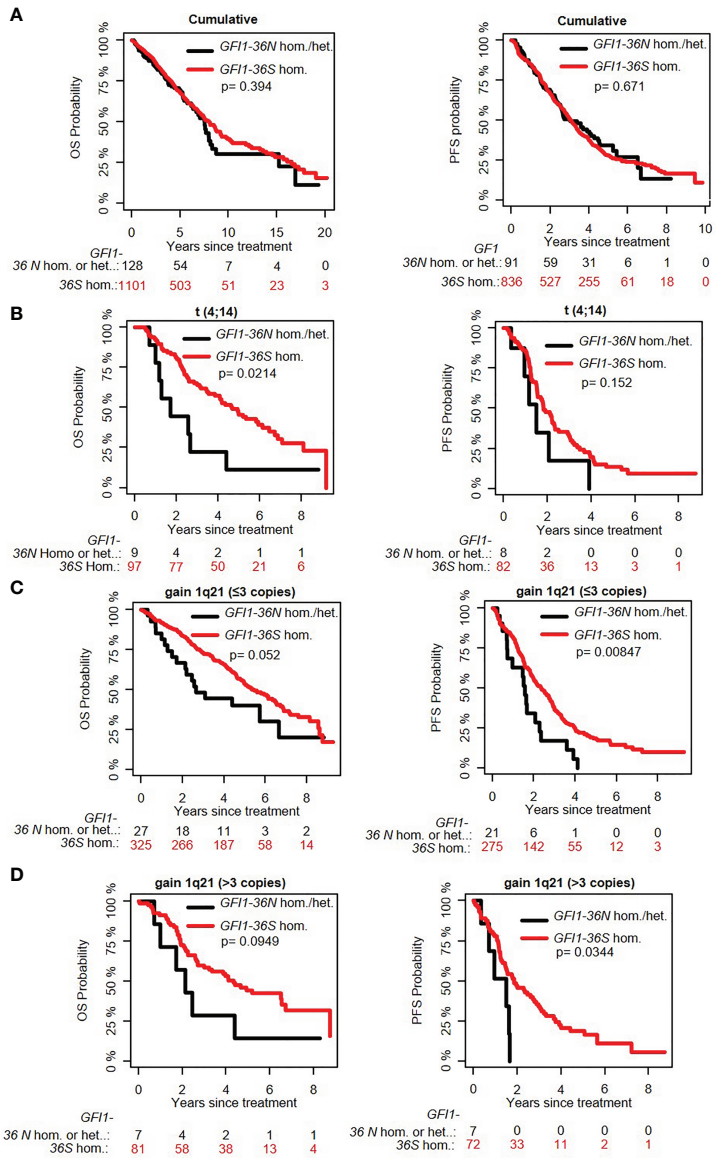

FIGURE 1 | Influence of the presence of GFI1-36N allele on PFS and OS of MM patient subgroups. **(A)** GFI1-36N did not influence OS and PFS in the entire cohort. **(B)** GFI1-36N negatively affects OS but not PFS in MM patients with t(4;14) translocation. **(C, D)** GFI1-36N negatively affects OS and PFS in MM patients with gain of 1q21 (≤3 copies and >3 copies).

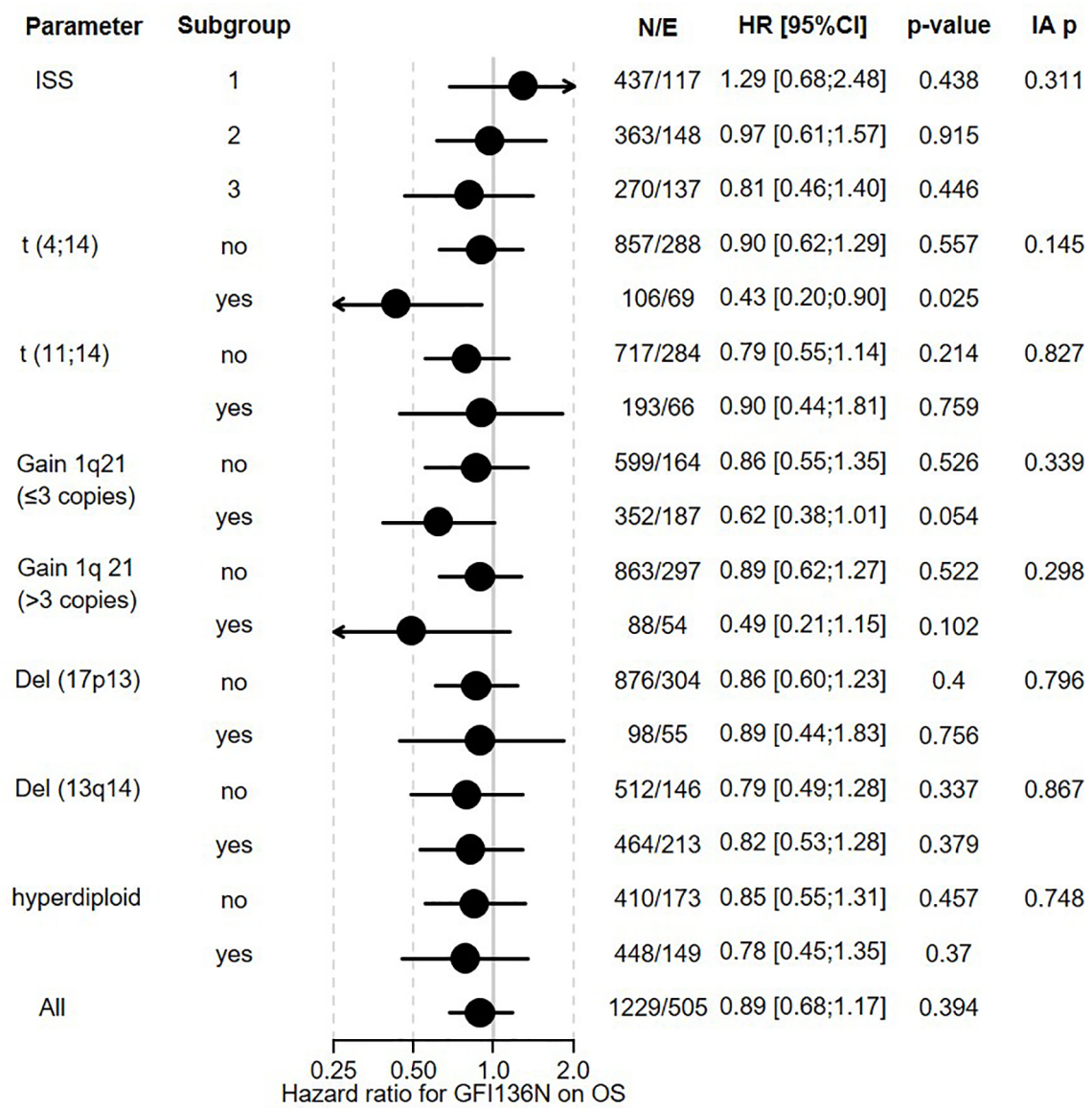

FIGURE 2 | Influence of GFI1-36N on OS of MM patients. GFI1-36N (homo or heterozygous) MM patients were stratified according to presence/absence/levels of different parameters, International Staging System (ISS), t(4;14), t(11;14), gain 1q21 (≤3 copies), or gain 1q21 (>3 copies), Del (17p13), Del (13q14), hyperdiploid and statistically evaluated for PFS. Hazard ratio including 95% confidence interval based on Cox regression is presented. IA p indicates test on the interaction between subgroups, N/E: Number of patients and events within the subgroup.

Therefore, we evaluated the prevalence of the GFI1-36N variant and if it contributed to the pathogenesis of MM. Interestingly, our results are in line with observations for AML. They indicate that GFI1-36N has a higher prevalence among MM patients compared to the unaffected population. Prevalence among control persons was slightly higher compared to our previous studies, which reported frequencies of *GFI1-36N* allele between 3-7% in the different control groups (4, 21). The frequency of the *GFI1-36N* allele among MM patients was similar to our previous reports in MDS and AML patients varying between 10-15% with an OR of 1.3-2 (4, 21). A similar frequency of the *GFI1-36N* allele among AML, MDS and MM patients points to a possible universal role of GFI1-36N predisposing or contributing to haematological malignancies. Our results with global gene expression pattern indicate that a similar mechanism might also explain the pathogenesis and therefore indicate that GFI1-36N appears to influence the pathogenesis of MM. It would therefore be well conceivable that the presence of a GFI1-36N protein prepares an epigenetic landscape for malignant transformation and mutation accumulation involving t(4,14) translocation, gain of 1q21 and thereby might contribute to an evolution of tumour cells. It remains to be elucidated whether

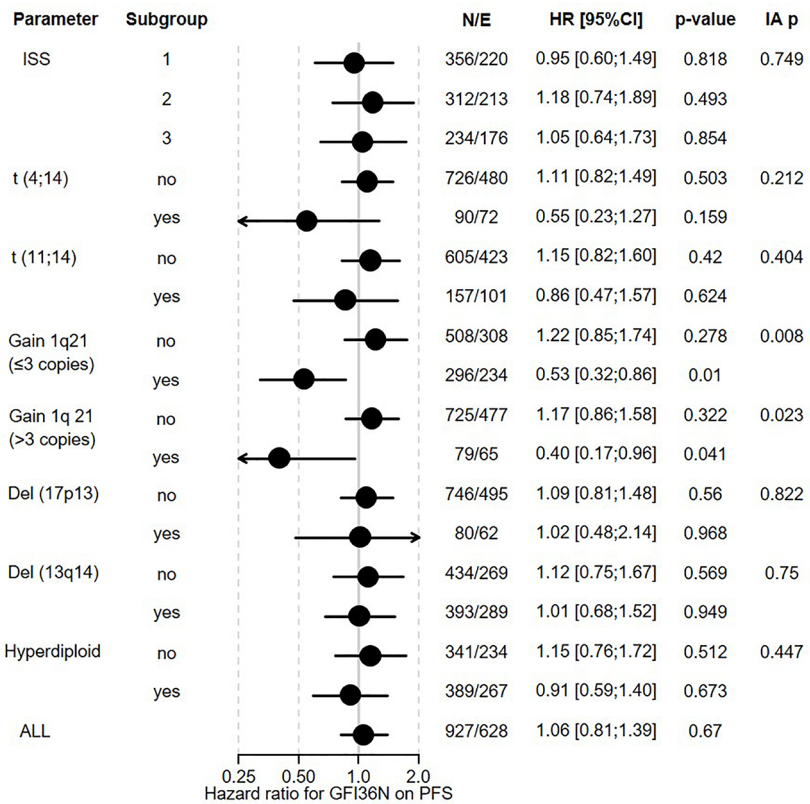

FIGURE 3 | Influence of GFI1-36N on PFS of different subgroups of MM patients. GFI1-36N (homo or heterozygous) MM patients were stratified according to presence/absence/levels of different parameters, International Staging System (ISS), t(4;14), t(11;14), gain 1q21 (≤3 copies), or gain 1q21 (>3 copies), Del (17p13), Del (13q14), hyperdiploid and statistically evaluated for PFS. Hazard ratio including 95% confidence interval based on Cox regression is presented. IA p: test on the interaction between subgroups, N/E: Number of patients and events within the subgroup.

TABLE 4 | Changes in gene expression of *GFI1-36N* homo- or heterozygous myeloma cells as compared to *GFI1-36S* homozygous cells.

Pathway	Genes (n)	Trend	p Value	FDR
Ras guanyl-nucleotide exchange factor activity	87	Up	9,44E-06	0,001987
DNA-binding transcription activator activity, RNA polymerase II-specific	230	Up	2,04E-05	0,003533
Histone demethylase activity	17	Up	2,74E-05	0,004463
Rho guanyl-nucleotide exchange factor activity	45	Up	3,1E-05	0,004977
RNA polymerase II regulatory region DNA binding	383	Up	3,52E-05	0,005439
RNA polymerase II regulatory region sequence-specific DNA binding	381	Up	4,49E-05	0,006491
Regulatory region nucleic acid binding	486	Up	5,98E-05	0,008347
Transcription regulatory region sequence-specific DNA binding	413	Up	6,11E-05	0,008423
Transcription regulatory region DNA binding	485	Up	6,35E-05	0,008459
Sequence-specific DNA binding	557	Up	6,82E-05	0,008957
Sequence-specific double-stranded DNA binding	438	Up	6,89E-05	0,008957
Mitochondrial respiratory chain	63	Down	2,44E-14	2,83E-10
Oxidative phosphorylation	103	Down	1,36E-13	7,88E-10
Respiratory chain complex	55	Down	2,85E-13	8,61E-10
ATP synthesis coupled electron transport	70	Down	4,51E-13	1,05E-09
Mitochondrial protein complex	203	Down	6,36E-13	1,09E-09
Mitochondrial ATP synthesis coupled electron transport	69	Down	6,6E-13	1,09E-09
Inner mitochondrial membrane protein complex	94	Down	9,55E-13	1,38E-09
Respiratory electron transport chain	84	Down	1,44E-12	1,86E-09
Mitochondrial inner membrane	367	Down	9,1E-12	1,05E-08
Mitochondrial respiratory chain	63	Down	2,44E-14	2,83E-10
Oxidative phosphorylation	103	Down	1,36E-13	7,88E-10

FDR, False discovery rate.

our findings with an elevated frequency of GFI1-36N in myeloma patients and its potential influence on the disease course of t(14;16) and gain 1q21, can be replicated in other independent cohorts. However it could be that GFI1-36N is a general factor predisposing to development of myeloid malignancies and myeloma.

DATA AVAILABILITY STATEMENT

The analysed data-set have been published at the following link: https://www.ebi.ac.uk/arrayexpress/experiments/E-MTAB-2299/.

AUTHOR CONTRIBUTIONS

CK, CE, SN, MR, NW, AS, DH, AJ, AF, KH, TH, MH, GL, HG, and SH provided and analysed the data. CK and SH designed the study and wrote the manuscript. All authors contributed to the article and approved the submitted version.

FUNDING

DH was supported by Deutsche Forschungsgemeinschaft (SFB/TRR79) the German Federal Ministry of Education ("CLIOMMICS" (01ZX1309 and 01ZX1609) as well as "CAMPSIMM" (01ES1103)). KH is supported by the European Union's Horizon 2020 research and innovation programme, grant No 856620. CK is supported by the Jose Carreras Leukaemia Foundation (DJCLS 17R/2018), partially by the Deutsche Krebshilfe (70112392), Deutsche Forschungsgemeinschaft (KH331/2-3), and the intramural funding of the Faculty of Medicine at University Hospital of Muenster (Kha2/002/20).

ACKNOWLEDGMENTS

The authors thank Maria Dörner, Ewelina Nickel, and Birgit Schneiders for technical assistance in the enrichment of CD138-positive plasma cells, Véronique Pantesco for performing DNA-microarrays, and the Transcriptomics Platform at INSERM Montpellier.

REFERENCES

1. Moroy T, Khandanpour C. Role of GFI1 in Epigenetic Regulation of MDS and AML Pathogenesis: Mechanisms and Therapeutic Implications. *Front Oncol* (2019) 9:824. doi: 10.3389/fonc.2019.00824
2. Chattopadhyay S, Thomsen H, Yadav P, da Silva Filho MI, Weinhold N, Nöthen MM, et al. Genome-Wide Interaction and Pathway-Based Identification of Key Regulators in Multiple Myeloma. *Commun Biol* (2019) 2:89. doi: 10.1038/s42003-019-0329-2
3. Botezatu L, Michel LC, Helness A, Vadnais C, Makishima H, Hones JM, et al. Epigenetic Therapy as a Novel Approach for GFI136N-Associated Murine/Human AML. *Exp Hematol* (2016) 44:713–26.e714. doi: 10.1016/j.exphem.2016.05.004
4. Khandanpour C, Vassen L, Gaudreau M-C, Krongold J, van der Reijden B, Jansen J, et al. A Human Variant of Growth Factor Independence 1 (GFI136N) Predisposes to Myeloid Leukemia In Mice. *Blood* (2010) 116 (21):439. doi: 10.1182/blood.V116.21.997.997
5. Broderick P, Chubb D, Johnson DC, Weinhold N, Forsti A, Lloyd A, et al. Common Variation at 3p22.1 and 7p15.3 Influences Multiple Myeloma Risk. *Nat Genet* (2011) 44(1):58–61. doi: 10.1038/ng.993
6. Chubb D, Weinhold N, Broderick P, Chen B, Johnson DC, Forsti A, et al. Common Variation at 3q26.2, 6p21.33, 17p11.2 and 22q13.1 Influences Multiple Myeloma Risk. *Nat Genet* (2013) 45(10):1221–5. doi: 10.1038/ng.2733
7. Pertesi M, Went M, Hansson M, Hemminki K, Houlston RS, Nilsson B. Genetic Predisposition for Multiple Myeloma. *Leukemia* (2020) 34(3):697–708. doi: 10.1038/s41375-019-0703-6
8. Went M, Sud A, Forsti A, Halvarsson BM, Weinhold N, Kimber S, et al. Identification of Multiple Risk Loci and Regulatory Mechanisms Influencing Susceptibility to Multiple Myeloma. *Nat Commun* (2018) 9(1):3707. doi: 10.1038/s41467-018-04989-w
9. Rollig C, Knop S, Bornhauser M. Multiple Myeloma. *Lancet* (2015) 385:2197–208. doi: 10.1016/S0140-6736(14)60493-1
10. Palumbo A, Anderson K. Multiple Myeloma. *N Engl J Med* (2011) 364:1046–60. doi: 10.1056/NEJMra1011442
11. D'Souza S, del Prete D, Jin S, Sun Q, Huston AJ, Kostov FE, et al. Gfi1 Expressed in Bone Marrow Stromal Cells Is a Novel Osteoblast Suppressor in Patients With Multiple Myeloma Bone Disease. *Blood* (2011) 118(26):6871–80. doi: 10.1182/blood-2011-04-346775
12. Spooner CJ, Cheng JX, Pujadas E, Laslo P, Singh H. A Recurrent Network Involving the Transcription Factors PU.1 and Gfi1 Orchestrates Innate and Adaptive Immune Cell Fates. *Immunity* (2009) 31:576–86. doi: 10.1016/j.immuni.2009.07.011
13. Chng WJ, Dispenzieri A, Chim CS, Fonseca R, Goldschmidt H, Lentzsch S, et al. IMWG Consensus on Risk Stratification in Multiple Myeloma. *Leukemia* (2014) 28(2):269–77. doi: 10.1038/leu.2013.247
14. Shah V, Sherborne AL, Walker BA, Johnson DC, Boyle EM, Ellis S, et al. Prediction of Outcome in Newly Diagnosed Myeloma: A Meta-Analysis of the Molecular Profiles of 1905 Trial Patients. *Leukemia* (2018) 32(1):102–10. doi: 10.1038/leu.2017.179
15. Mai EK, Bertsch U, Durig J, Kunz C, Haenel M, Blau IW, et al. Phase III Trial of Bortezomib, Cyclophosphamide and Dexamethasone (VCD) Versus Bortezomib, Doxorubicin and Dexamethasone (PAd) in Newly Diagnosed Myeloma. *Leukemia* (2015) 29(8):1721–9. doi: 10.1038/leu.2015.80
16. Hose D, Beck S, Salwender H, Emde M, Bertsch U, Kunz C, et al. Prospective Target Assessment and Multimodal Prediction of Survival for Personalized and Risk-Adapted Treatment Strategies in Multiple Myeloma in the GMMG-MM5 Multicenter Trial. *J Hematol Oncol* (2019) 12(1):65. doi: 10.1186/s13045-019-0750-5
17. Wu D, Smyth GK. Camera: A Competitive Gene Set Test Accounting for Inter-Gene Correlation. *Nucleic Acids Res* (2012) 40:e133. doi: 10.1093/nar/gks461
18. Hanamura I, Stewart JP, Huang Y, Zhan F, Santra M, Sawyer JR, et al. Frequent Gain of Chromosome Band 1q21 in Plasma-Cell Dyscrasias Detected by Fluorescence *In Situ* Hybridization: Incidence Increases From MGUS to Relapsed Myeloma and is Related to Prognosis and Disease Progression Following Tandem Stem-Cell Transplantation. *Blood* (2006) 108(5):1724–32. doi: 10.1182/blood-2006-03-009910
19. Marchesini M, Ogoti Y, Fiorini E, Aktas Samur A, Nezi L, D'Anca M, et al. ILF2 Is a Regulator of RNA Splicing and DNA Damage Response in 1q21-Amplified Multiple Myeloma. *Cancer Cell* (2017) 32(1):88–100.e106. doi: 10.1016/j.ccell.2017.05.011
20. Fraszczak J, Vadnais C, Rashkovan M, Ross J, Beauchemin H, Chen R, et al. Reduced Expression But Not Deficiency of GFI1 Causes a Fatal Myeloproliferative Disease in Mice. *Leukemia* (2019) 33(1):110–21. doi: 10.1038/s41375-018-0166-1
21. Botezatu L, Michel LC, Makishima H, Schroeder T, Germing U, Haas R, et al. GFI1(36N) as a Therapeutic and Prognostic Marker for Myelodysplastic Syndrome. *Exp Hematol* (2016) 44:590–5.e591. doi: 10.1016/j.exphem.2016.04.001

Conflict of Interest: Author MH was employed by company Roche Diagnostics GmbH.

The remaining authors declare that the research was conducted in the absence of any commercial or financial relationships that could be construed as a potential conflict of interest.

Publisher's Note: All claims expressed in this article are solely those of the authors and do not necessarily represent those of their affiliated organizations, or those of the publisher, the editors and the reviewers. Any product that may be evaluated in this article, or claim that may be made by its manufacturer, is not guaranteed or endorsed by the publisher.

frontiers in Oncology

MINI REVIEW
published: 05 November 2021
doi: 10.3389/fonc.2021.704464

Mass Cytometry in Hematologic Malignancies: Research Highlights and Potential Clinical Applications

John M. Astle * *and Huiya Huang*

Department of Pathology, Medical College of Wisconsin, Milwaukee, WI, United States

Recent advances in global gene sequencing technologies and the effect they have had on disease diagnosis, therapy, and research have fueled interest in technologies capable of more broadly profiling not only genes but proteins, metabolites, cells, and almost any other component of biological systems. Mass cytometry is one such technology, which enables simultaneous characterization of over 40 parameters per cell, significantly more than can be achieved by even the most state-of-the-art flow cytometers. This mini-review will focus on how mass cytometry has been utilized to help advance the field of neoplastic hematology. Common themes among published studies include better defining lineage sub-populations, improved characterization of tumor microenvironments, and profiling intracellular signaling across multiple pathways simultaneously in various cell types. Reviewed studies highlight potential applications for disease diagnosis, prognostication, response to therapy, measurable residual disease analysis, and identifying new therapies.

Keywords: mass cytometry, cyTOF, hematologic, oncology, acute myeloid leukemia, myeloma, flow cytometry

OPEN ACCESS

Edited by:
Alejandro Gru,
University of Virginia Health System, United States

Reviewed by:
Ranganatha R. Somasagara,
North Carolina Central University, United States
Daniele Derudas,
Ospedale Oncologico Armando Businco, Italy

****Correspondence:***
John M. Astle
jastle@mcw.edu

Specialty section:
This article was submitted to Hematologic Malignancies, a section of the journal Frontiers in Oncology

Received: *03 May 2021*
Accepted: *20 October 2021*
Published: *05 November 2021*

Citation:
Astle JM and Huang H (2021) Mass Cytometry in Hematologic Malignancies: Research Highlights and Potential Clinical Applications. Front. Oncol. 11:704464. doi: 10.3389/fonc.2021.704464

INTRODUCTION AND OVERVIEW OF MASS CYTOMETRY

Mass cytometry, also known as cytometry by time-of-flight (CyTOF), combines many aspects of flow cytometry with key advantages of mass spectrometry to enable simultaneous detection of over 40 parameters per cell for up to millions of cells (1, 2). Rather than using antibodies labeled with fluorophores for detection as in flow cytometry, mass cytometry uses antibodies labeled with heavy metals. Detecting the presence and abundance of heavy metals by mass spectrometry minimizes the amount of signal that "spills over" from one parameter to another, significantly decreasing the problem of spectral overlap that plagues flow cytometry (see **Figure 1**). The large number of parameters that can now be reasonably detected on limited specimens enables more thorough characterization, providing a more systemic view of networked processes while at the same time higher resolution of cellular sub-populations and individual cells.

CyTOF was originally developed by Scott Tanner and colleagues at the University of Toronto (1). Simplified, the CyTOF technique begins by incubating fixed cell suspensions and antibodies labeled with heavy metals that are not present in normal biological systems. Rather than individual cells being exposed to a laser and the emitted light detected as in flow cytometry, the cells are nebulized into liquid droplets then vaporized, ionized, and sent through a time-of-flight mass spectrometer, which can determine the identity of each heavy metal based on how long it takes to reach a sensor.

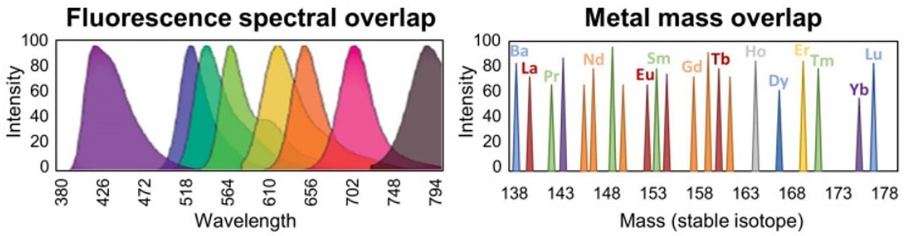

FIGURE 1 | Overcoming spectral overlap *via* mass cytometry. Significant spectral overlap complicates measurement of specific parameters when detecting emitted light from fluorophores in flow cytometry (left). Contamination of adjacent parameters is minimized *via* detection of heavy metal isotopes by mass cytometry (right). Figure adapted from (3).

This new technology first popped onto many people's radar after Gary Nolan's group at Stanford (in collaboration with Scott Tanner and others) published a seminal article showcasing the power of this novel technology (4). They stimulated cell populations with various stimuli and simultaneously measured 34 parameters per cell within a population of hematopoietic cells to show differential responses of individual cells and cell sub-populations to these stimuli. By utilizing SPADE analysis software, they were able to visualize an overview of the different cell types and differential expression of various proteins (**Figure 2**). Since that time, there have been continual improvements in technology and reagents, as well as software. Commonly used analysis software include SPADE (5–7), viSNE (8), Citrus (9, 10), and PhenoGraph (11).

This new technology has been utilized to study several different aspects of biology and disease, with many studies thus far emphasizing the characterization of novel subpopulations of various immune cell subsets, characterization of tumor microenvironments, and profiling intracellular signaling across multiple cell subpopulations. Various disease processes have been studied, including COVID-19 (12), Alzheimer disease (13), tuberculosis (14), rheumatoid arthritis (15), non-alcoholic steatohepatitis and hepatocellular carcinoma (16), just to name a few. Potential applications of CyTOF in clinical medicine have been reviewed (17). This mini-review will focus on studies characterizing hematologic malignancies and some of their findings relevant to disease diagnosis, prognostication, response to therapy, measurable residual disease (MRD) analysis, and potential new therapies.

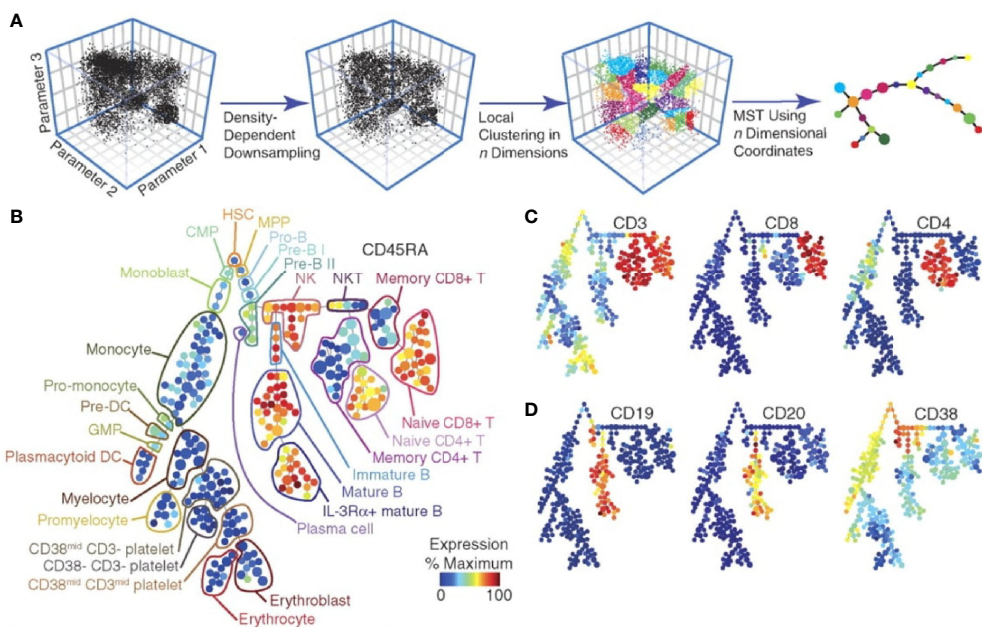

FIGURE 2 | SPADE analysis of multidimensional data. Overview of simplifying multi-dimensional data into a two-dimensional plot by SPADE analysis **(A)**. A tree plot constructed by SPADE software utilizing 13 cell surface markers identified hematopoietic cell populations **(B)**. Expression levels of specific markers can be visualized for each cellular sub-population **(C, D)**. Figure adapted from Bendall et al. (4), with permission.

RESEARCH HIGHLIGHTS IN HEMATOLOGIC MALIGNANCIES

Diagnosis

CyTOF has enabled profiling of cellular signaling states, tumor microenvironments, and immune responses to several diseases in a more global fashion than has been done with more traditional approaches, facilitating identification of disease biomarkers. These biomarkers have potential to aid in the diagnosis of various diseases. For example, Han et al. (18) identified disease-specific profiles of intracellular signaling activation that could aid in diagnosis of acute myeloid leukemia. Bailur et al. (19) profiled many markers simultaneously to show that leukemic cells created *via* CRISPR-induced MLL rearrangement were more similar to acute myeloid leukemia (AML) than acute lymphoblastic leukemia (ALL). A similar approach may aid in the distinction between AML and ALL in the subset of cases where this is difficult using currently utilized markers and flow cytometric approaches. Behbehani et al. (20) evaluated cell surface markers in patients with myelodysplastic syndrome (MDS) compared to healthy donors and showed aberrancies in 27 of 31 markers in patients with MDS, the presence of which may be helpful for diagnosing MDS. Van Leeuwen-Kerkhoff et al. (21) showed specific subsets of monocytes are decreased in MDS bone marrows and that these monocytes mediate expansion of a specific T-cell subset, suggesting the identification and quantitation of specific cell subsets may also aid in the diagnosis of MDS. Yang et al. (22) studied tumor microenvironments in follicular lymphoma (FL) and discovered at least 12 subsets of intratumoral CD4(+) T cells, three of which were unique to FL specimens. Subsequent study of FL identified a lack of plasmablasts in FL specimens compared to controls (23). Roussel et al. (24) compared tumor microenvironments of FL, diffuse large B-cell lymphoma (DLBCL) and classic Hodgkin lymphoma (cHL) and identified immune profiles specific to each lymphoma type, including the presence and abundance of monocyte subsets and T-cell subsets. These studies lend evidence to the idea that detecting the presence, absence, or relative abundance of non-neoplastic cell types within a tumor microenvironment can be useful for disease diagnosis.

Prognostication

CyTOF has also facilitated identification of biomarkers potentially helpful for disease prognostication. Levine et al. (11) published PhenoGraph software for analyzing CyTOF data, which enabled better identification and characterization of leukemic hematopoietic stem and progenitor cells (HSPCs). They showed that cell surface molecules indicating an HSPC immunophenotype are decoupled from intracellular signaling signatures of HSPCs in a significant subset of AML patient samples, and that the number of cells showing intracellular signaling markers of HSPCs correlates more closely with prognosis than when cell surface molecules are used to identify HSPCs. Around the same time Behbehani et al. (25) showed that core binding factor AMLs, which generally have a good prognosis, have an increased fraction of leukemic HSPCs in S-phase of the cell cycle while the relatively poor prognostic FLT3-ITD AMLs have a decreased S-phase fraction. Chretien et al. (26) showed that a "hypomature" NK cell profile or low expression of NKp30 is associated with poor survival in AML patients, while high expression of NKp30 without a hypomature profile is associated with longer survival. Good et al. (27) evaluated 60 primary diagnostic B-lymphoblastic leukemia (BLL) samples to identify 6 features able to predict patient relapse at diagnosis, improving currently established risk stratification methods. Bailur et al. (28) studied tumor microenvironments and identified immune profiles that correlated with disease risk in BLL. Van Leeuwen-Kerkhoff et al. (29) showed thrombomodulin expression on monocytes of MDS patients is associated with lower risk and better leukemia-free survival. Gullaksen et al. (30) profiled intracellular signal transduction in chronic myeloid leukemia (CML) and clear differences were noted between CML cells and healthy donor cells. Changes in signaling were detected within three hours of nilotinib therapy, and profiles identified after seven days of therapy correlated with BCR-ABL1 burden at 3 and 6 months, suggesting early signal transduction profiles may be useful for prognostication. Yang et al. (22) showed that naïve T cells within the tumor microenvironment of FL were associated with improved survival, while specific subsets of PD-1(+) T cells and loss of the costimulatory receptor CD27 on intratumoral T cells were associated with poor survival. Yang et al. (31) then showed that T-cell immunoglobulin and ITIM domain (TIGIT) is highly expressed on exhausted intratumoral T cells of FL and is associated with inferior survival. These studies show that the types of biomarkers identifiable by CyTOF for disease diagnosis such as intracellular signaling profiles and cellular profiles within tumor microenvironments may be helpful for disease prognostication.

Response to Therapy and Vaccination

CyTOF has been used to better characterize responses to various therapies, leading to better understanding of mechanisms of action as well as mechanisms of resistance to therapy. Saenz et al. (32) used CyTOF to help evaluate the response of post-myeloproliferative neoplasm secondary AML (sAML) cells to different therapies in a xenograft model, facilitating a broad and detailed characterization of drug responses, suggesting BET protein proteolysis-targeting chimera may be more effective than bromodomain inhibitor in treating this neoplasm. This group also showed decreased expression of Bcl-xL, CDK4/6, c-MYC, IL-7R, p-STAT5, and PIM1, and increased expression of BIM, HEXIM1, and p21 in BET inhibitor treated AML cells from sAML. Synergistic activity of BET inhibitor with the JAK inhibitor ruxolitinib is seen in sAML cells, and there is also synergistic activity of BET inhibitor and HSP90 inhibitor against ruxolitinib-resistant sAML cells. Zeng et al. (33) evaluated 24 primary AML samples to perform detailed characterization of mTOR inhibition in AML cells, and results pointed to cell signaling pathways dampening drug response. Edwards et al. (28) characterized CSF1R signaling to show anti-leukemic activity of CSF1R inhibitors occurs through inhibiting paracrine signaling from support cells. In 2020 Han et al. (34) showed that cobimetinib antagonized pERK and pS6 signaling, and was associated with increased BCL2 expression in leukemia

HSPCs in venetoclax-sensitive AML specimens. Borthakur et al. (35) published findings of a phase-I study of combined sorafenib, plerixafor, and G-CSF for AML, where CyTOF was used to identify resistant sub-clones and characterized signaling within these cells to show persistent Akt and/or ERK signaling. Rorby et al. (36) investigated the mechanism of synergistic activity of midostaurin in combination with daunorubicin and cytarabine, which has been shown to increase survival in FLT3-mutated AML patients. They showed that cytarabine appeared to antagonize midostaurin's effect on protein phosphorylation and increased surface expression of FLT3. Deng et al. (37) helped identify VEGFR2 signaling as the mechanism by which Apatinib exerts its anti-leukemic effect in BLL. Bandyopadhyay et al. (38) showed that avasimibe, an inhibitor of cholesterol esterification, synergistically suppressed CML cell proliferation, and led to downregulation of the MAPK signaling pathway, which likely sensitized CML cells to imatinib. Baughn et al. (39) identified loss of CD56 and CD66a and a signature of activation are associated with proteasome inhibitor resistance in a myeloma cell line suggesting these have potential as markers of resistance to proteasome inhibitor therapy. Adams et al. (40) characterized the myeloma tumor microenvironment and showed that daratumumab-treated patients have increased cytotoxic T cells and reduced immunosuppressive cell populations, consistent with immune modulation as a novel mechanism of action for daratumumab. Teh et al. (41) characterized regulators of cell death, mitosis, cell signaling, and cancer-related pathways in myeloma cells treated with dexamethasone or bortezomib to identify increased CREB and MCL-1 in treatment-resistant myeloma cells. Visram et al. (42) evaluated bone marrow from 13 newly diagnosed, 11 relapsed pre-daratumumab, and 13 triple-refractory myeloma patients and found that patients who are resistant to three lines of therapy have a distinct immune tumor microenvironment including decreased CD4(+) T cells and naïve T cells compared to newly diagnosed and relapsed but pre-daratumumab treated patients. This finding suggests that immune microenvironment signatures may help predict response to therapy. Finally, Alimam et al. (43) monitored immune responses to influenza A vaccine in 7 polycythemia vera (PV), 8 essential thrombocythemia (ET), and 4 myelofibrosis (MF) patients compared to 6 healthy donors, and evidence of impaired B- and T-memory cell responses in patients with myeloproliferative neoplasms was identified. The ability of CyTOF to broadly characterize numerous antigens and cells simultaneously greatly facilitates evaluation of responses to various therapies and even vaccinations. Several of these studies also highlight the ability of CyTOF data to elucidate the mechanism of action of drugs, and to identify potential predictors of response or resistance to therapy.

MRD Analysis

MRD analysis is typically performed using one or a combination of two distinct approaches. The first approach is to identify populations of cells that are immunophenotypically similar to the immunophenotype at diagnosis. This is the easier of the two approaches in many respects, but falls short when tumors modulate their immunophenotype, which some neoplasms do quite readily. The second approach is to identify immunophenotypes that are different from the immunophenotype of a normal cell counterpart to the tumor cell. For example, a "different-from-normal" approach to MRD analysis for AML would look for populations of aberrant HSPCs that display a different immunophenotype than normal HSPCs. A study by Ferrell et al. (44) highlighted the power of CyTOF for characterizing how versatile AML cells can be at modulating their immunophenotype. They characterized 46 samples from 5 AML patients before, during, and immediately after induction chemotherapy to show how the AML population and subpopulations modulated their immunophenotypes over time. Studies such as this not only characterize the degree of versatility with which cancers can modulate their immunophenotype, but may help identify new cancer-specific immunophenotypes and their frequency in studied populations. Unfortunately, the rate at which cells flow through CyTOF machines is roughly an order of magnitude slower than flow cytometers frequently used in clinical laboratories, limiting its utility for clinical use. However, CyTOF can facilitate the discovery of disease-specific immunophenotypes including specific combinations of immunophenotypes much more readily than other approaches due to the sheer number of antigens that can be monitored from a given, often limited, specimen. Despite the limited number of specimens that could be run in a day, a mass cytometer may be warranted for MRD detection in patients where MRD analysis has been hindered by the use of new antibody therapeutics. For example, antibodies targeting B-cell antigens are being used to treat B-cell lineage leukemias and lymphomas, and the antigens that these antibodies target (which are usually the same antigens used to identify the presence of these cell populations by flow cytometry) are often rendered useless as markers for MRD detection. The ability to identify cancer cell populations using combinations of other antigens by CyTOF could be extremely useful. Even if CyTOF machines are not used in clinical laboratories in the near future, software developed for CyTOF may prove useful for MRD detection. Amir et al. (8) showed that viSNE software can be used to visually distinguish leukemia from healthy bone marrow samples, and the potential of viSNE for identification of MRD was shown. Similarly, Bandyopadhyay et al. (45) utilized CyTOF to identify a subpopulation of cells in secondary AML that was not readily identified by manual gating approaches of two-dimensional plots, highlighting the power of software facilitating evaluation of multiple dimensions at once. As technological improvements increase acquisition rates, costs decrease, and data validating the value of high-parameter approaches to MRD analysis are published, clinical laboratories may in the not-too-distant future begin using CyTOF for MRD analysis.

Potential New Therapies

New discoveries identified *via* CyTOF analysis can point to potential new therapies, and potential new therapies can be tested in model cells and organisms to characterize their effects and side-effects across multiple signaling pathways in multiple cell types at once. Han et al. (18) identified distinct patterns of signaling activation within leukemia stem cells across AML samples and between AML and control samples. mTOR signaling was

identified as a possible therapeutic target as mTOR regulated proteins 4EBP1 and S6 were found to be phosphorylated in FLT3-ITD progenitor cells but not in controls. This study highlights the importance of using high dimensional cytometry to monitor multiple signaling pathways simultaneously to identify possible therapeutic targets. Zeng et al. (33), after identifying cell signaling pathways that dampen drug response during mTOR inhibitor administration, showed that targeting these pathways along with mTOR inhibition led to increased efficacy. Sarno et al. (46) set out to study why high expression of CRLF2 is associated with poor prognosis in patients with B-lymphoblastic leukemia/lymphoma, and identified coordinated signaling involving JAK/STAT, PI3K and CREB pathways downstream of CRLF2. The authors showed in primary leukemia cells that SRC/ABL inhibition was more effective at inhibiting the CRLF2-driven network than JAK or PI3K inhibition. Fisher et al. (47) identified increased activity of JAK-STAT, MAPK, PI3K and NFkB signaling in myelofibrosis (MF) and sAML cells. They identified constitutive and hypersensitive NFkB signaling in MF and sAML HSPCs, and found that inhibition of NFkB in CD34(+) HSPCs from MF patients suppressed myeloid colony formation, suggesting NFkB inhibition as a potential therapeutic approach in MF and sAML. They then monitored cytokine production in MF patient blood cells by CyTOF, and monocytes were found to overexpress many cytokines induced by thrombopoietin, TLR ligands, and tumor necrosis factor (48). All of these cytokines could be suppressed by inhibiting NFkB and/or MAPK signaling, suggesting this as a novel pharmacotherapy in MF. Teh et al. (41), after identifying increased CREB and MCL-1 in treatment-resistant myeloma cells, showed that combining an MCL-1 inhibitor to dexamethasone showed synergistic activity in killing primary myeloma cells from patients. These are just a few examples of how high-parameter profiling *via* CyTOF can help identify new potential therapies for diseases.

DISCUSSION

Mass cytometry has significantly increased our capacity to profile entire populations of cells at the individual cellular level. This can be extremely useful, particularly when the total number of cells for evaluation is limited, such as in clinical biopsy or fine needle aspirate specimens. However, it is important to recognize that CyTOF is not completely equivalent to flow cytometry with more measurable parameters. Slower acquisition rate, more complicated data analysis, and need for surrogates of forward and side scatter are a few of the caveats to the promise of mass cytometry for clinical use.

Review of the current literature has shown that only a few hematopoietic malignancies such as AML and plasma cell myeloma have been investigated *via* CyTOF in more than a handful of studies. Numerous diseases not mentioned in this mini-review could benefit from more detailed characterization made possible by this new technology. A major strength of CyTOF is in its ability to identify not only individual biomarkers but combinations of markers that together provide more systemic or global signatures of diseases or biological states (similar to gene expression profiling). These signatures may incorporate relative abundance of different cell subsets, expression levels of different proteins, and/or activation states of various cellular signaling pathways. Such expression profiles may be useful for disease diagnosis, prognostication, and predicting response to therapy. While the relatively slow acquisition rate of current CyTOF machines limits their utility for clinical MRD analysis, CyTOF provides a powerful mechanism for identifying disease-specific markers (i.e. leukemia-specific immunophenotypes) that can be used in routine flow cytometric MRD analysis. CyTOF has been particularly useful for characterization of tumor microenvironments. Continued research utilizing CyTOF will undoubtedly promote efforts to move this powerful technology into the clinic.

AUTHOR CONTRIBUTIONS

HH and JA contributed to the concept development, review of literature and writing of manuscript. All authors contributed to the article and approved the submitted version.

REFERENCES

1. Bandura DR, Baranov VI, Ornatsky OI, Antonov A, Kinach R, Lou X, et al. Mass Cytometry: Technique for Real Time Single Cell Multitarget Immunoassay Based on Inductively Coupled Plasma Time-of-Flight Mass Spectrometry. *Anal Chem* (2009) 81(16):6813–22. doi: 10.1021/ac901049w
2. Spitzer MH, Nolan GP. Mass Cytometry: Single Cells, Many Features. *Cell Cell Press* (2016) 165:780–91. doi: 10.1016/j.cell.2016.04.019
3. Blair TA, Frelinger AL, Michelson AD. Chapter 35 - Flow Cytometry. In: Michelson AD. Platelets (Fourth Edition). Academic Press (2019) 627–51. doi: 10.1016/B978-0-12-813456-6.00035-7
4. Bendall SC, Simonds EF, Qiu P, Amir EAD, Krutzik PO, Finck R, et al. Single-Cell Mass Cytometry of Differential Immune and Drug Responses Across a Human Hematopoietic Continuum. *Science* (2011) 332(6030):687–96. doi: 10.1126/science.1198704
5. Qiu P, Simonds EF, Bendall SC, Gibbs KD, Bruggner RV, Linderman MD, et al. Extracting a Cellular Hierarchy From High-Dimensional Cytometry Data With SPADE. *Nat Biotechnol* (2011) 29(10):886–93. doi: 10.1038/nbt.1991
6. Anchang B, Hart TDP, Bendall SC, Qiu P, Bjornson Z, Linderman M, et al. Visualization and Cellular Hierarchy Inference of Single-Cell Data Using SPADE. *Nat Protoc* (2016) 11(7):1264–79. doi: 10.1038/nprot.2016.066
7. Gautreau G, Pejoski D, Le Grand R, Cosma A, Beignon A-S, Tchitchek N. SPADEVizR: An R Package for Visualization, Analysis and Integration of SPADE Results. *Bioinf (Oxford England)* (2017) 33(5):779–81. doi: 10.1093/bioinformatics/btw708
8. Amir EAD, Davis KL, Tadmor MD, Simonds EF, Levine JH, Bendall SC, et al. ViSNE Enables Visualization of High Dimensional Single-Cell Data and Reveals Phenotypic Heterogeneity of Leukemia. *Nat Biotechnol* (2013) 31(6):545–52. doi: 10.1038/nbt.2594
9. Bruggner RV, Bodenmiller B, Dill DL, Tibshirani RJ, Nolan GP. Automated Identification of Stratifying Signatures in Cellular Subpopulations. *Proc Natl Acad Sci USA* (2014) 111(26):E2770-7. doi: 10.1073/pnas.1408792111
10. Polikowsky HG, Drake KA. Supervised Machine Learning With CITRUS for Single Cell Biomarker Discovery. *Methods Mol Biol (Clifton NJ)* (2019) 1989:309–32. doi: 10.1007/978-1-4939-9454-0_20

11. Levine JH, Simonds EF, Bendall SC, Davis KL, Amir EAD, Tadmor MD, et al. Data-Driven Phenotypic Dissection of AML Reveals Progenitor-Like Cells That Correlate With Prognosis. *Cell* (2015) 162(1):184–97. doi: 10.1016/j.cell.2015.05.047
12. Schulte-Schrepping J, Reusch N, Paclik D, Baßler K, Schlickeiser S, Zhang B, et al. Severe COVID-19 Is Marked by a Dysregulated Myeloid Cell Compartment. *Cell* (2020) 182(6):1419–40.e23. doi: 10.1016/j.cell.2020.08.001
13. Gate D, Saligrama N, Leventhal O, Yang AC, Unger MS, Middeldorp J, et al. Clonally Expanded CD8 T Cells Patrol the Cerebrospinal Fluid in Alzheimer's Disease. *Nature* (2020) 577(7790):399–404. doi: 10.1038/s41586-019-1895-7
14. Roy Chowdhury R, Vallania F, Yang Q, Lopez Angel CJ, Darboe F, Penn-Nicholson A, et al. A Multi-Cohort Study of the Immune Factors Associated With M. Tuberculosis Infection Outcomes. *Nature* (2018) 560(7720):644–8. doi: 10.1038/s41586-018-0439-x
15. Rao DA, Gurish MF, Marshall JL, Slowikowski K, Fonseka CY, Liu Y, et al. Pathologically Expanded Peripheral T Helper Cell Subset Drives B Cells in Rheumatoid Arthritis. *Nature* (2017) 542(7639):110–4. doi: 10.1038/nature20810
16. Pfister D, Núñez NG, Pinyol R, Govaere O, Pinter M, Szydlowska M, et al. NASH Limits Anti-Tumour Surveillance in Immunotherapy-Treated HCC. *Nature* (2021) 592(7854):450–56. doi: 10.1038/s41586-021-03362-0
17. Behbehani GK. Applications of Mass Cytometry in Clinical Medicine: The Promise and Perils of Clinical CyTOF. *Clinics Lab Med* (2017) 37:945–64. W.B. Saunders. doi: 10.1016/j.cll.2017.07.010
18. Han L, Qiu P, Zeng Z, Jorgensen JL, Mak DH, Burks JK, et al. Single-Cell Mass Cytometry Reveals Intracellular Survival/Proliferative Signaling in FLT3-ITD-Mutated AML Stem/Progenitor Cells. *Cytometry Part A* (2015) 87(4):346–56. doi: 10.1002/cyto.a.22628
19. Bailur JK, McCachren SS, Pendleton K, Vasquez JC, Lim HS, Duffy A, et al. Risk-Associated Alterations in Marrow T Cells in Pediatric Leukemia. *JCI Insight* (2020) 5(16):e140179. doi: 10.1172/jci.insight.140179
20. Behbehani GK, Finck R, Samusik N, Sridhar K, Fantl WJ, Greenberg PL, et al. Profiling Myelodysplastic Syndromes by Mass Cytometry Demonstrates Abnormal Progenitor Cell Phenotype and Differentiation. *Cytometry Part B - Clin Cytometry* (2020) 98(2):131–45. doi: 10.1002/cyto.b.21860
21. Van Leeuwen-Kerkhoff N, Westers TM, Poddighe PJ, Povoleri GAM, Timms JA, Kordasti S, et al. Reduced Frequencies and Functional Impairment of Dendritic Cell Subsets and non-Classical Monocytes in Myelodysplastic Syndromes. *Haematologica* (2021). doi: 10.3324/haematol.2020.268136
22. Yang ZZ, Kim HJ, Villasboas JC, Price-Troska T, Jalali S, Wu H, et al. Mass Cytometry Analysis Reveals That Specific Intratumoral CD4 + T Cell Subsets Correlate With Patient Survival in Follicular Lymphoma. *Cell Rep* (2019) 26(8):2178–93.e3. doi: 10.1016/j.celrep.2019.01.085
23. Wogsland CE, Greenplate AR, Kolstad A, Myklebust JH, Irish JM, Huse K. Mass Cytometry of Follicular Lymphoma Tumors Reveals Intrinsic Heterogeneity in Proteins Including HLA-DR and a Deficit in Nonmalignant Plasmablast and Germinal Center B-Cell Populations. *Cytometry Part B - Clin Cytometry* (2017) 92(1):79–87. doi: 10.1002/cyto.b.21498
24. Roussel M, Lhomme F, Roe CE, Bartkowiak T, Gravelle P, Laurent C, et al. Mass Cytometry Defines Distinct Immune Profile in Germinal Center B-Cell Lymphomas. *Cancer Immunol Immunother* (2020) 69(3):407–20. doi: 10.1007/s00262-019-02464-z
25. Behbehani GK, Samusik N, Bjornson ZB, Fantl WJ, Medeiros BC, Nolan GP. Mass Cytometric Functional Profiling of Acute Myeloid Leukemia Defines Cell-Cycle and Immunophenotypic Properties That Correlate With Known Responses to Therapy. *Cancer Discov* (2015) 5(9):988–1003. doi: 10.1158/2159-8290.CD-15-0298
26. Chretien AS, Fauriat C, Orlanducci F, Galseran C, Rey J, Borg GB, et al. Natural Killer Defective Maturation is Associated With Adverse Clinical Outcome in Patients With Acute Myeloid Leukemia. *Front Immunol* (2017) 8(MAY). doi: 10.3389/fimmu.2017.00573
27. Good Z, Sarno J, Jager A, Samusik N, Aghaeepour N, Simonds EF, et al. Single-Cell Developmental Classification of B Cell Precursor Acute Lymphoblastic Leukemia at Diagnosis Reveals Predictors of Relapse. *Nat Med* (2018) 24(4):474–83. doi: 10.1038/nm.4505
28. Edwards DK, Watanabe-Smith K, Rofelty A, Damnernsawad A, Laderas T, Lamble A, et al. CSF1R Inhibitors Exhibit Antitumor Activity in Acute Myeloid Leukemia by Blocking Paracrine Signals From Support Cells. *Blood* (2019) 133(6):588–99. doi: 10.1182/blood-2018-03-838946
29. van Leeuwen-Kerkhoff N, Westers TM, Poddighe PJ, de Gruijl TD, Kordasti S, van de Loosdrecht AA. Thrombomodulin-Expressing Monocytes are Associated With Low-Risk Features in Myelodysplastic Syndromes and Dampen Excessive Immune Activation. *Haematologica* (2020) 105(4):961–70. doi: 10.3324/haematol.2019.219303
30. Gullaksen SE, Skavland J, Gavasso S, Tosevski V, Warzocha K, Dumrese C, et al. Single Cell Immune Profiling by Mass Cytometry of Newly Diagnosed Chronic Phase Chronic Myeloid Leukemia Treated With Nilotinib. *Haematologica* (2017) 102(8):1361–7. doi: 10.3324/haematol.2017.167080
31. Yang Z-Z, Kim HJ, Wu H, Jalali S, Tang X, Krull JE, et al. TIGIT Expression Is Associated With T-Cell Suppression and Exhaustion and Predicts Clinical Outcome and Anti–PD-1 Response in Follicular Lymphoma. *Clin Cancer Res* (2020) 26(19):5217–31. doi: 10.1158/1078-0432.CCR-20-0558
32. Saenz DT, Fiskus W, Qian Y, Manshouri T, Rajapakshe K, Raina K, et al. Novel BET Protein Proteolysis-Targeting Chimera Exerts Superior Lethal Activity Than Bromodomain Inhibitor (BETi) Against Post-Myeloproliferative Neoplasm Secondary (s) AML Cells. *Leukemia* (2017) 31(9):1951–61. doi: 10.1038/leu.2016.393
33. Zeng Z, Konopleva M, Andreeff M. Single-Cell Mass Cytometry of Acute Myeloid Leukemia and Leukemia Stem/Progenitor Cells. In: *Methods in Molecular Biology*. Humana Press Inc (2017). p. 75–86.
34. Han L, Zhang Q, Dail M, Shi C, Cavazos A, Ruvolo VR, et al. Concomitant Targeting of BCL2 With Venetoclax and MAPK Signaling With Cobimetinib in Acute Myeloid Leukemia Models. *Haematologica* (2020) 105(3):697–707. doi: 10.3324/haematol.2018.205534
35. Borthakur G, Zeng Z, Cortes JE, Chen HC, Huang X, Konopleva M, et al. Phase 1 Study of Combinatorial Sorafenib, G-CSF, and Plerixafor Treatment in Relapsed/Refractory, FLT3-ITD-Mutated Acute Myelogenous Leukemia Patients. *Am J Hematol* (2020) 95(11):1296–303. doi: 10.1002/ajh.25943
36. Stone RM, Mandrekar SJ, Sanford BL, Laumann K, Geyer S, Bloomfield CD, et al. Midostaurin Plus Chemotherapy for Acute Myeloid Leukemia With a FLT3 Mutation. *New Engl J Med* (2017) 377(5):454–64. doi: 10.1056/NEJMoa1614359
37. Deng M, Zha J, Jiang Z, Jia X, Shi Y, Li P, et al. Apatinib Exhibits Anti-Leukemia Activity in Preclinical Models of Acute Lymphoblastic Leukemia. *J Trans Med* (2018) 16(1):47. doi: 10.1186/s12967-018-1421-y
38. Bandyopadhyay S, Li J, Traer E, Tyner JW, Zhou A, Oh ST, et al. Cholesterol Esterification Inhibition and Imatinib Treatment Synergistically Inhibit Growth of BCR-ABL Mutation-Independent Resistant Chronic Myelogenous Leukemia. *PloS One* (2017) 12(7):e0179558. doi: 10.1371/journal.pone.0179558
39. Baughn LB, Sachs Z, Noble-Orcutt KE, Mitra A, Van Ness BG, Linden MA. Phenotypic and Functional Characterization of a Bortezomib-Resistant Multiple Myeloma Cell Line by Flow and Mass Cytometry. *Leuk Lymphoma* (2017) 58(8):1931–40. doi: 10.1080/10428194.2016.1266621
40. Adams HC, Stevenaert F, Krejcik J, van der Borght K, Smets T, Bald J, et al. High-Parameter Mass Cytometry Evaluation of Relapsed/Refractory Multiple Myeloma Patients Treated With Daratumumab Demonstrates Immune Modulation as a Novel Mechanism of Action. *Cytometry Part A* (2019) 95(3):279–89. doi: 10.1002/cyto.a.23693
41. Teh CE, Gong JN, Segal D, Tan T, Vandenberg CJ, Fedele PL, et al. Deep Profiling of Apoptotic Pathways With Mass Cytometry Identifies a Synergistic Drug Combination for Killing Myeloma Cells. *Cell Death Differ* (2020) 27(7):2217–33. doi: 10.1038/s41418-020-0498-z
42. Visram A, Dasari S, Anderson E, Kumar S, Kourelis TV. Relapsed Multiple Myeloma Demonstrates Distinct Patterns of Immune Microenvironment and Malignant Cell-Mediated Immunosuppression. *Blood Cancer J* (2021) 11(3):45. doi: 10.1038/s41408-021-00440-4
43. Alimam S, Ann Timms J, Harrison CN, Dillon R, Mare T, DeLavallade H, et al. Altered Immune Response to the Annual Influenza A Vaccine in Patients With Myeloproliferative Neoplasms. *Br J Haematol* (2021) 193(1):150–4. doi: 10.1111/bjh.17096
44. Ferrell PB, Diggins KE, Polikowsky HG, Mohan SR, Seegmiller AC, Irish JM. High-Dimensional Analysis of Acute Myeloid Leukemia Reveals Phenotypic Changes in Persistent Cells During Induction Therapy. *PloS One* (2016) 11(4):e0153207. doi: 10.1371/journal.pone.0153207

45. Bandyopadhyay S, Fowles JS, Yu L, Fisher DAC, Oh ST. Identification of Functionally Primitive and Immunophenotypically Distinct Subpopulations in Secondary Acute Myeloid Leukemia by Mass Cytometry. *Cytometry Part B - Clin Cytometry* (2019) 96(1):46–56. doi: 10.1002/cyto.b.21743
46. Sarno J, Savino AM, Buracchi C, Palmi C, Pinto S, Bugarin C, et al. SRC/ABL Inhibition Disrupts CRLF2-Driven Signaling to Induce Cell Death in B-Cell Acute Lymphoblastic Leukemia. *Oncotarget* (2018) 9(33):22872–85. doi: 10.18632/oncotarget.25089
47. Fisher DAC, Malkova O, Engle EK, Miner CA, Fulbright MC, Behbehani GK, et al. Mass Cytometry Analysis Reveals Hyperactive NF Kappa B Signaling in Myelofibrosis and Secondary Acute Myeloid Leukemia. *Leukemia* (2017) 31 (9):1962–74. doi: 10.1038/leu.2016.377
48. Fisher DAC, Miner CA, Engle EK, Hu H, Collins TB, Zhou A, et al. Cytokine Production in Myelofibrosis Exhibits Differential Responsiveness to JAK-STAT, MAP Kinase, and Nfκb Signaling. *Leukemia* (2019) 33(8):1978–95. doi: 10.1038/s41375-019-0379-y

Conflict of Interest: The authors declare that the research was conducted in the absence of any commercial or financial relationships that could be construed as a potential conflict of interest.

frontiers in Oncology

ORIGINAL RESEARCH
published: 05 November 2021
doi: 10.3389/fonc.2021.746951

Database-Guided Analysis for Immunophenotypic Diagnosis and Follow-Up of Acute Myeloid Leukemia With Recurrent Genetic Abnormalities

Carmen-Mariana Aanei[1], Richard Veyrat-Masson[2], Cristina Selicean[3,4], Mirela Marian[4], Lauren Rigollet[1], Adrian Pavel Trifa[5,6], Ciprian Tomuleasa[3,7], Adrian Serban[1], Mohamad Cherry[1], Pascale Flandrin-Gresta[1], Emmanuelle Tavernier Tardy[8], Denis Guyotat[8] and Lydia Campos Catafal[1]*

[1] Laboratoire d'Hématologie, Centre Hospitalier Universitaire de Saint-Etienne, Saint-Etienne, France, [2] Laboratoire d'Hématologie, Centre Hospitalier Universitaire de Clermont-Ferrand, Clermont-Ferrand, France, [3] Department of Hematology, "Iuliu Haţieganu" University of Medicine and Pharmacy, Cluj-Napoca, Romania, [4] Laboratory of Hematology, Oncological Institute "Prof. Dr. Ion Chiricuţă", Cluj-Napoca, Romania, [5] Department of Medical Genetics, "Iuliu Haţieganu" University of Medicine and Pharmacy, Cluj-Napoca, Romania, [6] Department of Genetics, Oncological Institute "Prof. Dr. Ion Chiricuţă", Cluj-Napoca, Romania, [7] Department of Clinical Hematology, Oncological Institute "Prof. Dr. Ion Chiricuţă", Cluj-Napoca, Romania, [8] Département d'Hématologie Clinique, Institut de Cancérologie Lucien Neuwirth, Saint-Priest-en-Jarez, France

OPEN ACCESS

Edited by:
Andrew G. Evans, University of Rochester, United States

Reviewed by:
Cirino Botta, University of Palermo, Italy
Ritu Gupta, All India Institute of Medical Sciences, India

***Correspondence:**
Carmen-Mariana Aanei
cmaanei@gmail.com
orcid.org/0000-0003-1001-7597

Specialty section:
This article was submitted to Hematologic Malignancies, a section of the journal Frontiers in Oncology

Received: *25 July 2021*
Accepted: *13 October 2021*
Published: *05 November 2021*

Citation:
Aanei C-M, Veyrat-Masson R, Selicean C, Marian M, Rigollet L, Trifa AP, Tomuleasa C, Serban A, Cherry M, Flandrin-Gresta P, Tardy ET, Guyotat D and Campos Catafal L (2021) Database-Guided Analysis for Immunophenotypic Diagnosis and Follow-Up of Acute Myeloid Leukemia With Recurrent Genetic Abnormalities. Front. Oncol. 11:746951. doi: 10.3389/fonc.2021.746951

Acute myeloid leukemias (AMLs) are hematologic malignancies with varied molecular and immunophenotypic profiles, making them difficult to diagnose and classify. High-dimensional analysis algorithms might increase the utility of multicolor flow cytometry for AML diagnosis and follow-up. The objective of the present study was to assess whether a Compass database-guided analysis can be used to achieve rapid and accurate diagnoses. We conducted this study to determine whether this method could be employed to pilote the genetic and molecular tests and to objectively identify different-from-normal (DfN) patterns to improve measurable residual disease follow-up in AML. Three Compass databases were built using Infinicyt 2.0 software, including normal myeloid-committed hematopoietic precursors (n = 20) and AML blasts harboring the most frequent recurrent genetic abnormalities (n = 50). The diagnostic accuracy of the Compass database-guided analysis was evaluated in a prospective validation study (125 suspected AML patients). This method excluded AML associated with the following genetic abnormalities: t(8;21), t(15;17), inv(16), and *KMT2A* translocation, with 92% sensitivity [95% confidence interval (CI): 78.6%–98.3%] and a 98.5% negative predictive value (95% CI: 90.6%–99.8%). Our data showed that the Compass database-guided analysis could identify phenotypic differences between AML groups, representing a useful tool for the identification of DfN patterns.

Keywords: acute myeloid leukemia with recurrent genetic abnormalities, multicolor flow cytometry, Compass database-guided analysis, different-from-normal (DfN) approach, measurable (minimal) residual disease

1 INTRODUCTION

Acute myeloid leukemia (AML) refers to a heterogeneous group of malignant diseases characterized by the accumulation of aberrant hematopoietic progenitor cells, known as AML blasts, that cannot progress beyond various stages of maturation and are unable to develop into mature blood cells.

According to the current World Health Organization (WHO) criteria (1), an AML diagnosis depends on a combination of clinical findings, morphological evaluations of peripheral blood (PB) and bone marrow (BM) specimens, and cytogenetic (karyotype and fluorescent *in situ* hybridization (FISH)) and molecular analyses [polymerase chain reaction (PCR) and next-generation sequencing (NGS)].

At present, multicolor flow cytometry (MFC) is viewed as a complementary tool that can assist with the AML diagnostic process. MFC is typically used to define the blast cell lineage and can be used to identify phenotypic aberrations, known as leukemia-associated immunophenotypes (LAIPs), such as the presence of aberrant lymphoid markers, maturation asynchrony, or the absence of myeloid markers, which might be useful for assessing measurable residual disease (MRD) during AML treatment follow-up.

The evaluation of cytogenetics and mutational profiles represent reference methods for monitoring MRD in AML, allowing for the assessment of clonal evolution and the stratification of AML into prognostic subgroups to guide treatment approaches (2). Despite the high specificity and sensitivity of PCR-based methods for leukemic cells, their applicability is limited to the approximately 40% of AML patients that harbor one or more traceable molecular abnormalities, according to the European LeukaemiaNet (ELN) MRD Working Party (3). In addition, although complete remission rates have improved in recent years (approaching 80%) due to the application of therapeutic algorithms guided by molecular technologies, greater than 50% of adult patients with AML will undergo disease relapse after initial treatment (2). Therefore, interest exists in the development of MFC applications for disease monitoring in AML, with the potential to perform precise residual disease estimations below the current morphological assessment thresholds for determining complete remission. This method could refine prognostic assessments and direct postremission decision-making processes in AML (2).

However, despite the high applicability of MFC for MRD assessments in AML patients (>90% of all AML cases) compared with molecular MRD assessments (2), multicenter studies have shown a relatively high number of false-positive cases following MFC assessment, resulting in a low specificity of 71%, even when using standardized protocols, which is most likely due to differences in the subjective interpretation of MFC data (4).

To improve AML MRD detection by MFC, the ELN MRD Working Party has recommended combining the different-from-normal (DfN) approach with the LAIP assessment method (3). The major advantage of the DfN approach is that it can be applied even in cases with unknown blast phenotypes at diagnosis and can identify other abnormal immunophenotypic cells, in addition to residual blasts, which is not possible using the LAIP method, which focuses only on the detection of residual blasts carrying the immunophenotypic anomaly identified at diagnosis. Therefore, high-dimensional analysis algorithms may be useful for optimizing the MFC-MRD performance in AML (3).

New tools for MFC data analysis have recently been developed to objectively visualize immunophenotypic differences between abnormal cells from different pathologies. One such tool is Infinicyt Compass, which was developed by the EuroFlow™ (EF) Consortium, and allows for the recognition of complex immunophenotypic patterns through multivariate analyses of flow cytometric data.

The present study aimed to assess whether the Compass database analysis could be used to guide the genetic and molecular testing of AML to achieve a rapid and accurate diagnosis and to perform DfN analyses.

The results of this study showed that the comparison of new cases against reference databases composed of well-classified AML cases represents a user-friendly method that can facilitate the orientation of genetic and molecular biology testing to achieve a rapid, accurate diagnosis. In addition, the Compass database-guided analysis of MFC data can be used as a nonsubjective method for DfN evaluation.

2 MATERIALS AND METHODS

2.1 Study Design

The present study was conducted in three phases: construction of Compass databases; databases-guided analysis of new AML cases at initial diagnosis; and evaluation of database-guided DfN analysis (**Figure 1**).

2.2 Construction of the Databases

The Compass databases are composed of fcs-exported data files featuring characteristics of leukemic blasts from well-classified AML cases, according to WHO recommendations (1), including *t*(8;21) AML ($n = 8$), *t*(15;17) AML ($n = 19$), inv(16)/*t*(16;16) AML ($n = 12$), and AML with *MLL* gene translocations (*MLL*-r AML, $n = 11$); all samples were diagnosed by the Hematology Laboratory from the University Hospital of Saint-Etienne between 2013 and 2019. Normal myeloid hematopoietic precursor cells (my-HPCs) committed toward a neutrophil lineage ($CD45^{+low/int}$ $CD117^{+}$ $CD34^{+/-}$ $HLA\text{-}DR^{+int}$ $CD13^{+}$ $CD14^{-}$ $IREM2^{-}$ $CD33^{+}$ $CD36^{-}$), a monocyte lineage ($CD45^{+low/int}$ $CD117^{+}$ $CD34^{+/-}$ $HLA\text{-}DR^{+hi}$ $CD64^{+}$ $CD14^{-}$ $CD300e[IREM\text{-}2]^{-}$ $CD13^{+}$ $CD33^{+}$), and an erythroid lineage ($CD45^{-/+low}$ $CD117^{+}$ $CD34^{+/-}$ $HLA\text{-}DR^{+low/int}$ $CD36^{+}$ $CD105^{+}$ $CD33^{-}$ $CD35^{+low}$) were also included (**Figure 2**). The immunophenotypic characterization of my-HPCs using the EF AML/MDS panel was performed in the present study using normal BM samples obtained from healthy individuals with normal blood counts (eleven healthy BM donors (HDs) and nine patients undergoing sternotomy for cardiac surgery (CS)) from the University Hospitals of Saint-Etienne and Clermont-Ferrand, France. The strategy used for the selection of normal my-HPCs was based on recently published data (5, 6). Pregating for intact singlets, followed by the discrimination of normal my-HPCs, was

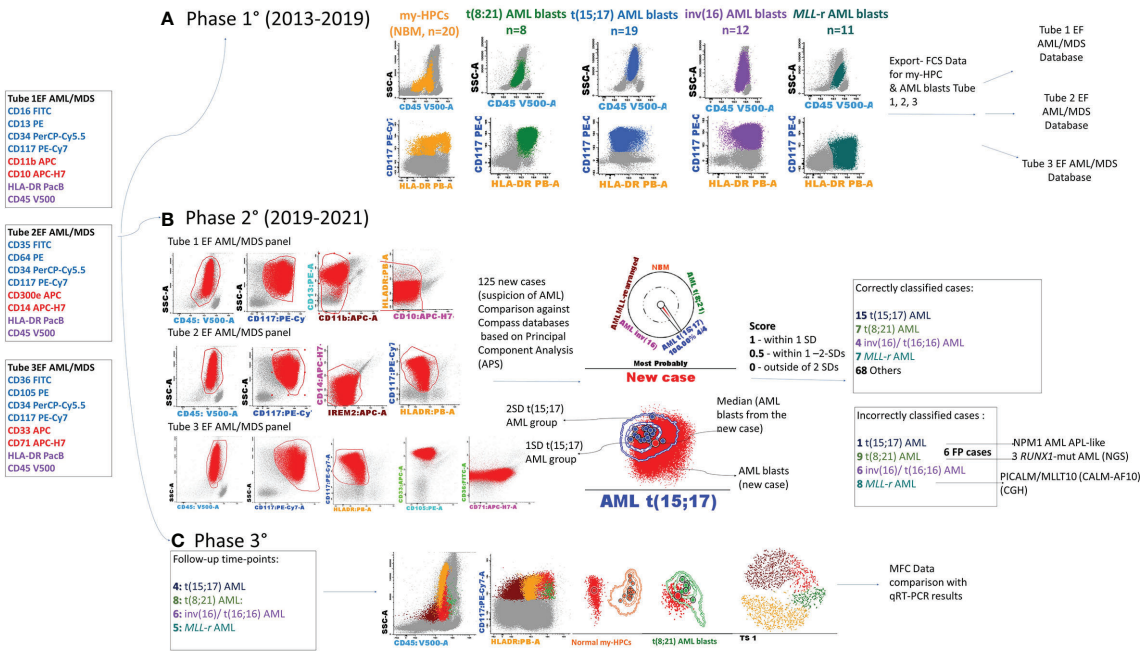

FIGURE 1 | Schematic overview of the study. The first three tubes of the EuroFlow (EF) AML/MDS antibody panel were used for the discrimination of acute myeloid leukemia (AML) blasts and normal myeloid-committed hematopoietic precursors (my-HPCs) in bone marrow aspirates obtained from patients with AML and healthy individuals. **(A)** Phase 1: Construction of the databases. The Compass databases were composed of fcs-exported files corresponding to leukemic blasts from well-classified AML cases, according to the WHO diagnostic recommendations, including *t*(8;21) AML (*n* = 8), *t*(15;17) AML (*n* = 19), inv(16)/*t*(16;16) AML (*n* = 12), AML with *MLL* gene translocations (*MLL*-r AML, *n* = 11), and normal my-HPCs (*n* = 20). **(B)** Phase 2: Samples from 125 patients with suspected AML were compared against the Compass databases based on APS plots. The blast events from each individual AML case were compared against each well-classified AML group and with the normal my-HPC populations using balanced APS plots. The similarity between blast events from the new case and any defined populations was scored based on the position of the median from the new case relative to the 1 and 2 standard deviation (SD) curves for the defined AML groups or normal my-HPC groups included in the database. A total of 101 cases were correctly classified, whereas 24 cases were incorrectly assigned to the wrong AML group or to the other group. The incorrectly assigned *t*(15;17) AML case was an *NPM1*$^{+}$ AML with an acute promyelocytic leukemia (APL)-like phenotype; the three false-positive *t*(8;21) AML cases were *RUNX1*-mutant AML cases, and for the false-positive *MLL*-r AML case, the array-comparative genomic hybridization (CGH) analysis identified a *PICALM/MLLT10* (*CALM-AF10*) fusion gene. **(C)** Phase 3: Evaluation of the Compass database-guided DfN analysis. Immunophenotypic data acquired at different MRD follow-up time points from four AML patients with different genetic abnormalities who were in cytological remission were used, including one *MLL*-r AML case, one *t*(8;21) AML case, one *t*(15;17) AML case, and one inv(16) AML case. Compass database-guided analysis was compared against quantitative reverse transcription–polymerase chain reaction (qRT-PCR).

performed using the Infinicyt 2.0 software based primarily on the backbone markers CD117, HLA-DR, and CD45, in addition to several lineage-specific markers, such as CD13 for neutrophil-committed HPCs; CD64 and CD33 for monocyte-committed HPCs; and CD105 and CD36 for erythroid-committed HPCs (**Figure 2**). Several exclusion gates were used to avoid the inclusion of undesirable events that may fall into the CD45^{+low} CD117^{+} HLA-DR^{+} blast gate, such as CD11b^{+} hypogranular neutrophils and basophils (tube 1), CD14^{+low} granulocytes and CD14^{+} IREM-2^{+} monocytes (tube 2), and CD10^{+} hematogones (tube 1) (**Figure 2**). Three databases corresponding to the first three tubes of the EF AML/MDS panel which are dedicated to the immunophenotypic analysis of the principals myeloid lineages were built from merged fcs files containing AML blasts from the four AML groups and the normal my-HPCs: tube 1 of the EF AML/MDS panel (neutrophil lineage), tube 2 of the EF AML/MDS panel (monocytic lineage), and tube 3 of the EF AML/MDS panel (erythroid cell lineage). The fcs files used to build the databases are available at FlowRepository (ID: FR-FCM-Z3JL).

Each group of cases was subsequently plotted in a balanced automatic population separator (APS), a principal component analysis (PCA) plot for comparisons with other groups included in the databases.

2.3 Database-Guided Analysis of New AML Cases at Initial Diagnosis

The BM samples used in this prospective study were obtained between January 2019 and June 2021 from 125 consecutive patients who were hospitalized with suspected AML at the Institut de Cancérologie Lucien Neuwirth, Saint-Priest-en-Jarez, the Estaing University Hospital of Clermont-Ferrand, France, and the Oncological Institute Prof. Dr. Ion Chiricuță, Cluj-Napoca, Romania.

Written informed consent was obtained from each patient and healthy donor (HD), as approved by the institutional procedures of the independent ethics committee and the Comité de Protection des Personnes - Ile de France (NCT03233074/17.07.2017).

All participants' characteristics are summarized in **Table 1** and detailed in **Table S1**.

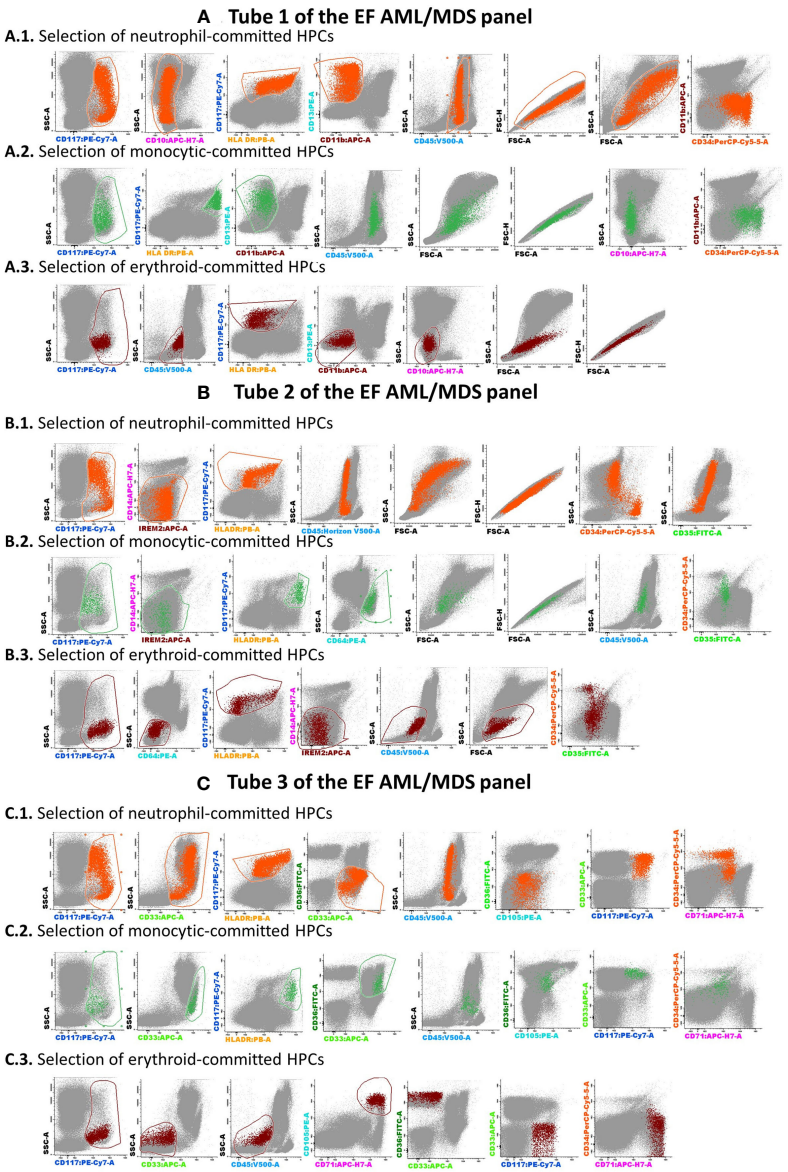

FIGURE 2 | The analysis strategy for the identification of normal myeloid-committed HPCs using Tubes 1–3 of the EF AML/MDS panel. The discrimination of normal my-HPCs was performed by Infinicyt 2.0 software, based primarily on the backbone markers CD117, human leukocyte antigen-DR (HLA-DR), and CD45. Several exclusion gates were used to avoid the inclusion of undesirable events that may fall into the blast gate, such as $CD11b^+$ hypogranular neutrophils and basophils (Tube 1), $CD14^{+low}$ granulocytes and $CD14^+$ CD300e (IREM-2)$^+$ monocytes (Tube 2), and $CD10^+$ hematogones (Tube 1). Bivariate dot plot histograms illustrating the HPCs committed toward a neutrophil lineage ($CD45^{+low/int}CD117^+CD34^{+/-}$HLA-$DR^{+int}CD13^+CD14^-$ IREM2$^-CD33^+CD36^-$; orange dots), a monocyte lineage ($CD45^{+low/int}CD117^+CD34^{+/-}$HLA-$DR^{+high}CD64^+CD14^-$CD300e/IREM-2$^-CD13^+CD33^+$; green dots), or an erythroid lineage ($CD45^{+low/-}CD117^+CD34^{+/-}$HLA-$DR^{+low/int}CD36^+CD105^+CD33^-CD35^{+low}$; dark-red dots). The other bone marrow cells are displayed in gray. **(A)** tube 1 EF AML/MDS panel; **(B)** tube 2 EF AML/MDS panel, **(C)** tube 3 EF AML/MDS panel.

The phenotypes of leukemic blasts obtained from new patients were compared against the phenotypes of AML blasts from four different cytogenetic groups and the most similar my-HPCs using the three databases.

AML blasts were selected according to $CD45^{+low}$ expression, CD117, HLA-DR positivity, and side scatter (SSC) characteristics, as previously described (7). Several exclusion gates were applied to avoid the inclusion of undesirable events, such as CD11b+ hypogranular neutrophils and basophils (tube 1), $CD14^{+low}$ granulocytes and $CD14^+$ IREM-2$^+$ monocytes (tube 2), and $CD10^+$ hematogones (tube 1) (**Figure 3**).

The AML blast events identified in each individual AML case were compared with each well-classified AML group and normal my-HPC populations using balanced APS plots.

The similarity between any two populations was scored based on the position of the median for the new AML blast events from

TABLE 1 | Characteristics of patients used for evaluation of the database-guided analysis.

	Parameter	Validation cohort	Database[a]
WHO diagnosis (*n*)	APL with PML-RARA	15	19
	AML with *t*(8;21)(q22;q22.1);RUNX1-RUNX1T1	7	8
	AML with inv(16)(p13.1q22) or *t*(16;16)(p13.1;q22);CBFB-MYH11	6	12
	KMT2A(MLL)-rearranged AML	7	11
	AML with mutated NPM1	16	
	Provisional entity: AML with mutated RUNX1	6	
	AML with biallelic mutations of CEBPA	1	
	AML-MRC	41	
	AML NOS	24	
	Blastic plasmacytoid dendritic cell neoplasm	1	
	Aggressive NK leukemia/lymphoma	1	
Gender	F	58	23
	M	67	27
Age (years)	Median	66	51
	Range	13—94	1–83
WBC (10^9/L)	Median	33.5	37.6
	Range	0.6–537.8	0.8–308.7

AML, acute myeloid leukemia; AML-MRC, AML with myelodysplasia-related changes; APL, acute promyelocytic leukemia; AML NOS, AML, not otherwise specified. [a]*Additional details can be found in* ***Table S1***.

each case relative to the 1 and 2 standard deviation (SD) curves for the AML groups and normal my-HPCs included in the database: falling within 1 SD was scored as 1 point (**Figure 4A**); falling within 1–2 SDs was scored as 0.5 point (**Figure 4B**); and falling outside of 2 SDs was scored as 0 points (**Figures 4C, D**).

After comparison with the AML phenotypes in the databases, the new AML cases were classified as follows:

Typical, clearly belonging to an AML group was used to described AML blast events that fell within 1 or within 1–2-SDs of a single AML group and outside of 2 SDs for all other groups based on the results of at least two of the three tubes from the EF AML/MDS panel (**Figure S1A**).

Atypical, oriented toward an AML group was used to describe AML blast events that fell within 1 SD or within 1–2 SDs for two or more AML groups; the case was assigned to the group with the

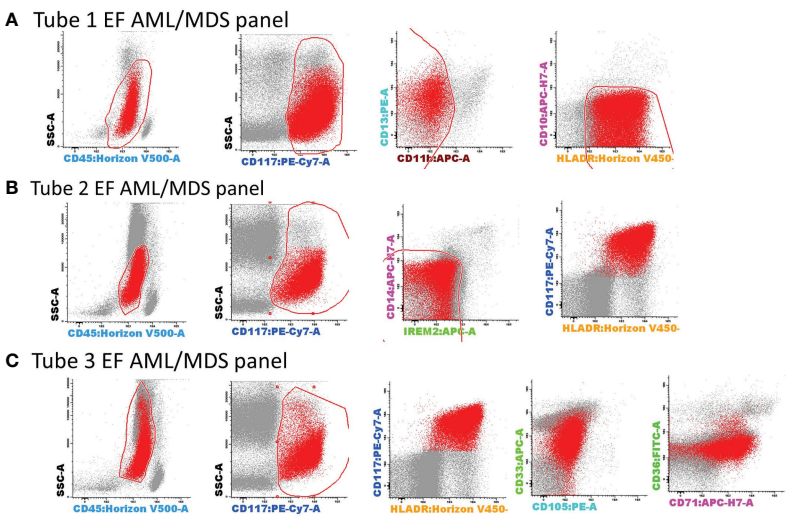

FIGURE 3 | Gating strategy for the selection of AML blasts using tubes 1–3 of the EF AML/MDS panel. AML blasts were selected based on the expression of backbone markers, CD117, human leukocyte antigen-DR (HLA-DR), and CD45^{+low}. Several exclusion gates were used to avoid the inclusion of undesirable events that may fall into the blast gate, such as CD11b$^+$ hypogranular neutrophils and basophils (tube 1), CD14^{+low} granulocytes and CD14$^+$CD300e (IREM-2)$^+$ monocytes (tube 2), and CD10$^+$ hematogones (tube 1). Bivariate dot plots illustrating a representative example of AML blast identification using the antibody combinations from tubes 1–3 of the EF AML/MDS panel. AML blasts (red dots), other singlet events (gray dots). **(A)** tube 1 EF AML/MDS panel; **(B)** tube 2 EF AML/MDS panel, **(C)** tube 3 EF AML/MDS panel.

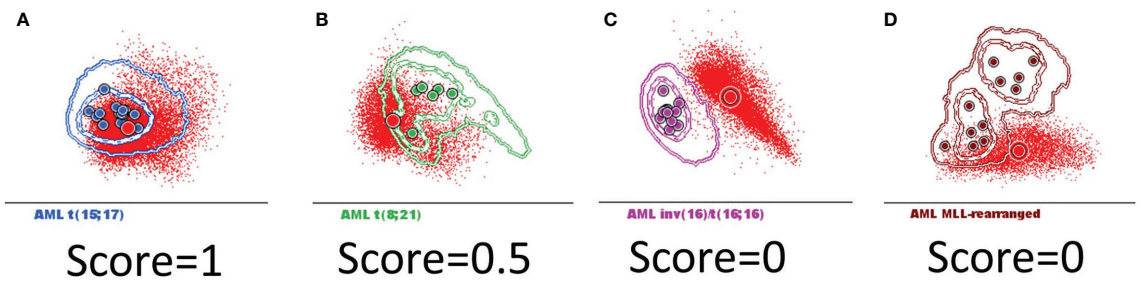

FIGURE 4 | The scoring system used to determine whether AML blasts from a new case can be classified in the defined AML groups harboring recurrent genetic abnormalities that were included in the Compass databases. Acute myeloid leukemia (AML) blasts from a new case (red dots and circles) were compared with the AML groups included in the databases: *t*(15;17) AML (blue), *t*(8;21) AML (green), inv(16)/*t*(16;16) AML (violet), and *MLL*-r AML (dark red). The circles represent the median values of individual cases. The dotted line represents the 1 standard deviation (SD) curve, and the solid line represents the 2 SD curve for the AML group. The similarity between the two populations was scored based on the position of the median for the new case blast events relative to the 1 and 2 SD curves for the AML groups that were included in the database: **(A)** falling within 1 SD was scored as 1 point; **(B)** falling within 1–2 SDs was scored as 0.5 points; and **(C, D)** falling outside of 2 SDs was scored as 0 points.

highest score obtained after combining the scores obtained for each of the three tubes of the EF AML/MDS panel (**Figure S1B**).

Other was used to describe AML blast events that fell outside of 2 SDs for all AML groups or within 1–2 SDs of any AML group based on the results of only one of the three tubes from the EF AML/MDS panel (**Figure S1C**).

The Compass database-guided results were compared with the final diagnoses for all suspected AML cases, which were established using a combination of morphological aspects, karyotypes, FISH analysis, and molecular biology data, according to WHO recommendations (1).

The results of comparisons between database-guided classifications and the final clinical diagnoses were classified as follows: *true positives*, when the AML group indicated by the Compass database-guided approach coincided with the final diagnosis; *false positives*, when the AML group indicated by the Compass database-guided approach was not confirmed by other diagnostic tests; *false negative*, when a final diagnosis was made in favor of an AML group featuring a genetic abnormality that was not identified by the Compass database-guided approach; and **true negative**, when the Compass database-guided approach did not identify an immunophenotype corresponding to any AML groups with recurrent genetic abnormalities, and no FISH or PCR tests detected any of the genetic abnormalities assessed in the study.

The false-positive and false-negative AML cases were thereafter re-evaluated using a neighborhood automatic population separator (NAPS) PCA-based plot.

2.4 Database-Guided DfN

We sought to evaluate whether the database-guided analysis could be used to identify DfN immunophenotypes during AML follow-up. We evaluated immunophenotypic data acquired at different MRD follow-up moments from four AML patients with different genetic abnormalities, including five time points for one with *MLL*-r AML, eight time points for one with *t*(8;21) AML, four time points for one with *t*(15;17) AML, and six time points for one with inv(16) AML. Nondebris, singlet, $CD117^+$ $HLA\text{-}DR^+$ my-HPCs were selected from each of the fcs files analysed for each patient, as described above (**Figure 2**). Events were evaluated for inclusion into one of the following groups, based on comparison with the developed Compass databases: normal my-HPCs, AML *t*(8;21), AML inv(16), AML *t*(15;17), and *MLL*-r AML (**Figures S2**–**S5**).

Events that fell outside of 2 SDs for normal my-HPCs but within 2 SDs of corresponding AML group were considerate DfN and classified into the AML blast group.

MFC data were compared with the results of quantitative reverse transcription-PCR (qRT-PCR).

2.5 Immunophenotyping

All samples were stained using the first three tubes of the EF AML/MDS antibody panel (7). Sample preparation and acquisition were performed according to the EF standard operating procedure and using the recommended EF instrument settings (8).

Appropriate instrument performance was confirmed by performing FranceFlow and EuroFlow quality assessments (9, 10).

At least 100,000 BM cells/tube were acquired using a three-laser, eight-color BD FACSCanto-II™ flow cytometer (BD Bioscience, San José, CA, USA) at each study site. Acquired cells were then analyzed using Infinicyt V2.0 (Cytognos, Salamanca, Spain).

2.6 Morphologic Examination

May-Grünwald-Giemsa-stained BM aspirate smears from each AML patient were examined under a light microscope by experienced pathologists and the diagnosis was established conforming WHO 2016 guidelines (1).

2.7 Cytogenetics Analysis

BM samples were obtained from all AML patients for cytogenetic (CG) analysis at the time of diagnosis. Karyotypes were analyzed

after 24 h of unstimulated culture using standard procedures. The chromosomes were stained by R- and G-banding. At least 20 metaphase events were analyzed. The results were interpreted and reported according to the International System for Human Cytogenetic Nomenclature (ISCN, 2013 and 2016) (11).

FISH was performed for promyelocytic leukemia/retinoic acid receptor α (*PML-RARA*; dual-color, dual-fusion probe, Abbott, Des Plaines, IL, USA), Runt-related transcription factor/RUNX1 partner transcriptional corepressor 1 (*RUNX1/RUNX1T1*; dual-color, dual-fusion probe, Metasystems Probes, Altlussheim, Germany), core-binding factor subunit beta (*CBFB*; dual-color, break-apart probe, Metasystems Probes, Altlussheim, Germany), and lysine methyltransferase 2A (*KMT2A*; dual-color, break-apart probe, Metasystems Probes, Altlussheim, Germany). Detection was performed on freshly harvested BM cells (metaphase and interphase). Twenty metaphase events and 200 nuclei were observed for each case.

2.8 Quantitative Reverse Transcription-Polymerase Chain Reaction

Multiparametric RT-PCR was performed to detect recurrent fusion transcripts in all newly diagnosed AMLs. In cases positive for any fusion products, qRT-PCR was performed to monitor treatment response. The panel tests included *PML/RARA*, *RUNX1-RUNX1T1 (AML1-ETO)*, *CBFB-MYH11* variant A, and *CBFB-MYH11* variant D. In brief, extracted RNA was analyzed by RT-PCR for the *PML/RARA*, *RUNX1-RUNX1T1 (AML1-ETO)*, and *CBFB-MYH11* fusion transcripts on an ABI HT platform (Applied Biosystems, Villebon Sur Yvette, France) and on an ABI 3500 DNA analyzer (Applied Biosystems, Thermo Fisher, Waltham, MA, USA). Quantitative values are expressed as a ratio of the fusion transcript level to the *ABL1* transcript level (%), and the sensitivity was determined to be 0.001%.

Wilms' tumor gene (*WT1*) expression levels were quantified in PB samples using qRT-PCR and normalized against total *ABL1* gene expression levels to monitor MRD for *KMT2A* (*MLL*)-rearranged AML cases.

2.9 Next-Generation Sequencing

Genomic DNA was tested for most AML cases at diagnosis by NGS using a custom-designed myeloid panel. The panel assessed 51 commonly mutated genes associated with myeloid malignancies: *ATM*, *ASXL1*, *BCOR*, *BCORL1*, *CALR*, *CBL*, *CEBPa*, *CSF3R*, *DDX41*, *DNMT3A*, *EPOR*, *ETNK1*, *ETV6*, *EZH2*, *FLT3*, *GATA1*, *GATA2*, *GNAS*, *HRAS*, *JAK2*, *IDH1*, *IDH2*, *KRAS*, *KDM6A*, *KIT*, *MPL*, *NF1*, *NFE2*, *NPM1*, *NRAS*, *PHF6*, *PPM1D*, *PTPN11*, *RAD21*, *RUNX1*, *SF3B1*, *SETBP1*, *SH2B3*, *SMC1A*, *SMC3*, *SRSF2*, *STAG1*, *STAG2*, *STATB5*, *TET2*, *THPO*, *TP53*, *U2AF1*, *U2AF2*, *WT1*, and *ZRSR2*.

Briefly, libraries were obtained by hybrid capture-based target enrichment (SureSelectXT Low Input, Agilent, Santa Clara, CA, USA), paired-end sequencing was performed on an Illumina MiSeq System (Chip V2-300; Illumina, San Diego, CA, USA), and sequence analysis was realized on an outsourced bioinformatics solution SeqOne (Hg19 alignment).

2.10 Statistical Analysis

A receiver operator characteristic (ROC) curve was generated to determine the ability of the Compass database-guided analysis to correctly classify new AML cases based on the established scoring system for this study.

The ROC curve, area under the curve (AUC), sensitivity, specificity, positive and negative predictive values, and likelihood ratios were estimated using MedCalc Software Ltd. Version 19.8 (Ostend, Belgium).

3 RESULTS

3.1 Prospective Validation Study

The resulting AML databases and the database-guided analysis tool were validated on 125 consecutive AML-suspected cases. The results were compared with the final diagnosis according to WHO 2016 guidelines that were established by each center. Overall, the distribution of the 125 cases across the various AML groups was as follows: 15 (12%) t(15;17) AML; 7 (5.6%) t(8;21) AML; 6 (4.8%) inv(16)/t(16;16) AML; 8 (6.4%) KMT2A(MLL) AML; 88 (70.4%) other AML; and 1 (0.8%) non-AML. The distribution across the database-guided result categories (typical, atypical, or other), based on the scoring algorithm described in the *Materials and Methods* section, is shown in **Table 2**.

When combining the Compass database-guided results obtained from the first three tubes of the EF AML/MDS panel, a true positive result was obtained in 33 (26.4%) cases, a true negative result was obtained in 67 (53.6%) cases, a false-positive result as obtained in 24 (19.2%) cases, and a false-negative result was obtained in one (0.8%) case. The Compass database-guided diagnosis allowed for correct classification with an AUC of 0.83 (95% confidence interval (CI): 0.75–0.89; $p < 0.001$; **Figure 5**). Overall, this method was able to exclude AML associated with *t*(8;21), *t*(15;17), inv(16)/*t*(16;16), and *KMT2A*(*MLL*) translocation with 92% sensitivity (95% CI: 78.6%–98.3%), a 98.5% negative predictive value (95% CI: 90.6%–99.8%), and a likelihood ratio for a negative test of 0.04 (95% CI: 0.01–0.28). The negative predictive value was 100% for t(15;17) and t(8;21) AMLs; and 99.1% (95% CI: 95.2%–99.9%) for inv(16)/t(16;16) and *KMT2A*(*MLL*) AMLs (95% CI: 94.6%–99.9%). Globally, a reduced positive predictive value (PPV) of approximately 58% (95% CI: 49%–66%) was observed [$PPV_{t(15;17)AML}$: 94% (95% CI: 68%–99%); $PPV_{KMT2A(MLL)AML}$: 47% (95% CI: 30%–64%); $PPV_{t(8;21)AML}$: 44% (95% CI: 29%–59%), and $PPV_{(inv16)/t(16;16)AML}$: 40% (95% CI: 21%–62%)].

A relatively increased number of false-positive cases were observed for the following AML groups: *t*(8;21) AML (9/118 negative cases), inv(16)/t(16;16) AML (6/119 negative cases), and *KMT2A*(*MLL*) AML (8/117 negative cases).

3.2 Detailed Evaluation of Discordant Cases

3.2.1 Re-Evaluation of the False-Positive *t*(8;21) AML Cases

Despite the perfect correspondence between the phenotypes of six discordant *t*(8;21) AML cases with the typical *t*(8;21) AML

TABLE 2 | Results of the database-guided analysis per AML category.

Compass result	AML category[a]				
	***t*(15;17) AML**	***t*(8;21) AML**	**inv(16) AML**	**KMT2A(MLL) AML**	**Other**
Typical	8 (6.4%)	6 (4.8%)	4 (3.2%)	3 (2.4%)	62 (49.6%)
Atypical	7[b] (5.6%)	1[b] (0.8%)	0[b] (0%)	4[b] (3.2%)	5[c] (4%)
Other	0 (0%)	0 (0%)	2 (1.6%)	1 (0.8%)	21[d] (16.8%)

AML, acute myeloid leukemia; t(15;17) AML, APL with PML-RARA; t(8;21) AML, AML with t(8;21)(q22;q22.1);RUNX1-RUNX1T1; inv(16) AML, AML with inv(16)(p13.1q22) or t(16;16)(p13.1;q22);CBFB-MYH11; MLL AML, KMT2A(MLL)-rearranged AML.

[a]*Number of cases and percentages within each AML category.*

[b]*Cases were the median of AML blast events fall within the 1 SD or 1–2 SDs of two or more AML groups; the assignment in a group being realized on the highest score obtained by summarizing the individual scores obtained in each of the three tubes.*

[c]*Uncertain cases were the median of AML blast events fall within the 1–2 SD of two or more AML groups and the final score for each AML group was less than 2.*

[d]*False-positive cases in the "Other" group.*

cases on the APS plots (the median of the blast events from these cases fell within 1 SD for the *t*(8;21) AML group), the NAPS diagrams (12) enabled the identification of several differences (**Figure 6**). NAPS showed clear distinctions between *t*(8;21) AML cases and these false-positive *t*(8;21) AML cases (except AML case 35) for markers from tube 1 of the EF AML/MDS panel, based on different patterns for HLA-DR (26%), and CD13 (25%) and differences in the SSC (26%) and forward scatter (FSC, 22%) parameters (**Figure 6A**). In addition, for markers in tube 3 of the EF AML/MDS panel, NAPS identified two distinct groups among the false-positive *t*(8; 21) AML cases, based on differences in CD33 and SSC (**Figure 6C**). Remarkably, when analyzing the NGS data for these cases, the cases closer to the *t*(8;21) AML group were found to harbor a somatic mutations clustering within the Runt domain (*RUNX1*-mutated AML cases: 36, 53, and 66; *RUNX1* nonmutated AML cases: 11, 35, and 74; **Table S1**). Of note, CD33 expression was lower in *RUNX1*-mutated cases, similar to that observed for *t*(8;21) AML blasts.

3.2.2 Re-Evaluation of the False-Positive inv(16)/*t*(16;16) AML Cases

When examining the false-positive inv(16)/t(16;16) AML cases, the NAPS diagram (**Figures 7A–C**) allowed for the identification of AML cases lacking the expression of CD13 or CD33 expression (**Figure 7A, C**); however, this difference in expression was not associated with any specific mutation patterns conforming with the NGS tests.

3.2.3 Re-Evaluation of the False-Positive *MLL*-r AML Cases

The wide variety of genetic abnormalities identified in the *MLL*-r group was reflected by large phenotypic variability (**Figure 8**), resulting in limited specificity and PPV values and an increased rate of false-positive results.

An interesting example from the *MLL*-r false-positive group is AML case 37 (**Figure S6**). A young adult woman patient presenting with multiple venous thromboses was hospitalized under emergency circumstances at the University Hospital of Saint-Etienne. A hemoglobin level of 6.4 g/dl was detected during a complete blood count test, and the PB smear examination revealed the presence of 64% blasts. Hemostasis tests revealed a D-dimer level >20,000 ng/ml, hypofibrinogenemia, and increased fibrin monomers >150 μg/ml. These findings resulted in suspicion of acute promyelocytic leukemia (APL), and complementary testing of the BM aspirate was performed with urgency. The morphological examination revealed the presence of undifferentiated blasts, and the immunophenotypic evaluation ruled out the *t*(15;17) AML phenotype. The Compass database-guided analysis guided the diagnosis toward the *MLL*-r AML group. Genetic and molecular tests confirmed the absence of *t*(15;17)(q24;q21) or *PML/RARA* rearrangement; however, the karyotype and FISH analyses did not reveal the presence of an *MLL* rearrangement, and an array-comparative genomic hybridization (CGH) analysis was performed. A *PICALM/MLLT10 (CALM-AF10)* fusion gene was identified.

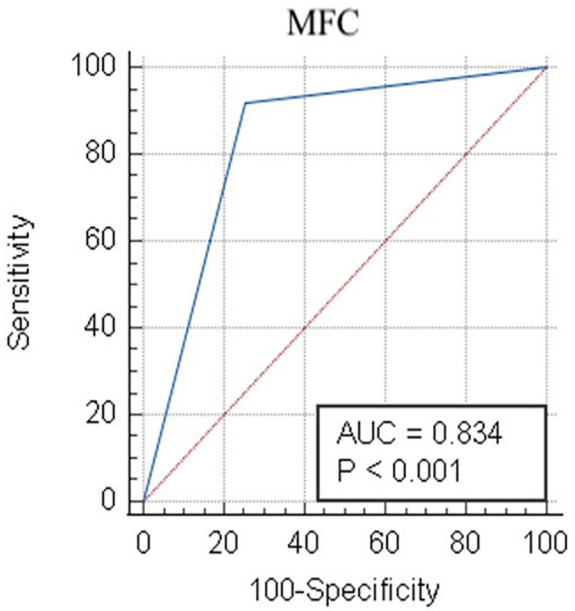

FIGURE 5 | Receiver operator characteristic evaluation of the performance of the Compass database-guided analysis for the correct classification of AML cases. Receiver operating characteristic (ROC) curve (blue line) comparing the results of the Compass database-guided analysis with those provided by FISH or PCR tests. The red diagonal line represents a random classifier. AML, acute myeloid leukemia; MFC, multicolor flow cytometry; AUC, area under the curve,

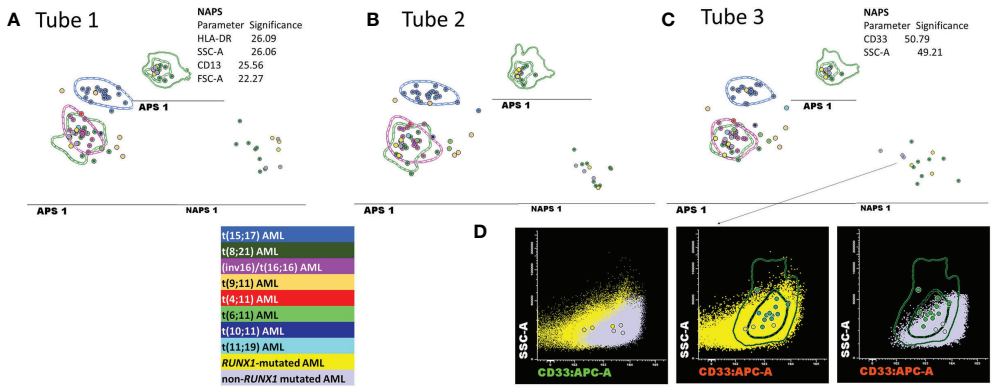

FIGURE 6 | Detailed evaluation of the false-positive *t*(8;21) AML cases. **(A–C)** APS plots showing the perfect overlap between the medians for the blast events from the false-positive *t*(8;21) AML cases (bright yellow and mauve circles) with those for the *t*(8;21) AML group (green circles, the dotted line represents the 1 standard deviation (SD) curve for the group) and for the inv(16)/*t*(16;16) AML group (violet circles, the dotted line represents the 1 SD curve of the group) using the first three tubes of the EF AML/MDS panel. In the tube 3 of EF AML/MDS panel, the neighborhood automatic population separator (NAPS) diagrams allow for the division of false-positive *t*(8;21) AML cases into two groups, according to the presence (bright yellow circles) or absence (mauve circles) of RUNX1 mutation according to NGS analysis. The tables show the contributions of each parameter to the separation of the false-positive *t*(8;21) AML blasts from the *t*(8;21) AML group in the NAPS diagrams, reflected as percentages. **(D)** Bivariate dot plots illustrating the differences in the CD33 and SSC parameters between *RUNX1*-mutated cases (yellow dots and circles representing the median CD33 expression for an individual case) and *RUNX1* nonmutated cases (mauve dots and circles representing the median CD33 expression for an individual case) compared with *t*(8;21) AML cases (green circles representing the median CD33 expression for an individual case; the dotted line represents the 1 SD curve, and the solid line represents the 2 SD curve for the AML group).

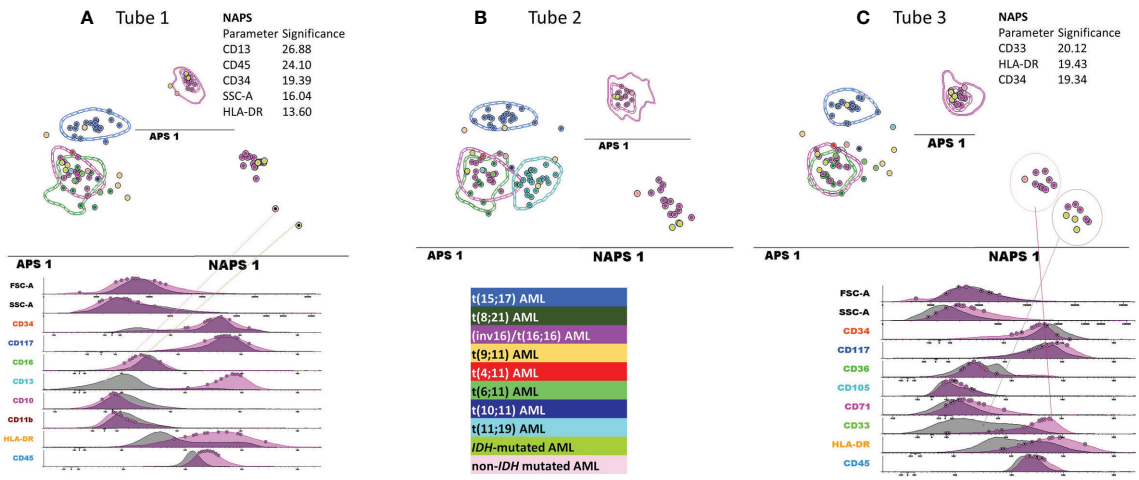

FIGURE 7 | Detailed evaluation of the false-positive inv(16)/t(16;16) AML cases. APS plots showing the overlap between the medians for the blast events from the false-positive inv(16)/t(16;16) AML cases (green-yellow, IDH mutated and pale rose circles, non-IDH mutated) with those for the inv(16)/t(16;16) AML group (violet circles, the dotted line represents the 1 standard deviation (SD) curve for the group), the t(8;21) AML group (green circles, the dotted line represents the 1 SD curve for the group) using the first three tubes of the EF AML/MDS panel **(A)** tube 1 EF AML/MDS panel; **(B)** tube 2 EF AML/MDS panel, **(C)** tube 3 EF AML/MDS panel.

3.2.4 Re-Evaluation of the False-Positive *t*(15;17) AML Case

An 80-year-old female patient (AML case 50) was transferred from a peripheral hospital to the University Hospital of Saint-Etienne with suspicion of APL. The hemostasis screening tests revealed a decrease in the prothrombin time and hypofibrinogenemia. Complementary tests were performed with urgency on PB and BM aspirate samples. Despite a preliminary orientation toward *t*(15;17) AML by the Compass database-guided analysis of the MFC results (**Figure S7**), cytogenetics analysis revealed a 46,XX, del(20)(q11q13)[20] karyotype, with no evidence of *PML-RARA* mutations by FISH or RT-PCR. NGS revealed pathogenic variants in nucleophosmin 1 (*NPM1*; type A) and FMS-like tyrosine kinase 3-internal tandem duplication (*FLT3-ITD*). An APL-like immunophenotype was previously described for AML with mutated *NPM1*, associated with significantly longer relapse-free

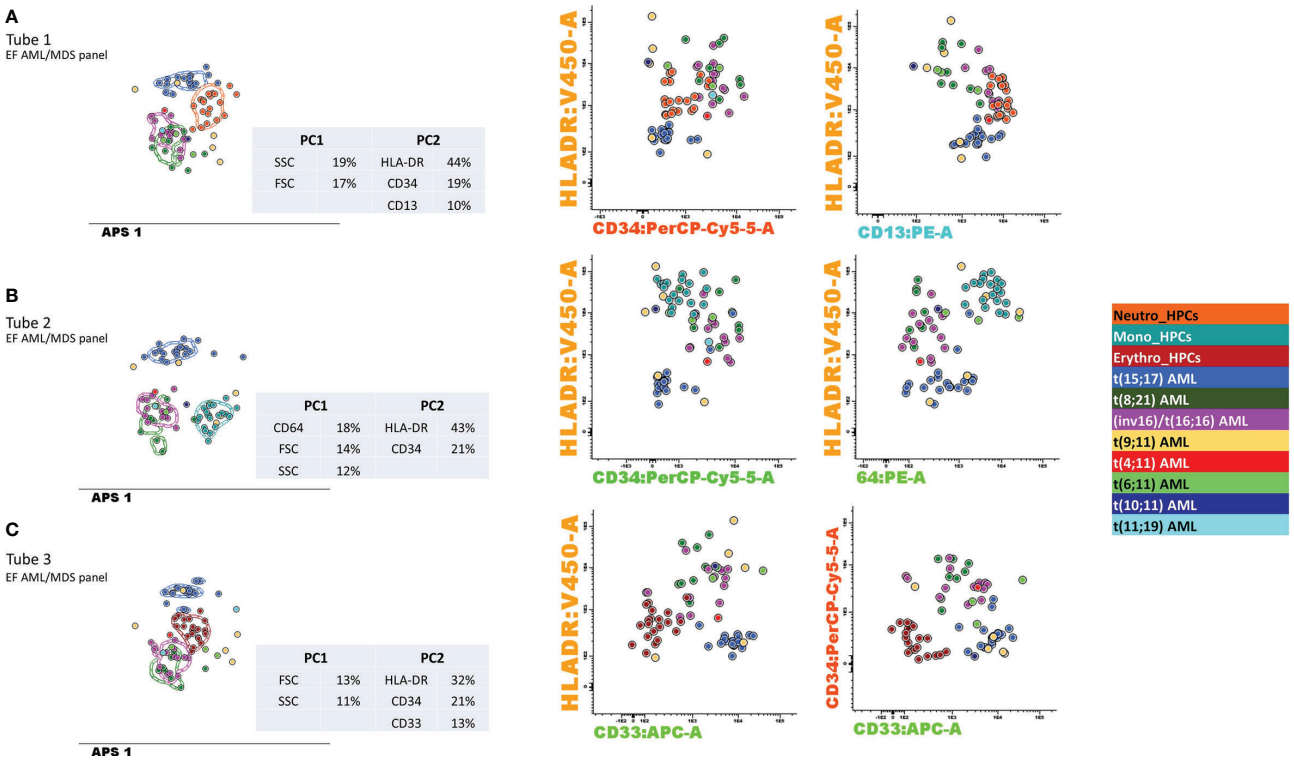

FIGURE 8 | Contribution of markers to the separation of blasts from different AML groups with recurrent genetic abnormalities and myeloid-committed normal HPCs. Samples were stained with antibodies from tubes 1–3 of the EuroFlow (EF) acute myeloid leukemia (AML)/myelodysplastic syndrome (MDS) panel. Bivariate dot plots and principal component analysis (APS) diagrams for 20 neutrophil-committed HPCs (orange), 20 monocyte-committed HPCs (turquoise), 20 erythroidcommitted HPCs (dark red), 19 t(15;17) AML cases (blue), 8 t(8;21) AML cases (dark green), 13 inv(16)/t(16;16) AML cases (violet), 5 t(19;11) AML cases (yellow), 1 t(4;11) AML cases (red), 3 t (6;11) AML cases (light green), 1 t(10;11) AML cases (dark blue), and 2 t(11;19) AML cases (light blue). showed good separation between neutrophil-committed HPCs and AML blasts using tube 1 of the EF AML/MDS panel, based on HLA-DR, CD34, and CD13 expression; between monocyte-committed HPCs and AML blasts using tube 2 of the EF AML/MDS panel, based on CD64, HLA-DR, and CD34 expression and between erythroid-committed HPCs and AML blasts using tube 3 of the EF AML/MDS panel, based on HLA-DR, CD34, and CD33 expression. The circles represent the median values of the blast events for an individual case. The dotted line represents the 1 standard deviation (SD) curve for the group, and the solid line represents the 2 SD curve. The tables show the contributions of each parameter to the first (PC1, *x*-axis) or second (PC2, *y*-axis) principal components, reflected as percentages. **(A)** tube 1 EF AML/MDS panel; **(B)** tube 2 EF AML/MDS panel, **(C)** tube 3 EF AML/MDS panel.

survival compared with patients lacking this phenotype (13) and a good response to all-trans retinoic acid (ATRA) therapy (14).

3.3 Contribution of Markers to the DfN Identification

The discriminatory power to distinguish between the different AML groups and normal my-HPCs included in the databases was assessed for the performance of DfN analysis using the Compass database-guided analysis. Tested antibody combinations were evaluated using balanced APS plots, using all eight markers and the FSC and SSC parameters for each tube of the EF AML/MDS panel (**Figure 8**).

Antibody combinations from the three tubes only provided a clear distinction between the blasts from different AML groups was for the *t*(15;17) AML group. Interestingly, a good separation was also observed between *t*(15;17) AML blasts and normal neutrophil-committed $CD13^+$ HPCs (tube 1 of the EF AML/MDS panel), normal monocyte-committed $CD64^+$ HPCs (tube 2 of the EF AML/MDS panel), and normal erythroid-committed $CD36^+$ $CD71^+$ $CD33^-$ HPCs (tube 3 of the EF AML/MDS panel). For tube 1 of the EF AML/MDS panel, the first principal component (PC1, *x*-axis) showed the major contributions of the SSC (19%) and FSC (17%) parameters, whereas the second principal component (PC2, *y*-axis) showed the major contributions of HLA-DR (44%), CD34 (19%), and CD13 (10%) for the separation of the *t*(15;17) AML group from normal neutrophil-committed HPCs and all other AML groups.

For tube 2 of the EF AML/MDS panel, the most discriminating markers identified in PC1 were CD64 (18%), FSC (14%), and SSC (12%), whereas PC2 included HLA-DR (43%) and CD34 (21%), resulting in the clear distinction between *t*(15;17) AML blasts, normal monocyte-committed HPCs, and blasts from other AML categories. For tube 3 of the EF AML/MDS panel, PC1 indicated that the most useful parameters for group separation were FSC (13%) and SSC (11%), whereas PC2 showed that the best discriminating factors for tube 3 of the EF

AML/MDS panel were HLA-DR (32%), CD34 (21%), and CD33 (13%), allowing for good separation between *t*(15;17) AML blasts, normal erythroid-committed HPCs, and blasts from other AML categories.

3.4 Compass Database-Guided DfN-MRD Evaluation in AML With Recurrent Genetic Abnormalities

In our study, the aberrant expression of lymphocytic markers on AML blasts was observed in a small number of cases: CD56 expression was observed in 13% of *t*(15;17) AML cases; the coexpression of CD19 and CD56 was observed in 28% of *t*(8;21) AML cases; the partial and low expression of CD19 was observed in 42% of *t*(8;21) AML cases; CD4 expression was observed in 7% of inv(16)/*t*(16;16) AML cases and in 18% of *MLL-r* AML cases; and CD7 expression was observed in 9% of all AML cases. Thus, performing MRD follow-up using these phenotypic aberrancies would only be applicable to a limited number of AML cases.

Therefore, we evaluated the utility of applying the Compass database-guided analysis based on the first three tubes of the EF AML/MDS panel to the detection of residual blasts in four AML cases harboring the most frequently detected genetic abnormalities.

3.4.1 Compass Database-Guided Analysis for the Detection of APL Residual Blasts by MFC Versus qRT-PCR Evaluation

Although the qRT-PCR evaluation of the *PML-RARA* fusion transcript of 10^{-4} was more sensitive, and a difference of 1 $\log_{10}$ was noticed between the qRT-PCR and those obtained for the MRD evaluation by MFC (**Figure S2**), the clinical relevance of these results was the same according to ELN MRD Working Party consensus, which recommended a threshold of 0.1% to distinguish "MRD-positive" from "MRD-negative" patients by MFC (4).

3.4.2 Compass Database-Guided Analysis for the Detection of *MLL*-r Residual Blasts by MFC Versus qRT-PCR Evaluation

For the *MLL*-r AML case, higher levels of residual blasts were detected by MFC than by *WT1* qRT-PCR at two time points before cytologic relapse occurred, and in other three time points, the values were aligned (**Figure S3**).

3.4.3 Compass Database-Guided Analysis for the Detection of *t*(8;21) Residual Blasts by MFC Versus qRT-PCR Evaluation

A better prediction for disease progression was achieved using the MFC-MRD evaluation compared with the qRT-PCR *RUNX1-RUNX1T1* evaluation in the *t*(8;21) AML case (**Figure S4**).

3.4.4 Compass Database-Guided Analysis for the Detection of inv(16) Residual Blasts by MFC Versus qRT-PCR Evaluation

The interpretation of DfN MFC data was most difficult for the inv(16) AML case because the isolation of events corresponding to residual blasts required the evaluation of multiple clusters on t-distributed stochastic neighbor embedding (t-SNE) graphs. In addition, in this case, we noticed discordances between the results obtained using the different EF AML/MDS tubes at the same time points (**Figure S5**). Despite these complications, overall, a good correlation was observed between the results obtained from the qRT-PCR and detection by MFC for identifying *CBFB-MYH11* and MRD.

4 DISCUSSION

The immunophenotypic characterization of AML blasts by MFC, combined with the morphological examination of BM aspirates, plays a critical role in the initial AML diagnosis and classification into different French–American–British (FAB) subgroups, which have been used for AML classification since 1976 (15).

However, relatively little is known regarding the associations between genetic alterations and distinct immunophenotypic profiles.

A lack of consensus regarding the choosing of AML immunophenotyping panels and data analysis strategies represent major drawbacks for AML classification. A collaborative effort within the EF consortium led to the development of the EF AML/MDS panel, which allows for the unequivocal identification of AML blasts and lineage assignments and the accurate evaluation of myeloid lineage maturation profiles (5, 9, 10). However, the discriminatory potential for this panel to differentiate between AML blasts and normal my-HPCs, in addition to the utility of the panel for AML blast classification across different cytogenetic groups, remains poorly explored.

Novel software for MFC data analysis has been developed by the EF group, which includes several analysis tools to facilitate phenotypic comparisons between pathological cells derived from different groups of diseases, with the ultimate aim of facilitating the performance of fast, objective, and reproducible diagnostic assessments. A database-guided analysis of MFC outcomes is capable of objectively analyzing all single leukemic events and classifying each event individually, providing a global image of the composition of the leukemic bulk, which can frequently be heterogeneous in AML (16). This method performs accurate, simultaneous measurements of the mean fluorescence values from eight different markers, and two scatter parameters (FSC and SSC) represent a more objective approach than expert-based interpretations, which considers arbitrary categorical classifications of negative versus positive and low versus bright patterns of marker expression for the dominant leukemic population (17).

The Compass database-guided analysis, which is based on a PCA algorithm, has been demonstrated to be effective in various studies, such as for acute leukemia orientation (16), B-cell chronic lymphoproliferative disorder classification (18), multiple myeloma diagnosis and monitoring (19), B-cell acute lymphoblastic leukemia follow-up (20), and MRD assessment in older patients with AML (21).

In this study, we sought to evaluate whether this method and the antibody combinations provided by the first three tubes of

the EF AML/MDS panel could be used to identify the most frequently identified recurrent genetic abnormalities in AML to rapidly orient cytogenetic and molecular tests and highlight the DfN characteristics of AML blast immunophenotypes.

Using the algorithm described here, the Compass database-guided diagnosis enabled the correct classification of AML types with an AUC of 0.83 (95% CI: 0.75–0.89; $p < 0.001$). The major advantage of this method was the ability to exclude certain recurrent genetic abnormalities from new AML cases, with 92% sensitivity and a 98.5% negative predictive value, which can prevent the performance of unnecessary, expensive, and time-consuming tests.

This method also allowed for the identification of *NPM1*-mutant AML cases with an APL-like immunophenotype, which might benefit from personalized therapy.

In addition, using this method, we observed a significant phenotypic heterogeneity among the various *MLL*-r AML cases, which is consistent with the prognostic variability associated with this AML type. This method could be useful for identifying immunophenotypic patterns associated with different translocations involving the *MLL* gene.

The application of the PCA-based algorithm to the four typical AML groups with recurrent genetic abnormalities that were included in the reference database highlighted the relative contributions of each marker included in the staining panel. The increased contributions of the SSC and FSC parameters highlighted the importance of rigorously standardizing these parameters over time and across instruments when performing multicenter studies.

In addition to SSC and FSC, the CD34, HLA-DR, CD13, CD64, and CD33 markers were identified as useful for separation among the four AML disease categories and for the DfN identification. Therefore, combining these markers into a single tube could be useful for improving both the identification of AML groups with recurrent genetic abnormalities and DfN monitoring.

However, a recently published study showed that the antibodies included in the first five tubes of the EF AML/MDS panel were not sufficiently effective to discriminate between normal my-HPCs and AML blasts. Phenotypically, normal $CD34^+$ HPCs isolated by fluorescence-activated cell sorting from patients with undetectable MRD possess substantial genetic abnormalities. Therefore, the identification of more specific leukemic antigens, together with improvements in MRD sensitivity using MFC and NGS data, remains necessary for the implementation of individualized treatments to prolong survival among older patients with AML (21).

Our preliminary data show that the Compass database-guided analysis represents a helpful tool for the identification of DfN, which may be useful for advancing MRD evaluations in AML.

According to our data, a similar approach has been applied for the detection of DfN patterns during MRD assessments in older AML patients. This method allowed the detection of DfN patterns and complete remission by MFC-MRD before morphological complete remission, serving as an independent prognostic factor in older AML patients. Therefore, this method can improve the sensitivity of MRD detection after semi-intensive therapy or hypomethylating agents (21).

The identification of phenotypic imprints for AML groups with recurrent genetic abnormalities may allow for the detection of leukemic blasts, even in the absence of phenotypic identification at diagnosis.

The antibody combination from the first three tubes of the EF AML/MDS panel has differential efficiencies for assessing MRD across different types of AML. Therefore, the use of multiple tubes could increase the efficiency of MRD evaluation using MFC.

The detection of AML MRD using the Compass database-guided analysis was superior to *WT1* qRT-PCR evaluation for predicting the risk of disease relapse in *MLL*-r AML.

In addition, previously published data show that qRT-PCR tests failed to predict disease progression in *t*(8;21) AML cases with low levels of MRD (22). In line with this study (22), we observed that the MFC method showed a constant low level of MRD positivity before relapse in the *t*(8;21) AML case, unlike the qRT-PCR method that indicated MRD levels below 10^{-4} at three different time points.

A good correlation was also observed between MRD evaluation by qRT-PCR and MFC in *t*(15;17) AML and inv (16) AML cases.

These preliminary results show that MRD evaluation in AML using MFC combined with Compass database-guided analysis should be considered to complement molecular biology for MRD detection.

The limited number of antibodies that can be combined into a single tube for routine MFC diagnostic purposes is a disadvantage of this method, as a relatively high number of unclassified events remains in the $CD45^{+low}$ gate, limiting the specificity and sensitivity of this method.

However, the findings of this study require large-scale validation in a multicenter study to gather sufficient quantities of sample data to establish a robust analytical model that can contribute to the development of supervised machine learning techniques capable of performing automated MFC interpretation for the objective detection of MRD in AML.

In conclusion, the first three tubes of the EF AML/MDS panel, combined with the Compass database-guided analysis:

- allows for the exclusion of frequent recurrent genetic abnormalities in new AML cases, with 92% sensitivity and a 98.5% negative predictive value, which can contribute to preventing the performance of unnecessary, expensive, and time-consuming tests;
- allows for the correct classification of *t*(15;17), *t*(8;21), inv (16)/*t*(16;16), and *MLL*-r AML groups with an AUC of 0.83 (95% CI: 0.75–0.89; $p < 0.00$);
- provides valuable clues and can direct the extensive genetic or molecular exploration of difficult cases, such as *MLL*-r AML;
- allows for the identification of $NPM1^+$ AML cases that have an APL-like phenotype and may benefit from ATRA therapy; and
- allows for the identification of DfN patterns, which may be useful for advancing MRD evaluations in AML.

DATA AVAILABILITY STATEMENT

The original contributions presented in the study are publicly available. This data can be found here: FlowRepository, ID: FR-FCM-Z3JL.

ETHICS STATEMENT

Written informed consent was obtained from each patient and healthy donor (HD), as approved by the institutional procedures of the independent ethics committee and the Comité de Protection des Personnes - Ile de France (NCT03233074/17.07.2017). The patients/participants provided their written informed consent to participate in this study.

AUTHOR CONTRIBUTIONS

Conceptualization: C-MA. Formal analysis: C-MA, RV-M, CS, MM, AT, LR, PF-G, AS, and MC. Validation: C-MA, RV-M, CS, MM, AT, LR, PF-G, AS, and MC. Clinical investigation: ET, DG, ad CT. Data curation: C-MA. Writing—original draft preparation: C-MA. Writing—review and editing: C-MA, RV-M, CS, MM, AT, LR, PF-G, AS, MC, ET, CT, LC, and DG. All authors have read and agreed to the published version of the manuscript.

FUNDING

Funding was provided by the Association Les Amis de Rémi (France).

ACKNOWLEDGMENTS

We thank BD Biosciences for providing some of the antibodies used in this study.

SUPPLEMENTARY MATERIAL

The Supplementary Material for this article can be found online at: https://www.frontiersin.org/articles/10.3389/fonc.2021.746951/full#supplementary-material

REFERENCES

1. Swerdlow SH, Campo E, Pileri SA, Lee Harris N, Stein H, Siebert R, et al. The 2016 Revision of the World Health Organization Classification of Lymphoid Neoplasms. *Blood* (2016) 127:2375–90. doi: 10.1182/blood-2016-01-643569
2. Voso MT, Ottone T, Lavorgna S, Venditti A, Maurillo L, Lo-Coco F, et al. MRD in AML: The Role of New Techniques. *Front Oncol* (2019) 2:655. doi: 10.3389/fonc.2019.00655
3. Schuurhuis GJ, Heuser M, Freeman S, Béné M-C, Buccisano F, Clooset J, et al. Minimal/measurable Residual Disease in AML: A Consensus Document From the European LeukemiaNet MRD Working Party. *Blood* (2018) 131 (12):1275–91. doi: 10.1182/blood-2017-09-801498
4. Brooimansa RA, van der Velden VHJ, Boeck N, Slomp J, Preijers F, te Marvelde JG, et al. Immunophenotypic Measurable Residual Disease (MRD) in Acute Myeloid Leukemia: Is Multicentric MRD Assessment Feasible? *Leukemia Res* (2019) 76:39–47. doi: 10.1016/j.leukres.2018.11.014
5. van Dongen J, Lhermitte L, Böttcher S, Almeida J, van der Velden VHJ, Flores-Montero J, et al. EuroFlow Antibody Panels for Standardised N-Dimensional Flow Cytometric Immunophenotyping of Normal, Reactive and Malignant Leukocytes. *Leukemia* (2012) 26:1908–75. doi: 10.1038/leu.2012.120
6. Kalina T, Flores-Montero J, van der Velden VH, Martin-Ayuso M, Böttcher S, Ritgen M, et al. EuroFlow Standardisation of Flow Cytometer Instrument Settings and Immunophenotyping Protocols. *Leukemia* (2012) 26:1986–2010. doi: 10.1038/leu.2012.122
7. Solly F, Angelot-Delettre F, Ticchioni M, Geneviève F, Rambaud H, Baseggio L, et al. Standardisation of Flow Cytometric Immunophenotyping for Hematological Malignancies: The FranceFlow Group Experience. *Cytometry A* (2019) 95:1008–18. doi: 10.1002/cyto.a.23844
8. Kalina T, Flores-Montero J, Lecrevisse Q, Pedreira CE, van der Velden VHJ, Novakova M, et al. Quality Assessment Program for EuroFlow Protocols: Summary Results of Four-Year (2010-2013) Quality Assurance Rounds. *Cytometry A* (2015) 87:145–56. doi: 10.1002/cyto.a.22581
9. Orfao A, Matarraz S, Pérez-Andrés M, Almeida J, Teodosio C, Berkowska MA, et al. Immunophenotypic Dissection of Normal Hematopoiesis. *J Immunol Methods* (2019) 475:112684. doi: 10.1016/j.jim.2019.112684
10. Matarraz S, Almeida J, Flores-Montero J, Lécrevisse Q, Guerri V, López A, et al. Introduction to the Diagnosis and Classification of Monocytic-Lineage Leukemias by Flow Cytometry. *Cytometry Part B (Clin Cytometry)* (2017) 92B:218–27. doi: 10.1002/cyto.b.21219
11. LG Shaffer, J McGowan-Jordan, M Schmid eds. *An International System for Human Cytogenetic Nomenclature (ISCN 2013)*. Basel, Switzerland: Karger Publishers (2016).
12. Pedreira CE, Sobral da Costa E, Lecreviset Q, Grigore G, Fluxad R, Verde J, et al. From Big flow Cytometry Datasets to Smart Diagnostic Strategies: The EuroFlow Approach. *J Immunol Methods* (2019) 475:112631. doi: 10.1016/j.jim.2019.07.003
13. Mason EF, Kuo FC, Hasserjian RP, Seegmiller AC, Pozdnyakova O. A Distinct Immunophenotype Identifies a Subset of NPM1-Mutated AML With TET2 or IDH1/2 Mutations and Improved Outcome. *Am J Hematol* (2017) 93:504–10. doi: 10.1002/ajh.25018
14. van Gils N, Verhagen HJMP, Smit L. Reprogramming Acute Myeloid Leukemia Into Sensitivity for Retinoic-Acid-Driven Differentiation. *Exp Hematol* (2017) 52:12–23. doi: 10.1016/j.exphem.2017.04.007
15. Bennett JM, Catovsky D, Daniel MT, Flandrin G, Galton DA, Gralnick HR, et al. Proposals for the Classification of the Acute Leukaemias. French-American-British (FAB) Co-Operative Group. *Br J Haematol* (1976) 33 (4):451–8. doi: 10.1111/j.1365-2141.1976.tb03563.x
16. Lhermitte L, Mejstrikova E, van der Sluijs-Gelling AJ, Grigore GE, Sedek L, Bras AE, et al. Automated Database-Guided Expert-Supervised Orientation for Immunophenotypic Diagnosis and Classification of Acute Leukemia. *Leukemia* (2018) 32(4):874–81. doi: 10.1038/leu.2017.313
17. Pedreira CE, Costa ES, Lecrevisse Q, van Dongen JJ, Orfao A. Overview of Clinical Flow Cytometry Data Analysis: Recent Advances and Future Challenges. *Trends Biotechnol* (2013) 31:415–25. doi: 10.1016/j.tibtech.2013.04.008
18. Costa ES, Pedreira CE, Barrena S, Lecrevisse Q, Flores J, Quijano S, et al. Automated Pattern-Guided Principal Component Analysis vs. Expert-Based Immunophenotypic Classification of B-Cell Chronic Lymphoproliferative Disorders: A Step Forward in the Standardisation of Clinical Immunophenotyping. *Leukemia* (2010) 24:1927–33. doi: 10.1038/leu.2010.160
19. Flores-Montero J, de Tute R, Paiva B, Perez JJ, Böttcher S, Wind H, et al. Immunophenotype of Normal vs. Myeloma Plasma Cells: Toward Antibody

Panel Specifications for MRD Detection in Multiple Myeloma. *Cytometry* (2016) Part B 90B:61– 72. doi: 10.1002/cyto.b.21265
20. Theunissen P, Mejstrikova E, Sedek L, van der Sluijs-Gelling AJ, Gaipa G, Bartels M, et al. Standardised Flow Cytometry for Highly Sensitive MRD Measurements in B-Cell Acute Lymphoblastic Leukemia. *Blood* (2017) 129 (3):347–57. doi: 10.1182/blood-2016-07-726307
21. Ouyang J, Goswami M, Peng J, Zuo Z, Daver N, Borthakur G, et al. Comparison of Multiparameter Flow Cytometry Immunophenotypic Analysis and Quantitative RT-PCR for the Detection of Minimal Residual Disease of Core Binding Factor Acute Myeloid Leukaemia. *Am J Clin Pathol* (2016) 145(6):769–77. doi: 10.1093/ajcp/aqw038

Conflict of Interest: The authors declare that the research was conducted in the absence of any commercial or financial relationships that could be construed as a potential conflict of interest.

Publisher's Note: All claims expressed in this article are solely those of the authors and do not necessarily represent those of their affiliated organizations, or those of the publisher, the editors and the reviewers. Any product that may be evaluated in this article, or claim that may be made by its manufacturer, is not guaranteed or endorsed by the publisher.

frontiers in Oncology

REVIEW
published: 23 November 2021
doi: 10.3389/fonc.2021.739441

Current Knowledge in Genetics, Molecular Diagnostic Tools, and Treatments for Mantle Cell Lymphomas

Shenon Sethi[1]*, *Zachary Epstein-Peterson*[2], *Anita Kumar*[2] and *Caleb Ho*[1]

[1] Department of Pathology, Memorial Sloan Kettering Cancer Center, New York, NY, United States, [2] Lymphoma Service, Department of Medicine, Memorial Sloan Kettering Cancer Center, New York, NY, United States

Mantle Cell lymphoma (MCL) is a mature B-cell lymphoma with a well-known hallmark genetic alteration in most cases, t (11,14)(q13q32)/*CCND1-IGH*. However, our understanding of the genetic and epigenetic alterations in MCL has evolved over the years, and it is now known that translocations involving *CCND2*, or cryptic insertion of enhancer elements of *IGK* or *IGL* gene, can also lead to MCL. On a molecular level, MCL can be broadly classified into two subtypes, conventional MCL (cMCL) and non-nodal MCL (nnMCL), each with different postulated tumor cell origin, clinical presentation and behavior, mutational pattern as well as genomic complexity. This article reviews both the common and rare alterations in MCL on a gene mutational, chromosomal arm, and epigenetic level, in the context of their contribution to the lymphomagenesis and disease evolution in MCL. This article also summarizes the important prognostic factors, molecular diagnostic tools, and treatment options based on the most recent MCL literature.

Keywords: mantle cell lymphoma, genetic, epigenetic, molecular diagnostics, immunochemotherapy, targeted therapy

OPEN ACCESS

Edited by:
Mina Luqing Xu,
Yale University, United States

Reviewed by:
Susanna Akiki,
Hamad Medical Corporation, Qatar
Alberto Zamo,
Julius Maximilian University of Würzburg, Germany

***Correspondence:**
Shenon Sethi
sethis@mskcc.org

Specialty section:
This article was submitted to Hematologic Malignancies, a section of the journal Frontiers in Oncology

Received: *10 July 2021*
Accepted: *29 October 2021*
Published: *23 November 2021*

Citation:
Sethi S, Epstein-Peterson Z, Kumar A and Ho C (2021) Current Knowledge in Genetics, Molecular Diagnostic Tools, and Treatments for Mantle Cell Lymphomas. Front. Oncol. 11:739441. doi: 10.3389/fonc.2021.739441

INTRODUCTION

Mantle cell lymphoma (MCL) is a relatively uncommon subtype of mature B-cell lymphoma with a heterogenous tumor behavior, with most behaving aggressively while others following an indolent clinical course. There have been a lot of advancements in the understanding of the genetics of MCL since the demonstration of t (11,14)(q13;q32)/*CCND1-IGH* as a hallmark feature of MCL in 1990s. The pathogenesis of MCL encompasses complex interactions between the tumor microenvironment, including stromal cells and T-cells, signaling *via* surface immunoglobulins, and tumor cell genetic alterations. Based on the proposed model of molecular pathogenesis, two subtypes of MCL have been recognized, which differ in their clinical and biologic behavior (1) (**Table 1**). The more common conventional MCL (cMCL) arises from expansion of pre-germinal center/naïve-like B cells that are characterized by frequent expression of the transcription factor SOX11, higher likelihood of unmutated immunoglobulin heavy chain variable region (*IGHV*), high genomic complexity, and an aggressive clinical behavior. The less common non-nodal (leukemic) variant (nnMCL), on the other hand, is derived from post-germinal center/memory-like B cells that are generally characterized by mutated *IGHV*, lack of SOX11 expression, low genomic complexity, and an indolent clinical behavior that is partially related to the lack of

TABLE 1 | Two molecular subtypes of mantle cell lymphoma (MCL).

	Conventional MCL (cMCL)	Non-nodal MCL (nnMCL)
Male: Female	3–4	1
Nodal presentation	82%	38%
Clinical presentation	Lymphadenopathy, extranodal	Leukemic, splenomegaly
Cell-of-origin	Naïve-like B cell	Memory-like B cell
Morphology	Classic/blastoid	Classic/blastoid/plasma cell differentiation
Immunophenotype	CD5+ (90–100%), CD200– (90%)	CD5– (25–50%), CD200+ (40–90%)
***IGHV* SHM status**	Unmutated or minimally mutated (IGHV identity >98%)	Hypermutated (IGHV identity <98%)
SOX11 expression	Positive	Negative
***ATM* mutation/11q22 deletion**	Common	Rare to Absent
TP53* mutation/17p13 deletion	Subset of cases	Subset of cases
***CCND1* SHM**	Uncommon	Common
Genomic complexity/Copy Number Alteration	Generally High	Generally Low
Clinical behavior	Aggressive	Stable/indolent

**A statistically significant difference in frequency has not been seen between cMCL and nnMCL.*
SHM, Somatic hypermutation.

angiogenic or tumor invasive properties (2–4). The progress in unraveling the pathogenesis and genetic alterations of MCL has also propelled new treatment modalities including molecularly targeted therapies and immunotherapies. This review focuses on the recent developments in the understanding of the mutational-, methylation-, and chromosomal-level alterations seen in MCL and the currently available molecular diagnostic tools and therapy options.

GENETICS AND PATHOGENESIS

CCND1 Translocation and Its Role in Pathogenesis

The translocation t (11,14)(q13;q32) is considered the primary oncogenic event in over 95% of MCL cases that results in the juxtaposition of immunoglobulin heavy-chain (*IGH*) enhancer region on 14q32 next to *CCND1* on 11q13, resulting in its overexpression (1, 5, 6). Irrespective of the molecular subtype, in approximately 90% of the cases, *CCND1* rearrangement (3) occurs in the pro/pre-B cell stage during *IGH* V(D)J recombination and is recombination-activating gene (RAG)-mediated, while in 10% of cases, the translocation occurs in mature B-cell stage during somatic hypermutation (SHM) or class switch recombination and is mediated by B cell-specific activation-induced cytidine deaminase (AID) machinery (3). The mechanism of *CCND1* rearrangment has no apparent clinical or biologic impact. The most common breakpoint on *IGH* locus involves the region between the *IGHD* and *IGHJ* gene segments and occurs during the initial step of *IGH* V(D)J recombination (3, 7). In some cases, the breakpoint occurs during the second step of *IGH* V(D)J recombination involving the region between the *IGHV* and *IGHD* gene segments. The most common breakpoint on 11q32 is located upstream from the *CCND1* gene within the major translocation cluster (MTC) (30% of cases), while in the remainder cases, the breakpoints are located either 5' or 3' to the MTC locus (3). Besides having *IGH* as a translocation partner, in a small number of cases, the translocation partner for *CCND1* is the immunoglobulin light chain kappa (*IGK*) or lambda (*IGL*) gene (**Figure 1A**). Furthermore, another small subset of cases does not exhibit *CCND1* translocation (so-called "Cyclin D1-Negative MCL"). Cases with these uncommon alterations will be discussed in the section *Diagnostic Challenges* below.

All types of *CCND1* translocations result in overexpression of *CCND1*, a proto-oncogene that regulates cell cycle transition from G1 to S phase and is often overexpressed or amplified in numerous cancers, including breast, lung, melanoma, and oral squamous cell carcinomas (8). Functions of cyclin D1 include control of cell growth, proliferation, transcription, DNA repair, and migration (9–11). Although Cyclin D1 is not essential for entry into cell cycle progression (12), its amplification/overexpression in human tumors is oncogenic as it allows cancer cells to proliferate independent of extracellular growth signaling cues (8). During lymphomagenesis, cyclin D1 requires cooperation of alterations in other genes, as supported by studies on transgenic mice, which showed that mice solely carrying *CCND1* rearrangement did not develop spontaneous lymphomas (13). The other key alterations that play a role in MCL pathogenesis include deletion of *CDKN2A* locus that encodes p16, a member of the INK4 family of cyclin-dependent kinase inhibitor, amplification of *BMI1* that inhibits *CDKN2A*, deregulation of *TP53 via* mutation or deletion, *MDM2* overexpression, and *ATM* deletion (1, 2, 5).

Recurrent Driver Mutations and the Main Altered Pathways

Nearly all MCLs carry at least one known driver alteration beside *CCND1* translocation, including gene mutations, copy number alterations (CNAs), and structural variants (SVs) (3). Although cMCL carry a significantly higher number of driver alterations as compared to nnMCL, the overall tumor mutational burden (which is calculated based on the number of point mutations) is similar in the two subtypes. Rather, the differences between the two primarily lie in the number of CNAs and SVs, which in general are higher in cMCL compared to nnMCL (3). Alterations in over 40 driver genes involving eight main pathways have been identified in MCL, namely: DNA damage response, proliferation,

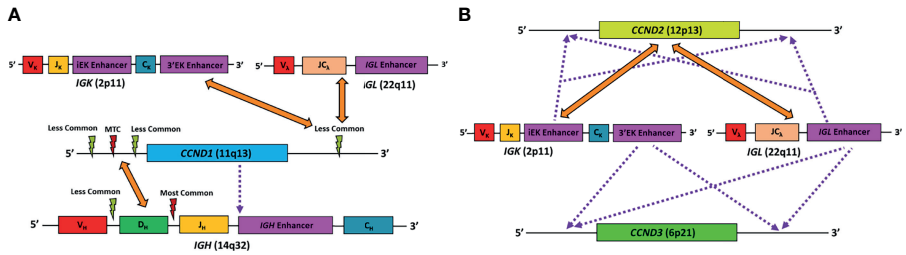

FIGURE 1 | Schematic diagram representing the known major genetic alterations leading to MCL. **(A)** Alterations found in conventional MCL. Orange arrows point to gene translocation partners, red lightning symbol represents major translocation breakpoint, light green lightning symbol represents minor translocation breakpoints, purple dotted line represents cryptic insertion of elements. In *CCND1-IGH*, the *IGH* breakpoints are mostly between the *IGHD* and *IGHJ* segments, while others are located between the *IGHV* and *IGHD* segments. The *CCND1* breakpoints are mostly in the region 5' to the gene, particularly in the major translocation cluster (MTC). In very rare case, *CCND1* coding region can be cryptically inserted into the *IGH* gene, resulting in CCND1 overexpression. Finally, *CCND1* can sometimes pair with *IGK* or *IGL* as translocation partner. In these cases, the *CCND1* breakpoints are more likely to be in the region 3' to the gene. **(B)** Alterations found in cyclin D1-negative MCL. Orange arrows point to gene translocation partners, and purple dotted line represents cryptic insertion of elements. *CCND2* mostly utilize *IGK* or *IGL*, rather than *IGH*, as translocation partners. On the other hand, conventional translocation of *CCND3* has not been reported in MCL. Alternatively, *IGK* or *IGL* enhancer elements can be cryptically inserted into the vicinity of the *CCND2* or *CCND3* gene, resulting in overexpression of the corresponding gene. VH, VK, Vλ, V gene segments of the *IGH, IGK*, and *IGL* genes, respectively; DH, D gene segment of the *IGH* gene; JH, JK, J gene segments of the *IGH* and *IGK* genes, respectively; JCλ, J and C gene segments of the *IGL* gene.

cell survival, chromatin remodeling, telomere maintenance, B-cell receptor/Toll-like receptor/NF-kB signaling, NOTCH and RNA regulation (3, 14). The most frequently mutated genes include: *ATM, TP53, CCND1* (SHM or *3'*UTR activation), *KMT2D, RB1, BIRC3, CDKN2A, CDKN1B, BCOR, NOTCH1*, and *TERT* alterations (promoter mutation, gain/amplification and translocations) (3, 14–17). More details are provided in **Table 2**. Most of the pathogenic mutations seen in MCL patients are somatic in nature. However, more recently, germline mutations in *ATM* and *CHEK2* have also been seen, which raises the possibility that germline mutations in these genes may lead to genetic predisposition to the development of MCL (3, 18). Nonetheless, currently any causal relationship remains speculatory rather than proven.

While mutational profile is not necessarily specific to a particular type of lymphoma, mutations in *CCND1, RB1, CTNNA2, NSD2*, and to a lesser degree, certain types of mutations in *ATM*, are predominantly seen in MCL in comparison to other common mature B- and T-cell lymphomas (14, 15). The presence of these mutations may be a helpful clue in rare diagnostically-challenging cases of MCL.

Alterations of *ATM*, a gene involved in the DNA damage repair pathway, are associated with shorter telomere length in MCL in comparison to MCL with wild-type *ATM*, and consequently, chromosomal instability has been found to be significantly more in MCL with mutated *ATM* (3, 18). Apart from *ATM*, there are likely other genes that also play a role in chromosomal instability, as suggested by the observation that high chromosomal instability can be associated with the blastoid variants of MCL irrespective of the *ATM* gene mutation status. Interestingly, *ATM* mutations are seen mostly in cMCL but not nnMCL, and are commonly truncating mutations or missense mutations involving the PI3K domain (1, 18). In contrast, even though *ATM* mutations are also seen in chronic lymphocytic leukemia (CLL), they are present at a much lower frequency (10–15% in CLL vs 40–75% in MCL) and commonly are missense mutations distributed in different areas of the genes.

Among the other frequent mutations found in MCL, *CCND1* SHM are predominantly seen in nnMCL (3, 14). Alterations in *TP53* have been reported to be either equally distributed among the two subtypes or slightly more enriched in nnMCL, along with *TERT* alterations (3, 14, 19).

Chromosomal Arm-Level Abnormalities

Overall, MCLs are characterized by frequent chromosomal arm-level abnormalities including gains of chromosomal arm 3q25-29, 7p22/*CARD11*, 8q24/*MYC*, 10p12/*BMI1*, 12q13/*CDK4*, 13q31/*MIR17HG*, and 18q21/*BCL2* and losses of 1p32, 6q/*TNFAIP3*, 9p21/*CDKN2A* and *CDKN2B*, 9q, 11q22/*ATM*, and *BIRC3*, 13q14/*RB1*, and 17p/*TP53* (20). Note that 13q14 loss is also common in CLL and not specific to MCL. Deletions involving 17p and 11q are often associated with *TP53* and *ATM* mutations, respectively (3, 14). The genomic landscape of cMCL is more complex as they carry a significantly higher number of CNAs and SVs than nnMCL. Due to high chromosomal instability, complex alterations such as chromoplexy and chromothripsis are also more frequently observed in cMCL, while breakage–fusion–bridge (BFB) cycles have only been seen in cMCL. The following alterations are exclusively seen in cMCL and not nnMCL: deletions of 1p, 10p, and 19p; and gain of 7p (3). **Table 3** summarizes the chromosomal arm-level abnormalities seen in MCL.

Molecular Subtypes of MCL

Distinguishing between the two subtypes of MCL is important prognostically and therapeutically. Among the two molecular subtypes, there are also several genes that are differentially expressed on a mRNA level. *HDGFRP3, FARP1, CSNK1E, SETMAR, HMGB3, LGALS3BP, PON2, CDK2AP1, DBN1, CNR1, CNN3, PLXNB1, DCHS1 NREP, MIML, FNBP1L, FHL1*,

TABLE 2 | Major driver alterations in MCL.

	Genes	Frequency
DNA damage response		
	ATM	41–50%
	TP53	19–28%
	SAMHD1	10%
Cell proliferation and survival		
	CCND1 SHM	26%
	CCND1 3'UTR activation	21%
	RB1	23%
	CDKN2A	21%
	MYC	15%
	CDKN1B	12%
	SYNE1	6%
	DAZAP1	4%
Chromatin remodeling		
	KMT2D	14–23%
	SP140	13%
	NSD2	10-12%
	SMARCA4	9%
	SMARCB1	4%
Telomere maintenance		
	TERT	15%
B-cell receptor/Toll-like receptor/NF-kB signaling		
	BCOR	22%
	CARD11	9%
	BIRC3	5%
	TRAF2	6-22%
NOTCH regulation		
	NOTCH1	5-14%
	NOTCH2	5%
RNA regulation		
	HNRPH1	6%
Protein ligase		
	UBR5	6-18%

and *SOX11* are upregulated in cMCL, while *CD200, BTLA*, and *SLAMF1* are upregulated in nnMCL (19, 21). Based on this differential gene expression pattern, Clot et al. developed a 16-gene assay (L-MCL16 assay) using the NanoString nCounter® platform (NanoString Technologies, Seattle, WA) that can utilize peripheral blood samples to distinguish between the two subtypes of MCL; however, one of the caveats is that it requires ≥60% tumor cell content (19), limiting the utility of this assay on a broader scale. It is also worth noting that a small number of patients in the validation cohort were in the

TABLE 3 | Major chromosomal-level alterations in MCL.

Chromosomal arm involved	Important genes involved	Frequency
Gains		
3q25–q29	*BCL6, TP63*	39%
7p22	*CARD11*	20%
8q24	*MYC*	19%
10p12	*BMI1*	9%
11q13	*CCND1*	9%
12q13–15	*CDK4, STAT6, KMT2D, MDM2*	5%
13q31	*MIR17HG*	8%
18q21	*BCL2*	10%
Losses		
1p32	*CDKN2C*	35%
6q	*TNFAIP3*	28%
9p21	*CDKN2A, CDKN2B*	23%
9q22	*CDC14B, FANCC, GAS1*	24%
11q22	*ATM, BIRC3*	34%
13q14	*RB1, SETDB2, DLEU1, DLEU2*	40%
13q33–q34	*CUL4A, ING1, IRS2*	35%
17p13	*TP53*	33%

"undetermined" category. As an alternative, a short 3-gene signature comprised of *SOX11, HDGFRP3*, and *DBN1* can also be used reliably to distinguish cMCL from nnMCL in leukemic samples with at least 30% involvement, where low expression profile is associated with the nnMCL subtype (22). The *RNA Gene Expression Profiling* section under *Important Molecular Diagnostic Tools for Genetic Alterations* below provides some important caveats related to gene expression profiling and the nCounter® platform.

Methylation Profile, Epigenetic Alterations, and SOX11 Expression

Besides looking at the gene expression profile and gene mutation pattern, the DNA methylation study represents another methodology that can shed insights on the tumor biology. Queiros et al. compared the DNA methylation profile of MCL cases and normal non-neoplastic B cells at different stages of maturation using principal component analysis of the first two main components. In the first principal component (PC), all MCL cases have been found to be more similar to germinal center-experienced B-cells, suggesting that MCL originates from cells with some degree of antigenic experience. However, the second PC showed that within MCL, the cases can be divided into two clusters that are biologically and clinically distinct. The first cluster represents mostly the cMCL, and as expected, has a pattern more resembling the germinal center-inexperienced cells, showing either the absence of or low but variable level of *IGHV* SHM. The second cluster represents most cases of nnMCL, and also as expected, has pattern more resembling the germinal center-experienced cells (3, 23).

One of the main distinguishing factors between cMCL and nnMCL is expression of SOX11, which is usually higher in the former and lower to absent in the latter. SOX11 expression alone is not reliable for classification, because there is a spectrum of SOX11 expression among cases in each subtype, and a subset of cMCL and nnMCL cases can have overlapping level of SOX11 expression (19). The mechanism of SOX11 expression is thought not to be due to gene mutation, but rather hypomethylation of a distant enhancer region of *SOX11*, leading to alteration of the 3-dimensional chromatin pattern with eventual activation of transcription of *SOX11*. This methylation change has been observed in cMCL, but is not seen in normal B-cells or most nnMCL (23). The precise role of SOX11 in MCL pathogenesis is still being explored. Mouse models overexpressing SOX11 have shown oligoclonal expansions of CD5+/CD23− B-cells, similar to MCL (24). SOX11 represses BCL6 expression, blocking the entry of B-cells into germinal center and thus may be integral for determining the cell of origin for MCL subtypes (25). Additionally, SOX11 promotes PAX5 expression, which in turn blocks plasmacytic differentiation, locking the cell in the mature B-cell stage, and has been previously implicated as an oncogenic mechanism in other B-cell lymphomas (26–28).

Tumor Microenvironment

The role of tumor microenvironment in lymphomagenesis and drug resistance has been previously demonstrated in several B-cell malignancies. Recent studies show that the stromal interactions in MCL *via* adhesion molecules and cytokines influence activation of multiple pathways including B-cell receptor (BCR) and NF-kB, promoting cell proliferation and survival as well as trafficking to tumor supportive tissue microenvironments. When compared to peripheral blood, it has been observed that the lymph node microenvironment in MCL fosters BCR and NF-kB signaling (29). In the bone marrow, another common site of MCL involvement, stromal cells upregulate expression of focal adhesion kinase (FAK), CXCR4 and CXCR5 chemokine receptors, and VLA-4 adhesion molecules, likely resulting in downstream activation of the NF-kB and PI3K/AKT pathways (30, 31). SOX11 also interacts with the microenvironment *via* the FAK/PI3K/AKT pathway axis to promote cell growth, angiogenesis and cell migration (25, 26, 32).

When active, these pathways may serve as potential targets for inhibition, offering alternate treatment strategies from conventional chemotherapy agents. Discussion of all these targets is beyond the scope of this review article, but one class of therapy, small molecular inhibitor of Bruton tyrosine kinase (BTK), an essential component for BCR signaling, has gained a lot of attention in recent years as a treatment for various B-cell lymphomas. One irreversible inhibitor in this class, ibrutinib, has shown efficacy in MCL, as well as in CLL and activated B-cell subtype of diffuse large B-cell lymphoma (33–37). Nevertheless, a subset of patient showed either intrinsic resistance or developed acquired resistance to ibrutinib. Other approved BTK inhibitors include zanubrutinib and acalabrutinib. Newer generation of BTK inhibitors are under development, and may potentially overcome the therapy resistance observed with ibrutinib. These were will be discussed more in the *Current Treatment Options* section below.

DIAGNOSTIC CHALLENGES

Cryptic *CCND1* Rearrangements

At most institutions, the diagnosis of MCL relies on demonstrating the classic histopathologic features and tumor cell immunophenotype (CD5+, cyclin D1+, CD23−, SOX11+/−), but many also perform *IGH*/*CCND1* dual-color dual-fusion fluorescence *in situ* hybridization (FISH) and/or *CCND1* break-apart probe studies to confirm the diagnosis. However, it is important to keep in mind that very rare cases of MCL with cyclin D1 overexpression detectable at the protein level, may have cryptic *CCND1* insertional event into the *IGH* locus that escapes detection by conventional FISH probes or karyotype analysis (38) (**Figure 1A**). These cryptic rearrangements may be more easily detected by whole genome sequencing (WGS) instead.

CCND1 Translocations With Non-*IGH* Partners

There are rare reports of MCL with translocations involving *CCND1* and *IGK* (chromosome 2) or *IGL* (chromosome 22) instead of *IGH* (chromosome 14), analogous to *IGK/MYC* or

IGL/MYC translocations seen in Burkitt lymphoma (39–43) (**Figure 1A**). A case of MCL with t(11, 12) (q13;p11.2) has also been reported (44). The 11q32 breakpoints for these variant translocations are mostly located in the 3' region, which contrasts with the breakpoints associated with conventional *IGH/CCND1* translocation that are centromeric (5') from the *CCND1* gene (39, 43). These cases would lack the expected fusion signal pattern by *IGH/CCND1* dual-color dual-fusion FISH, but a helpful clue in such cases would be the presence of an extra signal for *CCND1* as a consequence of one intact and one split *CCND1* signal. Use of *CCND1* break-apart probe, *IGK/IGL* break-apart probes or *IGK/CCND1* or *IGL/CCND1* dual-color dual-fusion probes could help prove the presence of these variant translocations, and aid in the diagnosis of MCL (**Figure 2**). While very rare, instead of conventional gene translocation involving *CCND1*, cryptic insertion of *IGK* and *IGL* enhancers in the vicinity of *CCND1* can occur, which also leads to cyclin D1 overexpression and MCL phenotype, and would be missed by *CCND1* break-apart probe (45). Such cases may be detectable only with *IGK/IGL* break-apart probes, *IGK/CCND1* or *IGL/CCND1* dual-color dual-fusion probes, or WGS assays.

Non-*CCND1* Translocation/Cyclin D1-Negative MCL

A minor subgroup of MCL lacks *CCND1* translocation as well as cyclin D1 expression (so-called "cyclin D1-negative MCL"). This subgroup has otherwise similar morphologic, phenotypic (including expression of *SOX11*) and genomic profiles as the cyclin D1-positive MCL (46–49). Nearly all of these cases show overexpression of either cyclin D2 or cyclin D3. Immunohistochemistry for cyclin D2 or cyclin D3 may serve as a screening tool for such cases. The major alteration in these cases involves the translocation of *CCND2* (55–70% of cyclin D1-negative MCL) with an immunoglobulin gene, preferably with *IGK* and *IGL* rather than *IGH*. Most of the *CCND2* translocations can be detected by break-apart probes (*CCND2* or *IGK/IGL*). In the remaining cases, the lymphomas harbor cryptic insertion of enhancer elements of *IGK* or *IGL* into the vicinity of the *CCND2 or CCND3* genes (**Figure 1B**). Due to the small size of the inserted enhancer element, such cases will be missed by conventional break-apart probes and require the use of either special customized *IGK* enhancer-*CCND2/CCND3* fusion probes or WGS for detection (46, 47) (**Figure 2**). Older studies describing cyclin D1-negative MCL, confirmed by gene expression signature, and demonstrating cyclin D2 or D3 overexpression but lacking demonstrable rearrangement by conventional break-apart probes, possibly represented such cases (49).

Even more rare are cyclin D1-negative cases (<10%) lacking protein expression of cyclin D1, cyclin D2 and cyclin D3. Such cases show concomitant upregulation of *CCNE1* and *CCNE2*, but lack a demonstrable relevant structural rearrangement (46). These cases show high genomic complexity and are associated with blastoid morphology (46).

Immunohistochemical (IHC) stains for SOX11, cyclin D2 and cyclin D3 may be helpful as part of the secondary panel in cyclin D1-negative lymphoid malignancies that have other features suggestive of MCL. Unlike cyclin D1, neither SOX11, cyclin D2 nor cyclin D3 expression is specific for MCL. Cyclin D2 or D3 expression can also be seen in CLL, follicular lymphoma or splenic marginal zone lymphoma. SOX11 expression has been reported in T-cell and B-cell lymphoblastic lymphoma/leukemia, Burkitt lymphoma, T-cell prolymphocytic leukemia, and rarely in classic Hodgkin lymphoma. Nevertheless, as compared to other B-cell lymphomas, with the exception for some cases of Burkitt lymphomas, the SOX11 mRNA levels in MCL is much higher (48).

Cyclin D1-Negative Immunostaining Despite t (11; 14)

Finally, an uncommon but potential pitfall in the diagnosis of MCL is the lack of cyclin D1 positivity by IHC stain despite the presence of t (11,14) detected by genetic studies, along with high CCND1 mRNA expression and SOX11 expression. Some

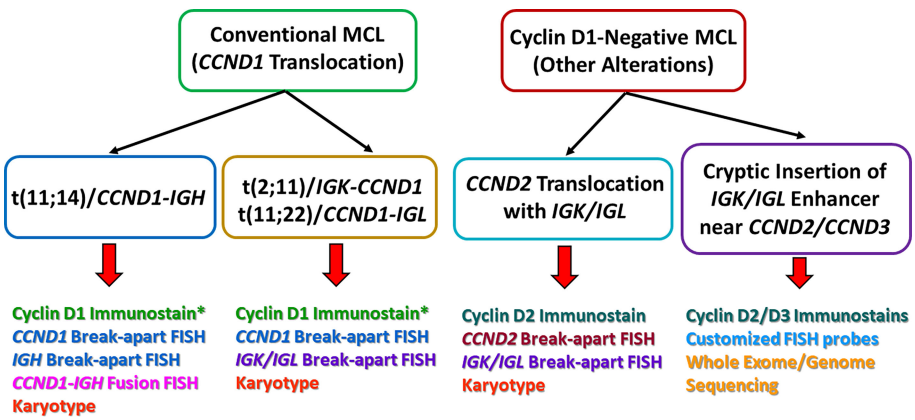

FIGURE 2 | A comparison of the major genetic alterations between conventional mantle cell lymphoma (MCL) and cyclin D1-negative MCL. The bottom of the picture also listed some of the common methods for detection. *In rare cases, MCL can harbor the *CCND1-IGH* translocation, but cyclin D1 immunostain can be negative. This can be due to poor viability of tumor cells, technical issues, as well as mutations within the *CCND1* gene that alter the immunostain antibody epitope.

potential explanations include mutations in *CCND1* that significantly alter the 3D protein structure of the IHC antibody-binding epitope, suboptimal staining due to technical issues with instrumentation or IHC antibody, and pre-analytical factors such as poor formalin fixation, or low tumor cell viability. One of the most commonly-used commercially-available cyclin D1 IHC antibodies (clone SP4) is a monoclonal antibody that binds to the C-terminus portion of cyclin D1. Mutations that alter the 3' end of *CCND1*, such as *CCND1* p.D292P, can alter the C-terminus portion of the cyclin D1 protein, and can impair binding of this antibody, resulting in a false negative IHC result (50). In such cases, the use of alternative antibodies that bind to the N-terminus of cyclin D1 will circumvent the problem.

Another mechanism for cyclin D1 IHC false negativity is related to mutations that can affect selected isoforms of *CCND1*. Alternative splicing of *CCND1* produces two major isoforms, the long isoform (cyclin D1a) and the short isoform (cyclin D1b). The short isoform derives from a splicing event that skips exon 5 and includes part of intron 4. Consequentially, cyclin D1b lacks the epitope for the C-terminal-binding cyclin D1 antibody. A defect in the expression of cyclin D1a isoform, which has been seen in association with the *CCND1* p.L6P mutation, has been found to be another reason for cyclin D1 immunostain false negativity, due to the presence of predominantly cyclin D1b isoform that lacks the appropriate antibody epitope (50).

PROGNOSTIC FACTORS

Histologic Subtypes of MCL

For practical purposes, the morphologic spectrum of MCL can be broadly divided into the classic and aggressive histologic variants. MCLs with blastoid and pleomorphic morphology are considered aggressive, as they exhibit inferior survival and response to chemotherapy (51, 52). These aggressive variants may arise *de novo* or from progression of an underlying classic variant of MCL, and are associated with high degree of aneuploidy and mutation burden, including *KMT2D* and *KMT2B* mutations (53). Jain et al. performed whole-exome sequencing (WES) in 183 patients of MCL with aggressive histology and found that mutations in *NOTCH2, NOTCH3*, and *UBR5* were exclusive to the blastoid and pleomorphic variants. Additionally, they reported that aggressive histology MCL with Ki-67 proliferation index ≥50% have exclusive mutations in *CCND1, NOTCH1, TP53, SPEN, SMARCA4, RANBP2, KMT2C, NOTCH2, NOTCH3*, and *NSD2* (53). It is also worth noting that since treatments for lymphomas can alter the tumor cell morphology, morphologic features may not be as reliable in predicting aggressive behavior and genomic complexity in the setting of post-treatment relapsed/refractory (R/R) MCL.

Molecular Subtypes and Genomic Complexity

As mentioned previously, the two molecular subtypes of MCL, cMCL and nnMCL differ in *IGHV* SHM status, gene expression profile and genomic complexity, and are usually associated with aggressive and indolent behavior, respectively (3, 54, 55). Time to treatment and overall survival (OS) from the time of diagnosis is significantly longer for nnMCL patients than cMCL (19, 22). The literature showed that a 5-year OS for cMCL ranged from 32 to 40%, and for nnMCL ranged from 59 to75% (22, 54). Nevertheless, nnMCL may acquire additional genetic alterations and undergo transformation to aggressive variants that confer worse prognoses (see *Secondary Genetic Events* below).

Although the total number of mutated driver genes does not have an impact on prognosis, chromosomal instability in the form of BFB and chromothripsis or high number of CNA and SV are associated with a shorter OS in MCL[3]. The number of CNA (>7), or presence of BFB shows independent prognostic value in multivariate analysis (3). This is also in keeping with the observation that the more aggressive blastoid variant of MCL has higher number of copy number gains and losses (56) (see *Histologic Subtypes of MCL* above).

Proliferative Activity and DNA Methylation Burden

Immunohistochemical evaluation of Ki-67 proliferative index is part of routine evaluation of MCL as per the European Mantle Cell Lymphoma Pathology Panel, because it is a strong prognostic factor for OS and progression-free survival (PFS) independent of the Mantle Cell Lymphoma International Prognostic Index (MIPI). Consequently, a combination of Ki-67 and MIPI (biologic MIPI) provides a better risk stratification into four groups with significantly different prognoses (51). A Ki-67 >30% is the currently accepted cut-off for high-risk behavior (57).

Tumor cell proliferation can also be assessed on a gene expression level. A gene signature comprised of 20 genes that has been identified as a strong predictor of survival. It is highly expressed in proliferating cells (such as *CDC2, ASPM*, tubulin α, etc.) and correlates with mitotic index, further validating the role of proliferation rate in determining the clinical course in MCL (58). A similar proliferation assay (MCL35), developed by Scott et al., utilizes the NanoString nCounter® platform (NanoString Technologies, Seattle, WA) to assess expression of 17 genes on MCL formalin-fixed paraffin-embedded (FFPE) tissue (expression of 18 other housekeeping genes was also assessed for normalization purposes, for a total of 35 genes assessed). This assay classifies patients treated with R-CHOP (rituximab, cyclophosphamide, doxorubicin, vincristine, and prednisone) into the high-risk, standard-risk, and low-risk groups, and the stratification was thought to have independent prognostication value from the MIPI score (59). The RNA *Gene Expression Profiling* section under *Important Molecular Diagnostic Tools for Genetic Alterations* below provides some important caveats related to gene expression profiling and the nCounter® platform.

Finally, the strength of a proliferation signature, which is predictive of inferior survival in MCL, correlates with the strength of the BCR signaling as well (29). The highly proliferative MCLs show high levels of cyclin D1 mRNA, with

the short, truncated variant of cyclin D1a isoform preferentially expressed. This short isoform has a longer half-life and consequently prolongs the oncogenic effect of cyclin D1 (60). The proliferative activity also determines the DNA methylation burden, which has been found to be an independent prognostic factor in MCL. High DNA methylation burden has stronger prognostic value than that of *IGHV* mutation rate and patient's age, and is associated with a worse clinical outcome (3, 23).

Secondary Genetic Events

Even in the generally indolent subtype of MCL, nnMCL, the tumors may acquire additional genetic alterations, such as *TP53* mutations and 17p deletions, that may impart an aggressive behavior (22, 54). *TP53* alterations have been shown to be an independent adverse risk factor in MCL irrespective of high Ki-67, high MIPI score or blastoid morphology (14, 61). Other known chromosomal- and mutational-level alterations associated with shorter OS include: loss of *CDKN2A*, loss of *RB1*, loss of 13q33-q34, loss of 9q22-q31, rearrangement of *MYC*, gain of 18q21-q22, and *SP140* mutations (3). In a recent study, *MYC* gene rearrangements, but not extra copies of *MYC*, were found to have a negative impact on OS in multivariate analysis (62).

From a therapeutic target standpoint, some of the secondary genetic alterations involving the BCR signaling, PIK3-AKT, canonical and non-canonical NF-kB pathways such as *NSD2, NOTCH2, UBR5, BIRC3, TRAF2, MAP2K14, KMT2D, CARD11, SMARCA4*, and *BTK*, have been found to be associated with ibrutinib resistance (63). These alterations pose therapeutic challenges, and their detection can help identify patients in need of alternative treatment regimens.

On the other hand, the prognostic role of other secondary genetic events are either more controversial or less established due to limited data available. For example, some studies have reported a negative impact of *NOTCH1* mutations in univariate analysis (14, 64) and in a multivariate Cox regression model that also included IPI and histology (16), while in others, *NOTCH1* mutations did not carry an independent prognostic value due to co-occurrence with *TP53* mutations (61). *NOTCH2* mutations occur independently of *NOTCH1* mutations, and have been found to have significantly lower 3-year OS than the non-mutated cases (0 vs 62%, P = 0.0002 in *NOTCH2*-mutated and wild-type cases, respectively). In one prospective randomized control study of young patients, *KMT2D* mutations were found to be an independent prognostic marker of OS and PFS despite intensive immunochemotherapy and autologous stem cell transplant (61).

Most of the existing literature thus far have focused on the role of *TP53* alterations in MCL. In current clinical practice, in the context of genetic alterations, only *TP53* abnormalities influence treatment decisions (see *Frontline Treatment for MCL* section under *Current Treatment Options* below). Also, a major limitation in many of the existing studies is that it remains unclear if subclonal/low-level alterations in the genes have the same prognostic impact as having the alterations in the entire disease clone. The therapeutic implications of gene alterations other than *TP53* certainly deserve further and more thorough evaluations.

Variant Translocations/Cryptic Enhancer Insertions

Overall, due to rarity of cases and treatment heterogeneity of MCL with variant translocations or cryptic enhancer insertions reported in the literature, any conclusion regarding their prognoses should be interpreted with caution. The few reported cases of MCL with variant *CCND1* translocations involving *IGK* or *IGL* instead of *IGH* mostly presented as nnMCL and followed a relatively indolent clinical course (39–43). However, no statistical difference in OS has been found among *CCND1* translocated and non-*CCND1* translocated cases. Furthermore, cases with *CCND2* translocations or cryptic insertions of *IGK/IGL* enhancer elements near *CCND2/CCND3* are associated with a similar OS as the *CCND1*-translocated cases (46).

Measurable/Minimal Residual Disease

Although not part of current routine management strategies, laboratory techniques for assessing MRD may serve as alternatives to 18 fluorodeoxyglucose positron emission tomography/computed tomography (18FDG PET-CT) for lymphoma response assessment and clinical decision making. In the context of MCL, measurement of molecular MRD is usually performed on peripheral blood or bone marrow, using methodology such as high sensitivity flow cytometry, allele-specific oligonucleotide polymerase chain reaction (PCR) or next-generation sequencing (NGS)-based *IGH* clonal rearrangement assay. Each of these can serve as a highly sensitive tool for monitoring tumor response to therapy at all time points during induction and consolidation. These diagnostic tools have been particularly helpful in the design of clinical trials to assess the efficacy of existing and novel drug regimens, and aid in tailoring the intensity and combinations of various frontline treatments. MRD assessment by molecular assays on peripheral blood or bone marrow samples, following initial immunochemotherapy, has been shown to be a strong independent prognostic factor and predictor of sustained clinical response and progression-free survival. However, MRD in MCL is still an emerging concept and prospective randomized clinical trials (such as NCT03267433) are warranted to design and evaluate MRD-guided treatment strategies (65–68). Further details on molecular MRD assays can be found in the section *IGHV Somatic Hypermutation (SHM) Assessment and NGS-Based MRD Assay* below.

IMPORTANT MOLECULAR DIAGNOSTIC TOOLS FOR GENETIC ALTERATIONS

Overview

Based on the most recent National Comprehensive Cancer Network (NCCN) guidelines (v.5.2021), besides relevant cell

marker assessment by flow cytometry/IHC and cytogenetics karyotype/FISH studies for confirming a diagnosis of MCL, the only molecular testing considered essential is *TP53* gene sequencing, for patients with expected aggressive clinical course (69) (see *Frontline Treatment for MCL* section under *Current Treatment Options* below). *IGHV* sequencing for determination of SHM status is considered helpful under certain circumstances, particularly for determination of clinically indolent MCL. Otherwise, additional molecular studies are considered optional. Other studies such as RNA gene expression and DNA methylation profiling are not performed routinely for clinical purposes, but can aid in the understanding of tumor pathogenesis.

Mutational Profiling

Detection of mutations in tumor cells can be performed by a variety of methodology, such as allele-specific PCR for detection of specific known mutations, Sanger sequencing for detection of mutation within a specific region, and NGS assays (also known as massive parallel sequencing). Different sequencing platforms and assay kits are available commercially, and discussion of each will be beyond the scope of this article. However, for the purpose of detection of *TP53* mutations, which are distributed throughout the gene rather than being confined to a few codons, Sanger sequencing and NGS assays are usually utilized, rather than allele-specific PCR. Sanger sequencing can be helpful for confirmation of findings, but in general it has worse technical detection sensitivity, is more costly, and inefficient in processing a large number of samples, as compared to the widely-used NGS assays (70).

For NGS assays, the sequencing strategy can be broadly classified into: 1. Targeted sequencing—enrichment of specific genes/exons by amplicon (PCR-based) or hybrid-capture techniques; 2. WES—enrichment of all exonic and surrounding region; 3. WGS—covering the entire genome, including the noncoding and intronic regions. In general, WGS yields the greatest breadth of information, is best suited for detecting larger gene insertions/deletions and SVs, and less prone to certain technical artifacts seen in targeted sequencing and WES. However, it is currently the most costly and time-consuming method for analyses, and due to lower overall coverage, may miss variants in samples with relatively low tumor content, or subclonal, low-level variants (70). Targeted sequencing has been favored in some clinical laboratories, due to the ability to detect variants at lower allele frequencies, lower cost, and the shorter amount of time needed for analyses, which has translated to faster report generation and sample turnaround time. If a targeted sequencing assay is chosen, it should be confirmed that important driver genes in MCL are covered by the assay (See **Table 2**).

Regardless of the breadth of sequencing regions, mutational profiling could be performed by sequencing of the tumor sample only, or paired sequencing of a normal control with the tumor sample. Analysis of a patient's paired normal and tumor sample allows most germline variants to be identified and filtered out during analyses (71). The main advantage of this approach is that only somatic variants, which are more likely to be pathogenic, are eventually included in the clinical reports. In addition, separate analysis can be performed on the sequencing data from the normal sample for detection of clinically significant germline/inherited variants (72). For paired tumor-normal sequencing of MCL, since there is a possibility of circulating tumor cells, caution should be made if blood sample is used as normal control, which is commonly used in the sequencing of non-hematologic neoplasms. Rather, alternative normal control, such as saliva or buccal swab, should be considered instead.

Finally, it is worth pointing out that the terms "mutation" and "variant" should not be used interchangeably. "Variant" is a broader term that describes nucleotide changes as compared to the reference sequence, and does not imply pathogenicity of the change. The American College of Medical Genetics and Genomics (ACMG) and the Association for Molecular Pathology (AMP) advocated for a 5-tier classification of variants, which include: pathogenic, likely pathogenic, uncertain significance, likely benign, or benign (73). The classification of variants is particularly important for tumor-only sequencing assays, in which germline benign variants (some of which are also known as polymorphisms) can be detected. In the absence of paired tumor-normal sequencing, to help distinguish between somatic and germline benign variants, the variant allele frequencies can be used in conjunction with information from publicly-available databases of somatic variants (e.g., COSMIC: https://cancer.sanger.ac.uk/cosmic), and several population-based databases of germline variants (e.g., dbSNP: https://www.ncbi.nlm.nih.gov/snp; gnomAD: https://gnomad.broadinstitute.org; The International Genome Sample Resource/The 1000 Genomes Project: https://www.internationalgenome.org). As a general rule, due to the clinical implication of assigning a variant as pathogenic, it is recommended to do so only when there is a reasonably high level of confidence in it being so (e.g., listing in multiple reliable databases of known pathogenic variants, available literature on functional studies on that particular variant).

IGHV Somatic Hypermutation Assessment and NGS-Based MRD Assay

Historically, much of the knowledge of *IGHV* SHM assessment arose from the data for CLL, where the *IGHV* SHM status has served as a key prognostic marker for the past two decades (74). In CLL as well as MCL, the *IGHV* SHM status also appears to be stable over time, regardless of therapy, and has traditionally been assessed by Sanger sequencing of the *IGH* gene VDJ segments. As clinical laboratories increasingly incorporate NGS-based assays into their workflow, and the corresponding sequencing instruments in their laboratories, *IGHV* sequencing by NGS method has also gained in popularity as a replacement for Sanger sequencing.

In terms of *IGHV* sequencing by NGS method, several commercial assays are available, and the same assay is often used for *IGH* clonal rearrangement (B-cell clonality) detection, as well as MRD detection of the known *IGH* disease clone in a post-treatment or follow-up sample. Different assays employ

different strategies, but the basic principles remain the same: the use of PCR primer sets to flank and amplify the *IGH* gene VDJ segments [usually the forward primer set is either upstream to or within the framework 1, 2, or 3 (FR1, FR2 or FR3) region of the V segment, or the D segment, while the reverse primer set is in the J gene segment] (75). Some assays may employ multiple primer sets to different regions of the *IGH* gene to overcome the problem of poor primer annealing that can result from high-level somatic mutations within the *IGH* gene. After sequencing, the disease-associated clonal sequence is identified and compared to a reference database, to determine the % of SHM as compared to the germline sequence. The patient- and disease-specific clonal sequence can also be saved, and searched for at very low level in subsequent samples, which form the basis of MRD detection. Besides commercial assays, in recent years, the European Research Initiative on CLL (ERIC) and the EuroClonality-NGS Working Group have collaborated to develop the appropriate primer sets and analysis pipeline for clonal sequence characterization and SHM determination from a NGS-based *IGHV* sequencing assay (74).

RNA Gene Expression Profiling

Somewhat analogous to the different DNA sequencing strategies mentioned above, global RNA gene expression can be performed to provide a global picture of the different alterations as compared to normal control/non-neoplastic tissue, but is mostly done in research settings. Targeted RNA gene expression profile is more feasible in the clinical setting, although in the case of MCL, it is not currently widely used for routine cases. This may be partially related to the need for RNA extraction from FFPE or blood, which is not performed at some smaller laboratories. For testing on archival FFPE samples, RNA is also not as well-preserved over time, compared to DNA.

Both MCL35 (59) and L-MCL16 (19) assays mentioned previously were designed using the NanoString nCounter® platform and require specific instrumentation from the manufacturer. This is in contrast to the sequencing instrumentation for NGS-based assays, where the same instruments can potentially be adapted for a variety of assays and serve multiple purposes (e.g., targeted mutation profiling assays using reagents/kits from different manufacturers, as well as *IGHV* sequencing by NGS method).

Single Nucleotide Polymorphism (SNP) Array

SNP array as a method of assessing CNAs has several advantages over conventional karyotype. First of all, while conventional karyotype requires fresh cell cultures, SNP array is a DNA-based assay, and therefore can be performed on existing extracted DNA, or on DNA extracted from FFPE tissue. With routine, conventional G-band karyotyping, chromosomal change >10 Mb can be detected; on the other hand, with newer SNP array assays, the average inter-marker distance is 680 bp, allowing a much higher resolution in detecting small areas of chromosomal-level gain/loss (76). Furthermore, SNP array can detect copy neutral-loss of heterozygosity (CN-LOH), as well as provide information on the level of copy number gain/loss, which are not possible by karyotyping. Nevertheless, unlike karyotype, SNP array cannot detect balanced translocation with no net loss of chromosomal material, and certainly not the partners involved in a translocation. Compared to FISH studies, which are usually much more targeted, and each set of probes assess alterations in a single chromosome, gene, or specific translocation, SNP array has the advantage of providing a broad overview of CNAs across all the chromosomes. On the flip side, since FISH studies assess for alterations in individual cells, in the context of fresh tissue studies, FISH studies can detect abnormalities at a much lower level than SNP array. This can be a consideration for samples with low tumor content, where the extracted DNA originated from a mixture of tumor and non-neoplastic cells, hampering the ability for SNP array to detect abnormalities.

CURRENT TREATMENT OPTIONS

Overview

The treatment approach and therapeutic landscape for patients with newly diagnosed and R/R MCL has changed substantially in recent years, largely due to pivotal new therapies and deepened understanding into the molecular alterations in MCL to inform their use. Besides conventional immunochemotherapy (IC), current treatments also include molecularly targeted therapies such as ibrutinib (BTK inhibitor) and venetoclax (BCL-2 inhibitor) and more recently, immune effector cells such as the chimeric antigen receptor (CAR)-modified T-cell product brexucabtagene autoleucel directed against CD19. Of note, clinical trial participation at any stage of treatment is generally encouraged given the rarity of MCL and the pressing need to improve outcomes in this disease.

Frontline Treatment for MCL

A number of considerations inform the therapeutic recommendations for patients with newly diagnosed MCL who require treatments. Of note, variability exists across treatment centers in this initial treatment approach. In current practice, the greatest patient- and tumor-specific factors of interest are the patient's age, frailty/comorbidity, and goals for care, as well as factors alluded to in the *Prognostic Factors* section above, namely clinical and biologic features of the disease, including tumor *TP53* alteration status.

Standard frontline treatments include IC or rituximab-lenalidomide (77). Younger, fit patients seeking maximal response duration generally receive multiagent IC followed by autologous stem cell rescue (HDT/ASCR). Conventional IC regimens include R-DHAP (78) (rituximab, dexamethasone, cytarabine, platinum), alternating R-CHOP/R-DHAP (52), and dose-intensified R-CHOP plus cytarabine (79). Maintenance rituximab is typically given post-HDT/ASCR based on data from Le Gouill et al. demonstrating improvements in PFS, event-free survival, and OS (78) with this approach. Of note, given uncertainty regarding the effect of HDT/ASCR on OS, an

ongoing randomized study (NCT03267433) is evaluating a MRD-based transplant approach wherein MRD-negative patients following IC are randomized to either rituximab maintenance or HDT/ASCR. Details of MRD molecular testing have been discussed in earlier sections of this review.

Transplant-ineligible patients or those seeking less intensive treatments commonly receive rituximab plus bendamustine (80); in select cases (for example, averse to IC or especially frail or comorbid), patients can also receive rituximab plus the immunomodulatory agent lenalidomide (77).

The clinical importance of *TP53* status is delineated in data from the Nordic Lymphoma Group (64) who evaluated the impact of *TP53* alterations in a cohort of patients who underwent intensive IC followed by HDT/ASCR. They demonstrated poor outcomes in these patients, with a median OS of less than 2 years and a cumulative incidence of relapse of 50% at 1 year. Other groups have demonstrated similar findings (61, 81) to reinforce the prognostic importance of *TP53* alterations. Based on these findings, IC + HDT/ASCR consolidation is not recommended; rather, treatment with novel agents in the context of a clinical trial is favored for upfront treatment of patients with *TP53*-altered MCL.

Treatment for Relapsed or Refractory MCL

For patients with R/R MCL, the treatment recommendations are highly individualized, and are primarily driven by the extent of disease/symptomatology; time to relapse; response, tolerability, and category/number of prior therapies received; and patient age/frailty/comorbidity and goals for care. Clinically, R/R MCL is characterized by progressive shortening of response duration with subsequent lines of treatment (82) and represents an unmet clinical need. Patients who have experienced favorable PFS with upfront IC may be treated with second-line IC, given the potential for achieving long responses again (83). More commonly, patients are treated with targeted agents. Approved agents (frequently combined with rituximab) include the BTK inhibitors ibrutinib, zanubrutinib, and acalabrutinib (33), the Bcl-2 inhibitor venetoclax (84), and the immunomodulatory agent lenalidomide (**Table 4**) (85). Additionally, many of these agents are being used in combination based on noteworthy preliminary data from ongoing trials [ibrutinib + lenalidomide + rituximab (35) and ibrutinib + venetoclax (37)]. The recent approval of brexucabtagene autoleucel and promising early data for lisocabtagene maraleucel are major landmarks in treating MCL given promising efficacy and tolerability in early results from trials (86, 87). For example, among 32 patients who received lisocabtagene maraleucel (median number prior therapies = 3), the response rate was 84%, including 59% complete response (87). Longer follow-up data are awaited to define the durability of responses with these agents and to inform proper sequencing with other agents in the R/R setting. Future investigations will likely investigate the use of CAR-T cells earlier in the care of patients with MCL (currently only approved for patients with R/R MCL), potentially targeting higher-risk MCL subtypes such as *TP53*-altered or blastoid morphology. Finally, for eligible patients with multiply relapsed MCL, there are supportive data for allogeneic stem cell transplantation, however, the role for this approach along with other therapies will likely evolve given the promise of CAR T-cell therapy.

TABLE 4 | Approved targeted therapies for MCL.

Agent	OR rate	CR rate	Median DOR	Median PFS	Citation
Ibrutinib	69.7%	27.0%	21.8 months	12.5 months	(36)
Acalabrutinib	81%	43%	26 months	20 months	(33)
Zanubrutinib	84%	68.6%	19. months	22.1 months	(76)
Venetoclax	53%	18%	8.1 months	3.2 months	(84)
Lenalidomide	40%	5%	16.1 months	8.7 months	(85)

OR, Overall Response; CR, Complete Response; DOR, Duration of Response; PFS, Progression Free Survival.

CONCLUSIONS

Although MCLs are characterized in most cases by t (11,14) (q13q32)/*CCND1-IGH*, other variant translocations and cryptic insertion of enhancer elements can also lead to MCL. There are certain common gene mutations and chromosomal-level alterations for MCLs. Although specific alterations may be more common in either the cMCL or nnMCL subtype, cMCL as a group has higher genomic complexity and higher average number of CNAs on a chromosomal level. As these alterations are accumulated over time during tumor progression, they can affect tumor aggressiveness and prognostication. Many alterations can be detected using widely-available clinical molecular diagnostic tools, including SNP array and targeted/WES assays. On the other hand, studies such as methylation profile assays, are currently mostly performed in the research settings. Nevertheless, detection of relevant genetic alterations is crucial for prognostication and therapy selection. Different frontline and refractory/relapsed treatment options are available for MCL, including immunochemotherapies, targeted therapies, immune effector cell therapy, and stem cell transplantation.

AUTHOR CONTRIBUTIONS

SS performed the literature review and wrote the manuscript for this review article. ZE-P and AK researched and wrote the *Current Treatment Options* section. CH researched and wrote the *Important Molecular Diagnostic Tools for Genetic Alterations* section, as well as oversaw the writing of the manuscript in the capacity of the senior author. All authors contributed to the article and approved the submitted version.

FUNDING

The authors have been supported by the Comprehensive Cancer Center Core Grant (P30 CA008748) at Memorial Sloan Kettering Cancer Center (MSKCC) from the National Institute of Health, USA (Grant recipient: CT).

REFERENCES

1. Swerdlow SH, Campo E, Harris NL, Jaffe ES, Pileri SA, Stein H, et al. *WHO Classification of Tumours of Haematopoietic and Lymphoid Tissues. Revised 4th Edition*. Lyon, France: IARC (2017).
2. Veloza L, Ribera-Cortadam I, Campom E. Mantle Cell Lymphoma Pathology Update in the 2016 WHO Classification. *Ann Lymphoma* (2019) 3:3–3. doi: 10.21037/aol.2019.03.01
3. Nadeu F, Martin-Garcia D, Clot G, Diaz-Navarro A, Duran-Ferrer M, Navarro A, et al. Genomic and Epigenomic Insights Into the Origin, Pathogenesis, and Clinical Behavior of Mantle Cell Lymphoma Subtypes. *Blood* (2020) 136(12):1419–32. doi: 10.1182/blood.2020005289
4. Puente XS, Jares P, Campo E. Chronic Lymphocytic Leukemia and Mantle Cell Lymphoma: Crossroads of Genetic and Microenvironment Interactions. *Blood* (2018) 131(21):2283–96. doi: 10.1182/blood-2017-10-764373
5. Jares P, Colomer D, Campo E. Molecular Pathogenesis of Mantle Cell Lymphoma. *J Clin Invest* (2012) 122(10):3416–23. doi: 10.1172/JCI61272
6. Royo C, Salaverria I, Hartmann EM, Rosenwald A, Campo E, Bea S. The Complex Landscape of Genetic Alterations in Mantle Cell Lymphoma. *Semin Cancer Biol* (2011) 21(5):322–34. doi: 10.1016/j.semcancer.2011.09.007
7. Kuppers R, Dalla-Favera R. Mechanisms of Chromosomal Translocations in B Cell Lymphomas. *Oncogene* (2001) 20(40):5580–94. doi: 10.1038/sj.onc.1204640
8. Santarius T, Shipley J, Brewer D, Stratton MR, Cooper CS. A Census of Amplified and Overexpressed Human Cancer Genes. *Nat Rev Cancer* (2010) 10(1):59–64. doi: 10.1038/nrc2771
9. Meyerson M, Harlow E. Identification of G1 Kinase Activity for Cdk6, a Novel Cyclin D Partner. *Mol Cell Biol* (1994) 14(3):2077–86. doi: 10.1128/MCB.14.3.2077
10. Resnitzky D, Gossen M, Bujard H, Reed SI. Acceleration of the G1/S Phase Transition by Expression of Cyclins D1 and E With an Inducible System. *Mol Cell Biol* (1994) 14(3):1669–79. doi: 10.1128/MCB.14.3.1669
11. Musgrove EA, Caldon CE, Barraclough J, Stone A, Sutherland RL. Cyclin D as a Therapeutic Target in Cancer. *Nat Rev Cancer* (2011) 11(8):558–72. doi: 10.1038/nrc3090
12. Kozar K, Ciemerych MA, Rebel VI, Shigematsu H, Zagozdzon A, Sicinska E, et al. Mouse Development and Cell Proliferation in the Absence of D-Cyclins. *Cell* (2004) 118(4):477–91. doi: 10.1016/j.cell.2004.07.025
13. Lovec H, Grzeschiczek A, Kowalski MD, Möröy T. Cyclin D1/bcl-1 Cooperates With Myc Genes in the Generation of B-Cell Lymphoma in Transgenic Mice. *EMBO J* (1994) 13(15):3487–95. doi: 10.1002/j.1460-2075.1994.tb06655.x
14. Bea S, Valdes-Mas R, Navarro A, Salaverria I, Martin-Garcia D, Jares P, et al. Landscape of Somatic Mutations and Clonal Evolution in Mantle Cell Lymphoma. *Proc Natl Acad Sci USA* (2013) 110(45):18250–5. doi: 10.1073/pnas.1314608110
15. Zhang J, Jima D, Moffitt AB, Liu Q, Czader M, Hsi ED, et al. The Genomic Landscape of Mantle Cell Lymphoma Is Related to the Epigenetically Determined Chromatin State of Normal B Cells. *Blood* (2014) 123(19):2988–96. doi: 10.1182/blood-2013-07-517177
16. Kridel R, Meissner B, Rogic S, Boyle M, Telenius A, Woolcock B, et al. Whole Transcriptome Sequencing Reveals Recurrent NOTCH1 Mutations in Mantle Cell Lymphoma. *Blood* (2012) 119(9):1963–71. doi: 10.1182/blood-2011-11-391474
17. Meissner B, Kridel R, Lim RS, Rogic S, Tse K, Scott DW, et al. The E3 Ubiquitin Ligase UBR5 Is Recurrently Mutated in Mantle Cell Lymphoma. *Blood* (2013) 121(16):3161–4. doi: 10.1182/blood-2013-01-478834
18. Camacho E, Hernandez L, Hernandez S, Tort F, Bellosillo B, Bea S, et al. ATM Gene Inactivation in Mantle Cell Lymphoma Mainly Occurs by Truncating Mutations and Missense Mutations Involving the Phosphatidylinositol-3 Kinase Domain and Is Associated With Increasing Numbers of Chromosomal Imbalances. *Blood* (2002) 99(1):238–44. doi: 10.1182/blood.V99.1.238
19. Clot G, Jares P, Gine E, Navarro A, Royo C, Pinyol M, et al. A Gene Signature That Distinguishes Conventional and Leukemic Nonnodal Mantle Cell Lymphoma Helps Predict Outcome. *Blood* (2018) 132(4):413–22. doi: 10.1182/blood-2018-03-838136
20. Stilgenbauer S, Nickolenko J, Wilhelm J, Wolf S, Weitz S, Döhner K, et al. Expressed Sequences as Candidates for a Novel Tumor Suppressor Gene at Band 13q14 in B-Cell Chronic Lymphocytic Leukemia and Mantle Cell Lymphoma. *Oncogene* (1998) 16(14):1891–7. doi: 10.1038/sj.onc.1201764
21. Fernandez V, Salamero O, Espinet B, Sole F, Royo C, Navarro A, et al. Genomic and Gene Expression Profiling Defines Indolent Forms of Mantle Cell Lymphoma. *Cancer Res* (2010) 70(4):1408–18. doi: 10.1158/0008-5472.CAN-09-3419
22. Royo C, Navarro A, Clot G, Salaverria I, Gine E, Jares P, et al. Non-Nodal Type of Mantle Cell Lymphoma Is a Specific Biological and Clinical Subgroup of the Disease. *Leukemia* (2012) 26(8):1895–8. doi: 10.1038/leu.2012.72
23. Queiros AC, Beekman R, Vilarrasa-Blasi R, Duran-Ferrer M, Clot G, Merkel A, et al. Decoding the DNA Methylome of Mantle Cell Lymphoma in the Light of the Entire B Cell Lineage. *Cancer Cell* (2016) 30(5):806–21. doi: 10.1016/j.ccell.2016.09.014
24. Kuo PY, Jatiani SS, Rahman AH, Edwards D, Jiang Z, Ahr K, et al. SOX11 Augments BCR Signaling to Drive MCL-Like Tumor Development. *Blood* (2018) 131(20):2247–55. doi: 10.1182/blood-2018-02-832535
25. Palomero J, Vegliante MC, Eguileor A, Rodriguez ML, Balsas P, Martinez D, et al. SOX11 Defines Two Different Subtypes of Mantle Cell Lymphoma Through Transcriptional Regulation of BCL6. *Leukemia* (2016) 30(7):1596–9. doi: 10.1038/leu.2015.355
26. Vegliante MC, Palomero J, Perez-Galan P, Roue G, Castellano G, Navarro A, et al. SOX11 Regulates PAX5 Expression and Blocks Terminal B-Cell Differentiation in Aggressive Mantle Cell Lymphoma. *Blood* (2013) 121(12):2175–85. doi: 10.1182/blood-2012-06-438937
27. Morrison AM, Jäger U, Chott A, Schebesta M, Haas OA, Busslinger M. Deregulated PAX-5 Transcription From a Translocated IgH Promoter in Marginal Zone Lymphoma. *Blood* (1998) 92(10):3865–78. doi: 10.1182/blood.V92.10.3865
28. Busslinger M, Klix N, Pfeffer P, Graninger PG, Kozmik Z. Deregulation of PAX-5 by Translocation of the Emu Enhancer of the IgH Locus Adjacent to Two Alternative PAX-5 Promoters in a Diffuse Large-Cell Lymphoma. *Proc Natl Acad Sci USA* (1996) 93(12):6129–34. doi: 10.1073/pnas.93.12.6129
29. Saba NS, Liu D, Herman SEM, Underbayev C, Tian X, Behrend D, et al. Pathogenic Role of B-Cell Receptor Signaling and Canonical NF-Kb Activation in Mantle Cell Lymphoma. *Blood* (2016) 128(1):82–92. doi: 10.1182/blood-2015-11-681460
30. Kurtova AV, Tamayo AT, Ford RJ, Burger JA. Mantle Cell Lymphoma Cells Express High Levels of CXCR4, CXCR5, and VLA-4 (CD49d): Importance for Interactions With the Stromal Microenvironment and Specific Targeting. *Blood* (2009) 113(19):4604–13. doi: 10.1182/blood-2008-10-185827
31. Rudelius M, Rosenfeldt MT, Leich E, Rauert-Wunderlich H, Solimando AG, Beilhack A, et al. Inhibition of Focal Adhesion Kinase Overcomes Resistance of Mantle Cell Lymphoma to Ibrutinib in the Bone Marrow Microenvironment. *Haematologica* (2018) 103(1):116–25. doi: 10.3324/haematol.2017.177162
32. Balsas P, Palomero J, Eguileor A, Rodriguez ML, Vegliante MC, Planas-Rigol E, et al. SOX11 Promotes Tumor Protective Microenvironment Interactions Through CXCR4 and FAK Regulation in Mantle Cell Lymphoma. *Blood* (2017) 130(4):501–13. doi: 10.1182/blood-2017-04-776740
33. Wang M, Rule S, Zinzani PL, Goy A, Casasnovas O, Smith SD, et al. Durable Response With Single-Agent Acalabrutinib in Patients With Relapsed or Refractory Mantle Cell Lymphoma. *Leukemia* (2019) 33(11):2762–6. doi: 10.1038/s41375-019-0575-9
34. Agarwal R, Chan YC, Tam CS, Hunter T, Vassiliadis D, Teh CE, et al. Dynamic Molecular Monitoring Reveals That SWI-SNF Mutations Mediate Resistance to Ibrutinib Plus Venetoclax in Mantle Cell Lymphoma. *Nat Med* (2019) 25(1):119–29. doi: 10.1038/s41591-018-0243-z
35. Jerkeman M, Eskelund CW, Hutchings M, Räty R, Wader KF, Laurell A, et al. Ibrutinib, Lenalidomide, and Rituximab in Relapsed or Refractory Mantle Cell Lymphoma (PHILEMON): A Multicentre, Open-Label, Single-Arm, Phase 2 Trial. *Lancet Haematol* (2018) 5(3):e109–16. doi: 10.1016/S2352-3026(18)30018-8
36. Rule S, Dreyling M, Goy A, Hess G, Auer R, Kahl B, et al. Ibrutinib for the Treatment of Relapsed/Refractory Mantle Cell Lymphoma: Extended 3.5-Year Follow Up From a Pooled Analysis. *Haematologica* (2019) 104(5):e211–4. doi: 10.3324/haematol.2018.205229

37. Tam CS, Anderson MA, Pott C, Agarwal R, Handunnetti S, Hicks RJ, et al. Ibrutinib Plus Venetoclax for the Treatment of Mantle-Cell Lymphoma. *New Engl J Med* (2018) 378(13):1211–23. doi: 10.1056/NEJMoa1715519
38. Peterson JF, Baughn LB, Ketterling RP, Pitel BA, Smoley SA, Vasmatzis G, et al. Characterization of a Cryptic IGH/CCND1 Rearrangement in a Case of Mantle Cell Lymphoma With Negative CCND1 FISH Studies. *Blood Adv* (2019) 3(8):1298–302. doi: 10.1182/bloodadvances.2019031450
39. Wlodarska I, Meeus P, Stul M, Thienpont L, Wouters E, Marcelis L, et al. Variant T(2,11)(P11;Q13) Associated With the IgK-CCND1 Rearrangement Is a Recurrent Translocation in Leukemic Small-Cell B-Non-Hodgkin Lymphoma. *Leukemia* (2004) 18(10):1705–10. doi: 10.1038/sj.leu.2403459
40. Marrero WD, Cruz-Chacon A, Cabanillas F. Mantle Cell Lymphoma With t(11,22) (Q13;Q11.2) an Indolent Clinical Variant? *Leuk Lymphoma* (2018) 59 (10):2509–11. doi: 10.1080/10428194.2018.1427863
41. Espinet B, Salaverria I, Bea S, Ruiz-Xiville N, Balague O, Salido M, et al. Incidence and Prognostic Impact of Secondary Cytogenetic Aberrations in a Series of 145 Patients With Mantle Cell Lymphoma. *Genes Chromosomes Cancer* (2010) 49(5):439–51. doi: 10.1002/gcc.20754
42. Rocha CK, Praulich I, Gehrke I, Hallek M, Kreuzer KA. A Rare Case of t(11,22) in a Mantle Cell Lymphoma Like B-Cell Neoplasia Resulting in a Fusion of IGL and CCND1: Case Report. *Mol Cytogenet* (2011) 4(1):8. doi: 10.1186/1755-8166-4-8
43. Komatsu H, Iida S, Yamamoto K, Mikuni C, Nitta M, Takahashi T, et al. A Variant Chromosome Translocation at 11q13 Identifying PRAD1/cyclin D1 as the BCL-1 Gene. *Blood* (1994) 84(4):1226–31. doi: 10.1182/blood.V84.4.1226.1226
44. Menke JR, Vasmatzis G, Murphy S, Yang L, Menke DM, Tun HW, et al. Mantle Cell Lymphoma With a Novel T(11,12)(Q13;P11.2): A Proposed Alternative Mechanism of CCND1 Up-Regulation. *Hum Pathol* (2017) 64:207–12. doi: 10.1016/j.humpath.2017.01.001
45. Fuster C, Martin-Garcia D, Balague O, Navarro A, Nadeu F, Costa D, et al. Cryptic Insertions of the Immunoglobulin Light Chain Enhancer Region Near CCND1 in T (11,14)-Negative Mantle Cell Lymphoma. *Haematologica* (2020) 105(8):e408–11. doi: 10.3324/haematol.2019.237073
46. Martin-Garcia D, Navarro A, Valdes-Mas R, Clot G, Gutierrez-Abril J, Prieto M, et al. CCND2 and CCND3 Hijack Immunoglobulin Light-Chain Enhancers in Cyclin D1(-) Mantle Cell Lymphoma. *Blood* (2019) 133 (9):940–51. doi: 10.1182/blood-2018-07-862151
47. Salaverria I, Royo C, Carvajal-Cuenca A, Clot G, Navarro A, Valera A, et al. CCND2 Rearrangements Are the Most Frequent Genetic Events in Cyclin D1 (-) Mantle Cell Lymphoma. *Blood* (2013) 121(8):1394–402. doi: 10.1182/blood-2012-08-452284
48. Mozos A, Royo C, Hartmann E, De Jong D, Baro C, Valera A, et al. SOX11 Expression Is Highly Specific for Mantle Cell Lymphoma and Identifies the Cyclin D1-Negative Subtype. *Haematologica* (2009) 94(11):1555–62. doi: 10.3324/haematol.2009.010264
49. Fu K, Weisenburger DD, Greiner TC, Dave S, Wright G, Rosenwald A, et al. Cyclin D1-Negative Mantle Cell Lymphoma: A Clinicopathologic Study Based on Gene Expression Profiling. *Blood* (2005) 106(13):4315–21. doi: 10.1182/blood-2005-04-1753
50. Iaccarino I, Afify L, Aukema SM, Reddemann K, Schütt P, Flür M, et al. t(11,14)-Positive Mantle Cell Lymphomas Lacking Cyclin D1 (CCND1) Immunostaining Because of a CCND1 Mutation or Exclusive Expression of the CCND1b Isoform. *Haematologica* (2018) 103(9):e432–5. doi: 10.3324/haematol.2018.192435
51. Hoster E, Rosenwald A, Berger F, Bernd HW, Hartmann S, Loddenkemper C, et al. Prognostic Value of Ki-67 Index, Cytology, and Growth Pattern in Mantle-Cell Lymphoma: Results From Randomized Trials of the European Mantle Cell Lymphoma Network. *J Clin Oncol* (2016) 34(12):1386–94. doi: 10.1200/JCO.2015.63.8387
52. Hermine O, Hoster E, Walewski J, Bosly A, Stilgenbauer S, Thieblemont C, et al. Addition of High-Dose Cytarabine to Immunochemotherapy Before Autologous Stem-Cell Transplantation in Patients Aged 65 Years or Younger With Mantle Cell Lymphoma (MCL Younger): A Randomised, Open-Label, Phase 3 Trial of the European Mantle Cell Lymphoma Network. *Lancet* (2016) 388(10044):565–75. doi: 10.1016/S0140-6736(16)00739-X
53. Jain P, Zhang S, Kanagal-Shamanna R, Ok CY, Nomie K, Nogueras-Gonzalez G, et al. Genomic Profiles and Clinical Outcomes of *De Novo* Blastoid/Pleomorphic MCL Are Distinct From Those of Transformed MCL. *Blood Adv* (2020) 4(6):1038–50. doi: 10.1182/bloodadvances.2019001396
54. Navarro A, Clot G, Royo C, Jares P, Hadzidimitriou A, Agathangelidis A, et al. Molecular Subsets of Mantle Cell Lymphoma Defined by the IGHV Mutational Status and SOX11 Expression Have Distinct Biologic and Clinical Features. *Cancer Res* (2012) 72(20):5307–16. doi: 10.1158/0008-5472.CAN-12-1615
55. Orchard J, Garand R, Davis Z, Babbage G, Sahota S, Matutes E, et al. A Subset of T (11,14) Lymphoma With Mantle Cell Features Displays Mutated IgVH Genes and Includes Patients With Good Prognosis, Nonnodal Disease. *Blood* (2003) 101(12):4975–81. doi: 10.1182/blood-2002-06-1864
56. Bea S, Ribas M, Hernandez JM, Bosch F, Pinyol M, Hernandez L, et al. Increased Number of Chromosomal Imbalances and High-Level DNA Amplifications in Mantle Cell Lymphoma Are Associated With Blastoid Variants. *Blood* (1999) 93(12):4365–74. doi: 10.1182/blood.V93.12.4365
57. Determann O, Hoster E, Ott G, Bernd HW, Loddenkemper C, Hansmann ML, et al. Ki-67 Predicts Outcome in Advanced-Stage Mantle Cell Lymphoma Patients Treated With Anti-CD20 Immunochemotherapy: Results From Randomized Trials of the European MCL Network and the German Low Grade Lymphoma Study Group. *Blood* (2008) 111(4):2385–7. doi: 10.1182/blood-2007-10-117010
58. Rosenwald A, Wright G, Wiestner A, Chan WC, Connors JM, Campo E, et al. The Proliferation Gene Expression Signature Is a Quantitative Integrator of Oncogenic Events That Predicts Survival in Mantle Cell Lymphoma. *Cancer Cell* (2003) 3(2):185–97. doi: 10.1016/S1535-6108(03)00028-X
59. Scott DW, Abrisqueta P, Wright GW, Slack GW, Mottok A, Villa D, et al. New Molecular Assay for the Proliferation Signature in Mantle Cell Lymphoma Applicable to Formalin-Fixed Paraffin-Embedded Biopsies. *J Clin Oncol* (2017) 35(15):1668–77. doi: 10.1200/JCO.2016.70.7901
60. Wiestner A, Tehrani M, Chiorazzi M, Wright G, Gibellini F, Nakayama K, et al. Point Mutations and Genomic Deletions in CCND1 Create Stable Truncated Cyclin D1 mRNAs That Are Associated With Increased Proliferation Rate and Shorter Survival. *Blood* (2007) 109(11):4599–606. doi: 10.1182/blood-2006-08-039859
61. Ferrero S, Rossi D, Rinaldi A, Bruscaggin A, Spina V, Eskelund CW, et al. KMT2D Mutations and TP53 Disruptions Are Poor Prognostic Biomarkers in Mantle Cell Lymphoma Receiving High-Dose Therapy: A FIL Study. *Haematologica* (2020) 105(6):1604–12. doi: 10.3324/haematol.2018.214056
62. Wang L, Tang G, Medeiros LJ, Xu J, Huang W, Yin CC, et al. MYC Rearrangement But Not Extra MYC Copies Is an Independent Prognostic Factor in Patients With Mantle Cell Lymphoma. *Haematologica* (2020) 106 (5):1381–9. doi: 10.3324/haematol.2019.243071
63. Hershkovitz-Rokah O, Pulver D, Lenz G, Shpilberg O. Ibrutinib Resistance in Mantle Cell Lymphoma: Clinical, Molecular and Treatment Aspects. *Br J Haematol* (2018) 181(3):306–19. doi: 10.1111/bjh.15108
64. Eskelund CW, Dahl C, Hansen JW, Westman M, Kolstad A, Pedersen LB, et al. TP53 Mutations Identify Younger Mantle Cell Lymphoma Patients Who Do Not Benefi T From Intensive Chemoimmunotherapy. *Blood J Am Soc Hematol* (2017) 130(17):1903–10. doi: 10.1182/blood-2017-04-779736
65. Kumar A, Bantilan KS, Jacob AP, Park A, Schoninger SF, Sauter C, et al. Noninvasive Monitoring of Mantle Cell Lymphoma by Immunoglobulin Gene Next-Generation Sequencing in a Phase 2 Study of Sequential Chemoradioimmunotherapy Followed by Autologous Stem-Cell Rescue. *Clin Lymphoma Myeloma Leukemia* (2021) 21(4):230–7.e12. doi: 10.1016/j.clml.2020.09.007
66. Merryman RW, Edwin N, Redd R, Bsat J, Chase M, LaCasce A, et al. Rituximab/bendamustine and Rituximab/Cytarabine Induction Therapy for Transplant-Eligible Mantle Cell Lymphoma. *Blood Adv* (2020) 4(5):858–67. doi: 10.1182/bloodadvances.2019001355
67. Hoster E, Pott C. Minimal Residual Disease in Mantle Cell Lymphoma: Insights Into Biology and Impact on Treatment. *Hematology* (2016) 2016 (1):437–45. doi: 10.1182/asheducation-2016.1.437
68. Pott C, Hoster E, Delfau-Larue MH, Beldjord K, Böttcher S, Asnafi V, et al. Molecular Remission Is an Independent Predictor of Clinical Outcome in Patients With Mantle Cell Lymphoma After Combined Immunochemotherapy: A European MCL Intergroup Study. *Blood* (2010) 115(16):3215–23. doi: 10.1182/blood-2009-06-230250

69. National Comprehensive Cancer Network (NCCN). Clinical Practice Guidelines in Oncology (NCCN Guidelines). *B-Cell Lymphomas* (2021) 4. Available at: https://www.nccn.org/guidelines/guidelines-detail?category=1&id=1480.
70. Kumar KR, Cowley MJ, Davis RL. Next-Generation Sequencing and Emerging Technologies. *Semin Thromb Hemost* (2019) 45(7):661–73. doi: 10.1055/s-0039-1688446
71. Cheng DT, Mitchell TN, Zehir A, Shah RH, Benayed R, Syed A, et al. Memorial Sloan Kettering-Integrated Mutation Profiling of Actionable Cancer Targets (MSK-IMPACT): A Hybridization Capture-Based Next-Generation Sequencing Clinical Assay for Solid Tumor Molecular Oncology. *J Mol Diagn* (2015) 17(3):251–64. doi: 10.1016/j.jmoldx.2014.12.006
72. Mandelker D, Zhang L, Kemel Y, Stadler ZK, Joseph V, Zehir A, et al. Mutation Detection in Patients With Advanced Cancer by Universal Sequencing of Cancer-Related Genes in Tumor and Normal DNA vs Guideline-Based Germline Testing. *JAMA* (2017) 318(9):825–35. doi: 10.1001/jama.2017.11137
73. Richards S, Aziz N, Bale S, Bick D, Das S, Gastier-Foster J, et al. Standards and Guidelines for the Interpretation of Sequence Variants: A Joint Consensus Recommendation of the American College of Medical Genetics and Genomics and the Association for Molecular Pathology. *Genet Med* (2015) 17(5):405–24. doi: 10.1038/gim.2015.30
74. Davi F, Langerak AW, Langlois de Septenville A, Kolijn PM, Hengeveld PJ, Chatzidimitriou A, et al. Immunoglobulin Gene Analysis in Chronic Lymphocytic Leukemia in the Era of Next Generation Sequencing. *Leukemia* (2020) 34(10):2545–51. doi: 10.1038/s41375-020-0923-9
75. Ho C, Arcila ME. Minimal Residual Disease Detection of Myeloma Using Sequencing of Immunoglobulin Heavy Chain Gene VDJ Regions. *Semin Hematol* (2018) 55(1):13–8. doi: 10.1053/j.seminhematol.2018.02.007
76. Song Y, Zhou K, Zou D, Zhou J, Hu J, Yang H, et al. Treatment of Patients With Relapsed or Refractory Mantle–Cell Lymphoma With Zanubrutinib, a Selective Inhibitor of Bruton's Tyrosine Kinase. *Clin Cancer Res* (2020) 26(16):4216–24. doi: 10.1158/1078-0432.CCR-19-3703
77. Ruan J, Martin P, Shah B, Schuster SJ, Smith SM, Furman RR, et al. Lenalidomide Plus Rituximab as Initial Treatment for Mantle-Cell Lymphoma. *N Engl J Med* (2015) 373(19):1835–44. doi: 10.1056/NEJMoa1505237
78. Le Gouill S, Thieblemont C, Oberic L, Moreau A, Bouabdallah K, Dartigeas C, et al. Rituximab After Autologous Stem-Cell Transplantation in Mantle-Cell Lymphoma. *N Engl J Med* (2017) 377(13):1250–60. doi: 10.1056/NEJMoa1701769
79. Eskelund CW, Kolstad A, Jerkeman M, Räty R, Laurell A, Eloranta S, et al. 15-Year Follow-Up of the Second Nordic Mantle Cell Lymphoma Trial (MCL 2): Prolonged Remissions Without Survival Plateau. *Br J Haematol* (2016) 175(3):410–8. doi: 10.1111/bjh.14241
80. Villa D, Sehn LH, Savage KJ, Toze CL, Song K, den Brok WD, et al. Bendamustine and Rituximab as Induction Therapy in Both Transplant-Eligible and-Ineligible Patients With Mantle Cell Lymphoma. *Blood Adv* (2020) 4(15):3486–94. doi: 10.1182/bloodadvances.2020002068
81. Delfau-Larue M-H, Klapper W, Berger F, Jardin F, Briere J, Salles G, et al. High-Dose Cytarabine Does Not Overcome the Adverse Prognostic Value of CDKN2A and TP53 Deletions in Mantle Cell Lymphoma. *Blood J Am Soc Hematol* (2015) 126(5):604–11. doi: 10.1182/blood-2015-02-628792
82. Kumar A, Sha F, Toure A, Dogan A, Ni A, Batlevi CL, et al. Patterns of Survival in Patients With Recurrent Mantle Cell Lymphoma in the Modern Era: Progressive Shortening in Response Duration and Survival After Each Relapse. *Blood Cancer J* (2019) 9(6):1–10. doi: 10.1038/s41408-019-0209-5
83. Czuczman MS, Goy A, Lamonica D, Graf DA, Munteanu MC, van der Jagt RH. Phase II Study of Bendamustine Combined With Rituximab in Relapsed/Refractory Mantle Cell Lymphoma: Efficacy, Tolerability, and Safety Findings. *Ann Hematol* (2015) 94(12):2025–32. doi: 10.1007/s00277-015-2478-9
84. Eyre TA, Walter HS, Iyengar S, Follows G, Cross M, Fox CP, et al. Efficacy of Venetoclax Monotherapy in Patients With Relapsed, Refractory Mantle Cell Lymphoma After Bruton Tyrosine Kinase Inhibitor Therapy. *Haematologica* (2019) 104(2):e68. doi: 10.3324/haematol.2018.198812
85. Trněný M, Lamy T, Walewski J, Belada D, Mayer J, Radford J, et al. Lenalidomide Versus Investigator's Choice in Relapsed or Refractory Mantle Cell Lymphoma (MCL-002; SPRINT): A Phase 2, Randomised, Multicentre Trial. *Lancet Oncol* (2016) 17(3):319–31. doi: 10.1016/S1470-2045(15)00559-8
86. Wang M, Munoz J, Goy A, Locke FL, Jacobson CA, Hill BT, et al. KTE-X19 CAR T-Cell Therapy in Relapsed or Refractory Mantle-Cell Lymphoma. *N Engl J Med* (2020) 382(14):1331–42. doi: 10.1056/NEJMoa1914347
87. Palomba M, Gordon L, Siddiqi T. Safety and Preliminary Efficacy in Patients With Relapsed/Refractory Mantle Cell Lymphoma Receiving Lisocabtagene Maraleucel in TRANSCEND NHL 001. *Blood* (2020) 136(Supplement1):10–1. doi: 10.1182/blood-2020-136158

Conflict of Interest: ZE-P received salary support through the AACR-AstraZeneca Lymphoma Research Fellowship and the Lymphoma Research Foundation LSRMP. AK has stocks and other ownership interests in Bridgebio Pharma, consulting or advisory role for Celgene, Kite Pharma (a Gilead company), AstraZeneca, and research funding from: AbbVie/Genetech, Adaptive Biotechnologies, Celgene, Seattle Genetics, AstraZeneca, Pharmacyclics. CH serves on the Hematopathology advisory board for Blueprint Medicines, received honorarium from Invivoscribe, Inc. and Maryland Society of Pathologists, and is a current employee of Loxo Oncology at Lilly.

The remaining author declares that the research was conducted in the absence of any commercial or financial relationships that could be construed as a potential conflict of interest.

frontiers in Oncology

REVIEW
published: 08 December 2021
doi: 10.3389/fonc.2021.719140

Tumor Microenvironment of Lymphomas and Plasma Cell Neoplasms: Broad Overview and Impact on Evaluation for Immune Based Therapies

*Sudhir Perincheri**

Department of Pathology, Yale School of Medicine, New Haven, CT, United States

Lymphomas and plasma cell neoplasms are a heterogenous group of malignancies derived from lymphocytes. They are a significant cause of patient morbidity and mortality. Advances in morphologic, immunophenotypic and molecular techniques have led to better understanding of the pathogenesis and diagnosis of these neoplasms. Advances in treatment, particularly immune-based therapies, increasingly allow for targeted therapies of these diseases. Mechanistic studies using animal models and clinical trials have revealed the importance of the tumor microenvironment on disease pathogenesis, progression, and response to therapy in these malignancies. Simultaneous progress in diagnostic techniques has made it feasible to generate high-resolution, high-throughput data from the tumor microenvironment with spatial context. As the armamentarium of targeted therapies and diagnostic techniques grows, there is potential to harness these advances to better stratify patients for targeted therapies, including immune-based therapies, in hematologic malignancies.

Keywords: tumor microenvironment, immune based therapies, lymphomas, plasma cell neoplasms, biomarkers

OPEN ACCESS

Edited by:
Julia T. Geyer,
Weill Cornell Medical Center,
United States

Reviewed by:
Caleb Ho,
Loxo Oncology, Inc., United States
Yen-Chun Liu,
St. Jude Children's Research Hospital,
United States

***Correspondence:**
Sudhir Perincheri
sudhir.perincheri@yale.edu

Specialty section:
This article was submitted to Hematologic Malignancies, a section of the journal Frontiers in Oncology

Received: *01 June 2021*
Accepted: *16 November 2021*
Published: *08 December 2021*

Citation:
Perincheri S (2021) Tumor Microenvironment of Lymphomas and Plasma Cell Neoplasms: Broad Overview and Impact on Evaluation for Immune Based Therapies. Front. Oncol. 11:719140. doi: 10.3389/fonc.2021.719140

INTRODUCTION

Lymphomas and plasma cell neoplasms are a heterogenous group of malignancies arising from lymphocytes at various stages of development. Depending on the cell of origin, morphology and immunophenotype, they are broadly categorized into non-Hodgkin lymphomas, Hodgkin lymphomas and plasma cell neoplasms (1). Non-Hodgkin lymphomas include the sub-categories of non-Hodgkin B-cell lymphomas (B-NHL) that comprise majority of cases in this group and T-cell/Natural-killer (T/NK) lymphomas. As a group, non-Hodgkin lymphomas are the seventh most common type of cancer in the United States and are expected to account for 81,560 new cases and 20,720 deaths in 2021 (2). Hodgkin lymphomas are rarer and are expected to account for 8,830 new cases and 960 deaths. For plasma cell neoplasms the corresponding numbers are 34,920 new cases and 12,410 deaths, respectively in 2021 (3, 4). The clinical course and prognosis for these heterogenous group of neoplasms is highly dependent on factors such as the specific type of disease, age, ethnicity and geographic location (1). Advances in our understanding of the molecular

pathology of these diseases has resulted in considerable progress in the treatment of these diseases. Immune-based therapies using monoclonal antibodies have become part of treatment regimens for these diseases (discussed in greater detail below). More recently, greater understanding of the tumor microenvironment in these diseases has led to development of immune system modulatory agents with therapeutic potential (3, 4). Future treatment regimens are likely to rely on combinatorial strategies using these agents. These developments are going to necessitate the development of novel diagnostic and prognostic tools to facilitate optimal treatment.

TUMOR MICROENVIRONMENT IN LYMPHOMAS AND PLASMA CELL NEOPLASMS

Scientific research on molecular mechanisms has expanded our understanding of cancer pathogenesis leading to advances in diagnostics and therapy. More recently, there has been increasing focus in delineating the components of the tumor microenvironment in enabling tumorigenesis and progression (5). These have led to development of several immune based therapies that have shown encouraging results both in epithelial and hematologic malignancies (6).

Tumor Microenvironment in Lymphomas

The tumor heterogeneity of non-Hodgkin lymphomas is reflected in the tumor microenvironment. The histologic architecture of lymph node and extra-nodal lymphoid organs is generally comprised of B-cell predominant follicles and interfollicular T-cells (**Figure 1A**). Naive B cells exposed to antigen home to follicles where they interact with follicular dendritic cells that are antigen presenting cells. Further maturation of B-cells occurs within germinal centers where they switch-off expression of the anti-apoptotic BCL2 protein rendering them vulnerable to apoptosis. Following the process of somatic mutation and affinity maturation, B-cells either undergo apoptosis or differentiate into memory/marginal zone B-cells found in the marginal zone around the germinal centers or into long-lived plasma cells (1). Macrophages present in the germinal centers remove the apoptotic cells giving rise to the characteristic tingible body macrophages seen in benign follicles (**Figure 1A**). Morphologically, lymphomas are characterized by architectural effacement of normal lymphoid tissue. The spatial distribution of tumor cells in lymphomas is variable. Their distribution may reflect the distribution of the cell of origin as in follicular lymphomas (**Figure 1B**) (7). Follicular lymphomas are derived from follicular germinal center B-cells. Typically, these tumors arise due to an IGH-BCL2 translocation leading to BCL2 overexpression in contrast to the BCL2 switch-off seen in normal follicles (8). Spatially the follicular lymphoma cells are seen within enlarged follicles. In contrast, marginal zone lymphomas that arise from post-germinal center B-cells show an expansion of the marginal zone around the follicles. The growth of neoplastic cells in marginal zone lymphomas is often due to continuous antigenic stimulation e.g., persistent *Helicobacter pylori* infection. While eradication of the underlying infection often leads to cure, over time marginal zone lymphomas can acquire translocations that lead to cell autonomous signaling independent of the microenvironment, leading to refractory disease. In contrast to follicular and marginal zone lymphomas, the tissue architecture is diffusely effaced in diffuse large B-cell lymphomas (**Figure 1C**). The cellular composition of lymphomas is also variable. In B-NHLs, the tumor is predominantly comprised of neoplastic B-cells with fewer admixed T-cells, macrophages and stroma that comprise the tumor microenvironment. In contrast, in Classic Hodgkin lymphoma (cHL) the neoplastic Hodgkin Reed-Sternberg (HRS) cells typically form only a minor subset of the neoplastic infiltrate. The substantial cellular component of the tumor is a characteristic polymorphous population of small lymphocytes, plasma cells, histiocytes and admixed granulocytes that constitutes a morphologically unique microenvironment (**Figure 1D**).

These morphologic pattens reflect different tumor microenvironments that result from genetic aberrations in these neoplasms and the external stimuli needed for survival, proliferation, and immune response evasion. Lymphoma cells have been shown to influence their microenvironment by their ability to use homing and trafficking mechanisms to spatially colonize milieus characteristic of their non-malignant counterparts. These include expression of various adhesion molecules as well as cytokines and cytokine receptors that regulate lymphocyte trafficking between various tissue compartments (9–13). After colonization, tumor cells can shift the tissue milieu to one that promotes cell survival and growth, and immune response evasion (14–17). Cell growth results from signaling through cell surface receptors such as the B-cell receptor and Toll-like receptor as well as cytokines released from stromal cells (18–21). The evasion of immune response occurs by various mechanisms including down-regulation of major histocompatibility complex molecules, recruitment of T-regulatory cells (T-regs) at the expense of T-helper cells, and expression of programmed cell death ligands PD-L1 and PD-L2 that bind to programmed cell death protein 1 (PD-1) on CD4-positive T cells and cytotoxic T lymphocytes to induce a state of T-cell exhaustion (22–28).

Despite similar spatial localization of neoplastic cells in some lymphomas when compared to their non-malignant counterparts, there can be significant differences in their respective microenvironments. For example, the tumor microenvironment in the neoplastic follicles in follicular lymphoma has been shown to be significantly different than normal germinal centers with respect to T-cells and macrophages. Specifically, there appears to be an increase in T-regs and immune-suppressive monocytes at the expense of T-helper cells in neoplastic follicles (14, 15, 17). In cHL, the secretion of cytokines produced by and in response to HRS cells is thought to result in the characteristic polymorphous milieu that also promotes cell survival (13). Cytokines such as CCL5, CCL17 and CCL22 recruit CD4+ T-cells that constitute

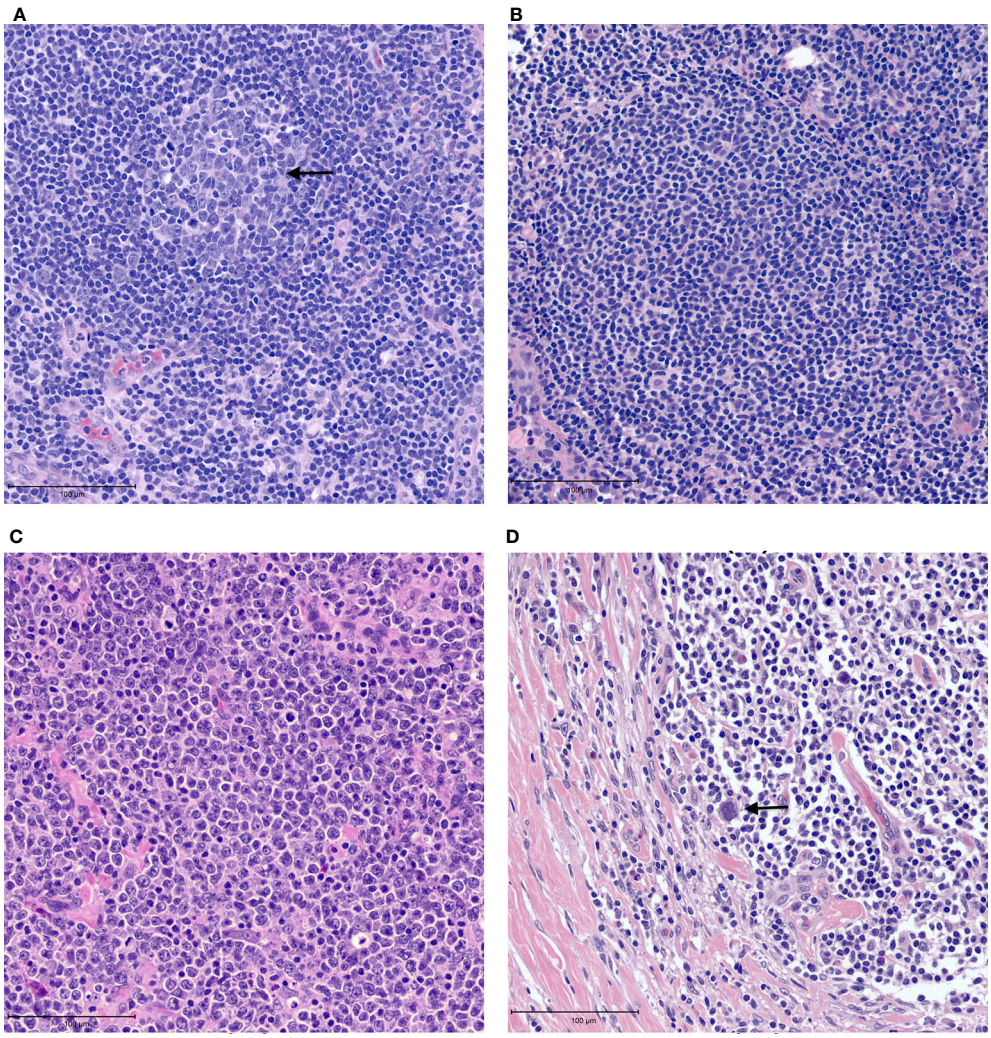

FIGURE 1 | Examples of tumor microenvironment in lymphomas. **(A)** Benign lymph node with a germinal center containing tangible body macrophages (arrow). **(B)** Follicular lymphoma with neoplastic follicle. **(C)** Diffuse large B cell lymphoma showing tissue effacement by large, neoplastic cells with very few admixed small lymphocytes. **(D)** Classic Hodgkin lymphoma showing rare Reed-Sternberg cells (arrow) in a background of small lymphocytes and histiocytes with fibrosis.

the major population of the tumor milieu. CSF1 and CX3CL1 recruit eosinophils and macrophages. Fibrosis, most prominently seen in the nodular sclerosis variant of cHL, is attributed to activation and proliferation of fibroblasts by IL-13, TNF-α and fibroblast growth factors by HRS cells (13). Interaction between membrane-bound or secreted ligands from the microenvironment and cell surface receptors on HRS cells results in activation of canonical signaling pathways such as the JAK-STAT, NF-kB and BCR pathways. These ligand-based mechanisms are complimented by gene mutations that cause constitutional activation of these signaling pathways (29). In highly aggressive tumors such as Burkitt lymphoma, the tumor cells often acquire mutations that result in cell autonomous growth signals (30). Most cases of Burkitt lymphoma harbor translocations of the MYC gene, typically juxtaposing it with enhancer genes of the IGH locus, and less frequently the IGK and IGL loci resulting in upregulation of c-myc, its target genes and target microRNAs. These and other mutations result in cell-autonomous growth signaling. These tumors are, therefore, less likely to need stromal signals for survival resulting in a characteristically sparse tumor microenvironment (31–34).

A better understating of expression, distribution, and interaction of PD-1 and PD-L1 in the tumor microenvironment has been critical in the development of immune checkpoint blockade therapy (CBT) in cancer therapy. CBT involves blockade of the PD-1/PD-L1 axis to enhance the therapeutic effects of anti-tumor immune response (35). PD-1 is expressed predominantly on activated T cells, natural killer cells, dendritic cells, macrophages, and B-cell subsets. PD-L1 is expressed on a wide variety of hematopoietic and non-hematopoietic cells including stromal cells and can also be expressed by tumor cells. In the context of lymphomas, PD-1 expression is seen in tumor infiltrating lymphocytes, as well as the neoplastic cells in

some types of B- and T-cell lymphomas (36). PD-L1 expression is seen in a wide variety of neoplastic cells in various lymphomas including cHL, Primary mediastinal large B cell lymphoma, and extra-nodal NK-T cell lymphomas among others (37). PD-L1 expression is also seen in some immune cells within the tumor microenvironment including tumor infiltrating lymphocytes as well as tumor associated macrophages (TAMs).

Tumor Microenvironment in Plasma Cell Neoplasms

Unlike lymphomas that often present in nodal tissues, plasma cell neoplasms are primarily diseases of the bone marrow. The marrow stromal niche in plasma cell neoplasm is occupied by a variety of cells including T-regs, NK cells, macrophages, dendritic cells, bone marrow stromal cells, endothelial cells, osteoblasts, and osteoclasts embedded in an extracellular matrix (38–40). The stromal niche has been shown to influence homing and adhesion of plasma cells by expression of adhesion molecules and cytokines (41–43). It also appears to aid immune evasion by mechanisms similar to those seen in lymphomas. For example, increased T-regs have been reported in the peripheral blood of neoplasms patients with plasma cell neoplasms (44). Interaction between myeloma cells and T-regs results T-reg expansion by a type 1IFN-dependent positive feedback loop (45). In response to stromal signals, plasma cell neoplasms cells express PD-L1 that interacts with PD-1 protein in T-cells, leading to immune exhaustion (46, 47). A caveat to these observations is that they are based on qRT-PCR and flow cytometry studies on small sample sets that include both patient samples and cell lines; larger studies are needed to validate these observations.

IMMUNE-BASED THERAPY IN LYMPHOMAS AND PLASMA CELL NEOPLASMS

Current therapy for non-Hodgkin lymphomas is dependent on various factors including the pathologic subtype of lymphoma, stage at presentation, and performance status of the patients. The treatment can range from watchful waiting to combination modality regimens followed by stem cell transplant. Salvage regimens are used to treat relapsed disease (48). Therapy for Hodgkin lymphoma is also influenced by stage and risk factors and can range from chemotherapy alone to combination modality treatment, and salvage therapy for progressive disease (49). Treatment for symptomatic myeloma typically involves immunomodulatory drugs and proteasome inhibitors (50, 51). For all three entities, immune based therapies are increasingly part of the therapeutic armamentarium in treatment regimens (3, 40).

Immune-Based Therapy in Lymphomas

Immune based therapies have been used for treatment of lymphomas for more than two decades (3). The earliest success was with rituximab, a chimeric monoclonal antibody targeting the B-cell marker CD20 (52–55). Since then, several other antibodies targeting B- and T-cell markers including CD30, CD19 and CCCR4 have been evaluated in lymphoma treatment with many such drugs receiving regulatory approval (56–59). Initial targeted monoclonal antibodies used complement dependent cytotoxicity or antibody-dependent cytotoxicity for anti-tumor effect. More recently, attempts have been made to increase their efficacy by conjugating them to cytotoxic drugs (60, 61). Bispecific T cell engager antibodies (BiTEs) that are designed to target both tumor antigens and T-cells to bring the tumor cells in close physical proximity to the T cells for enhanced anti-tumoral effects are also being evaluated (62, 63). There is mechanistic evidence that the tumor microenvironment can impact response to therapy. In cell-culture based studies CXCR-4 dependent interaction of lymphoma cells with stromal cells has been shown to protect lymphoma cells from anti-CD20 monoclonal antibody induced apoptosis (64). Studies have also shown induction of microRNAs impacting levels of proapoptotic proteins and upregulation of cell survival signals (65). As in solid organ epithelial tumors, there is intense interest in harnessing the power of CBT in lymphoid malignancies. Downstream signaling from the PD-1 receptor in T cells due to PDL-1 overexpression in tumor cells leads to immune exhaustion and helps tumors evade immune response. Blockade of this signaling pathway with monoclonal antibodies targeting either the PD-1 receptor or its ligand is predicted to enhance antitumor immune response (35). The results of immune checkpoint blockade in lymphomas have been mixed. The strongest response has been seen in lymphomas associated with high PDL-1 expression including Hodgkin lymphoma, primary mediastinal large B cell lymphoma and EBV-associated lymphoproliferative disorders (66–71). In contrast, the efficacy of CBT in other lymphomas such as DLBCL and chronic lymphocytic leukemia (CLL) have been less impressive (72, 73). Other strategies targeting the host immune response to lymphoma are being evaluated e.g., antibodies to the CD47 molecule that suppresses macrophage-induced phagocytosis by binding to signal regulatory protein-alpha (74).

The data with engineered adoptive cell therapies is promising in lymphoma therapy. Details of chimeric antigen receptor T cells (CAR-T) based therapy have been reviewed elsewhere (75). Briefly, CAR-Ts are created by transducing genetic material into patient's own T-cells using lentiviral or retroviral vectors. The chimeric receptor contains an antigen binding extracellular domain that targets a tumor antigen coupled to an intracellular signaling domain, including chimeric domains derived from costimulatory proteins. This design allows the CAR-T cells to respond to tumor antigen without MHC presentation. The CAR-T cells are infused after lymphodepletion chemotherapy. Upon antigen recognition, the receptors cluster together to trigger a T-cell activating signaling cascade. CAR-T therapy targeting CD19 has been approved for the treatment of relapsed refractory aggressive B-NHLs and acute lymphoblastic leukemia following impressive and sustained response in clinical trials (76–78). Prospective clinical trials to evaluate expanded use

of CAR-T as an alternative to stem cell transplant and in other B-NHLs are ongoing including combinatorial strategies with CBT and immunomodulatory therapy (3). Lack of long-term response due to emergence of target antigen negative cells (also known as antigen escape) has led to combinatorial antigen targeting including CD19 and CD20 or CD19 and CD22 (79–81). In contrast to CBT, CAR-T responses in Hodgkin lymphoma and T-cell lymphomas have not been impressive (82, 83).

Other immune based therapeutics in lymphoma include immunomodulators and small molecule inhibitors such as lenalidomide and ibrutinib. Lenalidomide and other thalidomide analogs exhibit immune modulatory effects by altering cytokine production, regulating T cell co-stimulation and augmenting NK cell cytotoxicity (84, 85). Ibrutinib and acalabrutinib are small molecule inhibitors that inhibit Bruton tyrosine kinase (BTK) that is part of the B cell receptor signaling pathway (86–89). In addition, ibrutinib can modulate immune response by increasing Th1 T cell response at the expense of Th2 T cell response by blocking IL-2 inducible kinase (90). Finally, observations in non-Hodgkin lymphomas have shown that treatment with these kinase inhibitors leads to the mobilization of lymphoma cells from their stromal niches into the bloodstream which may be an added component of their efficacy (91).

Immune-Based Therapy in Plasma Cell Neoplasms

Several immunotherapy approaches are being used in treatment of plasma cell neoplasms, both as part of standard-of-care treatments and in clinical trials (92). Lenalidomide is used in first line treatment of both standard-risk and high-risk plasma cell neoplasms (51). Targeted antibodies are now FDA-approved for treatment of plasma cell neoplasms. Anti-CD38 antibodies (daratumumab) in combination with immunomodulators has shown improved outcomes in relapsed refractory plasma cell neoplasms. The mechanism of action includes complement- and antibody-mediated cytotoxicity, and suppression of T-regs and regulatory myeloid populations (93). In contrast to B-NHLs results of CBT therapy in plasma cell neoplasms have been less impressive (94, 95). Combination immunotherapy approaches after autologous stem cell transplant are being evaluated based on encouraging data from preclinical trials (96). Immune modulatory drugs are now routinely used in treatment of symptomatic myeloma in combination regimens where they induce plasma cell apoptosis in addition to immune stimulatory effects. Other immunomodulatory regimens are being evaluated in early clinical trials. CAR-T therapy targeting B cell maturation antigen (BCMA) has shown promise (97, 98). BCMA is expressed primarily in plasmablasts and plasma cells in the bone marrow with no detectable expression in naïve B cells and hematopoietic cells (99, 100). The BCMA expression levels are much higher in neoplastic plasma cells compared to normal plasma cells. In response to signaling from its ligands APRIL and BAFF, BCMA signaling leads to activation of pro-survival pathways (38). Despite impressive early response in trials, persistent and durable response has not been seen, likely due to antigen escape and immunosuppressive effect of the bone marrow tumor microenvironment (101). Other immunomodulatory techniques targeting BCMA including targeted antibodies, BiTE antibodies, and CAR-T therapies to other antigens such as CD138 are under clinical development (102, 103).

IMPACT ON DIAGNOSTICS, PROGNOSTICS, AND BIOMARKERS

The diagnostic work-up of lymphomas and plasma cell neoplasms incorporates morphologic evaluation, immunophenotyping by tissue immunohistochemistry and multiparametric flow cytometry, and ancillary studies. The ancillary studies include cytogenetics, fluorescence *in situ* hybridization (FISH), molecular studies such as PCR for immunoglobulin heavy chain rearrangement, and targeted mutation detection for specific disease entities (104). While substantial information about disease behavior and prognosis can be obtained by these studies, they may provide only limited information regarding the tumor microenvironment and the potential for response to immune based therapies. There is a need to broaden the diagnostic and prognostic modalities to better predict disease response to immune-based therapies in lymphomas and plasma cell neoplasms. Some specific diagnostic modalities and their potential applications are briefly discussed below. While some techniques can be applied routinely in clinical diagnostic labs at the current time, other techniques exist currently more in the realm of clinical research that with time will probably supplant the current techniques.

Immunophenotyping

Immunohistochemistry (IHC) which involves interrogation of formalin-fixed paraffin embedded (FFPE) tissue with specific antibodies for specific antigens, and multiparametric flow cytometry are indispensable tools in clinical hematopathology diagnostic labs (104). These methods have potential utilities in assessing tissue for response to immune-based therapy. In solid organ tumors involving the lung and genitourinary tract for example, an FDA-approved immunohistochemistry based diagnostic assay for PD-L1 is used to predict response to CBT (105, 106). There are currently no FDA-approved IHC diagnostic assays to identify patients that will respond to CBT in hematologic malignancies. Analysis of PD-1 and PD-L1 expression patterns in hematologic malignancies show promising albeit sometimes contradictory results. For example, high proportion of PD-L1 positive macrophages or PD-1-positive T-cells is associated with favorable outcomes in primary testicular lymphoma (107). Similarly in a cohort of *de novo* DLBCL, increased myeloid derived PD-L1 cells correlated with STAT3 and macrophage gene expression, and improved outcomes in a subset of patients (108). A study utilizing 3-marker fluorescent multiplex immunohistochemistry coupled with automated immunofluorescent analysis concluded that the PD-1/PD-L1 expression and interaction is associated with adverse prognosis in DLBCLs with significant T cell infiltration (109). The variability of results in some of these studies may be attributable to

the different antibody clones and experimental methods used in these studies illustrating the need for standardization of these assays across clinical labs prior to widespread diagnostic use. The fact that many of the antigens targeted by immune-based therapies such as CD20, CD19 and CD30 are evaluated during routine lymphoma diagnostic workup is fortuitous. However, the utility of IHC assays to predict disease response to CBT and targeted immunotherapy in hematologic neoplasms is limited in the absence of prospective studies. While it is logical to assume that immunopositivity and the level of antigen expression as assessed by immunophenotyping will correlate with disease response, one should be cautious with such assumptions. Individual studies looking at the correlation of antigen expression by IHC and response to targeted therapy have sometimes shown variable correlation as in the case of CD30 (110, 111). Additionally, lab-to-lab variability in the individual clones of antibody used and in staining protocols can lead to subjective interpretation and poor reproducibility of IHC and flow cytometry studies (112–114). On the other hand, immunomodulatory techniques themselves have potential to impact diagnostic assessment by these techniques. For example, CD20 staining can yield negative IHC results after treatment with rituximab due to antigen masking and down-regulation of CD20 expression (115). Bright CD38 expression is often used in assessing plasma cells by flow cytometry; treatment by daratumumab can lead to interference and artifactual results with laboratory assays for monitoring disease (116, 117). As the arsenal of targeted antibodies grows, diagnosticians need to be keenly aware of such iatrogenic artifacts during diagnostic and prognostic work up. Documentation of increased macrophages, cytotoxic T cells and NK cells by IHC has been shown to correlate with outcomes in cHL (118–121). Current immunohistochemical workup in clinical labs typically uses one antibody on one slice of tissue at a time on glass slides. The development of high-throughput, multiplex immunohistochemical methods opens the possibility of simultaneous evaluation of multiple markers on a single slice of tissue. The individual markers can be evaluated for their expression status and spatial distribution facilitating assessment of the tumor microenvironment by immunophenotypic methods (122–124). Immunophenotypic evaluation may also have utility in predicting response in CAR-T therapy. For example, a population of $CD27^{+}PD\text{-}1^{-}CD8^{+}$ cells expressing high levels of the IL-6 receptor has been shown to correlate with therapeutic response (125).

Digital and Computational Pathology

IHC assays performed on FFPE tissue are easy to adopt in anatomic pathologic labs. However, interlaboratory variability in protocols and subjective variation in manual interpretation can lead to poor reproducibility of assays with impact on treatment and clinical course. The evolution of digital pathology where whole slide imaging scanners are used to digitize glass slides and render images in digital formats has aided the development of automated, reproducible, computer aided diagnostic tools that promise to be the next frontier in tissue-based diagnostics (126). WSI technology builds images of whole slides by stitching together multiple images of tissue sections on slides (127). WSI scanners have now been approved by the FDA for purposes of rendering anatomic pathology diagnoses (128). The College of American Pathology has published guidelines for validation and adoption of digital pathology techniques in clinical settings (129). Digital analyses tools including machine learning algorithms can be applied on digitized histology images for reproducible and quantitative assessment of tumors and their microenvironment. Multiplex approaches can yield high-complexity data with regard to spatial expression of multiple markers in the tumor microenvironment (130). In cHL for example, multiplex IF has shown the association of tumor microenvironment with CTLA-4-positive T cells that are PD-1 negative (131). Data shows that multiplex methods may be better at predicting response to CBT than standard IHC or gene expression profiling methods (132). These analyses can be extended to assess response to immunotherapy by assessing for distribution of components of the immune system such as regulatory T cells and macrophages. A limiting factor in the development and application of machine learning algorithms in computer aided diagnosis is the need for large, high quality data sets to train these algorithms (133). The performance metrics and portability of these algorithms across datasets can also be impacted by pre-analytic variables such as slide scan quality, need for additional image processing and input from human pathologists for accurate interpretation (134, 135). While multiplex IF provides high-resolution data about the tumor microenvironment, complexity of analyses, cost and time considerations currently limit the applicability of this technique in clinical settings. For practical purposes, gene expression analysis is currently utilized to assess characteristic signatures in diagnostic settings.

Molecular Techniques

Ancillary molecular techniques are a significant part of current diagnostic workflow in lymphoid and plasma cell malignancies (104). The presence of specific cytogenetic abnormalities, specific gene mutations, and other molecular findings such as IGH hypermutation status impact disease prognosis in various lymphomas and plasma cell neoplasms, and factor into the calculation of risk stratification scores of individual entities (1). These studies reveal little about the effect of tumor microenvironment on disease course since the spatial context is often lost with these techniques. However, studies have shown the potential utility of gene expression profiles that appear to reflect the tumor microenvironment in predicting response to immune based therapies. For example, in DLBCL gene expression profiles derived from non-malignant cells have shown association with response to R-CHOP therapy. A signature enriched for genes associated with components of the extracellular matrix deposition and histiocytic infiltration was associated with good behavior whereas a signature associated with angiogenesis was associated with poor prognosis (136). Similarly in follicular lymphoma, gene expression profiles associated with macrophages are correlated with different prognoses. Expression of a set of genes enriched for T-cell markers and genes highly expressed in macrophages was associated with better prognosis while a signature enriched for genes highly expressed in dendritic cells, macrophages or both was associated with worse prognosis (137). The refinement of

techniques that allow for spatial single cell sequencing from FFPE tissue with the potential to deliver high-resolution molecular data of the tumor microenvironment with spatial context are particularly exciting developments in this realm (138). Techniques such as CODEX (for CO-Detection by indEXing) that utilizes DNA barcodes, fluorescent dNTP analogs and an *in-situ* polymerization based indexing procedure to iteratively detect antibody binding events have recently been described (139). This methodology allows for single cell antigen quantification in tissue sections, and unlimited levels of multiplexing to map cell types in tissues. The continued development of multiplexed and high-dimensional imaging methods, and their application in translational research are likely to lead to a better understanding of the tumor microenvironment in malignancies and their impact on response to therapy (140).

The power of using a combinatorial approach to dissect tumor microenvironment in lymphoid malignancies is demonstrated by a recent study that used FISH, chromogenic IHC, and multiplex immunofluorescence microscopy with cell phenotyping followed by spatial analyses of the cell phenotypic data to characterize the PD1/PD-L1 pathway in the tumor microenvironment of a multi-institutional cohort of T-cell/histiocyte-rich large B-cell lymphomas (THRLBCL) (141). The authors found frequent PD-L1/PD-L2 copy gain or amplification in the large malignant B-cells of THRLBCL. Using sophisticated spatial image analyses to characterize the distribution of immune cells and their PD1/PDL1 expression status, the authors were able to develop spatially resolved immune signatures that distinguish TCRLBCL from cHL and DLBCL.

CONCLUSION

Recent advances in our understanding of the tumor microenvironment have led to better understanding of pathogenesis of lymphomas and plasma cell neoplasms. Concurrent advances in immune based therapies have highlighted the importance on the tumor microenvironment on disease course and response to therapy. Advances in diagnostic modalities are likely to lead to better biomarker identification, patient risk stratification and theranostic prediction in hematologic malignancies.

AUTHOR CONTRIBUTIONS

The author researched the topic and wrote the manuscript.

FUNDING

Salary support for the author was provided by the Department of Pathology, Yale School of Medicine, Yale University.

REFERENCES

1. Steven H, Swerdlow EC, Lee Harris N, Jaffe ES, Pileri SA, Stein H, et al. *WHO Classification of Tumors of Hematopoietic and Lymphoid Tissues. 4th Edition*. In: Bosman FT, Jaffe ES, Lakhani SR, Ohgaki H, editors. Lyon: IARC (2017).
2. National Cancer Institute. Surveillance, Epidemiology, and End Results Program. In: *Cancer Stat Facts: Non-Hodgkin Lymphoma* (2021). Available at: https://seer.cancer.gov/statfacts/html/nhl.html (Accessed September 13, 2021).
3. Ansell SM, Lin Y. Immunotherapy of Lymphomas. *J Clin Invest* (2020) 130 (4):1576–85. doi: 10.1172/JCI129206
4. Scott DW, Gascoyne RD. The Tumour Microenvironment in B Cell Lymphomas. *Nat Rev Cancer* (2014) 14(8):517–34. doi: 10.1038/nrc3774
5. Hanahan D, Weinberg RA. Hallmarks of Cancer: The Next Generation. *Cell* (2011) 144(5):646–74. doi: 10.1016/j.cell.2011.02.013
6. Waldman AD, Fritz JM, Lenardo MJ. A Guide to Cancer Immunotherapy: From T Cell Basic Science to Clinical Practice. *Nat Rev Immunol* (2020) 20 (11):651–68. doi: 10.1038/s41577-020-0306-5
7. Su W, Spencer J, Wotherspoon AC. Relative Distribution of Tumour Cells and Reactive Cells in Follicular Lymphoma. *J Pathol* (2001) 193(4):498–504. doi: 10.1002/path.820
8. Choi SM, Betz BL, Perry AM. Follicular Lymphoma Diagnostic Caveats and Updates. *Arch Pathol Lab Med* (2018) 142(11):1330–40. doi: 10.5858/arpa.2018-0217-RA
9. Pals ST, de Gorter DJ, Spaargaren M. Lymphoma Dissemination: The Other Face of Lymphocyte Homing. *Blood* (2007) 110(9):3102–11. doi: 10.1182/blood-2007-05-075176
10. Lopez-Giral S, Quintana NE, Cabrerizo M, Alfonso-Perez M, Sala-Valdes M, De Soria VG, et al. Chemokine Receptors That Mediate B Cell Homing to Secondary Lymphoid Tissues Are Highly Expressed in B Cell Chronic Lymphocytic Leukemia and Non-Hodgkin Lymphomas With Widespread Nodular Dissemination. *J Leukoc Biol* (2004) 76(2):462–71. doi: 10.1189/jlb.1203652
11. Rehm A, Anagnostopoulos I, Gerlach K, Broemer M, Scheidereit C, Johrens K, et al. Identification of a Chemokine Receptor Profile Characteristic for Mediastinal Large B-Cell Lymphoma. *Int J Cancer* (2009) 125(10):2367–74. doi: 10.1002/ijc.24652
12. Rehm A, Mensen A, Schradi K, Gerlach K, Wittstock S, Winter S, et al. Cooperative Function of CCR7 and Lymphotoxin in the Formation of a Lymphoma-Permissive Niche Within Murine Secondary Lymphoid Organs. *Blood* (2011) 118(4):1020–33. doi: 10.1182/blood-2010-11-321265
13. Steidl C, Connors JM, Gascoyne RD. Molecular Pathogenesis of Hodgkin's Lymphoma: Increasing Evidence of the Importance of the Microenvironment. *J Clin Oncol* (2011) 29(14):1812–26. doi: 10.1200/JCO.2010.32.8401
14. Yang ZZ, Novak AJ, Ziesmer SC, Witzig TE, Ansell SM. CD70+ Non-Hodgkin Lymphoma B Cells Induce Foxp3 Expression and Regulatory Function in Intratumoral CD4+CD25 T Cells. *Blood* (2007) 110(7):2537–44. doi: 10.1182/blood-2007-03-082578
15. Yang ZZ, Novak AJ, Ziesmer SC, Witzig TE, Ansell SM. Malignant B Cells Skew the Balance of Regulatory T Cells and TH17 Cells in B-Cell Non-Hodgkin's Lymphoma. *Cancer Res* (2009) 69(13):5522–30. doi: 10.1158/0008-5472.CAN-09-0266
16. Yang ZZ, Novak AJ, Stenson MJ, Witzig TE, Ansell SM. Intratumoral CD4+CD25+ Regulatory T-Cell-Mediated Suppression of Infiltrating CD4 + T Cells in B-Cell Non-Hodgkin Lymphoma. *Blood* (2006) 107(9):3639–46. doi: 10.1182/blood-2005-08-3376
17. Ai WZ, Hou JZ, Zeiser R, Czerwinski D, Negrin RS, Levy R. Follicular Lymphoma B Cells Induce the Conversion of Conventional CD4+ T Cells to T-Regulatory Cells. *Int J Cancer* (2009) 124(1):239–44. doi: 10.1002/ijc.23881
18. Kuppers R. Mechanisms of B-Cell Lymphoma Pathogenesis. *Nat Rev Cancer* (2005) 5(4):251–62. doi: 10.1038/nrc1589

19. Ngo VN, Young RM, Schmitz R, Jhavar S, Xiao W, Lim KH, et al. Oncogenically Active MYD88 Mutations in Human Lymphoma. *Nature* (2011) 470(7332):115–9. doi: 10.1038/nature09671
20. Yan Q, Huang Y, Watkins AJ, Kocialkowski S, Zeng N, Hamoudi RA, et al. BCR and TLR Signaling Pathways Are Recurrently Targeted by Genetic Changes in Splenic Marginal Zone Lymphomas. *Haematologica* (2012) 97 (4):595–8. doi: 10.3324/haematol.2011.054080
21. Schwaller J, Went P, Matthes T, Dirnhofer S, Donze O, Mhawech-Fauceglia P, et al. Paracrine Promotion of Tumor Development by the TNF Ligand APRIL in Hodgkin's Disease. *Leukemia* (2007) 21(6):1324–7. doi: 10.1038/sj.leu.2404627
22. Riemersma SA, Jordanova ES, Schop RF, Philippo K, Looijenga LH, Schuuring E, et al. Extensive Genetic Alterations of the HLA Region, Including Homozygous Deletions of HLA Class II Genes in B-Cell Lymphomas Arising in Immune-Privileged Sites. *Blood* (2000) 96 (10):3569–77. doi: 10.1182/blood.V96.10.3569
23. Steidl C, Shah SP, Woolcock BW, Rui L, Kawahara M, Farinha P, et al. MHC Class II Transactivator CIITA Is a Recurrent Gene Fusion Partner in Lymphoid Cancers. *Nature* (2011) 471(7338):377–81. doi: 10.1038/nature09754
24. Challa-Malladi M, Lieu YK, Califano O, Holmes AB, Bhagat G, Murty VV, et al. Combined Genetic Inactivation of Beta2-Microglobulin and CD58 Reveals Frequent Escape From Immune Recognition in Diffuse Large B Cell Lymphoma. *Cancer Cell* (2011) 20(6):728–40. doi: 10.1016/j.ccr.2011.11.006
25. Wilkinson ST, Vanpatten KA, Fernandez DR, Brunhoeber P, Garsha KE, Glinsmann-Gibson BJ, et al. Partial Plasma Cell Differentiation as a Mechanism of Lost Major Histocompatibility Complex Class II Expression in Diffuse Large B-Cell Lymphoma. *Blood* (2012) 119(6):1459–67. doi: 10.1182/blood-2011-07-363820
26. Rimsza LM, Roberts RA, Miller TP, Unger JM, LeBlanc M, Braziel RM, et al. Loss of MHC Class II Gene and Protein Expression in Diffuse Large B-Cell Lymphoma Is Related to Decreased Tumor Immunosurveillance and Poor Patient Survival Regardless of Other Prognostic Factors: A Follow-Up Study From the Leukemia and Lymphoma Molecular Profiling Project. *Blood* (2004) 103(11):4251–8. doi: 10.1182/blood-2003-07-2365
27. Green MR, Monti S, Rodig SJ, Juszczynski P, Currie T, O'Donnell E, et al. Integrative Analysis Reveals Selective 9p24.1 Amplification, Increased PD-1 Ligand Expression, and Further Induction *via* JAK2 in Nodular Sclerosing Hodgkin Lymphoma and Primary Mediastinal Large B-Cell Lymphoma. *Blood* (2010) 116(17):3268–77. doi: 10.1182/blood-2010-05-282780
28. Diepstra A, Poppema S, Boot M, Visser L, Nolte IM, Niens M, et al. HLA-G Protein Expression as a Potential Immune Escape Mechanism in Classical Hodgkin's Lymphoma. *Tissue Antigens* (2008) 71(3):219–26. doi: 10.1111/j.1399-0039.2008.01005.x
29. Liu Y, Abdul Razak FR, Terpstra M, Chan FC, Saber A, Nijland M, et al. The Mutational Landscape of Hodgkin Lymphoma Cell Lines Determined by Whole-Exome Sequencing. *Leukemia* (2014) 28(11):2248–51. doi: 10.1038/leu.2014.201
30. Schmitz R, Young RM, Ceribelli M, Jhavar S, Xiao W, Zhang M, et al. Burkitt Lymphoma Pathogenesis and Therapeutic Targets From Structural and Functional Genomics. *Nature* (2012) 490(7418):116–20. doi: 10.1038/nature11378
31. Greenough A, Dave SS. New Clues to the Molecular Pathogenesis of Burkitt Lymphoma Revealed Through Next-Generation Sequencing. *Curr Opin Hematol* (2014) 21(4):326–32. doi: 10.1097/MOH.0000000000000059
32. Salaverria I, Martin-Guerrero I, Wagener R, Kreuz M, Kohler CW, Richter J, et al. A Recurrent 11q Aberration Pattern Characterizes a Subset of MYC-Negative High-Grade B-Cell Lymphomas Resembling Burkitt Lymphoma. *Blood* (2014) 123(8):1187–98. doi: 10.1182/blood-2013-06-507996
33. Love C, Sun Z, Jima D, Li G, Zhang J, Miles R, et al. The Genetic Landscape of Mutations in Burkitt Lymphoma. *Nat Genet* (2012) 44(12):1321–5. doi: 10.1038/ng.2468
34. Richter J, Schlesner M, Hoffmann S, Kreuz M, Leich E, Burkhardt B, et al. Recurrent Mutation of the ID3 Gene in Burkitt Lymphoma Identified by Integrated Genome, Exome and Transcriptome Sequencing. *Nat Genet* (2012) 44(12):1316–20. doi: 10.1038/ng.2469
35. Pardoll DM. The Blockade of Immune Checkpoints in Cancer Immunotherapy. *Nat Rev Cancer* (2012) 12(4):252–64. doi: 10.1038/nrc3239
36. Xie M, Huang X, Ye X, Qian W. Prognostic and Clinicopathological Significance of PD-1/PD-L1 Expression in the Tumor Microenvironment and Neoplastic Cells for Lymphoma. *Int Immunopharmacol* (2019) 77:105999. doi: 10.1016/j.intimp.2019.105999
37. Chen BJ, Chapuy B, Ouyang J, Sun HH, Roemer MG, Xu ML, et al. PD-L1 Expression Is Characteristic of a Subset of Aggressive B-Cell Lymphomas and Virus-Associated Malignancies. *Clin Cancer Res* (2013) 19(13):3462–73. doi: 10.1158/1078-0432.CCR-13-0855
38. Garcia-Ortiz A, Rodriguez-Garcia Y, Encinas J, Maroto-Martin E, Castellano E, Teixido J, et al. The Role of Tumor Microenvironment in Multiple Myeloma Development and Progression. *Cancers (Basel)* (2021) 13(2):217. doi: 10.3390/cancers13020217
39. Kawano Y, Moschetta M, Manier S, Glavey S, Gorgun GT, Roccaro AM, et al. Targeting the Bone Marrow Microenvironment in Multiple Myeloma. *Immunol Rev* (2015) 263(1):160–72. doi: 10.1111/imr.12233
40. Lomas OC, Tahri S, Ghobrial IM. The Microenvironment in Myeloma. *Curr Opin Oncol* (2020) 32(2):170–5. doi: 10.1097/CCO.0000000000000615
41. Pellegrino A, Ria R, Di Pietro G, Cirulli T, Surico G, Pennisi A, et al. Bone Marrow Endothelial Cells in Multiple Myeloma Secrete CXC-Chemokines That Mediate Interactions With Plasma Cells. *Br J Haematol* (2005) 129 (2):248–56. doi: 10.1111/j.1365-2141.2005.05443.x
42. Roccaro AM, Sacco A, Purschke WG, Moschetta M, Buchner K, Maasch C, et al. SDF-1 Inhibition Targets the Bone Marrow Niche for Cancer Therapy. *Cell Rep* (2014) 9(1):118–28. doi: 10.1016/j.celrep.2014.08.042
43. Roccaro AM, Mishima Y, Sacco A, Moschetta M, Tai YT, Shi J, et al. CXCR4 Regulates Extra-Medullary Myeloma Through Epithelial-Mesenchymal-Transition-Like Transcriptional Activation. *Cell Rep* (2015) 12(4):622–35. doi: 10.1016/j.celrep.2015.06.059
44. Feyler S, von Lilienfeld-Toal M, Jarmin S, Marles L, Rawstron A, Ashcroft AJ, et al. CD4(+)CD25(+)FoxP3(+) Regulatory T Cells Are Increased Whilst CD3(+)CD4(-)CD8(-)alphabetaTCR(+) Double Negative T Cells Are Decreased in the Peripheral Blood of Patients With Multiple Myeloma Which Correlates With Disease Burden. *Br J Haematol* (2009) 144(5):686–95. doi: 10.1111/j.1365-2141.2008.07530.x
45. Kawano Y, Zavidij O, Park J, Moschetta M, Kokubun K, Mouhieddine TH, et al. Blocking IFNAR1 Inhibits Multiple Myeloma-Driven Treg Expansion and Immunosuppression. *J Clin Invest* (2018) 128(6):2487–99. doi: 10.1172/JCI88169
46. Tamura H, Ishibashi M, Yamashita T, Tanosaki S, Okuyama N, Kondo A, et al. Marrow Stromal Cells Induce B7-H1 Expression on Myeloma Cells, Generating Aggressive Characteristics in Multiple Myeloma. *Leukemia* (2013) 27(2):464–72. doi: 10.1038/leu.2012.213
47. Liu J, Hamrouni A, Wolowiec D, Coiteux V, Kuliczkowski K, Hetuin D, et al. Plasma Cells From Multiple Myeloma Patients Express B7-H1 (PD-L1) and Increase Expression After Stimulation With IFN-{Gamma} and TLR Ligands *via* a MyD88-, TRAF6-, and MEK-Dependent Pathway. *Blood* (2007) 110(1):296–304. doi: 10.1182/blood-2006-10-051482
48. Zelenetz AD, Gordon LI, Abramson JS, Advani RH, Bartlett NL, Caimi PF, et al. NCCN Guidelines Insights: B-Cell Lymphomas, Version 3.2019. *J Natl Compr Canc Netw* (2019) 17(6):650–61. doi: 10.6004/jnccn.2019.0029
49. Hoppe RT, Advani RH, Ai WZ, Ambinder RF, Armand P, Bello CM, et al. Hodgkin Lymphoma, Version 2.2020, NCCN Clinical Practice Guidelines in Oncology. *J Natl Compr Canc Netw* (2020) 18(6):755–81. doi: 10.6004/jnccn.2020.0026
50. Rajkumar SV, Kumar S. Multiple Myeloma Current Treatment Algorithms. *Blood Cancer J* (2020) 10(9):94. doi: 10.1038/s41408-020-00359-2
51. Rajkumar SV. Multiple Myeloma: 2020 Update on Diagnosis, Risk-Stratification and Management. *Am J Hematol* (2020) 95(5):548–67. doi: 10.1002/ajh.25791
52. McLaughlin P, Grillo-Lopez AJ, Link BK, Levy R, Czuczman MS, Williams ME, et al. Rituximab Chimeric Anti-CD20 Monoclonal Antibody Therapy for Relapsed Indolent Lymphoma: Half of Patients Respond to a Four-Dose Treatment Program. *J Clin Oncol* (1998) 16(8):2825–33. doi: 10.1200/JCO.1998.16.8.2825
53. Colombat P, Salles G, Brousse N, Eftekhari P, Soubeyran P, Delwail V, et al. Rituximab (Anti-CD20 Monoclonal Antibody) as Single First-Line Therapy for Patients With Follicular Lymphoma With a Low Tumor Burden: Clinical

and Molecular Evaluation. *Blood* (2001) 97(1):101–6. doi: 10.1182/blood.V97.1.101
54. Hiddemann W, Kneba M, Dreyling M, Schmitz N, Lengfelder E, Schmits R, et al. Frontline Therapy With Rituximab Added to the Combination of Cyclophosphamide, Doxorubicin, Vincristine, and Prednisone (CHOP) Significantly Improves the Outcome for Patients With Advanced-Stage Follicular Lymphoma Compared With Therapy With CHOP Alone: Results of a Prospective Randomized Study of the German Low-Grade Lymphoma Study Group. *Blood* (2005) 106(12):3725–32. doi: 10.1182/blood-2005-01-0016
55. Coiffier B, Lepage E, Briere J, Herbrecht R, Tilly H, Bouabdallah R, et al. CHOP Chemotherapy Plus Rituximab Compared With CHOP Alone in Elderly Patients With Diffuse Large-B-Cell Lymphoma. *N Engl J Med* (2002) 346(4):235–42. doi: 10.1056/NEJMoa011795
56. Salles G, Duell J, Gonzalez Barca E, Tournilhac O, Jurczak W, Liberati AM, et al. Tafasitamab Plus Lenalidomide in Relapsed or Refractory Diffuse Large B-Cell Lymphoma (L-MIND): A Multicentre, Prospective, Single-Arm, Phase 2 Study. *Lancet Oncol* (2020) 21(7):978–88. doi: 10.1016/S1470-2045(20)30225-4
57. Ishida T, Joh T, Uike N, Yamamoto K, Utsunomiya A, Yoshida S, et al. Defucosylated Anti-CCR4 Monoclonal Antibody (KW-0761) for Relapsed Adult T-Cell Leukemia-Lymphoma: A Multicenter Phase II Study. *J Clin Oncol* (2012) 30(8):837–42. doi: 10.1200/JCO.2011.37.3472
58. Ogura M, Ishida T, Hatake K, Taniwaki M, Ando K, Tobinai K, et al. Multicenter Phase II Study of Mogamulizumab (KW-0761), a Defucosylated Anti-Cc Chemokine Receptor 4 Antibody, in Patients With Relapsed Peripheral T-Cell Lymphoma and Cutaneous T-Cell Lymphoma. *J Clin Oncol* (2014) 32(11):1157–63. doi: 10.1200/JCO.2013.52.0924
59. Kim YH, Bagot M, Pinter-Brown L, Rook AH, Porcu P, Horwitz SM, et al. Mogamulizumab Versus Vorinostat in Previously Treated Cutaneous T-Cell Lymphoma (MAVORIC): An International, Open-Label, Randomised, Controlled Phase 3 Trial. *Lancet Oncol* (2018) 19(9):1192–204. doi: 10.1016/S1470-2045(18)30379-6
60. Younes A, Gopal AK, Smith SE, Ansell SM, Rosenblatt JD, Savage KJ, et al. Results of a Pivotal Phase II Study of Brentuximab Vedotin for Patients With Relapsed or Refractory Hodgkin's Lymphoma. *J Clin Oncol* (2012) 30(18):2183–9. doi: 10.1200/JCO.2011.38.0410
61. Connors JM, Jurczak W, Straus DJ, Ansell SM, Kim WS, Gallamini A, et al. Brentuximab Vedotin With Chemotherapy for Stage III or IV Hodgkin's Lymphoma. *N Engl J Med* (2018) 378(4):331–44. doi: 10.1056/NEJMoa1708984
62. Viardot A, Goebeler ME, Hess G, Neumann S, Pfreundschuh M, Adrian N, et al. Phase 2 Study of the Bispecific T-Cell Engager (BiTE) Antibody Blinatumomab in Relapsed/Refractory Diffuse Large B-Cell Lymphoma. *Blood* (2016) 127(11):1410–6. doi: 10.1182/blood-2015-06-651380
63. Budde LE, Wu D, Martin DB, Philip M, Shustov AR, Smith SD, et al. Bendamustine With Rituximab, Etoposide and Carboplatin (T(R)EC) in Relapsed or Refractory Aggressive Lymphoma: A Prospective Multicentre Phase 1/2 Clinical Trial. *Br J Haematol* (2018) 183(4):601–7. doi: 10.1111/bjh.15585
64. Mraz M, Zent CS, Church AK, Jelinek DF, Wu X, Pospisilova S, et al. Bone Marrow Stromal Cells Protect Lymphoma B-Cells From Rituximab-Induced Apoptosis and Targeting Integrin Alpha-4-Beta-1 (VLA-4) With Natalizumab can Overcome This Resistance. *Br J Haematol* (2011) 155(1):53–64. doi: 10.1111/j.1365-2141.2011.08794.x
65. Lwin T, Lin J, Choi YS, Zhang X, Moscinski LC, Wright KL, et al. Follicular Dendritic Cell-Dependent Drug Resistance of Non-Hodgkin Lymphoma Involves Cell Adhesion-Mediated Bim Down-Regulation Through Induction of microRNA-181a. *Blood* (2010) 116(24):5228–36. doi: 10.1182/blood-2010-03-275925
66. Zinzani PL, Ribrag V, Moskowitz CH, Michot JM, Kuruvilla J, Balakumaran A, et al. Safety and Tolerability of Pembrolizumab in Patients With Relapsed/Refractory Primary Mediastinal Large B-Cell Lymphoma. *Blood* (2017) 130(3):267–70. doi: 10.1182/blood-2016-12-758383
67. Ansell SM, Lesokhin AM, Borrello I, Halwani A, Scott EC, Gutierrez M, et al. PD-1 Blockade With Nivolumab in Relapsed or Refractory Hodgkin's Lymphoma. *N Engl J Med* (2015) 372(4):311–9. doi: 10.1056/NEJMoa1411087
68. Armand P, Shipp MA, Ribrag V, Michot JM, Zinzani PL, Kuruvilla J, et al. Programmed Death-1 Blockade With Pembrolizumab in Patients With Classical Hodgkin Lymphoma After Brentuximab Vedotin Failure. *J Clin Oncol* (2016) 34(31):3733–9. doi: 10.1200/JCO.2016.67.3467
69. Armand P, Engert A, Younes A, Fanale M, Santoro A, Zinzani PL, et al. Nivolumab for Relapsed/Refractory Classic Hodgkin Lymphoma After Failure of Autologous Hematopoietic Cell Transplantation: Extended Follow-Up of the Multicohort Single-Arm Phase II CheckMate 205 Trial. *J Clin Oncol* (2018) 36(14):1428–39. doi: 10.1200/JCO.2017.76.0793
70. Chen R, Zinzani PL, Fanale MA, Armand P, Johnson NA, Brice P, et al. Phase II Study of the Efficacy and Safety of Pembrolizumab for Relapsed/Refractory Classic Hodgkin Lymphoma. *J Clin Oncol* (2017) 35(19):2125–32. doi: 10.1200/JCO.2016.72.1316
71. Younes A, Santoro A, Shipp M, Zinzani PL, Timmerman JM, Ansell S, et al. Nivolumab for Classical Hodgkin's Lymphoma After Failure of Both Autologous Stem-Cell Transplantation and Brentuximab Vedotin: A Multicentre, Multicohort, Single-Arm Phase 2 Trial. *Lancet Oncol* (2016) 17(9):1283–94. doi: 10.1016/S1470-2045(16)30167-X
72. Ansell SM, Minnema MC, Johnson P, Timmerman JM, Armand P, Shipp MA, et al. Nivolumab for Relapsed/Refractory Diffuse Large B-Cell Lymphoma in Patients Ineligible for or Having Failed Autologous Transplantation: A Single-Arm, Phase II Study. *J Clin Oncol* (2019) 37(6):481–9. doi: 10.1200/JCO.18.00766
73. Ding W, LaPlant BR, Call TG, Parikh SA, Leis JF, He R, et al. Pembrolizumab in Patients With CLL and Richter Transformation or With Relapsed CLL. *Blood* (2017) 129(26):3419–27. doi: 10.1182/blood-2017-02-765685
74. Advani R, Flinn I, Popplewell L, Forero A, Bartlett NL, Ghosh N, et al. CD47 Blockade by Hu5F9-G4 and Rituximab in Non-Hodgkin's Lymphoma. *N Engl J Med* (2018) 379(18):1711–21. doi: 10.1056/NEJMoa1807315
75. Feins S, Kong W, Williams EF, Milone MC, Fraietta JA. An Introduction to Chimeric Antigen Receptor (CAR) T-Cell Immunotherapy for Human Cancer. *Am J Hematol* (2019) 94(S1):S3–9. doi: 10.1002/ajh.25418
76. Neelapu SS, Tummala S, Kebriaei P, Wierda W, Gutierrez C, Locke FL, et al. Chimeric Antigen Receptor T-Cell Therapy - Assessment and Management of Toxicities. *Nat Rev Clin Oncol* (2018) 15(1):47–62. doi: 10.1038/nrclinonc.2017.148
77. Schuster SJ, Bishop MR, Tam CS, Waller EK, Borchmann P, McGuirk JP, et al. Tisagenlecleucel in Adult Relapsed or Refractory Diffuse Large B-Cell Lymphoma. *N Engl J Med* (2019) 380(1):45–56. doi: 10.1056/NEJMoa1804980
78. Park JH, Riviere I, Gonen M, Wang X, Senechal B, Curran KJ, et al. Long-Term Follow-Up of CD19 CAR Therapy in Acute Lymphoblastic Leukemia. *N Engl J Med* (2018) 378(5):449–59. doi: 10.1056/NEJMoa1709919
79. Bukhari A, El Chaer F, Koka R, Singh Z, Hutnick E, Ruehle K, et al. Rapid Relapse of Large B-Cell Lymphoma After CD19 Directed CAR-T-Cell Therapy Due to CD-19 Antigen Loss. *Am J Hematol* (2019) 94(10):E273–E5. doi: 10.1002/ajh.25591
80. Shalabi H, Kraft IL, Wang HW, Yuan CM, Yates B, Delbrook C, et al. Sequential Loss of Tumor Surface Antigens Following Chimeric Antigen Receptor T-Cell Therapies in Diffuse Large B-Cell Lymphoma. *Haematologica* (2018) 103(5):e215–8. doi: 10.3324/haematol.2017.183459
81. Shah NN, Johnson BD, Schneider D, Zhu F, Szabo A, Keever-Taylor CA, et al. Bispecific Anti-CD20, Anti-CD19 CAR T Cells for Relapsed B Cell Malignancies: A Phase 1 Dose Escalation and Expansion Trial. *Nat Med* (2020) 26(10):1569–75. doi: 10.1038/s41591-020-1081-3
82. Ramos CA, Ballard B, Zhang H, Dakhova O, Gee AP, Mei Z, et al. Clinical and Immunological Responses After CD30-Specific Chimeric Antigen Receptor-Redirected Lymphocytes. *J Clin Invest* (2017) 127(9):3462–71. doi: 10.1172/JCI94306
83. Wang CM, Wu ZQ, Wang Y, Guo YL, Dai HR, Wang XH, et al. Autologous T Cells Expressing CD30 Chimeric Antigen Receptors for Relapsed or Refractory Hodgkin Lymphoma: An Open-Label Phase I Trial. *Clin Cancer Res* (2017) 23(5):1156–66. doi: 10.1158/1078-0432.CCR-16-1365
84. Davies FE, Forsyth PD, Rawstron AC, Owen RG, Pratt G, Evans PA, et al. The Impact of Attaining a Minimal Disease State After High-Dose Melphalan and Autologous Transplantation for Multiple Myeloma. *Br J Haematol* (2001) 112(3):814–9. doi: 10.1046/j.1365-2141.2001.02530.x

85. Tai YT, Li XF, Catley L, Coffey R, Breitkreutz I, Bae J, et al. Immunomodulatory Drug Lenalidomide (CC-5013, IMiD3) Augments Anti-CD40 SGN-40-Induced Cytotoxicity in Human Multiple Myeloma: Clinical Implications. *Cancer Res* (2005) 65(24):11712–20. doi: 10.1158/0008-5472.CAN-05-1657
86. Burger JA, Barr PM, Robak T, Owen C, Ghia P, Tedeschi A, et al. Long-Term Efficacy and Safety of First-Line Ibrutinib Treatment for Patients With CLL/SLL: 5 Years of Follow-Up From the Phase 3 RESONATE-2 Study. *Leukemia* (2020) 34(3):787–98. doi: 10.1038/s41375-019-0602-x
87. Byrd JC, Harrington B, O'Brien S, Jones JA, Schuh A, Devereux S, et al. Acalabrutinib (ACP-196) in Relapsed Chronic Lymphocytic Leukemia. *N Engl J Med* (2016) 374(4):323–32. doi: 10.1056/NEJMoa1509981
88. Byrd JC, Furman RR, Coutre SE, Burger JA, Blum KA, Coleman M, et al. Three-Year Follow-Up of Treatment-Naive and Previously Treated Patients With CLL and SLL Receiving Single-Agent Ibrutinib. *Blood* (2015) 125(16):2497–506. doi: 10.1182/blood-2014-10-606038
89. Shanafelt TD, Wang XV, Kay NE, Hanson CA, O'Brien S, Barrientos J, et al. Ibrutinib-Rituximab or Chemoimmunotherapy for Chronic Lymphocytic Leukemia. *N Engl J Med* (2019) 381(5):432–43. doi: 10.1056/NEJMoa1817073
90. Dubovsky JA, Beckwith KA, Natarajan G, Woyach JA, Jaglowski S, Zhong Y, et al. Ibrutinib Is an Irreversible Molecular Inhibitor of ITK Driving a Th1-Selective Pressure in T Lymphocytes. *Blood* (2013) 122(15):2539–49. doi: 10.1182/blood-2013-06-507947
91. Chang BY, Francesco M, De Rooij MF, Magadala P, Steggerda SM, Huang MM, et al. Egress of CD19(+)CD5(+) Cells Into Peripheral Blood Following Treatment With the Bruton Tyrosine Kinase Inhibitor Ibrutinib in Mantle Cell Lymphoma Patients. *Blood* (2013) 122(14):2412–24. doi: 10.1182/blood-2013-02-482125
92. Minnie SA, Hill GR. Immunotherapy of Multiple Myeloma. *J Clin Invest* (2020) 130(4):1565–75. doi: 10.1172/JCI129205
93. Palumbo A, Chanan-Khan A, Weisel K, Nooka AK, Masszi T, Beksac M, et al. Daratumumab, Bortezomib, and Dexamethasone for Multiple Myeloma. *N Engl J Med* (2016) 375(8):754–66. doi: 10.1056/NEJMoa1606038
94. Lesokhin AM, Ansell SM, Armand P, Scott EC, Halwani A, Gutierrez M, et al. Nivolumab in Patients With Relapsed or Refractory Hematologic Malignancy: Preliminary Results of a Phase Ib Study. *J Clin Oncol* (2016) 34(23):2698–704. doi: 10.1200/JCO.2015.65.9789
95. D'Souza A, Hari P, Pasquini M, Braun T, Johnson B, Lundy S, et al. A Phase 2 Study of Pembrolizumab During Lymphodepletion After Autologous Hematopoietic Cell Transplantation for Multiple Myeloma. *Biol Blood Marrow Transplant* (2019) 25(8):1492–7. doi: 10.1016/j.bbmt.2019.04.005
96. Jing W, Gershan JA, Weber J, Tlomak D, McOlash L, Sabatos-Peyton C, et al. Combined Immune Checkpoint Protein Blockade and Low Dose Whole Body Irradiation as Immunotherapy for Myeloma. *J Immunother Cancer* (2015) 3(1):2. doi: 10.1186/s40425-014-0043-z
97. Brudno JN, Maric I, Hartman SD, Rose JJ, Wang M, Lam N, et al. T Cells Genetically Modified to Express an Anti-B-Cell Maturation Antigen Chimeric Antigen Receptor Cause Remissions of Poor-Prognosis Relapsed Multiple Myeloma. *J Clin Oncol* (2018) 36(22):2267–80. doi: 10.1200/JCO.2018.77.8084
98. Cohen AD, Garfall AL, Stadtmauer EA, Melenhorst JJ, Lacey SF, Lancaster E, et al. B Cell Maturation Antigen-Specific CAR T Cells Are Clinically Active in Multiple Myeloma. *J Clin Invest* (2019) 129(6):2210–21. doi: 10.1172/JCI126397
99. O'Connor BP, Raman VS, Erickson LD, Cook WJ, Weaver LK, Ahonen C, et al. BCMA Is Essential for the Survival of Long-Lived Bone Marrow Plasma Cells. *J Exp Med* (2004) 199(1):91–8. doi: 10.1084/jem.20031330
100. Friedman KM, Garrett TE, Evans JW, Horton HM, Latimer HJ, Seidel SL, et al. Effective Targeting of Multiple B-Cell Maturation Antigen-Expressing Hematological Malignances by Anti-B-Cell Maturation Antigen Chimeric Antigen Receptor T Cells. *Hum Gene Ther* (2018) 29(5):585–601. doi: 10.1089/hum.2018.001
101. Sidana S, Shah N. CAR T-Cell Therapy: Is It Prime Time in Myeloma? *Hematol Am Soc Hematol Educ Program* (2019) 2019(1):260–5. doi: 10.1182/hematology.2019000370
102. Sun C, Mahendravada A, Ballard B, Kale B, Ramos C, West J, et al. Safety and Efficacy of Targeting CD138 With a Chimeric Antigen Receptor for the Treatment of Multiple Myeloma. *Oncotarget* (2019) 10(24):2369–83. doi: 10.18632/oncotarget.26792
103. Gogishvili T, Danhof S, Prommersberger S, Rydzek J, Schreder M, Brede C, et al. SLAMF7-CAR T Cells Eliminate Myeloma and Confer Selective Fratricide of SLAMF7(+) Normal Lymphocytes. *Blood* (2017) 130(26):2838–47. doi: 10.1182/blood-2017-04-778423
104. Kroft SH, Sever CE, Bagg A, Billman B, Diefenbach C, Dorfman DM, et al. Laboratory Workup of Lymphoma in Adults. *Am J Clin Pathol* (2021) 155(1):12–37. doi: 10.1093/ajcp/aqaa191
105. Rimm DL, Han G, Taube JM, Yi ES, Bridge JA, Flieder DB, et al. A Prospective, Multi-Institutional, Pathologist-Based Assessment of 4 Immunohistochemistry Assays for PD-L1 Expression in Non-Small Cell Lung Cancer. *JAMA Oncol* (2017) 3(8):1051–8. doi: 10.1001/jamaoncol.2017.0013
106. Davis AA, Patel VG. The Role of PD-L1 Expression as a Predictive Biomarker: An Analysis of All US Food and Drug Administration (FDA) Approvals of Immune Checkpoint Inhibitors. *J Immunother Cancer* (2019) 7(1):278. doi: 10.1186/s40425-019-0768-9
107. Pollari M, Bruck O, Pellinen T, Vahamurto P, Karjalainen-Lindsberg ML, Mannisto S, et al. PD-L1(+) Tumor-Associated Macrophages and PD-1(+) Tumor-Infiltrating Lymphocytes Predict Survival in Primary Testicular Lymphoma. *Haematologica* (2018) 103(11):1908–14. doi: 10.3324/haematol.2018.197194
108. McCord R, Bolen CR, Koeppen H, Kadel EE3rd, Oestergaard MZ, Nielsen T, et al. PD-L1 and Tumor-Associated Macrophages in *De Novo* DLBCL. *Blood Adv* (2019) 3(4):531–40. doi: 10.1182/bloodadvances.2018020602
109. Li L, Sun R, Miao Y, Tran T, Adams L, Roscoe N, et al. PD-1/PD-L1 Expression and Interaction by Automated Quantitative Immunofluorescent Analysis Show Adverse Prognostic Impact in Patients With Diffuse Large B-Cell Lymphoma Having T-Cell Infiltration: A Study From the International DLBCL Consortium Program. *Mod Pathol* (2019) 32(6):741–54. doi: 10.1038/s41379-018-0193-5
110. Xu ML, Gabali A, Hsi ED, Fedoriw Y, Vij K, Salama ME, et al. Practical Approaches on CD30 Detection and Reporting in Lymphoma Diagnosis. *Am J Surg Pathol* (2020) 44(2):e1–e14. doi: 10.1097/PAS.0000000000001368
111. Xu ML, Acevedo-Gadea C, Seropian S, Katz SG. Expression of CD30 as a Biomarker to Predict Response to Brentuximab Vedotin. *Histopathology* (2016) 69(1):155–8. doi: 10.1111/his.12914
112. Tsao MS, Kerr KM, Kockx M, Beasley MB, Borczuk AC, Botling J, et al. PD-L1 Immunohistochemistry Comparability Study in Real-Life Clinical Samples: Results of Blueprint Phase 2 Project. *J Thorac Oncol* (2018) 13(9):1302–11. doi: 10.1016/j.jtho.2018.05.013
113. Doroshow DB, Bhalla S, Beasley MB, Sholl LM, Kerr KM, Gnjatic S, et al. PD-L1 as a Biomarker of Response to Immune-Checkpoint Inhibitors. *Nat Rev Clin Oncol* (2021) 18(6):345–62. doi: 10.1038/s41571-021-00473-5
114. Brunnstrom H, Johansson A, Westbom-Fremer S, Backman M, Djureinovic D, Patthey A, et al. PD-L1 Immunohistochemistry in Clinical Diagnostics of Lung Cancer: Inter-Pathologist Variability Is Higher Than Assay Variability. *Mod Pathol* (2017) 30(10):1411–21. doi: 10.1038/modpathol.2017.59
115. Hiraga J, Tomita A, Sugimoto T, Shimada K, Ito M, Nakamura S, et al. Down-Regulation of CD20 Expression in B-Cell Lymphoma Cells After Treatment With Rituximab-Containing Combination Chemotherapies: Its Prevalence and Clinical Significance. *Blood* (2009) 113(20):4885–93. doi: 10.1182/blood-2008-08-175208
116. van de Donk NW, Otten HG, El Haddad O, Axel A, Sasser AK, Croockewit S, et al. Interference of Daratumumab in Monitoring Multiple Myeloma Patients Using Serum Immunofixation Electrophoresis can be Abrogated Using the Daratumumab IFE Reflex Assay (DIRA). *Clin Chem Lab Med* (2016) 54(6):1105–9. doi: 10.1515/cclm-2015-0888
117. Kleinot W, Aguilera N, Courville EL. Daratumumab Interference in Flow Cytometry Producing a False Kappa Light Chain Restriction in Plasma Cells. *Lab Med* (2020) 52(4):403–9. doi: 10.1093/labmed/lmaa107
118. Chetaille B, Bertucci F, Finetti P, Esterni B, Stamatoullas A, Picquenot JM, et al. Molecular Profiling of Classical Hodgkin Lymphoma Tissues Uncovers Variations in the Tumor Microenvironment and Correlations With EBV

Infection and Outcome. *Blood* (2009) 113(12):2765–3775. doi: 10.1182/blood-2008-07-168096
119. Steidl C, Lee T, Shah SP, Farinha P, Han G, Nayar T, et al. Tumor-Associated Macrophages and Survival in Classic Hodgkin's Lymphoma. *N Engl J Med* (2010) 362(10):875–85. doi: 10.1056/NEJMoa0905680
120. Alvaro T, Lejeune M, Salvado MT, Bosch R, Garcia JF, Jaen J, et al. Outcome in Hodgkin's Lymphoma Can Be Predicted From the Presence of Accompanying Cytotoxic and Regulatory T Cells. *Clin Cancer Res* (2005) 11(4):1467–73. doi: 10.1158/1078-0432.CCR-04-1869
121. Kelley TW, Pohlman B, Elson P, Hsi ED. The Ratio of FOXP3+ Regulatory T Cells to Granzyme B+ Cytotoxic T/NK Cells Predicts Prognosis in Classical Hodgkin Lymphoma and Is Independent of Bcl-2 and MAL Expression. *Am J Clin Pathol* (2007) 128(6):958–65. doi: 10.1309/NB3947K383DJ0LQ2
122. Dixon AR, Bathany C, Tsuei M, White J, Barald KF, Takayama S. Recent Developments in Multiplexing Techniques for Immunohistochemistry. *Expert Rev Mol Diagn* (2015) 15(9):1171–86. doi: 10.1586/14737159.2015.1069182
123. Blom S, Paavolainen L, Bychkov D, Turkki R, Maki-Teeri P, Hemmes A, et al. Systems Pathology by Multiplexed Immunohistochemistry and Whole-Slide Digital Image Analysis. *Sci Rep* (2017) 7(1):15580. doi: 10.1038/s41598-017-15798-4
124. Stack EC, Wang C, Roman KA, Hoyt CC. Multiplexed Immunohistochemistry, Imaging, and Quantitation: A Review, With an Assessment of Tyramide Signal Amplification, Multispectral Imaging and Multiplex Analysis. *Methods* (2014) 70(1):46–58. doi: 10.1016/j.ymeth.2014.08.016
125. Fraietta JA, Lacey SF, Orlando EJ, Pruteanu-Malinici I, Gohil M, Lundh S, et al. Determinants of Response and Resistance to CD19 Chimeric Antigen Receptor (CAR) T Cell Therapy of Chronic Lymphocytic Leukemia. *Nat Med* (2018) 24(5):563–71. doi: 10.1038/s41591-018-0010-1
126. Parwani AV. Next Generation Diagnostic Pathology: Use of Digital Pathology and Artificial Intelligence Tools to Augment a Pathological Diagnosis. *Diagn Pathol* (2019) 14(1):138. doi: 10.1186/s13000-019-0921-2
127. Zarella MD, Bowman D, Aeffner F, Farahani N, Xthona A, Absar SF, et al. A Practical Guide to Whole Slide Imaging: A White Paper From the Digital Pathology Association. *Arch Pathol Lab Med* (2019) 143(2):222–34. doi: 10.5858/arpa.2018-0343-RA
128. Evans AJ, Bauer TW, Bui MM, Cornish TC, Duncan H, Glassy EF, et al. US Food and Drug Administration Approval of Whole Slide Imaging for Primary Diagnosis: A Key Milestone Is Reached and New Questions Are Raised. *Arch Pathol Lab Med* (2018) 142(11):1383–7. doi: 10.5858/arpa.2017-0496-CP
129. Evans AJ, Brown RW, Bui MM, Chlipala EA, Lacchetti C, Milner DA, et al. Validating Whole Slide Imaging Systems for Diagnostic Purposes in Pathology: Guideline Update From the College of American Pathologists in Collaboration With the American Society for Clinical Pathology and the Association for Pathology Informatics. *Arch Pathol Lab Med* (2021). doi: 10.5858/arpa.2020-0723-CP
130. Heindl A, Nawaz S, Yuan Y. Mapping Spatial Heterogeneity in the Tumor Microenvironment: A New Era for Digital Pathology. *Lab Invest* (2015) 95(4):377–84. doi: 10.1038/labinvest.2014.155
131. Patel SS, Weirather JL, Lipschitz M, Lako A, Chen PH, Griffin GK, et al. The Microenvironmental Niche in Classic Hodgkin Lymphoma Is Enriched for CTLA-4-Positive T Cells That Are PD-1-Negative. *Blood* (2019) 134(23):2059–69. doi: 10.1182/blood.2019002206
132. Lu S, Stein JE, Rimm DL, Wang DW, Bell JM, Johnson DB, et al. Comparison of Biomarker Modalities for Predicting Response to PD-1/PD-L1 Checkpoint Blockade: A Systematic Review and Meta-Analysis. *JAMA Oncol* (2019) 5(8):1195–204. doi: 10.1001/jamaoncol.2019.1549
133. Tizhoosh HR, Pantanowitz L. Artificial Intelligence and Digital Pathology: Challenges and Opportunities. *J Pathol Inform* (2018) 9:38. doi: 10.4103/jpi.jpi_53_18
134. Pantanowitz L, Quiroga-Garza GM, Bien L, Heled R, Laifenfeld D, Linhart C, et al. An Artificial Intelligence Algorithm for Prostate Cancer Diagnosis in Whole Slide Images of Core Needle Biopsies: A Blinded Clinical Validation and Deployment Study. *Lancet Digit Health* (2020) 2(8):e407–16. doi: 10.1016/S2589-7500(20)30159-X
135. Perincheri S, Levi AW, Celli R, Gershkovich P, Rimm D, Morrow JS, et al. An Independent Assessment of an Artificial Intelligence System for Prostate Cancer Detection Shows Strong Diagnostic Accuracy. *Mod Pathol* (2021) 34(8):1588–95. doi: 10.1038/s41379-021-00794-x
136. Lenz G, Wright G, Dave SS, Xiao W, Powell J, Zhao H, et al. Stromal Gene Signatures in Large-B-Cell Lymphomas. *N Engl J Med* (2008) 359(22):2313–23. doi: 10.1056/NEJMoa0802885
137. Dave SS, Wright G, Tan B, Rosenwald A, Gascoyne RD, Chan WC, et al. Prediction of Survival in Follicular Lymphoma Based on Molecular Features of Tumor-Infiltrating Immune Cells. *N Engl J Med* (2004) 351(21):2159–69. doi: 10.1056/NEJMoa041869
138. Liu Y, Yang M, Deng Y, Su G, Enninful A, Guo CC, et al. High-Spatial-Resolution Multi-Omics Sequencing *via* Deterministic Barcoding in Tissue. *Cell* (2020) 183(6):1665–81 e18. doi: 10.1016/j.cell.2020.10.026
139. Goltsev Y, Samusik N, Kennedy-Darling J, Bhate S, Hale M, Vazquez G, et al. Deep Profiling of Mouse Splenic Architecture With CODEX Multiplexed Imaging. *Cell* (2018) 174(4):968–81.e15. doi: 10.1016/j.cell.2018.07.010
140. Decalf J, Albert ML, Ziai J. New Tools for Pathology: A User's Review of a Highly Multiplexed Method for *in Situ* Analysis of Protein and RNA Expression in Tissue. *J Pathol* (2019) 247(5):650–61. doi: 10.1002/path.5223
141. Voorhees PM, Rodriguez C, Reeves B, Nathwani N, Costa LJ, Lutska Y, et al. Daratumumab Plus RVd for Newly Diagnosed Multiple Myeloma: Final Analysis of the Safety Run-in Cohort of GRIFFIN. *Blood Adv* (2021) 5(4):1092–6. doi: 10.1182/bloodadvances.2020003642

Conflict of Interest: The author declares that the research was conducted in the absence of any commercial or financial relationships that could be construed as a potential conflict of interest.

Publisher's Note: All claims expressed in this article are solely those of the authors and do not necessarily represent those of their affiliated organizations, or those of the publisher, the editors and the reviewers. Any product that may be evaluated in this article, or claim that may be made by its manufacturer, is not guaranteed or endorsed by the publisher.

Advantages of publishing in Frontiers

OPEN ACCESS
Articles are free to read for greatest visibility and readership

FAST PUBLICATION
Around 90 days from submission to decision

HIGH QUALITY PEER-REVIEW
Rigorous, collaborative, and constructive peer-review

TRANSPARENT PEER-REVIEW
Editors and reviewers acknowledged by name on published articles

Frontiers
Avenue du Tribunal-Fédéral 34
1005 Lausanne | Switzerland

Visit us: www.frontiersin.org
Contact us: frontiersin.org/about/contact

REPRODUCIBILITY OF RESEARCH
Support open data and methods to enhance research reproducibility

DIGITAL PUBLISHING
Articles designed for optimal readership across devices

FOLLOW US
@frontiersin

IMPACT METRICS
Advanced article metrics track visibility across digital media

EXTENSIVE PROMOTION
Marketing and promotion of impactful research

LOOP RESEARCH NETWORK
Our network increases your article's readership